

School of Molecular and Life Sciences

**Controlled Polymerisation of Arylacetylenes with Well-Defined
Rhodium Catalysts**

Nicholas Tan Sheng Loong

**This thesis is presented for the Degree of
Doctor of Philosophy
of
Curtin University**

September 2020

Declaration

To the best of my knowledge this thesis contains no material previously published by any other person except where due acknowledgement has been made.

I declare that this thesis is my own account of my research and contains as its main content work which has not been submitted for a degree or diploma in any university.

Signature:

Date: 7th September 2020

Abstract

This thesis details the synthesis of six new Rh(I)-vinyl and -aryl complexes and their extensive characterisation using a suite of multinuclear nuclear magnetic resonance spectroscopy techniques (which include but is not limited to, ^{103}Rh and 2D ^{31}P - ^{103}Rh heteronuclear multiple quantum correlation spectroscopy), single-crystal X-ray diffraction crystallography, X-ray powder diffraction, and elemental analysis. The primary focus of this thesis is the evaluation of these new Rh(I)-vinyl and -aryl complexes as initiators for the stereospecific (controlled) (co)polymerisation of phenylacetylenes (PA) and other substituted arylacetylene substrates.

Initially, a series of Rh(I)(nbd)(α -phenylvinylfluorenyl)(P(4- XC_6H_4) $_3$) (where nbd = 2,5-norbornadiene and X = F, CF_3 , (3,5- CF_3) $_2$) complexes were synthesised, characterised and evaluated for their ability to mediate the (controlled) polymerisation of PA. The study reveals that the complexes were active initiators for PA homopolymerisation but suffered low initiation efficiencies (IEs) which were attributed to steric and geometric factors arising from the bulky and conformationally locked nature of the α -phenylvinylfluorenyl initiating fragment, thus, hindering facile coordination of monomer.

To address this issue, we targeted the synthesis of Rh(I)(nbd)(2-phenylnaphthyl)(P(4- FC_6H_4) $_3$) complex that possesses an initiating fragment that is geometrically unrestricted; however, upon recrystallisation, the structural isomer, Rh(I)(nbd)(2-naphthylphenyl)(P(4- FC_6H_4) $_3$) was isolated. We proceeded to rationalise the mechanism which underpinned this observation and proposed that the formation of the structural isomer(s) was via 1,4-Rh atom migrations, or *ortho-to-ortho* C-H bond activations, which was supported by density functional theory

calculations. ^1H and $2\text{D } ^{31}\text{P}-^{103}\text{Rh}$ HMQC spectroscopy further identified a second, Rh(I)(3-phenylnaphthyl) isomer (and possibly a third minor structural isomer), which are a result of the same Rh-atom migratory processes. While unanticipated, the complex(es) were evaluated and determined to be active initiator(s) for the PA homopolymerisation with significantly improved IEs (though not quantitative, which was attributed to the formation of multiple (in)active species) over the Rh(I)- α -phenylvinylfluorenyl derivatives.

Building on these findings, we proceeded to investigate and targeted the synthesis of an alternative Rh(I)-aryl complex, Rh(I)(nbd)(Biphenyl)(P(4-FC₆H₄)₃). While it is potentially susceptible to 1,4-Rh atom migratory processes, the occurrence of such an event will yield chemically identical species. The Rh(I)-biphenyl complex was successfully prepared and isolated and was shown to be an active initiator for the homopolymerisation of PA with near-quantitative IEs observed, which was a significant improvement over its predecessors. The activity of Rh(I)-biphenyl was evaluated against the functional derivative 4-fluorophenylacetylene (4-FPA) was found to be active in homopolymerisation of 4-FPA. Poly(phenylacetylene-*block*-4-fluorophenylacetylene) was successfully prepared by sequential monomer addition, yielding a block copolymer with a low dispersity.

Finally, the structure-activity of the diene ligand of the Rh(I) complex was investigated by substituting the nbd diene ligand with tetrafluorobenzobarrelene (tfb), which has a relatively higher π -acidity. Rh(I)(tfb)(Biphenyl)(P(4-FC₆H₄)₃) complex was synthesised, characterised and subsequently evaluated as an initiator for the homopolymerisation of PA. The higher π -acidity of tfb diene ligand was demonstrated to enhance the activity of Rh(I) towards PA homopolymerisation, which was confirmed via polymerisation kinetic studies. In comparison to its structurally similar

Rh(I)-biphenyl complex bearing a nbd diene ligand, the activity was 8 to 16 times higher than previous Rh-vinyl and -aryl complexes, placing it first amongst the complexes, in terms of activity towards PA. The activity of this complex was also evaluated against a range of substituted (aryl)acetylenes, and was found to be active in the homopolymerisation for a majority of these monomers, exceptions being 2-ethynylthiophene and 4-ethynylaniline, which were found to be not amenable to polymerisation mediated by this Rh(I)-aryl species.

Overall, the resulting polyenes from the polymerisations mediated by each of these six new Rh(I)-vinyl and -aryl complexes possess high *cis-transoidal* stereoregularity with relatively narrow molecular weight distributions. Further, the ability of these complexes to mediate block (co)polymerisation to prepare diblock copolymers, is an indication of a controlled polymerisation process.

Acknowledgements

It has been a roller-coaster of emotions in the time leading up to the completion of this thesis. There was a lot of uncertainty, but one thing is for sure, I have made it, and it is all thanks to Prof. Andrew B. Lowe. Firstly, I would like to express my sincerest gratitude and thank him for the opportunity to do this research, it was challenging in the beginning, but your assurance and guidance help me persevere through it all. He also gave me constant and quick feedback until the last second while sacrificing his weekends, so that I may graduate on time. I am sorry for piling last-minute work on you and thank you for not giving up on me, for that, I am truly grateful to you. Secondly, I would also like to thank Prof. Mark Ogden and Associate Prof. Max Massi for their excellent co-supervision and for their prompt aid whenever I needed it throughout my PhD.

I would like to acknowledge and thank Dr. Gareth Nealon for his impeccable work in nuclear magnetic resonance spectroscopy, particularly, the ^{103}Rh and 2D ^{31}P - ^{103}Rh experiments. I also would like to thank Dr. Alexandre Sobolev and Dr. Stephen A. Moggach for their single-crystal X-ray diffraction crystallography contributions, Dr. Matthew R. Rowles for the X-ray powder diffraction work, Dr. Paolo Raiteri for his work on the gas-phase modelling, and Dr. Jason M. Lynam for his contribution on the DFT calculations presented in this thesis. I would also like to express my thanks to Dr. Peter Simpson, who had the patience to teach me the ropes of air-sensitive chemistry at the start of my PhD so that I was properly prepared to conduct the research presented in this thesis

To my family, especially my parents, who are 3,929 km away from me who supported me emotionally and financially when needed, which has given me the

strength and reason to push through the difficult times, I thank you. Finally, I would like to thank my partner, Alexis W. H. Chung, who help me with the final proof-reading, assurance, emotional support and encouragement during times of great distress and uncertainty.

Statement of Contribution by Others

Chapters 1-4 have been prepared as manuscripts for peer-reviewed publication in the scientific literature. These chapters are adaptations of submitted and published manuscripts, with the exception of formatting consistent with the thesis. Signature of authors approving of the candidate's contribution can be found at the end of this section. I have obtained permission from the copyright owners to use any third-party copyright material reproduced (adapted) in this thesis, and to use any of my own published work in which the copyright is held by another party. Permission for paper reproduction in this thesis can be found in Appendix B.

The study presented in Chapter 1 was published in the peer-reviewed journal, 'Angewandte Chemie International Edition' and 'Angewandte Chemie' on 16th March 2020:

Nicholas Sheng Loong Tan, Andrew B. Lowe '**Polymerizations Mediated by Well-defined Rhodium Complexes**' *Angewandte Chemie, International Edition* **2020**, *59*, 5008-5021. **DOI:** 10.1002/anie.201909909.

Nicholas Sheng Loong Tan, Andrew B. Lowe '**Durch definierte Rhodiumkomplexe vermittelte Polymerisationen**' *Angewandte Chemie*, **2020**, *132*, 5040-5052. **DOI:** 10.1002/ange.201909909.

Statement of contributions: The manuscript was written by Andrew B. Lowe and Nicholas Sheng Loong Tan. The manuscript was revised by all authors.

The study presented in Chapter 2 was published in the peer-reviewed journal, 'European Journal of Inorganic Chemistry' on 1st February 2019:

Nicholas Sheng Loong Tan, Peter V. Simpson, Gareth L. Nealon, Alexandre N. Sobolev, Paolo Raiteri, Massimiliano Massi, Mark I. Ogden, Andrew B. Lowe. **'Rhodium(I)- α -Phenylvinylfluorenyl Complexes: Synthesis, Characterization, and Evaluation as Initiators in the Stereospecific Polymerization of Phenylacetylene'** *European Journal of Inorganic Chemistry* **2019**, 592-601. DOI: 10.1002/ejic.201801411. Highlighted as a *Very Important Paper*.

Statement of contributions: The manuscript was written by Andrew B. Lowe and Nicholas Sheng Loong Tan. The manuscript was revised by all authors; experimental data (such as catalyst synthesis and polymerisation data) was collected and analysed by Nicholas Sheng Loong Tan with guidance from Andrew B. Lowe; gas-phase modelling data and analysis were provided by Paolo Raiteri; single-crystal XRD data and analysis were provided by Alexandre N. Sobolev; ^{103}Rh and 2D NMR experiments (such as ^{31}P - ^{103}Rh HMQC) data were provided by Gareth L. Nealon.

The study presented in Chapter 3 was published within the peer-reviewed journal, 'Dalton Transaction' on 18th October 2019:

Nicholas Sheng Loong Tan, Gareth L. Nealon, Matthew R. Rowles, Alexandre N. Sobolev, Jason M. Lynam, Mark I. Ogden, Massimiliano Massi, Andrew B. Lowe. **'A (2-(Naphthalen-2-yl)phenyl)rhodium(I) Complex formed by a Proposed Intramolecular 1,4-Ortho-to-Ortho' Rh Metal-atom Migration and its Efficacy as an Initiator in the Controlled Stereospecific**

Polymerization of Phenylacetylene’ Accepted for publication 18/10/2019.

Dalton Transactions **2019**, 48, 16437-16447. **DOI:** 10.1039/c9dt02953b.

Statement of contributions: The manuscript was written by Andrew B. Lowe and Nicholas Sheng Loong Tan. The manuscript was revised by all authors; experimental data (such as catalyst synthesis and polymerisation data) was collected and analysed by Nicholas Sheng Loong Tan with guidance from Andrew B. Lowe; DFT calculations were performed by Jason M. Lynam; continuous shape measures data and analysis were conducted by Mark I. Ogden; single-crystal XRD data and analysis were provided by Alexandre N. Sobolev; X-ray powder diffraction data was provided by Matthew R. Rowles; ^{103}Rh , 2D NMR experiments (such as ^{31}P - ^{103}Rh HMQC) data and structure assignments were provided by Gareth L. Nealon.

The study presented in Chapter 4 was published within the peer-reviewed journal, ‘ACS Macro Letters’ on 1st January 2020:

Nicholas Sheng Loong Tan, Gareth L. Nealon, Gemma Turner, Stephen Moggach, Mark I. Ogden, Massimiliano Massi, Andrew B. Lowe ‘**Rh(I)(2,5-Norbornadiene)(biphenyl)tris(4-fluorophenyl)phosphine: Synthesis, Characterization and Application as an Initiator in the Stereospecific (Co)Polymerization of Phenylacetylenes**’ *ACS Macro Letters* **2020**, 9, 56-60.
DOI: 10.1021/acsmacrolett.9b00975.

Statement of contributions: The manuscript was written by Andrew B. Lowe and Nicholas Sheng Loong Tan. The manuscript was revised by all authors; experimental data (such as catalyst synthesis and polymerisation data) was collected and analysed by Nicholas Sheng Loong Tan with guidance from Andrew B. Lowe; single-crystal XRD data and analysis were provided by Stephen Moggach and Gemma

Turner; ^{103}Rh , 2D NMR experiments (such as ^{31}P - ^{103}Rh HMQC) data and structure assignments were provided by Gareth L. Nealon.

Author 1

Name: Nicholas Tan Sheng Loong

Signature:

Date: 2nd September 2020

Author 2

Name: Andrew B. Lowe

Signature:

Date: 2nd September 2020

Author 3

Name: Massimiliano Massi

Signature:

Date: 3rd September 2020

Author 4

Name: Mark I. Ogden

Signature:

Date: 2nd September 2020

Author 5

Name: Gareth L. Nealon

Signature:

Date: 3rd September 2020

Author 6

Name: Jason M. Lynam

Signature:

Date: 2nd September 2020

Author 7

Name: Paolo Raiteri

Signature:

Date: 4th September 2020

Author 8

Name: Alexandre N. Sobolev

Signature:

Date: 3rd September 2020

Author 9

Name: Stephen A. Moggach

Signature:

Date: 15th September 2020

Author 10

Name: Peter V. Simpson

Signature:

Date: 7th September 2020

Author 11

Name: Matthew R. Rowles

Signature:

Date: 2nd September 2020

Author 12

Name: Gemma Turner

Signature:

Date: 2nd September 2020

Table of Contents

Declaration.....	i
Abstract.....	iii
Acknowledgements.....	vi
Statement of Contribution by Others.....	x
Table of Contents	xviii
List of Figures.....	xxiii
List of Schemes	xxxvi
List of Tables	xlii
Chapter 1	1
1.1 Transition Metal Complexes and Their Applications in Synthetic Chemistry... 1	
1.2 Introduction to Polymer Nomenclatures and Techniques	3
1.3 Insertion Polymerisation.....	8
1.3.1 Titanium-Based Catalysts (Ziegler-Natta) and Their Application in α -olefin Polymerisation	8
1.4 Olefin Metathesis Processes and Its Application in Metathesis Polymerisation	10
1.4.1 Ruthenium.....	11
1.1.1. Tungsten and Molydenum	21
1.1.1.1. W- Carbene Complexes for ROMP	21
1.1.1.2. Mo-Carbenes Complexes for ROMP.....	24

1.5	Metathesis vs Insertion Polymerisation of Substituted Acetylenes	26
1.5.1	Metathesis Ru-Based Initiators for The Polymerisation of Substituted Acetylenes	29
1.5.2	Group 6 (W and Mo) Metathesis Catalyst-Mediated Polymerisation of Substituted Acetylenes	34
1.5.3	Niobium (Nb) and Tantalum (Ta) Complexes for The Polymerisation of Acetylenes	39
1.6	Rhodium Catalysts for The (Co)Polymerisation of Acetylenes	40
1.6.1	Non-Controlled Stereospecific Polymerisation of Substituted Acetylenes. ..	40
1.6.2	Stereospecific Controlled Polymerisation by Rh Complexes	62
1.7	Research Objectives.....	88
1.8	References.....	89
Chapter 2	115
2.1	Introduction.....	115
2.2	Experimental.....	118
2.2.1	Materials.....	118
2.2.2	Rh(I)- α -phenylvinyl Fluorenyl Complexes.....	119
2.2.3	Modelling	122
2.2.4	Polymerisations	122
2.2.5	Homopolymerisation of Phenylacetylene	122
2.2.6	Multistage, Self-blocking of Polyphenylacetylene with Phenylacetylene...	123
2.2.7	NMR Measurements	123

2.2.8	Crystallography	124
2.2.9	Elemental Analysis.....	125
2.2.10	Size Exclusion Chromatography (SEC).....	126
2.3	Results and Discussion	127
2.3.1	Synthesis and Characterisation of Rh(I)- α -phenylvinyl Complexes.....	127
2.4	Conclusions	153
2.5	References.....	154
	Chapter 3	158
3.1	Introduction.....	158
3.2	Experimental.....	161
3.2.1	Materials.....	161
3.2.2	Attempted Synthesis of Rh(nbd)(2-PhNaphth)(P(4-FC ₆ H ₄) ₃)	161
3.2.3	Polymerisation Reactions.....	165
3.2.4	Computational Chemistry	165
3.2.5	NMR Measurements	166
3.2.6	Crystallography	167
3.2.7	X-ray Powder Diffraction	168
3.2.8	Elemental Analysis.....	168
3.2.9	Size Exclusion Chromatography (SEC).....	168
3.3	Results and Discussion	170
3.3.1	Synthesis and Characterisation of a Rh(I)-2-naphthylphenyl Species.....	170
3.3.2	Mechanistic and Computational Studies	181

3.3.3	Polymerisation Studies.....	185
3.4	Conclusions	196
3.5	References.....	197
	Chapter 4	203
4.1	Introduction.....	203
4.2	Experimental.....	206
4.2.1	Materials.....	206
4.2.2	Synthesis of Rh(I)(nbd)(Biphenyl)(P(4-FC ₆ H ₄) ₃).....	206
4.2.3	Polymerisation Studies.....	208
4.2.4	NMR Measurements	209
4.2.5	Crystallography	210
4.2.6	Elemental Analysis.....	211
4.2.7	Size Exclusion Chromatography (SEC).....	211
4.3	Results and Discussion	212
4.4	Conclusions	230
4.5	References.....	232
	Chapter 5	234
5.1	Introduction.....	234
5.2	Experimental.....	238
5.2.1	Materials.....	238
5.2.2	Synthesis of Tetrafluorobenzobarralene (tfb).	239
5.2.3	Synthesis of [Rh(tfb)Cl] ₂	240

5.2.4	Synthesis of Rh(I)(tfb)(Biphenyl)(P(4-FC ₆ H ₄) ₃)	241
5.2.5	Homopolymerisation of Phenylacetylene	243
5.2.6	Self-blocking of Polyphenylacetylene (PPA) with PA	243
5.2.7	NMR Measurements	244
5.2.8	Crystallography	245
5.2.9	Size Exclusion Chromatography (SEC).....	245
5.3	Results and Discussion	246
5.3.1	Synthesis of Dimer Complex [Rh(tfb)Cl] ₂	246
5.3.2	Synthesis of Target Complex Rh(I)(tfb)(Biphenyl)(P(4-FC ₆ H ₄) ₃)	251
5.3.3	Polymerisation Studies.....	257
5.4	Conclusions	280
5.5	References.....	283
	Chapter 6	286
6.1	References.....	295
	Appendix A	297
	Appendix B	299
	Appendix C	301

List of Figures

Figure 1-1. Illustration of the separation process for a polymer sample using size exclusion chromatography technique.....	4
Figure 1-2. SEC chromatogram plots the detector signal against elution volume or time.....	5
Figure 1-3. Selected examples of (oxa) norbornene and cyclopropene derivatives that have been reported in the literature.....	12
Figure 1-4. Grubbs catalysts from 1 st to 3 rd generation (3 , 4 , 5) and Hoveyda-Grubbs 1 st generation, 6 , discussed in this chapter.....	19
Figure 1-5. Selected examples of W-based complexes discussed in this section.....	21
Figure 1-6. Possible geometric structures of polyphenylacetylene.....	28
Figure 1-7. Monomers used in the polymerisations by Kasumata <i>et al.</i> ¹⁵³ to synthesise functionalised poly(phenylacetylene)s.....	31
Figure 1-8. Living polymerisation of various 1,2-disubstituted acetylenes by ternary Mo-halide based catalyst system.....	36
Figure 1-9. Selected examples of well-defined Mo-based complexes that mediate the living polymerisation of <i>ortho</i> -substituted phenylacetylenes and α,ω -dialkynes.....	39
Figure 1-10. Rh complexes used in the polymerisation of PA reported by Furlani <i>et al.</i> ¹⁹²⁻¹⁹⁴	41

Figure 1-11. Chemical structures of [Rh(nbd)Cl] ₂ , 20 , and [Rh(cod)Cl] ₂ , 21	42
Figure 1-12. Stereoregular polymerisations of PA derivatives yielding <i>cis-transoidal</i> materials mediated by the [Rh(nbd)Cl] ₂ /Et ₃ N catalyst system.	44
Figure 1-13. Cationic Rh complexes bearing amidine bases (1,8-diazabicyclo[5.4.0]undec-7-ene (DBU) and 1,5-diazabicyclo[4.3.0]non-5-ene (DBN)).	45
Figure 1-14 Dinuclear Rh complex bearing a cod diene ligand with pentafluorothiophenol bridging ligand and mononuclear Rh complex reported by Vilar <i>et al.</i> ²³¹	46
Figure 1-15. Structures of RhBp(cod) and RhTp(cod) (where Bp = bis(pyrazolylborate) and Tp = tris(pyrazolylborate)).....	49
Figure 1-16. A series of charged and non-charged mononuclear Rh(I) complexes bearing dibenzo[α,ϵ]cyclooctatetraene (dbcot) derived from dinuclear Rh complex 37	51
Figure 1-17 Selected examples of organorhodium catalyst bearing cod/nbd diene ligand with a tris(pyrazolyl)borate and their target monomers which have been grouped according to the activity of the catalyst towards them.....	52
Figure 1-18. Dinuclear Rh complexes employed as initiators for the polymerisation of PA.....	54
Figure 1-19. Structures of cationic and neutral variants of Rh(I) 1,4,7-triazacyclononane complexes reported by Gott <i>et al.</i> ²⁵⁰	58

Figure 1-20. Cationic Rh(I) complexes bearing hemilabile hetero-atom phosphine ligands reported by Jiménez <i>et al.</i> ²⁵¹	59
Figure 1-21. A series of neutral and cationic Rh complexes for application as initiators in the polymerisation of PA reported by Angoy <i>et al.</i> ²⁵²	60
Figure 1-22. A series of dinuclear Rh complexes for PA polymerisation reported by Wu <i>et al.</i> ²⁵³	61
Figure 1-23. Masuda-type Rh(I)-triphenyl derivatives.	70
Figure 1-24. Chemical structures of Rh(I) complexes with hemilabile heteroatom ligands with either phosphine or amino functional groups reported by Onishi <i>et al.</i> ²⁶⁵	73
Figure 1-25. The Dewar-Chatt-Duncanson model of bonding between a metal centre and an alkene.....	76
Figure 1-26. Chemical structure of Rh(tfb)(PhC=CPh ₂)(PPh ₃) derived from the [Rh(tfb)Cl] ₂ /LiCPh=CPh ₂ /PPh ₃ ternary mixture.	77
Figure 1-27. Chemical structures of 2,5-norbornadienerhodium(I) tetraphenylborate.	80
Figure 1-28. Chemical structures of Rh(I)-aryl species examined, evaluated and presented in the study by Onitsuka <i>et al.</i> ²⁸²	85
Figure 2-1. Chemical structures of Noyori's Rh(I)-phenylethynyl derivatives (76 and 77), Masuda's Rh(I)triphenylvinyl species (78a , 78b , 78c) and new fluorous- α -phenylvinylfluorenyl Rh(I) complexes (88b , 88d and 88e).....	116

Figure 2-2. ^1H NMR spectra, recorded in C_6D_6 , of $\text{Rh}(\text{nbd})(\text{CPh}=\text{CFlu})(\text{P}(4\text{-FC}_6\text{H}_4)_3)$ (88b). (A) The full ^1H NMR spectrum with key peaks highlighted and the measured integral values included; (B) the ^1H NMR spectrum covering the aromatic region from $\delta = 8.0$ to 6.4 ppm.	129
Figure 2-3. NMR spectra, recorded in C_6D_6 , of 88b (A) The $^{31}\text{P}\{^1\text{H}\}$ NMR spectrum with the rhodium-phosphorous coupling constant noted, and; (B) the ^{19}F NMR spectrum with the structure of the complex shown.....	131
Figure 2-4. NMR spectra of 88d (A) ^1H NMR spectrum of 88d recorded in CD_2Cl_2 ; (B) $^{31}\text{P}\{^1\text{H}\}$ NMR spectrum of 88d recorded in C_6D_6 ; (C) ^{19}F NMR spectrum of 88d recorded in C_6D_6	133
Figure 2-5. NMR spectra of 88e (A) ^1H NMR spectrum of 88e recorded in CD_2Cl_2 ; (B) $^{31}\text{P}\{^1\text{H}\}$ NMR spectrum of 88e recorded in C_6D_6 ; (C) ^{19}F NMR spectrum of 88e recorded in C_6D_6	134
Figure 2-6. (A) ^{103}Rh NMR spectrum of 88b , recorded in C_6D_6 at 298K; (B) ^{103}Rh NMR spectrum of 88d , recorded in CD_2Cl_2 at 298 K.	135
Figure 2-7. ^{31}P - ^{103}Rh HMQC spectrum of 88e recorded in CD_2Cl_2 at 298K.	136
Figure 2-8. ^{31}P - ^{103}Rh HMQC spectrum of 88d recorded in CD_2Cl_2 at 298K.....	137
Figure 2-9. ^{31}P - ^{103}Rh HMQC spectrum of 88b recorded in CD_2Cl_2 at 298K.....	138
Figure 2-10. OLEX ² representation of the X-ray crystal structure of 88b with 50 % probability ellipsoids and H atoms omitted for clarity. Selected bond lengths (Å): Rh(1)-P(1), 2.314(5); Rh(1)-C(52), 2.185(17); Rh(1)-C(57), 2.236(18); C(14)-F(1),	

1.354(2). Selected bond angles (deg): C(52)-Rh(1)-P(1), 171.13(5); C(57)-Rh(1)-P(1), 106.54(5); C(40)-Rh(1)-P(1), 92.99(5). 139

Figure 2-11. OLEX² representation of the X-ray crystal structure of **88d** with 50 % probability ellipsoids and H atoms omitted for clarity. Selected bond lengths (Å): Rh(1)-P(1), 2.301(4); Rh(1)-C(52), 2.168(15); Rh(1)-C(57), 2.217(15); C(17)-F(13), 1.330(2). Selected bond angles (deg): C(52)-Rh(1)-P(1), 171.42(4); C(57)-Rh(1)-P(1), 106.78(5); C(40)-Rh(1)-P(1), 92.97(4). 140

Figure 2-12. OLEX² representation of the X-ray crystal structure of **88e** with 50 % probability ellipsoids and H atoms omitted for clarity. Selected bond lengths (Å): Rh(1)-P(1), 2.305(6); Rh(1)-C(52), 2.165(2); Rh(1)-C(57), 2.250(2); C(151)-F(153), 1.326(4). Selected bond angles (deg): C(52)-Rh(1)-P(1), 167.53(7); C(57)-Rh(1)-P(1), 110.10(7); C(40)-Rh(1)-P(1), 89.74(7). 141

Figure 2-13. Energy-minimised, gas-phase molecular geometry of Rh(nbd)(CPh=CFlu)(P(4-CF₃C₆H₄)₃) (**88d**). The corresponding modelled geometry for **88b** is given in the Appendix A. 142

Figure 2-14. (A) SEC traces (RI signal), measured in THF, of a self-blocked PPA demonstrating retention of active chain ends; (B) ¹H NMR spectrum, recorded in *d*₆-benzene of the final, isolated ‘block’ copolymer highlighting the stereoregular structure as evidenced by the sharp singlet at δ = 6.19 ppm that is attributed to the backbone hydrogen in a *cis* conformation. 151

Figure 3-1. Masuda triphenylvinyl Rh(I) derivative, **78b**, Tan α-phenylvinylfluorenyl derivative, **88b**, a targeted 2-phenylnaphthyl Rh(I) species, **89**, and isolated 2-naphthylphenyl Rh(I) species, **90**. 159

Figure 3-2. OLEX² representation of the X-ray crystal structure of **90** with 50% probability ellipsoid and H-atoms omitted for clarity. Selected bond lengths (Å): Rh(1)-P(1), 2.294 (5); Rh(1)-C(51), 2.182 (2); Rh(1)-C(52), 2.152 (2); C(14)-F(14), 1.365 (3). Selected bond angles (deg): C(51)-Rh(1)-P(1), 168.06 (6); C(52)-Rh(1)-P(1), 132.78 (6); C(1)-Rh(1)-P(1), 90.24 (6). 171

Figure 3-3. X-ray powder diffraction spectra of Rh(nbd)(2-NaphthPh)(P(4-FC₆H₄)₃), **90**. In red is shown the predicted spectra based on the obtained single-crystal structure and in blue is the experimentally obtained spectra of a bulk sample of Rh(nbd)(2-NaphthPh)(P(4-FC₆H₄)₃). 172

Figure 3-4. NMR spectra, recorded in CD₂Cl₂, of Rh(nbd)(2-NaphthPh)(P(4-FC₆H₄)₃), **90**. (A) The full ¹H NMR spectrum with key peaks annotated. (B) the ¹H NMR spectrum covering the aromatic region δ = 8.5 to 6.0 ppm. 175

Figure 3-5 NMR spectra, recorded in CD₂Cl₂, of **90** (A) The ³¹P{¹H} NMR spectrum, and; (B) the ¹⁹F NMR spectrum of **90** showing three distinct signals for the isomeric forms of **89** and one signal attributed to the oxide of P(4-FC₆H₄)₃. 177

Figure 3-6. ³¹P-¹⁰³Rh{¹H, ¹⁰³Rh} HMQC NMR spectrum of **90** recorded in *d*₈-toluene. 178

Figure 3-7. Isomeric forms of **89** identified, and their structure elucidated in this work. 179

Figure 3-8. (A) The ³¹P{¹H} NMR spectrum, of P(4-FC₆H₄)₃, and; (B) the ¹⁹F NMR spectrum of P(4-FC₆H₄)₃. Relevant signals are annotated in the spectrums. 180

Figure 3-9. DFT-calculated pathway for the conversion of 89 to 90 and 91 . Calculations performed at the D3-pbe0/def2-TZVPP//bp86/SV(P) level with COSMO solvent correction in CH ₂ Cl ₂ . Energies are Gibbs energies at 298 K in units of kJ/mol. PAr ₃ = P(4-F-C ₆ H ₄) ₃ . DFT-predicted structure of 90 , showing the bond metrics of the agostic interaction (carbon grey, hydrogen white, fluorine green, phosphorus orange, rhodium dark green).....	183
Figure 3-10. (A) Pseudo-first-order kinetic plots for the homopolymerisation of PA, with target molecular weight of 10,000 at two different phosphine/Rh ratios; (B) the plots of number average molecular weight (M_n , as measured by SEC and reported as polystyrene equivalents) vs conversion.	189
Figure 3-11. Kinetic data for the homopolymerisation of PA with 90 for a target MW of 5,000 at [P]/[Rh] 10 and 20.	191
Figure 3-12. A series of SEC traces demonstrating the evolution of the molecular weight distribution with polymerisation time.	193
Figure 3-13. The four possible stereoisomers associated with polyphenylacetylenes.	194
Figure 3-14. ¹ H NMR spectrum of polyphenylacetylene, recorded in CDCl ₃ , prepared with 90 for a target molecular weight of 10,000 and [P]:[Rh] of 20 highlighting the high <i>cis-transoidal</i> stereoregularity.	195
Figure 4-1. Chemical structures of Masuda-type Rh(I)-vinyl complexes, 78b and 88 , recently reported Rh(I)aryl species 90 , and the structurally related aryl complex 92 (the focus of this chapter).....	204

Figure 4-2. OLEX² representation of the X-ray crystal structure of **92** with 50 % probability ellipsoids and H-atoms omitted for clarity. Selected bond lengths (Å): Rh(1)-P(1), 2.297(4); Rh(1)-C(32), 2.177(15); P(1)-C(13), 1.832(14); C(16)-F(3), 1.361(16). Selected bond angles (deg): C(32)-Rh(1)-P(1), 167.84(4); C(34)-Rh(1)-P(1), 104.96(5); C(19)-Rh(1)-P(1), 92.68(4). 213

Figure 4-3. (A) ¹H NMR spectrum of Rh(I)(nbd)(Biphenyl)(P(4-FC₆H₄)₃) recorded in CD₂Cl₂. (B) Expanded view of the aromatic region between δ = 8.0 - 6.5 ppm. 214

Figure 4-4. (A) ³¹P NMR spectrum of Rh(I)(nbd)(Biphenyl)(P(4-FC₆H₄)₃) recorded in C₆D₆, showing a doublet of quartets; (B) ¹⁹F NMR spectrum of Rh(I)(nbd)(Biphenyl)(P(4-FC₆H₄)₃) recorded in C₆D₆. 216

Figure 4-5. (A) ¹⁰³Rh spectrum (19.1 MHz) recorded in CD₂Cl₂, and (B) ³¹P-¹⁰³Rh{¹H} HMQC spectrum of complex **92**. 218

Figure 4-6. (A) Pseudo first-order kinetic plots for the homopolymerisation of PA in toluene at 30 °C with [P]/[Rh] = 5, 10 and 20; (B) evolution of the molecular weight distribution in the homopolymerisation of PA for a target molecular weight of 10,000 and [P]/[Rh] = 20. ([P] = [P(4-FC₆H₄)₃]) 222

Figure 4-7. *M_n* vs conversion plot for homopolymerisation of PA at 30 °C in toluene with (A) [P]/[Rh] = 5 (■); (B) [P]/[Rh] = 10 (□); (C) [P]/[Rh] = 20 (●), ([P] = [P(4-FC₆H₄)₃]) 224

Figure 4-8. (A) ¹H NMR, recorded in C₆D₆, of poly(4-fluorophenylacetylene) homopolymer, with the SEC trace of the homopolymer shown inset. Calculated *cis* content of 96 %. (B) ¹⁹F NMR of the poly(4-fluorophenylacetylene) homopolymer. 227

Figure 4-9. SEC traces for a polyphenylacetylene homopolymer (red) and an AB diblock copolymer with 4-fluorophenylacetylene formed by sequential monomer addition (blue).	228
Figure 4-10. ¹ H NMR spectrum, recorded in C ₆ D ₆ , of poly(phenylacetylene- <i>block</i> -4-fluorophenylacetylene) highlighting the <i>cis-transoidal</i> stereoregular nature of the copolymer microstructure. The ¹⁹ F NMR spectrum of the block copolymer is shown inset.	229
Figure 5-1. Chemical structure of isolable Rh(I)-based complexes described in this thesis with different diene moiety and initiating fragment. Norbornadiene (nbd) variant (top row), Rh(I)-vinyl complexes, 76 and 88 , and recently reported Rh(I)-aryl complexes, 90 and 92 . Tetrafluorobenzobarralene (tfb)/Tetrachlorobenzobarralene (tcb) variant (bottom row), Rh(I)-vinyl complex, 82 reported by Saeed <i>et al.</i> ² and Rh(I)-aryl complex, 93 , whose synthesis and evaluation as initiator for the homopolymerisation of PA will be discussed in this chapter.	235
Figure 5-2. ¹ H NMR spectrum recorded in CDCl ₃ for purified tfb ligand	247
Figure 5-3. ¹⁹ F NMR spectrum of purified tfb ligand in CDCl ₃	248
Figure 5-4. (A) ¹ H NMR spectrum of [Rh(tfb)Cl] ₂ in CDCl ₃ ; (B) ¹⁹ F NMR spectrum of [Rh(tfb)Cl] ₂ in CDCl ₃ . Relevant peaks highlighted in blue boxes. Two intense peaks at δ = 7.26 and 1.56 ppm (indicated with red boxes) are CHCl ₃ and HDO respectively.	249
Figure 5-5. (A) ¹ H NMR spectrum of Rh(I)(tfb)(Biphenyl)(P(4-FC ₆ H ₄) ₃) with the expanded aromatic region shown inset; (B) ³¹ P NMR spectrum of	

Rh(I)(tfb)(Biphenyl)(P(4-FC ₆ H ₄) ₃) showing a doublets of doublets around $\delta = 23.6$ ppm with $J_{P-Rh} = 193.4$ Hz.	252
Figure 5-6. ¹⁹ F NMR spectrum of Rh(I)(tfb)(Biphenyl)(P(4-FC ₆ H ₄) ₃), 93 with an expansion of the region from $\delta = -145$ to -165 ppm shown inset.	254
Figure 5-7. OLEX ² representation of Rh(I)(tfb)(Biphenyl)(P(4-FC ₆ H ₄) ₃), at 50 % probability ellipsoids and H atoms omitted for clarity. Selected bond lengths (Å): Rh(1)-P(1), 2.323(10); Rh(1)-C(C), 2.093(4); Rh(1)-C(H), 2.236(4); P(1)-C(D), 1.822(5); C(S)-F(3), 1.353(6). Selected bond angles (deg): C(B)-Rh(1)-P(1), 166.19(12); C(H)-Rh(1)-P(1), 111.11(12); C(C)-Rh(1)-P(1), 91.23(13).	255
Figure 5-8. ¹⁰³ Rh{ ¹ H- ³¹ P} NMR spectrum of Rh(I)(tfb)(Biphenyl)(P(4-FC ₆ H ₄) ₃), 93 , recorded in CD ₂ Cl ₂	256
Figure 5-9. ³¹ P- ¹⁰³ Rh HMQC NMR spectrum of Rh(I)(tfb)(Biphenyl)(P(4-FC ₆ H ₄) ₃), recorded in CD ₂ Cl ₂	257
Figure 5-10. Pseudo first-order kinetic plots for the homopolymerisation of PA in toluene at 30 °C with [P]/[Rh] = 10 and 20.	259
Figure 5-11. Normalised SEC traces showing the evolution of the molecular weight in the homopolymerisation of PA for a target molecular weight of 10,000 and at [P]/[Rh] = 20.	262
Figure 5-12. M_n vs conversions plots for homopolymerisation of PA at (A) [P]/[Rh] = 10; and (B) [P]/[Rh] = 20.....	263
Figure 5-13. SEC-traces for a self-blocking homopolymerisation of PA demonstrating retention of active chain ends.....	264

Figure 5-14. ^1H NMR spectrum recorded in CDCl_3 , of a self-block (co)polymer highlighting the <i>cis-transoidal</i> stereoregular structure as evidenced by a sharp singlet at $\delta = 6.19$ ppm that is attributed to the proton on the backbone of the polymer in a <i>cis</i> conformation.	265
Figure 5-15. Phenylacetylene (M1), 1-ethyl-4-ethynylbenzene (M2), 4-ethynylanisole (M3), 4-(trifluoromethoxy)phenylacetylene (M4), 3,4-dichlorophenylacetylene (M5), 4-ethynylaniline (M6), 4-ethynylbiphenyl (M7), 4-ethynylnaphthalene (M8) and 2-ethynylthiophene (M9).....	266
Figure 5-16 Normalised SEC traces of the evolution of molecular weight distribution in the homopolymerisation of M2 for a target molecular weight of 10,000 with $[\text{P}]/[\text{Rh}] = 20$	267
Figure 5-17. Pseudo-first order kinetic plot of homopolymerisation of M3 in toluene at $30\text{ }^\circ\text{C}$ with $[\text{P}]/[\text{Rh}] = 10$	269
Figure 5-18. ^1H NMR spectrum of poly(4-ethynylanisole), poly(M3), (A) recorded in C_6D_6 ; (B) recorded in CDCl_3	270
Figure 5-19. (A) Pseudo-first order kinetic plots for homopolymerisation of M4 with $[\text{P}]/[\text{Rh}] = 10$ and 20 ; (B) a series of SEC traces for the homopolymerisation of M4 at $[\text{P}]/[\text{Rh}] = 10$	272
Figure 5-20. (A) ^1H NMR spectrum; (B) ^{19}F NMR spectrum of poly(4-(trifluoromethoxy)phenylacetylene), poly(M4), recorded in CDCl_3	273

Figure 5-21. (A) SEC traces of a PPA homopolymer, poly(**PA1**) (red) and a poly(**PA1**)-*block*-poly(**M4**) (blue); (B) ¹H NMR spectrum, recorded in CDCl₃, of poly(**PA1**)-*block*-poly(**M4**) with the relevant *cis* protons highlighted. 276

Figure 5-22. (A) SEC traces of a PPA homopolymer, poly(**PA2**) (red) and a poly(**PA2**)-*block*-poly(**M5**) (blue); (B) ¹H NMR spectrum, recorded in CDCl₃, of poly(**PA2**)-*block*-poly(**M5**) with the relevant *cis* protons highlighted. 277

Figure 5-23. (A) SEC traces for a PPA homopolymer, poly(**PA3**) (red) and poly(**PA3**)-*block*-poly(**M2**) (blue); (B) ¹H NMR spectrum, recorded in CDCl₃, of poly(**PA3**)-*block*-poly(**M2**) with the relevant *cis* protons highlighted..... 280

Figure 6-1. The chemical structures of Masuda catalysts¹ (**78**) and three new Rh(I)-fluorenyl complexes bearing a fluorine functionalised phosphine (**88b**, **88d** and **88e** where **b** = P(4-FC₆H₄)₃; **d** = P(4-CF₃C₆H₄)₃; **e** = P(3,5-(CF₃)₂C₆H₃)₃). Initiating fragment highlighted in blue. 286

Figure 6-2. Chemical structure of targeted (2-phenylnaphthalene)Rh(I) derivative (**89**), isolated second isomeric form (2-naphthylphenyl)Rh(I) (**90**), and third isomeric form (3-phenylnaphthalene)Rh(I) (**91**) with the ‘vinyl’ moiety highlighted in red..... 288

Figure 6-3. Chemical structure of Rh(I)(Biphenyl)(nbd)(P(4-FC₆H₄)₃) (Biphenyl = biphenyl initiating fragment highlighted above in blue)..... 289

Figure 6-4. Chemical structure of Rh(tfb)(PhC=CPh₂)(P(4-FC₆H₄)₃) (**82**) and Rh(tfb)(Biphenyl)(P(4-FC₆H₄)₃) (**93**). Tetrafluorobenzobarralene (tfb, highlighted in red) ligand and initiating fragment highlighted in blue, respectively. 291

Figure A-1. Reported X-ray crystal structure for the Masuda complex
Rh(nbd)(CPh=CPh₂)PPh₃, **88a**..... 297

Figure A-2. Reported X-ray crystal structure for the Masuda complex
Rh(nbd)(CPh=CPh₂)P(4-ClC₆H₄)₃, **88c**..... 298

List of Schemes

Scheme 1-1. Insertion mechanism of Ziegler-Natta catalyst mediated polymerisation of ethylene. The coordination-insertion process proceeds via a metallocyclobutene intermediate (highlighted in red).....	8
Scheme 1-2. General mechanism of an olefin metathesis reaction mediated by a transition metal.....	10
Scheme 1-3. General reaction scheme of ROMP of norbornene.	11
Scheme 1-4. A general scheme for ROMP involving initiation, propagation and termination steps.	13
Scheme 1-5. ROMP of cyclooctene by 2 nd generation Grubbs catalyst (Ru-based) and the introduction of chain-end functionality using a chain transfer reagent (CTA) reported by Diallo <i>et al.</i> ⁷²	14
Scheme 1-6. Synthesis of the first well-defined ruthenium-based complex that facilitated ROMP.	15
Scheme 1-7. ROMP of norbornene by (PPh ₃)Cl ₂ Ru=CH-CH=CPh ₂ , 1	15
Scheme 1-8. Synthesis of a more active derivative of 1 via phosphine exchange to give 2	16
Scheme 1-9. ROMP of a silylether-functional norbornene and subsequent block (co)polymerisation mediated by 2	17

Scheme 1-10. ROMP of functionalised cyclooctene with Hoveyda-Grubbs 2 nd generation catalyst, 7 , and formation of macrocyclic oligo(cyclooctene)s from back-biting.	20
Scheme 1-11. Polymerisations of 1-methylnorbornene via ROMP with 9	22
Scheme 1-12. Polymerisation of <i>n</i> -alkyl norbornene dicarboxyimides via ROMP with 12	24
Scheme 1-13. The generally accepted mechanisms for the Rh-insertion polymerisation of phenylacetylene (top) and the Mo-mediated metathesis polymerisation of phenylacetylene (bottom).....	27
Scheme 1-14. General reaction scheme of the ruthenium-catalysed polymerisation of diacetylene derivatives.	30
Scheme 1-15. Proposed decomposition mechanism for ruthenium-alkoxybenzylidene complex during polymerisations and the chemical structure of the cyclotrimerisation product (shown inset).....	32
Scheme 1-16. Cyclopolymerisation of 1,6-heptadiyne by complex 5 and α,ω -dialkyne derivatives used in block (co)polymerisation experiments.....	33
Scheme 1-17. Proposed mechanism by Tamura <i>et al.</i> ¹⁷⁹ involving metal-carbonyl complexes for the polymerisation of alkynes with, and without, photoirradiation....	37
Scheme 1-18. Proposed mechanism for the formation of 5 and 6 membered rings during cyclopolymerisations of 1,6-heptadiyne derivatives mediated by Schrock-type Mo catalyst.....	38

Scheme 1-19. The polymerisation of PA with a zwitterionic rhodium complex in the presence of Et ₃ SiH as co-catalyst.....	48
Scheme 1-20. Polymerisation of PA, and its derivative, conducted with a ternary catalyst system comprising of [Rh(nbd)Cl] ₂ /Ph ₂ C=CPhLi/(C ₆ H ₄ - <i>m</i> -SO ₃ Na)Ph ₂ P) ..	50
Scheme 1-21. Preparation of cationic and neutral phosphine-imine Rh(I) complexes reported by Reddy <i>et al.</i> ²⁴⁷	55
Scheme 1-22. Preparation of a series of Rh(I)(cod) complexes bearing <i>N</i> -heterocyclic carbenes (NHCs) resulting in charged and neutral organorhodium species.	56
Scheme 1-23. Preparation of a Rh complex bearing an NHC and cod diene ligand.	57
Scheme 1-24. The polymerisation of PA with Rh(C≡CPh)(nbd)(PPh ₃) ₂ in the presence of DMAP, yielding stereoregular polymers.	62
Scheme 1-25. Reaction scheme representing the rapid, reversible dissociation of PPh ₃ from the inactive species, Rh(C≡CPh)(nbd)(PPh ₃) ₂ to active Rh(C≡CPh)(nbd)(PPh ₃).	63
Scheme 1-26. Reaction scheme of the homopolymerisation of PA by the [Rh(nbd)Cl] ₂ /PPh ₃ /LiCPh=Ph ₂ ternary catalyst system.....	65
Scheme 1-27. End-functionalisation achieved by replacing LiCPh=CPh ₂ with LiCPh=C(4-NMe ₂ -C ₆ H ₄) ₂	65
Scheme 1-28. Synthetic route to poly(phenylacetylene)- <i>block</i> -poly(β-propiolactone) via combination of Rh-mediated alkyne polymerisation and anionic polymerisation of the propiolactone moiety of the macroinitiator.	66

Scheme 1-29. The synthesis of star polymers via homopolymerisation of PA followed by cross-linking with a difunctional arylalkyne.....	69
Scheme 1-30. Block copolymerisation of a chiral arylacetylene with achiral acetylene via sequential monomer addition with Rh(nbd)(CPh=CPh ₂)(PPh ₃)/PPh ₃ as the initiating system.	71
Scheme 1-31. Chemical structures of a chiral arylacetylene, (A) (((1 <i>S</i> ,5 <i>S</i>)-6,6-dimethylbicyclo[3.1.1]heptan-2-yl)methyl)(4-ethynylphenyl)dimethylsilane and (B) achiral monomer (2-(dodecyloxy)-5-ethynyl-1,3-phenylene)dimethanol.	72
Scheme 1-32. Chemical structures of diene ligands: 2,5-norbornadiene (nbd); 1,5-cyclooctadiene (cod); <i>endo</i> -dicyclopentadiene (dcp); tetrafluorobenzobarrelene (tfb) and tetrachlorobenzobarrelene (tcb), and the homopolymerisation of phenylacetylene with bridged Rh complexes [Rh(diene)Cl] ₂	75
Scheme 1-33. Reaction scheme for the preparation of end-functionalised polyenes described by Taniguchi <i>et al.</i> ²⁷⁰ and selected examples of arylboronic acid and arylacetylenes used in this study.	79
Scheme 1-34. Polymerisation of simple alkyl propargyl amide substrates with well-defined Rh(nbd)(CPh=CPh ₂)(P(4-FC ₆ H ₄) ₃) (Masuda catalyst).	81
Scheme 1-35. The general synthetic route for the preparation of Rh(I)-aryl complexes of the type Rh(nbd)(aryl)(PPh ₃).	83
Scheme 1-36. The polymerisation of 2,5-substituted arylisocyanides monomers with Rh(nbd)(aryl)(PPh ₃).	84

Scheme 2-1. Outline for the synthesis of Rh(nbd)(CPh=Flu)(P(4-FC ₆ H ₄) ₃) (88b), Rh(nbd)(CPh=Flu)(P(4-CF ₃ C ₆ H ₄) ₃) (88d) and Rh(nbd)(CPh=Flu)(P(3,5-(CF ₃) ₂ C ₆ H ₃) ₃) (88e).....	127
Scheme 2-2. The homopolymerisation of phenylacetylene yielding highly stereoregular polyphenylacetylene with <i>cis-transoidal</i> configuration.	143
Scheme 2-3. The sequence of steps resulting in the formation of polyphenylacetylene from the precursor catalyst/initiator 88	147
Scheme 3-1. Outline for the synthesis of the target 2-phenylnaphthyl derivative, 89 , and chemical structure of the isolated, isomeric, 2-naphthylphenyl species, 90	170
Scheme 3-2. Proposed formation of (2-naphthylphenyl-1-yl)rhodium(I) (2,5-norbornadiene) <i>tris</i> -(<i>para</i> -fluorophenylphosphine), 90 , and (3-phenylnaphthalen-1-yl)rhodium(I)(2,5-norbornadiene) <i>tris</i> (<i>para</i> -fluorophenyl phosphine), 91 , via sequential 1,4-Rh atom migrations. PAr ₃ = P(4-FC ₆ H ₄) ₃	181
Scheme 3-3. “Merry-go-round” multiple alkylation on aromatic rings via Rh catalysis reported by Oguma <i>et al.</i> ³⁷	182
Scheme 3-4. Conditions for the polymerisation of phenylacetylene (PA) with 90	187
Scheme 4-1. Outline for the synthesis of the biphenyl derivative, 92	212
Scheme 5-1. Reaction of pentafluorobromobenzene with <i>n</i> -BuLi 1.6M in benzene to afford tetrafluorobenzobarrelene (tfb).....	246
Scheme 5-2. Synthetic pathway employed for the preparation of the Rh dimer [Rh(tfb)Cl] ₂	250

Scheme 5-3. Overview of the synthetic pathway adopted for the preparation of the target Rh complex Rh(I)(tfb)(Biphenyl)(P(4-FC₆H₄)₃). 251

List of Tables

Table 1-1. Summary of conditions, <i>cis</i> content, M_w , and \bar{D} for the homopolymerisation of PA with a series of NHC-functional Rh complexes.	56
Table 2-1. Summary of PA polymerisation conditions with 88b , 88d and 88e , SEC-measured molecular weights and dispersities, initiation efficiencies and NMR measured <i>cis</i> contents in the resulting polyphenylacetylene (co)polymers.	145
Table 3-1. Continuous Shape Measures values of Rh(L)(nbd)(PR ₃) complexes against the reference tetrahedral and square planar geometries.	173
Table 3-2. Summary of PA polymerisation conditions with 90 , SEC-measured molecular weights and dispersities, initiation efficiencies and NMR measured <i>cis</i> contents in the resulting polyphenylacetylene (co)polymers.	186
Table 4-1. Summary of PA polymerisation conditions with 92 , SEC-measured molecular weights and dispersities, initiation efficiencies and NMR measured <i>cis</i> contents in the resulting polyphenylacetylene (co)polymers.	220
Table 4-2. A comparison between 90 and 92 with their relevant k_{app} values listed. All polymerisations were conducted at 30 °C in toluene.	225
Table 5-1. Summary of homopolymerisations of PA (M1) with 93 conducted at 30 °C, in toluene.	258
Table 5-2. The apparent rate constant of propagation, k_{app} and calculated initiation efficiencies, for homopolymerisations of PA mediated by Rh(I)-aryl complexes reported in Chapter 3 and 4 compared to, Rh(I)(tfb)(Biphenyl)(P(4-FC ₆ H ₄) ₃), 93	260

Table 5-3. Summary of homopolymerisations of mono-substituted acetylenes with 93 conducted at 30 °C	268
Table 6-4. Summary of AB diblock copolymers synthesised by 93 in Chapter 5 ...	292

Chapter 1

Introduction

Part of the content in this chapter has been published in:

Angewandte Chemie International Edition and Angewandte Chemie (2020) with the title “Polymerisation Mediated by Well-defined Rhodium Complexes” and “Polymerisationen vermittelt durch wohl-definierte Rhodium Komplexe” (refer to Appendix C)

1.1 Transition Metal Complexes and Their Applications in Synthetic Chemistry

The primary focus of this thesis is the synthesis, and characterisation of new rhodium(I)-vinyl and rhodium(I)-aryl complexes and an evaluation of their efficacy as initiators on the (controlled) (co)polymerisation of arylacetylenes.

Broadly speaking, transition metal complexes plays a key role in modern synthetic chemistry as they give chemists access to new molecules with unique structures, better stereo control and incorporation of a broad range of functionalisation that would otherwise take longer to achieve due to the multi-steps synthesis (low efficiency) or simply near-impossible to achieve via conventional synthetic routes (such as concerted [6+2] cycloaddition reactions¹ which are thermally forbidden, but made possible by transition metal mediated reactions). These transition metal complexes often proved useful in the total synthesis of a complex natural product or yield important polymeric materials such as polyethylene and polypropene which are

used primarily for packaging applications such as plastic grocery bags, a modern day convenience, that has been ingrained in our daily lives.

Much of the advancement in synthetic chemistry can be attributed to transition metal complexes such as the Haber-Bosch process for ammonia production via iron (Fe)² catalyst, hydrogenation reactions of unsaturated fatty acids with nickel (Ni)³ or platinum (Pt)⁴, hydroformylation reaction of olefins with rhodium (Rh) catalysts⁵, hydrocarboxylation reactions of olefins (with cobalt (Co)⁶⁻⁹, Ni¹⁰, iron (Fe)¹¹, palladium (Pd)^{12, 13}, or iridium (Ir)⁸), hydroesterification reactions of olefins (Co^{9, 14} or palladium (Pd)¹⁵ ruthenium (Ru)^{9, 16, 17}), and a suite of cross-coupling/metathesis reactions (Suzuki-coupling reactions with Pd¹⁸⁻²⁴ or Ni²⁵⁻²⁹ which are useful for the synthesis of asymmetrical biaryls,³⁰⁻³⁴ Heck reaction with Pd for the reaction between organic halides and olefins,³⁵⁻³⁷ Kumada coupling reactions primarily with Ni³⁸⁻⁴⁹, Pd^{47, 50} or iron (Fe)⁵¹⁻⁵³ between Grignard reagents with organohalides, Sonogashira-coupling reactions with Pd and copper (Cu) as a co-catalyst for the coupling between terminal alkynes and aryl or vinyl halides⁵⁴⁻⁵⁶). The list is not meant to be exhaustive as it does not give justice to the contributions of transition metal chemistry and the researchers behind it all, but to demonstrate the profound implications it has in modern synthetic chemistry.

As noted, this thesis focusses on the synthesis and application of Rh complexes, examples of which are known to play a vital role in organic synthetic chemistry because they can facilitate certain reactions that are normally not possible via other means. For example, as mentioned earlier, the [6+2] cycloaddition reaction of 2-vinylcyclobutanones reported by Wender *et al.*⁵⁷ which is thermally forbidden is made possible by employing Wilkinson's catalyst, Rh(PPh₃)Cl, to catalyse the reaction. In this thesis, we will be discussing the synthesis, evaluation, and application

of new Rh(I)-vinyl and -aryl complexes as initiators for polymerisations of phenylacetylene (PA) and other aryl substituted acetylenes.

In this chapter, a brief overview of the relevant basic polymer chemistry terminology used in this thesis will be given. Then, an overview of insertion and metathesis polymerisation processes mediated by selected transition metals (ruthenium (Ru), molybdenum (Mo), tungsten (W), niobium (Nb), tantalum (Ta), and titanium (Ti)), their uses in polymerisation-related applications (such as ring-opening metathesis polymerisation (ROMP), and alkyne polymerisations). Finally, a thorough review of the development and application of rhodium (Rh) complexes as mediators in the controlled/non-controlled polymerisation of acetylenes and substituted acetylenes will be presented.

1.2 Introduction to Polymer Nomenclatures and Techniques

Today, synthetic polymer chemists have an extensive tool box of polymerisation techniques enabling the preparation of a near-infinite number of new materials. This thesis will deal specifically with controlled chain-growth insertion polymerisation mediated by Rh(I)-vinyl and -aryl complexes for the synthesis of polyarylacetylenes.

In polymer chemistry, the characterisation of the polymer is commonly acquired by size exclusion chromatography (SEC), which is a high-performance liquid chromatography (HPLC) technique that separates polymer sample based on their hydrodynamic volume, Figure 1-1. The heart of an SEC instrument is the chromatography column which is packed with gel beads (commonly cross-linked polystyrene beads) with porosities of a defined size range. Molecules that are smaller than the pore size, can interact with these pores, which increases its residential time in

the column, thus, eluting later; molecules that are larger than the pore size, will be excluded from the pores, thereby, eluting earlier, this is called the size exclusion limit. The separation process results in the fractionation of chains prior to their detection.

The drawback of SEC is that it requires calibration with near-monodisperse standards (usually polystyrene equivalents due commercial availability and convenience) before reliable data acquisition can be performed, thus, molecular weight of polymers is reported as polystyrene equivalents in this thesis.

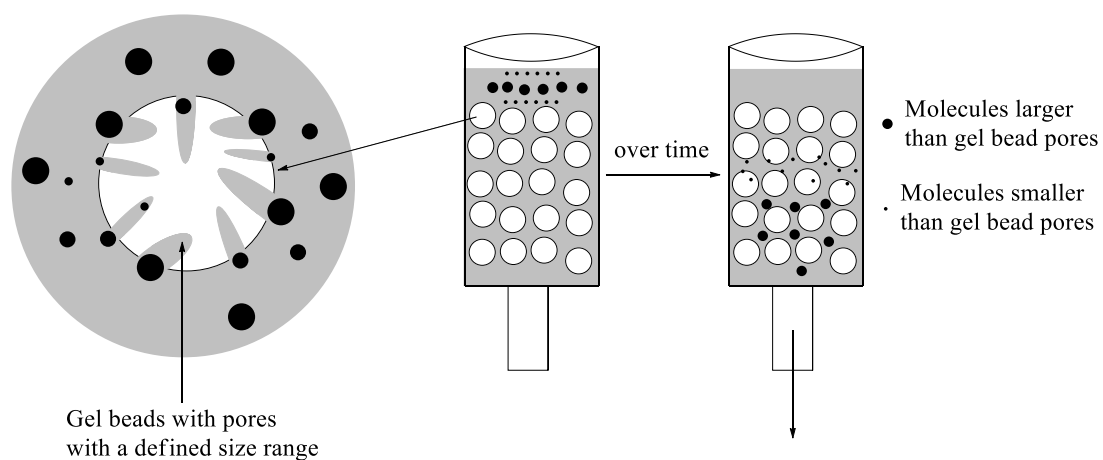


Figure 1-1. Illustration of the separation process for a polymer sample using size exclusion chromatography technique.

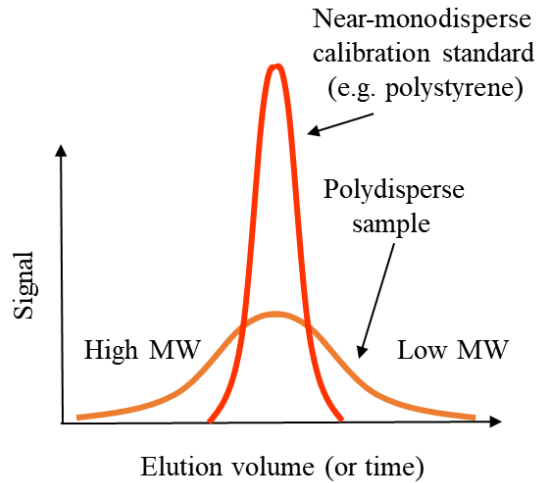


Figure 1-2. SEC chromatogram plots the detector signal against elution volume or time.

The detector response against the elution volume or time is plotted and interpreted by the SEC software. Figure 1-2, which then provides us information such as the number average molecular weight, M_n , the weighted average molecular weight, M_w , and the dispersity, D (ratio M_w/M_n). The M_n gives us the average molecular weight of the polymers and can be defined as:

$$M_n = \frac{\sum n_i M_i}{\sum n_i} \quad (1.1)$$

where n_i = the number of molecules

M_i = molecular weight of molecule

Referring to equation 1.1, the number average molecule weight, M_n , is the total of the *mole* fraction of each molecule multiply by its molecular weight, M_i . In contrast, the weighted average molecular weight, M_w , is the summation of the *weight* fraction of each molecule multiply by its molecular weight, M_i , and can be expressed as:

$$M_w = \frac{\sum w_i M_i}{\sum w_i} = \frac{\sum n_i M_i^2}{\sum n_i} \quad (1.2)$$

$$\text{where } w_i = \sum n_i M_i$$

The dispersity, \mathcal{D} , indicates the breadth of the molecular weight distribution (MWD) of the polymer, and is simply the ratio of M_w and M_n which can be expressed as:

$$\mathcal{D} = \frac{M_w}{M_n} \quad (1.3)$$

The closer to unity ($\mathcal{D} = 1.0$), the narrower the MWD or monodisperse the polymer sample is. Generally, the values obtained are relative to a set of polymer standards (such as low dispersity polystyrene (PS)) which have narrow MWD. This information is highly important because it is directly related to the polymer's properties such as its melting point, durability, ductility, colligative properties, osmotic pressure, and freezing point depression to name a few which affects the processability and the potential application of new polymeric materials.

Another commonly used term in this thesis is living polymerisation. According to the official IUPAC definition, outlined by Jenkins *et al.*,⁵⁸ a living polymerisation is a chain polymerisation from which chain transfer and chain termination are absent. Another related technical term is “controlled polymerisations”. A controlled polymerisation process is associated with several features that are often observed in such processes and include:

1. Linear pseudo-first-order kinetic plot, which implies that there is a constant number of propagating species in the system.
2. The molecular weight (MW) increases proportionally with monomer conversion. This indicates that there are no chain transfer or chain termination

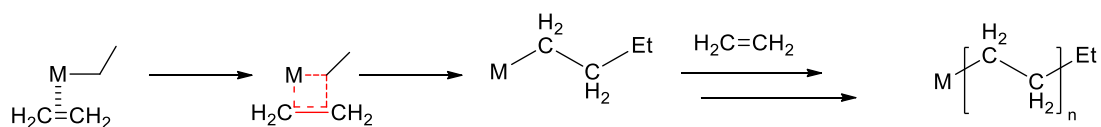
events occurring and the MW can be controlled via tuning the monomer-to-initiator ratio, $[M]/[I]$.

3. The formation of (co)polymers with narrow molecular weight distributions (MWDs). Narrow MWDs (low D_s), while desirable, it is not a formal prerequisite, but is a common feature in a controlled polymerisation process.
4. The retention of chain-end activity after all monomers are consumed, which facilitates the preparation of block copolymers and other advanced polymer architectures.

1.3 Insertion Polymerisation

1.3.1 Titanium-Based Catalysts (Ziegler-Natta) and Their Application in α -olefin Polymerisation

According to the accounts of the late John J. Eisch,⁵⁹ in the late 1940s, while experimenting with the synthesis of alkyl lithium salts for use in organic synthesis, Karl Ziegler was made aware that by performing organolithium reactions in pressurized ethylene, oligomers of α -olefins would be observed. It was not until 1953, shortly after his departure from working with “main group chemistry”, that he made a serendipitous discovery that when passing ethylene into a mixture of TiCl_4 and Et_2AlCl , which was then known as “Ziegler’s” catalyst, resulted in the deposition of polyethylene (PE). Giulio Natta, building upon Ziegler’s work, subsequently discovered the use of TiCl_3 instead of TiCl_4 , for propylene polymerisations.⁶⁰ Today, the use of Ti-based catalysis is for the (co)polymerisation of α -olefins and is referred to as Ziegler-Natta polymerisations, which is particularly important for the synthesis of polyethylene and polypropylene including ultra-high-molecular-weight PE (UHMWPE), high-density PE (HDPE), cross-linked PE, medium-density PE, and low-density PE.^{61, 62}

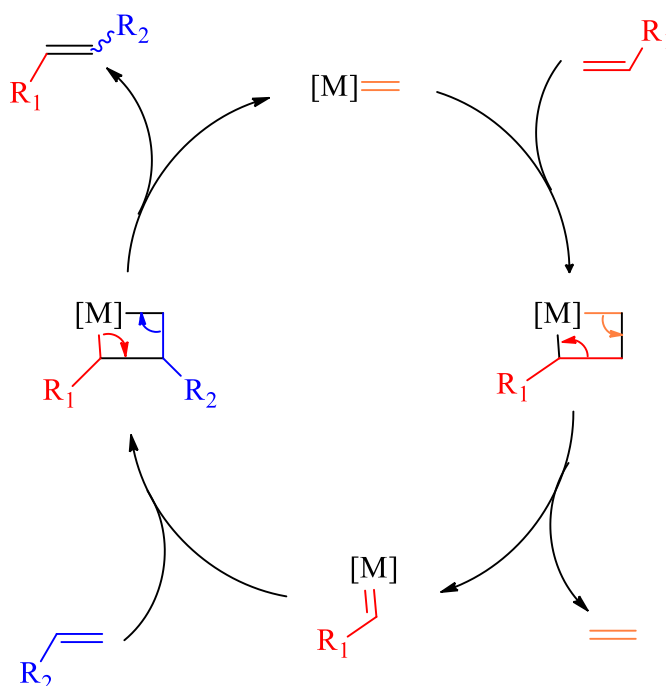


Scheme 1-1. Insertion mechanism of Ziegler-Natta catalyst mediated polymerisation of ethylene. The coordination-insertion process proceeds via a metallocyclobutene intermediate (highlighted in red).

Scheme 1-1 shows the general mechanism, also known today as the Cossee-Arlman mechanism,⁶³ illustrates the insertion processes of ethylene mediated by Ziegler-Natta catalysts (heterogeneous catalysts) or metallocenes (homogeneous catalysts). The principle behind this mechanism is the insertion of the coordinating monomer (an α -olefin, in this case) into a reactive metal-carbon σ -bond and the subsequent regeneration of a metal-carbon bond of the same character. The analogous steps of monomer insertion and regeneration are repeated, resulting in the polymerisation of ethylene.

1.4 Olefin Metathesis Processes and Its Application in Metathesis Polymerisation

In 1971, Chauvin and Hérisson proposed the first olefin metathesis mechanism by a transition metal, and is still widely accepted today.⁶⁴ The term “olefin metathesis” would be coined later by Calderon, Chen and Scott.⁶⁵



Scheme 1-2. General mechanism of an olefin metathesis reaction mediated by a transition metal.

Scheme 1-2 shows the general reaction scheme of an olefin metathesis reaction mediated by a transition metal. The mechanism involves a [2+2] cycloaddition of a C=C double bond and a transition metal carbene to form a metallocyclobutane intermediate, which then undergoes a cycloreversion reaction forming a new metal-carbene and eliminates a molecule of ethylene. This reaction is governed by Le Chatelier’s principle or the equilibrium law, and since ethylene is gaseous, can

essentially be driven to completion by applying vacuum to the system to remove the ethylene by-product.

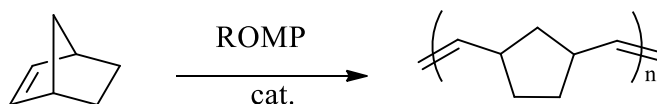
The olefin metathesis concept would later prove to be useful for polymerisations of α -olefins and cyclic olefins via ring-opening metathesis polymerisation (ROMP).

Ruthenium-based (Ru) complexes (Grubbs' 1st, 2nd, and 3rd generation catalysts and Hoveyda-Grubbs species) and molybdenum- (Mo) and tungsten-based (W) catalysts (Schrock's catalyst) have been used for the polymerisation of cyclic olefins, commonly norbornene derivatives via ring-opening metathesis polymerisations (ROMP). Their utilisation has also been seen in the polymerisation of terminal alkynes. This section will provide an overview of Grubbs-type and Schrock-type metathesis complexes as initiators for polymerisations of cyclic dienes, acyclic dienes and 1-alkynes.

1.4.1 Ruthenium

1.4.1.1 Ring-Opening Metathesis Polymerisation (ROMP)

ROMP is a type of chain-growth polymerisation of cyclic olefins. Historically, ROMP was first discovered by Anderson and Merckling who made a fortuitous observation that polymerizing norbornene with Ziegler-Natta ($\text{TiCl}_4/\text{EtMgBr}$) catalysts resulted in unsaturated polymers.⁶⁶



Scheme 1-3. General reaction scheme of ROMP of norbornene.

The reaction is driven by the energetically favourable relief of the ring strain and the energy release from the incorporation of monomer into the growing chain. For this reason, ROMP is a type of chain-growth polymerisation that is suited to cyclic-ene monomers of medium-to-high strain and includes three, four, five and eight membered rings or cyclic olefins as bicyclic monomers.⁶⁷ One of the most common monomers that are frequently used for ROMP are norbornene derivatives as these can be made relatively easy by Diels-Alder addition reactions, Figure 1-3.⁶⁷⁻⁷⁰

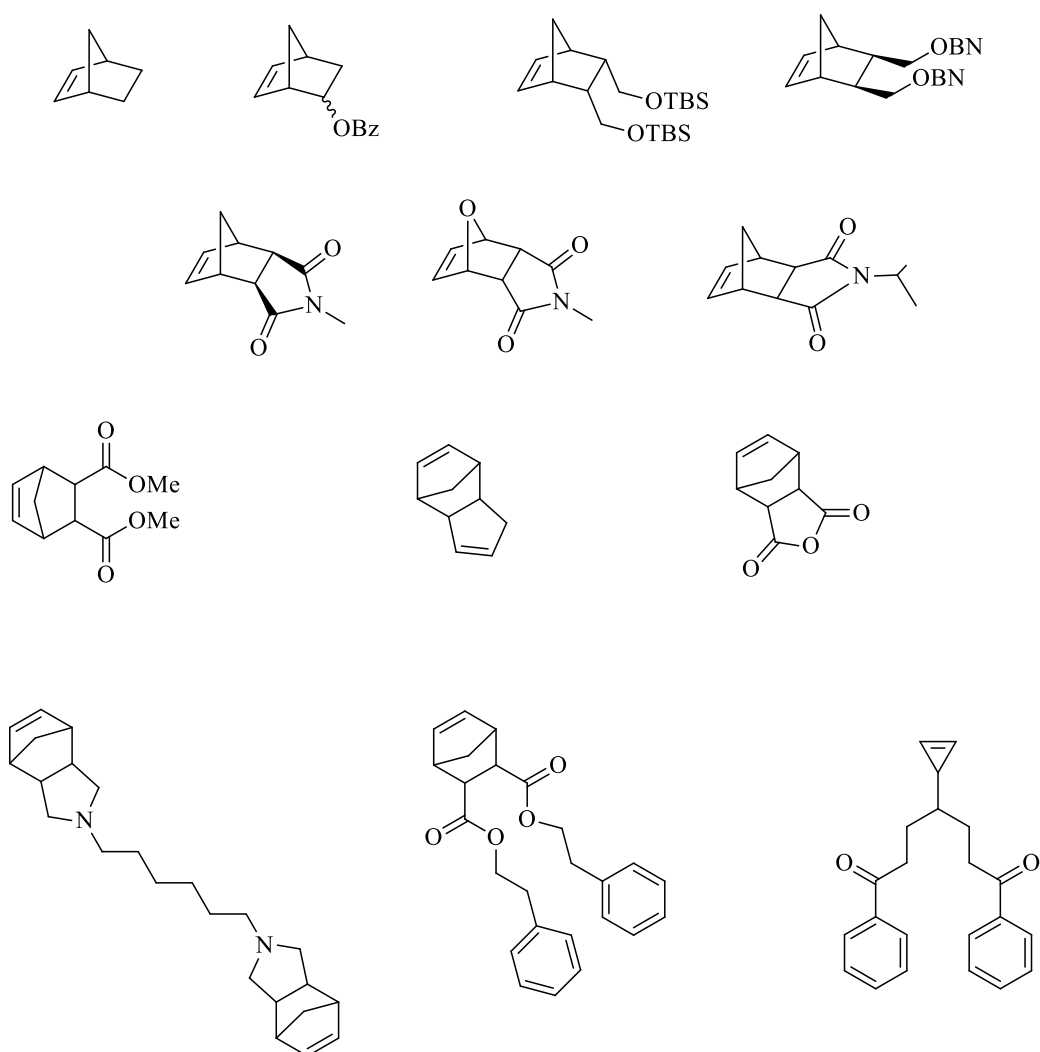
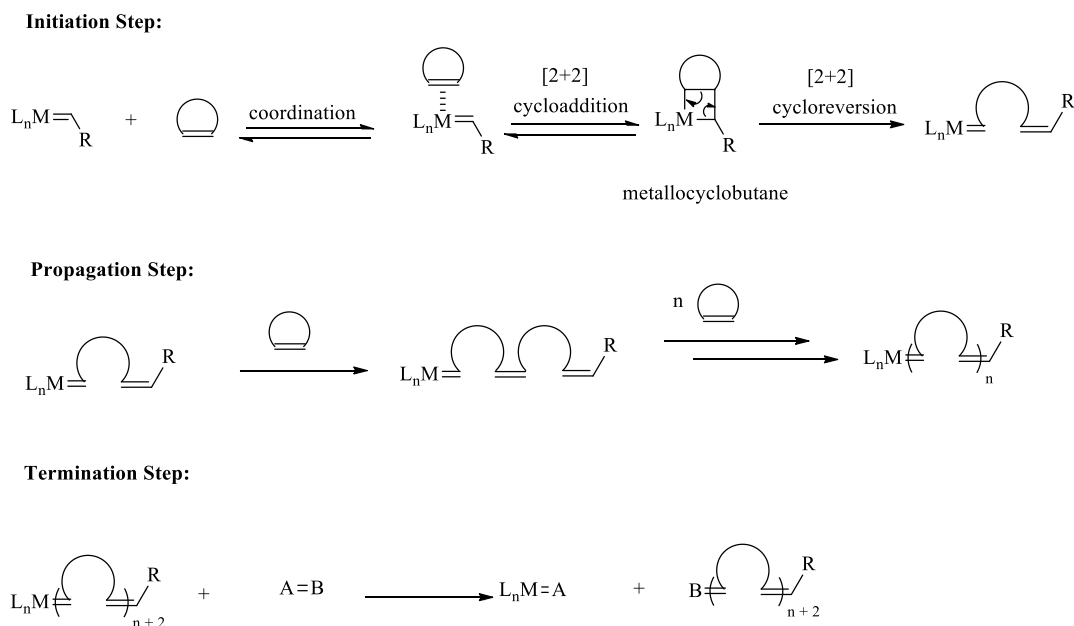


Figure 1-3. Selected examples of (oxa) norbornene and cyclopropene derivatives that have been reported in the literature.

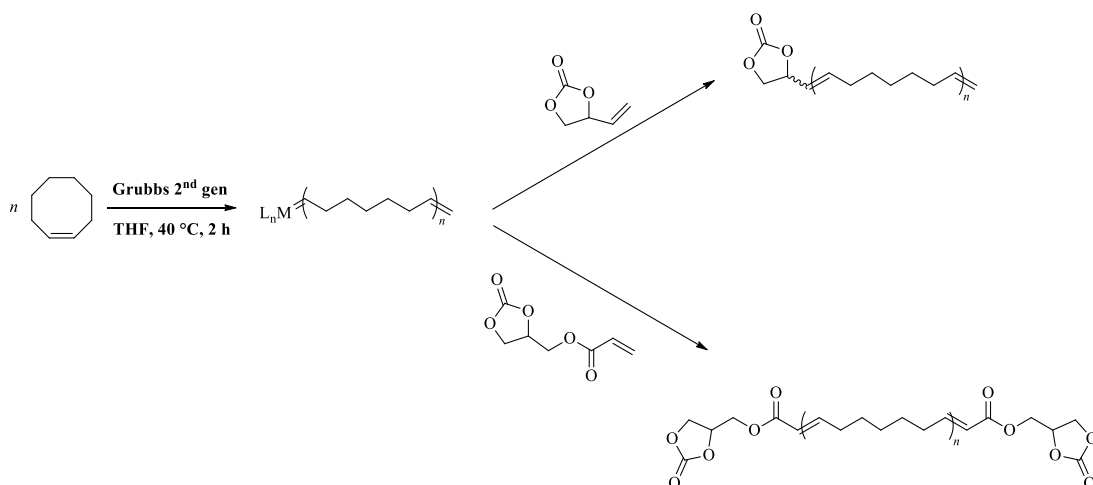


Scheme 1-4. A general scheme for ROMP involving initiation, propagation and termination steps.

The main difference between ROMP and olefin metathesis is that ROMP involves a cyclic olefin forming a metal-carbene bond that remains attached and forms the growing polymer chain. There are three key steps in the ROMP process: initiation, propagation and termination, Scheme 1-4. The initiation process begins with phosphine dissociation from the metal centre, then, π -coordination of the cyclic alkene, which then undergoes a [2+2] cycloaddition to form a cyclobutane intermediate. This intermediate, then undergoes a [2+2] cycloreversion to form a new metal-carbene species with an active growing chain.⁷¹ This new metal-carbene species can undergo the same sequences or steps resulting in propagation.

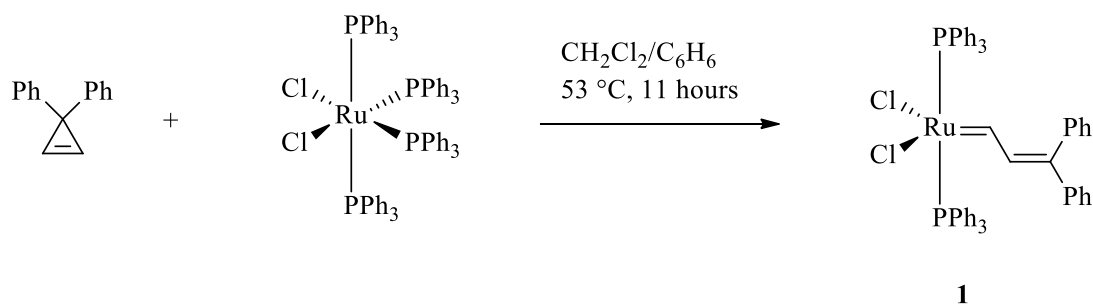
The termination step can occur in two ways: intermolecular or intramolecular chain transfer reaction, (“back-biting”). Intramolecular chain transfer reaction or “back-biting” occurs when the active terminus end of the metal-alkylidene reacts with an unsaturated bond in the same polymer backbone to form a macrocycle or cyclic

species, on the other hand, intermolecular chain transfer reaction occurs when the active terminus end of the alkylidene reacts with an unsaturated bond in a different polymer backbone, both of which results in a shortened polymer chain. This result in higher \bar{D} and lower than expected M_n of the polymers. Generally undesirable for polymerisations, intentional termination can be useful for synthesizing end-functionalised polymers through the use of an appropriate chain transfer agent, Scheme 1-5.



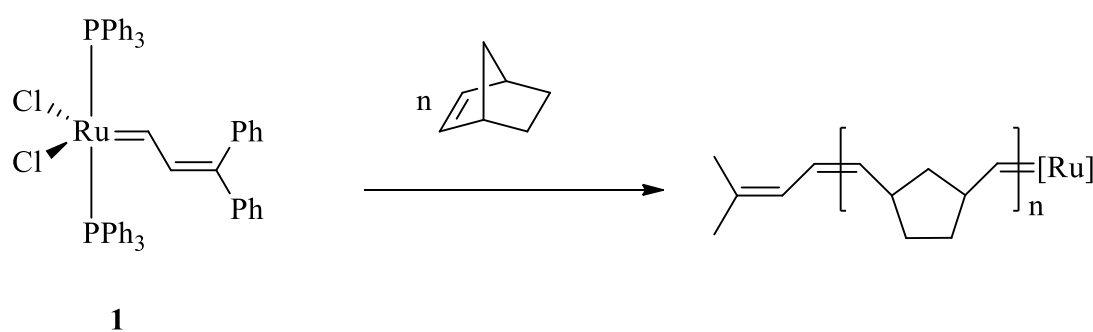
Scheme 1-5. ROMP of cyclooctene by 2nd generation Grubbs catalyst (Ru-based) and the introduction of chain-end functionality using a chain transfer reagent (CTA) reported by Diallo *et al.*⁷²

Nyugen *et al.*⁷³ reported the first well-defined Ru-based complex for metathesis reactions, Scheme 1-6, which was synthesised by reacting 3,3-diphenylcyclopropene with $(PPh_3)_3RuCl_2$, affording **1** in near-quantitative yields. **1** is readily stored in the solid-state indefinitely, and is stable in solution for an extended period of time if degassed and dry organic solvent is used. It is also known that **1** is tolerant towards water and polar functional groups including alcohols and ethers. More importantly, **1** is able to mediate living ROMP of norbornene with excellent activity.



Scheme 1-6. Synthesis of the first well-defined ruthenium-based complex that facilitated ROMP.

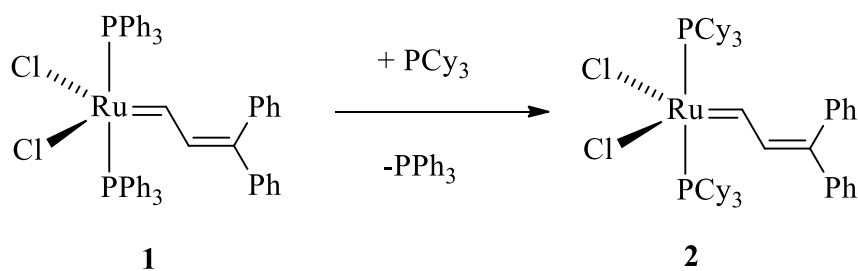
Scheme 1-7 shows the polymerisation of norbornene via ROMP mediated by **1**, conducted in a mixture of 1:8 $\text{CH}_2\text{Cl}_2/\text{C}_6\text{H}_6$ at room temperature to yield polynorbornene.⁷⁴ Subsequently, Louie *et al.*⁷⁵ reported the ROMP of other cyclic olefins including bicyclo[3.2.0]heptene and *trans*-cyclooctene, and with **1** being able to mediate living ROMP, block copolymers of both monomers were successfully synthesised.



Scheme 1-7. ROMP of norbornene by $(\text{PPh}_3)_3\text{Cl}_2\text{Ru}=\text{CH}-\text{CH}=\text{CPh}_2$, **1**.

While **1** was demonstrated to exhibit broad tolerance to a range of functionality and was capable of mediating living ROMP, it did not display the same excellent

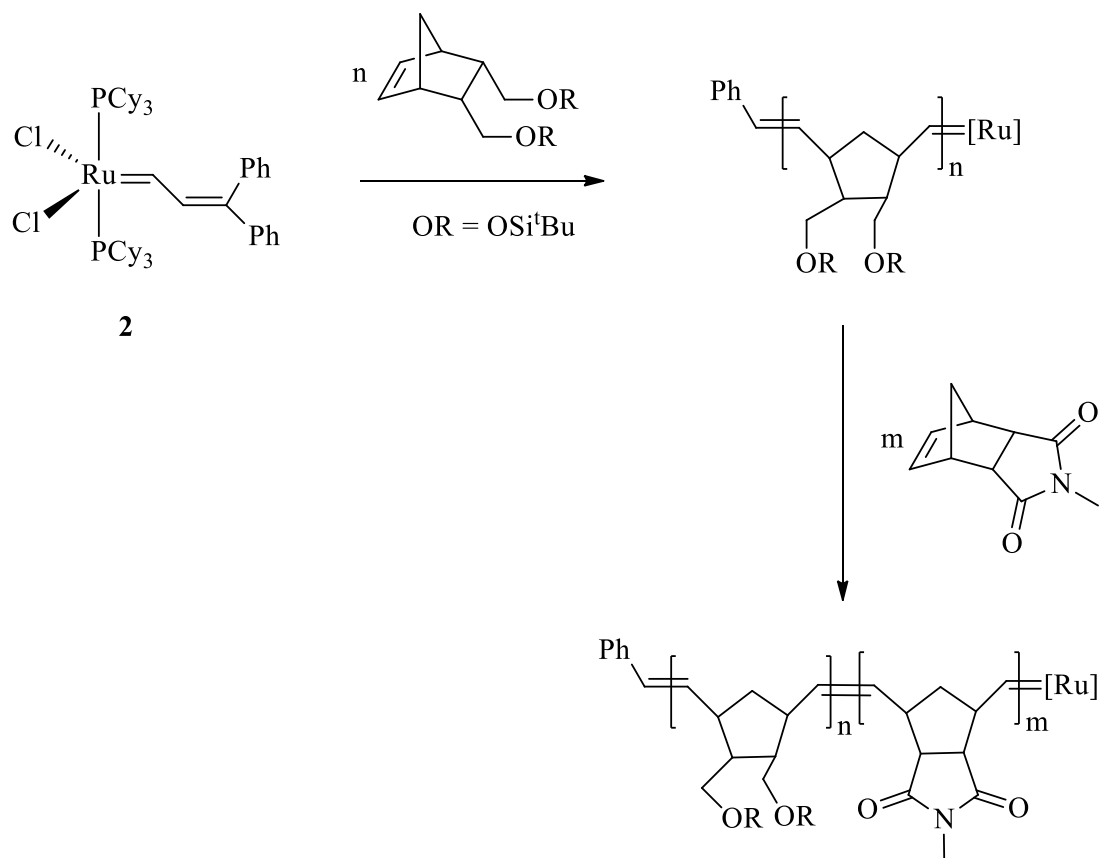
activity towards other cyclic olefins such as *cis*-cyclooctene, cyclooctadiene, 7-oxanorbornene derivatives and cyclopentene.⁷⁴ This led to the optimization of **1** by varying the substitution of ligands, altering the environment around the metal centre, in an effort to improve its activity towards other cyclic olefins. The same group later expanded on this contribution,⁷⁴ and discovered that by substituting triphenyl phosphine (PPh₃) with a more electron-rich phosphine like tricyclohexylphosphine (PCy₃), the activity of **1** could be significantly improved. The simple modification was accomplished easily by adding excess PCy₃ to **1** in solution so that phosphine exchange can be facilitated, Scheme 1-8.



Scheme 1-8. Synthesis of a more active derivative of **1** via phosphine exchange to give **2**.

Relatively, **2** was more ‘compatible’ with a broader range of functional groups and showed impressive tolerance towards organic acids, like acetic acid and inorganic acids such as diethyl ether solution of hydrochloric acid. Bielawski *et al.*⁷⁶ reported the synthesis of end-functionalised poly(norbornene)s or telechelic polymers via ROMP with **2**. While demonstrating increased activity towards norbornene, the rate of initiation of **2** was lower in comparison to **1**, resulting in large dispersities ($D = 2.10$) of the final (co)polymers. End functionalisation was readily accomplished using chain transfer agents (CTAs) such as allyl acetate, although, extensive (higher than expected)

chain transfers between high MW polymers and CTAs was observed. Despite the slow rate of initiation, **2** was capable of mediating living ROMP of norbornene derivatives with functionality as shown in the synthesis of polynorbornene with Si-containing functional group and subsequent block (co)polymerisation with *exo*-*N*-methylbicyclo[2.2.1]hept-6-ene2,3-dicarboxylimide, Scheme 1-9.⁷⁷



Scheme 1-9. ROMP of a silylether-functional norbornene and subsequent block (co)polymerisation mediated by **2**.

An alternative to **2** was prepared via the treatment of (PPh₃)₃RuCl₂ with diazobenzylidene and subsequent exchange of the phosphine ligands to obtain the more active derivative, **3**, Figure 1-4. It was reported by Schwab *et al.*^{78, 79} that this benzylidene derivative has a higher initiation rate than **2**. This minor modification to the structure led to the first generation of what is now known as the Grubbs catalysts.

The remarkable activity and compatibility of **3** towards polar functional groups was demonstrated in its application for the ROMP of a range of norbornene derivatives and cyclobutenes. Compatible functionalities include alcohol, amino, ester, amido and keto groups.⁸⁰⁻⁸⁴ In an effort to further improve the rate of initiation of **3**, Robson *et al.*⁸⁵ exploited the labile nature of the ligands, that is by adding phosphine ligands as a rate modifier during ROMP to reduce the rate of propagation as phosphine ligands and monomers will competitively coordinate to the Ru-centre. This solution proved to be effective as the ROMP of norbornenes resulted in poly(norbornene)s with \bar{D} as low as 1.04.⁸⁶

Continuing with an examination of the ligand environment in these Ru-based complexes,^{87, 88} the same group subsequently reported the 2nd generation of Grubbs catalysts,⁸⁹ **4**, in which a N-heterocyclic carbene (NHC) replaced one of the phosphine ligands. NHCs are known for their strong sigma-donation⁹⁰⁻⁹⁴ which provides more electron density at the metal centre and stabilises the transition state during metathesis events.

The Ru-based complex, **4**, was demonstrated to have extraordinary activity towards a range of cyclic olefins including *cis*-cyclooctadiene, 1,5-dimethylcyclooctadiene, 1,3,5,7-cyclooctatetraene.^{95, 96} albeit in an uncontrollable fashion with the dispersities in the resulting polymers typically in the range from \bar{D} of 1.60 to 3.20. The broad dispersities were due to the slow rate of initiation relative to propagation coupled with a propensity for chain termination reactions.

A 3rd generation Ru-based, Grubbs catalyst was reported by Love *et al.*,^{97, 98} **5**, the first phosphine-free Grubbs derivative is 1.25×10^6 times more active for cross-metathesis of acrylonitrile than **4**, which was attributed to rapid dissociation of the 3-bromo-pyridine ligand, which in turn increases the rate of initiation of **5**. For this

reason, the 3rd generation Grubbs catalyst has been employed for ROMP. For example, Choi and Grubbs⁶⁷ reported the ROMP of norbornene by **5**, affording polynorbornenes in high yield (ca. 90 %) with $D = 1.04$. Complex **5** is capable of mediating ROMP of a wide variety of functional norbornene derivatives, which resulted in ROMP polymers having dispersities around $D = 1.05$ with good control over the MW, as well as facilitating the synthesis of novel block copolymers via sequential monomer addition.

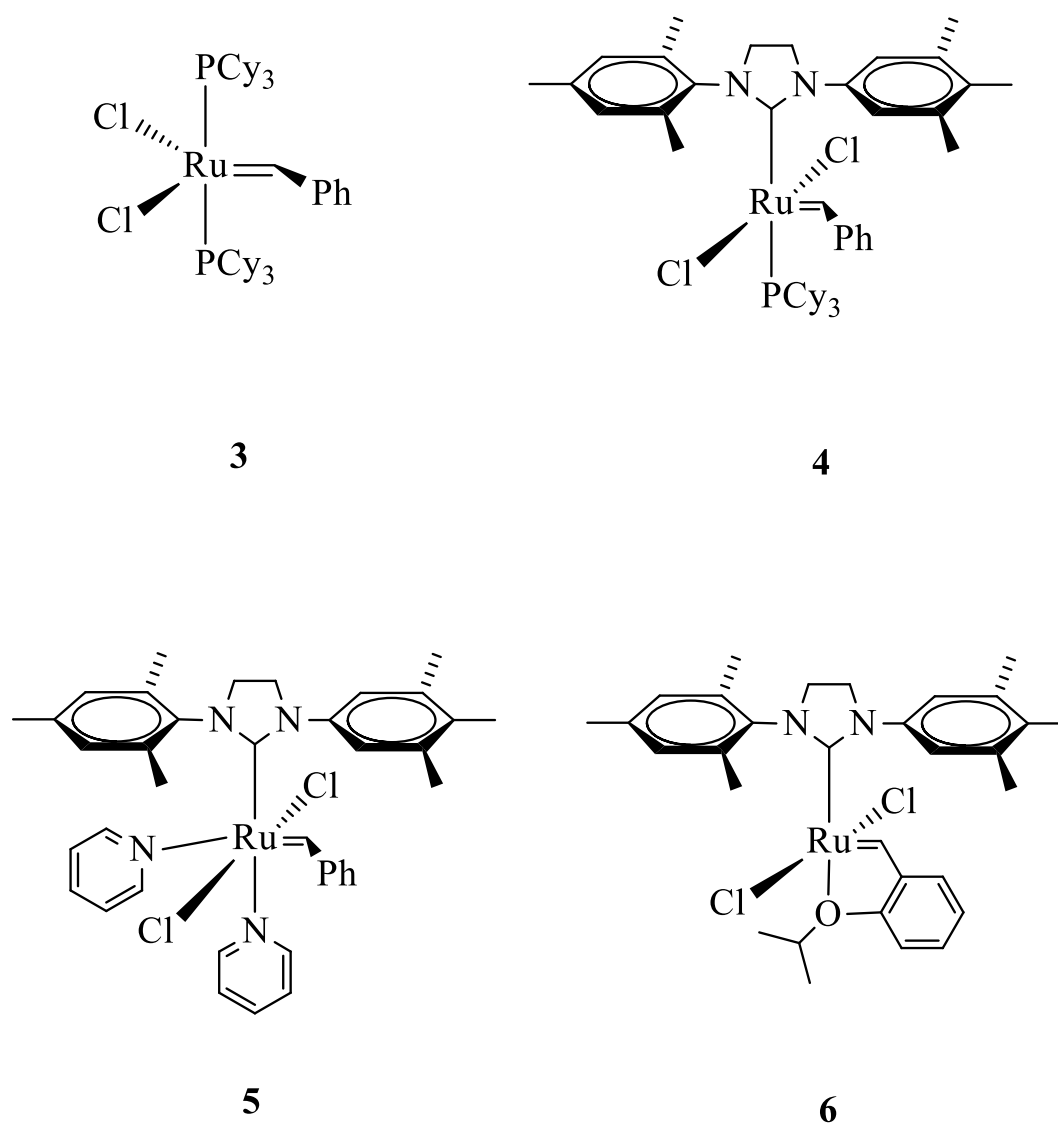
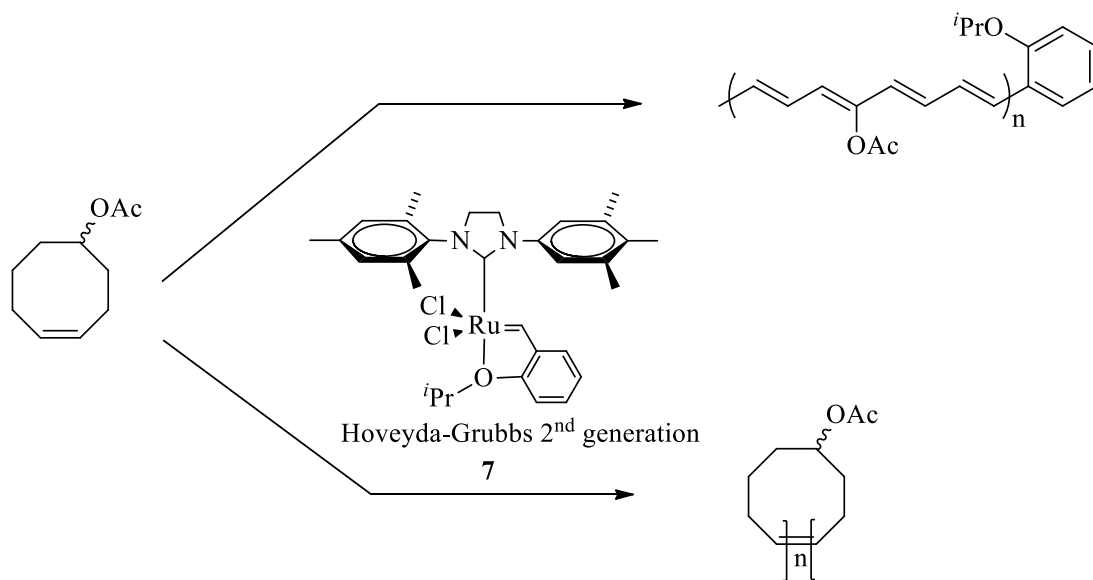


Figure 1-4. Grubbs catalysts from 1st to 3rd generation (**3**, **4**, **5**) and Hoveyda-Grubbs 1st generation, **6**, discussed in this chapter.

The Hoveyda-Grubbs catalyst, **6**, Figure 1-4, and subsequent generations/variations of **6** have been employed for ROMP, although is not the preferred initiator due to its low activity towards cyclooctene^{99, 100} and norbornenes.¹⁰¹ In addition, macrocyclic oligomers formed via backbiting have been observed with Hoveyda-Grubbs type catalysts.¹⁰² While macrocycle formation is generally undesirable, there are reported applications of macrocycles in drug delivery¹⁰³, and as lubricants.¹⁰⁴ As such, a recent example of applications of Hoveyda-Grubbs type catalysts to promote macrocycle formation was reported by Blencowe and Qiao,¹⁰⁵ detailing the synthesis of functionalised macrocyclic oligo(cyclooctene)s via Hoveyda-Grubbs 2nd generation catalysts, **7**, Scheme 1-10. Hoveyda-Grubbs catalysts are also known to facilitate the (co)polymerisation of norbornene and cyclooctene via alternating ROMP (AROMP) to produce novel alternating copolymers.⁹⁹



Scheme 1-10. ROMP of functionalised cyclooctene with Hoveyda-Grubbs 2nd generation catalyst, **7**, and formation of macrocyclic oligo(cyclooctene)s from backbiting.

1.1.1. Tungsten and Molybdenum

1.1.1.1. W- Carbene Complexes for ROMP

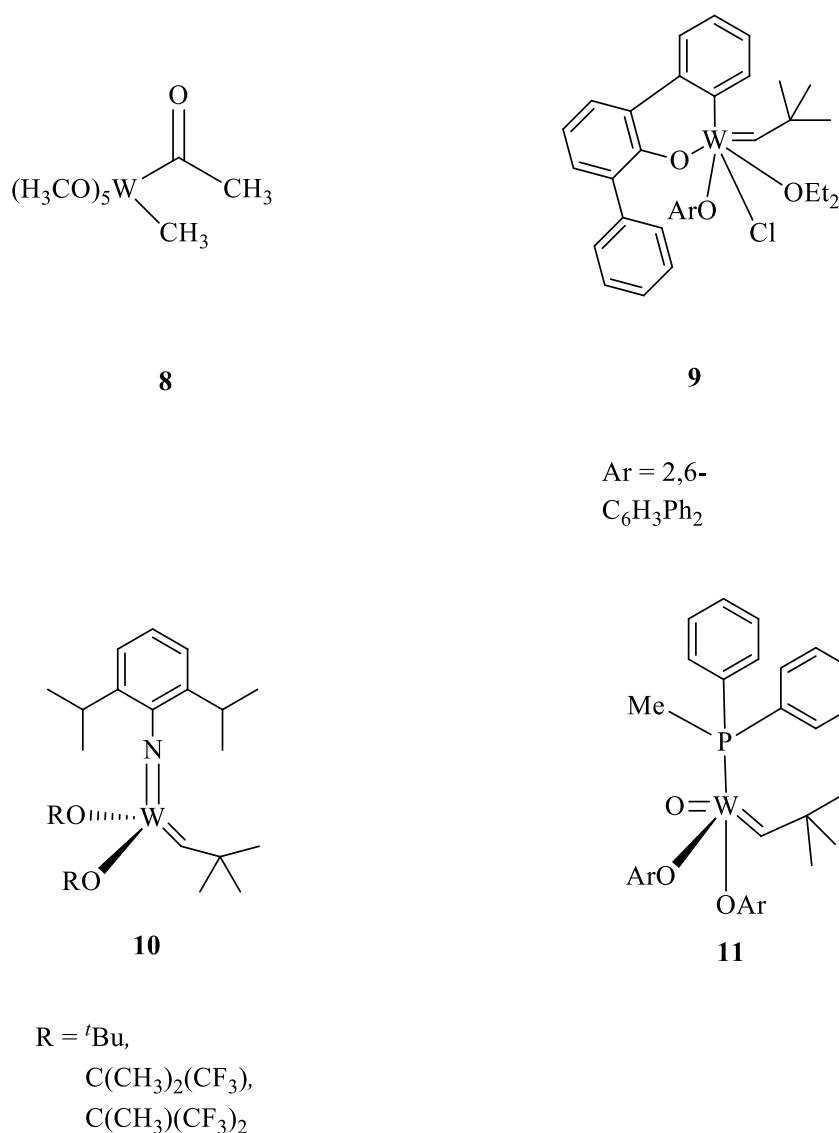
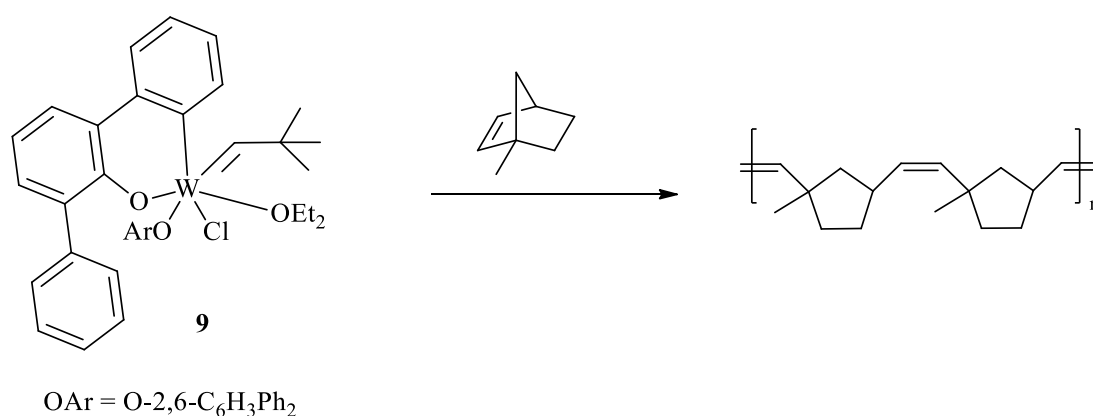


Figure 1-5. Selected examples of W-based complexes discussed in this section.

Fischer and Casey¹⁰⁶ reported the first well-defined W-based complex, Figure 1-5, **8**, which was able to mediate the non-controlled polymerisation of strained cyclic olefins including norbornenes, cyclobutene, cyclopentene, cycloheptene, and cyclooctene with large dispersities, presumably due to the secondary metathesis

reactions.¹⁰⁷ Since then hundreds of Fischer-type catalysts¹⁰⁸⁻¹¹¹ had been prepared, usually stabilised by a N- or O- containing carbene ligand.

During the 1970s, Schrock *et al.*¹¹² and Osborn *et al.*¹¹³⁻¹¹⁵ designed and developed new, well-defined W-based complexes based on the **8** structural motif which were then used to perform living ROMP of norbornene derivatives in the presence of a Lewis acid such as GaBr₃. A range of single component W-based initiators with a variety of aryloxy ligands that required no added Lewis acid was reported by Quignard *et al.*¹¹⁶ which showed increased functional group tolerance with the ability to polymerise norbornene with ester, nitrile and anhydride functional groups. Most notably, W complex, **9**, Figure 1-5, demonstrated high activity which facilitated the stereoregular polymerisation of norbornene with a propensity to form 100 % *cis* polymers as in the case of 1-methylnorbornene, Scheme 1-11, with head-to-tail configuration being preferred. However, the high activity proved to be problematic as it prevented the living polymerisation of norbornene due to secondary metathesis reactions.



Scheme 1-11. Polymerisations of 1-methylnorbornene via ROMP with **9**.

A new well-defined, W-based complex, **10**, Figure 1-5, bearing imido-alkoxy ligands was reported by Schrock *et al.*¹¹⁷⁻¹¹⁹ It was discovered that by increasing the

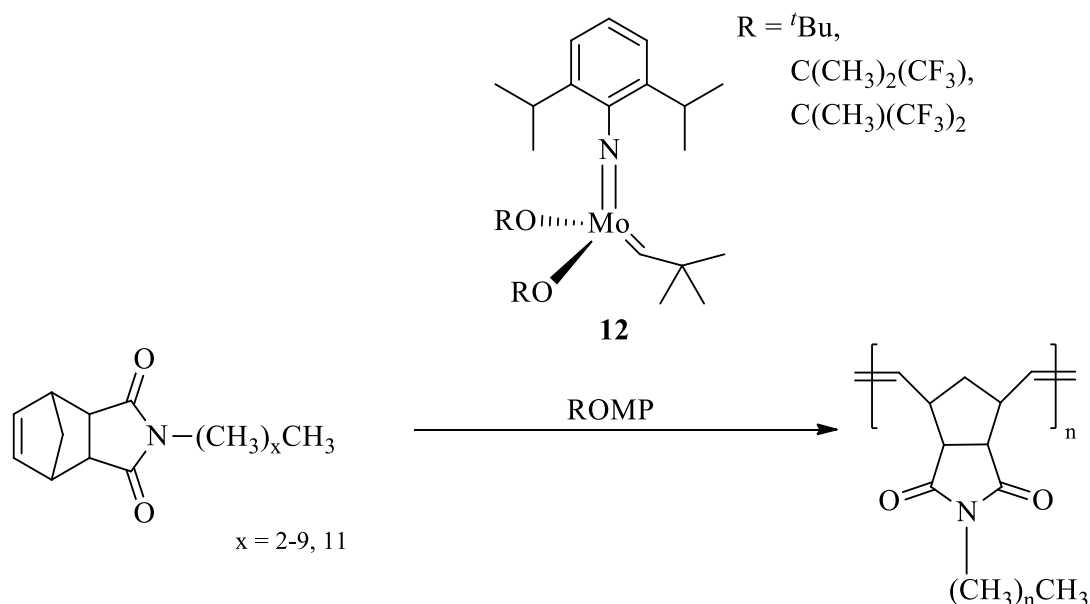
electrophilic character of the alkoxide ligands (such as using a fluorine functionalised derivative), the activity of the catalyst can be significantly improved for metathesis reactions and in particular ROMP of norbornene. Complex **10** with *tert*-butyl alkoxide ligands was found to mediate the living ROMP of norbornene with tunable molecular weight and dispersities as low as $\bar{D} = 1.03$; however, the fluorine functionalised **10** derivatives were found to suffer from slow initiation with a propensity to undergo secondary metathesis reactions during ROMP.

The same group reported the alkylidene complex, **11**, Figure 1-5.¹²⁰ Complex **11** was found to mediate the polymerisation of 2,3-dicarboxymethoxynorbornadiene and 2,3-bis(trifluoromethyl)norbornadiene in a living fashion, to give a highly stereoregular polymer with little to no evidence of secondary metathesis reactions as evidenced by the low dispersities ($\bar{D} = 1.01$). Cyclopentene is a challenging cyclic olefin to polymerise due to relatively low ring-strain but these W-based catalysts were able to mediate the living ROMP of cyclopentene, conducted at $-40\text{ }^{\circ}\text{C}$ with complex **10** bearing a *tert*-butyl alkoxide, resulting in polymers with $\bar{D} = 1.08$. The polymerisation was conducted at lower temperature to prevent secondary metathesis reactions such as back-biting reactions.¹²¹⁻¹²⁴

In contrast, cyclobutene was readily amenable to ROMP with **10** due to significant ring-strain. As a result, the activity of these catalysts towards cyclobutene is vastly increased, and requires the addition of a labile Lewis base such as trimethylphosphine (without Lewis base added, large \bar{D} s were observed) to modulate the reaction by competitively inhibiting olefin metathesis, thereby, increasing the rate of initiation and reducing the occurrences of secondary metathesis reactions.¹²⁵

1.1.1.2. Mo-Carbenes Complexes for ROMP

In addition to W-based carbenes, there has been significant interests in Mo-based species such as complex **12**, reported by Schrock *et al.*¹²⁶ Although complex **12** is structurally similar to **11**, it is compatible with a range of functionality including ether, cyano, imide, amide, ester, ketal and halogen groups.¹²⁷⁻¹²⁹ Access to monomers (such as norbornene with *endo* substituents) that were previously not amenable to ROMP mediated by W-based carbenes, is now available with complex **12**; resulting ROMP of these norbornene derivatives with complex **12** resulted in polymers with low dispersities (ranging from $D = 1.04$ to 1.19) with controllable MW.



Scheme 1-12. Polymerisation of *n*-alkyl norbornene dicarboxyimides via ROMP with **12**.

In terms of the tunability of Mo-based complexes, they share similarities with their W-based counterparts in that the alkoxide ligand modulates their activity, with more electron withdrawing alkoxide ligands increasing the metathesis activity. This is shown when complex **12** bearing a C(CH₃)(CF₃)₂ alkoxide was employed in the

polymerisations of *n*-alkyl norbornene dicarboxyimides via ROMP, Scheme 1-12. The resulting polymers had high dispersities, typically around *D*s of 1.30 to 2.10, which was attributed to a fast initiation step of **12** bearing fluorinated alkoxide ligands.^{130, 131}

Mo-based ROMP initiators have also been found to polymerise other less reactive cyclic olefins such as cyclopentene. Complex **12** with *tert*-butyl alkoxide ligands reported by Trzaska *et al.*,¹³² was able to polymerise cyclopentene to afford poly(1-pentenylene) with a low dispersity (*D* < 1.10). Similar to the W-based analogue of **12**, the ROMP reaction needed a Lewis base to induce living ROMP but differs in that the polymerisation temperature required for efficient ROMP with **12** was room temperature versus -40 °C with complex **11**. Since **12** is capable of living ROMP, access to block copolymers are available; Diblock copolymers of poly(cyclopentene) and poly(ethylidenenorbornene) were successfully synthesised and exhaustive hydrogenation of the block copolymers afforded regions of linear polyethylene backbone and star polymer backbone which led to crystalline and amorphous regions in the polymer.

The polymerisation of cyclobutenes via ROMP with **12** have been reported.^{133, 134} In general, they are amenable to ROMP but with little control over the MW and dispersities due to rapid rates of propagation compared to the rate of initiation, stemming from the high ring-strain of the cyclobutenes. The authors noted that **12** bearing a fluorine functionalised alkoxide ligands, afforded better control over the MW when it comes to ROMP of these cyclobutene derivatives.^{135, 136} Other cyclic olefins that are of interest in ROMP, are cyclopropenes. The ROMP with **12** bearing *tert*-butyl alkoxide ligands was reported by Singh *et al.*,¹³⁷ with resulting polymers having low dispersities (*D* = < 1.05) with good control over the MW and quantitative polymer yields. The ROMP of cyclopropene was also found to be living in nature, as

evidenced by the successful synthesis of block copolymers from a combination 3-methyl-3-phenylcyclopropenes, dicarbomethoxynorbornadiene, 3-(2-methoxyethyl)-3-methylcyclopropene, and methyltetracyclododecene with low MWD ($\bar{D} = < 1.10$)

1.5 Metathesis vs Insertion Polymerisation of Substituted Acetylenes

Interest in acetylene polymerisations began as early as 1955, with the first reported synthesis of polyacetylene by Giulio Natta¹³⁸ employing a Ziegler-Natta catalyst system ($\text{Ti}(\text{O}i\text{Bu})_4/\text{AlEt}_3$). The resulting polymers were a black powder which was insoluble and infusible. Later, Shirakawa, Ito and Ikeda reported the preparation thin films of polyacetylenes using a very high concentration of the same catalytic system previously employed by Natta but, in this instance, without stirring.^{138, 139} With this method, a thin copper-coloured film can be obtained from the polymerisation of acetylene conducted at < -78 °C. According to IR and Raman spectroscopic studies, this thin copper-coloured film was revealed to be *cis* in nature, while, a silvery thin film possessing predominantly *trans* configuration can be obtained via *cis-trans* thermal isomerisation at > 150 °C.¹³⁹ The primary interest in these materials is their potential semi-conducting property, and upon oxidation with halogens electrical conductivity can be further enhanced.¹⁴⁰ The drawback of polyacetylenes are their insolubility and instability in air, making them challenging to characterise.¹³⁹⁻¹⁴⁴

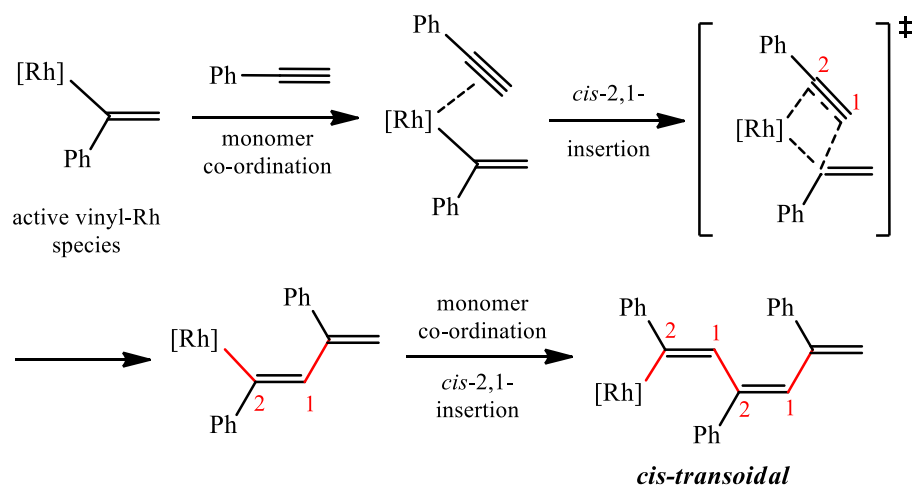
For this reason, research efforts were diverted to the polymerisation of substituted acetylenes that are more stable and soluble and easier to characterise. One of the most widely examined substituted acetylenes is phenylacetylenes (PA) because:

1. Poly(phenylacetylene)s (PPAs) are soluble in most common organic solvents such as CH_2Cl_2 and toluene.

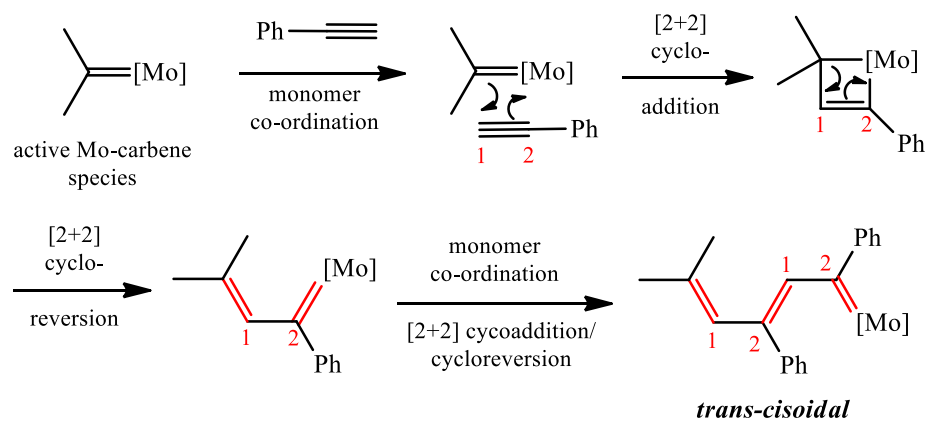
2. PPAs are generally stable in air, particularly in the solid-state, facilitating characterisation of their properties.

As such, there is extensive literature regarding the preparation and properties of PPAs, and its derivatives.

Insertion polymerisation mechanism



Metathesis polymerisation mechanism



Scheme 1-13. The generally accepted mechanisms for the Rh-insertion polymerisation of phenylacetylene (top) and the Mo-mediated metathesis polymerisation of phenylacetylene (bottom).

There are two distinct mechanistic pathways available for transition-metal mediated polymerisations of PA, and that is the metathesis and insertion processes, Scheme 1-13. As such, there are four possible geometric structures of substituted poly(acetylene)s as a result of the different transition metal pathways available and that is *cis-transoidal*, *cis-cisoidal*, *trans-transoidal* and *trans-cisoidal*, Figure 1-6. For reference, *cis*- and *trans*- refers to the geometric isomerism about the double bond (highlighted in blue), while *cisoidal* or *transoidal* refers to the configuration about the single bond. In general, metathesis-type polymerisation results in *trans-transoidal* and *trans-cisoidal* structures, while insertion-type polymerisation results in *cis-transoidal* and *cis-cisoidal* products.

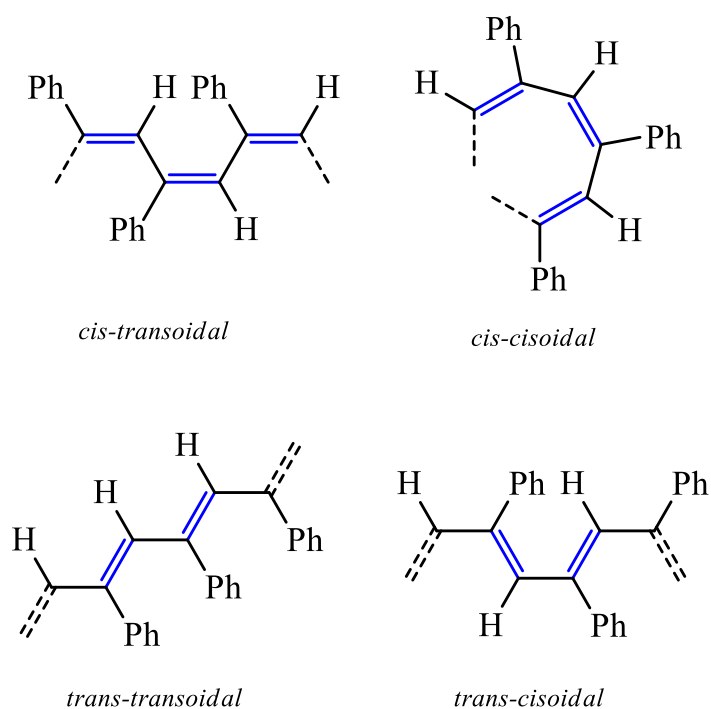


Figure 1-6. Possible geometric structures of polyphenylacetylene.

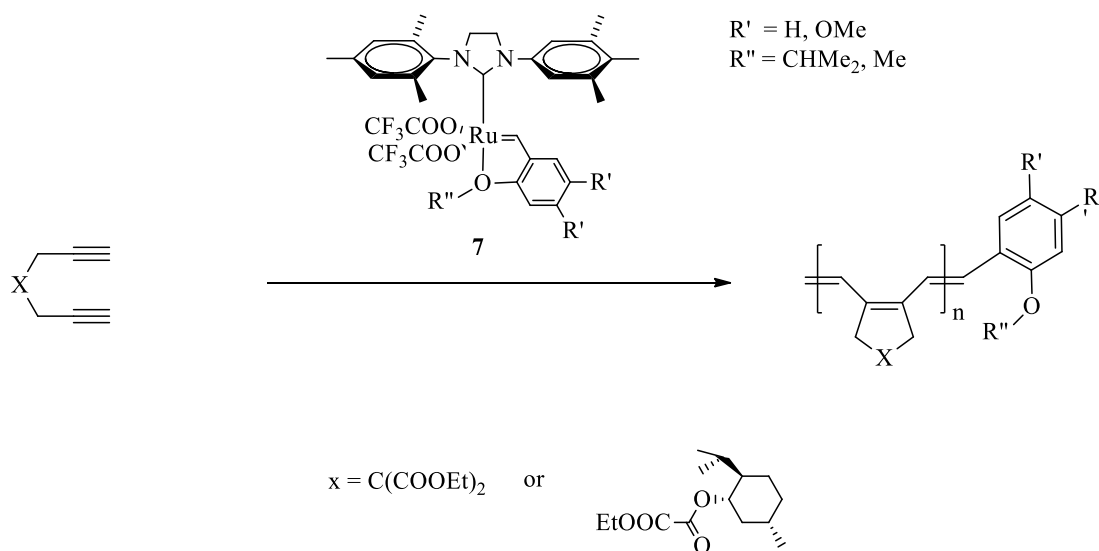
It was elucidated by Motoshige *et al.*¹⁴⁵⁻¹⁴⁸ that the conformation about the single bond in these polyenes are not restricted to their original configuration (*cisoid* or *transoid*) but can be altered via the type of catalyst used or post polymerisation

processes such as heat-treatment, and even the type of solvent (e.g. toluene or chloroform) used to dissolve the polymers.

1.5.1 Metathesis Ru-Based Initiators for The Polymerisation of Substituted Acetylenes

There is a noticeable dearth of reports of Ru-mediated polymerisation of acetylenes, or substituted derivatives. Yamaguchi *et al.*¹⁴⁹ reported the attempted polymerisation of -OH or -COOH functionalised alkynes employing [(Cp)RuCl₂]₂ (Cp = permethylcyclopentadienyl), which yielded a brown polymer of various MWs, multimodal SEC traces, and dispersities too broad to measure, clearly indicative of uncontrolled polymerisation. In addition, the reaction yielded small amounts of 1,2,4- and 1,3,5-benzenetricarboxylic acids, which are cyclotrimerisation products, with the mechanism of formation elucidated by Kirchner *et al.*,¹⁵⁰ which was Ru-catalysed of a [4+2] reaction via metallacyclopentatriene transition state. Subsequently, Schuehler *et al.*¹⁵¹ reported an attempt at the synthesis of poly(acetylene)s via **3**, **4**, and **5**, Figure 1-4. Poly(acetylene)s were obtained from **5** but not from **3** and **4**, however, the authors did not report the MW and dispersities but focussed on the characterisation of the physical properties of the thin-layer of poly(acetylene)s such as conductivity and morphologies under a scanning electron microscope (SEM).

Krause *et al.*¹⁵² employed a modified Hoveyda-Grubbs catalyst, **7**, that could cyclopolymerise diethyl dipropargyl malonate in stereoregular manner (high trans selectivity with respect to the *N*-heterocyclic carbene) with end-functionalised cyclopolymer obtained in quantitative yields. In addition, complex **7** displayed good control over the MW, Scheme 1-14; furthermore, the M_n vs conversion plot was linear in some cases, suggesting living character.



Scheme 1-14. General reaction scheme of the ruthenium-catalysed polymerisation of diacetylene derivatives.

Katsumata *et al.*¹⁵³ utilised the 1st generation Hoveyda-Grubbs catalysts **6** to polymerise disubstituted acetylenes with ester and amide functionalities. In general, the polymerisations attempted did yield polymers but in poor yields (5-48 %) and the resulting dispersities were, on average, around \bar{D} of 1.70.

Zhang *et al.*¹⁵⁴ reported the uncontrolled polymerisation of phenylacetylenes mediated by complex **7**, which was previously employed by Krause *et al.* for α,ω -dialkynes. Polymerisation yielded PPA with \bar{D} s > 2.00, and with predominantly *trans* backbone configuration.

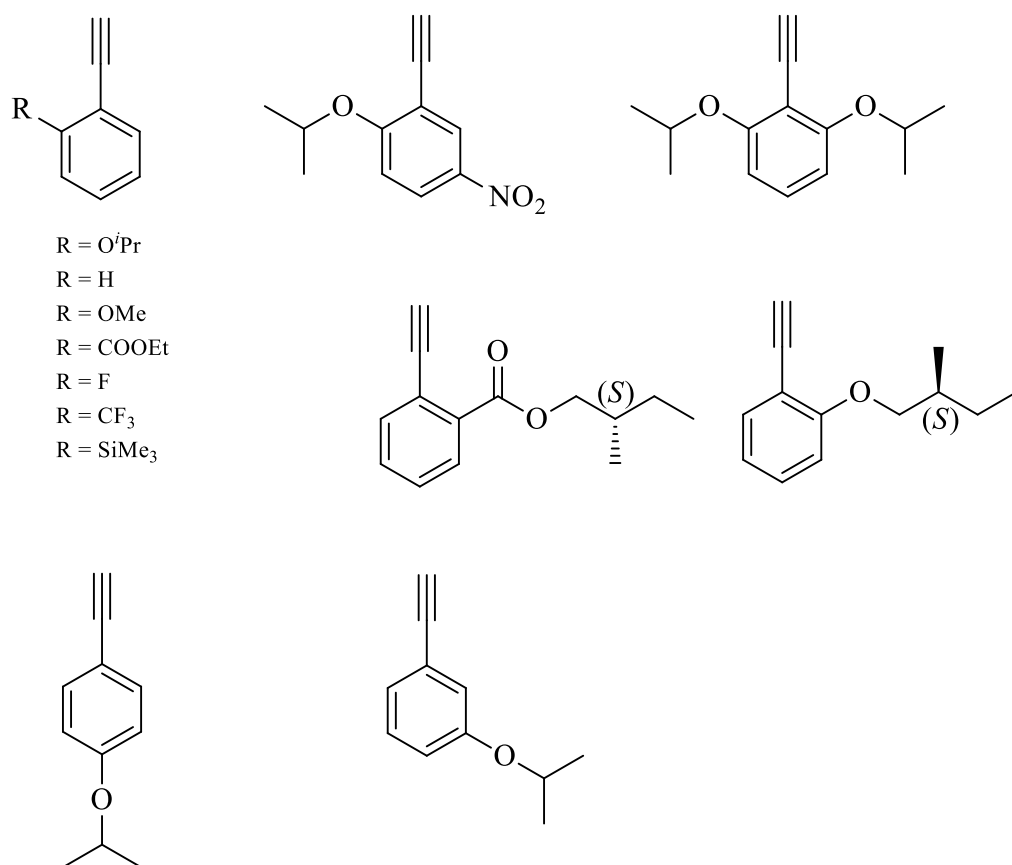
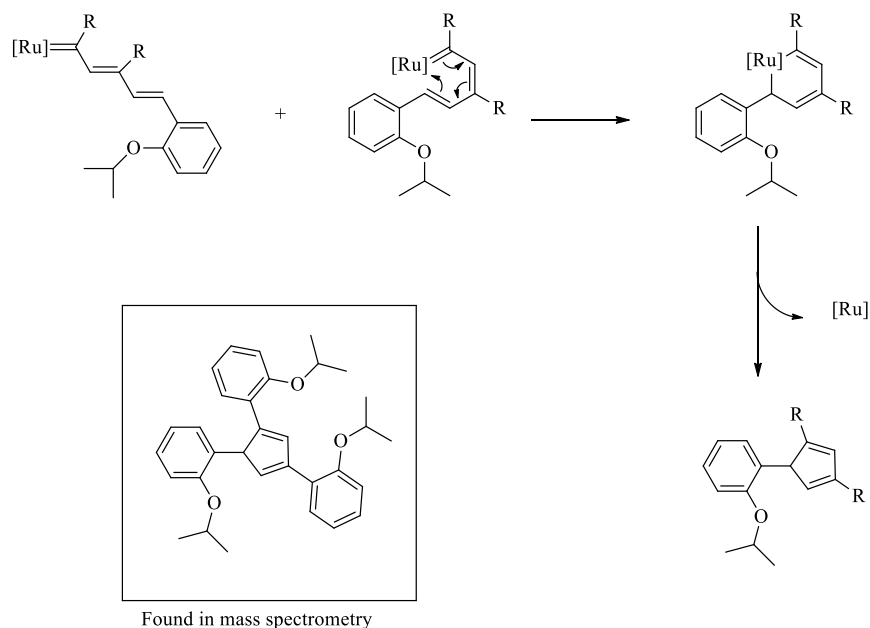


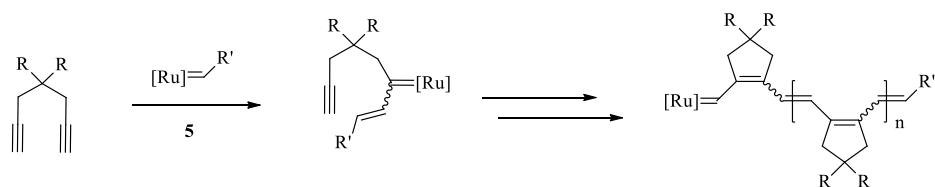
Figure 1-7. Monomers used in the polymerisations by Kasumata *et al.*¹⁵³ to synthesise functionalised poly(phenylacetylene)s.

Kasumata *et al.*¹⁵³ described the Ru-mediated polymerisation of a series of *ortho*-substituted PPAs, Figure 1-7. The ¹H NMR of the resulting polymers from the Ru-mediated polymerisations were not well-defined (broad signals and no prominent H backbone signal) which is indicative of high *trans* content in the polymer backbone, as expected for metathesis polymerisation. The majority of the polymerisations yielded trace polymers that were generally not characterisable. Those that were characterised were either oligomeric or had broad dispersities with \bar{D} as high as 4.79. This was attributed to termination or side reactions associated with the conversion of the metathesis active alkylidenes into metathesis inactive cyclopentadienes via cyclotrimerisation processes, Scheme 1-15.

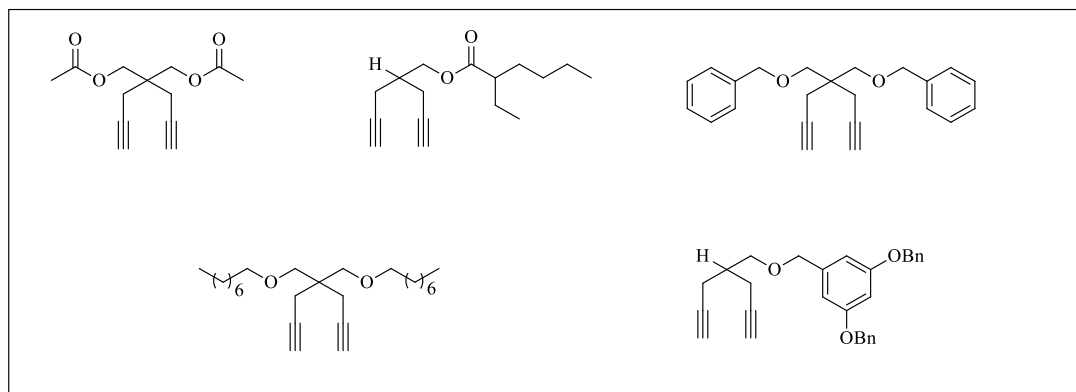


Scheme 1-15. Proposed decomposition mechanism for ruthenium-alkoxybenzylidene complex during polymerisations and the chemical structure of the cyclotrimerisation product (shown inset).

Complex **5** was found to mediate the living cyclopolymerisation of α,ω -dialkynes such as 1,6-heptadiyne in THF and DCM, Scheme 1-16, as reported by Kang *et al.*¹⁵⁵ The MW of the product could be controlled by the ratio of monomer-to-initiator, $[M]/[I]$, with resulting materials having low D_s of ca. 1.15 and quantitative conversions. In addition, diblock copolymers of various α,ω -dialkyne derivatives were successfully synthesised as a result of living nature of the polymerisations.



α,ω -alkynes derivatives:



Scheme 1-16. Cyclopolymerisation of 1,6-heptydiyne by complex **5** and α,ω -dialkyne derivatives used in block (co)polymerisation experiments.

In summary, Ru-mediated polymerisation is a viable synthetic route to *trans*-rich polyenes, but there are currently few examples in which (co)polymerisation proceeds in a controlled fashion.

1.5.2 Group 6 (W and Mo) Metathesis Catalyst-Mediated Polymerisation of Substituted Acetylenes

Group 6 metal complexes active in the polymerisation of substituted acetylenes can be divided into their respective groups, namely metal-carbene complexes (Schrock-type carbene complexes), metal-halide complexes, and metal-carbonyl complexes. Their mechanism of action was proposed to be metathesis in nature and examples have been reported to be convenient for the polymerisation of sterically hindered substituted acetylenes but not for less sterically hindered monomers like phenylacetylenes and acetylenes with a propensity to form cyclotrimers via cyclotrimerisation reactions.¹⁵⁶

The bulk of the initial studies on the application of Mo- and W-based halide complexes in the polymerisations of substituted acetylenes were conducted by the Masuda group, who demonstrated that relatively high molecular weight poly(phenylacetylene)s (PPAs) ($M_n > 10,000$) could be obtained easily if tetraphenyltin, Ph_4Sn , or water was used as a co-catalyst.^{157, 158} It was also found that internal alkynes such as phenylpropyne were susceptible to polymerisation, which produced moderate yield poly(phenylpropyne)s with a predominantly *trans* geometrical structure.¹⁵⁹ Balcar and Pacovska¹⁶⁰ reported the use of tungsten(IV)tetrachloride, WCl_4 dissolved in 1,4-dioxane (an increase in the activity of WCl_4 is seen if dissolved in oxygen-containing solvents, particularly in 1,4-dioxane) which had a significantly higher activity over the $\text{WCl}_6/\text{Ph}_4\text{Sn}$ system, resulting in PPAs with very high molecular weight ($M_n = 200,000$) with quantitative yields. It was subsequently reported that the $\text{WOCl}_4/\text{Ph}_4\text{Sn}$ system yielded very high MW PPAs (M_n around 1,000,000) when polymerised in 1,4-dioxane.¹⁶¹ Masuda, Kawa, and Higashimura reported the synthesis of poly(propionic acid) by MoCl_5 with Ph_4Sn ,

BuSn₄ or Ph₃Sb as catalysts in 1,4-dioxane which appreciably improved polymer yield.¹⁶²

In light of this discovery, many derivatives of the metal-halide catalyst systems thereafter, incorporated oxygen-containing compound (such as 1,4-dioxane, *t*-BuOH and EtOH) with a co-catalyst (such as *n*-Bu₄Sn, *n*-Bu₃SnCl, Ph₄Sn, Et₃AlCl, EtAlCl₂, Et₃SiH, Ph₃SiH, N-BuLi, Et₃Zn, EtMgBr, Ph₃Sb, and Ph₃Bi) in their design and some even exhibited living polymerisation characteristics.¹⁶³⁻¹⁶⁹ For example, Masuda *et al.*¹⁷⁰ reported the polymerisation of 1-chloro-1-alkynes, Figure 1-8, employing a ternary catalyst system comprising of MoOCl₄/*n*-Bu₄Sn/EtOH, resulting in polymers with *D*s ranging from 1.15 to 1.25 with controllable MW of the polymer, which can be as high as $M_n = 400,000$. Furthermore, the polymerisation was living in nature as the successive addition of monomer after each polymerisation was accompanied by a systematic increase in the MW of the polymer. The successful synthesis of triblock copolymers of 1-chloro-1-hexyne and 1-chloro-1-hexadecyne corroborated these findings. The previous examples highlight classical systems that contain two or more components for effective polymerisation (living or otherwise). While frequently demonstrated to be highly active, however, it is a complex system with an undetermined mechanism for the formation of the presumed active metal-carbene species, M=CCl₃ (where M = Mo or W).

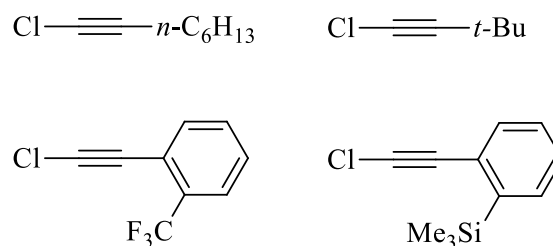
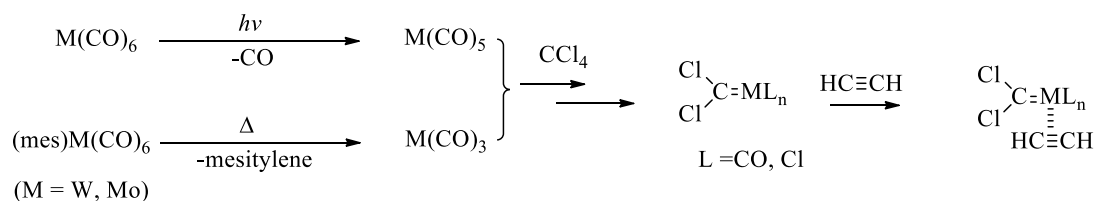


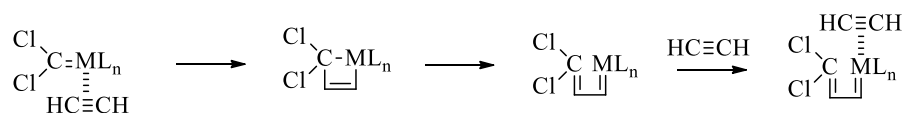
Figure 1-8. Living polymerisation of various 1,2-disubstituted acetylenes by ternary Mo-halide based catalyst system.

Metal-carbonyl complexes, on the other hand, are more stable towards air and moisture, though their activity is not on par with their metal halide counterparts. They are also known to be metathesis active towards norbornenes, cycloalkenes and acetylenes.^{171, 172} Early development of metal-carbonyl catalyst systems were conducted in chloroform, CCl₄, or dichlorodiphenylmethane, Ph₂CCl₂,¹⁷² and required photoirradiation to produce the active metal-carbene species, M=CCl₃ (where M = Mo or W).¹⁷³ For example, Mo(CO)₆-CCl₄-*hν* or W(CO)₆-CCl₄-*hν* systems were developed by Masuda *et al.*¹⁷⁴ and were reported to initiate the polymerisation of 1,6-dibromo-1-hexyne and 6-bromo-1-hexyne with moderate to high polymer yields (60-80 %), although the Mo(CO)₆-CCl₄-*hν* catalytic system was only shown to be able to polymerise the less sterically hindered monomer, 6-bromo-1-hexyne. Concurrently, the development of metal-carbonyl systems using additives in chlorine-containing compounds¹⁷⁵⁻¹⁷⁸ or by employing organo-metal-carbonyl complexes¹⁷⁹⁻¹⁸² such as (mesitylene)W(CO)₃ or (nbd)Mo(CO)₃ (where nbd = 2,5-norbornadiene) in CCl₄ were reported, both of which required no photoirradiation to be activated. The proposed mechanism for *hν* activation of such complexes is shown in Scheme 1-17.

Initiation:



Propagation:



Scheme 1-17. Proposed mechanism by Tamura *et al.*¹⁷⁹ involving metal-carbonyl complexes for the polymerisation of alkynes with, and without, photoirradiation.

Schrock-type catalysts such as Mo- and W-carbene complexes are highly active initiators for the polymerisation of suitable substituted acetylenes but can be difficult to handle (highly unstable in air and towards moisture) and synthetic procedures are complex due to the required use of impeccable air-sensitive techniques. A controlled polymerisation of α,ω -alkynes mediated by the well-defined Mo-based complex, **12**, was described by Fox *et al.*¹⁶⁴ who reported the successful polymerisation of 1,6-heptadiyne derivatives, which yielded cyclopolymerisation products quantitatively with dispersities typically around D of 1.20. The cyclised polymers were found to have a distribution of 5 and 6 membered rings in an almost 1:1 ratio. A mechanism proposing the origins of these products is shown in Scheme 1-18. Furthermore, with the ability to prepare block copolymers and linear M_n vs monomer conversion plots corroborate the living nature of these cyclopolymerisations.

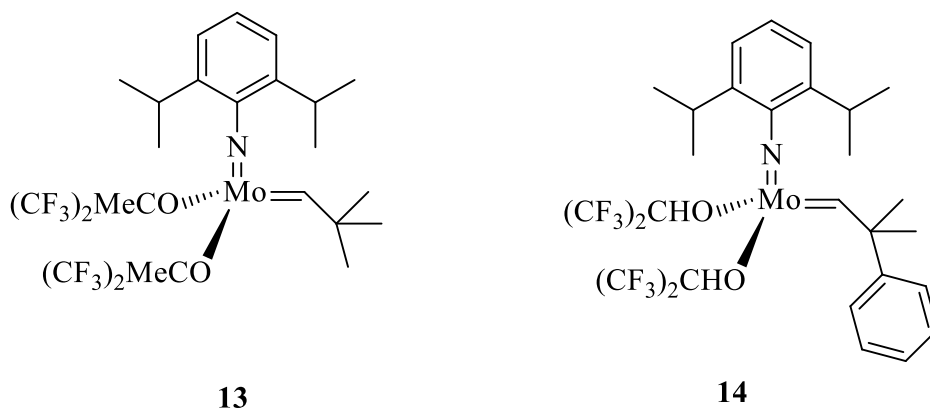


Figure 1-9. Selected examples of well-defined Mo-based complexes that mediate the living polymerisation of *ortho*-substituted phenylacetylenes and α,ω -dialkynes.

1.5.3 Niobium (Nb) and Tantalum (Ta) Complexes for The Polymerisation of Acetylenes.

Nb- and Ta-based complexes such as metal-halides with a (co)catalyst (similar to those employed for W- and Mo-based halides), are well known for their ability to mediate the polymerisation of sterically bulky disubstituted acetylenes but have a propensity to cyclotrimerize monosubstituted acetylenes. The proposed explanation for these occurrences is simply that the steric bulk of disubstituted acetylenes inhibits cyclotrimerization reactions. The various monomers that have been polymerised by Nb- or Ta-based catalyst systems are diphenylacetylene and its derivatives, 1-phenyl-1-propyne, -butyne and -1-octyne, and 2-,3- and 4-octynes.¹⁸⁷⁻¹⁹⁰

Their unique feature is the ability to polymerise substituted acetylenes to high MW polymers. TaCl₅ and NbCl₅ on their own polymerise 1-trimethylsilyl-1-propyne, yielding homopolymer with M_n of 100,000 to 1,000,000, while a TaCl₅/Ph₃Bi catalyst system, M_n as high as 4,000,000 can be achieved.¹⁹¹ Another instance of high MW

polymers was reported by Fujimori *et al.*,¹⁸⁹ who employed a NbCl₅/*n*-Bu₄Sn catalyst system and yielded polymers with $M_n = 1,000,000$.

While Nb- and Ta-based complexes are active for the polymerisation of acetylenes, they have a low functional group tolerance especially towards highly polar or protic functional groups. As such, their applications are limited, other than their exceptional ability to polymerise bulky non-polar/protic disubstituted acetylenes to very high MW.¹⁵⁶

1.6 Rhodium Catalysts for The (Co)Polymerisation of Acetylenes

1.6.1 Non-Controlled Stereospecific Polymerisation of Substituted Acetylenes.

The literature is quite extensive on the application of Rh complexes as initiators for the polymerisation of substituted acetylenes owing to their low oxophilicity, stability to moisture, excellent compatibility with a broad array of functional groups, and generally, produce highly stereoregular polymers, with *cis-transoidal* geometry. In this section is detailed the history of Rh catalysts in polymerisations of PA and its derivatives. In addition, the recent development of Rh catalyst systems and their practical applications in synthesising functional materials will be discussed.

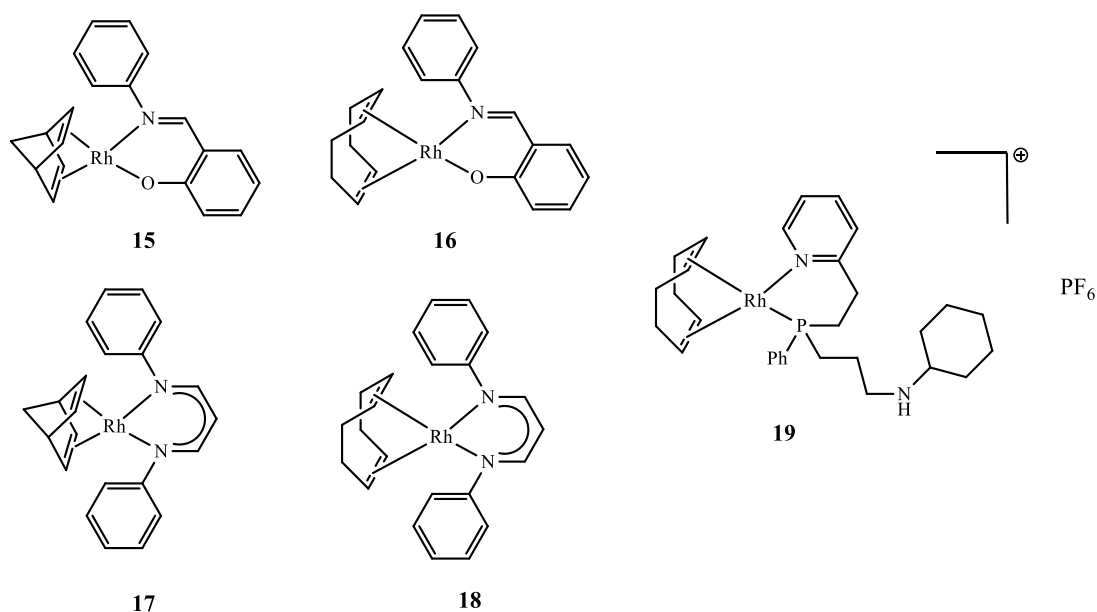


Figure 1-10. Rh complexes used in the polymerisation of PA reported by Furlani *et al.*¹⁹²⁻¹⁹⁴

The first attempted polymerisation of PA with Rh complexes was reported by Kern¹⁹⁵ in which thermal initiation with Wilkinson's catalyst, Rh(Cl)(PPh₃)₃, was detailed. In this instance, the formation of oligomers with an M_n of 1,100 was observed. This report was followed by Furlani *et al.*¹⁹²⁻¹⁹⁴ who reported the application of Rh complexes bearing chelating ligands, **15** to **18**, and a cationic Rh species, **19**, Figure 1-10. All five complexes were demonstrated to polymerise PA with M_n s ranging from 10,000 to 100,000 in the presence of a base such as NaOH. In addition, these researchers were the first to elucidate the geometrical structure of PPAs, prepared with Rh species, and were high in *cis* content (> 98 %).

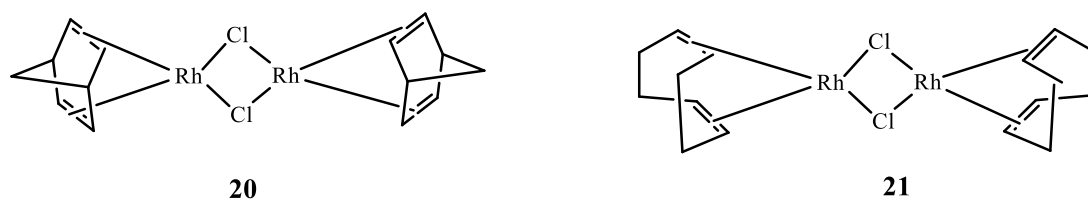


Figure 1-11. Chemical structures of $[\text{Rh}(\text{nbd})\text{Cl}]_2$, **20**, and $[\text{Rh}(\text{cod})\text{Cl}]_2$, **21**.

The synthesis of a high MW PPA with a M_n of ca. 1,000,000 (polymer yield was 100 %) was reported by Tabata *et al.*¹⁹⁶ The Rh catalyst system employed in this study was a combination of $[\text{Rh}(\text{nbd})\text{Cl}]_2$ (where nbd = 2,5-norbornadiene), **20**, Figure 1-11, with triethylamine as a co-catalyst. Interestingly, the highest polymer MW achieved was a M_n of ca. 4,420,000 but polymer yields were low (< 10 %) with large dispersities, a mixture of *cis-cisoidal* (red powder) and *cis-transoidal* PPA (yellow-orange powder) structures. The same group also reported the stereoregular polymerisation of PA, *p*-MeOPA (*p*-methoxyphenylacetylene), *p*-ClPA (*p*-chlorophenylacetylene) with $M_w = 260,000$ with $[\text{Rh}(\text{nbd})\text{Cl}]_2$, $[\text{Rh}(\text{cod})\text{Cl}]_2$ and $[\text{Rh}(\text{bis-cot})\text{Cl}]_2$ (where bis-cot = 1,3,5,7-cyclooctatetraene and cod = 1,5-cyclooctadiene), **21**, Figure 1-11, using triethylamine as co-catalyst and concluded that both **20** and **21** were active for this monomer (but **20** giving higher polymer yields than **21**).¹⁹⁷ These catalysts are also reportedly active for (*E*)-*p*-[(*p*-methoxyphenyl)-2-ethynyl].¹⁹⁸ Due to the highly stereoregular nature of the PPA obtained from this system, interesting ordered structures such as columnar PPA¹⁹⁹ and helical PPA²³⁰ can be obtained.

Building on these findings, Kanki *et al.*²⁰⁰ investigated the effects of adding co-catalysts such as Et_3N , organolithium reagents, Grignard reagents and others in the polymerisation of PA mediated by $[\text{Rh}(\text{nbd})\text{Cl}]_2$. It was found that adding alkyl compounds such as organolithium and Grignard reagents were effective, and yielded

high MW polymers. This was attributed to the formation of an active Rh-alkyl species, which served as the active initiator. The authors also investigated the effect of adding triphenylphosphine (PPh₃) to the polymerisation and found that it retarded the polymerisation significantly, which was actually useful for kinetic studies as the polymerisation was too fast to observe in the absence of PPh₃. It was proposed that PPh₃ acted as a rate modifier by retardation of the rate of propagation. Progressively increasing the concentration of PPh₃, lowered the MW of the final PPAs, which they attributed it to the presence of a larger quantity of long-lived propagating species as a result of stabilisation of a tetracoordinate Rh species (assumed to be Rh(diene)(PPh₃)₂, where diene = cod or nbd) by PPh₃.

Thereafter, the **20**/Et₃N catalyst system has been utilised in many applications in the literature with simple minor modifications such as using a different co-catalyst due, in part, to its versatility and ease of use. For example, Kong *et al.*²⁰¹ utilised the **20**/Et₃N catalyst system for the synthesis of substituted PPA to study their anticipated liquid crystalline properties, Figure 1-12, although no such properties were observed with these PPA derivatives. In addition, they were the first to provide experimental evidence for head-to-tail linkages of the monomeric units in the PPA via a combination of differential scanning calorimetry, ¹H NMR spectroscopy and size exclusion chromatography (SEC). In another example, Karim *et al.*²⁰² described the polymerisations of azomethine-containing PA with this catalytic system, but was found to only oligomerise these PA derivatives albeit with a highly stereoregular *cis-transoidal* geometry.

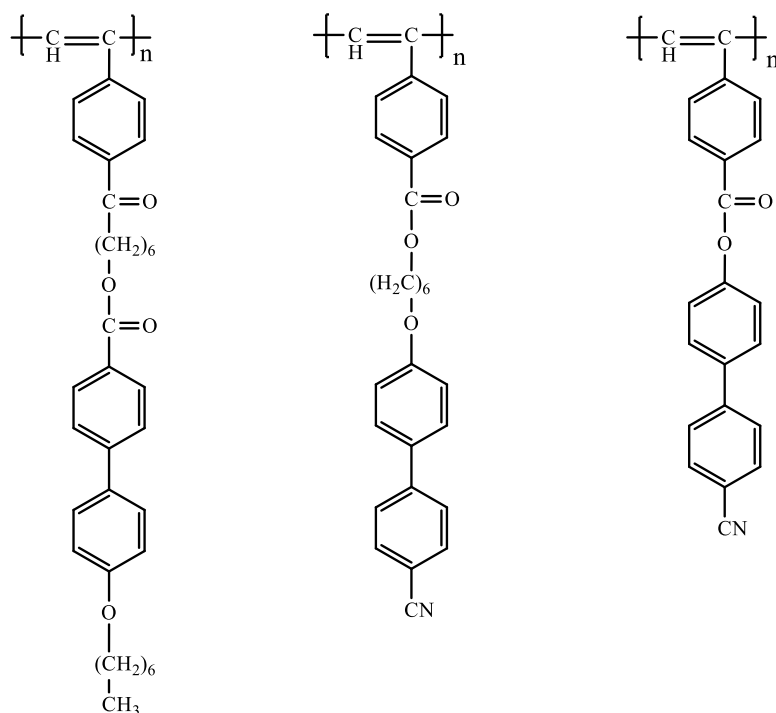


Figure 1-12. Stereoregular polymerisations of PA derivatives yielding *cis-transoidal* materials mediated by the $[\text{Rh}(\text{nbd})\text{Cl}]_2/\text{Et}_3\text{N}$ catalyst system.

Other notable applications of this Rh catalyst system include (co)polymerisations of PA with C60 (fullerene) to study the resulting “(co)polymers” conductivity,^{203, 204} polymerisations of PA conducted in pressurised liquid CO_2 ,²⁰⁵ synthesis of gas permeable membranes with PPA derivatives bearing silyl pendant groups,²⁰⁶ the synthesis of an effective heterogeneous catalyst system with **21** immobilised on a polymer substrate (polybenzimidazole)²⁰⁷ or mesoporous molecular sieves or metal-organic framework,²⁰⁸⁻²¹⁰ synthesis of biomimetic polymers based on PPA derivatives,²¹¹⁻²¹⁷ preparation of helix-sense PPA with pendant groups (such as -OH, 1-aza-15-crown-5 ether),²¹⁸⁻²²¹ synthesis of an optically active helical PPA derivative for the separation of enantiomers and asymmetric catalysis,²²²⁻²²⁸ and synthesis of the helical PPA with mesogenic properties bearing chiral ruthenium complexes as pendant groups.²²⁹

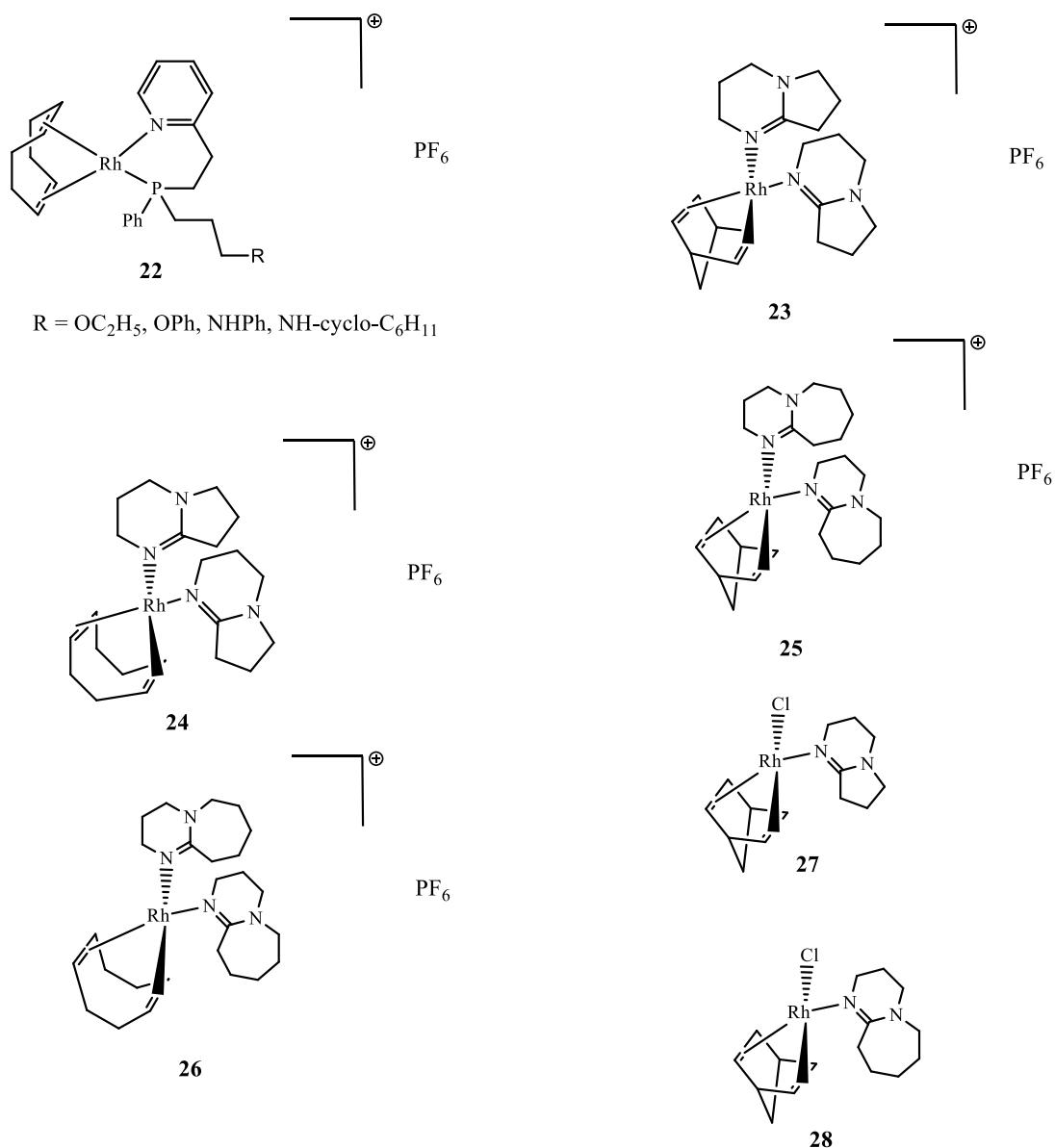


Figure 1-13. Cationic Rh complexes bearing amidine bases (1,8-diazabicyclo[5.4.0]undec-7-ene (DBU) and 1,5-diazabicyclo[4.3.0]non-5-ene (DBN)).

Building on the work from Furlani *et al.*,¹⁹²⁻¹⁹⁴ on Rh(I) salts for the polymerisation of PA, such as **19**, Schiendermeier and Haupt²³⁰ described the synthesis of a range of cationic Rh complexes, Figure 1-13, which were used in the polymerisation of PA. The cationic Rh complexes, **22** to **26**, and the non-charged Rh chloride derivatives, **27** and **28**, were shown to be very active towards PA, yielding

very high MW PPA (M_w ranged from 180,000 to 1,800,000) with high *cis-transoidal* stereoregularity. The high MW was assumed to be the result of low initiation efficiencies (IE) associated with these complexes.

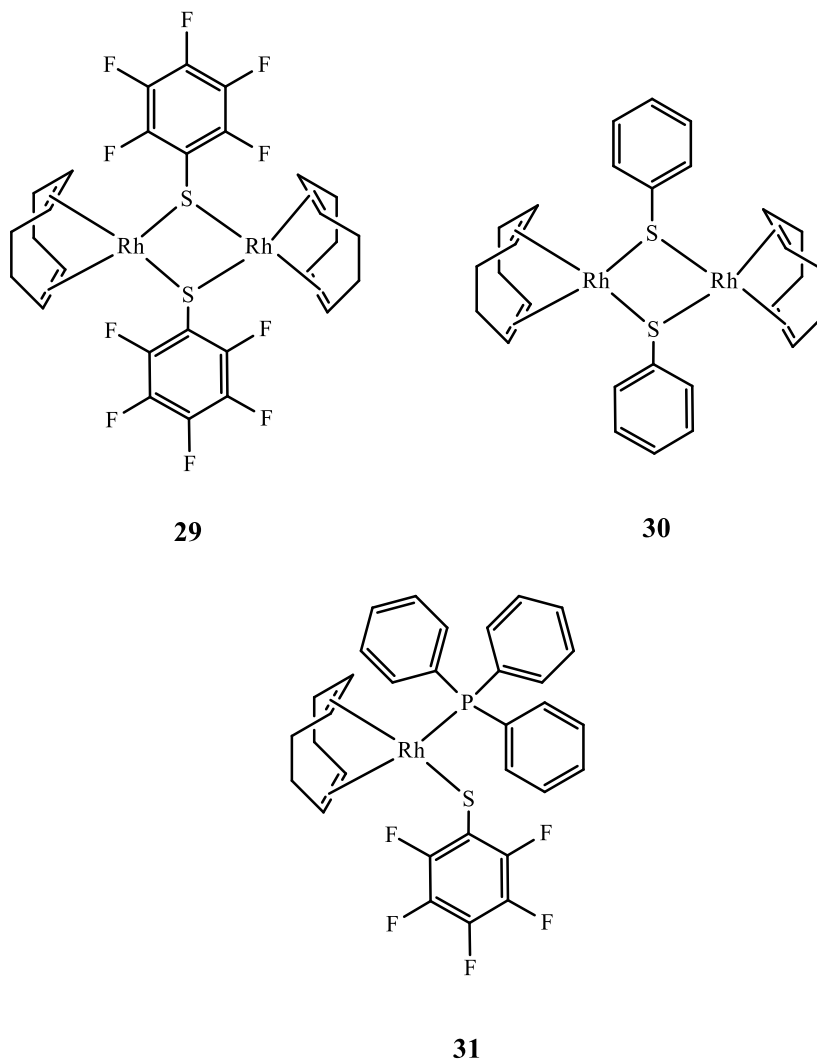
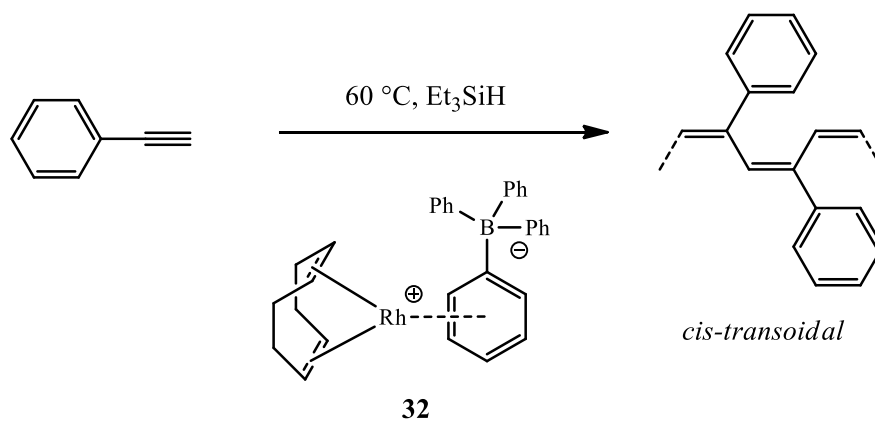


Figure 1-14 Dinuclear Rh complex bearing a cod diene ligand with pentafluorothiophenol bridging ligand and mononuclear Rh complex reported by Vilar *et al.*²³¹

Vilar *et al.*^{231, 232} reported the polymerisation of PA mediated by di- μ -pentafluorothiophenolate bis(cod) Rh(I), **29**, and the mononuclear Rh complexes, **30** and **31**, Figure 1-14. The obtained PPA had an M_n of 10,000 or 35,000 in dioxane and

THF respectively, although, the polymer yield was only around 50 %. These catalyst systems suffer from chain transfer reactions as evident by the decrease in polymer MW over time as monomer conversion increases. The geometrical structure of the PPAs was determined by IR spectroscopy and found to be *cis-transoidal* in nature, consistent with the previous catalysts of the same class reported by Furlani *et al.*¹⁹²

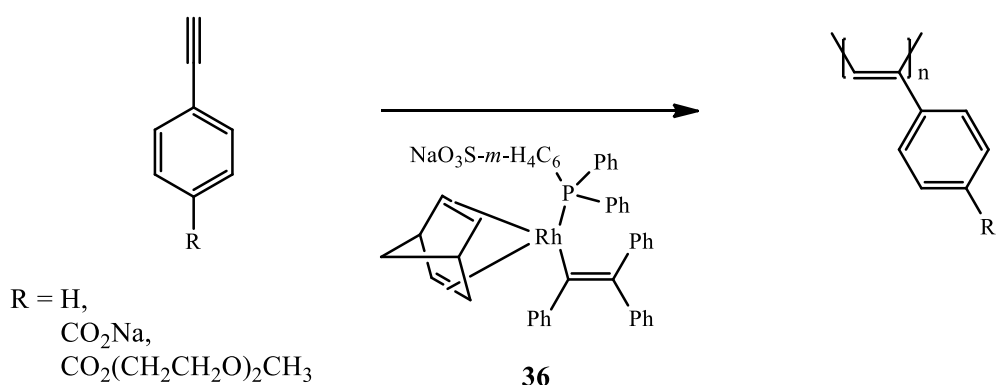
Following this, Goldberg and Alper²³³ reported the polymerisation of PA under hydrosilylation conditions using a zwitterionic Rh complex, **32**, Scheme 1-19. The reaction was conducted at elevated temperatures of 60 °C, 80 °C and 100 °C with Et₃SiH added as the co-catalyst with polymerisation proceeding for 16 to 24 hours. Resulting PPAs generally had large *D*s, and ranged from 1.70 to 5.00, with *M*_{ns} of 1,600 to 18,700 and polymer yields less than 70 %. It was determined that chain termination reactions are occurring, which were evident from the lower than expected *M*_n and low monomer conversions, even with longer reaction times. The authors noted that the PPAs were predominantly *cis-transoidal* as determined by IR spectroscopy and ¹H NMR using the methodology described by Simionescu *et al.*²³⁴ with the exception of PPAs obtained at 100 °C polymerisation which was rich in *trans* backbone C=C bonds. This observation is well-documented and has been extensively studied by Percec *et al.*²³⁵⁻²³⁷ who investigated heat-induced *cis-trans* isomerisation of PPA under a range of experimental conditions.



Scheme 1-19. The polymerisation of PA with a zwitterionic rhodium complex in the presence of Et₃SiH as co-catalyst.

Due to growing concerns regarding the use of toxic organic solvents such as benzene and associated negative impacts on the environment,²³⁸ some research groups in this field have directed their efforts to synthesising water-soluble organorhodium initiators for the polymerisation of PA and its derivatives. For example, Tang *et al.* reported the first polymerisation of PA in aqueous media by water-soluble organorhodium complexes such as Rh(nbd)(tos)(H₂O) (where tos = *p*-toluenesulfonate). The resulting PPA from on water polymerisations had large dispersities, *D* of 2.80 to 5.50, with *M_n* values as high as 77,100 (polymer yield = 80 %). Overall, the activity of these organorhodium initiators had higher activity in aqueous media (water), followed by THF (polar solvent) and toluene (non-polar solvent). The resulting PPAs had high stereoregularity with *cis* contents in the range of 86 to 100 %.

In a related example, Mastrorilli *et al.*²³⁹ reported the first PA polymerisations in an ionic liquid, employing Rh(nbd)(acac)Cl (where acac = acetylacetonate). This catalyst gave high polymer yields. (ca. 90 %), in contrast to those previously reported by Tang *et al.* (highest polymer yield was ca. 60 %). The polymers obtained were,



Scheme 1-20. Polymerisation of PA, and its derivative, conducted with a ternary catalyst system comprising of [Rh(nbd)Cl]₂/Ph₂C=CPhLi/(C₆H₄-*m*-SO₃Na)Ph₂P)

Kanki *et al.*²⁴² reported the application of a ternary catalyst system comprised of [Rh(nbd)Cl]₂/Ph₂C=CPhLi/(C₆H₄-*m*-SO₃Na)PPh₂ with a speculated structure for the active species, **36**, for the polymerisation of PA, Scheme 1-20. This was derived from a similar ternary catalyst system that mediated the living polymerisation of PA.²⁴³ However, the water-soluble ternary catalyst system did not mediate the living/controlled polymerisation of PA in aqueous media. The polymerisation of PA only commenced when the temperature was raised to 60 °C, producing PPA with an M_n of 8,200 and $D = 1.7$. The activity of complex **36** in THF was significantly improved, with PPA having M_n of 110,000, which corresponds to an initiator efficiency (IE) of 0.023. ¹H NMR spectroscopy reveals *cis-cisoidal* structures from polymer resulting from polymerisation at 60 °C. The author proceeded to investigate the activity of this ternary catalyst system towards an oligo(ethylene glycol)-substituted acetylene and obtained a water-soluble polymer with M_n of 14,500 and average polymer yield of 75 %, but no D value was mentioned. The author attributed to the lower than expected activity in water was due to heterogeneous phases resulting

from immiscibility of the solvents, which provided less-than-ideal conditions for polymerisation.

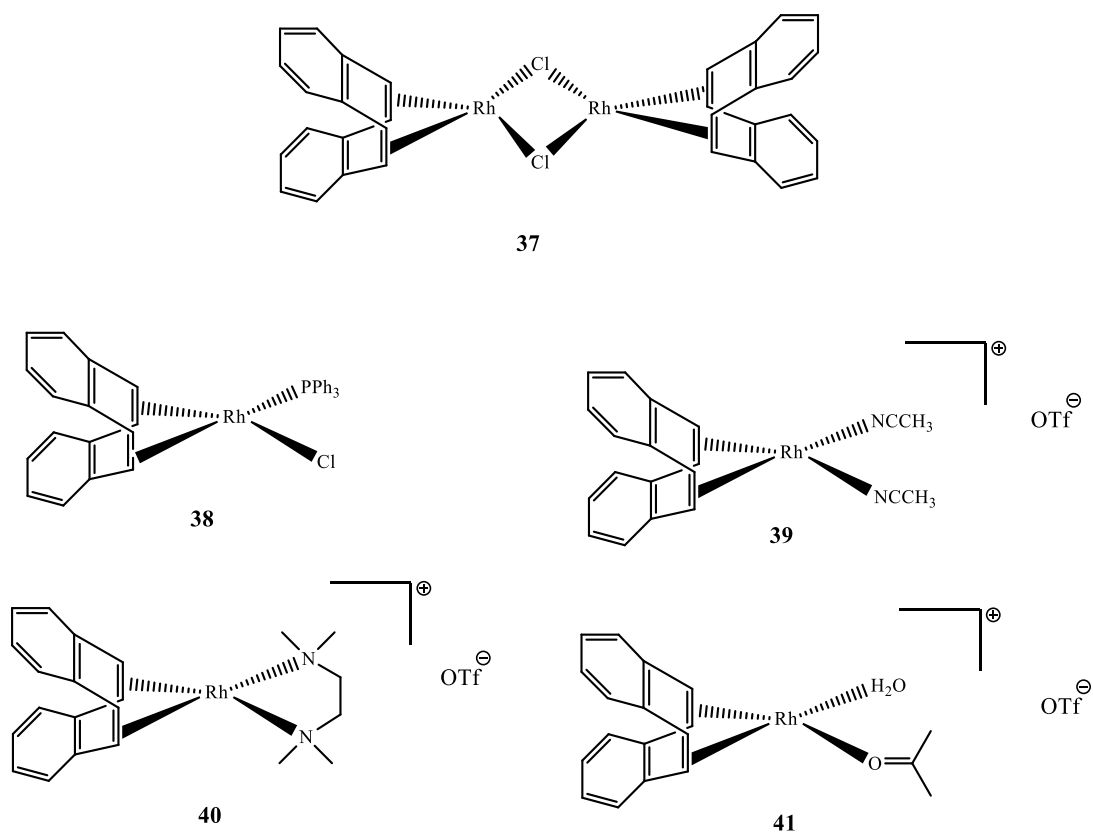


Figure 1-16. A series of charged and non-charged mononuclear Rh(I) complexes bearing dibenzo[α,ϵ]cyclooctatetraene (dbcot) derived from dinuclear Rh complex **37**.

Zhang *et al.*²⁴⁴ reported the synthesis of a series of water-soluble cationic Rh complex bearing acidic diene ligands such as dibenzo[α,ϵ]cyclooctatetraene (dbcot), Figure 1-16, which were employed in the polymerisation of PA. Complexes **37** to **41** were 163 times more active in water than in organic solvents (toluene, THF or CH_2Cl_2) and yielded PPA with generally large D_s ranging from 2.00 to 4.00 and slightly reduced *cis* content but still stereoregular. The activity of complex **39** was further explored with PA derivatives such as *m*-MePA (3-methylphenylacetylene), *p*-MeOPA, *p*-FPA (*p*-fluorophenylacetylene) and *p*-CIPA in water and THF.

some cases, it has been also shown to be optimal in ionic liquids. Katayama *et al.*²⁴¹ described the synthesis of cationic Rh complexes bearing a tris(pyrazolyl)borate ligand, Figure 1-17, and were found to mediate the stereospecific polymerisation of PA, producing PPAs with M_n s of 28,000, high *cis* content (> 99 %), and large D s at ca. 2.00. Polymer yields were quantitative with **42a**, **42b**, and **42c**. However, **43**, in which a cod diene ligand was replaced with an nbd ligand, was found to be inactive. Complexes **42** were also found to be active towards other ring-substituted phenylacetylenes, Figure 1-17, producing quantitative polymer yields of the respective monomers with generally large dispersities but similar to PA. The activity of **42** and **43** towards additional substituted acetylenes was investigated. They were found not to be active towards tri-substituted phenylacetylenes, with substituents at *ortho* and *para* positions, nor with α,ω -dialkyne. The preparation of a Rh(I) complex bearing heteroscorpionate trispyrazolylborate ligands was described by Ruman *et al.*²⁴⁵ and displayed similar catalytic activity and results.

The preparation of dinuclear Rh complexes was described by Yao *et al.*,²⁴⁶ Figure 1-18. They were investigated for their efficacy as initiators for PA polymerisations and were found to be active with one exception, Rh complex **47**, which was explained by the coordinatively saturated Rh centre. No specific MW values were given but the authors noted that the resulting PPAs were *cis-transoidal* in nature.

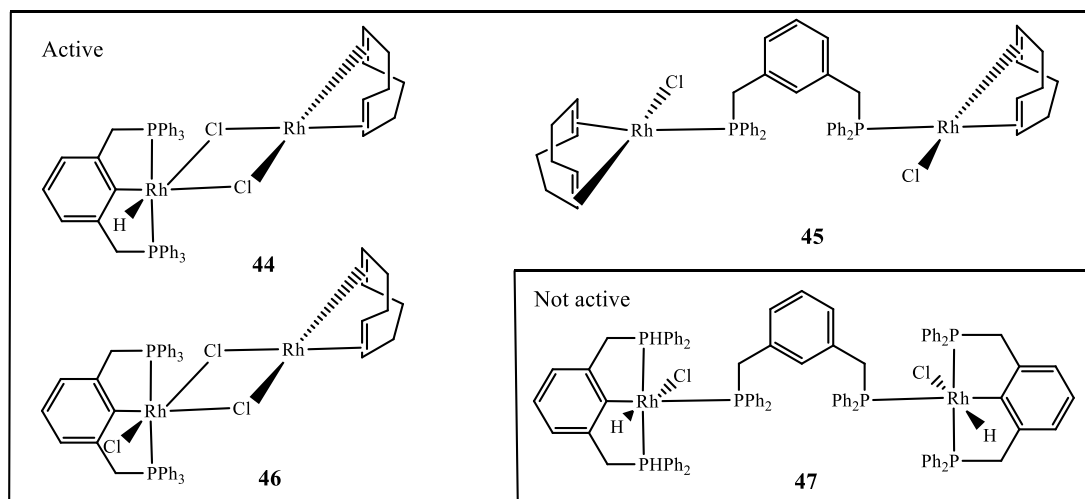
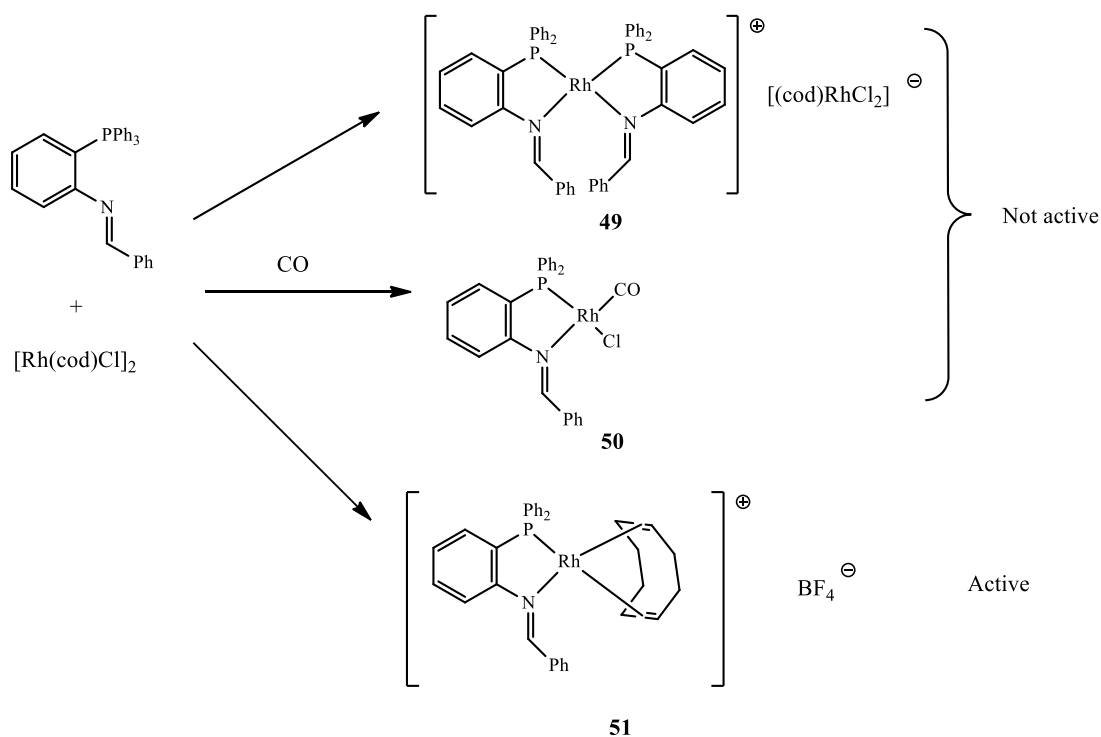


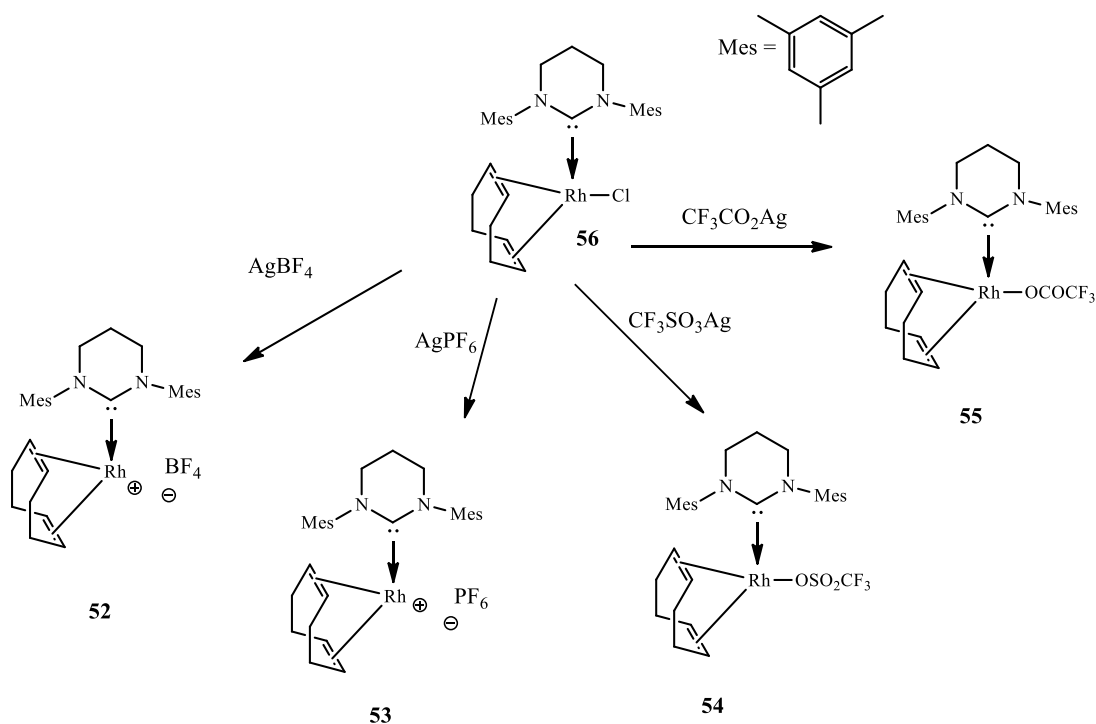
Figure 1-18. Dinuclear Rh complexes employed as initiators for the polymerisation of PA.

Reddy *et al.*²⁴⁷ reported the synthesis of a cationic phosphine-imine Rh(I) complexes, Scheme 1-21, with **49** and **50** determined to be inactive towards PA. Only the Rh(I) complex bearing a tetrafluoroborate counterion, **51**, was active. The resulting PPA was stereoregular (*cis-transoidal*) with large *Ds* ranging from 2.00 to 4.50, suggesting uncontrolled polymerisation.



Scheme 1-21. Preparation of cationic and neutral phosphine-imine Rh(I) complexes reported by Reddy *et al.*²⁴⁷

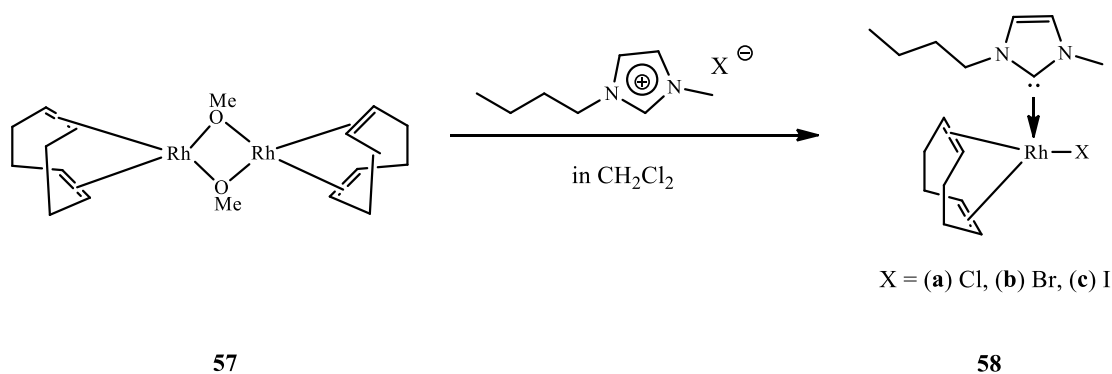
There is a scarcity in reports of Rh(I)-carbene complexes suitable for the polymerisation of PA. Zhang *et al.*¹⁵⁴ described the preparation of a series of Rh(I)cod complexes bearing an NHC ligand, Scheme 1-21. Polymerisations were conducted in a range of organic solvents and aqueous media. As can be seen in Table 1-1, charged Rh species such as Rh complexes **52** and **53**, generally yielded PPA with a larger M_w in aqueous media (Table 1-1, entry 1 and 4) than in organic solvent (Table 1-1, entry 3 and 5). On average, apart from PPA resulting from complex **54** (Table 1-1, entry 6), dispersities were generally $D > 2.00$. Polymerisations conducted in aqueous media, yielded PPA with high *cis-transoidal* stereoregularity (Table 1-1, entry 1 and 4), while polymerisations performed in CH_2Cl_2 resulted in moderately stereoregular products (Table 1-1, entry 3, 5, 6, and 7)



Scheme 1-22. Preparation of a series of Rh(I)(cod) complexes bearing *N*-heterocyclic carbenes (NHCs) resulting in charged and neutral organorhodium species.

Table 1-1. Summary of conditions, *cis* content, M_w , and \bar{D} for the homopolymerisation of PA with a series of NHC-functional Rh complexes.

Entry	Complex	Solvent	Temperature (°C)	<i>Cis</i> content (%)	M_w	\bar{D}
1	52	H ₂ O/MeOH	23	100	138,200	2.71
3	52	CH ₂ Cl ₂	23	77	67,200	2.31
4	53	H ₂ O/MeOH	23	100	115,800	2.48
5	53	CH ₂ Cl ₂	23	75	16,700	1.95
6	55	CH ₂ Cl ₂	40	64	25,000	1.55
7	56	CH ₂ Cl ₂	40	71	115,000	2.88



Scheme 1-23. Preparation of a Rh complex bearing an NHC and cod diene ligand.

Another Rh(I)-carbene complex was reported by Gil *et al.*,²⁴⁸ who detailed the preparation of complex **58** which was synthesised by the reaction of complex **57** with [bmim]X (where X = Cl, Br, I) in CH₂Cl₂ at room temperature, Scheme 1-23. The polymerisation of PA with complexes **58a** and **58b**, resulted in PPA with $M_{w,s}$ of 19,100 and 26,700, respectively. In contrast, complex **58b** did not show significant activity by itself. However, upon addition of a phosphorous ligand such as PPh₃ or triphenylphosphite, P(OPh)₃, a significant increase in catalytic activity was observed, and PPA with a M_w of 26,000, comparable to the **58a** and **58b** was obtained. Increasing the phosphorous ligand-to-catalyst ratio, resulted in the displacement of the cod diene ligand, and polymer yield was significantly reduced and was attributed to the formation of an inactive Rh(I) species, speculated to be *cis*-[Rh(bmim)(P(OPh)₃)₂]. The same group expanded upon this contribution and reported the use of **57** in ionic liquids with of a co-catalyst such as Et₃N and free cod diene ligands. The authors reported a positive impact on the polymer yield (97 % in ionic [mokt]BF₄) overall with the use of Et₃N which represents an improvement over the previously reported dinuclear Rh complex of the same class, complex **21**.²⁴⁹

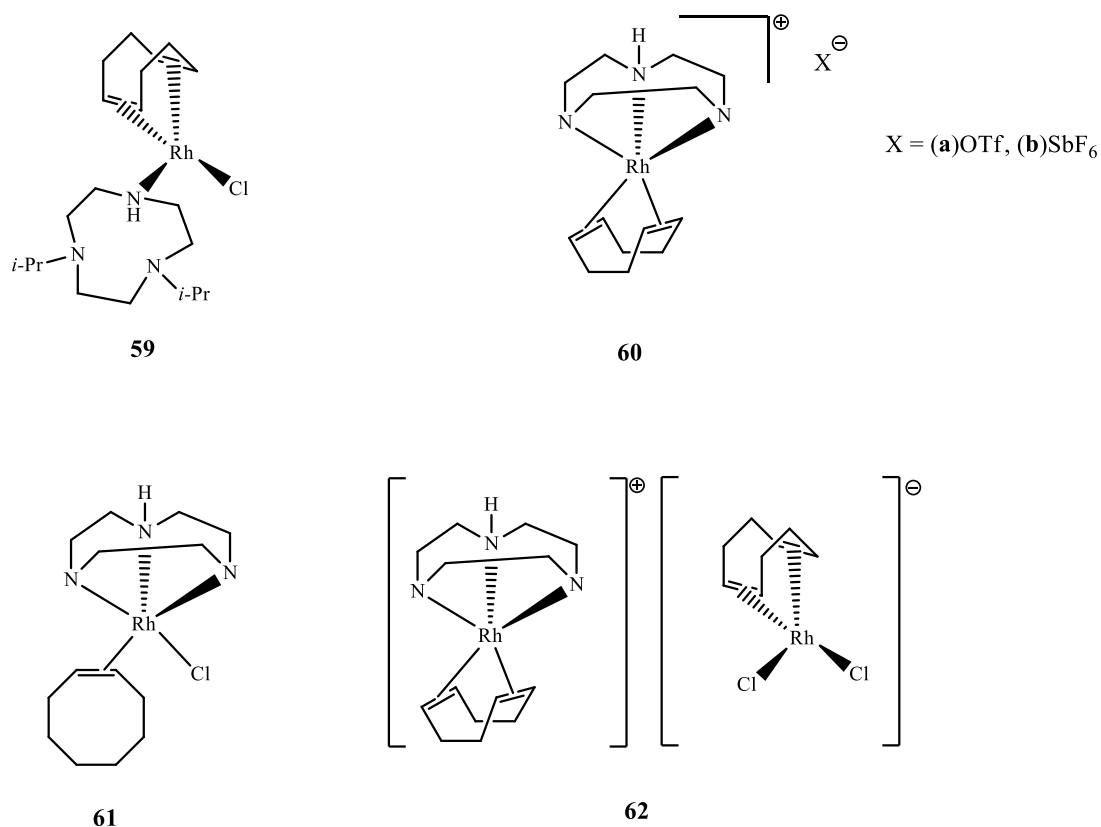


Figure 1-19. Structures of cationic and neutral variants of Rh(I) 1,4,7-triazacyclononane complexes reported by Gott *et al.*²⁵⁰

Gott *et al.*²⁵⁰ describe the preparation of charged, **60** and **62**, and non-charged, **59** and **61**, derivatives of a Rh complex bearing a 1,4,7-triazacyclononane and codiene ligands, Figure 1-19. With the exception of **61**, all complexes were active towards PA but only yielded low MW products with M_n averaging around 1,437, coupled with large dispersities ($\mathcal{D} > 2.00$). The stereoregularity of the PPAs obtained with these complexes were surprisingly low and averaged around 50 % *cis* content which is in distinct contrast with other Rh(I) complexes.

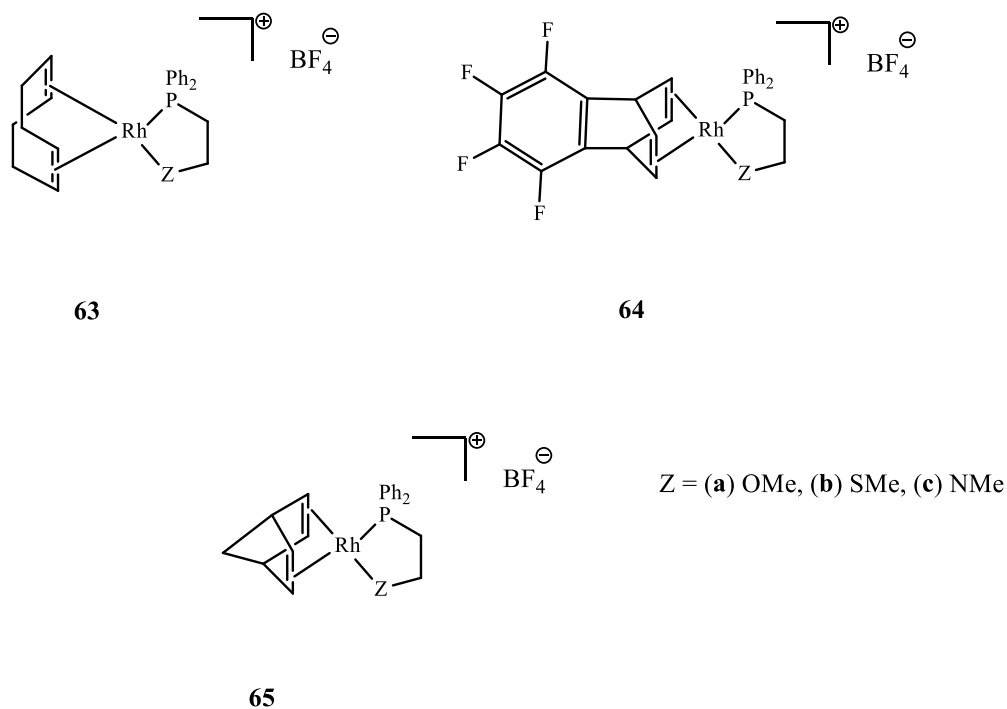


Figure 1-20. Cationic Rh(I) complexes bearing hemilabile hetero-atom phosphine ligands reported by Jiménez *et al.*²⁵¹

Jiménez *et al.*²⁵¹ reported the synthesis of a series of cationic Rh complexes bearing hemilabile hetero-atom phosphine ligands, **63** to **65**. PA homopolymerisation mediated by **63a** yielded PPA with a bimodal MWD and a high average MW of 165,000 ($\bar{D} = 1.13$) and lower MW of 24,000 ($\bar{D} = 2.17$) for polymerisation in THF. Similar results were reported for **63c** in wet toluene. Complexes **63b**, **64c** and **65c** were all active (all polymer yields were quantitative) but yielded PPAs with broad MWD ($\bar{D} > 1.50$) and corresponding IEs of 0.12, 0.01 and < 0.01 , respectively. All polymers were stereoregular with 99 % *cis* content on average.

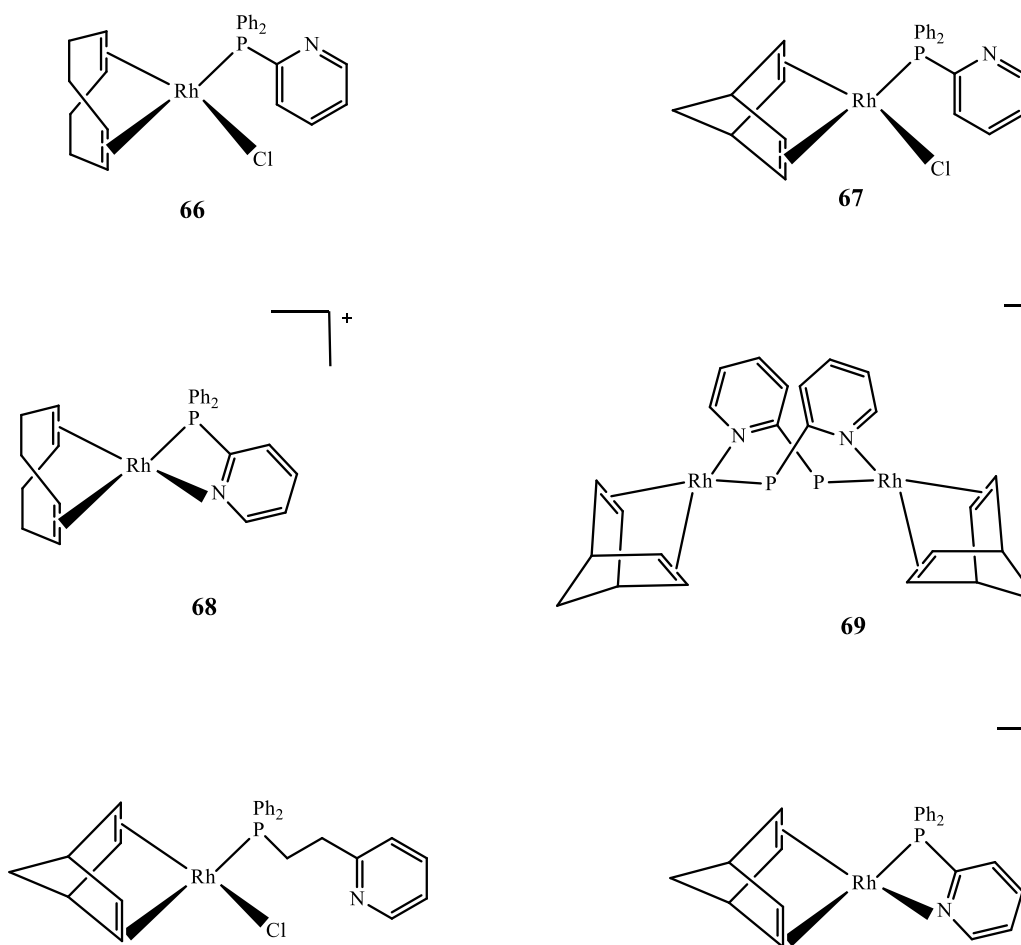


Figure 1-21. A series of neutral and cationic Rh complexes for application as initiators in the polymerisation of PA reported by Angoy *et al.*²⁵²

Angoy *et al.*²⁵² reported the preparation of a series of neutral and cationic Rh complexes and their utilisation as initiators in the polymerisation of PA, Figure 1-21. Complexes **66** to **71** (apart from **68** and **69**) were active initiators for PA homopolymerisation but yielded PPAs with MWs ranging from M_n of 100,000 to 1,000,000. Complexes **68** and **69** were completely inactive, but upon addition of 10 equivalents of *i*PrNH₂, proceeded to give PPA with high MW ($M_n = 246,000$ and 145,000 respectively) and *D*s of 1.39 for both. However, SEC traces of PPA resulting from **69** showed a bimodal MWD. All complexes were found to suffer from low IEs,

and the reason for this was elucidated by density functional theory (DFT) calculations performed by the author for complex **68**, and showed that the energy barrier for the initial insertion (initiation step) was 4 kcal⁻¹ higher than the barrier for the insertion into the Rh-vinyl bond in the propagation step.

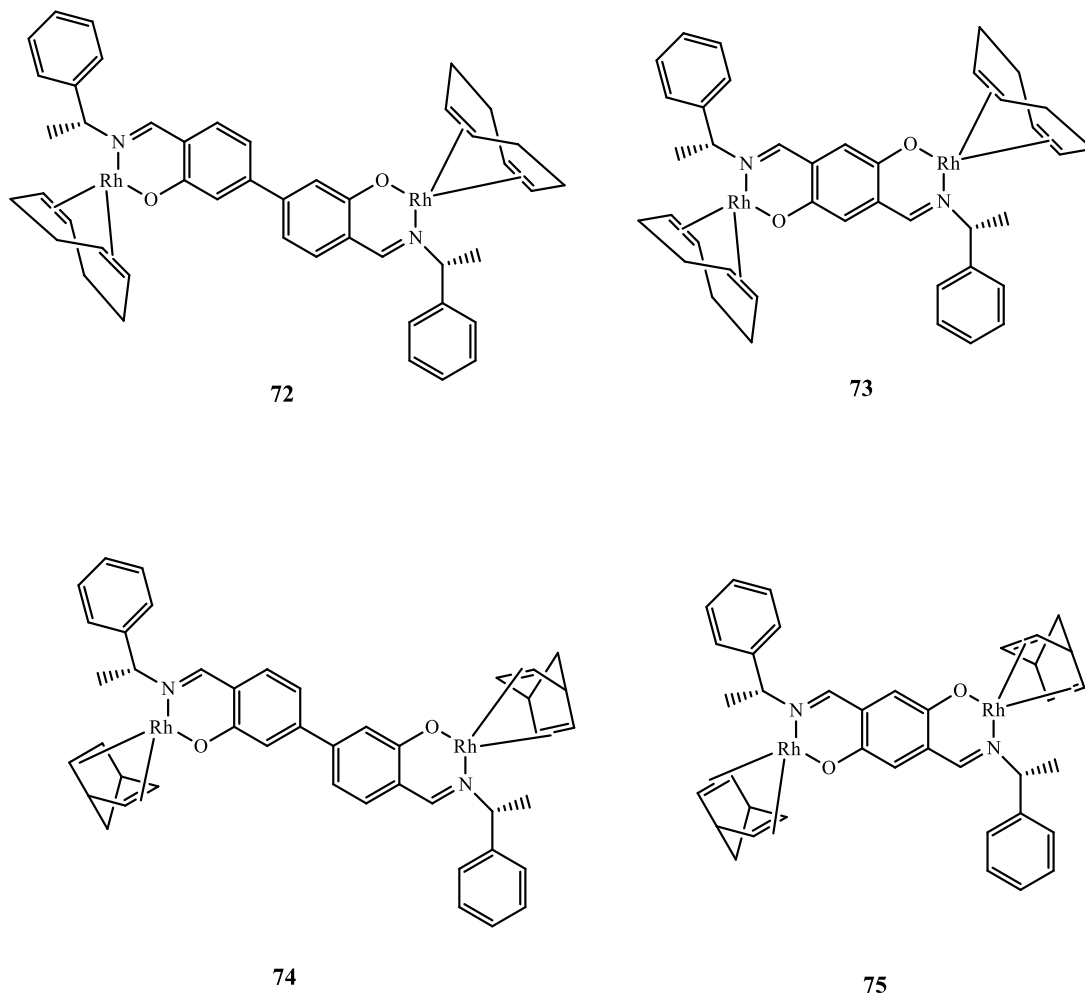
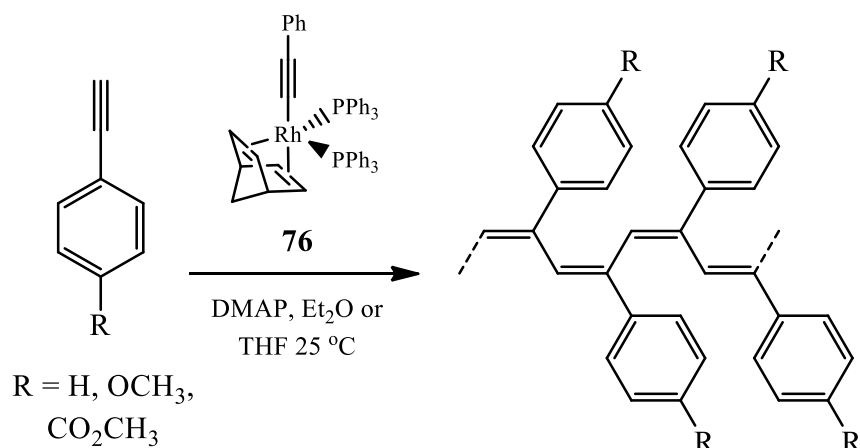


Figure 1-22. A series of dinuclear Rh complexes for PA polymerisation reported by Wu *et al.*²⁵³

Wu *et al.*²⁵³ reported the first observation of a cooperative effect in a binuclear Rh complex, **75**, for the polymerisation of PA. In multinuclear polymerisation catalysis, the cooperative effect can manifest itself as increased catalytic activity, regio- or stereoselectivity, MW control, dispersity control, and effective control over

chain-transfer reactions to create intentional branching via chain shuttling processes.²⁵³ In this case, complex **75** exhibited at least 1.5 to 3.7 times the activity of complexes **72** to **74**. However, the resulting PPA had low molecular weights, even with quantitative polymer yields, and generally large *D*s, ranging from 1.50 to 4.30. All polymers were stereoregular and had high *cis* content > 87 %. The synergistic effects associated with complex **75** and the mechanism behind the cooperative effect are still undetermined and is a work in progress.

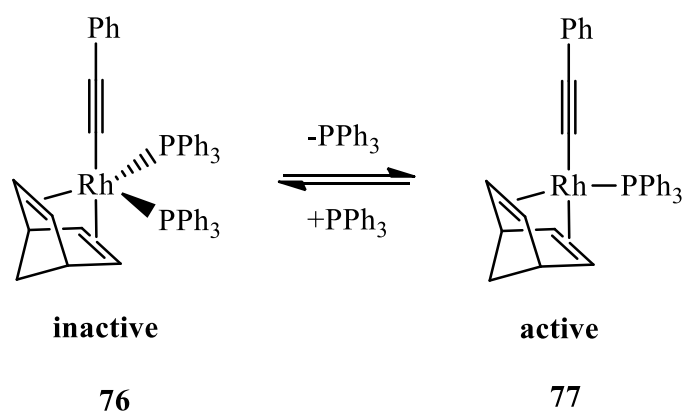
1.6.2 Stereospecific Controlled Polymerisation by Rh Complexes



Scheme 1-24. The polymerisation of PA with $\text{Rh}(\text{C}\equiv\text{CPh})(\text{nbd})(\text{PPh}_3)_2$ in the presence of DMAP, yielding stereoregular polymers.

The first literature example concerning the controlled, stereospecific polymerisation of PA by a rhodium species was from Kishimoto *et al.*²⁵⁴ $\text{Rh}(\text{C}\equiv\text{CPh})(\text{nbd})(\text{PPh}_3)_2$, **76**, Scheme 1-24, was prepared from the reaction of $[\text{Rh}(\text{nbd})\text{Cl}]_2$, PPh_3 and $\text{LiC}\equiv\text{CPh}$ in diethyl ether and isolated in a 77 % yield. The complex adopts a slightly distorted trigonal bipyramidal geometry in the solid-state with the phenylethynyl ligand and one C=C associated with nbd occupying the axial

positions, Scheme 1-24. The homopolymerisation of PA and several *para*-substituted derivatives, with **76** in the presence of DMAP was reported with polymerisations proceeding rapidly at ambient temperatures, in diethyl ether, yielding homopolymer essentially quantitatively with an SEC-measured M_n of 14,900 and \bar{D} of 1.15. Similar results were noted for polymerisations in THF and with alternative phenylacetylene substrates. While broadly exhibiting features associated with a controlled polymerisation, the authors noted that initiation efficiencies (IE) were non-quantitative and reported to be in the range 33-56% (although we note that quantitative initiation is *not* a formal requirement for a polymerisation to be accurately termed controlled).



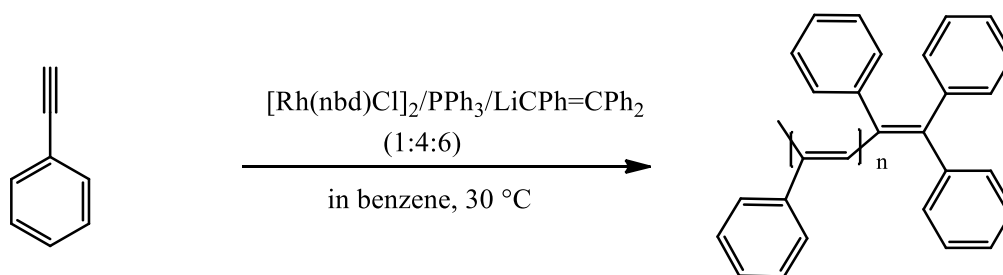
Scheme 1-25. Reaction scheme representing the rapid, reversible dissociation of PPh_3 from the inactive species, $\text{Rh}(\text{C}\equiv\text{CPh})(\text{nbd})(\text{PPh}_3)_2$ to active $\text{Rh}(\text{C}\equiv\text{CPh})(\text{nbd})(\text{PPh}_3)$.

Recognising that the active initiating species is not the pentacoordinate complex, **76**, but the tetracoordinate complex, **77**, Scheme 1-25, formed by the rapid, reversible dissociation of one of the PPh_3 ligands, Kishimoto *et al.*²⁵⁵ reported a ternary catalyst system in which the active initiating species is generated *in situ*. The homopolymerisation of PA proceeded rapidly at room temperature in THF with $[\text{Rh}(\text{nbd})(\text{OCH}_3)]_2$, PPh_3 and DMAP in a ratio of 1:1:10 yielding a head-to-tail, *cis-transoidal* stereoregular polymer with an SEC-measured M_n of 6,900 and $\bar{D} = 1.11$.

The IEs for **77** were estimated to be ~ 0.72 , which is double that observed for **76**. The authors attempted to isolate the active species but were not successful, due to its instability. However, oligomeric species bearing a tetracoordinate Rh fragment derived from **77** was isolated, which confirmed the initiation and propagation steps for this ternary catalyst system were identical to those for **76**.

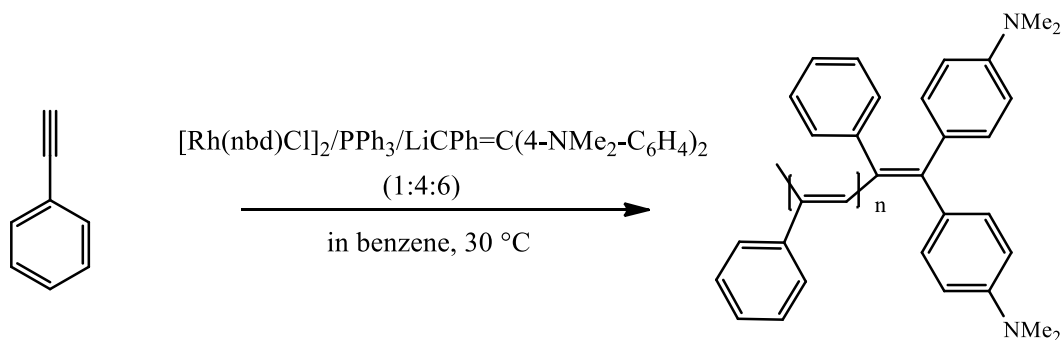
Following these initial disclosures, the same group reported a detailed study on the mechanism and structure of the resulting polyenes in polymerisations mediated by **76** and **77**.²⁵⁶ The role of DMAP was shown to be critical, through stoichiometric studies, in achieving controlled polymerisations yielding polymeric products with low D s. Although the pentacoordinate species, **76**, is moderately active for the polymerisation of PA, in the absence of DMAP, it yielded a high MW polymer with a measured M_n of 175,000 and $D = 2.45$. The reduced level of control in the absence of DMAP was attributed to the formation of a binuclear rhodacyclopentadiene complex which was not an active initiator.

The initiating systems described by Kishimoto *et al.*,²⁵⁵ while clearly seminal contributions, are arguably limited in terms of the reported IEs and with respect to accessible end-functional (co)polymers. The latter is due to the fact that while inspection of the active tetracoordinate complex might suggest that polymerisation proceeds via monomer insertion into the Rh-phenylethynyl bond (i.e. the phenylethynyl group can be viewed as the initiating fragment and thus end-functional polymers should be accessible by using a functional phenylethynyl ligand), the resulting polymers bear hydride at the initiating terminus implying a multistep initiation process that ultimately does not result in incorporation of the phenylethynyl group.

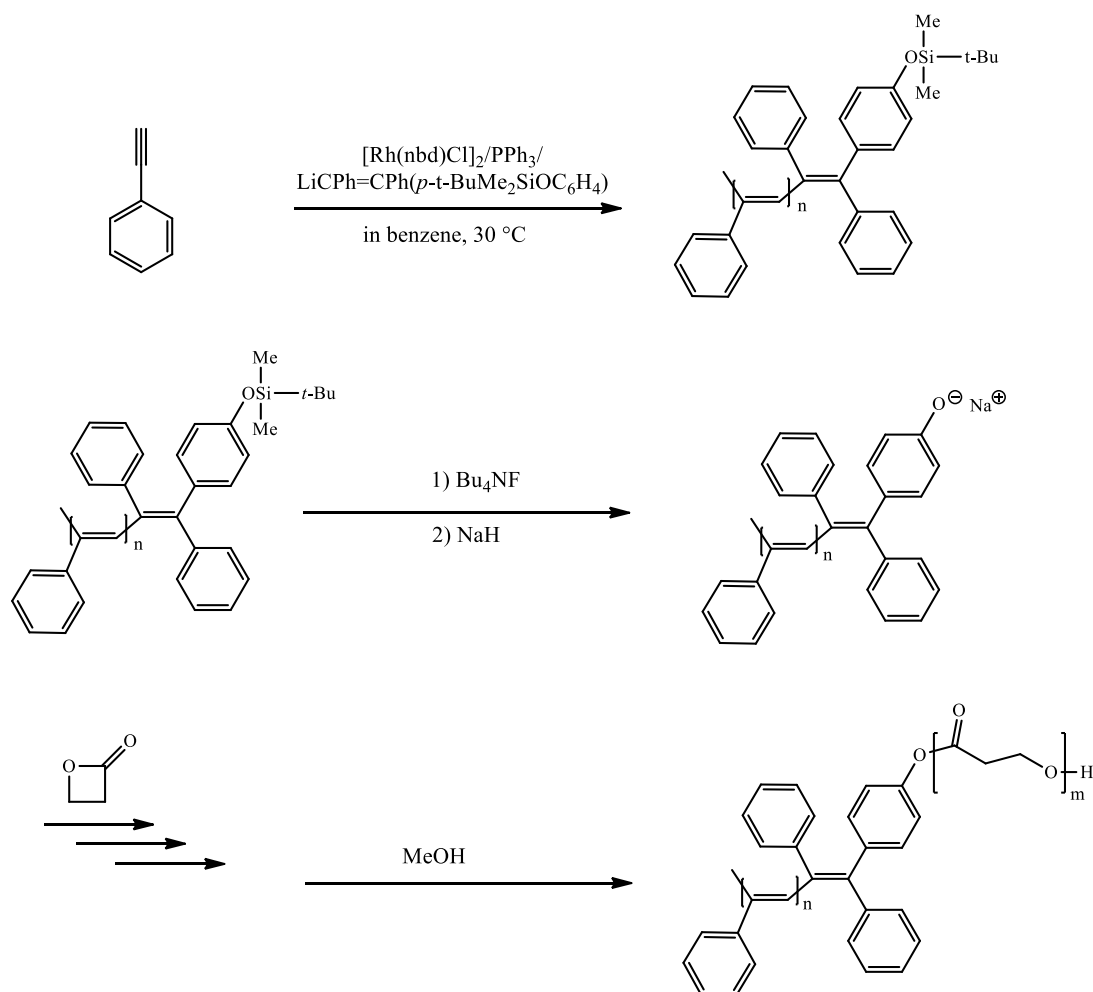


Scheme 1-26. Reaction scheme of the homopolymerisation of PA by the $[\text{Rh}(\text{nbd})\text{Cl}]_2/\text{PPh}_3/\text{LiCPh}=\text{CPh}_2$ ternary catalyst system.

Based on the assumption that the active site in the Rh-mediated polymerisation of PA is a vinylrhodium species, Misumi and Masuda²⁴³ reported a ternary catalytic system prepared from $[\text{Rh}(\text{nbd})\text{Cl}]_2$, PPh_3 and $\text{LiCPh}=\text{CPh}_2$ in benzene or toluene that was shown to mediate the homo- and co-polymerisation of PA in a controlled fashion yielding polymers with low D_s and with quantitative initiation, Scheme 1-26. While the crystal structure of the actual catalytic species was not reported in this initial disclosure, it was noted that a Rh species was isolated from the ternary mixture and its structure confirmed to be $\text{Rh}(\text{nbd})(\text{CPh}=\text{CPh}_2)(\text{PPh}_3)$ based on NMR spectroscopic analysis. The crystal structure of this complex was reported sometime later by Kumazawa *et al.*²⁵⁷ who also conducted a detailed examination of the end-group structure in polyphenylacetylenes prepared with the well-defined isolated catalyst.



Scheme 1-27. End-functionalisation achieved by replacing $\text{LiCPh}=\text{CPh}_2$ with $\text{LiCPh}=\text{C}(4\text{-NMe}_2\text{-C}_6\text{H}_4)_2$.



Scheme 1-28. Synthetic route to poly(phenylacetylene)-*block*-poly(β -propiolactone) via combination of Rh-mediated alkyne polymerisation and anionic polymerisation of the propiolactone moiety of the macroinitiator.

In addition to demonstrating quantitative initiation, Misumi and Masuda highlighted the ability to prepare end-functional polyphenylacetylene. This was accomplished by replacing $\text{LiCPh}=\text{CPh}_2$ with the amino-functional vinylolithium $\text{LiCPh}=\text{C}(4\text{-NMe}_2\text{-C}_6\text{H}_4)_2$ in the ternary catalytic mixture, see Scheme 1-27. Targeting a low molecular weight product, the authors clearly demonstrated the efficient (quantitative) incorporation of this functional group via ^1H NMR spectroscopy. While an effective approach for the preparation of end-functional polyphenylacetylenes, the

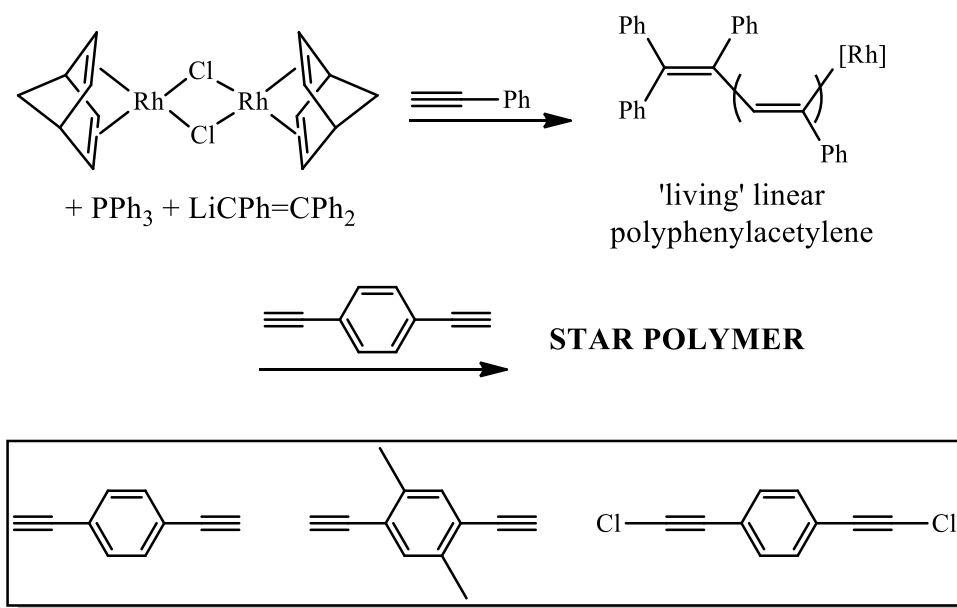
major drawback of this synthetic route is the lack of commercially available functional triarylvinyllithium species that serve as the precursors to the vinyl lithium species, and as such need to be synthesised. In the case of the above example, the target $\text{BrCPh}=\text{C}(4\text{-NMe}_2\text{-C}_6\text{H}_4)_2$ precursor was prepared via a multistep procedure and isolated in a 10.5 % yield. In another example of end-functionalisation, the synthesis of polyphenylacetylene-*block*-poly(β -propiolactone) copolymers was reported by Kanki, Misumi and Masuda²⁵⁸ employing the $[\text{Rh}(\text{nbdc})\text{Cl}]_2/p\text{-tert-BuMe}_2\text{SiOC}_6\text{H}_4\text{PhC}=\text{CPhLi}/\text{PPh}_3$ ternary catalytic system, Scheme 1-28.

The use of this siloxy-functional triarylvinyl species yielded well-defined polyphenylacetylene bearing the siloxy functional group at the initiating chain end; its incorporation, as determined by ^1H NMR analysis, was determined to be essentially quantitative. Removal of the protecting siloxy group yielded the corresponding phenol-end-functional material which, after treatment with NaH to yield the corresponding phenolate, was employed as a macroinitiator for the subsequent ring-opening polymerisation of β -propiolactone. Block copolymerisation was verified by a combination of NMR and FTIR spectroscopic analysis. Unfortunately, no cross-over efficiencies were reported nor any D data provided for the final block copolymers.

Following the initial report,²⁴³ Misumi and co-workers²⁵⁹ reported a detailed study of the effects of each component in such ternary catalytic systems. In the case of the ene/diene ligand component in $\text{Rh}(\text{diene/ene})/\text{LiPh}=\text{CPh}_2/\text{PPh}_3$, it was reported that substituting norbornadiene (nbd) for 1,5-cyclooctadiene (cod) gave an active catalytic system resulting in 100 % conversion of phenylacetylene to the corresponding polymer but at the expense of losing control associated with the molecular weight distribution with the product having a measured D of 2.45, while replacing norbornadiene with two cyclooctene ligands yielded an inactive species.

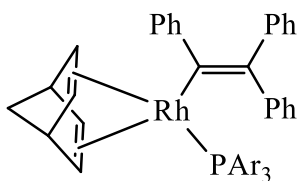
The effect of substituents at the α and β positions on the vinyl lithium species was likewise investigated. It was found that bulky substituents at the α position (preferably a Ph group) with at least one substituent on the β position were necessary to achieve a well-controlled polymerisation of phenylacetylene. However, *only* the triphenylvinyl species, i.e. the active species derived from the original $[\text{Rh}(\text{nbd})\text{Cl}]_2/\text{LiPh}=\text{CPh}_2/\text{PPh}_3$ ternary mixture, gave a system that exhibited quantitative initiation with the remaining ternary mixtures yielding active species with IEs covering the range 0.072-0.30.

The effect of the structure of the phosphine ligand has a less pronounced effect on the level of control in such ternary catalytic systems at least for PPh_3 and simple tris *para*-substituted derivatives. For example, the use of PPh_3 , $\text{P}(4\text{-ClC}_6\text{H}_4)_3$, $\text{P}(4\text{-FC}_6\text{H}_4)_3$, $\text{P}(4\text{-CH}_3\text{C}_6\text{H}_4)_3$, and $\text{P}(4\text{-MeOC}_6\text{H}_4)_3$ in ternary mixtures yielded, in all instances, active species giving quantitative conversion of PA with 100 % IE and essentially identical D s of 1.16. There was, however, an observed, but not unexpected, kinetic impact associated with changing the phosphine ligand structure. As the basicity of the phosphine ligand decreases the rate of polymerisation increases, a feature associated with the fact that the phosphine ligand serves as a competitive binding species with monomer – the lower the basicity of the phosphine the lower the effective competitive binding and thus increase in rate of polymerisation. For the ligands noted, and under identical polymerisation conditions, the rate of polymerisation increased in the order: $\text{P}(4\text{-FC}_6\text{H}_4)_3 > \text{PPh}_3 > \text{P}(4\text{-ClC}_6\text{H}_4)_3 > \text{P}(4\text{-CH}_3\text{C}_6\text{H}_4)_3 > \text{P}(4\text{-MeOC}_6\text{H}_4)_3$.



Scheme 1-29. The synthesis of star polymers via homopolymerisation of PA followed by cross-linking with a difunctional arylalkyne.

The broader utility of the $[\text{Rh}(\text{nbd})\text{Cl}]_2/\text{PPh}_3/\text{LiCPh}=\text{Ph}_2$ ternary catalyst system for the synthesis of star and star-block copolymers, was reported by Kanki and Masuda,²⁶⁰ Scheme 1-29. Polymerisation of phenylacetylene for a target M_n of 5,100 ($[\text{M}]_0/[\text{Rh}] = 50$) yielded “living” polyphenylacetylene with an SEC-measured M_n of 5,350 and D of 1.13. Subsequent addition of five equivalents of 1,4-diethynylbenzene (DEB) (based on Rh) resulted in crosslinking and isolation of a new material with an M_n of 37,500 and D of 1.2 (this species contained < 3 % of linear polyphenylacetylene chains). Substituting DEB with 1,4-diethynyl-2,5-dimethylbenzene also yielded star products although with up to 25 % linear chains. This was attributed to the reduced reactivity of 2-methylphenylacetylene towards Rh catalysts compared to phenylacetylene. No star formation was observed when 1,4-bis(chloroethynyl)benzene was employed as the linking agent.



where Ar = (a) PPh₃, (b) P(4-FC₆H₄)₃,
(c) P(4-ClC₆H₄)₃

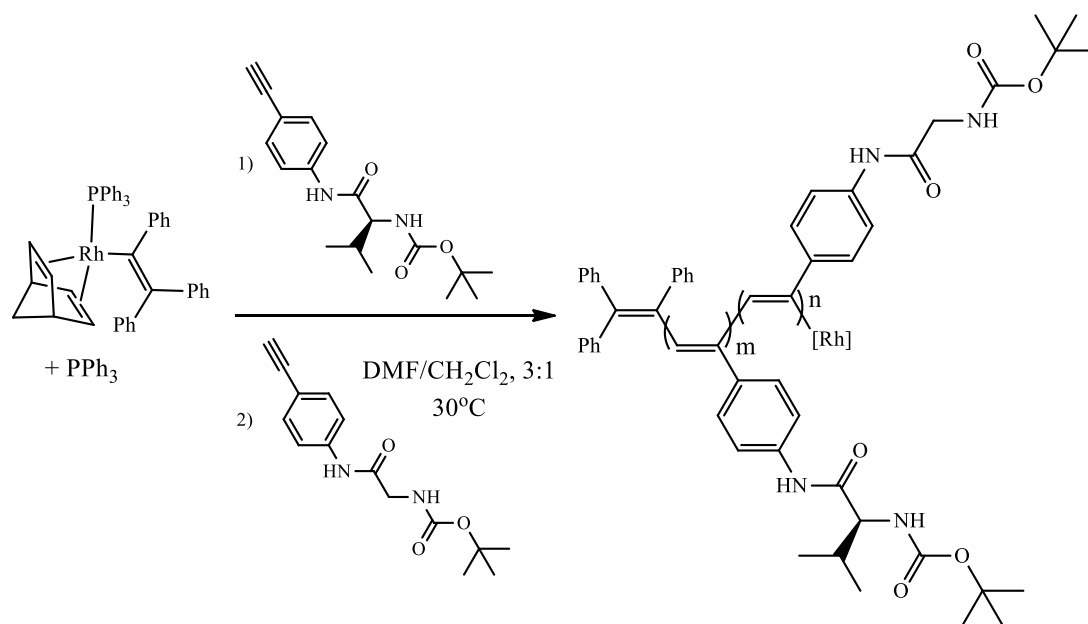
78

Figure 1-23. Masuda-type Rh(I)-triphenyl derivatives.

Following the report regarding the effect of the individual components in ternary catalytic mixtures of the general type Rh complex/phosphine/vinyl lithium, Miyake, Misumi and Masuda²⁶¹ examined catalysts bearing halogen functionalised phosphine ligands. In particular the authors focused on the synthesis, isolation and application of Rh(nbd)(CPh=CPh₂)(PAr₃), **78b** and **78c** (where Ar = (b) P(4-FC₆H₄)₃, (c) P(4-ClC₆H₄)₃) Figure 1-23. Both Rh(I)-vinyl catalysts were isolated from the corresponding ternary mixtures, and in the case of the chloro derivative a crystal structure was reported with the complex adopting a distorted square planar geometry consistent with the ‘parent’ Rh(nbd)(CPh=CPh₂)(PPh₃) species. The **78b** and **78c** derivatives were subsequently shown to effectively mediate the controlled polymerisation of phenylacetylene with essentially quantitative initiation yielding highly stereoregular *cis-transoidal* polymers with tunable molecular weights and low *D*s. Interestingly, the well-defined, isolated Rh(I) species were reported to be more effective than the corresponding ternary mixtures which, most notably, exhibited lower IEs.

It should be noted that polymerisations performed with the isolated Rh complexes are typically conducted in the presence of added excess phosphine that serves as a co-controlling agent and rate modifier. For example, it was reported that a

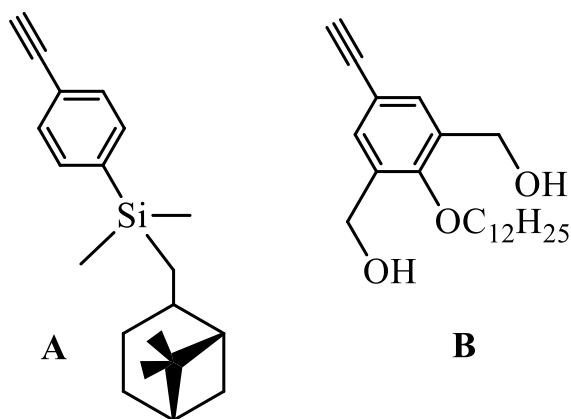
ratio of $[P(4-XC_6H_4)_3]/[Rh]$ (where $X = F$ or Cl) of at least 5 was essential in achieving the living polymerisation of phenylacetylene as well as yielding polymers with low \overline{D}_s . Polymerisations conducted with higher ratios of free phosphine also proceeded in a controlled manner but at a reduced rate as the effect of competitive phosphine binding became more dominant.



Scheme 1-30. Block copolymerisation of a chiral arylacetylene with achiral acetylene via sequential monomer addition with $Rh(nbd)(CPh=CPh_2)(PPh_3)_2$ as the initiating system.

While phenylacetylene, and in some instances simple substituted derivatives, are the monomer substrates of choice when demonstrating the effectiveness of new Rh(I) complexes as initiators, such species do exhibit a broader applicability although still remain largely under-utilised. For example, Kumazawa and co-workers²⁶² detailed the application of **78a**/ PPh_3 as the initiating species in the block copolymerisation of the chiral monomer *N-tert*-butoxycarbonyl-L-valine 4-ethynylanilide with the achiral comonomer *N-tert*-butoxycarbonylglycine 4-ethynylanilide. A series of homo- and

block copolymers, Scheme 1-30, were prepared of tuneable composition and molecular weight and, in most instances, the final materials possessed narrow molecular weight distributions with $\mathcal{D} \leq 1.25$. Interestingly, the authors demonstrated chirality amplification in the block copolymers with chirality transfer from the chiral block to the achiral block clearly evident. The chirality transfer was rationalised in terms of the energy difference between conformers with and without a helix turn as determined by DFT calculations.



Scheme 1-31. Chemical structures of a chiral arylacetylene, **(A)** (((1*S*,5*S*)-6,6-dimethylbicyclo[3.1.1]heptan-2-yl)methyl)(4-ethynylphenyl)dimethylsilane and **(B)** achiral monomer (2-(dodecyloxy)-5-ethynyl-1,3-phenylene)dimethanol.

In related work Liu *et al.*²⁶³ reported the use of $\text{Rh}(\text{nbd})(\text{CPh}=\text{CPh}_2)(\text{P}(4\text{-FC}_6\text{H}_4)_3)$ as an initiating species in the preparation of AB diblock copolymers in which the A block was a chiral species based on (((1*S*,5*S*)-6,6-dimethylbicyclo[3.1.1]heptan-2-yl)methyl)(4-ethynylphenyl)-dimethylsilane, **A** Scheme 1-31) and the B block on achiral (2-(dodecyloxy)-5-ethynyl-1,3-phenylene)dimethanol, **B** Scheme 1-31. Well defined AB diblock copolymers of tunable composition were prepared with measured \mathcal{D} s in the range $1.29 \leq \mathcal{D} \leq 1.73$. Similar to the work of Kumazawa and co-workers,²⁶²

the use of a chiral **A** block induced chirality in the **B** block of monomer **B**. However, distinct from the previous report, the poly(**A-block-B**) copolymers possessed a *cis-transoidal*(**A** block)/*cis-cisoidal* (**B** block) stereoregular structure – the first example of its kind prepared by helix-sense selective polymerisation.

Onishi and co-workers²⁶⁴ reported a series of novel Rh(I) catalysts containing a butylene bridge between the nbd ligand and a co-ordinating phosphine or amino functional group, of general formula [$\{\text{nbd}-(\text{CH}_2)_4\text{-X}\}\text{RhR}$] where **79**: X = PPh₂, R = Cl; **80**: X = NPh₂, R = Cl; **81**: X = PPh₂, R = triphenylvinyl, Figure 1-24.

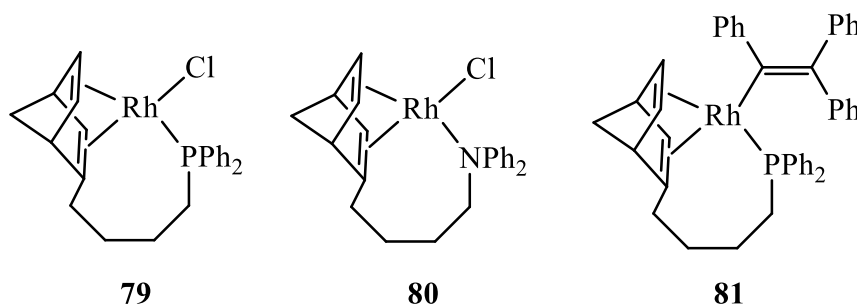
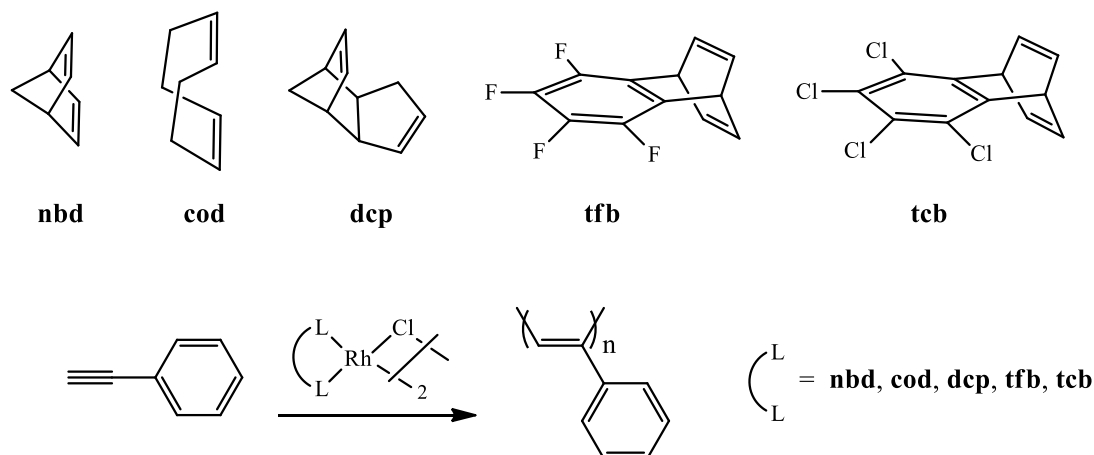


Figure 1-24. Chemical structures of Rh(I) complexes with hemilabile heteroatom ligands with either phosphine or amino functional groups reported by Onishi *et al.*²⁶⁵

All three of these species were evaluated as initiators in the (co)polymerisation of phenylacetylene. The Rh(nbd-(CH₂)₄-PPh₂)Cl complex, **79**, Figure 1-24, in the absence of any additive, displayed low catalytic activity with a measured monomer conversion of < 1 % after 24 hours in THF at 30 °C. In contrast, the nitrogen analogue, Rh(nbd-(CH₂)₄-NPh₂)Cl, **80** Figure 1-24, polymerised phenylacetylene quantitatively with an isolated yield of 83 %, *D* of 1.7 and initiation efficiency of 0.21. The Rh(I)-vinyl derivative, Rh(CPh=CPh₂)(nbd-(CH₂)₄-PPh₂), **81**, Figure 1-24, gave polymer yields of 94 % with quantitative conversion of monomers and a relatively low *D* of 1.3; however, the IE, while higher than **80**, was non-quantitative at 0.6.

According to the authors, the low IE observed for **80** was due to a low population of the active 14e mononuclear complex generated via coordination of the amino group to the Rh centre akin to NEt₃ in the [Rh(nbd)Cl]₂/NEt₃ catalyst system. In the case of **79**, Rh(nbd-(CH₂)₄-PPh₂)Cl, the low activity was attributed to the slow formation of the Rh-C≡CPh species which serves as the initiating species in the polymerisation of PA. In contrast, and consistent with previous examples of Rh(I)-vinyl, Masuda-type, complexes, the Rh(CPh=CPh₂)(nbd-(CH₂)₄-PPh₂) species with a structural resemblance to the active propagating chain end facilitates the smooth insertion of phenylacetylene monomer into the Rh-C bond of the metal centre and triphenylvinyl group. Initiator **81** is the first example of a well-defined Rh complex with a tridentate ligand for this specific application and also represents the only current example of a Rh(I)-triphenylvinyl complex able to mediate the controlled polymerisation of phenylacetylene without the addition of extra free phosphine.

All examples highlighted thus far have been Rh-based catalysts containing nbd or cod as the diene ligand. We note that while nbd catalysts are able to mediate the polymerisation of phenylacetylene (and derivatives) in a controlled or non-controlled fashion, cod-based catalysts only effect non-controlled (co)polymerisation – there are no known examples of well-defined cod-analogues of complexes **76**, **77**, **78**, **79**, **80**, **81** capable of mediating the controlled polymerisation of arylacetylenes. The effect of diene ligands in complexes of the type [Rh(diene)Cl]₂ for the polymerisation of phenylacetylene employing the series of dienes shown in Scheme 1-32 was reported by Saeed, Shiotsuki and Masuda,²⁶⁶ with the principle aim of developing novel catalytic systems.



Scheme 1-32. Chemical structures of diene ligands: 2,5-norbornadiene (**nbd**); 1,5-cyclooctadiene (**cod**); *endo*-dicyclopentadiene (**dcp**); tetrafluorobenzobarrelene (**tfb**) and tetrachlorobenzobarrelene (**tcb**), and the homopolymerisation of phenylacetylene with bridged Rh complexes $[\text{Rh}(\text{diene})\text{Cl}]_2$.

The **tfb** and **tcb** derivatives, $[\text{Rh}(\text{tfb})\text{Cl}]_2$ and $[\text{Rh}(\text{tcb})\text{Cl}]_2$, were found to be significantly more active than the conventional $[\text{Rh}(\text{nbd})\text{Cl}]_2$ and $[\text{Rh}(\text{cod})\text{Cl}]_2$ species. For example, in polymerisations conducted in toluene at 30 °C for one minute in the presence of one equivalent of NEt_3 under otherwise identical conditions yielded for the **nbd** catalyst, PPA in a yield of 69 % (SEC-measured M_n of 118,000, \bar{D} of 1.85); while the **cod** catalyst yielded PPA in a 5 % yield (M_n of 22,000, \bar{D} of 2.16), the **dcp** complex only gave a trace of polymer while the **tfb** and **tcb** derivatives both effected *quantitative* conversion with the former yielding a homopolymer with an M_n of 281,000 and \bar{D} of 1.70, while the **tcb** complex yielded a homopolymer with an M_n of 227,000 and corresponding \bar{D} of 1.79 (note: all polymers have the expected high degree of *cis-transoidal* stereoregularity). This was the first demonstration of catalytic systems exhibiting a superior activity over the well-established $[\text{Rh}(\text{nbd})\text{Cl}]_2$ complex. The authors also examined the effect of solvent and co-catalyst additive with, in all

cases the activity profiles following the same trend with catalyst activity increasing in the order **tfb** \approx **tcb** > **nbd** > **cod** > **dcp**. Based on this observation, the authors proposed that the difference in catalytic activity between the different complexes was due to the difference in π -acidity of the diene ligands. The bonding model in such metal-alkene complexes is shown in Figure 1-25.

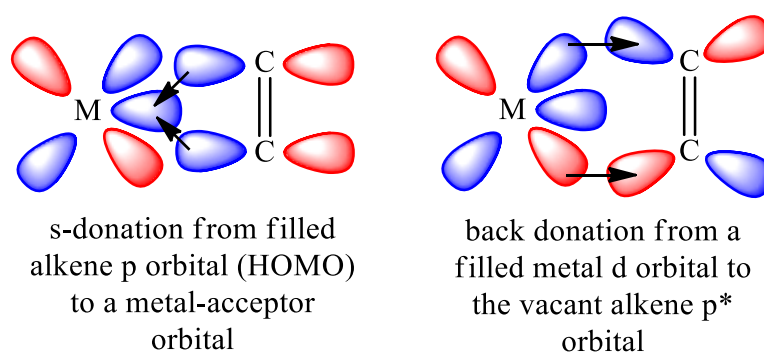
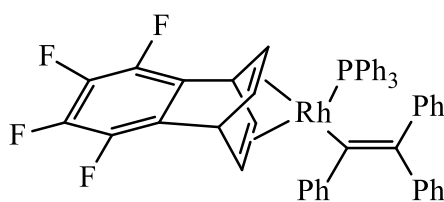


Figure 1-25. The Dewar-Chatt-Duncanson model of bonding between a metal centre and an alkene.

The net result of the back-donation from the metal to the alkene is a reduction in the electron density at the metal centre, i.e. an increase in electrophilic character. The degree of back-donation is determined, at least in part, by the π -acidity of the alkene, i.e. the ability of the ligand to accept electrons into the π^* (LUMO) orbital ($d-\pi^*$ overlap). As such, the π -acidity can be estimated from the energy of the LUMO. In this contribution the authors reported the LUMO energies (in eV) to be (in order from lowest to highest): 0.21 (**tfb**) < 0.48 (**tcb**) < 0.79 (**nbd**) < 0.90 (**cod**) < 1.09 (**dcp**), entirely consistent with the above order of observed polymerisation activity and highlights that of the five ligands **tfb** is expected to be the most π -acidic.



82

Figure 1-26. Chemical structure of $\text{Rh}(\text{tfb})(\text{PhC}=\text{CPh}_2)(\text{PPh}_3)$ derived from the $[\text{Rh}(\text{tfb})\text{Cl}]_2/\text{LiCPh}=\text{CPh}_2/\text{PPh}_3$ ternary mixture.

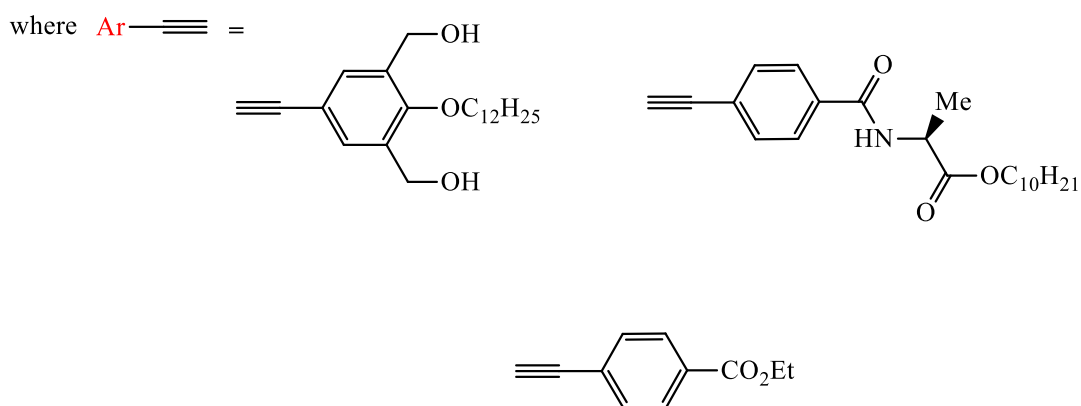
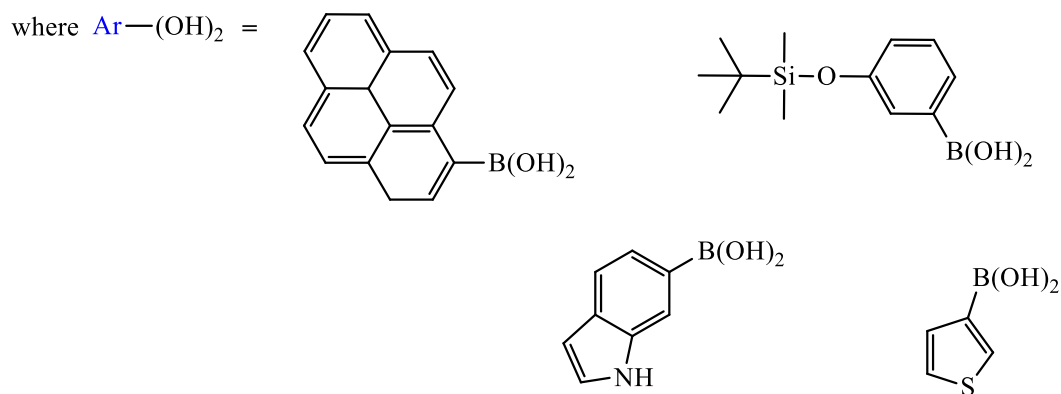
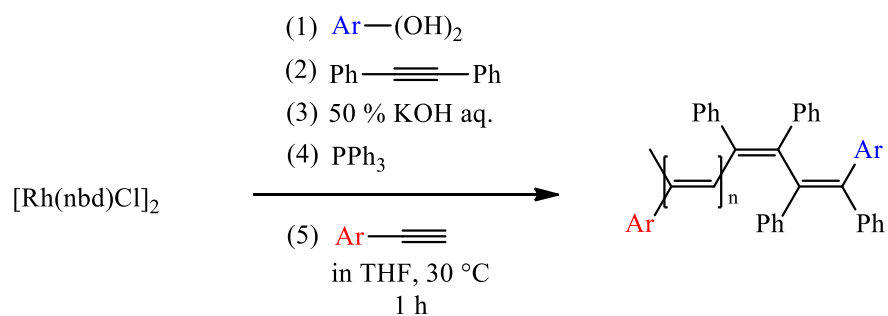
As a natural extension of the above study, the same authors detailed the synthesis of a well-defined **tfb**-based Rh catalytic system.²⁶⁷ Saeed, Shiotsuki and Masuda reported a ternary catalyst system derived from $[\text{Rh}(\text{tfb})\text{Cl}]_2$, PPh_3 and $\text{LiCPh}=\text{CPh}_2$ along with the well-defined Rh(I)-vinyl catalyst, $\text{Rh}(\text{tfb})(\text{CPh}=\text{CPh}_2)(\text{PPh}_3)$, **82**, Figure 1-26, isolated from the ternary mixture. Although the crystal structure of $\text{Rh}(\text{tfb})(\text{CPh}=\text{CPh}_2)(\text{PPh}_3)$ was not reported it was presumed to have a square planar geometry in line with the above highlighted Rh(I)-vinyl species.

An evaluation of the activity of the ternary catalytic mixture in the homopolymerisation of PA revealed that PPAs prepared under such conditions yielded product with essentially quantitative initiation (estimated IE of 0.96), i.e. controllable molecular weights, \bar{D} s as low as 1.03, and *cis-transoidal* contents $\geq 99\%$. For both the ternary catalyst system and the isolated complex, multistage polymerisation of PA experiments were conducted and confirmed the living nature of the polymerisations as did the pseudo-first order kinetic plots and evolution of \bar{D} as a function of conversion. A particularly salient, and somewhat unique, feature of polymerisations conducted with the $\text{Rh}(\text{tfb})(\text{CPh}=\text{CPh}_2)(\text{PPh}_3)/\text{PPh}_3$ initiating system was the observed high activity, and IE, even at low concentration. For example, homopolymerisation of PA

at $[M]_0/[Rh]$ of 4,000 (theoretical M_n of 408,560) yielded a polymer with an SEC-measured M_n of 401,000 (calculated IE of 0.98) and \bar{D} of 1.12.

While other reports exist detailing the use of **tfb**-functional Rh catalysts for the preparation of PPAs (typically in a non-controlled fashion),^{251,268,269} the above highlighted report remains, to the best of our knowledge, the only example in which a well-defined isolable Rh(I)-vinyl complex, or ternary mixture with the *in situ* generation of the active **tfb**-Rh(I)-vinyl species, has been noted and that has been demonstrated to be effective in the controlled polymerisation of phenylacetylene yielding materials with near-quantitative *cis-transoidal* stereoregularity. This suggests that there is significant scope and opportunity for the further development and evaluation of new **tfb** and **tcb**-based catalytic systems for this target application.

Recently, a convenient alternative for the preparation of end functionalised PPAs with precise architecture/structure was presented by Taniguchi *et al.*²⁷⁰ This synthetic route involves a one pot reaction with the active species generated *in situ*. To achieve this, $[Rh(nbd)Cl]_2$ is reacted with a functional arylboronic acid followed by the reaction with 2 to 3 equivalents of diphenylacetylene in the presence of 50 % aqueous solution of KOH and at least 3 equivalents of PPh_3 , thus, generating an active species with structural similarities to well-defined Rh(I) catalyst **78**. Polymerisation is then initiated by the addition of PA to this mixture in THF at 30 °C, which proceeds in a controlled fashion, yielding highly stereoregular PPAs (*cis* content > 95 %) with \bar{D} s typically < 1.10.



Scheme 1-33. Reaction scheme for the preparation of end-functionalised polyenes described by Taniguchi *et al.*²⁷⁰ and selected examples of arylboronic acid and arylacetylenes used in this study.

Referring to Scheme 1-33, it can be seen that a range of functionality can be introduced, from the bulky multi-ring aryl species to a silyl group, which can be utilised in further functionalisation, for example, via deprotection of the silyl group to a phenolate, then proceeding to perform a condensation reaction to obtain a new end-functionalised polymer. Furthermore, the living nature of the polymerisations was confirmed via the standard methodology (multistage polymerisation, linear pseudo-first order kinetics and M_n vs conversion). The authors also demonstrated that this multicomponent catalyst system was active towards a broad range of substituted arylacetylenes, Scheme 1-33, which include highly polar functional groups such as amides and esters, yielding end-functionalised polyenes quantitatively with narrow MWDs ($1.06 < \bar{D} < 1.28$), controllable MW and highly stereoregular microstructures (*cis* content > 95 %).

While certain Rh catalysts are clearly highly effective species for the (non)controlled (co)polymerisation of arylacetylene substrates their applicability does extend beyond this important monomer class. In addition to arylacetylenes, propargyl esters and amides have been reported to be suitable substrates although typically polymerize in a non-controlled fashion, yielding polymers with reduced stereoregularity (compared to phenylacetylenes).

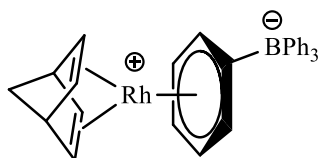
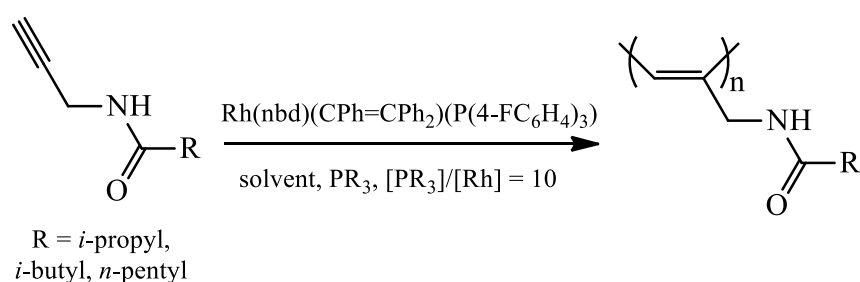


Figure 1-27. Chemical structures of 2,5-norbornadienylrhodium(I) tetraphenylborate.

For example, a series of poly(propargyl ester)s were reported by Zhang *et al.*²⁷¹ obtained using the nbd-tetraphenylborate Rh catalyst, Figure 1-27. For example,

homopolymerisation of propargyl hexanoate with 2,5-norbornadienerhodium(I) tetraphenylborate in THF under a range of conditions yielded poly(propargyl hexanoate) with yields of 42-77 %, SEC-measured M_n s of 4,900-28,000, D s spanning the range 1.83 to 4.70 and *cis* contents of 48-88 % with little, if any, clear direct correlation between any of these features. Reports employing the same catalyst for both propargyl esters and amides, from Masuda and co-workers,²⁷²⁻²⁷⁵ have focused on amino-acid derived monomers and emphasised the structure and properties of the final materials rather than the fundamental features of polymerisation. However, we note that within this body of work examples are given in which polymers are isolated with 100 % monomer conversion and reported D s < 1.20 which suggests that under certain conditions polymerisation of this monomer family proceeds in a controlled (or pseudo-controlled) manner.

Nakazato *et al.*²⁷⁶ reported the application of the well-defined Masuda complex $\text{Rh}(\text{nbd})(\text{CPh}=\text{CPh}_2)(\text{P}(4\text{-FC}_6\text{H}_4)_3)$, **78c**, the fluorine analogue of the catalysts shown in Figure 1-23, for the polymerisation of three simply alkyl propargyl amide monomers, Scheme 1-34.



Scheme 1-34. Polymerisation of simple alkyl propargyl amide substrates with well-defined $\text{Rh}(\text{nbd})(\text{CPh}=\text{CPh}_2)(\text{P}(4\text{-FC}_6\text{H}_4)_3)$ (Masuda catalyst).

As a representative example, the polymerisation of the *iso*-butyl derivative, in CHCl_3 at 30 °C with five equivalents of added PPh_3 as a rate modifier gave a 100 %

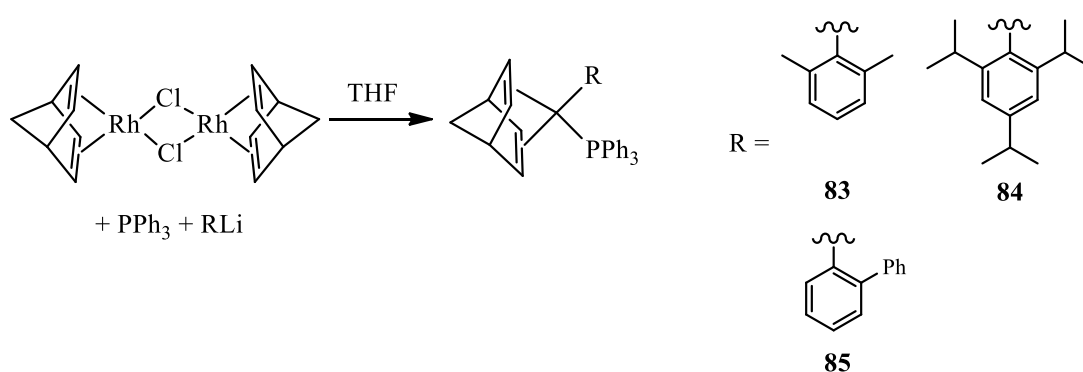
yield of polymer product with an M_n of 17,300 (IE of 0.8, although we note that molecular weights were measured by SEC and reported as polystyrene equivalents) and \bar{D} of 1.36. The fundamental features of this polymerisation were examined under identical conditions except polymerisation was conducted at 0 °C. Under such conditions, the polymerisation of the *iso*-butyl monomer was complete after 60 min, exhibited linear pseudo-first order kinetics (although the plot did not pass through the origin suggesting non-ideal polymerisation), \bar{D} decreased with conversion (although are consistently higher than might be expected), and polymerisation resumed upon the addition of a second charge of monomer which also polymerised to completion.

While the authors presented the molecular weight vs. conversion plot as a linear plot it is, arguably, better represented as a two-stage plot with an initial steep increase in the measure molecular weight. This is perhaps also more consistent with the non-ideal kinetic plot and suggests that there may be some non-controlled polymerisation occurring in the early stages of the process. However, it is clear that the polymerisations do appear to proceed with many of the key hallmark features associated with a controlled polymerisation and we reiterate that quantitative initiation nor low dispersity are formally prerequisites for a polymerisation to be termed 'controlled'. The authors proposed that the less-than ideal dispersities were likely due to a larger k_p/k_t ratio than might be commonly associated with other controlled polymerisation processes.

Thus far in this chapter, we have explored the applications of Rh catalyst systems which can be broadly classified as Rh-vinyl complexes (-vinyl referring to the type of initiating fragment). The effectiveness of Rh catalysts as initiators for the controlled (or non-controlled) (co)polymerisation of PA and its derivatives has been clearly demonstrated, however, this is not the whole gamut of its potential. Other

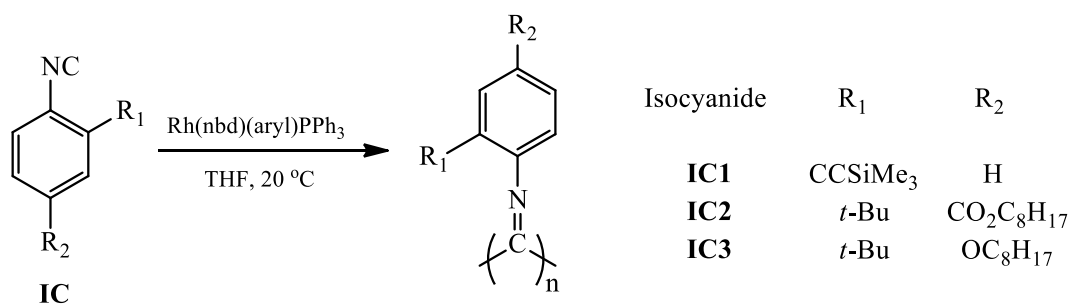
alkynes such as α,ω -dialkynes,²⁴¹ have been examined, and demonstrated to be amenable to polymerisation by Rh complexes, albeit in an uncontrolled fashion. Another important subset of acetylenic monomers are the arylisocyanides, which have been demonstrated to have a propensity to form materials with helical structures^{277, 278} when polymerised by transition metal complexes with, for example, Ni(II),²⁷⁹ and Pt(II)²⁸⁰ complexes.

Yamamoto, Onitsuka and Takahashi²⁸¹ reported the synthesis of three Rh(I)-aryl complexes and their application as initiators for the polymerisation of three different, substituted arylisocyanides monomers. Scheme 1-35, shows the synthetic outline for the preparation of the Rh complexes. Such Rh(I)-aryl species are prepared via the same general route as the well-defined Rh(I)-vinyl complexes described earlier, namely, from the reaction between $[\text{Rh}(\text{nbd})\text{Cl}]_2$, a triarylphosphine (PPh_3) and an aryllithium (versus a vinyl lithium in the case of the Rh(I)-vinyl complexes), with the noted $\text{Rh}(\text{nbd})(2,6\text{-Me}_2\text{C}_6\text{H}_3)\text{PPh}_3$ complex **83**, isolated in a 96 % yield. The reported crystal structure of this Rh(I)-aryl species shows that the complex adopts a square planar geometry that is entirely consistent with the Rh(I)-vinyl complexes.



Scheme 1-35. The general synthetic route for the preparation of Rh(I)-aryl complexes of the type $\text{Rh}(\text{nbd})(\text{aryl})(\text{PPh}_3)$.

All three Rh(I)-aryl complexes were subsequently evaluated as initiating species in the polymerisation of three different arylisocyanides, Scheme 1-36.



Scheme 1-36. The polymerisation of 2,5-substituted arylisocyanides monomers with Rh(nbd)(aryl)(PPh₃).

The polymerisation of **IC1** (2-((trimethylsilyl)ethynyl)phenyl isocyanide) with Rh(nbd)(2,6-Me₂C₆H₃)(PPh₃), **83**, Scheme 1-36, generally proceeded smoothly provided the polymerisation was performed with 10 equivalents of added free PPh₃. For example, for an **IC1**/Rh of 25 and PPh₃/Rh of 10, under the conditions noted in Scheme 1-36, resulted in 100 % conversion of monomer to polymer with the product having an SEC measured M_n of 4,700 and \bar{D} of 1.12. While this is reported as a polystyrene-equivalent molecular weight we note that the authors were able to perform end-group analysis and established that the IE for Rh(nbd)(aryl)(PPh₃)/PPh₃ was essentially quantitative. In the absence of added PPh₃, the yield dropped and in addition to polymer a significant amount of oligomers was formed highlighting the need for added phosphine in order to ensure smooth polymerisation. Increasing the **IC1**/Rh ratio to 50, 75 and finally 100 resulted in a systematic increase in the final M_n of the polymer although was accompanied by a noticeable increase in the \bar{D} from 1.19 to 1.26 to 1.47 at **IC1**/Rh = 100. Similar polymerisation results were obtained for the homopolymerisations of monomers **IC2** and **IC3**. Attempts to prepare block

copolymers, verifying at least in part, the controlled nature of the polymerisations, failed, suggesting that polymerisation was not controlled and that chain end decomposition was likely occurring during polymerisation. Unfortunately, no kinetic data was reported that would have supported, or verified, this supposition.

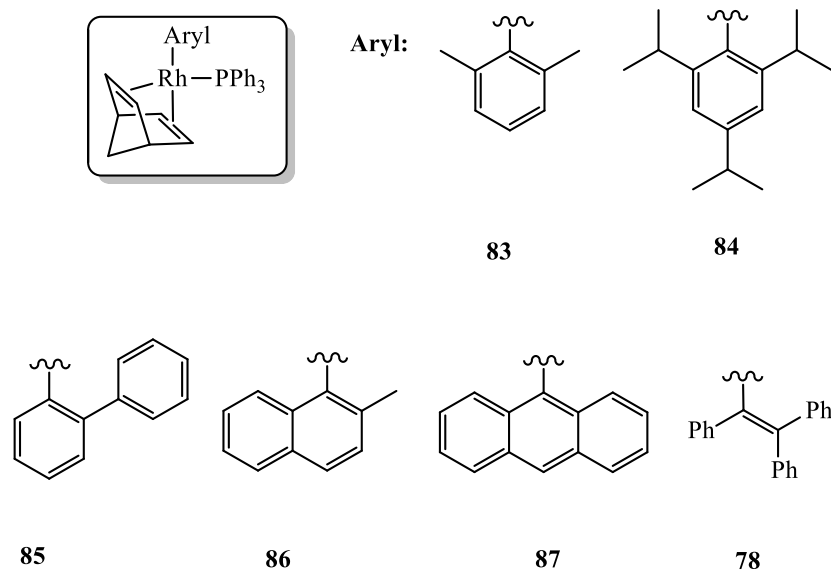


Figure 1-28. Chemical structures of Rh(I)-aryl species examined, evaluated and presented in the study by Onitsuka *et al.*²⁸²

In a follow-up paper Onitsuka *et al.*²⁸² detailed a study in which they expanded both the catalyst pool and the number of arylisocyanides. Figure 1-28 shows the structures of the six Rh complexes examined and includes the three species shown in Scheme 1-35, two new derivatives Rh(nbd)(2-MeNaphthyl)(PPh₃) and Rh(nbd)(9-Anthra)(PPh₃) (where 2-MeNaphthyl = 2-Methyl-1-Naphthyl and 9-Anthra = 9-Anthracenyl) and the original well-defined Rh(I)-vinyl Masuda complex, Rh(nbd)(CPh=CPh₂)(PPh₃).

As a general observation, all the noted complexes (including the Masuda-vinyl derivative) effectively mediated the polymerisation of arylisocyanides *provided* there

was a bulky substituent in one of the *ortho* positions in the isocyanide monomer. Attempted polymerisation of 2,6-dimethylphenylisocyanide with Rh(nbd)(2,6-Me₂C₆H₃)(PPh₃), for example, resulted in no observed conversion. In cases where polymerisation was effective, the resulting polymers had tunable molecular weights and *D*s spanned the range 1.16-1.53. In no instance was any oligomeric by-product observed for the above complexes. The controlled nature of the polymerisations was clearly demonstrated with the *M_n* vs conversion plots being linear and measured values agreeing almost perfectly with the theoretical values at all conversions. Consistent with the preliminary report, initial attempts to effect block copolymer formation by sequential monomer addition failed, further confirming that the active site slowly decomposed, and became particularly problematic at high conversion. However, the authors demonstrated that the active chain end could be efficiently stabilized in the presence of a large excess of added PPh₃ allowing block copolymer formation. For example, the authors reported that the three-step sequential addition of 50 equivalents of **IC2** to Rh(nbd)(2,4,6-*i*-Pr₃C₆H₂)(PPh₃) in the presence of 400 equivalents of PPh₃ resulted in the step-wise formation of polymer with *M_n*s of 21,300, 38,000 and 50,900 with corresponding *D*s of 1.19, 1.20 and 1.29. Further, an AB diblock copolymer of **IC2** (A block) with 2-*tert*-butyl-4-(cyclohexyloxycarbonyl)phenyl isocyanide (B block) was successfully prepared, quantitatively, under similar conditions with (Rh(nbd)(2,4,6-*iso*-Pr₃C₆H₂)(PPh₃), **84**, Figure 1-28, as initiator, 400 equivalents of PPh₃, THF, 20 °C).

The tri-*iso*-propyl Rh derivative, **84**, has also been employed as the initiating species in the helix sense selective (co)polymerisation of bulky aryl isocyanide monomers with chiral ester or amide groups, yielding materials of variable molecular weight and low-to-medium dispersities.²⁸³ For example, polymerisation of (*S*)-octan-

2-yl 3-(*tert*-butyl)-4-isocyanobenzoate (100 equivalents) with **84** with 40 equivalents of PPh₃ based on [Rh] in THF at 20° C resulted in the quantitative conversion of monomer to polymer with the homopolymer having an M_n of 43,600 and \bar{D} of 1.40. The specific rotation, $[\alpha]_D$, of the chiral monomer was determined to be +32 while $[\alpha]_D$ for the corresponding homopolymer was measured at -178 indicating that the polymerisation resulted in the generation of chirality other than that associated with the pendent ester groups. The CD (circular dichromism) spectrum of the homopolymer exhibited a strong Cotton effect in the 250-400 nm region while nothing was observed for the monomer in this region. The authors noted that the Cotton effect around 350 nm is associated with the $n-\pi^*$ transition of imino groups characteristic of helical poly(aryl isocyanide)s. The authors also demonstrated that the structure of the chiral ester groups, and specifically the monomer purity, precise location of the chiral centre and the length of the alkyl chain, had a direct impact on the helical sense selectivity.

Despite the efficacy of these Rh(I)-aryl species as initiators for the polymerisation of arylisocyanides, there have yet to be reports of the evaluation and application of these well-defined Rh(I)-aryl species (**83**, **84**, **85**, **86**, and **87**) as initiators for the polymerisation of arylacetylenes (such as PA) in the literature which we will examine in future chapters.

1.7 Research Objectives

It was clearly shown in this chapter that there are numerous reports of uncontrolled polymerisation of PA and its derivatives by ill-defined and well-defined Rh catalyst systems. In contrast, there exists a noticeable dearth of reported living controlled polymerisations of arylacetylenes. Misumi *et al.*²⁸⁴ has shown that the initiating fragment of the Rh(I) catalyst can be modified to introduce new end-functionalisation to PPA, which should provide ample opportunities to prepared novel well-defined Rh(I) derivatives. As such, these are the current research objectives:

1. To synthesise, isolate and characterise new Rh(I) derivatives based on the Masuda catalyst structural motif via modification of their ligand chemical structure.
2. To evaluate these new isolable well-defined Rh(I) derivatives as initiators for the controlled polymerisation of phenylacetylenes.
3. To determine if the applicability of these Rh(I) initiators is transferrable to other substituted arylacetylenes while retaining features of a controlled polymerisation process.

1.8 References

1. Anand, A.; Singh, P.; Kumar, V.; Bhargava, G., Transition metal catalyzed [6 + 2] cycloadditions. *RSC Advances* **2019**, 9 (44), 25554-25568.
2. Haber, F., *Thermodynamik technischer Gasreaktionen*. De Gruyter: 1905.
3. Alonso, F.; Yus, M., Hydrogenation of olefins with hydrated nickel chloride, lithium and a catalytic amount of naphthalene. *Tetrahedron Letters* **1996**, 37 (38), 6925-6928.
4. Pradier, C. M.; Berthier, Y., Hydrogenation of olefins on platinum. *Journal of Catalysis* **1991**, 129 (2), 356-367.
5. van der Veen, L. A.; Kamer, P. C. J.; van Leeuwen, P. W. N. M., Hydroformylation of internal olefins to linear aldehydes with novel rhodium catalysts. *Angewandte Chemie International Edition* **1999**, 38 (3), 336-338.
6. Forster, D.; Hershman, A.; Morris, D. E., Mechanistic pathways in the catalysis of olefin hydrocarboxylation by rhodium, iridium, and cobalt complexes. *Catalysis Reviews* **1981**, 23 (1-2), 89-105.
7. Vigranenko, Y. T.; Gvozдовskii, G. N., Hydrocarboxylation of olefins in the presence of a catalyst based on a cobalt carbonylpyridine complex. *Petroleum Chemistry* **2002**, 42 (4), 246-252.
8. Hou, J.; Ee, A.; Feng, W.; Xu, J.-H.; Zhao, Y.; Wu, J., Visible-light-driven alkyne hydro-/carbocarbonylation using CO₂ via iridium/cobalt dual catalysis for divergent heterocycle synthesis. *Journal of The American Chemical Society* **2018**, 140 (15), 5257-5263.
9. Hidai, M.; Fukuoka, A.; Koyasu, Y.; Uchida, Y., Homogeneous multimetallic catalysts : part 6. Hydroformylation and hydroesterification of olefins by homogeneous cobalt-ruthenium bimetallic catalysts. *Journal of Molecular Catalysis* **1986**, 35 (1), 29-37.
10. Elman, A. R.; Batov, A. E., Olefin hydrocarboxylation under mild conditions in nickel complex solutions. *Kinetics and Catalysis* **2008**, 49 (3), 386-390.
11. Baibich, I. M.; Garcia, R. R. P., Olefin hydrogenation with iron carbonyls as catalysts. *Journal of the Brazilian Chemical Society* **1997**, 8 (1), 215-218.
12. Bianchini, C.; Mantovani, G.; Meli, A.; Oberhauser, W.; Brüggeller, P.; Stampfl, T., Novel diphosphine-modified palladium catalysts for oxidative carbonylation of styrene to methyl cinnamate *Dalton : An International Journal of Inorganic Chemistry* **2001**, 2001 (5), 690-698.
13. Tsuji, J., Organopalladium chemistry in the '60s and '70s†. *New Journal of Chemistry* **2000**, 24 (3), 127-135.

14. van Rensburg, H.; Hanton, M.; Tooze, R.; Foster, D. F., Cobalt catalyzed hydroesterification of a wide range of olefins. In *DGMK International Conference on Catalysis - Innovative Applications in Petrochemistry and Refining*, DE, 2011; pp 261-268.
15. Pruvost, R.; Boulanger, J.; Léger, B.; Ponchel, A.; Monflier, E.; Ibert, M.; Mortreux, A.; Sauthier, M., Biphasic palladium-catalyzed hydroesterification in a polyol phase : selective synthesis of derived monoesters. *ChemSusChem* **2015**, *8* (12), 2133-2137.
16. Ko, S.; Na, Y.; Chang, S., A novel chelation-assisted hydroesterification of alkenes via ruthenium catalysis. *Journal of The American Chemical Society* **2002**, *124* (5), 750-751.
17. Profir, I.; Beller, M.; Fleischer, I., Novel ruthenium-catalyst for hydroesterification of olefins with formates. *Organic and Biomolecular Chemistry* **2014**, *12* (36), 6972-6976.
18. Fu, L.; Cao, X.; Wan, J.-P.; Liu, Y., Synthesis of enaminone-Pd(II) complexes and their application in catalysing aqueous Suzuki-Miyaura cross coupling reaction. *Chinese Journal of Chemistry* **2020**, *38* (3), 254-258.
19. Ma, S.; Zhou, T.; Li, G.; Szostak, M., Suzuki-Miyaura cross-coupling of amides using well-defined, air-stable [(PR₃)₂Pd(II)X₂] precatalysts. *Advanced Synthesis and Catalysis* **2020**, *362* (9), 1887-1892.
20. Clavé, G.; Pelissier, F.; Campidelli, S.; Grison, C., Ecocatalyzed Suzuki cross coupling of heteroaryl compounds. *Green Chemistry* **2017**, *19* (17), 4093-4103.
21. Wang, T.; Yang, S.; Xu, S.; Han, C.; Guo, G.; Zhao, J., Palladium catalyzed Suzuki cross-coupling of benzyltrimethylammonium salts via C–N bond cleavage. *Royal Society of Chemistry Advances* **2017**, *7* (26), 15805-15808.
22. Savitha, B.; Sajith, A. M.; Joy, M. N.; Khader, K. K. A.; Muralidharan, A.; Padusha, M. S. A.; Bodke, Y. D., Palladium-catalyzed Suzuki cross-coupling of 2-halo-deazapurines with potassium organotrifluoroborate salts in the regioselective synthesis of imidazo[4,5-b]pyridine analogues. *Australian Journal of Chemistry* **2016**, *69* (6), 618-630.
23. Qiu, P.; Zhao, J. Y.; Shi, X.; Duan, X. H., An efficient water-soluble surfactant-type palladium catalyst for Suzuki cross-coupling reactions in pure water at room temperature. *New Journal of Chemistry* **2016**, *40* (8), 6568-6572.
24. Lei, P.; Meng, G.; Szostak, M., General method for the Suzuki–Miyaura cross-coupling of amides using commercially available, air- and moisture-stable palladium/NHC (NHC = *N*-heterocyclic carbene) complexes. *American Chemical Society Catalysis* **2017**, *7* (3), 1960-1965.

25. Prajapati, P. K.; Saini, S.; Jain, S. L., Nickel mediated palladium free photocatalytic Suzuki-coupling reaction under visible light irradiation. *Journal of Materials Chemistry A* **2020**, *8* (10), 5246-5254.
26. Lu, X.-Y.; Yan, L.-Y.; Li, J.-S.; Li, J.-M.; Zhou, H.-p.; Jiang, R.-C.; Liu, C.-C.; Lu, R.; Hu, R., Base-free Ni-catalyzed Suzuki-type cross-coupling reactions of epoxides with boronic acids. *Chemical Communications* **2020**, *56* (1), 109-112.
27. Akkarasamiyo, S.; Margalef, J.; Samec, J. S. M., Nickel-catalyzed Suzuki-Miyaura cross-coupling reaction of naphthyl and quinolyl alcohols with boronic acids. *Organic Letters* **2019**, *21* (12), 4782-4787.
28. Ho, G.-M.; Sommer, H.; Marek, I., Highly e-selective, stereoconvergent nickel-catalyzed Suzuki-Miyaura cross-coupling of alkenyl ethers. *Organic Letters* **2019**, *21* (8), 2913-2917.
29. Schwarzer, M. C.; Konno, R.; Hojo, T.; Ohtsuki, A.; Nakamura, K.; Yasutome, A.; Takahashi, H.; Shimasaki, T.; Tobisu, M.; Chatani, N.; Mori, S., Combined theoretical and experimental studies of nickel-catalyzed cross-coupling of methoxyarenes with arylboronic esters via C-O bond cleavage. *Journal of The American Chemical Society* **2017**, *139* (30), 10347-10358.
30. Cammidge, A. N.; Crépy, K. V. L., The first asymmetric Suzuki cross-coupling reaction. *Chemical Communications* **2000**, *2000* (18), 1723-1724.
31. Callam, C. S.; Lowary, T. L., Suzuki cross-coupling reactions : synthesis of unsymmetrical biaryls in the organic laboratory. *Journal of Chemical Education* **2001**, *78* (7), 947.
32. Zhou, Y.; Wang, S.; Wu, W.; Li, Q.; He, Y.; Zhuang, Y.; Li, L.; Pang, J.; Zhou, Z.; Qiu, L., Enantioselective synthesis of axially chiral multifunctionalized biaryls via asymmetric Suzuki-Miyaura coupling. *Organic Letters* **2013**, *15* (21), 5508-5511.
33. Li, Y.; Pan, B.; He, X.; Xia, W.; Zhang, Y.; Liang, H.; Subba Reddy, C. V.; Cao, R.; Qiu, L., Pd-catalyzed asymmetric Suzuki-Miyaura coupling reactions for the synthesis of chiral biaryl compounds with a large steric substituent at the 2-position. *Beilstein Journal of Organic Chemistry* **2020**, *16* (1), 966-973.
34. Chen, Q.; Wu, S.; Yan, S.; Li, C.; Abduhulam, H.; Shi, Y.; Dang, Y.; Cao, C., Suzuki-Miyaura cross-coupling of sulfoxides. *American Chemical Society Catalysis* **2020**, *10* (15), 8168-8176.
35. Heck, R. F., Palladium-catalyzed reactions of organic halides with olefins. *Accounts of Chemical Research* **1979**, *12* (4), 146-151.
36. Heck, R. F., Palladium-catalyzed vinylation of organic halides. In *Organic Reactions*, Dauben, W. G., Ed. John Wiley and Sons: New Jersey, US, 1982; Vol. 27, pp 345-390.

37. Shaikh, T.; Hong, F. E., Palladium(II)-catalyzed Heck reaction of aryl halides and arylboronic acids with olefins under mild conditions. *Beilstein Journal of Organic Chemistry* **2013**, *9* (1), 1578-1588.
38. Dawson, D. D.; Oswald, V. F.; Borovik, A. S.; Jarvo, E. R., Identification of the active catalyst for nickel-catalyzed stereospecific Kumada coupling reactions of ethers. *Chemistry : A European Journal* **2020**, *26* (14), 3044-3048.
39. Iffland, L.; Petuker, A.; Gastel, M.; Apfel, U.-P., Mechanistic implications for the Ni(I)-catalyzed Kumada cross-coupling reaction. *Inorganics* **2017**, *5* (4), 78.
40. Piontek, A.; Ochędzan-Siodłak, W.; Bisz, E.; Szostak, M., Nickel-catalyzed C(sp²)-C(sp³) Kumada cross-coupling of aryl tosylates with alkyl Grignard reagents. *Advanced Synthesis and Catalysis* **2019**, *361* (10), 2329-2336.
41. Wu, Z.; Si, T.; Xu, G.; Xu, B.; Tang, W., Ligand-free nickel-catalyzed Kumada couplings of aryl bromides with tert-butyl Grignard reagents. *Chinese Chemical Letters* **2019**, *30* (3), 597-600.
42. Fiorito, D.; Folliet, S.; Liu, Y.; Mazet, C., A general nickel-catalyzed Kumada vinylation for the preparation of 2-substituted 1,3-dienes. *American Chemical Society Catalysis* **2018**, *8* (2), 1392-1398.
43. Eno, M. S.; Lu, A.; Morken, J. P., Nickel-catalyzed asymmetric Kumada cross-coupling of symmetric cyclic sulfates. *Journal of The American Chemical Society* **2016**, *138* (25), 7824-7827.
44. Ye, X.; Yuan, Z.; Zhou, Y.; Yang, Q.; Xie, Y.; Deng, Z.; Peng, Y., Nickel-catalyzed Kumada cross-coupling reaction for the synthesis of 2,4-diarylquinazolines. *Journal of Heterocyclic Chemistry* **2016**, *53* (6), 1956-1962.
45. Dawson, D. D.; Jarvo, E. R., Stereospecific nickel-catalyzed cross-coupling reactions of benzylic ethers with isotopically-labeled Grignard reagents. *Organic Process Research and Development* **2015**, *19* (10), 1356-1359.
46. Stamatopoulos, I.; Giannitsios, D.; Psycharis, V.; Raptopoulou, C. P.; Balcar, H.; Zukal, A.; Svoboda, J.; Kyritsis, P.; Vohlřidal, J., A Kumada coupling catalyst, [Ni{(Ph₂-P)₂N(CH₂)₃Si(OCH₃)₃-P,P'}Cl₂], bearing a ligand for direct immobilization onto siliceous mesoporous molecular sieves. *European Journal of Inorganic Chemistry* **2015**, *2015* (18), 3038-3044.
47. Dai, W.; Xiao, J.; Jin, G.; Wu, J.; Cao, S., Palladium- and Nickel-catalyzed Kumada cross-coupling reactions of gem-difluoroalkenes and monofluoroalkenes with Grignard reagents. *The Journal of Organic Chemistry* **2014**, *79* (21), 10537-10546.
48. Zhang, M.-M.; Gong, J.; Song, R.-J.; Li, J.-H., Synthesis of internal alkynes by Pd(PPh₃)₄/TMEDA-catalyzed Kumada cross-coupling of alkynyl halides with Grignard reagents. *European Journal of Organic Chemistry* **2014**, *2014* (30), 6769-6773.

49. Wu, D.; Wang, Z.-X., P,N,N-Pincer nickel-catalyzed cross-coupling of aryl fluorides and chlorides. *Organic and Biomolecular Chemistry* **2014**, *12* (33), 6414-6424.
50. Rathod, J.; Sharma, P.; Pandey, P.; Singh, A. P.; Kumar, P., Highly active recyclable SBA-15-EDTA-Pd catalyst for Mizoroki-Heck, Stille and Kumada C–C coupling reactions. *Journal of Porous Materials* **2017**, *24* (4), 837-846.
51. Achanta, S., Basu, D., Neelam, U.K., Budhdev, R.R., Bhattacharya, A. and Bandichhor, R., Development of Iron-Catalyzed Kumada Cross-coupling for the Large-Scale Production of Aliskiren Intermediate. In *Organometallic Chemistry in Industry*, 2020; pp 121-136.
52. Nugent, J.; Shire, B. R.; Caputo, D. F. J.; Pickford, H. D.; Nightingale, F.; Houlsby, I. T. T.; Mousseau, J. J.; Anderson, E. A., Synthesis of all-carbon disubstituted bicyclo[1.1.1]pentanes by iron-catalyzed Kumada cross-coupling. *Angewandte Chemie International Edition* **2020**, *59* (29), 11866-11870.
53. Bisz, E.; Szostak, M., Iron-catalyzed C(sp²)–C(sp³) cross-coupling of chlorobenzenesulfonamides with alkyl Grignard reagents : entry to alkylated aromatics. *The Journal of Organic Chemistry* **2019**, *84* (3), 1640-1646.
54. Schilz, M.; Plenio, H., A guide to Sonogashira cross-coupling reactions : the influence of substituents in aryl bromides, acetylenes, and phosphines. *The Journal of Organic Chemistry* **2012**, *77* (6), 2798-2807.
55. Sakai, N.; Annaka, K.; Konakahara, T., Palladium-catalyzed coupling reaction of terminal alkynes with aryl iodides in the presence of indium tribromide and its application to a one-pot synthesis of 2-phenylindole. *Organic Letters* **2004**, *6* (10), 1527-1530.
56. Lin, B.-N.; Huang, S.-H.; Wu, W.-Y.; Mou, C.-Y.; Tsai, F.-Y., Sonogashira reaction of aryl and heteroaryl halides with terminal alkynes catalyzed by a highly efficient and recyclable nanosized MCM-41 anchored palladium bipyridyl complex. *Molecules* **2010**, *15* (12), 9157-9173.
57. Wender, P. A.; Correa, A. G.; Sato, Y.; Sun, R., Transition Metal-Catalyzed [6+2] Cycloadditions of 2-Vinylcyclobutanones and Alkenes: A New Reaction for the Synthesis of Eight-Membered Rings. *Journal of the American Chemical Society* **2000**, *122* (32), 7815-7816.
58. Jenkins, A. D.; Kratochvíl, P.; Stepto, R. F. T.; Suter, U. W., Glossary of basic terms in polymer science (IUPAC Recommendations 1996). *Pure and Applied Chemistry* **1996**, *68* (12), 2287.
59. Eisch, J. J., Fifty years of Ziegler–Natta polymerization : from serendipity to science. a personal account. *Organometallics* **2012**, *31* (14), 4917-4932.

60. Natta, G., A New Class of Polymers of α -Olefins with an Exceptional Regularity of Structure. In *Stereoregular Polymers and Stereospecific Polymerizations*, Natta, G.; Danusso, F., Eds. Pergamon: Oxford, UK, 1967; pp 5-18.
61. Agboola, O.; Sadiku, R.; Mokrani, T.; Amer, I.; Imoru, O., Polyolefins and the environment. In *Polyolefin Fibres 2ed.*; Ugbolue, S. C. O., Ed. Woodhead Publishing: Cambridge, UK, 2017; pp 89-133.
62. Raucci, M. G.; Gloria, A.; De Santis, R.; Ambrosio, L.; Tanner, K. E., Introduction to biomaterials for spinal surgery. In *Biomaterials for spinal surgery*, Ambrosio, L.; Tanner, E., Eds. Woodhead Publishing: Cambridge, UK, 2012; pp 1-38.
63. Cossee, P., Ziegler-Natta catalysis I. mechanism of polymerization of α -olefins with Ziegler-Natta catalysts. *Journal of Catalysis* **1964**, 3 (1), 80-88.
64. Jean-Louis Hérisson, P.; Chauvin, Y., Catalyse de transformation des oléfines par les complexes du tungstène. II. Télomérisation des oléfines cycliques en présence d'oléfines acycliques. *Die Makromolekulare Chemie* **1971**, 141 (1), 161-176.
65. Calderon, N.; Chen, H. Y.; Scott, K. W., Olefin metathesis : a novel reaction for skeletal transformations of unsaturated hydrocarbons. *Tetrahedron Letters* **1967**, 8 (34), 3327-3329.
66. Anderson, A. W.; Merckling, N. G. Polymeric bicyclo-(2, 2, 1)-2-heptene. U.S Patent 2,721,189, 18 October 1955, 1955.
67. Choi, T.-L.; Grubbs, R. H., Controlled living ring-opening-metathesis polymerization by a fast-initiating ruthenium catalyst. *Angewandte Chemie International Edition* **2003**, 42 (15), 1743-1746.
68. Jacobson, H.; Stockmayer, W. H., Intramolecular reaction in polycondensations. I. the theory of linear systems. *The Journal of Chemical Physics* **1950**, 18 (12), 1600-1606.
69. Bozhenkova, G. S.; Samochernova, A. P.; Ashirov, R. V.; Lyapkov, A. A., Polymers based on norbornene derivatives. *Procedia Chemistry* **2015**, 15, 8-13.
70. Yu, H.; Lin, S.; Sun, D.; Pan, Q., Synthesis of norbornene derivatives and their polymers via ROMP of norbornene derivatives. *High Performance Polymers* **2020**, 32 (6), 729-737.
71. Bielawski, C. W.; Grubbs, R. H., Living ring-opening metathesis polymerization. *Progress in Polymer Science* **2007**, 32 (1), 1-29.
72. Diallo, A. K.; Annunziata, L.; Fouquay, S.; Michaud, G.; Simon, F.; Brusson, J.-M.; Guillaume, S. M.; Carpentier, J.-F., Ring-opening metathesis polymerization of cyclooctene derivatives with chain transfer agents derived from glycerol carbonate. *Polymer Chemistry* **2014**, 5 (7), 2583-2591.

73. Nguyen, S. T.; Johnson, L. K.; Grubbs, R. H.; Ziller, J. W., Ring-opening metathesis polymerization (ROMP) of norbornene by a group VIII carbene complex in protic media. *Journal of The American Chemical Society* **1992**, *114* (10), 3974-3975.
74. Nguyen, S. T.; Grubbs, R. H.; Ziller, J. W., Syntheses and activities of new single-component, ruthenium-based olefin metathesis catalysts. *Journal of The American Chemical Society* **1993**, *115* (21), 9858-9859.
75. Louie, J.; Grubbs, R. H., Metathesis of electron-rich olefins : structure and reactivity of electron-rich carbene complexes. *Organometallics* **2002**, *21* (11), 2153-2164.
76. Bielawski, C. W.; Benitez, D.; Morita, T.; Grubbs, R. H., Synthesis of end-functionalized poly(norbornene)s via ring-opening metathesis polymerization. *Macromolecules* **2001**, *34* (25), 8610-8618.
77. Kanaoka, S.; Grubbs, R. H., Synthesis of block copolymers of silicon-containing norbornene derivatives via living ring-opening metathesis polymerization catalyzed by a ruthenium carbene complex. *Macromolecules* **1995**, *28* (13), 4707-4713.
78. Schwab, P.; Grubbs, R. H.; Ziller, J. W., Synthesis and applications of $\text{RuCl}_2(=\text{CHR}')(\text{PR}_3)_2$: the influence of the alkylidene moiety on metathesis activity. *Journal of The American Chemical Society* **1996**, *118* (1), 100-110.
79. Schwab, P.; France, M. B.; Ziller, J. W.; Grubbs, R. H., A series of well-defined metathesis catalysts—synthesis of $[\text{RuCl}_2(=\text{CHR}')(\text{PR}_3)_2]$ and its reactions. *Angewandte Chemie International Edition* **1995**, *34* (18), 2039-2041.
80. Lynn, D. M.; Kanaoka, S.; Grubbs, R. H., Living ring-opening metathesis polymerization in aqueous media catalyzed by well-defined ruthenium carbene complexes. *Journal of The American Chemical Society* **1996**, *118* (4), 784-790.
81. Weck, M.; Schwab, P.; Grubbs, R. H., Synthesis of ABA triblock copolymers of norbornenes and 7-oxanorbornenes via living ring-opening metathesis polymerization using well-defined, bimetallic ruthenium catalysts. *Macromolecules* **1996**, *29* (5), 1789-1793.
82. Maughon, B. R.; Grubbs, R. H., Ruthenium alkylidene initiated living ring-opening metathesis polymerization (ROMP) of 3-substituted cyclobutenes. *Macromolecules* **1997**, *30* (12), 3459-3469.
83. Maughon, B. R.; Weck, M.; Mohr, B.; Grubbs, R. H., Influence of backbone rigidity on the thermotropic behavior of side-chain liquid crystalline polymers synthesized by ring-opening metathesis polymerization. *Macromolecules* **1997**, *30* (2), 257-265.

84. Weck, M.; Mohr, B.; Maughon, B. R.; Grubbs, R. H., Synthesis of discotic columnar side-chain liquid crystalline polymers by ring-opening metathesis polymerization (ROMP). *Macromolecules* **1997**, *30* (21), 6430-6437.
85. Robson, D. A.; Gibson, V. C.; Davies, R. G.; North, M., A new and highly efficient Grubbs initiator for ring-opening metathesis polymerization. *Macromolecules* **1999**, *32* (19), 6371-6373.
86. Bielawski, C. W.; Grubbs, R. H., Increasing the initiation efficiency of ruthenium-based ring-opening metathesis initiators : effect of excess phosphine. *Macromolecules* **2001**, *34* (26), 8838-8840.
87. Dias, E. L.; Nguyen, S. T.; Grubbs, R. H., Well-defined ruthenium olefin metathesis catalysts : mechanism and activity. *Journal of The American Chemical Society* **1997**, *119* (17), 3887-3897.
88. Sanford, M. S.; Ulman, M.; Grubbs, R. H., New insights into the mechanism of ruthenium-catalyzed olefin metathesis reactions. *Journal of The American Chemical Society* **2001**, *123* (4), 749-750.
89. Scholl, M.; Ding, S.; Lee, C. W.; Grubbs, R. H., Synthesis and activity of a new generation of ruthenium-based olefin metathesis catalysts coordinated with 1,3-dimesityl-4,5-dihydroimidazol-2-ylidene ligands. *Organic Letters* **1999**, *1* (6), 953-956.
90. Herrmann, W. A.; Köcher, C., N-heterocyclic carbenes. *Angewandte Chemie International Edition* **1997**, *36* (20), 2162-2187.
91. Weskamp, T.; Schattenmann, W. C.; Spiegler, M.; Herrmann, W. A., A novel class of ruthenium catalysts for olefin metathesis. *Angewandte Chemie International Edition* **1998**, *37* (18), 2490-2493.
92. Arduengo, A. J., Looking for stable carbenes : the difficulty in starting anew. *Accounts of Chemical Research* **1999**, *32* (11), 913-921.
93. Huang, J.; Schanz, H.-J.; Stevens, E. D.; Nolan, S. P., Stereoelectronic effects characterizing nucleophilic carbene ligands bound to the Cp*₂RuCl (Cp* = η⁵-C₅Me₅) moiety : a structural and thermochemical investigation. *Organometallics* **1999**, *18* (12), 2370-2375.
94. Bourissou, D.; Guerret, O.; Gabbai, F. P.; Bertrand, G., Stable carbenes. *Chemical Reviews* **2000**, *100* (1), 39-92.
95. Scherman, O. A.; Grubbs, R. H., Polycyclooctatetraene (polyacetylene) produced with a ruthenium olefin metathesis catalyst. *Synthetic Metals* **2001**, *124* (2-3), 431-434.
96. Bielawski, C. W.; Grubbs, R. H., Highly efficient ring-opening metathesis polymerization (ROMP) using new ruthenium catalysts containing N-heterocyclic carbene ligands. *Angewandte Chemie International Edition* **2000**, *39* (16), 2903-2906.

97. Love, J. A.; Morgan, J. P.; Trnka, T. M.; Grubbs, R. H., A practical and highly active ruthenium-based catalyst that effects the cross metathesis of acrylonitrile. *Angewandte Chemie International Edition* **2002**, *41* (21), 4035-4037.
98. Sanford, M. S.; Love, J. A.; Grubbs, R. H., A versatile precursor for the synthesis of new ruthenium olefin metathesis catalysts. *Organometallics* **2001**, *20* (25), 5314-5318.
99. Vasiuta, R.; Stockert, A.; Plenio, H., Alternating ring-opening metathesis polymerization by Grubbs-type catalysts with N-penttiptyceny, N-alkyl-NHC ligands. *Chemical Communications* **2018**, *54* (14), 1706-1709.
100. Torker, S.; Müller, A.; Chen, P., Building stereoselectivity into a chemoselective ring-opening metathesis polymerization catalyst for alternating copolymerization. *Angewandte Chemie International Edition* **2010**, *49* (22), 3762-3766.
101. Zamal, H. H.; Barba, D.; Aissa, B.; Haddad, E.; Rosei, F., Cure kinetics of poly (5-ethylidene-2-norbornene) with 2nd generation Hoveyda-Grubbs' catalyst for self-healing applications. *Polymer* **2018**, *153*, 1-8.
102. Song, A.; Parker, K. A.; Sampson, N. S., Cyclic alternating ring-opening metathesis polymerization (CAROMP). rapid access to functionalized cyclic polymers. *Organic Letters* **2010**, *12* (17), 3729-3731.
103. Fox, M. E.; Szoka, F. C.; Fréchet, J. M. J., Soluble polymer carriers for the treatment of cancer : the importance of molecular architecture. *Accounts of Chemical Research* **2009**, *42* (8), 1141-1151.
104. Bahr, S.; Doyle, N.; Wang, J.; Winckler, S.; Takekoshi, T.; Wang, Y.-F. Macrocyclic polyester oligomers as carriers and/or flow modifier additives for thermoplastics. 20 September 2007, 2007.
105. Blencowe, A.; Qiao, G. G., Ring-opening metathesis polymerization with the second generation Hoveyda-Grubbs catalyst : an efficient approach toward high-purity functionalized macrocyclic oligo(cyclooctene)s. *Journal of The American Chemical Society* **2013**, *135* (15), 5717-5725.
106. Fischer, E. O.; Maasböl, A., On the existence of a tungsten carbonyl carbene complex. *Angewandte Chemie International Edition* **1964**, *3* (8), 580-581.
107. Katz, T. J.; Lee, S. J.; Acton, N., Stereospecific polymerizations of cycloalkenes induced by a metal-carbene. *Tetrahedron Letters* **1976**, *17* (47), 4247-4250.
108. Fischer, E. O., Structure, bonding and reactivity of (stable) transition metal carbonyl carbene complexes. *Pure and Applied Chemistry* **1970**, *24* (2), 407-424.

109. Fischer, E. O., Recent aspects of transition metal carbonyl carbene complexes. *Pure and Applied Chemistry* **1972**, 30 (3), 353-372.
110. Fischer, E. O., Selectivity and specificity in chemical reactions of carbene and carbyne metal complexes. *Pure and Applied Chemistry* **1978**, 50 (9), 857-870.
111. Fischer, E. O., On the way to carbene and carbyne complexes. In *Advances in organometallic chemistry*, Stone, F. G. A.; West, R., Eds. Academic Press: Cambridge, US, 1976; Vol. 14, pp 1-32.
112. Rocklage, S. M.; Fellmann, J. D.; Rupprecht, G. A.; Messerle, L. W.; Schrock, R. R., Multiple metal-carbon bonds. 19. how niobium and tantalum complexes of the type $M(\text{CHCMe}_3)(\text{PR}_3)_2\text{Cl}_3$ can be modified to give olefin metathesis catalysts. *Journal of The American Chemical Society* **1981**, 103 (6), 1440-1447.
113. Kress, J.; Osborn, J. A., Stereochemically nonrigid tungsten alkylidene complexes. barriers to rotation about the tungsten carbon double bond. *Journal of The American Chemical Society* **1987**, 109 (13), 3953-3960.
114. Kress, J.; Wesolek, M.; Osborn, J. A., Tungsten (IV) carbenes for the metathesis of olefins. direct observation and identification of the chain carrying carbene complexes in a highly active catalyst system. *Journal of The Chemical Society : Chemical Communications* **1982**, 1982 (9), 514-516.
115. Kress, J.; Osborn, J. A., Tungsten carbene complexes in olefin metathesis : a cationic and chiral active species. *Journal of The American Chemical Society* **1983**, 105 (20), 6346-6347.
116. Quignard, F.; Leconte, M.; Basset, J.-M., Synthesis and catalytic properties of $\text{W}(\text{OAr})_2\text{Cl}_2(\text{CHCMe}_3)(\text{OR}_2)$ and $\text{W}(\text{OAr})_2\text{Cl}(\text{CHCMe}_3)(\text{CH}_2\text{CMe}_3)(\text{OR}_2)$ (Ar = 2,6-disubstituted phenyl; R = Et or Pri), new uni-component catalysts for metathesis of acyclic and cyclic olefins, with or without functional groups. *Journal of The Chemical Society : Chemical Communications* **1985**, 1985 (24), 1816-1817.
117. Schrock, R. R., Living ring-opening metathesis polymerization catalyzed by well-characterized transition-metal alkylidene complexes. *Accounts of Chemical Research* **1990**, 23 (5), 158-165.
118. Schaverien, C. J.; Dewan, J. C.; Schrock, R. R., Multiple metal-carbon bonds. 43. well-characterized, highly active, lewis acid free olefin metathesis catalysts. *Journal of The American Chemical Society* **1986**, 108 (10), 2771-2773.
119. Schrock, R. R.; DePue, R. T.; Feldman, J.; Schaverien, C. J.; Dewan, J. C.; Liu, A. H., Preparation and reactivity of several alkylidene complexes of the type $\text{W}(\text{CHR}')(\text{N}-2,6\text{-C}_6\text{H}_3\text{-iso-Pr}_2)(\text{OR})_2$ and related tungstacyclobutane complexes. controlling metathesis activity through the choice of alkoxide ligand. *Journal of The American Chemical Society* **1988**, 110 (5), 1423-1435.

120. O'Donoghue, M. B.; Schrock, R. R.; LaPointe, A. M.; Davis, W. M., Preparation of well-defined, metathetically active oxo alkylidene complexes of tungsten. *Organometallics* **1996**, *15* (5), 1334-1336.
121. Schrock, R. R.; Krouse, S. A.; Knoll, K.; Feldman, J.; Murdzek, J. S.; Yang, D. C., Controlled ring-opening metathesis polymerization by molybdenum and tungsten alkylidene complexes. *Journal of Molecular Catalysis* **1988**, *46* (1), 243-253.
122. Schrock, R. R.; Yap, K. B.; Yang, D. C.; Sitzmann, H.; Sita, L. R.; Bazan, G. C., Evaluation of cyclopentene-based chain-transfer agents for living ring-opening metathesis polymerization. *Macromolecules* **1989**, *22* (8), 3191-3200.
123. Dounis, P.; Feast, W. J., A route to low polydispersity linear and star polyethylenes via ring-opening metathesis polymerization. *Polymer* **1996**, *37* (12), 2547-2554.
124. Trzaska, S. T.; Lee, L.-B. W.; Register, R. A., Synthesis of narrow-distribution "perfect" polyethylene and its block copolymers by polymerization of cyclopentene. *Macromolecules* **2000**, *33* (25), 9215-9221.
125. Wu, Z.; Wheeler, D. R.; Grubbs, R. H., Living ring-opening metathesis polymerization of cyclobutene: the thermodynamic effect of a reversibly binding ligand. *Journal of The American Chemical Society* **1992**, *114* (1), 146-151.
126. Schrock, R. R.; Murdzek, J. S.; Bazan, G. C.; Robbins, J.; DiMare, M.; O'Regan, M., Synthesis of molybdenum imido alkylidene complexes and some reactions involving acyclic olefins. *Journal of The American Chemical Society* **1990**, *112* (10), 3875-3886.
127. Bazan, G. C.; Oskam, J. H.; Cho, H. N.; Park, L. Y.; Schrock, R. R., Living ring-opening metathesis polymerization of 2,3-difunctionalized 7-oxanorbornenes and 7-oxanorbornadienes by $\text{Mo}(\text{CHCMe}_2\text{R})(\text{NC}_6\text{H}_3\text{-iso-Pr}_{2,6})(\text{O-tert-Bu})_2$ and $\text{Mo}(\text{CHCMe}_2\text{R})(\text{NC}_6\text{H}_3\text{-iso-Pr}_{2,6})(\text{OCMe}_2\text{CF}_3)_2$. *Journal of The American Chemical Society* **1991**, *113* (18), 6899-6907.
128. Bazan, G. C.; Khosravi, E.; Schrock, R. R.; Feast, W. J.; Gibson, V. C.; O'Regan, M. B.; Katz, T. J.; Davis, W. M., Living ring-opening metathesis polymerization of 2,3-difunctionalized norbornadienes by $\text{Mo}(\text{:CHBu-tert})(\text{:NC}_6\text{H}_3\text{Pr-iso}_{2,6})(\text{OBu-tert})_2$. *Journal of The American Chemical Society* **1990**, *112* (23), 8378-8387.
129. Bazan, G. C.; Schrock, R. R.; Cho, H. N.; Gibson, V. C., Polymerization of functionalized norbornenes employing $\text{Mo}(\text{CH-t-Bu})(\text{NAr})(\text{O-t-Bu})_2$ as the initiator. *Macromolecules* **1991**, *24* (16), 4495-4502.
130. Khosravi, E.; Al-Hajaji, A. A., Ring opening metathesis polymerisation of n-alkyl norbornene dicarboxyimides using well-defined initiators. *Polymer* **1998**, *39* (23), 5619-5625.

131. Khosravi, E.; Feast, W. J.; Al-Hajaji, A. A.; Leejarkpai, T., ROMP of n-alkyl norbornene dicarboxyimides : from classical to well-defined initiators, an overview. *Journal of Molecular Catalysis A : Chemical* **2000**, *160* (1), 1-11.
132. Trzaska, S. T.; Lee, L.-B. W.; Register, R. A., Synthesis of narrow-distribution “perfect” polyethylene and its block copolymers by Polymerization of cyclopentene. *Macromolecules* **2000**, *33* (25), 9215-9221.
133. Wu, Z.; Grubbs, R. H., Preparation of alternating copolymers from the ring-opening metathesis polymerization of 3-methylcyclobutene and 3,3-dimethylcyclobutene. *Macromolecules* **1995**, *28* (10), 3502-3508.
134. Alder, R. W.; Allen, P. R.; Khosravi, E., Preparation of poly[(1,1-dipropyl)butane-1,4-diyl], $(\text{Pr}_2\text{CCH}_2\text{CH}_2\text{CH}_2)_n$, via regiospecific ring opening polymerisation of 3,3-dipropylcyclobutene. *Journal of The Chemical Society : Chemical Communications* **1994**, *1994* (10), 1235-1236.
135. Perrott, M. G.; Novak, B. M., Living ring-opening metathesis polymerizations of 3,4-difunctional cyclobutenes. *Macromolecules* **1995**, *28* (9), 3492-3494.
136. Perrott, M. G.; Novak, B. M., Living ring-opening metathesis polymerizations of 3,4-disubstituted cyclobutenes and synthesis of polybutadienes with protic functionalities. *Macromolecules* **1996**, *29* (5), 1817-1823.
137. Singh, R.; Czekelius, C.; Schrock, R. R., Living ring-opening metathesis polymerization of cyclopropenes. *Macromolecules* **2006**, *39* (4), 1316-1317.
138. Natta, G.; Mazzanti, G.; Corradini, P., *Atti della accademia nazionale dei lincei. classe di scienze fisiche, matematiche e naturali* **1958**, (25), 3.
139. Ito, T.; Shirakawa, H.; Ikeda, S., Simultaneous polymerization and formation of polyacetylene film on the surface of concentrated soluble Ziegler-type catalyst solution. *Journal of Polymer Science : Polymer Chemistry Edition* **1974**, *12* (1), 11-20.
140. Chiang, C. K.; Fincher, C. R.; Park, Y. W.; Heeger, A. J.; Shirakawa, H.; Louis, E. J.; Gau, S. C.; MacDiarmid, A. G., Electrical conductivity in doped polyacetylene. *Physical Review Letters* **1977**, *39* (17), 1098-1101.
141. Saxman, A. M.; Liepins, R.; Aldissi, M., Polyacetylene : its synthesis, doping and structure. *Progress in Polymer Science* **1985**, *11* (1), 57-89.
142. Shirakawa, H.; Ikeda, S., Infrared spectra of poly(acetylene). *Polymer Journal* **1971**, *2* (2), 231-244.
143. Ito, T.; Shirakawa, H.; Ikeda, S., Thermal cis–trans isomerization and decomposition of polyacetylene. *Journal of Polymer Science : Polymer Chemistry Edition* **1975**, *13* (8), 1943-1950.

144. Shirakawa, H.; Ito, T.; Ikeda, S., Raman scattering and electronic spectra of poly(acetylene). *Polymer Journal* **1973**, *4* (4), 460-462.
145. Motoshige, A.; Mawatari, Y.; Yoshida, Y.; Seki, C.; Matsuyama, H.; Tabata, M., Irreversible helix rearrangement from cis-transoid to cis-cisoid in poly(p-n-hexyloxyphenylacetylene) induced by heat-treatment in solid phase. *Journal of Polymer Science Part A : Polymer Chemistry* **2012**, *50* (15), 3008-3015.
146. Motoshige, R.; Mawatari, Y.; Motoshige, A.; Yoshida, Y.; Sasaki, T.; Yoshimizu, H.; Suzuki, T.; Tsujita, Y.; Tabata, M., Mutual conversion between stretched and contracted helices accompanied by a drastic change in color and spatial structure of poly(phenylacetylene) prepared with a [Rh(nbd)Cl]₂-amine catalyst. *Journal of Polymer Science Part A : Polymer Chemistry* **2014**, *52* (6), 752-759.
147. Mawatari, Y.; Motoshige, A.; Yoshida, Y.; Motoshige, R.; Sasaki, T.; Tabata, M., Structural determination of stretched helix and contracted helix having yellow and red colors of poly(2-ethynyl-naphthalene) prepared with a [Rh(norbornadiene)Cl]₂-triethylamine catalyst. *Polymer* **2014**, *55* (10), 2356-2361.
148. Motoshige, A.; Mawatari, Y.; Yoshida, Y.; Motoshige, R.; Tabata, M., Synthesis and solid state helix to helix rearrangement of poly(phenylacetylene) bearing n-octyl alkyl side chains. *Polymer Chemistry* **2014**, *5* (3), 971-978.
149. Yamaguchi, I.; Osakada, K.; Yamamoto, T., Ruthenium complex catalyzed polymerization of OH or COOH group containing alkynes to give functionalized poly(acetylene)s. *Inorganica Chimica Acta* **1994**, *220* (1), 35-40.
150. Kirchner, K.; Calhorda, M. J.; Schmid, R.; Veiros, L. F., Mechanism for the cyclotrimerization of alkynes and related reactions catalyzed by CpRuCl. *Journal of The American Chemical Society* **2003**, *125* (38), 11721-11729.
151. Schuehler, D. E.; Williams, J. E.; Sponsler, M. B., Polymerization of acetylene with a ruthenium olefin metathesis catalyst. *Macromolecules* **2004**, *37* (17), 6255-6257.
152. Krause, J. O.; Zarka, M. T.; Anders, U.; Weberskirch, R.; Nuyken, O.; Buchmeiser, M. R., Simple synthesis of poly(acetylene) latex particles in aqueous media. *Angewandte Chemie International Edition* **2003**, *42* (48), 5965-5969.
153. Katsumata, T.; Shiotsuki, M.; Masuda, T., Polymerization of diphenylacetylenes with polar functional groups by the Grubbs-Hoveyda Ru carbene catalyst. *Macromolecular Chemistry and Physics* **2006**, *207* (14), 1244-1252.
154. Zhang, Y.; Wang, D.; Wurst, K.; Buchmeiser, M. R., Polymerization of phenylacetylene by novel Rh (I)-, Ir (I)- and Ru (IV) 1,3-R₂-3,4,5,6-tetrahydropyrimidin-2-ylidenes (R=mesityl, 2-propyl) : influence of structure on activity and polymer structure. *Journal of Organometallic Chemistry* **2005**, *690* (24), 5728-5735.

155. Kang, E.-H.; Yu, S. Y.; Lee, I. S.; Park, S. E.; Choi, T.-L., Strategies to enhance cyclopolymerization using third-generation Grubbs catalyst. *Journal of The American Chemical Society* **2014**, *136* (29), 10508-10514.
156. Masuda, T.; Zhang, A., Polymerization of substituted acetylenes. In *Handbook of metathesis*, Grubbs, R. H.; Wenzel, A. G.; O'Leary, D. J.; Khosravi, E., Eds. Wiley-VCH Verlag GmbH & Co. KGaA: Weinheim, DE, 2015; pp 375-390.
157. Masuda, T.; Hasegawa, K.-i.; Higashimura, T., Polymerization of phenylacetylenes. I. polymerization of phenylacetylene catalyzed by WCl_6 and $MoCl_5$. *Macromolecules* **1974**, *7* (6), 728-731.
158. Masuda, T.; Thieu, K.-Q.; Sasaki, N.; Higashimura, T., Polymerization of phenylacetylenes. 4. effects of tetraphenyltin and initiation mechanism in the WCl_6 -catalyzed polymerization. *Macromolecules* **1976**, *9* (4), 661-664.
159. Sasaki, N.; Masuda, T.; Higashimura, T., Polymerization of phenylacetylenes. 5. polymerization of phenylpropyne catalyzed by tungsten hexachloride-tetraphenyltin. *Macromolecules* **1976**, *9* (4), 664-667.
160. Balcar, H.; Pacovská, M., Pure WCl_4 -catalyst for polymerization of norbornene and monosubstituted acetylenes. *Journal of Molecular Catalysis A : Chemical* **1997**, *115* (1), 101-105.
161. Sedláček, J.; Pacovská, M.; Vohlídal, J.; Grubišić-Gallot, Z.; Žigon, M., Polymerization of phenylacetylene with $WOCl_4$ /tetraphenyltin catalyst in benzene/1,4-dioxane. synthesis of high-molecular-weight poly(phenylacetylene). *Macromolecular Chemistry and Physics* **1995**, *196* (5), 1705-1712.
162. Masuda, T.; Kawai, M.; Higashimura, T., Polymerization of propiolic acid and its derivatives catalysed by $MoCl_5$. *Polymer* **1982**, *23* (5), 744-747.
163. Masuda, T.; Fujimori, J. I.; Rahman, M. Z. A.; Higashimura, T., Living polymerization of [o-(trimethylsilyl)phenyl]acetylene by molybdenum-based three-component catalysts. *Polymer Journal* **1993**, *25* (5), 535-539.
164. Fox, H. H.; Wolf, M. O.; O'Dell, R.; Lin, B. L.; Schrock, R. R.; Wrighton, M. S., Living cyclopolymerization of 1,6-heptadiyne derivatives using well-defined alkylidene complexes : polymerization mechanism, polymer structure, and polymer properties. *Journal of The American Chemical Society* **1994**, *116* (7), 2827-2843.
165. Nakano, M.; Masuda, T.; Higashimura, T., Stereospecific living polymerization of tert-butylacetylene by molybdenum-based ternary catalyst systems. *Macromolecules* **1994**, *27* (6), 1344-1348.
166. Hayano, S.; Masuda, T., Living polymerization of [o-(trifluoromethyl)phenyl]acetylene by $WOCl_4$ -based catalysts such as $WOCl_4$ -n-Bu₄Sn-t-BuOH (1:1:1). *Macromolecules* **1999**, *32* (22), 7344-7348.

167. Gal, Y.-S.; Lee, W.-C.; Jin, S.-H.; Lee, H.-J.; Kim, S.-Y.; Kim, D.-W.; Ko, J.-M.; Chun, J.-H., Polymerisation of Acetylene Derivatives by Metallocene Catalysts: Polymerisation of Phenylacetylene by Bis(cyclopentadienyl)molybdenum Dichloride-based Catalyst System. *Journal of Macromolecular Science, Part A* **2001**, *38* (3), 263-279.
168. Minaki, N.; Hayano, S.; Masuda, T., Living polymerization of several substituted acetylenes by CpMoCl₄-based catalysts. *Polymer* **2002**, *43* (12), 3579-3583.
169. Matusiak, R.; Keller, A., Cyclotrimerization of phenylacetylene and living polymerization of tert-butylacetylene by Mo₂(O₂CCH₃)₄-Lewis acid systems. *Journal of Molecular Catalysis A : Chemical* **2003**, *195* (1), 29-35.
170. Masuda, T.; Yoshimura, T.; Higashimura, T., Living polymerization of 1-chloro-1-alkynes by MoOCl₄-n-Bu₄Sn-EtOH catalyst. *Macromolecules* **1989**, *22* (9), 3804-3806.
171. Misumi, Y.; Tamura, K.; Nakako, H.; Masuda, T., Metathesis polymerization of substituted acetylenes and norbornene by M(CO)₆-Ph₂CCl₂-hv (M=Mo, W) catalysts. *Polymer Journal* **1998**, *30* (7), 581-584.
172. Tamura, K.; Misumi, Y.; Masuda, T., M(CO)₆-RCl-hv catalysts (M = W, Mo; RCl= PhCCl₃, Ph₂CCl₂) : new catalyst systems for the metathesis polymerization of substituted acetylenes and cycloalkenes. *Chemical Communications* **1996**, *1996* (3), 373-374.
173. Masuda, T., Substituted polyacetylenes : synthesis, properties, and functions. *Polymer Reviews* **2017**, *57* (1), 1-14.
174. Kawasaki, M.; Masuda, T.; Higashimura, T., Polymerization of 6-Bromo-1-hexyne and 1,6-Dibromo-1-hexyne. *Polymer Journal* **1983**, *15* (10), 767-770.
175. Vosloo, H. C. M.; du Plessis, J. A. K., Influence of temperature and phenol on the polymerization of phenylacetylene catalyzed by Mo(CO)₆. *Journal of Molecular Catalysis* **1993**, *79* (1), 7-12.
176. Vosloo, H. C. M.; du Plessis, J. A. K., Polymerization of phenylacetylene catalyzed by Mo(CO)₆. *Polymer Bulletin* **1993**, *30* (3), 273-278.
177. van Schalkwyk, C.; Vosloo, H. C. M.; du Plessis, J. A. K., W(O-2,6-C₆H₃X₂)₂Cl₄/Bu₄Sn as metathesis catalyst of 1-alkenes. *Journal of Molecular Catalysis A : Chemical* **1998**, *133* (1), 167-173.
178. Szymańska-Buzar, T.; Głowiak, T., Synthesis and reactivity of Mo-Sn compounds : X-ray crystal structure of a novel [Mo(SnCl₃)₂(CO)₂(NC₂H₅)₃]. *Journal of Organometallic Chemistry* **1999**, *575* (1), 98-107.

179. Tamura, K.; Masuda, T.; Higashimura, T., Polymerization of substituted acetylenes by (mesitylene)M(CO)₃ (M=W, Mo). *Polymer Bulletin* **1993**, *30* (5), 537-544.
180. Nakako, H.; Misumi, Y.; Masuda, T.; Bencze, L.; Szalai, G., Novel group 6 transition metal catalysts, MCl₂(CO)₃(AsPh₃)₂ (M=W, Mo), for the metathesis polymerization of substituted acetylenes. *Polymer Journal* **1998**, *30* (7), 577-580.
181. Xu, K.; Peng, H.; Lam, J. W. Y.; Poon, T. W. H.; Dong, Y.; Xu, H.; Sun, Q.; Cheuk, K. K. L.; Salhi, F.; Lee, P. P. S.; Tang, B. Z., Transition metal carbonyl catalysts for polymerizations of substituted acetylenes. *Macromolecules* **2000**, *33* (19), 6918-6924.
182. Czeluśniak, I.; Szymańska-Buzar, T.; Kenwright, A.; Khosravi, E., Ring-opening metathesis polymerization of 5,6-bis(chloromethyl)-norbornene by tungsten(II) and molybdenum(II) complexes. *Catalysis Letters* **2002**, *81* (3), 157-161.
183. Schrock, R. R.; Luo, S.; Zanetti, N. C.; Fox, H. H., Living polymerization of (o-(trimethylsilyl)phenyl)acetylene using "small alkoxide" molybdenum(VI) initiators. *Organometallics* **1994**, *13* (9), 3396-3398.
184. Schrock, R. R.; Luo, S.; Lee, J. C.; Zanetti, N. C.; Davis, W. M., Living polymerization of (o-(trimethylsilyl)phenyl)acetylene by molybdenum imido alkylidene complexes. *Journal of The American Chemical Society* **1996**, *118* (16), 3883-3895.
185. Fox, H. H.; Schrock, R. R., Living cyclopolymerization of diethyl dipropargylmalonate by Mo(CH-t-Bu)(NAr)[OCMe(CF₃)₂]₂ in dimethoxyethane. *Organometallics* **1992**, *11* (8), 2763-2765.
186. Schattenmann, F. J.; Schrock, R. R.; Davis, W. M., Preparation of biscarboxylato imido alkylidene complexes of molybdenum and cyclopolymerization of diethyldipropargylmalonate to give a polyene containing only six-membered rings. *Journal of The American Chemical Society* **1996**, *118* (13), 3295-3296.
187. Masuda, T.; Niki, A.; Isobe, E.; Higashimura, T., Effect of organometallic cocatalysts on the polymerization of 1-phenyl-1-propyne by tantalum pentachloride (TaCl₅) and niobium pentachloride (NbCl₅). *Macromolecules* **1985**, *18* (11), 2109-2113.
188. Niki, A.; Masuda, T.; Higashimura, T., Effects of organometallic cocatalysts on the polymerization of disubstituted acetylenes by TaCl₅ and NbCl₅. *Journal of Polymer Science Part A : Polymer Chemistry* **1987**, *25* (6), 1553-1562.
189. Fujimori, J. I.; Masuda, T.; Higashimura, T., Synthesis of poly[1-(trimethylsilyl)-1-propyne] with a narrow molecular weight distribution by using NbCl₅ catalyst in cyclohexane. *Polymer Bulletin* **1988**, *20* (1), 1-6.

190. Tachimori, H.; Masuda, T., Synthesis and properties of a poly(diphenylacetylene) containing carbazolyl groups. *Journal of Polymer Science Part A : Polymer Chemistry* **1995**, *33* (12), 2079-2085.
191. Nagai, K.; Masuda, T.; Nakagawa, T.; Freeman, B. D.; Pinnau, I., Poly[1-(trimethylsilyl)-1-propyne] and related polymers: synthesis, properties and functions. *Progress in Polymer Science* **2001**, *26* (5), 721-798.
192. Furlani, A.; Licoccia, S.; Russo, M. V.; Camus, A.; Marsich, N., Rhodium and platinum complexes as catalysts for the polymerization of phenylacetylene. *Journal of Polymer Science Part A : Polymer Chemistry* **1986**, *24* (5), 991-1005.
193. Furlani, A.; Napoletano, C.; Russo, M. V.; Feast, W. J., Stereoregular polyphenylacetylene. *Polymer Bulletin* **1986**, *16* (4), 311-317.
194. Furlani, A.; Napoletano, C.; Russo, M. V.; Camus, A.; Marsich, N., The influence of the ligands on the catalytic activity of a series of RhI complexes in reactions with phenylacetylene: Synthesis of stereoregular poly(phenyl) acetylene. *Journal of Polymer Science Part A : Polymer Chemistry* **1989**, *27* (1), 75-86.
195. Kern, R. J., Preparation and properties of isomeric polyphenylacetylenes. *Journal of Polymer Science Part A-1: Polymer Chemistry* **1969**, *7* (2), 621-631.
196. Yang, W.; Tabata, M.; Kobayashi, S.; Yokota, K.; Shimizu, A., Synthesis of ultra-high-molecular-weight aromatic polyacetylenes with [Rh(norbornadiene)Cl]₂-triethylamine and solvent-induced crystallization of the obtained amorphous polyacetylenes. *Polymer Journal* **1991**, *23* (9), 1135-1138.
197. Tabata, M.; Yang, W.; Yokota, K., ¹H-NMR and UV studies of Rh complexes as a stereoregular polymerization catalysts for phenylacetylenes : effects of ligands and solvents on its catalyst activity. *Journal of Polymer Science Part A : Polymer Chemistry* **1994**, *32* (6), 1113-1120.
198. Rodríguez, J. G.; Lafuente, A.; Arranz, J., Synthesis and polymerization of (*E*)-p-[(*p*-methoxyphenyl)-2-ethenyl]phenylacetylene with Ziegler–Natta, rhodium, and palladium complexes. *Journal of Polymer Science Part A : Polymer Chemistry* **2005**, *43* (24), 6438-6444.
199. Tabata, M.; Sone, T.; Sadahiro, Y.; Yang, W.; Kobayashi, S.; Inaba, Y.; Yokota, K., Synthesis of Columnar Polyacetylenes by Rh Complex Catalyst. *Japanese Journal of Polymer Science and Technology* **1997**, *54* (12), 863-874.
200. Kanki, K.; Misumi, Y.; Masuda, T., Remarkable cocatalytic effect of organometallics and rate control by triphenylphosphine in the Rh-catalyzed polymerization of phenylacetylene. *Macromolecules* **1999**, *32* (7), 2384-2386.
201. Kong, X.; Lam, J. W. Y.; Tang, B. Z., Synthesis, mesomorphism, isomerization, and aromatization of stereoregular poly{[4-({[6-({[4'-(heptyl)oxy-4-biphenyl]carbonyl}oxy)-hexyl]oxy}carbonyl)phenyl]acetylene}. *Macromolecules* **1999**, *32* (6), 1722-1730.

202. Karim, S. M. A.; Nomura, R.; Masuda, T., Synthesis and properties of poly(phenylacetylene)s with pendant imino groups. *Polymer Bulletin* **1999**, *43* (4), 305-310.
203. Xu, H.; Tang, B. Z., Syntheses and optical properties of poly(C₆₀-Co-phenylacetylene)s. *Journal of Macromolecular Science Part A* **2007**, *A36* (9), 1197-1207.
204. Nishimura, T.; Ohsawa, S.; Maeda, K.; Yashima, E., A helical array of pendant fullerenes on a helical poly(phenylacetylene) induced by non-covalent chiral interactions. *Chemical Communications* **2004**, *2004* (6), 646-647.
205. Hori, H.; Six, C.; Leitner, W., Rhodium-catalyzed phenylacetylene polymerization in compressed carbon dioxide. *Macromolecules* **1999**, *32* (10), 3178-3182.
206. Kwak, G.; Masuda, T., Synthesis, chiroptical properties, and high gas permeability of poly(phenylacetylene) with bulky chiral silyl groups. *Macromolecules* **2000**, *33* (18), 6633-6635.
207. Sedláček, J.; Pacovská, M.; Rádová, D.; Balcar, H.; Biffis, A.; Corain, B.; Vohlídal, J., Polybenzimidazole-supported [Rh(cod)Cl]₂ complex : effective catalyst for the polymerization of substituted acetylenes. *Chemistry : A European Journal* **2002**, *8* (2), 366-371.
208. Balcar, H.; Sedláček, J.; Svoboda, J.; Žilková, N.; Rathousky, J.; Vohlídal, J., Hybrid catalysts for acetylenes polymerization prepared by anchoring [Rh(cod)Cl]₂ on MCM-41, MCM-48 and SBA-15 mesoporous molecular sieves - the effect of support structure on catalytic activity in polymerization of phenylacetylene and 4-ethynyl-N-{4-[(trimethylsilyl)ethynyl]benzylidene}aniline. *Collection of Czechoslovak Chemical Communications* **2003**, *68* (10), 1861-1876.
209. Balcar, H.; Čejka, J.; Sedláček, J.; Svoboda, J.; Zedník, J.; Bastl, Z.; Bosáček, V. r.; Vohlídal, J., [Rh(cod)Cl]₂ complex immobilized on mesoporous molecular sieves MCM-41-a new hybrid catalyst for polymerization of phenylacetylene. *Journal of Molecular Catalysis A : Chemical* **2003**, *203* (1), 287-298.
210. Zhang, L.; Cao, Q.; Gao, F.; Dong, Y.; Li, X., Self-supported rhodium catalysts based on a microporous metal-organic framework for polymerization of phenylacetylene and its derivatives. *Polymer Chemistry* **2020**, *11* (16), 2904-2913.
211. Lai, L. M.; Lam, J. W. Y.; Qin, A.; Dong, Y.; Tang, B. Z., Synthesis, helicity, and chromism of optically active poly(phenylacetylene)s carrying different amino acid moieties and pendant terminal groups. *The Journal of Physical Chemistry B* **2006**, *110* (23), 11128-11138.
212. Lam, J. W. Y.; Lai, L. M.; Tang, B. Z., Synthesis, liquid crystallinity, and chiroptical properties of sterol-containing polyacetylenes. *Proceedings of SPIE : The International Society for Optical Engineering* **2006**, *6332*, 1-10.

213. Li, B.; Cheuk, K.; Ling, L.-S.; Chen, J.; Xiao, X.; Bai, C.-L.; Tang, B., Synthesis and hierarchical structures of amphiphilic polyphenylacetylenes carrying L-valine pendants. *Macromolecules* **2003**, *36* (1), 77-85.
214. Lai, L. M.; Lam, J. W. Y.; Tang, B. Z., Synthesis and chiroptical properties of L-valine-containing poly(phenylacetylene)s with (a)chiral pendant terminal groups. *Journal of Polymer Science Part A : Polymer Chemistry* **2006**, *44* (6), 2117-2129.
215. Sato, T.; Aoki, T.; Teraguchi, M.; Kaneko, T.; Kim, S.-Y., Role of chiral amine cocatalysts in the helix-sense-selective polymerization of a phenylacetylene using a catalytic system. *Polymer* **2004**, *45* (24), 8109-8114.
216. Lai, L. M.; Lam, J. W. Y.; Cheuk, K. K. L.; Sung, H. H. Y.; Williams, I. D.; Tang, B. Z., Optically active polyacetylene : synthesis and helical conformation of a poly(phenylacetylene) carrying L-alanyl-L-alanine pendants. *Journal of Polymer Science Part A : Polymer Chemistry* **2005**, *43* (16), 3701-3706.
217. Chen, J.; Cheuk, K. K.-L.; Tang, B. Z., Synthesis and characterization of poly(phenylacetylene)s carrying oligo(ethylene oxide) pendants. *Journal of Polymer Science Part A : Polymer Chemistry* **2006**, *44* (3), 1153-1167.
218. Aoki, T.; Kaneko, T.; Maruyama, N.; Sumi, A.; Takahashi, M.; Sato, T.; Teraguchi, M., Helix-sense-selective polymerization of phenylacetylene having two hydroxy groups using a chiral catalytic system. *Journal of The American Chemical Society* **2003**, *125* (21), 6346-6347.
219. Nonokawa, R.; Oobo, M.; Yashima, E., Helicity induction on a poly(phenylacetylene) derivative bearing aza-15-crown-5 ether pendants in organic solvents and water. *Macromolecules* **2003**, *36* (17), 6599-6606.
220. Maeda, K.; Kamiya, N.; Yashima, E., Poly(phenylacetylene)s bearing a peptide pendant : helical conformational changes of the polymer backbone stimulated by the pendant conformational change. *Chemistry : A European Journal* **2004**, *10* (16), 4000-4010.
221. Maeda, K.; Tamaki, S.; Tamura, K.; Yashima, E., Helicity induction and memory of the macromolecular helicity in a polyacetylene bearing a biphenyl pendant. *Chemistry : An Asian Journal* **2008**, *3* (3), 614-624.
222. Kobayashi, S.; Itomi, K.; Morino, K.; Iida, H.; Yashima, E., Polymerization of an optically active phenylacetylene derivative bearing an azide residue by click reaction and reaction with a rhodium catalyst. *Chemical Communications* **2008**, *2008* (26), 3019-3021.
223. Kawamura, H.; Takeyama, Y.; Yamamoto, M.; Kurihara, H.; Morino, K.; Yashima, E., Chirality responsive helical poly(phenylacetylene) bearing L-proline pendants. *Chirality* **2011**, *23* (1E), E35-E42.

224. Onimura, K.; Shintaku, K.; Rattanatraicharoen, P.; Yamabuki, K.; Oishi, T., Asymmetric polymerizations of chiral 4-benzyl-2-ethynylloxazoline with rhodium catalyst and chiroptical properties of the polymers. *Chirality* **2011**, *23* (1E), E43-E51.
225. Rattanatraicharoen, P.; Shintaku, K.; Yamabuki, K.; Oishi, T.; Onimura, K., Synthesis and chiroptical properties of helical poly(phenylacetylene) bearing optically active chiral oxazoline Pendants. *Polymer* **2012**, *53* (13), 2567-2573.
226. Tang, Z.; Iida, H.; Hu, H.-Y.; Yashima, E., Remarkable enhancement of the enantioselectivity of an organocatalyzed asymmetric Henry reaction assisted by helical poly(phenylacetylene)s bearing cinchona alkaloid pendants via an amide linkage. *American Chemical Society Macro Letters* **2012**, *1* (2), 261-265.
227. Teraguchi, M.; Tanioka, D.; Kaneko, T.; Aoki, T., Helix-sense-selective polymerization of achiral phenylacetylenes with two N-alkylamide groups to generate the one-handed helical polymers stabilized by intramolecular hydrogen bonds. *American Chemical Society Macro Letters* **2012**, *1* (11), 1258-1261.
228. Abe, Y.; Aoki, T.; Jia, H.; Hadano, S.; Namikoshi, T.; Kakihana, Y.; Liu, L.; Zang, Y.; Teraguchi, M.; Kaneko, T., Chiral teleinduction in asymmetric polymerization of 3,5-bis(hydroxymethyl)phenylacetylene having a chiral group via a very long and rigid spacer at 4-position. *Chemistry Letters* **2012**, *41* (3), 244-246.
229. Sakurai, S.-i.; Ohira, A.; Suzuki, Y.; Fujito, R.; Nishimura, T.; Kunitake, M.; Yashima, E., Synthesis and property of helical poly(phenylacetylene)s bearing chiral ruthenium complexes and real space imaging of meso- and nanoscopic structures by atomic force microscopy. *Journal of Polymer Science Part A : Polymer Chemistry* **2004**, *42* (18), 4621-4640.
230. Schniedermeier, J.; Haupt, H. J., New rhodium(I)- π -chelate complexes with coordinated amidine bases (dbu,dbn) and their catalytic properties to polymerize phenylacetylene. *Journal of Organometallic Chemistry* **1996**, *506* (1), 41-47.
231. Vilar, R.; Salcedo, R.; Gaviño, R.; Ogawa, T., Polymerization of phenylacetylene with Di- μ -pentafluorothiophenolate bis (1,5-cyclooctadiene) rhodium (I) and its analogues. *European Polymer Journal* **1994**, *30* (11), 1237-1242.
232. Escudero, A.; Vilar, R.; Salcedo, R.; Ogawa, T., Effects of substituent groups and substituted benzenes on the polymerization of phenylacetylenes initiated by di- μ -pentafluorothiophenolate bis(1,5-cyclooctadiene) rhodium(I). *European Polymer Journal* **1995**, *31* (11), 1135-1138.
233. Goldberg, Y.; Alper, H., Polymerisation of phenylacetylene catalysed by a zwitterionic rhodium(I) complex under hydrosilylation conditions. *Journal of the Chemical Society : Chemical Communications* **1994**, *1994* (10), 1209-1210.
234. Simionescu, C. I.; Percec, V.; Dumitrescu, S., Polymerization of acetylenic derivatives. XXX. isomers of polyphenylacetylene. *Journal of Polymer Science Part A : Polymer Chemistry* **1977**, *15* (10), 2497-2509.

235. Simionescu, C. I.; Percec, V., Thermal *cis*–*trans* isomerization of *cis*–*transoidal* polyphenylacetylene. *Journal of Polymer Science : Polymer Chemistry Edition* **1980**, *18* (1), 147-155.
236. Percec, V.; Rudick, J. G.; Nombel, P.; Buchowicz, W., Dramatic decrease of the *cis* content and molecular weight of *cis*–*transoidal* polyphenylacetylene at 23 °C in solutions prepared in air. *Journal of Polymer Science Part A: Polymer Chemistry* **2002**, *40* (19), 3212-3220.
237. Percec, V.; Rudick, J. G.; Peterca, M.; Wagner, M.; Obata, M.; Mitchell, C. M.; Cho, W.-D.; Balagurusamy, V. S. K.; Heiney, P. A., Thermoreversible *cis*–*cisoidal* to *cis*–*transoidal* isomerization of helical dendronized polyphenylacetylenes. *Journal of The American Chemical Society* **2005**, *127* (43), 15257-15264.
238. Tobiszewski, M.; Namieśnik, J.; Pena-Pereira, F., Environmental risk-based ranking of solvents using the combination of a multimedia model and multi-criteria decision analysis. *Green Chemistry* **2017**, *19* (4), 1034-1042.
239. Mastrorilli, P.; Nobile, C. F.; Gallo, V.; Suranna, G. P.; Farinola, G., Rhodium(I) catalyzed polymerization of phenylacetylene in ionic liquids. *Journal of Molecular Catalysis A : Chemical* **2002**, *184* (1), 73-78.
240. Trzeciak, A. M.; Ziółkowski, J. J., Polymerization of phenylacetylene catalysed by RhTp(cod) and RhBp(cod) in ionic liquids : effect of alcohols and of tetraammonium halides. *Applied Organometallic Chemistry* **2004**, *18* (3), 124-129.
241. Katayama, H.; Yamamura, K.; Miyaki, Y.; Ozawa, F., Stereoregular polymerization of phenylacetylenes catalyzed by [hydridotris(pyrazolyl)borato]rhodium(I) complexes. *Organometallics* **1997**, *16* (20), 4497-4500.
242. Kanki, K.; Nakazato, A.; Nomura, R.; Sanda, F.; Masuda, T., Polymerization of substituted phenylacetylenes with a novel, water-soluble Rh–vinyl complex in water. *Journal of Polymer Science Part A : Polymer Chemistry* **2004**, *42* (9), 2100-2105.
243. Misumi, Y.; Masuda, T., Living polymerization of phenylacetylene by novel rhodium catalysts. quantitative initiation and introduction of functional groups at the initiating chain end. *Macromolecules* **1998**, *31* (21), 7572-7573.
244. Zhang, P.; Wang, H.; Shi, X.; Yan, X.; Wu, X.; Zhang, S.; Yao, B.; Feng, X.; Zhi, J.; Li, X.; Tong, B.; Shi, J.; Wang, L.; Dong, Y., On-water polymerization of phenylacetylene catalyzed by Rh complexes bearing strong π -acidic dibenzo[a,e]cyclooctatetraene ligand. *Journal of Polymer Science Part A : Polymer Chemistry* **2017**, *55* (4), 716-725.
245. Ruman, T.; Ciunik, Z.; Trzeciak, A. M.; Wołowicz, S.; Ziółkowski, J. J., Complexes of heteroscorpionate trispyrazolylborate ligands. part 10. structures and fluxional behavior of rhodium(I) complexes with heteroscorpionate

trispyrazolylborate ligands, Tp' 'Rh(LL) (LL = (CO)₂ or COD). *Organometallics* **2003**, 22 (5), 1072-1080.

246. Yao, J.; Wong, W. T.; Jia, G., Preparation of some dinuclear rhodium complexes with the orthometallated ligand [2,6-(PPh₂CH₂)₂C₆H₃]⁻ and their catalytic activity for polymerization of phenylacetylene. *Journal of Organometallic Chemistry* **2000**, 598 (2), 228-234.

247. Reddy, K. R.; Lin, C.-F.; Lee, G.-H.; Peng, S.-M.; Chen, J.-T.; Liu, S.-T., Cationic phosphine-imine podium(I) complexes and their activity on catalysis of phenylacetylene polymerization. *Journal of The Chinese Chemical Society* **2001**, 48 (6A), 997-1002.

248. Gil, W.; Lis, T.; Trzeciak, A. M.; Ziółkowski, J. J., Structure and catalytic activity of rhodium(I) carbene complexes in polymerization of phenylacetylene. *Inorganica Chimica Acta* **2006**, 359 (9), 2835-2841.

249. Gil, W.; Trzeciak, A. M.; Ziółkowski, J. J., Catalytic polymerization of phenylacetylene with dimeric [Rh(OMe)(cod)]₂ complex in ionic liquids. *Applied Organometallic Chemistry* **2006**, 20 (11), 766-770.

250. Gott, A. L.; McGowan, P. C.; Temple, C. N., Controlling the coordination mode of 1,4,7-triazacyclononane complexes of rhodium and iridium and evaluating their behavior as phenylacetylene polymerization catalysts. *Organometallics* **2008**, 27 (12), 2852-2860.

251. Jiménez, M. V.; Pérez-Torrente, J. J.; Bartolomé, M. I.; Vispe, E.; Lahoz, F. J.; Oro, L. A., Cationic rhodium complexes with hemilabile phosphine ligands as polymerization catalyst for high molecular weight stereoregular poly(phenylacetylene). *Macromolecules* **2009**, 42 (21), 8146-8156.

252. Angoy, M.; Jiménez, M. V.; Modrego, F. J.; Oro, L. A.; Passarelli, V.; Pérez-Torrente, J. J., Mechanistic investigation on the polymerization of phenylacetylene by 2-diphenylphosphinopyridine rhodium(I) catalysts: understanding the role of the cocatalyst and alkynyl intermediates. *Organometallics* **2018**, 37 (16), 2778-2794.

253. Wu, X.; Zhang, P.; Yang, Z.; Zhang, S.; Liu, H.; Chi, W.; Li, X.; Dong, Y.; Qiu, N.; Yan, L., Polymerization of phenylacetylenes by binuclear rhodium catalysts with different para-binucleating phenoxyiminato linkages. *Polymer chemistry* **2019**, 10 (30), 4163-4172.

254. Kishimoto, Y.; Eckerle, P.; Miyatake, T.; Ikariya, T.; Noyori, R., Living polymerization of phenylacetylenes initiated by Rh(C≡CC₆H₅)(2,5-norbornadiene)[P(C₆H₅)₃]₂. *Journal of The American Chemical Society* **1994**, 116 (26), 12131-12132.

255. Kishimoto, Y.; Miyatake, T.; Ikariya, T.; Noyori, R., An efficient rhodium(I) initiator for stereospecific living polymerization of phenylacetylenes. *Macromolecules* **1996**, 29 (14), 5054-5055.

256. Kishimoto, Y.; Eckerle, P.; Miyatake, T.; Kainosho, M.; Ono, A.; Ikariya, T.; Noyori, R., Well-controlled polymerization of phenylacetylenes with organorhodium(I) complexes : mechanism and structure of the polyenes. *Journal of The American Chemical Society* **1999**, *121* (51), 12035-12044.
257. Kumazawa, S.; Rodriguez Castanon, J.; Onishi, N.; Kuwata, K.; Shiotsuki, M.; Sanda, F., Characterization of the polymerization catalyst [(2,5-norbornadiene)Rh{C(Ph)=CPh₂}(PPh₃)] and identification of the end structures of poly(phenylacetylenes) obtained by polymerization using this catalyst. *Organometallics* **2012**, *31* (19), 6834-6842.
258. Kanki, K.; Misumi, Y.; Masuda, T., Synthesis of poly(phenylacetylene)-block-poly(b-propiolactone) by use of Rh-catalyzed living polymerization of phenylacetylene. *Inorganica Chimica Acta* **2002**, *336*, 101-104.
259. Misumi, Y.; Kanki, K.; Miyake, M.; Masuda, T., Living Polymerization of Phenylacetylene by Rhodium-based Ternary Catalysts, (Diene)Rh(I) Complex/Vinylolithium/Phosphorous Ligand. Effect of Catalyst Components. *Macromol. Chem. Phys.* **2000**, *201*, 2239-2244.
260. Kanki, K.; Masuda, T., Synthesis of conjugated star polymer and star block copolymers based on the living polymerization of phenylacetylenes with a Rh catalyst. *Macromolecules* **2003**, *36* (5), 1500-1504.
261. Miyake, M.; Misumi, Y.; Masuda, T., Living polymerization of phenylacetylene by isolated rhodium complexes, Rh[C(C₆H₅)=C(C₆H₅)₂](nbd)(4-XC₆H₄)₃P (X = F, Cl). *Macromolecules* **2000**, *33* (18), 6636-6639.
262. Kumazawa, S.; Rodriguez Castanon, J.; Shiotsuki, M.; Sato, T.; Sanda, F., Chirality amplification in helical block copolymers. synthesis and chiroptical properties of block copolymers of chiral/achiral acetylene monomers. *Polymer Chemistry* **2015**, *6* (32), 5931-5939.
263. Liu, L.; Zhang, G.; Aoki, T.; Wang, Y.; Kaneko, T.; Teraguchi, M.; Zhang, C.; Dong, H., Synthesis of One-Handed Helical Block Copoly(substituted acetylene)s Consisting of Dynamic *cis-transoidal* and Static *cis-cisoidal* Block: Chiral Teleinduction in Helix-Sense-Selective Polymerization Using a Chiral Living Polymer as an Initiator. *ACS Macro Letts.* **2016**, *5*, 1381-1385.
264. Onishi, N.; Shiotsuki, M.; Masuda, T.; Sano, N.; Sanda, F., Polymerization of Phenylacetylenes Using Rhodium Catalysts Coordinated by Norbornadiene Linked to a Phosphino or Amino Group. *Organometallics* **2013**, *32*, 846-853.
265. Onishi, N.; Shiotsuki, M.; Masuda, T.; Sano, N.; Sanda, F., Polymerization of phenylacetylenes using rhodium catalysts coordinated by norbornadiene linked to a phosphino or amino group. *Organometallics* **2013**, *32* (3), 846-853.
266. Saeed, I.; Shiotsuki, M.; Masuda, T., Effect of Diene Ligands in the Rhodium-Catalyzed Polymerization of Phenylacetylene. *Macromolecules* **2006**, *39*, 8977-8981.

267. Saeed, I.; Shiotsuki, M.; Masuda, T., Living polymerization of phenylacetylene with tetrafluorobenzobarrelene ligand-containing rhodium catalyst systems featuring the synthesis of high molecular weight polymer. *Macromolecules* **2006**, *39* (25), 8567-8573.
268. Onishi, N.; Shiotsuki, M.; Sanda, F.; Masuda, T., Polymerization of phenylacetylenes with rhodium zwitterionic complexes : enhanced catalytic activity by p-acidic diene ligands. *Macromolecules* **2009**, *42* (12), 4071-4076.
269. Shiotsuki, M.; Onishi, N.; Sanda, F.; Masuda, T., Living polymerization of phenylacetylenes catalyzed by cationic rhodium complexes bearing tetrafluorobenzobarrelene. *Polymer Journal* **2011**, *43* (1), 51-57.
270. Taniguchi, T.; Yoshida, T.; Echizen, K.; Takayama, K.; Nishimura, T.; Maeda, K., Facile and versatile synthesis of end-functionalized poly(phenylacetylene)s: a multicomponent catalytic system for well-controlled living polymerization of phenylacetylenes. *Angewandte Chemie International Edition* **2020**, *59* (22), 8670-8680.
271. Zhang, W.; Tabei, J.; Shiotsuki, M.; Masuda, T., Synthesis of poly(propargyl esters) with rhodium catalysts and their characterization. *Polymer Bulletin* **2006**, *57* (4), 463-472.
272. Sanda, F.; Terada, K.; Masuda, T., Synthesis, chiroptical properties, and pH responsibility of aspartic acid- and glutamic acid-based helical polyacetylenes. *Macromolecules* **2005**, *38* (20), 8149-8154.
273. Sanda, F.; Araki, H.; Masuda, T., Serine-based helical polyacetylenes. effect of hydroxyl group on the secondary structure. *Macromolecules* **2005**, *38* (25), 10605-10608.
274. Sanda, F.; Araki, H.; Masuda, T., Synthesis and properties of serine- and threonine-based helical polyacetylenes. *Macromolecules* **2004**, *37* (23), 8510-8516.
275. Gao, G.; Sanda, F.; Masuda, T., Synthesis and properties of amino acid-based polyacetylenes. *Macromolecules* **2003**, *36* (11), 3932-3937.
276. Nakazato, A.; Saeed, I.; Shiotsuki, M.; Sanda, F.; Masuda, T., Polymerization of *N*-propargylamides with a Rh-vinyl complex : confirmation of the presence of long-lived active species. *Macromolecules* **2004**, *37* (11), 4044-4047.
277. Yashima, E.; Maeda, K.; Iida, H.; Furusho, Y.; Nagai, K., Helical polymers : synthesis, structures, and functions. *Chemical Reviews* **2009**, *109* (11), 6102-6211.
278. Schwartz, E.; Koepf, M.; Kitto, H. J.; Nolte, R. J. M.; Rowan, A. E., Helical poly(isocyanides): past, present and future. *Polymer Chemistry* **2011**, *2* (1), 33-47.
279. Asaoka, S.; Joza, A.; Minagawa, S.; Song, L.; Suzuki, Y.; Iyoda, T., Fast Controlled Living Polymerization of Arylisocyanide Initiated by Aromatic

Nucleophile Adduct of Nickel Isocyanide Complex. *ACS Macro Letters* **2013**, 2 (10), 906-911.

280. Xue, Y.-X.; Chen, J.-L.; Jiang, Z.-Q.; Yu, Z.; Liu, N.; Yin, J.; Zhu, Y.-Y.; Wu, Z.-Q., Living polymerization of arylisocyanide initiated by the phenylethynyl palladium(II) complex. *Polymer Chemistry* **2014**, 5 (22), 6435-6438.

281. Yamamoto, M.; Onitsuka, K.; Takahashi, S., Polymerization of aryl isocyanides possessing bulky substituents at an *ortho* position initiated by organorhodium complexes. *Organometallics* **2000**, 19 (23), 4669-4671.

282. Onitsuka, K.; Yamamoto, M.; Mori, T.; Takei, F.; Takahashi, S., Living polymerization of bulky aryl isocyanide with arylrhodium complexes. *Organometallics* **2006**, 25 (5), 1270-1278.

283. Onitsuka, K.; Mori, T.; Yamamoto, M.; Takei, F.; Takahashi, S., Helical Sense Selective Polymerization of Bulky Aryl Isocyanide Possessing Chiral Ester or Amide Groups Initiated by Arylrhodium Complexes. *Macromolecules* **2006**, 39, 7224-7231.

284. Misumi, Y.; Kanki, K.; Miyake, M.; Masuda, T., Living polymerization of phenylacetylene by rhodium-based ternary catalysts, (diene)Rh(I) complex/vinyl lithium/phosphorous ligand. effect of catalyst components. *Macromolecular Chemistry and Physics* **2000**, 201 (17), 2239-2244.

Every reasonable effort has been made to acknowledge the owners of copyright material. I would be pleased to hear from any copyright owner who has been omitted or incorrectly acknowledged.

Chapter 2

Synthesis, Characterisation and Evaluation of Rh(I)- α -Phenylvinylfluorenyl Complexes as Initiators in the Controlled Polymerisations of Phenylacetylene

The content of this chapter has been published in:

European Journal of Inorganic Chemistry (2019) with the title “Rh(I)- α -Phenylvinylfluorenyl Complexes: Synthesis, Characterisation and Evaluation as Initiators in the Stereospecific Polymerisation of Phenylacetylene” (refer to Appendix C)

2.1 Introduction

There is growing interest in the (co)polymerisation of phenylacetylene (PA), and functional derivatives thereof, by rhodium-based catalysts. The literature describing the preparation and characterisation of poly(phenylacetylene)s (PPAs) is extensive due, in part, to their ease of handling, low oxophilicity of Rh catalysts, good functional group compatibility, combined with the stability and processability of the resulting PA (co)polymers. The literature contains a considerable volume of reports of rhodium-based catalysts that mediate the non-controlled polymerisation of PAs and their functional derivatives; however, there is a paucity of literature pertaining to the stereospecific controlled (co)polymerisation of this important monomer class.

The first reported controlled, stereospecific, homopolymerisation of PA by a rhodium-catalyst system was reported by Kishimoto and co-workers employing **76**, Figure 2-1,¹ which mediated the (co)polymerisation in a controlled fashion (as judged by size exclusion chromatography (SEC) data and the ability to prepare block copolymers via sequential monomer addition using an isolated PPA homopolymer with active chain ends) although the initiation efficiencies (IEs) were not quantitative and ranged from 33 – 56 %. The same group then expanded upon this seminal contribution and reported a non-isolable tetracoordinate Rh species, **77**, which polymerised PA at the feed ratio of 1:50, with a higher initiation efficiency (72 %) than **76**, and afforded PPA bearing a head-to-tail *cis-transoidal* configuration.²

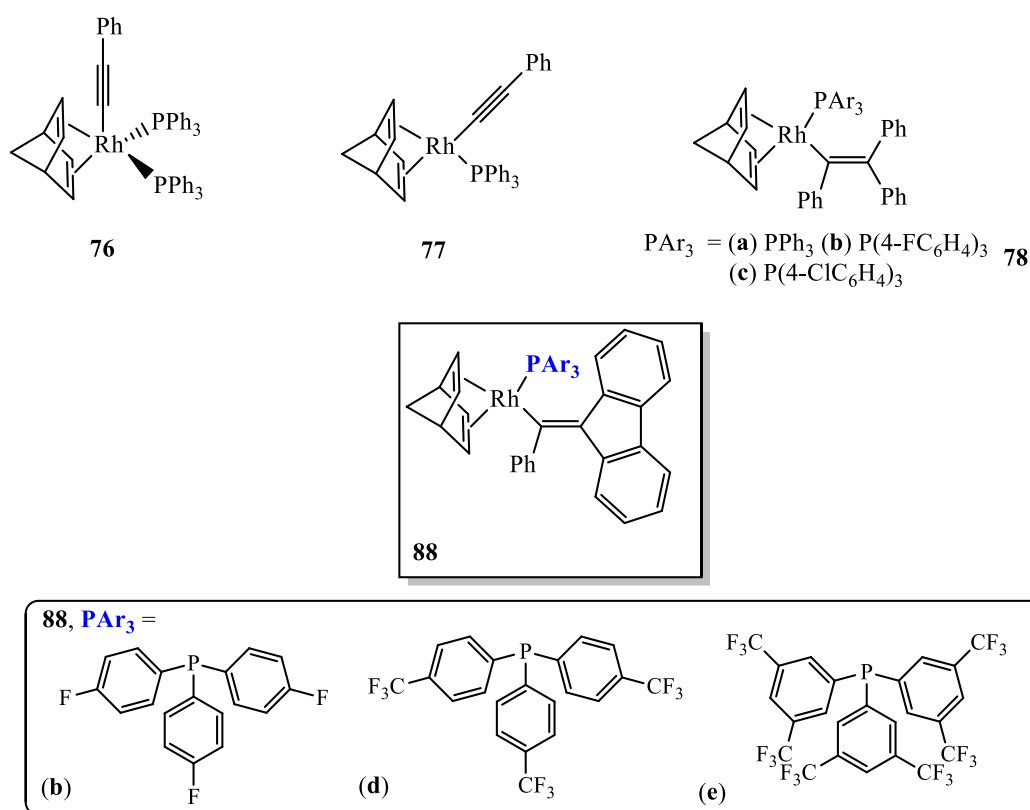


Figure 2-1. Chemical structures of Noyori's Rh(I)-phenylethynyl derivatives (**76** and **77**), Masuda's Rh(I)triphenylvinyl species (**78a**, **78b**, **78c**) and new fluorous- α -phenylvinylfluorenyl Rh(I) complexes (**88b**, **88d** and **88e**).

Inferring that polymerisation proceeded via a tetracoordinate vinylrhodium species generated *in situ*, Misumi and Masuda reported a novel ternary Rh catalyst system, based on $[\text{Rh}(\text{nbd})\text{Cl}]_2$, PPh_3 and $\text{LiCPh}=\text{CPh}_2$ which was able to mediate the stereospecific controlled polymerisation of PA with quantitative initiation efficiency.³ The chemical structure of the active species in this ternary catalyst system was assumed to be **78a**, Figure 2-1. This important finding was then expanded upon by the same group in which a more detailed examination of the ligand components in this system was reported by Misumi *et al.*⁴

Following this, Miyake, Misumi and Masuda reported the first isolable Rh(I)-vinyl complexes from this family of catalysts.⁴ The isolated catalysts, **78b** and **78c** Figure 2-1, were able to mediate the polymerisation of PA in a controlled fashion over a range of temperatures (15 – 60 °C) and different solvent systems. The polymerisations yielded PPA with tunable molecular weights and, \bar{D}_s , as low as 1.05.

In this chapter, the synthesis, characterisation and use, as initiators for PA (co)polymerisation, of three new Rh(I)-vinyl complexes bearing fluorenyl functionality with fluorine-functionalised phosphine ligands is described. Systematic characterisation of the complexes was performed via a combination of ^1H , ^{31}P , ^{19}F , ^{103}Rh NMR spectroscopy and 2D ^{31}P - ^{103}Rh and ^{31}P - $^{103}\text{Rh}\{^{103}\text{Rh}\}$ heteronuclear multiple quantum correlation (HMQC) experiments, elemental analysis and single crystal X-ray analysis. This is followed by an evaluation of the complexes as initiators in the polymerisation of PA, characterisation of the resulting polymers via SEC for molecular weight determination and ^1H NMR spectroscopy for determining stereoregularity and configuration.

2.2 Experimental

2.2.1 Materials

n-Butyllithium (*n*-BuLi, 1.6 M solution in hexane, Sigma-Aldrich), 9-(bromo(phenyl)methylene)-9*H*-fluorene, (C₁₂H₈)C=CPhBr (FluC=CPhBr, Matrix Scientific, 95 %), [Rh(nbd)Cl]₂ (nbd = 2,5-norbornadiene, 98 %, Strem Chemicals), tris(*para*-fluorophenyl)phosphine (P(4-FC₆H₄)₃, 98 %, Aldrich), tris(*para*-trifluoromethylphenyl) phosphine (P(4-CF₃C₆H₄)₃, 97 %, Aldrich), and tris[3,5-bis(trifluoromethyl)phenyl]phosphine (P(3,5-(CF₃)₂C₆H₃)₃, 97 %, Strem Chemicals), were used as received. Phenylacetylene (CH≡CPh, 98 % Aldrich) was purified by passage over a column of basic alumina and then stored in a fridge until needed. The Masuda complex,⁴ Rh(nbd)(CPh=CPh₂)(P(4-FC₆H₄)₃), was prepared as detailed below for **88b** except triphenylbromoethylene was used in place of FluC=CPhBr.

THF, diethyl ether and CH₂Cl₂ were dried using a PureSolv MD5 solvent purification system (Innovative Technology, Inc.), collected, degassed via the freeze-pump-thaw technique and stored under dry nitrogen until needed. Toluene (99.8 %, Sigma-Aldrich) was degassed via the freeze-pump-thaw technique and stored under dry nitrogen until needed.

All glassware was pre-dried in an oven at 50 °C and flame dried under vacuum prior to use. All reactions were performed using standard Schlenk line techniques.

2.2.2 Rh(I)- α -phenylvinyl Fluorenyl Complexes

2.2.2.1 Synthesis of Complex Rh(nbd)(CPh=CFlu)(P(4-FC₆H₄)₃)

Synthesis of Rh(nbd)(CPh=CFlu)(P(4-FC₆H₄)₃): The target complex was prepared according to the method of Miyake et al.⁴

To a round bottomed flask equipped with a Teflon-coated magnetic stir-bar was added FluC=CPhBr (333 mg, 1.0 mmol) and diethyl ether (20.0 mL) under a dry nitrogen atmosphere. The flask was cooled to 0 °C and *n*-BuLi (1.6 M solution in hexane, 1.25 mL, 2.0 mmol) was cannula transferred and the mixture allowed to react for 30 min yielding FluC=CPhLi.

To a separate round bottomed flask equipped with a magnetic stir-bar containing dry toluene (15.0 mL) was added [Rh(nbd)Cl]₂ (92.2 mg, 0.2 mmol) and P(4-FC₆H₄)₃ (253 mg, 0.8 mmol). The mixture was then stirred vigorously for 15 min at ambient temperature yielding the intermediate Rh species, Rh(nbd)Cl(P(4-FC₆H₄)₃).

The lithiated species, FluC=CPhLi, was added, via cannula, to the solution containing Rh(nbd)Cl(P(4-FC₆H₄)₃) and allowed to stir at ambient temperature for 1 hour. Subsequently the reaction solution was cannula transferred and filtered through a short plug of neutral activated alumina 90, under an inert atmosphere, to give a clear orange solution. Solvents were removed under high vacuum on a Schlenk line yielding a dark coloured viscous liquid. To this crude product was added ethanol (25.0 mL) and the mixture stirred vigorously for 30 min. during which time an orange precipitate formed. The precipitate was collected via a Hirsch funnel and washed with a small amount of additional ethanol. The Rh(I) complex Rh(nbd)(CPh=CFlu)(P(4-FC₆H₄)₃) (**88b**) was isolated by recrystallisation from CH₂Cl₂/*n*-pentane employing a solvent layering technique.

Yield: 140.0 mg, 46 %. Anal. Calcd. for $C_{45}H_{33}F_3PRh$: C, 70.69 %; H, 4.35 %. Found: C, 70.38 %; H, 4.07 %. 1H NMR (400.1 MHz, C_6D_6), δ (ppm): 9.24 (dd, $J = 7.4, 1.1$ Hz, 1H), 7.77 (dt, $J = 7.5, 1.0$ Hz, 1H), 7.71 (dt, $J = 7.4, 0.9$ Hz, 1H), 7.46 (td, $J = 7.4, 1.1$ Hz, 1H), 7.33 (td, $J = 7.4, 1.1$ Hz, 1H), 7.26 – 7.19 (m, 7H), 7.10 (td, $J = 7.4, 1.0$ Hz, 1H), 7.07 – 6.98 (m, 2H), 6.92 (dddd, $J = 7.3, 4.3, 2.9, 1.2$ Hz, 2H), 6.67 – 6.63 (m, 1H), 6.60 – 6.50 (m, 7H), 4.51 – 4.38 (m, 2H), 3.84 (td, $J = 3.8, 1.9$ Hz, 1H), 3.56 – 3.48 (m, 2H), 3.30 – 3.24 (m, 1H), 1.24 (dt, $J = 8.2, 1.6$ Hz, 1H), 1.19 – 1.14 (m, 1H). $^{31}P\{^1H\}$ NMR (162.0 MHz, C_6D_6) δ (ppm): 26.6 (d, $J = 190.4$ Hz). ^{19}F NMR (376.5 MHz, C_6D_6), δ (ppm): -109.9 (s). ^{103}Rh (19.1 MHz, C_6D_6 , 25 °C), δ (ppm): -7862 (d, $J = 190.4$ Hz; 372 ppm if referenced to Rh metal).

2.2.2.2 Synthesis of $Rh(nbd)(CPh=CFlu)(P(4-CF_3C_6H_4)_3)$

*Synthesis of $Rh(nbd)(CPh=CFlu)(P(4-CF_3C_6H_4)_3)$: The target complex was prepared as detailed above for **88b** except $P(4-FC_6H_4)_3$ was replaced with $P(4-CF_3C_6H_4)_3$.*

The Rh(I) complex $Rh(nbd)(CPh=CFlu)(P(4-CF_3C_6H_4)_3)$ (**88d**) was isolated by recrystallisation from CH_2Cl_2/n -pentane. Yield: 322.0 mg, 88 %. Anal. Calcd for $C_{48}H_{33}F_9PRh$: C, 63.03 %; H, 3.64 %; Found: C, 62.03 %; H, 3.57 %. 1H NMR (400.1 MHz, CD_2Cl_2), δ (ppm): 8.76 (dt, $J = 7.3, 0.8$ Hz, 1H), 7.85 – 7.75 (m, 1H), 7.75 – 7.68 (m, 1H), 7.56 (dt, $J = 7.5, 0.9$ Hz, 1H), 7.47 (dt, $J = 7.5, 0.9$ Hz, 1H), 7.43 – 7.37 (m, 6H), 7.37 – 7.33 (m, 5H), 7.32 – 7.27 (m, 1H), 7.23 (td, $J = 7.4, 1.1$ Hz, 1H), 7.13 (tt, $J = 7.4, 1.3$ Hz, 1H), 7.02 (qd, $J = 7.5, 1.3$ Hz, 2H), 6.81 (dt, $J = 7.6, 1.6$ Hz, 1H), 6.74 (ddd, $J = 8.4, 7.2, 1.2$ Hz, 1H), 6.33 (dt, $J = 7.9, 1.5$ Hz, 1H), 6.09 (dd, $J = 7.9, 0.9$ Hz, 1H), 4.56 (qd, $J = 3.7, 1.8$ Hz, 1H), 4.43 – 4.39 (m, 1H), 4.15 (dq, $J = 3.6, 1.9$

Hz, 1H), 3.93 (tq, $J = 3.3, 1.6$ Hz, 1H), 3.78 – 3.72 (m, 2H), δ 1.56 (dt, $J = 8.3, 1.5$ Hz, 1H), 1.47 – 1.43 (m, 1H); $^{31}\text{P}\{^1\text{H}\}$ NMR (162.0 MHz, C_6D_6 , 25 °C), δ (ppm): 29.8 (d, $J = 188.8$ Hz). ^{19}F NMR (376.5 MHz, C_6D_6 , 25 °C), δ (ppm): -62.84 (s). ^{103}Rh (19.1 MHz, CD_2Cl_2 , 25 °C), δ (ppm): -7870 (d, $J = 188.8$ Hz; 365 ppm if referenced to Rh metal).

2.2.2.3 Synthesis of Complex $\text{Rh}(\text{nbd})(\text{CPh}=\text{CFlu})(\text{P}(3,5\text{-CF}_3\text{C}_6\text{H}_4)_3)$

*Synthesis of $\text{Rh}(\text{nbd})(\text{CPh}=\text{CFlu})(\text{P}(3,5\text{-(CF}_3)_2\text{C}_6\text{H}_3)_3)$: The target complex was prepared as detailed above for **88b** except $\text{P}(4\text{-FC}_6\text{H}_4)_3$ was replaced with $\text{P}(3,5\text{-(CF}_3)_2\text{C}_6\text{H}_3)_3$.*

The Rh(I) complex $\text{Rh}(\text{nbd})(\text{CPh}=\text{CFlu})(\text{P}(3,5\text{-(CF}_3)_2\text{C}_6\text{H}_3)_3)$ (**88e**) was purified by recrystallisation from CH_2Cl_2 /methanol via a solvent layering technique. Yield: 112 mg, 25 %. Anal. Calcd. for $\text{C}_{51}\text{H}_{30}\text{F}_{18}\text{PRh}$: C, 54.76 %; H, 2.70 %; Found: C, 54.12 %; H, 2.60 %. ^1H NMR (400.1 MHz, C_6D_6), δ (ppm): ^1H NMR (400 MHz, C_6D_6) δ 8.43 (d, $J = 7.2$ Hz, 1H), 8.11 (dd, $J = 12.2, 1.6$ Hz, 1H), 7.94 (s, 6H), 7.62 – 7.58 (m, 2H), 7.55 (s, 3H), 7.49 (d, $J = 7.4$ Hz, 1H), 7.45 (dt, $J = 7.6, 1.0$ Hz, 1H), 7.33 (td, $J = 7.6, 1.2$ Hz, 1H), 7.09 – 7.03 (m, 1H), 6.99 (td, $J = 7.6, 1.2$ Hz, 1H), 6.88 (dt, $J = 7.7, 1.6$ Hz, 1H), 6.82 (td, $J = 7.7, 1.2$ Hz, 1H), 6.57 (d, $J = 7.9$ Hz, 1H), 6.44 (dd, $J = 7.7, 1.6$ Hz, 1H), 4.35 (d, $J = 4.6$ Hz, 1H), 4.32 – 4.28 (m, 1H), 3.43 (d, $J = 4.6$ Hz, 1H), 3.40 (s, 2H), 3.27 (s, 1H), 1.12 (dt, $J = 8.5, 1.6$ Hz, 1H), 1.05 (dd, $J = 8.5, 1.7$ Hz, 1H). $^{31}\text{P}\{^1\text{H}\}$ NMR (162.0 MHz, C_6D_6), δ (ppm): 33.08 (d, $J = 198.6$ Hz). ^{19}F NMR (376.5 MHz, C_6D_6), δ (ppm): -62.92 (s). ^{103}Rh (19.1 MHz, CD_2Cl_2 , 25 °C), δ (ppm): -7861 (determined indirectly by HMQC; 373 ppm if referenced to Rh metal).

2.2.3 Modelling

The geometry of the complexes obtained by single crystal X-ray crystallography were relaxed in vacuum using the 6-311G** basis set of the light atoms while Rh was treated with the Stuttgart-Dresden effective core potential.⁵ The vibrational frequencies have been calculated to ensure that the final configuration was a stable minimum. The final relaxed geometries were then employed to calculate the bonding energies using the triple-zeta Dunning's correlation consistent basis sets (cc-pVTZ),⁶ the counterpoise correction was also included.⁷

2.2.4 Polymerisations

All (co)polymerisations were carried out under a dry nitrogen atmosphere in a pre-dried Schlenk flask.

2.2.5 Homopolymerisation of Phenylacetylene

Below is given a typical procedure for the homopolymerisation of phenylacetylene with a Rh(I)-vinyl catalyst.

A solution of phenylacetylene (0.184 g, 1.80 mmol) in THF or toluene (2.5 mL) was added to a solution of Rh catalyst (0.015 g, 0.02 mmol) and free additional phosphine – P(4-FC₆H₄)₃ in the case of Rh(nbd)(CPh=CFlu)(P(4-FC₆H₄)₃) for example (0.031 g, 0.10 mmol) dissolved in THF or toluene (2.5 mL) in a Schlenk flask equipped with a magnetic stir bar. The flask was immersed in a pre-heated oil bath set at 30 °C and allowed to react for 1 hour after which the polymerisation was stopped via the addition of a small volume of acetic acid. The polymer was isolated by precipitation into a large volume of methanol, filtered by gravity filtration and dried to constant weight in a vacuum oven at 40 °C overnight.

2.2.6 Multistage, Self-blocking of Polyphenylacetylene with Phenylacetylene

A solution of phenylacetylene (0.184 g, 1.80 mmol) in THF (2.5 mL) was added to a solution of Rh catalyst (0.015 g, 0.02 mmol) and free additional phosphine – P(4-FC₆H₄)₃ in the case of Rh(nbd)(CPh=CFlu)(P(4-FC₆H₄)₃) for example (124 mg, 0.39 mmol) in THF (2.5 mL) in a Schlenk flask immersed in a pre-heated oil-bath set at 30 °C. After 1 hour an aliquot was withdrawn (1.0 mL) and the polymer isolated by precipitation into methanol (20 mL) containing a small amount of acetic acid. Then, a second feed of phenylacetylene (0.184 g, 1.80 mmol) in THF (2.5 mL) was added to the remaining polymerisation solution and ‘block’ copolymerisation allowed to proceed for 1 hour. Subsequently the polymerisation was quenched with acetic acid and the ‘copolymer’ precipitated into a large volume of methanol. The copolymer was isolated by filtration and dried to a constant weight *in vacuo*.

2.2.7 NMR Measurements

¹H, ³¹P, and ¹⁹F NMR spectra were recorded at 298K on a Bruker Avance 400 spectrometer. The data were processed with Bruker’s TopSpin 3.1 software. ¹⁰³Rh NMR were acquired at 298K on a Bruker Avance IIIHD (600 MHz for ¹H) at 19.1 MHz using a commercial 5 mm triple resonance broadband probe (doubly tuned ¹H/³¹P outer coil, with inner broadband coil) with 90° pulses of 27.5 μs and 18.4 μs for ¹⁰³Rh and ³¹P respectively. ¹⁰³Rh chemical shifts, δ, are given in ppm relative to frequency ratio, $\mathcal{E} = 3.186447^8$ (as an aide to the reader, the chemical shifts for the commonly used reference $\mathcal{E} = 3.160000$ (Rh metal) are also given) and were determined, where possible, by direct detection (using an anti-ringing experiment, Bruker pulse sequence aring) or by four pulse ³¹P-¹⁰³Rh HMQC experiments with and without ¹⁰³Rh

decoupling during acquisition. The transmitter frequency offset and t_1 increments were varied to ensure that no signals were folded. All ^{103}Rh data were processed using Bruker's Topspin 3.5 or MestReNova software packages. Exponential line broadening of 10 Hz was applied to 1D ^{103}Rh data, with 2D data zero filled, Gaussian broadened by 10 Hz and treated with sine-squared window function during processing. Coupling constants reported herein are given as absolute values but are likely to be negative in sign for $^1J_{\text{Rh-P}}$.⁹

2.2.8 Crystallography

Crystallographic data for the structures were collected at 100(2) K on an Oxford Diffraction Gemini or Xcalibur diffractometer using Mo K α radiation, Lp and absorption corrections applied. The structures were solved by direct methods and refined against F^2 with full-matrix least-squares procedures using the program suite SHELX-2014.¹⁰ Unless stated, anisotropic displacement parameters were employed for the non-hydrogen atoms. All hydrogen atoms were added at calculated positions and refined by use of a riding model with isotropic displacement parameters based on those of the parent atom. CCDC 1865950-1865952 deposits contain supplementary crystallographic data, and can be obtained free of charge via <https://www.ccdc.cam.ac.uk/structures/>, or from the Cambridge Crystallographic Data Centre, 12 Union Road, Cambridge CB2 1EZ, U.K.; fax: (+44) 1223-336-033; or e-mail: deposit@ccdc.cam.ac.uk.

Crystal data for **88b**: $\text{C}_{45}\text{H}_{33}\text{F}_3\text{PRh}$, $M = 764.59$, $0.218 \times 0.200 \times 0.134 \text{ mm}^3$, triclinic, space group $P-1$ (No. 2), $\alpha = 10.3698(2)$, $\beta = 10.8798(3)$, $\gamma = 17.8743(4) \text{ \AA}$, $\alpha = 76.930(2)$, $\beta = 77.883(2)$, $\gamma = 83.054(2)^\circ$, $V = 1914.88(8) \text{ \AA}^3$, $Z = 2$, $D_c = 1.326 \text{ g cm}^{-3}$, $m = 0.532 \text{ mm}^{-1}$. $F_{000} = 780$, MoK α radiation, $\lambda = 0.71073 \text{ \AA}$, $2\theta \text{ max} = 65.3^\circ$,

39697 reflections collected, 12915 unique ($R_{\text{int}} = 0.0456$). Final $Goof = 1.000$, $R1 = 0.0404$, $wR2 = 0.0874$, R indices based on 10608 reflections with $I > 2\sigma(I)$ (refinement on F^2), $|\Delta\rho|_{\text{max}} = 1.1(1) \text{ e } \text{\AA}^{-3}$, 455 parameters, 1 restraint. CCDC number 1865951.

Crystal data for **88d**: $\text{C}_{48}\text{H}_{33}\text{F}_9\text{PRh}$, $M = 914.62$, orange prism, $0.386 \times 0.215 \times 0.152 \text{ mm}^3$, monoclinic, space group $P2_{1/c}$ (No. 14), $\alpha = 19.6621(3)$, $\beta = 16.2263(2)$, $\gamma = 12.5354(2) \text{ \AA}$, $\beta = 104.996(2)^\circ$, $V = 3863.13(10) \text{ \AA}^3$, $Z = 4$, $D_c = 1.573 \text{ g cm}^{-3}$, $\mu = 0.563 \text{ mm}^{-1}$. $F_{000} = 1848$, MoK α radiation, $\lambda = 0.71073 \text{ \AA}$, $2\theta_{\text{max}} = 65.4^\circ$, 85622 reflections collected, 13411 unique ($R_{\text{int}} = 0.0380$). Final $Goof = 1.002$, $R1 = 0.0337$, $wR2 = 0.0861$, R indices based on 11430 reflections with $I > 2\sigma(I)$ (refinement on F^2), $|\Delta\rho|_{\text{max}} = 0.98(8) \text{ e } \text{\AA}^{-3}$, 586 parameters, 132 restraints. CCDC number 1865952.

Crystal data for **88e**: $\text{C}_{51}\text{H}_{30}\text{F}_{18}\text{PRh}$, $M = 1118.63$, orange prism, $0.281 \times 0.252 \times 0.167 \text{ mm}^3$, triclinic, space group $P-1$ (No. 2), $\alpha = 12.5332(4)$, $\beta = 13.0550(4)$, $\gamma = 16.0370(5) \text{ \AA}$, $\alpha = 79.006(3)$, $\beta = 69.692(3)$, $\gamma = 64.893(3)^\circ$, $V = 2225.45(14) \text{ \AA}^3$, $Z = 2$, $D_c = 1.669 \text{ g cm}^{-3}$, $\mu = 0.533 \text{ mm}^{-1}$. $F_{000} = 1116$, MoK α radiation, $\lambda = 0.71073 \text{ \AA}$, $2\theta_{\text{max}} = 64.6^\circ$, 41817 reflections collected, 14683 unique ($R_{\text{int}} = 0.0376$). Final $Goof = 1.001$, $R1 = 0.0507$, $wR2 = 0.1157$, R indices based on 12467 reflections with $I > 2\sigma(I)$ (refinement on F^2), $|\Delta\rho|_{\text{max}} = 1.6(1) \text{ e } \text{\AA}^{-3}$, 658 parameters, 324 restraints. CCDC number 1865950.

2.2.9 Elemental Analysis

Elemental microanalyses were performed on a Perkin Elmer 2400 Series II CHNS/O Analyser in CHN mode with helium as a carrier gas.

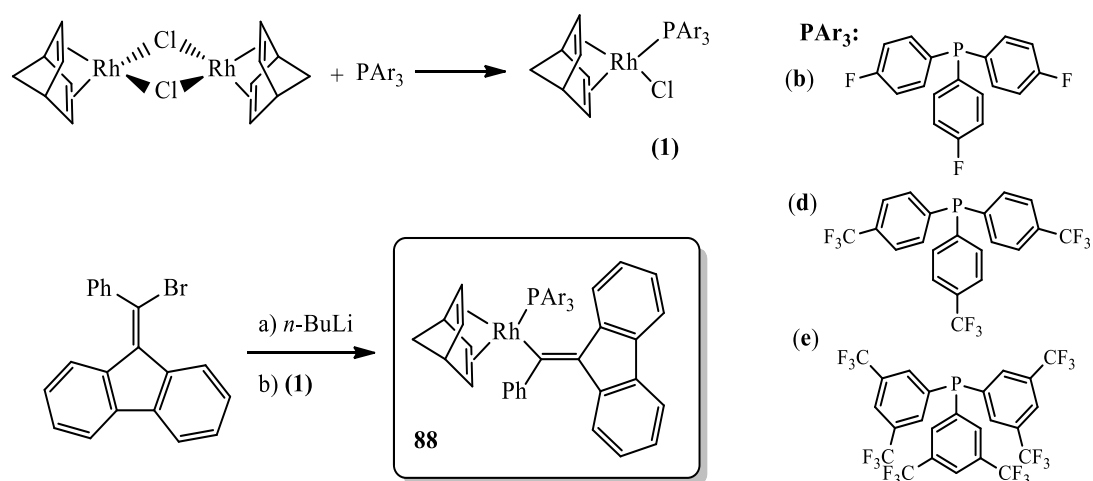
2.2.10 Size Exclusion Chromatography (SEC)

Size exclusion chromatography (SEC) was performed on a Shimadzu modular system consisting of a 4.0 mm × 3.0 mm Phenomenex Security Guard™ Cartridge guard column and two linear phenogel columns (10³ and 10⁴ Å pore size) in tetrahydrofuran (THF) operating at a flow rate of 1.0 mL/min and 40 °C using a RID-20A refractive index detector, a SPD-M20A prominence diode array detector and a miniDAWN TREOS multi-angle static light scattering (MALLS) detector. The system was calibrated with a series of narrow molecular weight distribution polystyrene standards with molecular weights ranging from 0.27 to 66 kg mol⁻¹. Chromatograms were analysed by Lab Solutions SEC software.

2.3 Results and Discussion

2.3.1 Synthesis and Characterisation of Rh(I)- α -phenylvinyl Complexes

Three new Rh(I)- α -phenylvinyl complexes containing fluorenyl functionality on the β -vinylcarbon, in combination with fluorinated triarylphosphine ligands, were synthesised as outlined in Scheme 2-1.



Scheme 2-1. Outline for the synthesis of $\text{Rh}(\text{nbd})(\text{CPh}=\text{Flu})(\text{P}(\text{4-FC}_6\text{H}_4)_3)$ (**88b**), $\text{Rh}(\text{nbd})(\text{CPh}=\text{Flu})(\text{P}(\text{4-CF}_3\text{C}_6\text{H}_4)_3)$ (**88d**) and $\text{Rh}(\text{nbd})(\text{CPh}=\text{Flu})(\text{P}(\text{3,5-(CF}_3)_2\text{C}_6\text{H}_3)_3)$ (**88e**).

$[\text{Rh}(\text{nbd})\text{Cl}]_2$ was first reacted with a fluorine functional triphenylphosphine of choice ($\text{P}(\text{4-FC}_6\text{H}_4)_3$, $\text{P}(\text{4-CF}_3\text{C}_6\text{H}_4)_3$ or $\text{P}(\text{3,5-(CF}_3)_2\text{C}_6\text{H}_3)_3$) to give intermediate tetracoordinate Rh(I) species $[\text{Rh}(\text{nbd})(\text{PAR}_3)\text{Cl}]$ (1). $n\text{-BuLi}$ -mediated lithiation of 9-(bromo(phenyl)methylene)-9H-fluorene followed by reaction with (1) gave the target Rh(I)- α -phenylvinylfluorenyl-functional complexes (**88b**, **88d**, **88e** where **b** = F, **d** = CF_3 , **e** = $(\text{CF}_3)_2$) and refers to the nature of the fluorine species on the phosphine

ligand). In all instances, the Rh(I)-vinyl complexes were isolated as orange powders by a washing process with EtOH, or in the case of **88e** by column chromatography, and subsequently recrystallised from CH₂Cl₂/pentane or CH₂Cl₂/methanol solvent mixtures. For all complexes, X-ray quality crystals were obtained, facilitating solid-state structure determination, *vide infra*.

All complexes were characterised via a combination of techniques including NMR spectroscopy (¹H, ³¹P, ¹⁹F, ¹⁰³Rh and 2D ³¹P-¹⁰³Rh/³¹P-¹⁰³Rh{¹⁰³Rh} HMQC), elemental analysis and X-ray crystallography. Figure 2-2 and Figure 2-3 show the ¹H, ³¹P{¹H}, and ¹⁹F spectra of Rh(nbd)(CPh=CFlu)(P(4-FC₆H₄)₃) (**88b**), measured in C₆D₆, with key identifying signals highlighted. Similarly, data for **88d** and **88e**, verifying their structure, are shown in Figure 2-4 and Figure 2-5, respectively. The full ¹H NMR spectrum of **88b** is given at the top in Figure 2-2A with an expansion of the aromatic region (plotted between δ = 8.0 and 6.4 ppm) given directly below, Figure 2-2B. In the full spectrum a distinct signal is observed at δ = 9.24 ppm, which appears as a doublet, assigned to a single H labelled **A**, that is associated with the fluorenyl functional group. The remaining labelled peaks (**B**, **C**, **D**, and **E**) can be assigned to the norbornadiene ligand, see structure at the top of Figure 2-2A. All peaks integrate in the expected ratio.

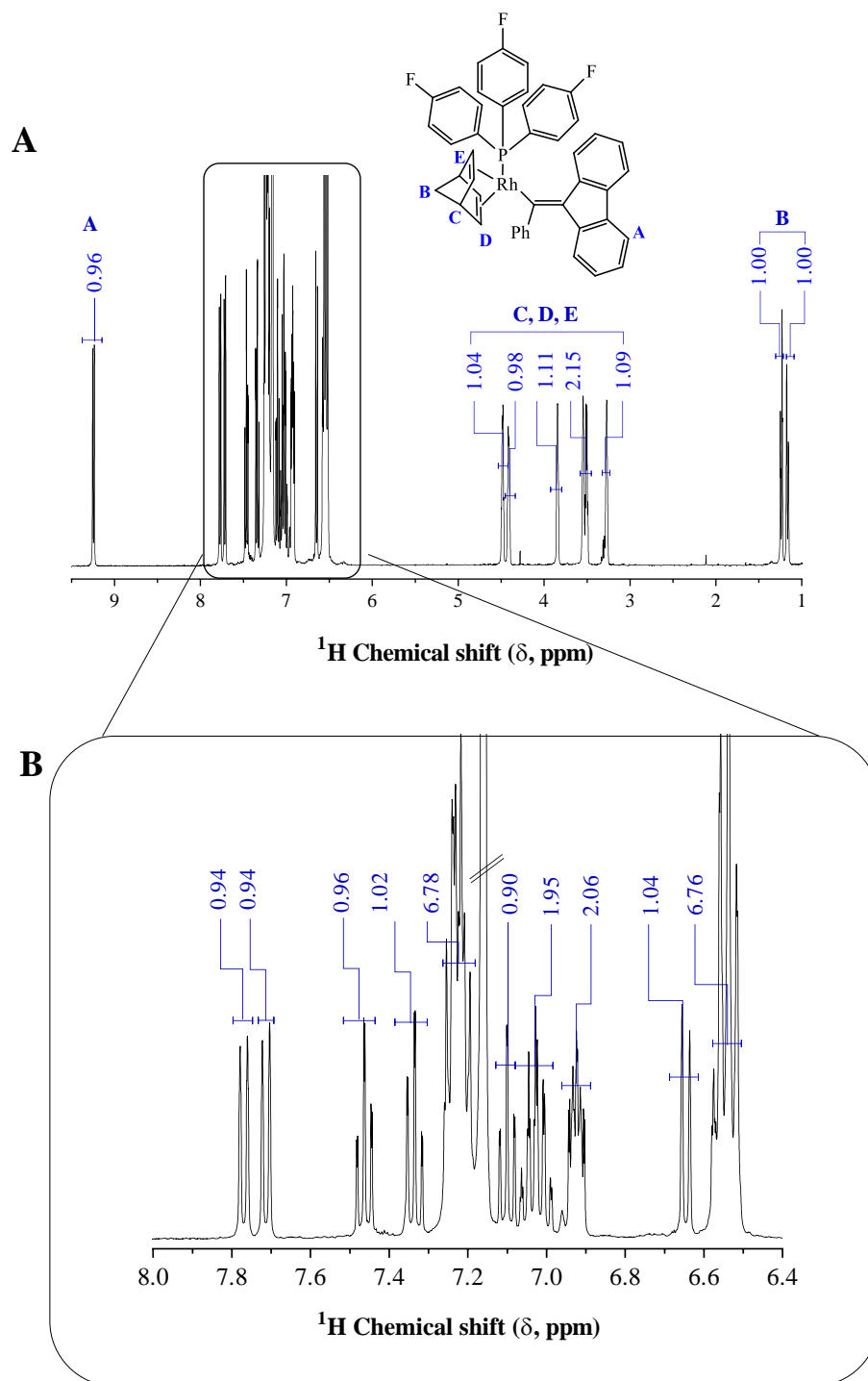


Figure 2-2. ¹H NMR spectra, recorded in C₆D₆, of Rh(nbd)(CPh=CFlu)(P(4-FC₆H₄)₃) (**88b**). (A) The full ¹H NMR spectrum with key peaks highlighted and the measured integral values included (blue); (B) the ¹H NMR spectrum covering the aromatic region from δ = 8.0 to 6.4 ppm.

The ^1H NMR spectrum covering the region $\delta = 8.0 - 6.4$ ppm is complex, Figure 2-2B. It is within this region that signals associated with the remaining 24 aromatic H's appear, i.e. those present on the phosphine ligand, the α -phenylvinyl group and the remaining fluorenyl H's. However, all signals integrate in the expected ratio, confirming the structure.

The $^{31}\text{P}\{^1\text{H}\}$ NMR spectrum of **88b** is shown in Figure 2-3A. A set of doublets is observed arising from coupling between Rh and P, with signals centred at ~ 27.0 and 25.8 ppm with a corresponding $^1J_{\text{Rh-P}}$ value of 190.4 Hz. This differs from the Masuda derivative, $\text{Rh}(\text{nbd})(\text{CPh}=\text{CPh}_2)(\text{PPh}_3)$, as reported by Kumazawa *et al.*,¹¹ in which the $^{31}\text{P}\{^1\text{H}\}$ NMR spectrum presents as a pair of doublets at 26.9 and 26.3 ppm at ambient temperature (measured in d_8 -toluene) with $^1J_{\text{Rh-P}}$ coupling constants of 183 and 187 Hz; this was attributed to the presence of two conformational isomers as determined by variable temperature NMR with the two sets of peaks coalescing at 89 °C. However, both the chemical shifts and coupling constant of **88b** are consistent with previously reported values for Rh(I)-vinyl complexes with a single phosphine ligand for our target application. The ^{19}F NMR spectrum, Figure 2-3B, shows a sharp singlet at $\delta = -109.95$ ppm (along with ^{13}C satellites arising from ^{19}F - ^{13}C coupling¹²).

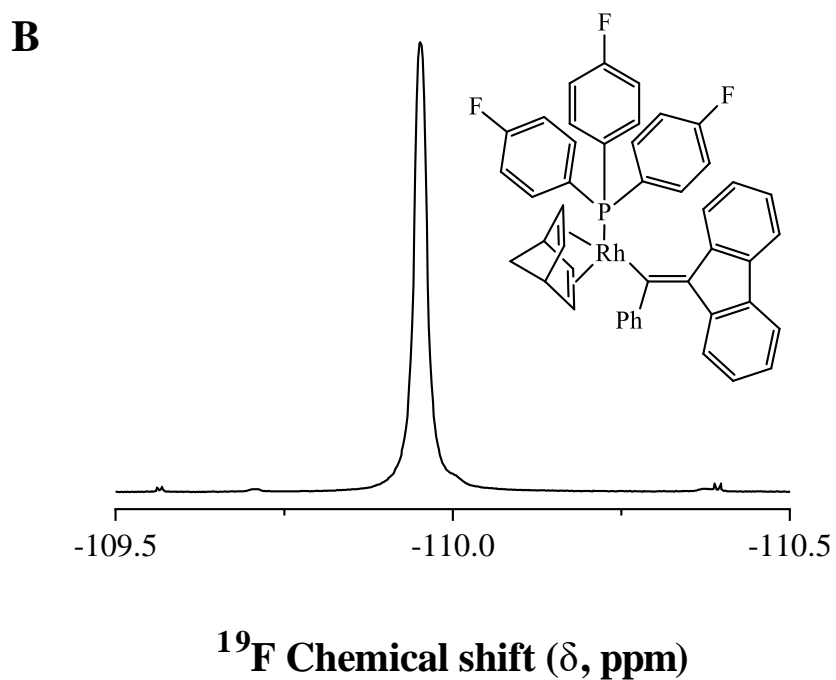
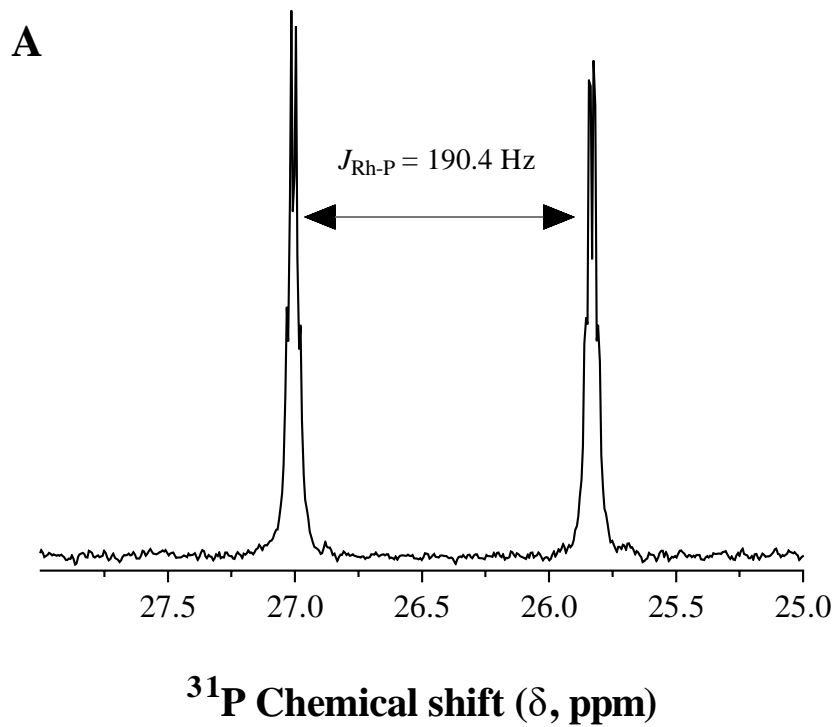


Figure 2-3. NMR spectra, recorded in C_6D_6 , of **88b** (A) The $^{31}\text{P}\{^1\text{H}\}$ NMR spectrum with the rhodium-phosphorous coupling constant noted, and; (B) the ^{19}F NMR spectrum with the structure of the complex shown.

Figure 2-4A and Figure 2-5A show the ^1H NMR spectrum of **88d** and **88e**, recorded in C_6D_6 . In both spectrums, the peaks in the region between $\delta = 5.0 - 3.0$ ppm are associated with the olefinic H's and methine H's and the pair of doublets observed in the region between $\delta = 2.0 - 1.0$ ppm are associated with the methylene H's on the norbornadiene.

Like **88b**, **88d** and **88e** have a prominent doublet at $\delta = 8.76$ ppm and $\delta = 8.43$ ppm respectively, arising from the H atom labelled **A** from the fluorenyl moiety of the α -phenylvinyl group. The signals within the region $\delta = 8.0 - 6.4$ ppm are associated with the 24 aromatic H's of the phosphine ligand, the α -phenylvinyl group and the remaining fluorenyl H's. All signals integrate in the expected ratio, confirming the structure.

The $^{31}\text{P}\{^1\text{H}\}$ NMR spectrum of **88d** is shown in Figure 2-4B. A set of doublets is observed arising from coupling between Rh and P, with signals centred at ~ 31.0 and 29.0 ppm with a corresponding $^1J_{\text{Rh-P}}$ value of 188.8 Hz. The ^{19}F NMR spectrum, Figure 2-4C, shows a sharp singlet at $\delta = -62.84$ ppm.

Similarly, the $^{31}\text{P}\{^1\text{H}\}$ NMR spectrum of **88e** is shown in Figure 2-5B. A set of doublets is observed, with signals centred at ~ 31.0 and 29.0 ppm with a corresponding $^1J_{\text{Rh-P}}$ value of 198.6 Hz. The ^{19}F NMR spectrum, Figure 2-5C, shows a sharp singlet at $\delta = -62.92$ ppm.

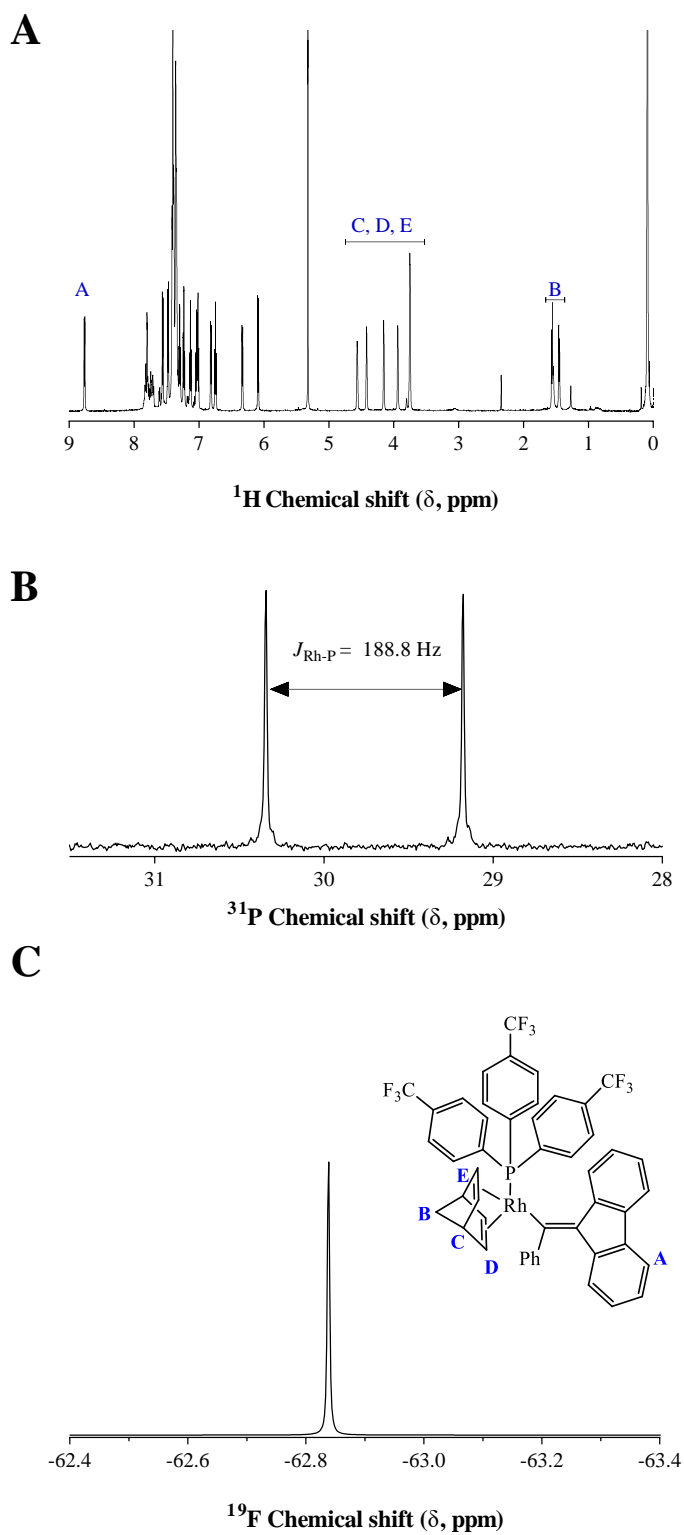


Figure 2-4. NMR spectra of **88d** (A) ^1H NMR spectrum of **88d** recorded in CD_2Cl_2 ; (B) $^{31}\text{P}\{^1\text{H}\}$ NMR spectrum of **88d** recorded in C_6D_6 ; (C) ^{19}F NMR spectrum of **88d** recorded in C_6D_6 .

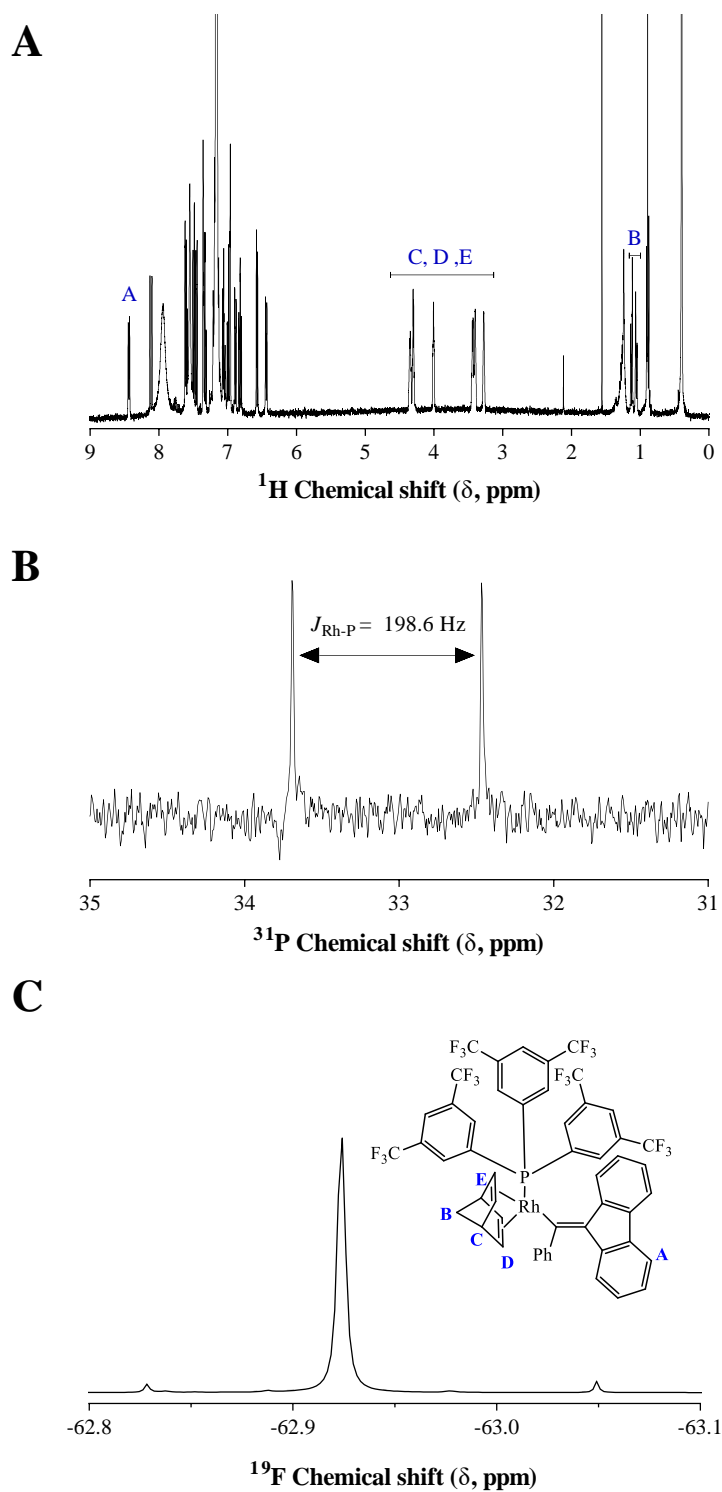


Figure 2-5. NMR spectra of **88e** (A) ^1H NMR spectrum of **88e** recorded in CD_2Cl_2 ; (B) $^{31}\text{P}\{^1\text{H}\}$ NMR spectrum of **88e** recorded in C_6D_6 ; (C) ^{19}F NMR spectrum of **88e** recorded in C_6D_6 .

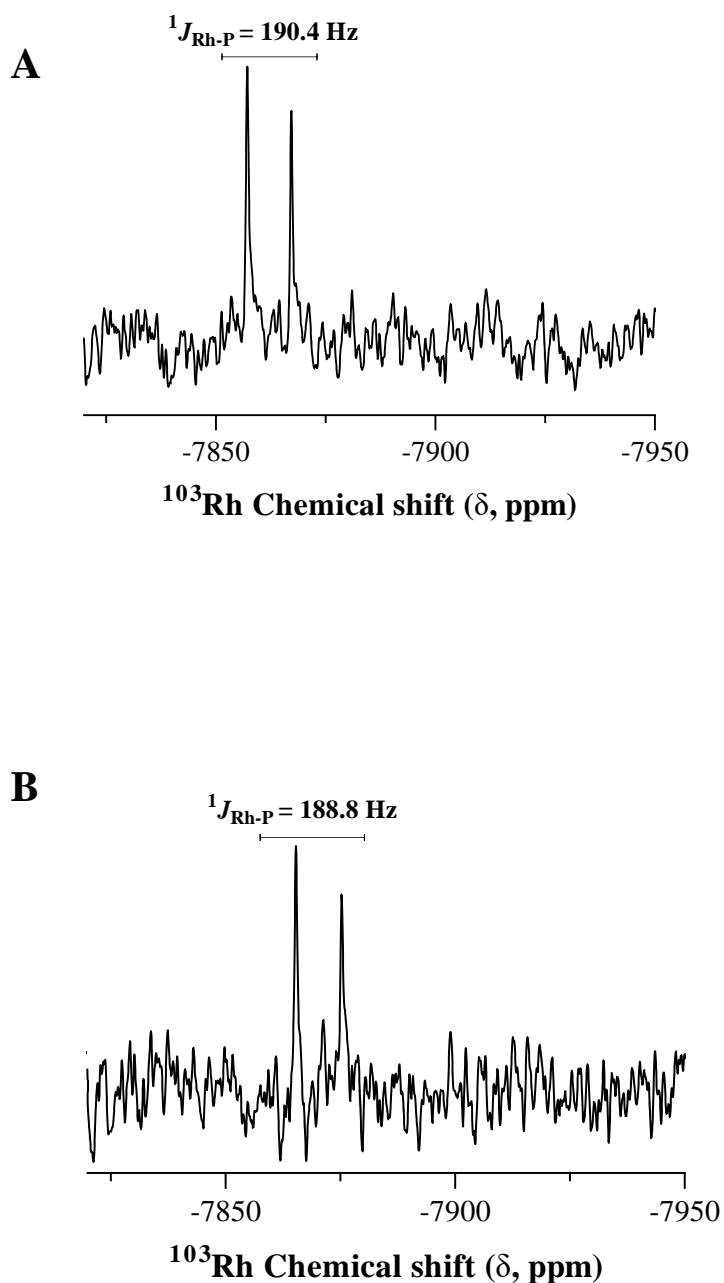


Figure 2-6. (A) ^{103}Rh NMR spectrum of **88b**, recorded in C_6D_6 at 298K; (B) ^{103}Rh NMR spectrum of **88d**, recorded in CD_2Cl_2 at 298 K.

Rhodium has one NMR-active spin $-1/2$ nucleus, ^{103}Rh , which is 100% abundant. While direct observation of ^{103}Rh is possible, it suffers from low sensitivity and a large chemical shift range (of ca. 12,000 ppm). An alternative to direct observation is the application of a 2D polarisation transfer technique, such as

heteronuclear multiple quantum coherence (HMQC). In such experiments the sensitivity of the ^{103}Rh nuclei can be enhanced considerably if bonded to a nucleus with a high gyromagnetic ratio such as ^{31}P (by a factor of almost 600), ^{19}F or ^1H , facilitating more ready detection of the ^{103}Rh nuclei.^{9, 13, 14} In the case of **88b** and **88d** sufficiently concentrated solutions were prepared facilitating direct observation of the ^{103}Rh nuclei. Figure 2-6A shows the ^{103}Rh spectrum of **88b**, while Figure 2-6B shows that of **88d**. In the case of the former, a doublet is observed centred at $\delta = -7862$ ppm, that arises due to coupling with ^{31}P . The absolute value of the $^1J_{\text{Rh-P}}$ coupling constant was determined to be 190.4 Hz, consistent with the value measured by ^{31}P NMR, *vide supra*. A similar observation was made for **88d** with the doublet centred around $\delta = -7870$ ppm with a corresponding $^1J_{\text{Rh-P}}$ coupling constant of 188.8 Hz.

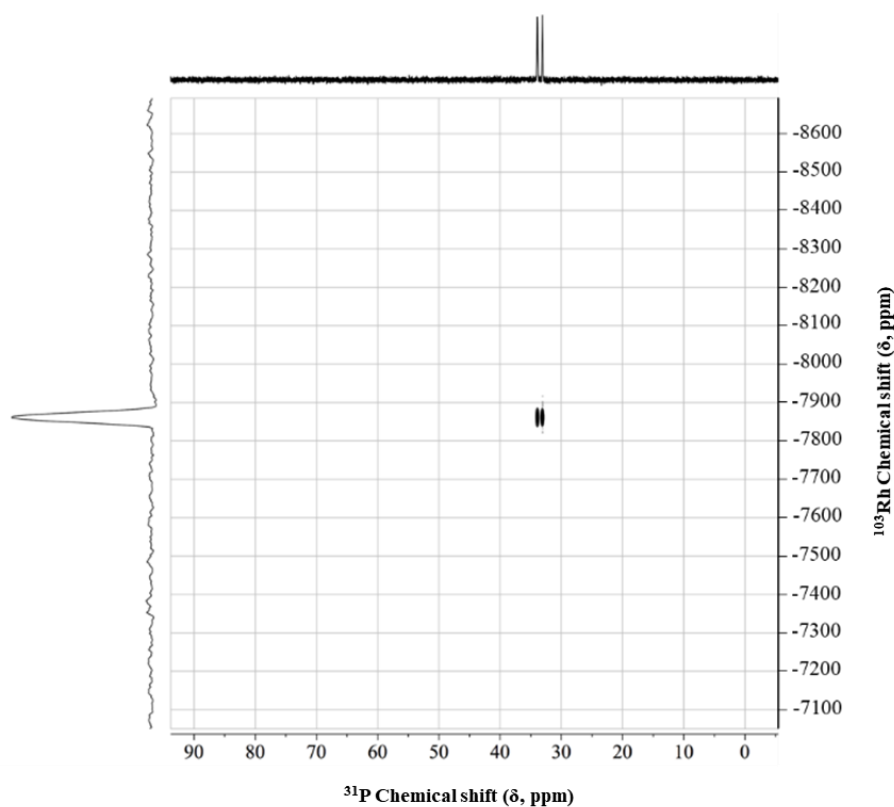


Figure 2-7. ^{31}P - ^{103}Rh HMQC spectrum of **88e** recorded in CD_2Cl_2 at 298K.

Direct measurement of the ^{103}Rh spectrum for **88e** was not readily achieved in a reasonable timeframe but the $|^1J_{\text{Rh-P}}|$ coupling constant of 198.6 Hz was noted.

However, the ^{31}P - ^{103}Rh HMQC spectrum in CD_2Cl_2 was readily acquired, Figure 2-7, giving a ^{103}Rh chemical shift of $\delta = -7861$ ppm and a coupling constant comparable to that determined using ^{31}P NMR.

Similarly, this methodology was employed for **88d** and **88b**, Figure 2-8 and Figure 2-9 respectively. The ^{31}P - ^{103}Rh HMQC spectrum for both **88b** and **88d** was readily acquired in CD_2Cl_2 , giving identical ^{103}Rh chemical shifts to those values acquired from direct observation of the ^{103}Rh nucleus. Similarly, the coupling constants for both acquisitions are comparable to those determined using ^{31}P NMR. This demonstrates that indirect observation (2D ^{31}P - ^{103}Rh HMQC) is a suitable alternative to direct observation of the ^{103}Rh nucleus.

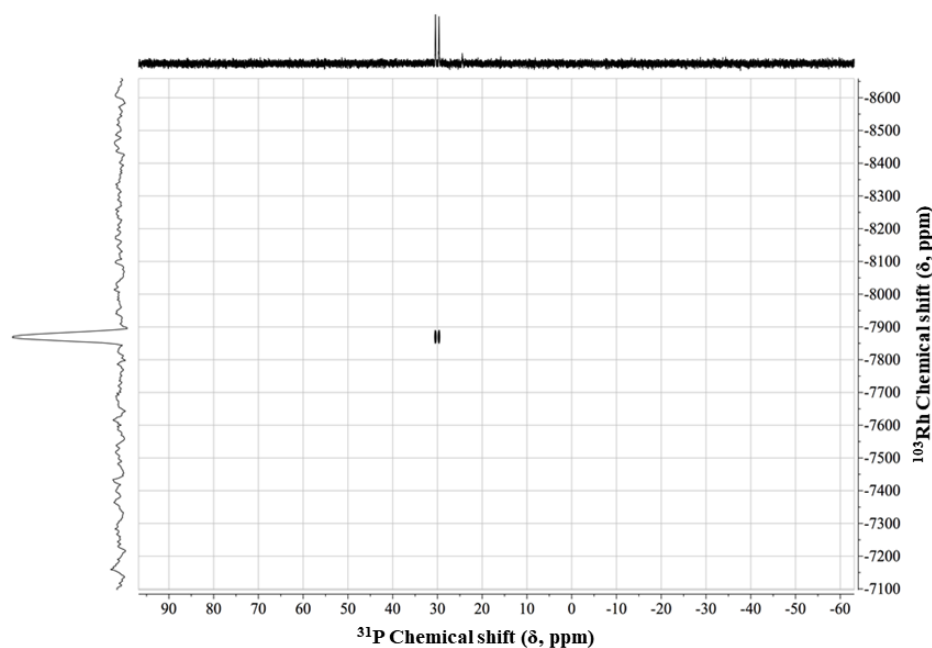


Figure 2-8. ^{31}P - ^{103}Rh HMQC spectrum of **88d** recorded in CD_2Cl_2 at 298K.

The ^{103}Rh chemical shifts for **88b**, **88d** and **88e** differ by less than 10 ppm, which is consistent with the similarities observed in the metal coordination geometries

in the solid-state. Furthermore, it appears that the changes in the fluorination pattern of the phosphine ligand do not appreciably alter the electronic environment about the Rh metal centre.

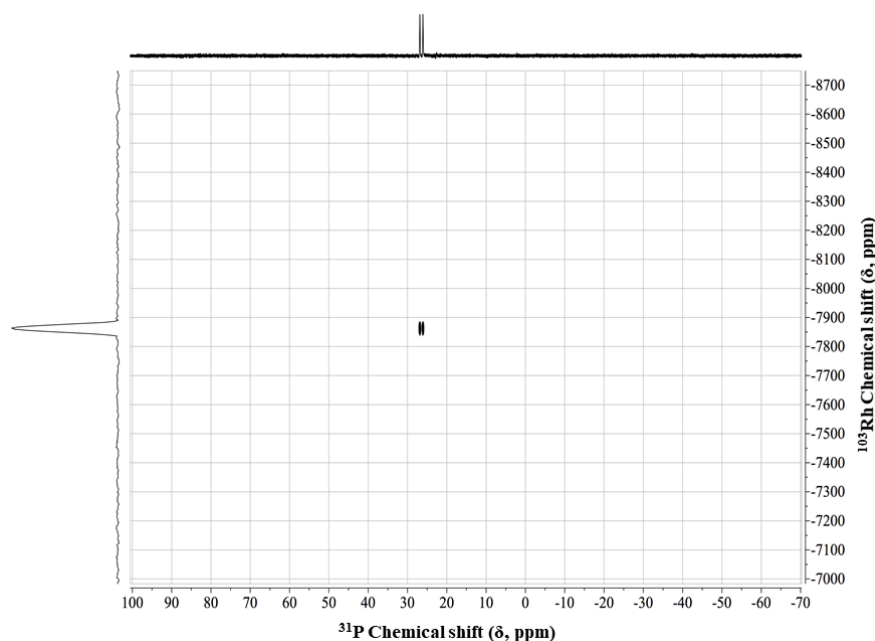


Figure 2-9. ^{31}P - ^{103}Rh HMQC spectrum of **88b** recorded in CD_2Cl_2 at 298K.

While crystal structures of the derivatives $\text{Rh}(\text{nbd})(\text{CPh}=\text{CPh}_2)(\text{PPh}_3)$ (**78a** Figure 2-1) and $\text{Rh}(\text{nbd})(\text{CPh}=\text{Ph}_2)(\text{P}(4\text{-ClC}_6\text{H}_4)_3)$ (**78c** Figure 2-1) have been reported,^{4, 11} Miyake, Misumi and Masuda noted that they were unable to obtain X-ray quality crystals for the analogous fluorine derivative, $\text{Rh}(\text{nbd})(\text{CPh}=\text{Ph}_2)(\text{P}(4\text{-FC}_6\text{H}_4)_3)$.¹⁵ In contrast, each of these new fluorine functional Rh(I)- α -phenylvinylfluorenyl complexes was readily crystallised, enabling the solid-state structures to be determined. Figure 2-10, Figure 2-11 and Figure 2-12 show the X-ray crystal structures obtained for **88b**, **88d** and **88e** respectively. All three complexes have similar solid-state structures, adopting a slightly distorted square planar geometry, consistent with the crystal structures reported for the Masuda derivatives.^{11, 15}

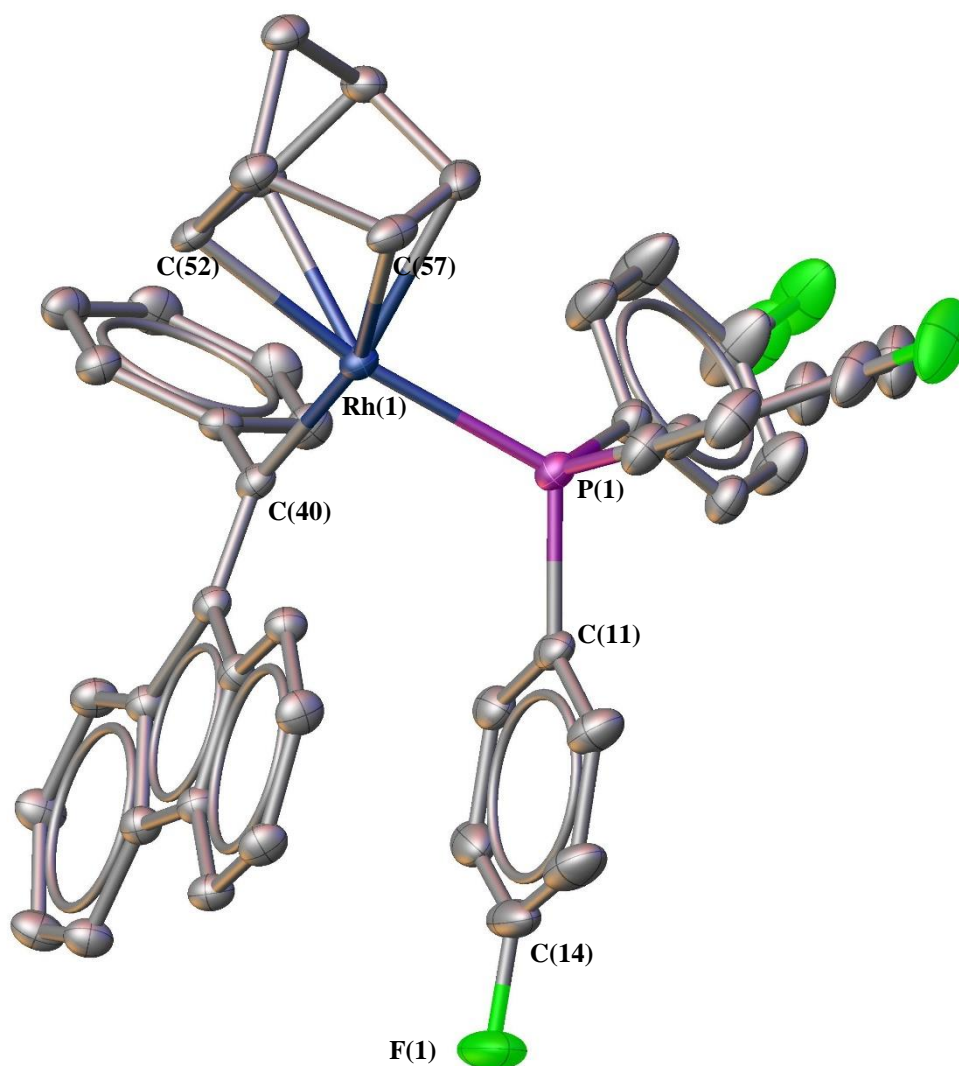


Figure 2-10. OLEX² representation of the X-ray crystal structure of **88b** with 50 % probability ellipsoids and H atoms omitted for clarity. Selected bond lengths (Å): Rh(1)-P(1), 2.314(5); Rh(1)-C(52), 2.185(17); Rh(1)-C(57), 2.236(18); C(14)-F(1), 1.354(2). Selected bond angles (deg): C(52)-Rh(1)-P(1), 171.13(5); C(57)-Rh(1)-P(1), 106.54(5); C(40)-Rh(1)-P(1), 92.99(5).

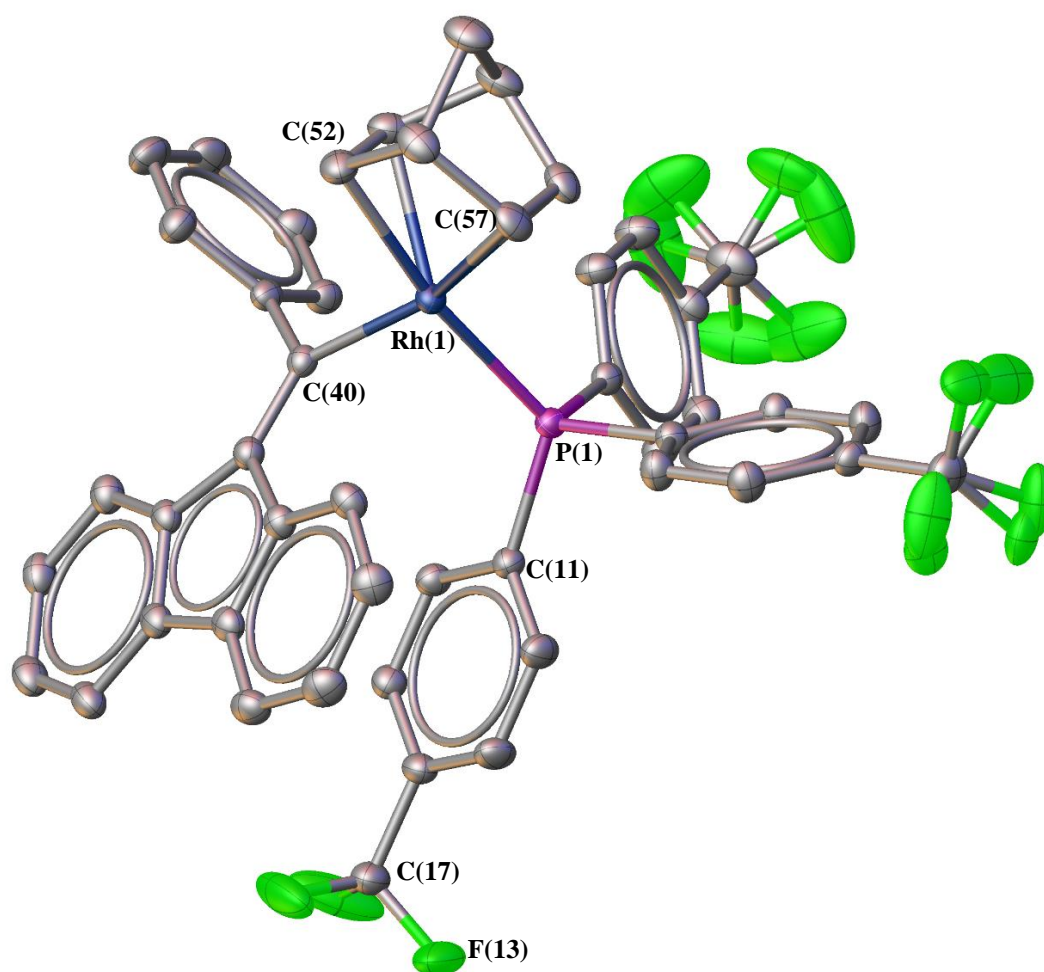


Figure 2-11. OLEX² representation of the X-ray crystal structure of **88d** with 50 % probability ellipsoids and H atoms omitted for clarity. Selected bond lengths (Å): Rh(1)-P(1), 2.301(4); Rh(1)-C(52), 2.168(15); Rh(1)-C(57), 2.217(15); C(17)-F(13), 1.330(2). Selected bond angles (deg): C(52)-Rh(1)-P(1), 171.42(4); C(57)-Rh(1)-P(1), 106.78(5); C(40)-Rh(1)-P(1), 92.97(4).

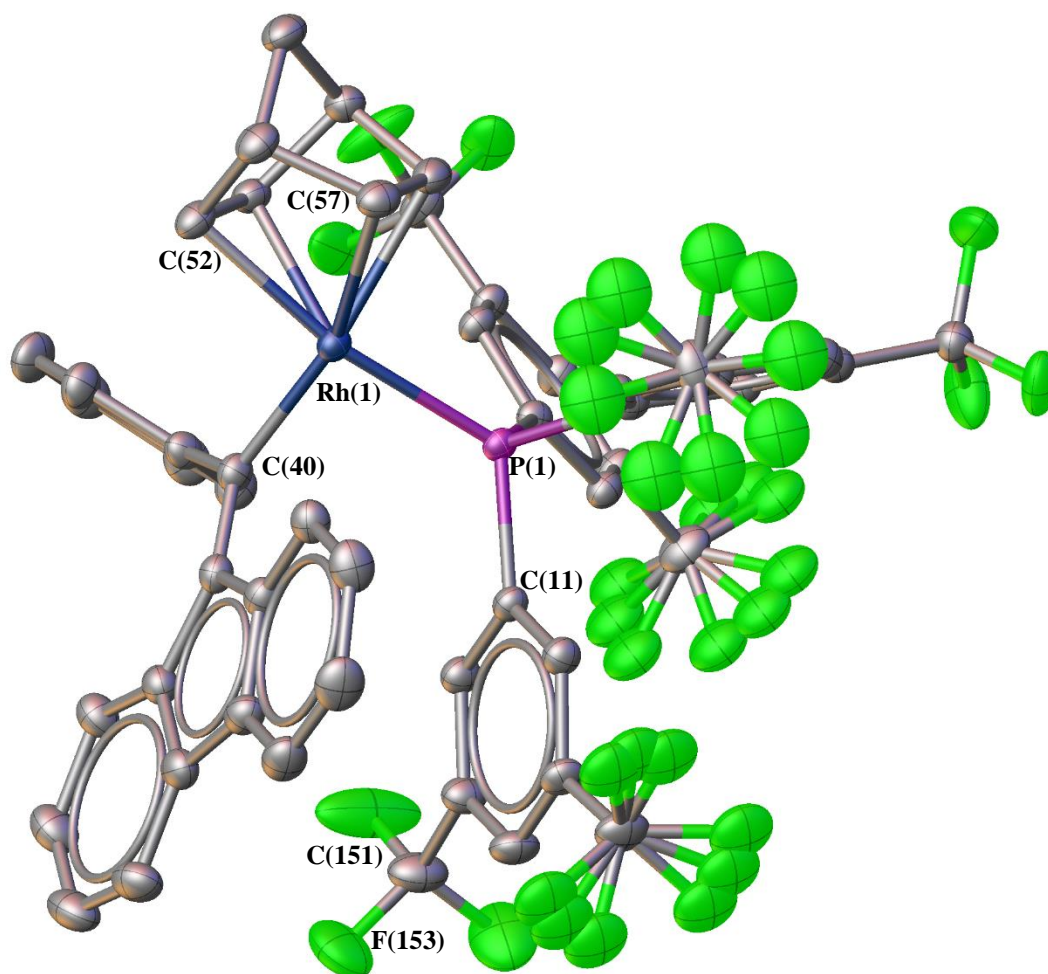


Figure 2-12. OLEX² representation of the X-ray crystal structure of **88e** with 50 % probability ellipsoids and H atoms omitted for clarity. Selected bond lengths (Å): Rh(1)-P(1), 2.305(6); Rh(1)-C(52), 2.165(2); Rh(1)-C(57), 2.250(2); C(151)-F(153), 1.326(4). Selected bond angles (deg): C(52)-Rh(1)-P(1), 167.53(7); C(57)-Rh(1)-P(1), 110.10(7); C(40)-Rh(1)-P(1), 89.74(7).

There are two structural differences between these α -phenylvinylfluorenyl derivatives and the Masuda-type triphenylvinyl analogues. Firstly, the fluorenyl group is conformationally locked and is coplanar with the vinyl bond – such a geometric restriction is not present in the Masuda species with both β -phenyl groups able to freely rotate (the reported X-crystal structures for $\text{Rh}(\text{nbd})(\text{CPh}=\text{CPh}_2)(\text{PPh}_3)$ and $\text{Rh}(\text{nbd})(\text{CPh}=\text{CPh}_2)(\text{P}(4\text{-ClC}_6\text{H}_4)_3)$ are shown in Appendix A¹⁵). Secondly, there is the apparent presence of through-space π - π interactions, at least in the solid-state, between the fluorenyl ring and one of the aromatic rings of the phosphine ligands (centroid-centroid distances, interplanar angles: **88b**, 3.60 Å, 9.65°; **88e**, 3.55 Å, 9.39°). The presence of these interactions is supported, at least in part, by gas-phase modelling, *vide infra*.

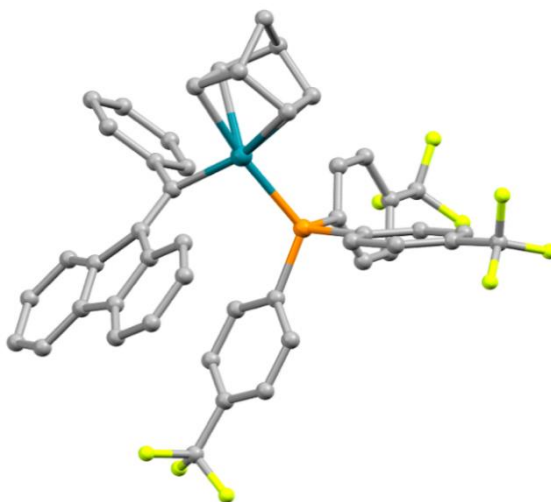
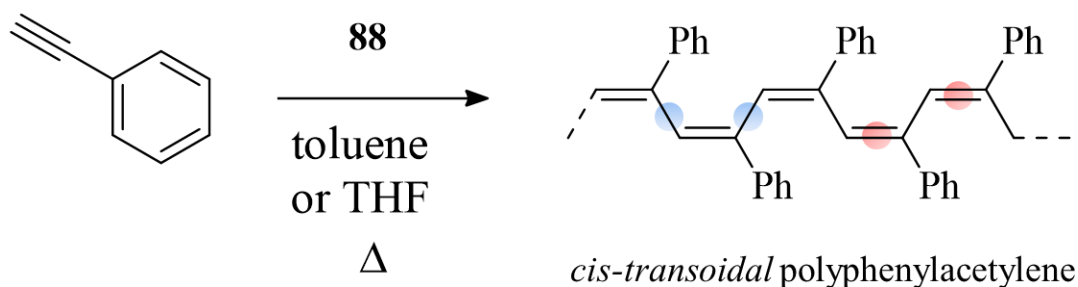


Figure 2-13. Energy-minimised, gas-phase molecular geometry of $\text{Rh}(\text{nbd})(\text{CPh}=\text{CFlu})(\text{P}(4\text{-CF}_3\text{C}_6\text{H}_4)_3)$ (**88d**). The corresponding modelled geometry for **88b** is given in the Appendix A.

The structure and presence of through-space π - π interactions between the fluorenyl functional group and one aromatic group associated with the phosphine ligand was supported by molecular modelling. For example, Figure 2-13, shows the energy-minimised, gas-phase, modelled geometry of **88d** and is clearly almost identical to the X-ray crystal structure (the phosphine ligand binding energy, ignoring solvent effects was determined to be -31.0 kcal/mol).

In two of the three crystal structures, **88d** and **88e**, we observe positional disorder associated with the fluorine functional groups of the phosphine ligand. Such disorder is not uncommon and can be especially prevalent in species with *tert*-butyl and/or CF_3 functional groups, with the highly symmetrical nature of such species coupled with the relatively low energy barrier for rotation about their three-fold symmetry axes the principle cause of the observed disorder.¹⁶⁻¹⁹



Scheme 2-2. The homopolymerisation of phenylacetylene yielding highly stereoregular polyphenylacetylene with *cis-transoidal* configuration.

With three new fluorine functional Rh(I)- α -phenylvinylfluorenyl complexes successfully prepared and characterised, their efficacy as initiators was evaluated in the stereospecific (co)polymerisation of phenylacetylene (PA), Scheme 2-2. Initially, the homopolymerisation of PA with the Masuda derivative **78b** (Figure 2-1) under conditions identical to those reported in the literature was examined (toluene as solvent, T = 30 °C, [Rh] = 2.0 mM, [PA] = 0.50 mM, [Rh]/[P] = 1/5, and polymerisation time = 60 min.)¹⁵ to confirm the efficiency and effectiveness of the experimental approach adopted.

Under these conditions, the resulting PPA has a theoretical M_n of 25,000 at 100 % monomer conversion and assuming quantitative initiation. SEC analysis of the isolated PPA gave an experimentally determined M_n of 24,500, M_w of 25,500 and a corresponding D of 1.04, entry 1 Table 2-1. ¹H NMR spectroscopic analysis of the obtained PPA indicated that it was highly stereoregular with a calculated²⁰ *cis* content of 96 %. A second control experiment was conducted targeting a lower PPA MW (M_n theoretical of 9,300 at quantitative conversion) to confirm the ability to tune MW. This yielded a PPA with an SEC-measured M_n of 9,100 and corresponding D of 1.04, entry 2 Table 2-1.

Table 2-1. Summary of PA polymerisation conditions with **88b**, **88d** and **88e**, SEC-measured molecular weights and dispersities, initiation efficiencies and NMR measured *cis* contents in the resulting polyphenylacetylene (co)polymers.

Entry	Rh species	[P]/[Rh]	Polym. Temp. (°C)	Polym. solvent	Theoretical MW ^a	M_n (SEC) ^b	M_w (SEC) ^b	Dispersity (\mathcal{D}) ^b	Rh initiation efficiency ^c	<i>cis</i> content (%) ^d
1	78b	5	30	toluene	25,000	24,500	25,500	1.04	1.00	96
2	78b	5	30	toluene	9,300	9,100	9,500	1.04	1.00	nd ^e
3	88b	5	30	toluene	10,000	62,800	65,000	1.03	0.16	78
4	88b	5	40	toluene	9,300	71,000	83,500	1.18	0.13	94
5	88b	5	50	toluene	9,300	59,500	73,500	1.24	0.16	90
6	88b	5	60	toluene	9,300	49,000	62,500	1.27	0.19	88
7	88b	20	60	toluene	9,300	35,900	50,100	1.39	0.26	85
8	88d	5	30	toluene	9,300	47,900	63,000	1.31	0.19	90
9	88e	5	30	THF	9,300	16,500	20,100	1.21	0.56	96
10	88b	5	30	THF	9,000	19,600	25,500	1.30	0.46	94
11	88b	5	40	THF	9,000	35,100	43,200	1.23	0.26	92
12	88b	10	40	THF	9,300	27,300	34,100	1.25	0.34	93
13	88b	20	40	THF	9,300	18,600	24,100	1.30	0.50	95
14	88b	10	50	THF	9,300	34,400	41,900	1.22	0.27	92
15	88b	20	50	THF	9,300	45,800	48,900	1.07	0.20	93

a. Calculated as M_n = mass (g) monomer/moles of **88** and assuming 100 % initiation efficiency.

b. As measured by size exclusion chromatography: eluent THF operated at a flow rate of 1.0 mL/min, instrument calibrated with narrow molecular weight distribution polystyrene standards. Dispersity (\mathcal{D}) = M_w/M_n

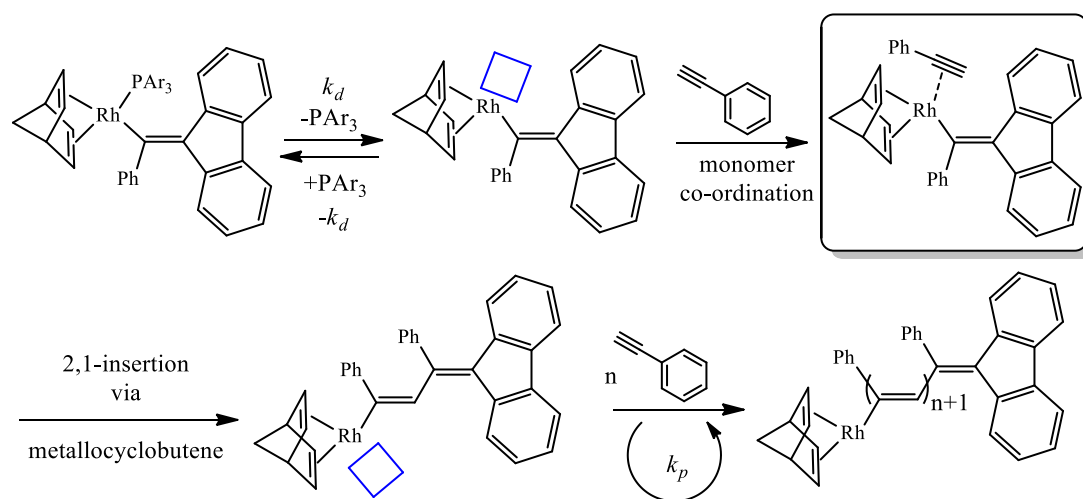
c. Calculated from the ratio of theoretical to measured (SEC determined) M_n 's.

d. As determined by ¹H NMR spectroscopy according to C. I. Simionescu, V. Percec and S. Dumitrescu, *J. Polym. Sci., Part A: Polym. Chem.*, 1977, **15**, 2497-2509.

e. Not determined

Subsequently, the initiating ability/efficiency of **88b** was examined under identical conditions to those employed for **78b**, Table 1 entry 3. Interestingly, while **88b** was active, it exhibited a low initiation efficiency (IE) of ca. 0.16 (based on the molecular weight as determined by SEC) although did yield highly stereoregular PPA with a low dispersity. The low IE was surprising; however, Misumi and co-workers⁴ reported that changing the substitution pattern on the vinyl group in ternary systems of [Rh(nbd)Cl]₂/vinyl-Li/PPh₃ had a significant effect on the IE of the *in situ*-generated active species with values dropping from near quantitative for triphenylvinyl lithium to values more typically in the range 0.2 – 0.3 even for similar species such as (1,2-diphenyl)vinyl lithium, while still maintaining a low dispersity.

This observation from Misumi *et al.*⁴ was proposed to be a direct result of the stability of the vinyl-Li species generated in such ternary systems (with the triphenylvinyl Li species being optimal) and, presumably, the subsequent formation of the actual catalytically active species. However, in these isolated fluorenyl derivatives, the low activity cannot be rationalised in terms of the stability of a vinyl-Li species. The low efficiency could, conceivably, be caused by various factors including catalyst decomposition in solution (although this is not consistent with observations regarding **88**) but is more likely a result of the energetics associated with the initiation process.



Scheme 2-3. The sequence of steps resulting in the formation of polyphenylacetylene from the precursor catalyst/initiator **88**.

The initiation step in such co-ordination polymerisation processes is the stage in which the catalyst (or precatalyst) is converted to the active propagating species. The sequence of processes leading to the formation of PPA is shown in Scheme 2-3. In solution, **88** becomes ‘activated’ by phosphine ligand dissociation (a reversible process) with an associated rate constant, k_d , resulting in a Rh species with a vacant co-ordination site. In the presence of (excess) PA, the monomer will co-ordinate and undergo a 2,1-insertion into the Rh- α -phenylcarbon bond. The net result of these three processes is chain initiation and in the presence of excess PA, propagation, i.e. chain growth, will ensue.

Since phosphine ligand dissociation and subsequent PA coordination is assumed to be rapid, it is hypothesised that the low efficiency of the **88** species is associated with the first (perhaps also second) monomer insertion into the Rh-C bond, although such insertions of PA into a Rh- sp^2 hybridised carbon bond have been reported to be facile.²¹

It is proposed that the bulky, and conformationally locked, fluorenyl functionality sterically hinders efficient insertion. While 2,1-insertion is the well-

established mode of propagation in such polymerisations, theoretical studies suggest that a transition state in which conjugative insertion occurs is energetically favoured. This requires the phenyl group of PA to locate on the square planar face of the Rh complex and be coplanar with the PA C≡C and the Rh atom.²¹ This may be hindered in these fluorenyl derivatives. However, once PA insertion has occurred subsequent insertions become more energetically favourable as the fluorenyl group moves further away from the active site, the conjugation length increases and, as noted by Onishi *et al.*, the presence of through space electron donation from the phenyl group to the Rh centre.²² If this proposal is correct then it suggests that a similar level of activity would likely be observed for the **88d** and **88e**. Indeed, for **88d** mediated homopolymerisation of PA under the same conditions (entry 8 Table 2-1), the isolated PPA had an SEC-measured M_n of 47,900 (an initiation efficiency of 0.19) with a corresponding \bar{D} of 1.31.

Miyake, Misumi and Masuda¹⁵ noted that PA homopolymerisations with **78b** proceeded smoothly over the temperature range 30-60 °C. In an effort to improve the IE, **88b** was further examined under conditions noted above except polymerisations were performed at 40, 50 and 60 °C, Table 2-1 entries 4-6. While an improvement is observed with increasing temperature (the IE increases from 0.13 at 40 °C to 0.16 at 50 °C and 0.19 at 60 °C), it is still not quantitative and represents only marginal improvements over homopolymerisation at 30 °C. There also appears to be an undesirable effect on the dispersity and stereoregularity with increasing polymerisation temperature – the former increases from 1.18 to 1.27, and the latter decreases from 94 to 88 %. The decrease in *cis*-content at elevated temperatures has been documented previously by Percec *et al.*²³ in a study on the thermal isomerisation

of PPA in solution under an inert atmosphere (argon and nitrogen-based atmosphere) leading to a decrease of *cis*-content.

Miyake, Misumi and Masuda¹⁵ also reported that the homopolymerisation of PA with **78b** was essentially unaffected by the nature of the polymerisation solvent with polymerisations proceeding in a controlled fashion with (near) quantitative IE to give polymers with low dispersities. The only observed effect was related to the kinetics of polymerisation with rates falling marginally with increasing dielectric constant of the reaction medium.

Homopolymerisations of PA was subsequently examined with **88b** in THF, Table 2-1 entries 10-15. Broadly, the use of THF resulted in higher IE with values spanning the range 0.26 – 0.50 and increased stereoregularity with *cis* contents as high as 95 %. In the case of polymerisations performed at 40 °C, a near doubling of the IE was observed when 20 equivalents of free phosphine versus five were employed albeit at the expense of slightly broader molecular weight distributions. These results suggest that in contrast to the Masuda-type triphenylvinyl derivatives, the polymerisation solvent does impact the level of control for PA polymerisations mediated by the fluorenyl derivatives. Next, a single PA homopolymerisation was conducted with **88e** in THF at 30 °C with five equivalents of added free phosphine, Table 2-1 entry 9. Of all the conditions examined, this polymerisation proceeded with the highest initiation efficiency (0.56) and yielded the most stereoregular PPA product with a measured *cis* content of 96 %.

While the initiation efficiencies of the **88** complexes were less than quantitative, the highly stereoregular nature of the products, their high yields and low dispersities do suggest controlled polymerisation. One key feature indicative of a controlled polymerisation process is the ability to prepare AB diblock copolymers (or more advanced architectures) by sequential monomer addition; successful blocking, ideally quantitatively, confirms retention of active chain ends.

To examine this feature, a self-blocking experiment was performed in which PA was initially homopolymerised in THF at 40 °C in the presence of **88b** and 20 equivalents of free phosphine. After 1 hour, an aliquot was withdrawn and analysed by SEC, Figure 2-14A, with the formed PPA having a measured M_n just over 17,000 and a corresponding \mathcal{D} of 1.34. Subsequently, a second charge of PA was added to the vessel and the polymerisation allowed to proceed for a further 60 min. Termination with acetic acid and isolation by precipitation yielded a final material with an SEC-measured M_n of 46,900 and \mathcal{D} of 1.19.

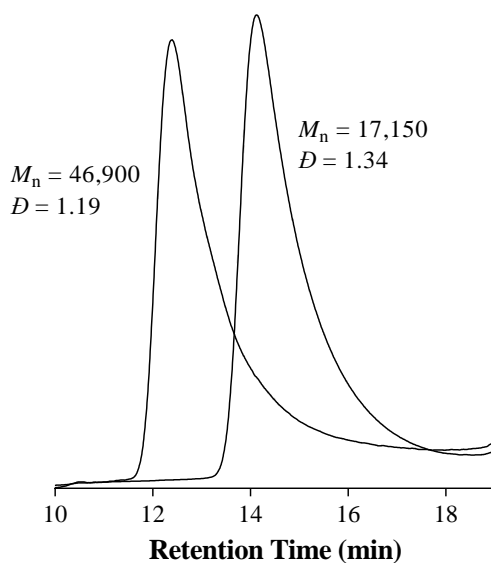
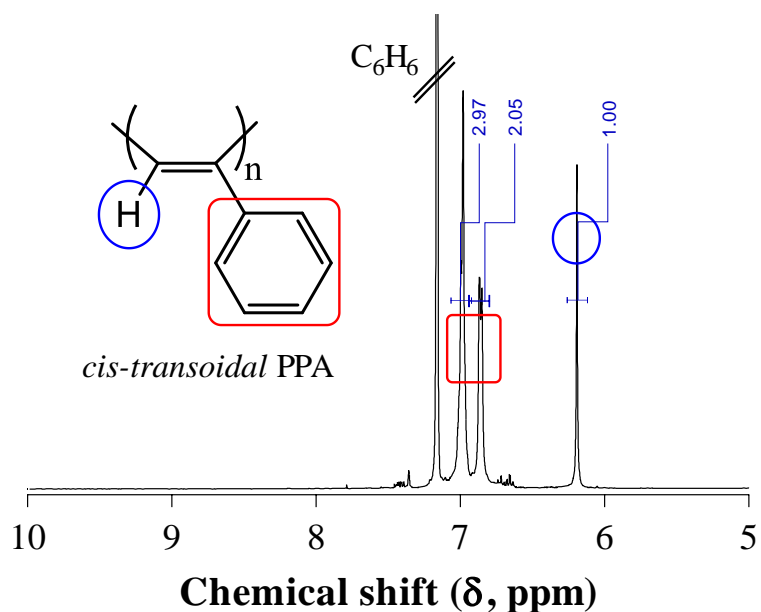
A**B**

Figure 2-14. (A) SEC traces (RI signal), measured in THF, of a self-blocked PPA demonstrating retention of active chain ends; (B) ^1H NMR spectrum, recorded in d_6 -benzene of the final, isolated 'block' copolymer highlighting the stereoregular structure as evidenced by the sharp singlet at $\delta = 6.19$ ppm that is attributed to the backbone hydrogen in a *cis* conformation. Measured integral values are annotated in blue.

Importantly, a clear shift in the chromatograms to lower retention time (higher molecular weight) was observed after the addition and polymerisation of the second batch of monomer with little, if any, evidence of homopolymer impurity, Figure 2-14A, this confirms retention of active chain ends after the initial homopolymerisation of the first batch of PA and also indicates near-quantitative 'reinitiation' following the addition of the second charge of monomer; both features are indicative of a controlled polymerisation process. Consistent with the prior polymerisations, the isolated material was highly stereoregular with a calculated *cis* content of 96%. The ¹H NMR spectrum, recorded in C₆D₆, of the isolated PPA is shown in Figure 2-14B. The highly regular structure is confirmed by the presence of the sharp singlet at $\delta = 6.19$ ppm coupled with the two sharp resonances at ca. 6.9-7.0 ppm. The former is attributed to the backbone H in a *cis* conformation while the latter are the aromatic hydrogens on the phenyl ring. This is entirely in-line with previous reports in which, for example, the presence of any significant *trans* backbone H's results in very significant broadening in the aromatic region.²⁴

2.4 Conclusions

In this chapter we have described the synthesis of three new Rh(I)- α -phenylvinyl complexes containing different fluorine-functional triarylphosphine ligands. All complexes have been characterised in detail via a combination of NMR spectroscopy (^1H , ^{19}F , ^{31}P , ^{103}Rh , ^{31}P - ^{103}Rh HMQC and ^{31}P - $^{103}\text{Rh}\{^{103}\text{Rh}\}$ HMQC), elemental analysis and X-ray crystallography. All new species have similar solid-state structures and the general square planar geometry which was confirmed by modelling. The Rh(I) complexes were examined as initiators for the stereoregular polymerisation of phenylacetylene (PA) with an emphasis on Rh(nbd)(CPh=CFlu)(P(4-FC₆H₄)) (**88b**). All Rh species were active as initiators yielding polyphenylacetylene with *cis* contents as high as 96 % although initiation efficiencies spanned the range 0.13-0.56 and were dependent on the reaction conditions. It was also clearly demonstrated that solvent effects play a role in regulating the IEs of **88**, for example, under identical conditions ([P]/[Rh] = 5 at 30 °C) polymerisations mediated by **88b** in THF resulted in higher IEs (0.46) than in toluene (0.16). In addition, the ability to prepare block copolymers via sequential monomer addition confirms the controlled nature of the polymerisations mediated by **88**.

2.5 References

1. Kishimoto, Y.; Eckerle, P.; Miyatake, T.; Ikariya, T.; Noyori, R., Living polymerization of phenylacetylenes initiated by $\text{Rh}(\text{C}\equiv\text{CC}_6\text{H}_5)(2,5\text{-norbornadiene})[\text{P}(\text{C}_6\text{H}_5)_3]_2$. *Journal of The American Chemical Society* **1994**, *116* (26), 12131-12132.
2. Kishimoto, Y.; Miyatake, T.; Ikariya, T.; Noyori, R., An efficient rhodium(I) initiator for stereospecific living polymerization of phenylacetylenes. *Macromolecules* **1996**, *29* (14), 5054-5055.
3. Misumi, Y.; Masuda, T., Living polymerization of phenylacetylene by novel rhodium catalysts. quantitative initiation and introduction of functional groups at the initiating chain end. *Macromolecules* **1998**, *31* (21), 7572-7573.
4. Misumi, Y.; Kanki, K.; Miyake, M.; Masuda, T., Living polymerization of phenylacetylene by rhodium-based ternary catalysts, (diene)Rh(I) complex/vinyl lithium/phosphorous ligand. effect of catalyst components. *Macromolecular Chemistry and Physics* **2000**, *201* (17), 2239-2244.
5. Andrae, D.; Haeusserman, U.; Dolg, M.; Stoll, H.; Preuss, H., Energy-adjusted ab initio pseudopotentials for the second and third row transition elements. *Theoretica Chimica Acta* **1990**, *77* (2), 123-141.
6. Dunning, T. H., Gaussian basis sets for use in correlated molecular calculations. I. the atoms boron through neon and hydrogen. *The Journal of Chemical Physics* **1989**, *90* (2), 1007-1023.
7. Boys, S. F.; Bernardi, F., The calculation of small molecular interactions by the differences of separate total energies. some procedures with reduced errors. *Molecular Physics* **1970**, *100* (1), 65-73.
8. Harris, R. K.; Becker, E. D.; Cabral de Menezes, S. M.; Granger, P.; Hoffman, R. E.; Zilm, K. W., Further conventions for NMR shielding and chemical shifts (IUPAC recommendations 2008). *Magnetic Resonance in Chemistry* **2008**, *46* (6), 582-598.
9. Carlton, L., Rhodium-103 NMR. In *Annual Reports on NMR Spectroscopy*, Webb, G. A., Ed. Academic Press: Cambridge, US, 2008; Vol. 63, pp 49-178.
10. Sheldrick, G. M., Crystal structure refinement with *SHELXL*. *Acta Crystallographica Section C : Structural Chemistry* **2015**, *71* (1), 3-8.
11. Kumazawa, S.; Rodriguez Castanon, J.; Onishi, N.; Kuwata, K.; Shiotsuki, M.; Sanda, F., Characterization of the polymerization catalyst $[(2,5\text{-norbornadiene})\text{Rh}\{\text{C}(\text{Ph})=\text{CPh}_2\}(\text{PPh}_3)]$ and identification of the end structures of poly(phenylacetylenes) obtained by polymerization using this catalyst. *Organometallics* **2012**, *31* (19), 6834-6842.

12. Harris, R. K., Fluorine NMR spectroscopy : studies of ¹³C satellite spectra. *Journal of Molecular Spectroscopy* **1963**, *10* (1), 309-319.
13. Ernsting, J. M.; Gaemers, S.; Elsevier, C. J., ¹⁰³Rh NMR spectroscopy and its application to rhodium chemistry. *Magnetic Resonance in Chemistry* **2004**, *42*, 721-736.
14. von Philipsborn, W., Transition metal NMR spectroscopy : a probe into organometallic structure and catalysis. *Pure and Applied Chemistry* **1986**, *58* (4), 513-528.
15. Miyake, M.; Misumi, Y.; Masuda, T., Living polymerization of phenylacetylene by isolated rhodium complexes, Rh[C(C₆H₅)=C(C₆H₅)₂](nbd)(4-XC₆H₄)₃P (X = F, Cl). *Macromolecules* **2000**, *33* (18), 6636-6639.
16. Corona-Armenta, A. T.; Ordoñez, M.; López, J. A.; Cervantes, J.; Serrano, O., Synthesis and characterization of *m*-terphenyl (1,3-diphenylbenzene) compounds containing trifluoromethyl groups. *Helvetica Chimica Acta* **2015**, *98* (3), 359-367.
17. Eujen, R.; Hoge, B.; Brauer, D. J., Preparation and NMR spectra of the (trifluoromethyl)argentates(III) [Ag(CF₃)_nX_{4-n}]⁻, with X = CN (n = 1-3), CH₃, C≡CC₆H₁₁, Cl, Br (n = 2, 3), and I (n = 3), and of related silver(III) compounds. structures of [PPh₄][trans-Ag(CF₃)₂(CN)₂] and [PPh₄][Ag(CF₃)₃(CH₃)]. *Inorganic Chemistry* **1997**, *36* (7), 1464-1475.
18. Wang, X.; Mallory, F. B.; Mallory, C. W.; Beckmann, P. A.; Rheingold, A. L.; Francl, M. M., CF₃ rotation in 3-(trifluoromethyl)phenanthrene. x-ray diffraction and ab initio electronic structure calculations. *The Journal of physical Chemistry A* **2006**, *110* (11), 3954-3960.
19. Brouwer, E. B.; Enright, G. D.; Ratcliffe, C. I.; Ripmeester, J. A., Dynamic molecular recognition in solids : a synoptic approach to structure determination in p-tert-butylcalix[4]arene-toluene. *Supramolecular Chemistry* **1996**, *7* (1), 79-83.
20. Simionescu, C. I.; Percec, V.; Dumitrescu, S., Polymerization of acetylenic derivatives. XXX. isomers of polyphenylacetylene. *Journal of Polymer Science Part A : Polymer Chemistry* **1977**, *15* (10), 2497-2509.
21. Ke, Z.; Abe, S.; Ueno, T.; Morohuma, K., Rh-catalyzed polymerization of phenylacetylene : theoretical studies of the reaction mechanism, regioselectivity, and stereoregularity. *Journal of The American Chemical Society* **2011**, *133* (20), 7926-7941.
22. Onishi, N.; Shiotsuki, M.; Masuda, T.; Sano, N.; Sanda, F., Polymerization of phenylacetylenes using rhodium catalysts coordinated by norbornadiene linked to a phosphino or amino group. *Organometallics* **2013**, *32* (3), 846-853.
23. Percec, V.; Rudick, J. G.; Nombel, P.; Buchowicz, W., Dramatic decrease of the cis content and molecular weight of cis-transoidal polyphenylacetylene at 23 °C in

solutions prepared in air. *Journal of Polymer Science Part A: Polymer Chemistry* **2002**, *40* (19), 3212-3220.

24. Tang, B. Z.; Poon, W. H.; Leung, S. M.; Leung, W. H.; Peng, H., Synthesis of stereoregular poly(phenylacetylene)s by organorhodium complexes in aqueous media. *Macromolecules* **1997**, *30* (7), 2209-2212.

Every reasonable effort has been made to acknowledge the owners of copyright material. I would be pleased to hear from any copyright owner who has been omitted or incorrectly acknowledged.

Chapter 3

Controlled Polymerisation of Phenylacetylenes Catalysed by a (2-(Naphthalen-2-yl)phenyl)rhodium(I) Complex Formed by a Proposed Intramolecular 1,4-*Ortho*-to-*Ortho*' Rh Metal-atom Migration.

The content of this chapter has been published in:

Dalton Transaction (2019) with the title “A (2-(Naphthalen-2-yl)phenyl)rhodium(I) Complex formed by a Proposed Intramolecular 1,4-*Ortho*-to-*Ortho*' Rh Metal-atom Migration and its Efficacy as an Initiator in the Controlled Stereospecific Polymerisation of Phenylacetylene” (refer to Appendix C)

3.1 Introduction

In the previous chapter, the preparation of three new Rh(I)- α -phenylvinylfluorenyl complexes based on the Masuda structural motif was described, see Figure 3-1, **88b** as an example. It was noted that although **88b**, and its derivatives, was structurally similar to **78b**, complex **88b** displayed low initiation efficiencies with values ranging from 16 – 56 % depending on polymerisation conditions, although the resulting phenylacetylene polymers did have high *cis-transoidal* content with SEC measured dispersities, D , as low as 1.03. These Chapter 2 results suggest that its more than meeting the substitution criteria outlined by Misumi *et al.*¹ that is important in

tuning catalytic activity and a more detailed understanding of the initiating fragment is clearly necessary.

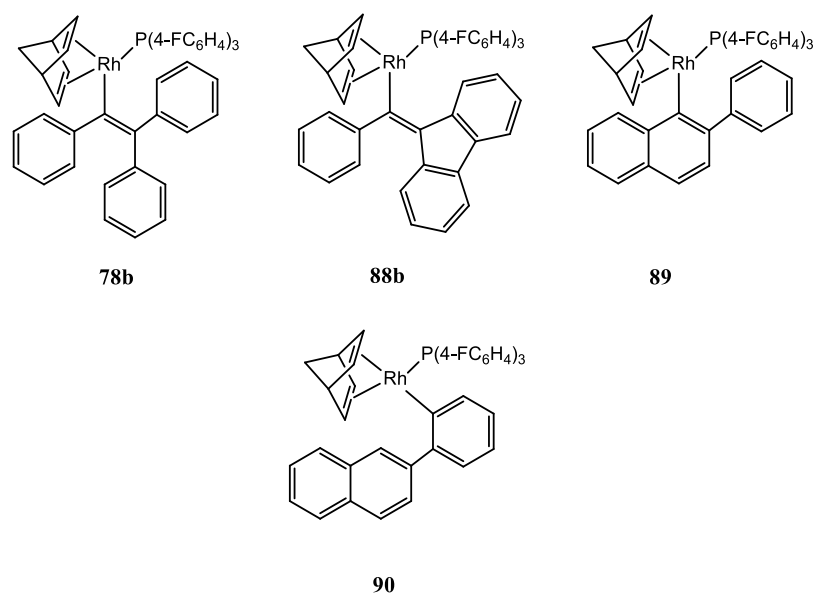


Figure 3-1. Masuda triphenylvinyl Rh(I) derivative, **78b**, Tan α -phenylvinylfluorenyl derivative, **88b**, a targeted 2-phenylnaphthyl Rh(I) species, **89**, and isolated 2-naphthylphenyl Rh(I) species, **90**.

The observed disparity in the activity between **88b** and **78b** was hypothesised to be due to the conformationally locked nature of the fluorenyl group on the β -vinyl carbon, which inhibited the effective co-ordination of incoming monomer and as such impacted the initiation and early propagation processes.

This chapter details work involved in testing this proposition with the synthesis of a novel Rh(I) complex, Rh(nbd)(2-PhNaphth)(P(4-FC₆H₄)₃), (2-PhNaphth = 2-phenylnaphthalen-1-yl), **89** Figure 3-1, where the phenyl group on the β -vinyl carbon, which is now a part of the aromatic naphthyl group, is freely rotating and part of the initiating fragment. Herein, will be detailed the attempted synthesis of the targeted 2-phenylnaphthyl Rh(I) species, **89**, the mechanistic rationale for the isolation of the structural isomer **90**, *vide infra*, an isomeric 2-naphthylphenylrhodium(I)-aryl

derivative and the presence of a third structural isomer, the 3-phenylnaphthyl derivative formed in solution via sequential Rh-atom migrations. Finally, the novel Rh(I)-aryl complex was evaluated to determine its efficacy in mediating the controlled polymerisation of PAs. As of writing, this is the first example in which a Rh(I)-aryl complex of this type has been evaluated as a polymerisation initiator for PA although similar Rh(I)-aryl species are known to mediate the controlled polymerisation of bulky aryl isocyanides^{2,3}

3.2 Experimental

3.2.1 Materials

n-Butyllithium (*n*-BuLi, 1.6 M solution in hexane, Sigma-Aldrich), 1-bromo-2-phenylnaphthalene ($C_6H_5(C_{10}H_6Br)$) (98 % Tokyo Chemical Industry), $[Rh(nbd)Cl]_2$ (*nbd* = 2,5-norbornadiene, 98 %, Strem Chemicals), and tris(*para*-fluorophenyl)phosphine ($P(4-FC_6H_4)_3$, 98 %, Sigma-Aldrich) were used as received. Phenylacetylene ($CH\equiv CPh$, 98 %, Sigma-Aldrich) was purified by passage over a column of basic alumina and then stored in a fridge until needed.

THF, diethyl ether and CH_2Cl_2 were dried using a PureSolv MD5 solvent purification system (Innovative Technology, Inc.), collected, degassed via the freeze-pump-thaw technique and stored under dry nitrogen until needed. Toluene (99.8 %, Sigma-Aldrich) was degassed via the freeze-pump-thaw technique and stored under dry nitrogen until needed. All glassware was pre-dried in an oven at 120 °C and then flamed dried under vacuum before use. All reactions were performed using standard Schlenk line techniques.

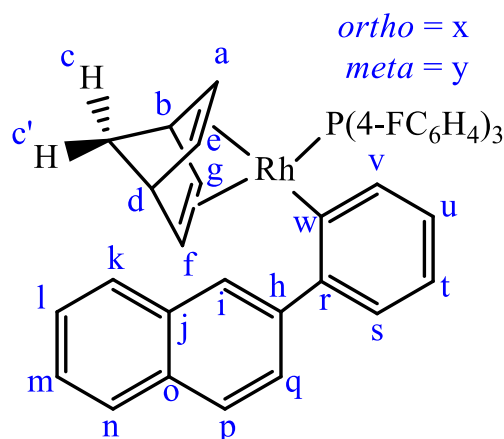
3.2.2 Attempted Synthesis of $Rh(nbd)(2-PhNaphth)(P(4-FC_6H_4)_3)$

$Rh(nbd)(2-PhNaphth)(P(4-FC_6H_4)_3)$, **89**, was prepared following the procedure recently reported, and described in Chapter 2, for the preparation of $Rh(I)$ - α -phenylvinylfluorenyl derivatives.⁴

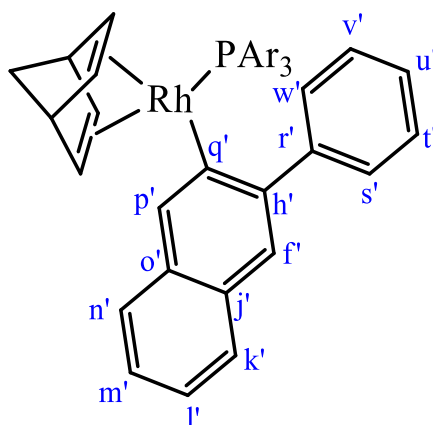
To a round-bottomed flask equipped with a Teflon-coated magnetic stir bar was added 1-bromo-2-phenylnaphthalene (293 mg, 1.03 mmol) and diethyl ether (20.0 mL) under a dry nitrogen atmosphere. The flask was cooled to 0 °C, and *n*-BuLi (1.6 M solution in hexane, 1.25 mL, 2.0 mmol) was cannula transferred and the mixture allowed to react for 30 min yielding $C_6H_5(C_{10}H_6Li)$.

To a separate round-bottomed flask equipped with a magnetic stir-bar containing dry toluene (15.0 mL) was added $[\text{Rh}(\text{nbd})\text{Cl}]_2$ (210 mg, 0.45 mmol) and $\text{P}(4\text{-FC}_6\text{H}_4)_3$ (411 mg, 1.30 mmol). The mixture was then stirred vigorously for 15 min at ambient temperature yielding the intermediate Rh species, $\text{Rh}(\text{nbd})(\text{P}(4\text{-FC}_6\text{H}_4)_3)\text{Cl}$.

The lithiated species, $\text{C}_6\text{H}_5(\text{C}_{10}\text{H}_6\text{Li})$, was added, via cannula, to the solution containing $\text{Rh}(\text{nbd})(\text{P}(4\text{-FC}_6\text{H}_4)_3)\text{Cl}$ and allowed to stir at ambient temperature overnight. Subsequently, the reaction solution was cannula transferred and filtered through a short plug of neutral activated alumina 90, under an inert atmosphere, yielding a clear orange solution. Solvents were concentrated under high vacuum on a Schlenk line yielding a dark viscous liquid. To the residue was added CH_2Cl_2 (2.5 mL) and the Rh(I) complex, **90**, the 2-naphthylphenyl structural isomer, was isolated following recrystallisation from CH_2Cl_2 /methanol via a solvent layering technique. Yield: 209.8 mg, 64 %. CH elemental analysis: % C_{theor} : 68.92, % C_{found} : 68.20; % H_{theor} : 4.37, % H_{found} : 4.33.



Rh(nbd)(2-NaphthPh)(P(4-FC₆H₄)₃), **90**: ¹H NMR (600 MHz, CD₂Cl₂), δ (ppm): 9.14 (s, 1H, H_i), 8.06 (d, *J* = 8.2 Hz, 1H, H_k), 7.89 (d, *J* = 8.1 Hz, 1H, H_n), 7.60 (d, *J* = 8.3 Hz, 1H, H_p), 7.59 (m, 1H, H_l), 7.54 (ddd, *J* = 8.1, 6.8, 1.3 Hz, 1H, H_m), 7.25 (dt, *J* = 7.2, 1.6 Hz, 1H, H_v), 7.06 (dd, *J* = 7.4, 1.4 Hz, 1H, H_s), 6.99 (dd, *J* = 8.3, 1.8 Hz, 1H, H_q), 6.88 (m, 1H, H_t), 6.84 (td, *J* = 7.2, 1.4 Hz, 1H, H_u), 6.74 (m, 6H, H_y), 4.97-4.94 (m, 1H, H_g), 6.60 (m, 6H, H_x), 4.13 (dt, *J* = 7.5, 3.8 Hz, 1H, H_f), 4.04 (s, 1H, H_d), 3.83 (s, 1H, H_b), 3.55 (m, 1H, H_a), 3.54 (m, 1H, H_e), 1.60 (dt, *J* = 8.1, 1.7 Hz, 1H, H_{c'}), 1.35-1.32 (m, 1H, H_c); ¹³C NMR (151 MHz, CD₂Cl₂), δ (ppm): 172.3 (dd, *J* = 33.5, 13.2 Hz, C_w), 163.4 (dd, *J* = 249.5, 1.9 Hz, C-F), 147.2 (dd, *J* = 3.0, 1.9 Hz, C_r), 145.9 (d, *J* = 2.2 Hz, C_h), 136.2 (dd, *J* = 2.4, 1.8 Hz, C_v), 135.9 (dd, *J* = 14.2, 8.1 Hz, C_x), 135.0 (C_j), 133.22 (C_o), 130.1 (dd, *J* = 35.3, 3.2 Hz, C-P), 128.6 (C_k), 128.1 (C_n), 127.9 (C_p), 127.6 (C_s), 126.4 (C_l), 125.7 (C_m), 125.2 (d, *J* = 1.7 Hz, C_u), 124.7 (C_q), 122.2 (C_t), 116.2 (d, *J* = 1.4 Hz, C_i), 115.2 (dd, *J* = 20.9, 10.2 Hz, C_y), 75.4 (dd, *J* = 5.3, 3.2 Hz, C_e), 75.0 (dd, *J* = 5.7, 1.4 Hz, C_a), 72.4 (dd, *J* = 15.1, 1.4 Hz, C_g), 64.9 (t, *J* = 4.7 Hz, C_c), 55.5 (dd, *J* = 19.1, 6.9 Hz, C_f), 51.5 (d, *J* = 3.3 Hz, C_b), 51.1 (d, *J* = 3.9 Hz, C_d); ¹⁹F NMR (565 MHz, CD₂Cl₂), δ (ppm): -112.4 (m); ³¹P{¹H} NMR (243 MHz, CD₂Cl₂), δ (ppm): 24.4 (dq, *J*_{P-Rh} = 189.9, *J*_{P-F} = 3.3 Hz); ¹⁰³Rh NMR (19.1 MHz, *d*₈-toluene), δ (ppm): -7688 (547 ppm if referenced to Rh metal).



Rh(nbd)(3-PhNaphth)(P(4-FC₆H₄)₃), **91**: ¹H NMR (600 MHz, CD₂Cl₂), δ (ppm): 7.84 – 7.87 (m, 2H, H_{w'+s'}), 7.65 (d, *J* = 8.0 Hz, 1H, H_{k'}), 7.43 (s, 1H, H_{p'}), 7.42 (s, 1H, H_{i'}), 7.42-7.39 (m, 4H, H_{v'+t'}, H_{u'}, H_{n'}), 7.24-7.23 (m, 1H, H_{m'}), 7.19 (dd, *J* = 8.7, 6.8 Hz, 1H, H_{l'}), 6.90-6.85 (m, 12H, H_{x'}, H_{y'}), 4.97 (m, 1H, H_{a'}), 3.88 (dd, *J* = 4.2, 3.4 Hz, H_{f'}), 3.82-3.74 (m, 3H, H_{e'}, H_{b'}, H_{d'}), 3.61 (dd, *J* = 8.3, 4.2 Hz, H_{g'}), 1.52 (m, 1H, H_{c'}), 1.32 (m, 1H, H_{c''}); ¹³C NMR (151 MHz, CD₂Cl₂), δ (ppm): 169.4 (dd, *J* = 33.7, 13.1 Hz, C_{q'}), 163.8 (dd, *J* = 250.1, 1.6 Hz, C-F), 147.6 (d, *J* = 1.6 Hz, C_{r'}), 147.1(C_{h'}), 135.9, (dd, *J* = 14.3, 7.9 Hz, C_{x'}), 133.6 (m, C_{p'}), 132.5 (C_{o'}), 131.1 (C_{j'}), 130.4 (d, *J* = 35.8 Hz, C-P), 129.4 (C_{v'+t'}), 128.1 (C_{k'}), 127.3 (C_{u'}), 125.8 (C_{n'}), 124.9 (C_{m'}), 124.4 (C_{i'}), 123.1 (C_{l'}), 122.7 (C_{w'+s'}), 115.4 (dd, *J* = 21.2, 10.2 Hz, C_{y'}), 75.2 (m, C_{g'}), 74.0 (m, C_{f'}), 72.3 (m, C_{a'}), 65.2 (t, *J* = 4.6 Hz, C_{c'}), 56.4 (dd, *J* = 19.6, 7.4 Hz, C_{e'}), 51.1 (m, C_{b'}), 51.0 (d, *J* = 4.0 Hz, C_{d'}); ¹⁹F NMR (565 MHz, CD₂Cl₂), δ (ppm): -112.21 (m); ³¹P{¹H} NMR (243 MHz, CD₂Cl₂), δ (ppm): 23.23 (dq, *J*_{P-Rh} = 189.8, *J*_{P-F} = 2.9 Hz); ¹⁰³Rh NMR (19 MHz, *d*₈-toluene), δ (ppm): -7682. (544 ppm if referenced to Rh metal).

3.2.3 Polymerisation Reactions

All (co)polymerisations were carried out under a dry nitrogen atmosphere in glassware pre-dried in an oven at 120 °C. Below is given a typical procedure for the homopolymerisation of phenylacetylene with **90**:

A solution of phenylacetylene (0.184 g, 1.80 mmol) in toluene (2.5 mL) was added to a solution of **90** (0.015 g, 0.02 mmol) and free phosphine (P(4-FC₆H₄)₃) (0.031 g, 0.10 mmol) dissolved in toluene (2.5 mL) in a Schlenk flask equipped with a magnetic stir bar. The flask was then immersed in a pre-heated oil bath set at 30 °C and polymerisation allowed to proceed for 90 min. An aliquot (0.1 mL) was withdrawn every 5-10 min and was added to a vial of deuterated chloroform (0.5 mL) containing a small volume of acetic acid (2.0 µL). After 90 min, the polymerisation was terminated by the addition of acetic acid. The final polymer was isolated by precipitation into a large volume of methanol, isolated by gravity filtration and dried to constant weight in a vacuum oven at 40 °C overnight. Monomer conversions were determined by ¹H NMR spectroscopy, and molecular weights and dispersity were determined by size exclusion chromatography.

3.2.4 Computational Chemistry

All calculations were performed using the TURBOMOLE V6.4 package using the resolution of identity (RI) approximation.⁵⁻¹²

Initial optimisations were performed at the (RI-)BP86/SV(P) level, followed by frequency calculations at the same level. Transition states were located by initially performing a constrained minimisation (by freezing internal coordinates that change most during the reaction) of a structure close to the anticipated transition state. This was followed by a frequency calculation to identify the transition vector to follow

during a subsequent transition state optimisation. A final frequency calculation was then performed on the optimised transition-state structure. All minima were confirmed as such by the absence of imaginary frequencies, and all transition states were identified by the presence of only one imaginary frequency. Dynamic Reaction Coordinate analysis confirmed that transition states were connected to the appropriate minima. Single-point calculations on the (RI-)BP86/SV(P) optimised geometries were performed using the hybrid PBE0 functional and the flexible def2-TZVPP basis set. The (RI-)PBE0/def2-TZVPP SCF energies were corrected for their zero-point energies, thermal energies and entropies (obtained from the (RI-)BP86/SV(P)-level frequency calculations). A 28 electron quasi-relativistic ECP replaced the core electrons of Rh. No symmetry constraints were applied during optimisations. Solvent corrections were applied with the COSMO dielectric continuum model¹³ and dispersion effects modelled with Grimme's D3 method.^{14, 15}

3.2.5 NMR Measurements

NMR spectra were recorded at 298K on a Bruker Avance IIIHD (600 MHz for ¹H). The data were processed with Bruker's TopSpin 3.5 or MestReNova software packages. ¹H, ¹³C, ¹⁹F, and ³¹P spectra were collected on a commercial broadband probe, whereas the ¹⁰³Rh NMR was acquired at 19.1 MHz using a commercial 5 mm triple resonance broadband probe (doubly tuned ¹H/³¹P outer coil with inner broadband coil) with 90° pulses of 27.5 μs and 18.4 μs for ¹⁰³Rh and ³¹P respectively. ¹⁰³Rh chemical shifts, δ, are given in ppm relative to frequency ratio, $\mathcal{E} = 3.186447^{16}$ and derived indirectly from the ³¹P-¹⁰³Rh HMQC experiments (the chemical shift for the commonly used reference $\mathcal{E} = 3.160000$ (Rh metal) is also given) by four pulse ³¹P-¹⁰³Rh HMQC experiments with ¹⁰³Rh and ¹H decoupling during acquisition. The

transmitter frequency offset and t_1 increments were varied to ensure that no signals were folded. Exponential line broadening of 10 Hz was applied to 1D ^{103}Rh data, with 2D data zero filled, Gaussian broadened by 10 Hz and treated with spine-squared window function during processing. Coupling constants reported herein are given as absolute values but are likely to be negative in sign for $^1J_{\text{Rh-P}}$.¹⁷

3.2.6 Crystallography

A crystalline sample of **90** was measured at 100(2) K on an Oxford Diffraction Xcalibur diffractometer using Mo-K α radiation, $\lambda = 0.71073 \text{ \AA}$, Lp and absorption corrections applied. The structure was solved and refined against F^2 with full-matrix least-squares using the program suite SHELX-2014.¹⁸ Anisotropic thermal displacement parameters were employed for the non-hydrogen atoms. All hydrogen atoms were added at calculated positions and refined by the use of a riding model with isotropic displacement parameters based on those of the parent atom. CCDC 1902529 deposit contains supplementary crystallographic data, and can be obtained free of charge via <https://www.ccdc.cam.ac.uk/structures/>, or from the Cambridge Crystallographic Data Centre, 12 Union Road, Cambridge CB2 1EZ, U.K.; fax: (+44) 1223-336-033; or e-mail: deposit@ccdc.cam.ac.uk

Crystal data for Rh(nbd)(2-NaphthPh)(P(4-FC₆H₄)₃) (C₄₂H₃₃F₃PRh, CH₂Cl₂): C₄₂H₃₃Cl₂F₃PRh, $M = 799.46$, yellow needle, 0.210 x 0.115 x 0.099 mm³, monoclinic, space group $P2_1/n$ (No. 14), $a = 11.7509(1)$, $b = 21.0929(2)$, $c = 13.9381(1) \text{ \AA}$, $\beta = 96.153(1)^\circ$, $V = 3434.80(5) \text{ \AA}^3$, $Z = 4$, $D_c = 1.546 \text{ g cm}^{-3}$, $\mu = 0.747 \text{ mm}^{-1}$. $F_{000} = 1624$, $T = 100(2) \text{ K}$, $2\theta_{\text{max}} = 64.7^\circ$, 71355 reflections collected, 11686 unique ($R_{\text{int}} = 0.0492$).

Final $Goof = 1.000$, $R1 = 0.0397$, $wR2 = 0.0916$, R indices based on 9483 reflections with $I > 2\sigma(I)$ (refinement on F^2), $|\Delta\rho|_{\max} = 1.1(1) \text{ e } \text{\AA}^{-3}$, 442 parameters, 0 restraints.

3.2.7 X-ray Powder Diffraction

Powder diffraction data was collected with a Bruker D8 diffractometer using copper $K\alpha$ radiation at room temperature over the range $5 - 80^\circ 2\theta$ with a step size of $0.01^\circ 2\theta$. Approximately 30 mg of as-crystallised sample was placed on a silicon low-background holder and spun at 1 Hz during data collection. The data was modelled by the Rietveld^{19, 20} method with TOPAS,^{21, 22} using the current single-crystal structure. Unit cell parameters were refined with atomic coordinates remaining fixed. A preferred orientation correction²³ was applied to correct model intensities.

3.2.8 Elemental Analysis

Elemental microanalyses were performed on a Perkin Elmer 2400 Series II CHNS/O Analyser in CHN mode with helium as a carrier gas.

3.2.9 Size Exclusion Chromatography (SEC)

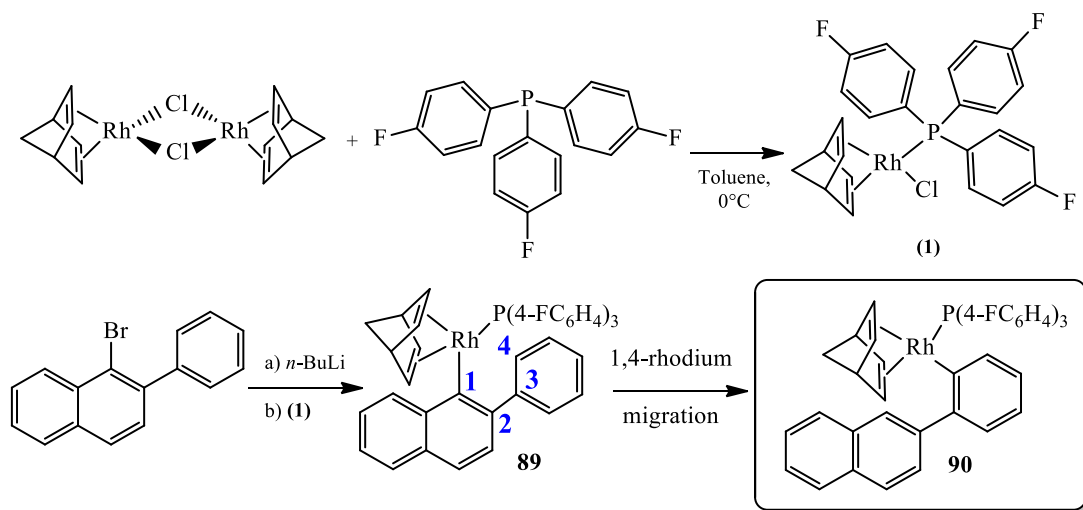
SEC was performed on a Shimadzu modular system consisting of a $4.0 \text{ mm} \times 3.0 \text{ mm}$ Phenomenex Security GuardTM Cartridge guard column and two linear phenogel columns (10^3 and 10^4 \AA pore size) in tetrahydrofuran (THF) operating at a flow rate of 1.0 mL/min and 40°C using a RID-20A refractive index detector, a SPD-M20A prominence diode array detector and a miniDAWN TREOS multi-angle static light scattering (MALLS) detector. The system was calibrated with a series of narrow molecular weight distribution polystyrene standards with molecular weights ranging

from 0.27 to 66 kg mol⁻¹. Chromatograms were analysed by Lab Solutions SEC software.

3.3 Results and Discussion

3.3.1 Synthesis and Characterisation of a Rh(I)-2-naphthylphenyl Species

Species



Scheme 3-1. Outline for the synthesis of the target 2-phenylnaphthyl derivative, **89**, and chemical structure of the isolated, isomeric, 2-naphthylphenyl species, **90**.

The synthetic route employed for the preparation of the target Rh(I)-aryl complex **89** is shown in Scheme 3-1. The reaction of commercially available $[\text{Rh}(\text{nbd})\text{Cl}]_2$ with the fluorine functionalised phosphine $\text{P}(\text{4-FC}_6\text{H}_4)_3$ yielded the intermediate tetra-coordinate Rh(I) species $\text{Rh}(\text{nbd})(\text{P}(\text{4-FC}_6\text{H}_4)_3)\text{Cl}$, (**1**). Reaction of 1-bromo-2-phenylnaphthalene with $n\text{-BuLi}$ gave the corresponding lithiated 2-phenylnaphthalene derivative that when reacted with (**1**) was anticipated to yield the target complex **89**. Interestingly, after isolation and recrystallisation, X-ray crystal structure analysis, Figure 3-2, indicated the presence of **90**, a structural isomer of the target complex **89**.

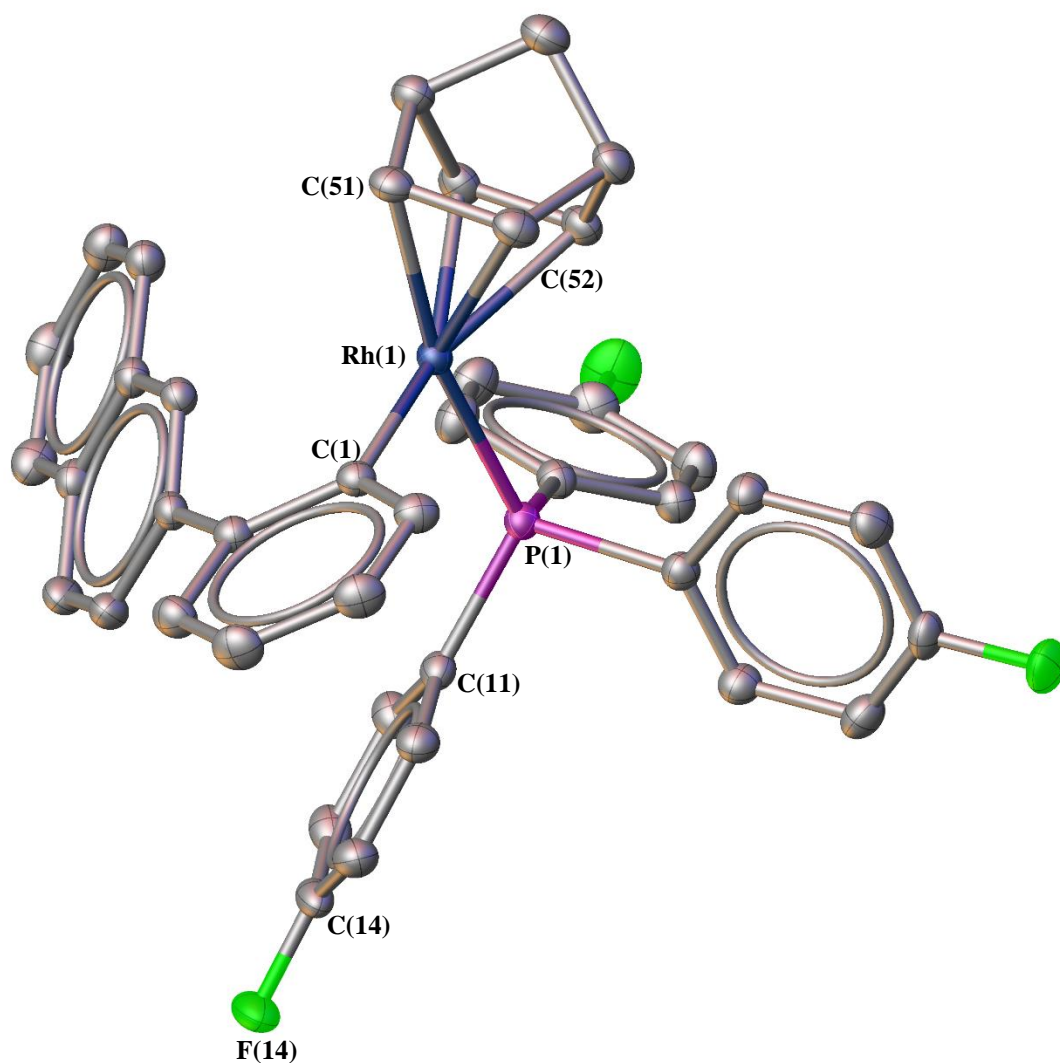


Figure 3-2. OLEX² representation of the X-ray crystal structure of **90** with 50% probability ellipsoid and H-atoms omitted for clarity. Selected bond lengths (Å): Rh(1)-P(1), 2.294 (5); Rh(1)-C(51), 2.182 (2); Rh(1)-C(52), 2.152 (2); C(14)-F(14), 1.365 (3). Selected bond angles (deg): C(51)-Rh(1)-P(1), 168.06 (6); C(52)-Rh(1)-P(1), 132.78 (6); C(1)-Rh(1)-P(1), 90.24 (6).

While **90** was not the target species, the characterisation of the complex was performed. It can be seen from the crystal structure in Figure 3-2 that the recrystallised species has a slightly distorted square planar geometry consistent with previous reports of similar Rh(I) species.^{4, 24} X-ray powder diffraction characterisation of a bulk sample of **90**, Figure 3-3, was consistent with the single-crystal structure, Figure 3-2, with remaining intensity mismatches likely due to large crystallites in the powder or slight changes in crystal structure due to the temperature difference between powder and single-crystal data collection.

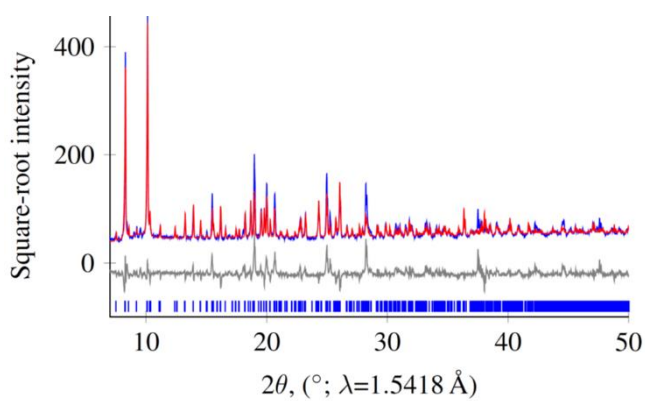


Figure 3-3. X-ray powder diffraction spectra of Rh(nbd)(2-NaphthPh)(P(4-FC₆H₄)₃), **90**. In red is shown the predicted spectra based on the obtained single-crystal structure and in blue is the experimentally obtained spectra of a bulk sample of Rh(nbd)(2-NaphthPh)(P(4-FC₆H₄)₃).

Table 3-1. Continuous Shape Measures values of Rh(L)(nbd)(PR₃) complexes against the reference tetrahedral and square planar geometries.

Complex	CSD Refcode	Reference	Tetrahedral	Square Planar
L = Phenyl derivative				
(90)	–	This work	25.047	2.952
[Rh(2-Me-1-Naphth)(nbd)PPh ₃]	LEDSIX	10.1021/om0509692	30.697	1.723
[Rh(<i>m</i> -Xylene)(nbd)PPh ₃]	QEMTEH	10.1021/om0005809	32.761	1.744
[Rh(C ₆ F ₅)(nbd)PCy ₃]	RUPYAE	10.1039/C5DT01981H	28.736	2.091
L = α -phenylvinylfluorenyl				
[Rh(L)(nbd)(P(4-FC ₆ H ₄) ₃)] (88b)	XITVAA	10.1002/ejic.201801411	26.231	2.555
[Rh(L)(nbd)(P(4-(CF ₃)C ₆ H ₄) ₃)] (88d)	XITVEE	10.1002/ejic.201801411	25.518	2.664
[Rh(L)(nbd)(P(3,5-(CF ₃)C ₆ H ₃) ₃)] (88e)	XITTUS	10.1002/ejic.201801411	23.556	3.527
L = triphenylvinyl				
[[Rh(CPh=CPh ₂)(nbd)(CH ₂) ₄ PPh ₂]	HEZBAR	10.1021/om301147n	25.763	2.552
[Rh(CPh=CPh ₂)(nbd)(PPh ₃)]	QIDCEN	10.1021/om300642b	22.125	4.015
[Rh(CPh=CPh ₂)(nbd)(P(4-IC ₆ H ₄) ₃)]	PERHEC	10.1021/ma000497x	21.23	4.519

A tetrahedral-square planar continuous shape measure analysis²⁵ was performed comparing **90** to complexes similar to **78b** and **88b** (Table 3-1), as well as three other structurally characterised Rh(nbd)(Ar)(PR₃) complexes: Rh(nbd)(2-Me-1-Naphth)(PPh₃),³ Rh(nbd)(*m*-xylene)(PPh₃),² and Rh(nbd)(C₆H₅)(PCy₃)²⁶ (Cy = cyclohexyl). While all are appropriately described as having distorted square planar geometries, complexes with triphenylvinyl ligands, **78b**, are the most significantly distorted towards tetrahedral geometry and those with an aromatic ring directly coordinated the least distorted. Of the latter class, it is notable that **90** is the most distorted of these, presumably because of the bulky naphthyl substituent, placing it amongst the α -phenylvinylfluorenyl derivatives, **88b** (see Table 3-1).

Multinuclear NMR spectroscopy (¹H, ¹³C, ¹⁹F, ³¹P, and various 2D techniques) were employed to characterise **90**. Figure 3-4 shows the ¹H NMR spectrum of **90** recorded in CD₂Cl₂; the full ¹H NMR spectrum is given at the top in Figure 3-4A with an expansion of the aromatic region (plotted between $\delta = 8.5$ to 6.0 ppm) given directly below, Figure 3-4B. In the full spectrum, a distinct signal at $\delta = 9.14$ ppm, which appears as a singlet, assigned to a single H labelled **i** (see annotated structure in Figure 3-4A), that is associated with the 2-naphthylphenyl functional group. The remaining labelled peaks (**a**, **b**, **c**, **c'**, **d**, **e**, **f**, **g**) can be assigned to the norbornadiene ligand. The full peak assignments are given in the experimental section along with the ¹³C, ¹⁹F, ³¹P and ¹⁰³Rh chemical shifts of **90**.

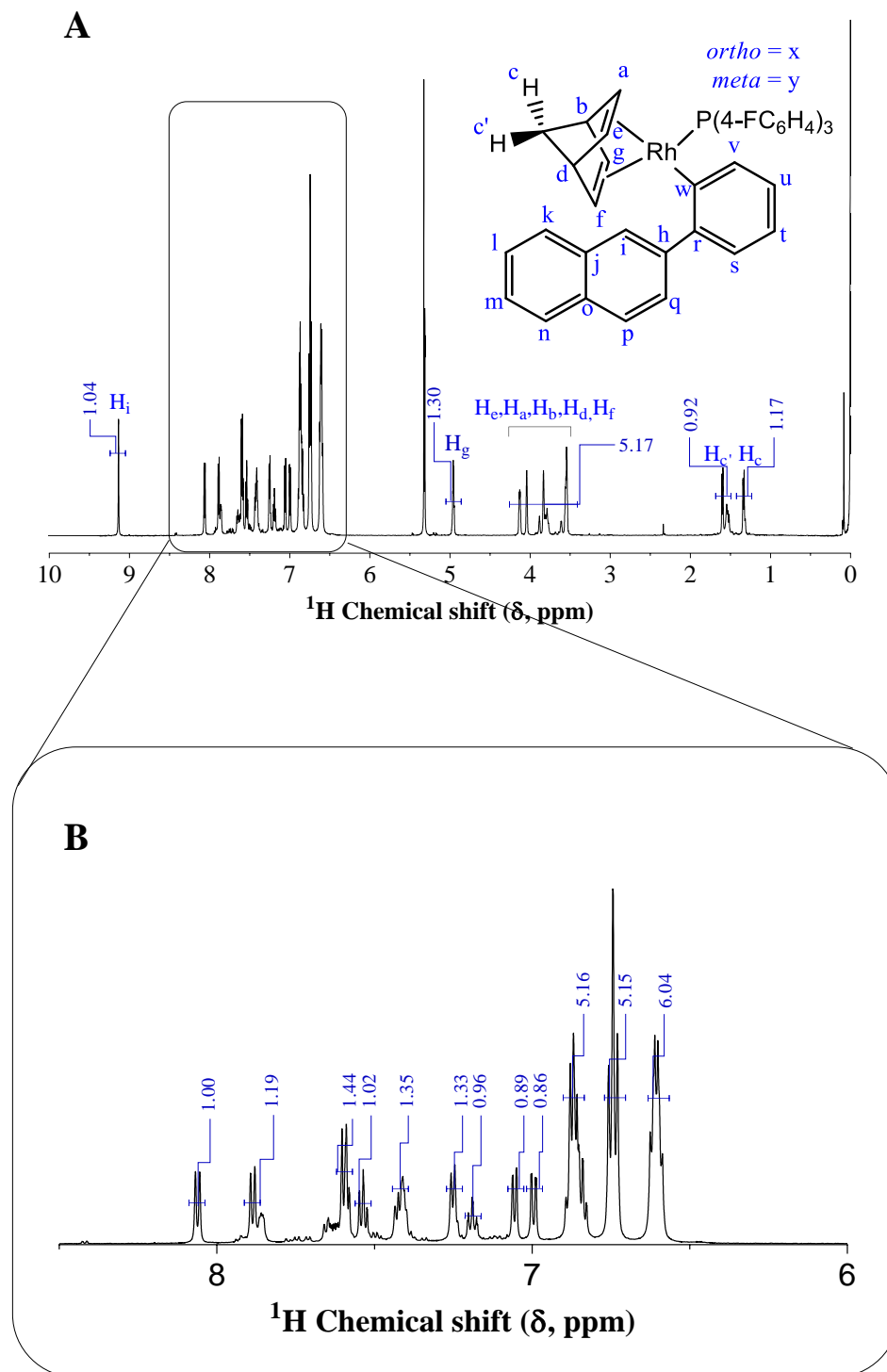


Figure 3-4. NMR spectra, recorded in CD_2Cl_2 , of $\text{Rh}(\text{nbd})(2\text{-NaphthPh})(\text{P}(4\text{-FC}_6\text{H}_4)_3)$, **90**. (A) The full ^1H NMR spectrum with key peaks annotated. (B) the ^1H NMR spectrum covering the aromatic region $\delta = 8.5$ to 6.0 ppm with measured integral values annotated in blue.

The $^{31}\text{P}\{^1\text{H}\}$ NMR spectrum of **90** is shown in Figure 3-5A. Three pairs of doublets are observed at 29.5 (3rd isomeric species), 24.4 (major isomeric species, **90**), and 23.2 ppm (2nd isomeric species, **91**) with a corresponding $^1J_{\text{Rh-P}}$ value of 176.2, 189.9 and 189.8 Hz respectively. A singlet observed at 25.3 ppm is attributed to the presence of phosphine oxide ($\text{P}(=\text{O})(4\text{-FC}_6\text{H}_4)_3$). Both the chemical shifts and coupling constant of **90** are consistent with previously reported values for Rh(I)- α -phenylvinylfluorenyl complexes, **88**, reported in Chapter 2. The ^{19}F NMR spectrum, Figure 3-5B, shows four distinct signals at -112.4 (major isomeric species, **90**), -112.21 (2nd isomeric species, **91**), -110.04 (3rd isomeric species) and -107.3 ppm (phosphine oxide, $\text{P}(=\text{O})(4\text{-FC}_6\text{H}_4)_3$).

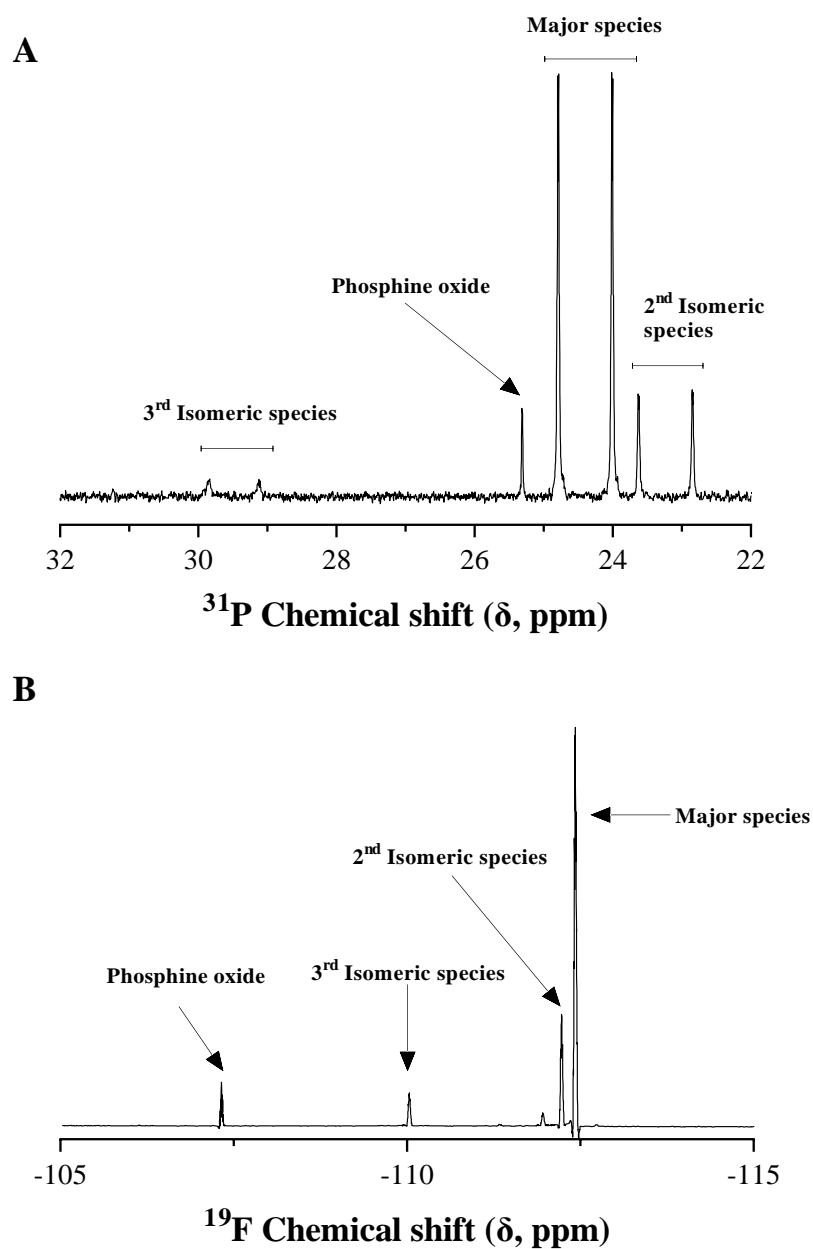


Figure 3-5 NMR spectra, recorded in CD_2Cl_2 , of **90** (A) The $^{31}\text{P}\{^1\text{H}\}$ NMR spectrum, and; (B) the ^{19}F NMR spectrum of **90** showing three distinct signals for the isomeric forms of **89** and one signal attributed to the oxide of $P(4\text{-FC}_6\text{H}_4)_3$.

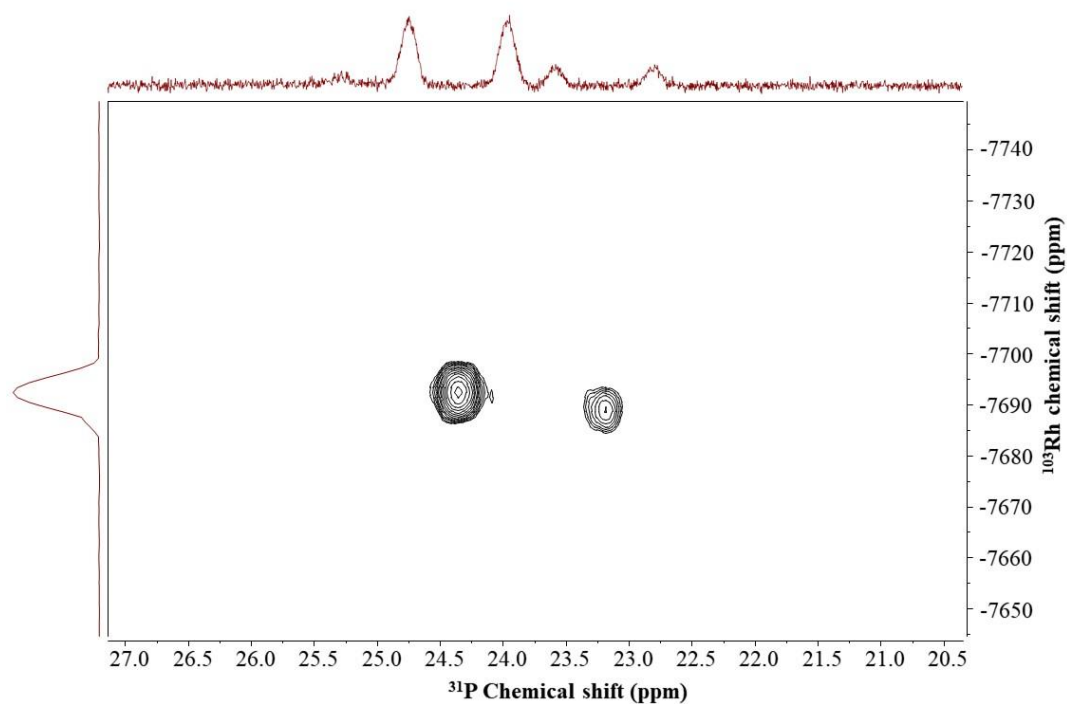


Figure 3-6. ^{31}P - $^{103}\text{Rh}\{^1\text{H}, ^{103}\text{Rh}\}$ HMQC NMR spectrum of **90** recorded in d_8 -toluene.

Interestingly, the ^1H , ^{13}C , $^{31}\text{P}\{^1\text{H}\}$ and ^{31}P - $^{103}\text{Rh}\{^1\text{H}, ^{103}\text{Rh}\}$ spectra, indicated the presence of more than one species in solution even though samples were prepared with recrystallised complex. Figure 3-6 shows the measured ^{31}P - $^{103}\text{Rh}\{^1\text{H}, ^{103}\text{Rh}\}$ HMQC spectrum of **90**. As mentioned, there are clearly two main phosphorous species present, in a ratio of 4:1, and both are coupled to Rh (the presence of a third species (ca. 5%) was also detected in the $^{31}\text{P}\{^1\text{H}\}$, and $^{19}\text{F}\{^1\text{H}\}$ spectrum of **90**, Figure 3-5A and Figure 3-5B, but was not observable in the HMQC experiment, Figure 3-6. Initially, the possibility that the two major species observed in Figure 3-6 were rotamers was considered – this has previously been observed by Kumazawa *et al.* in their detailed structural characterisation of $\text{Rh}(\text{nbd})(\text{CPh}=\text{CPh}_2)(\text{PPh}_3)$.²⁷ However, variable temperature (VT) $^{31}\text{P}\{^1\text{H}\}$, ^1H and ^{31}P - ^{103}Rh HMQC NMR experiments proved inconclusive as compound decomposition took place during heating to 90 °C in d_8 -toluene and no signal coalescence was observed.

Based, therefore, on the ^1H , ^{13}C and 2D techniques employed to characterise **90**, it was concluded that the major species present in solution is *Rh(nbd)(2-NaphthPh)(P(4-FC₆H₄)₃)* **90** (ca. 75%) Figure 3-7, while the minor species is a second structural isomer of **89**, (3-phenylnaphthalen-1-yl)rhodium(I)(2,5-norbornadiene) *tris(para*-fluorophenylphosphine), **91** (ca. 19%) Figure 3-7, and a possibility of a very minor species, a third structural isomer (ca. 5%). Finally, a smaller phosphorous peak centred around 25.4 ppm that is not coupled to Rh was noted and is attributed to the presence of the phosphine oxide (this is more clearly observed in the full $^{31}\text{P}\{^1\text{H}\}$ of the complex and $^{31}\text{P}\{^1\text{H}\}$ of the phosphine ligand, Figure 3-5A and Figure 3-8A. The signals for the phosphine oxide in the ^{19}F NMR spectrum of the complex and phosphine ligand are also noted in Figure 3-5B and Figure 3-8B for reference.)

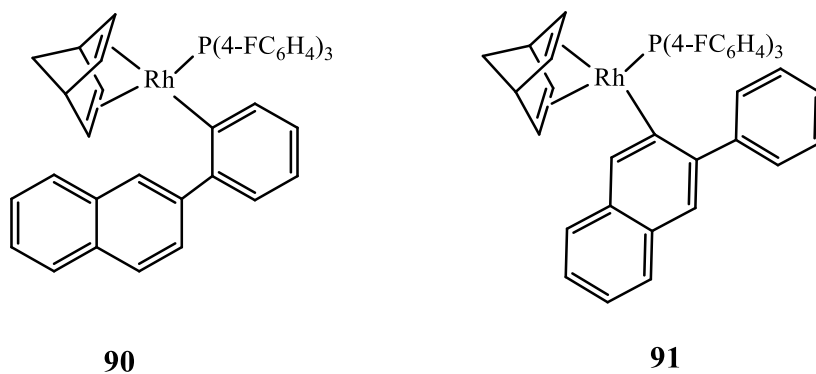


Figure 3-7. Isomeric forms of **89** identified, and their structure elucidated in this work.

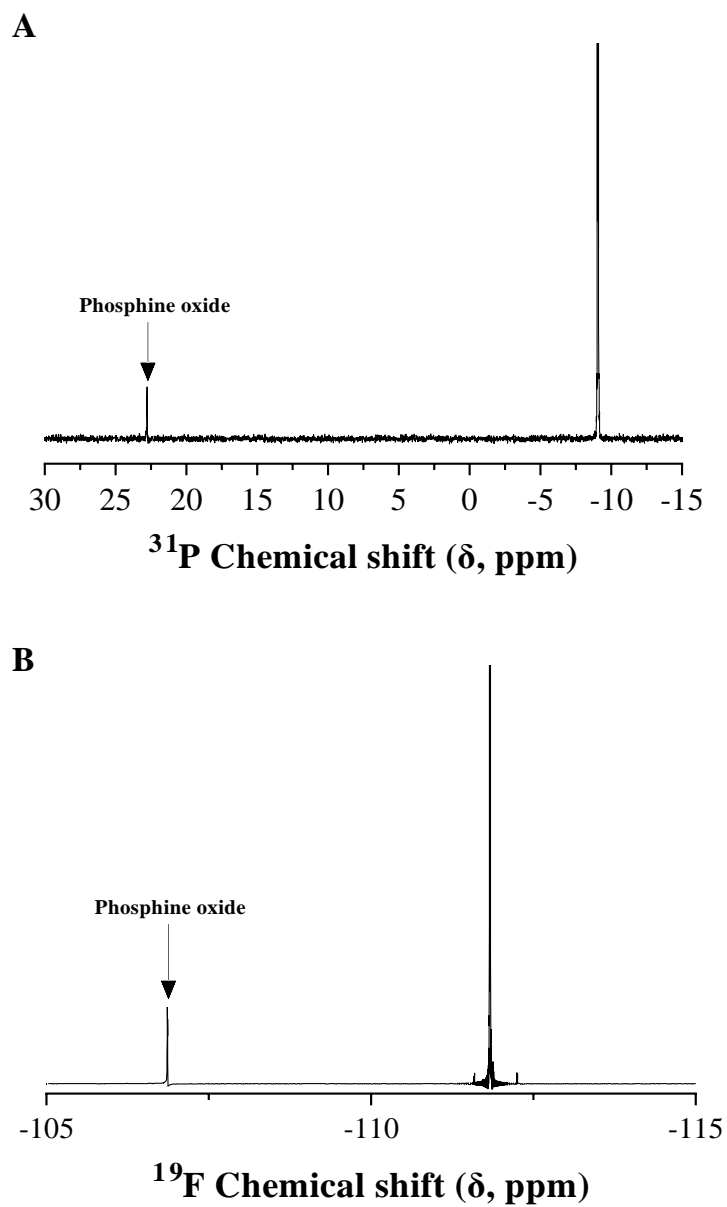
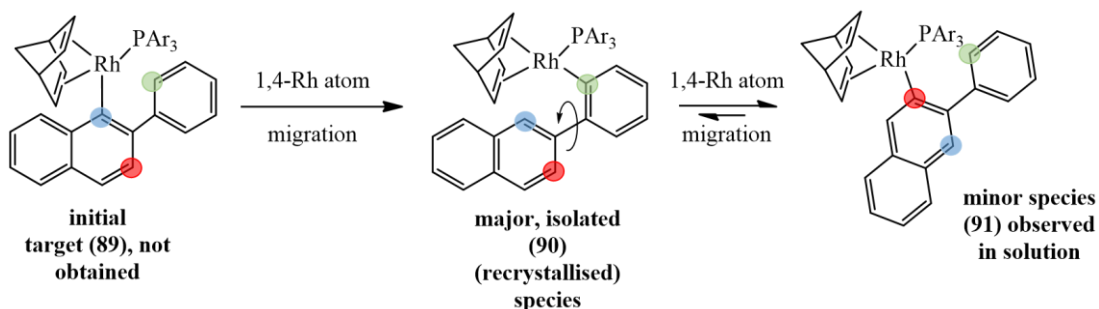


Figure 3-8. (A) The $^{31}\text{P}\{^1\text{H}\}$ NMR spectrum, of $\text{P}(4\text{-FC}_6\text{H}_4)_3$, and; (B) the ^{19}F NMR spectrum of $\text{P}(4\text{-FC}_6\text{H}_4)_3$. Relevant signals are annotated in the spectrums.

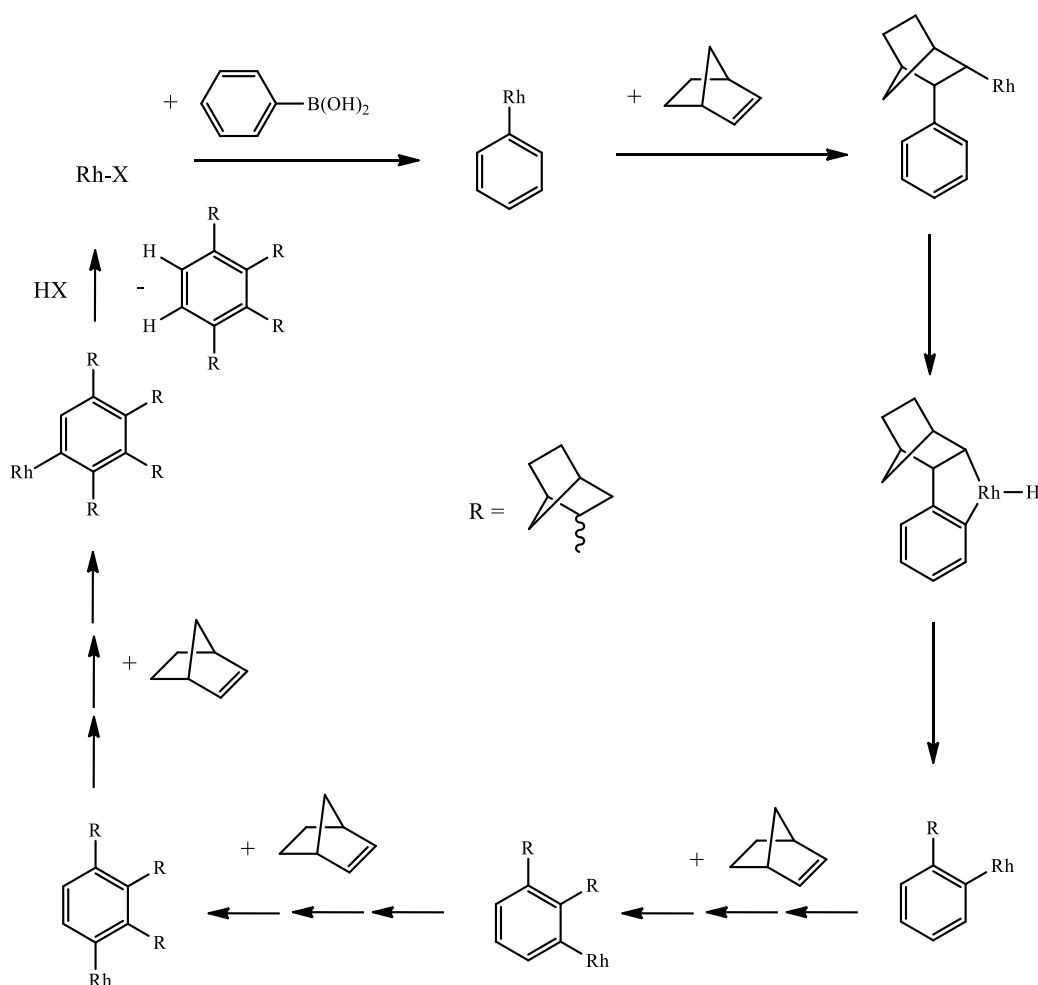
3.3.2 Mechanistic and Computational Studies



Scheme 3-2. Proposed formation of (2-naphthylphenyl-1-yl)rhodium(I)(2,5-norbornadiene)*tris*-(*para*-fluorophenylphosphine), **90**, and (3-phenylnaphthalen-1-yl)rhodium(I)(2,5-norbornadiene)*tris*(*para*-fluorophenyl phosphine), **91**, via sequential 1,4-Rh atom migrations. PAR₃ = P(4-FC₆H₄)₃.

While unanticipated, it is proposed that **90** and **91** are formed from **89** via sequential intramolecular 1,4-Rh metal-atom migrations or *ortho*-to-*ortho*' C-H bond activations, Scheme 3-2. This is an important feature of this synthesis since transition metal-mediated C-H bond activations²⁸⁻³³ play an increasingly important role in modern chemical syntheses and, mechanistically, reaction pathways involving metal (catalyst) atom migrations have been proposed to rationalise product formation with pertinent examples including reactions mediated by Pd³⁴ or Rh catalysts.³⁵ In the case of Rh-catalysed reactions, examples of 1,3-,³⁶ 1,4-,³⁷⁻⁴³ and 1,5^{44, 45} migrations have been reported. For example, Oguma *et al.*³⁷ reported that alkylation of phenylboronic acid, with norbornene, catalysed by [Rh(cod)Cl]₂/dppp (cod: cyclooctadiene; dppp: bis(diphenylphosphino)propane) yielded predominantly, under appropriate conditions, the 1,2,3,4-tetraalkylated product, Scheme 3-3. The formation of the polyalkylated species was rationalised in terms of insertion of the ene into the sp²C-[Rh] bond (as expected) followed by a 1,4-Rh atom migration to the next adjacent

phenyl ring C followed by further norbornene insertion etc. Alkylation stopped after four insertion/migration steps due to steric hindrance.



Scheme 3-3. “Merry-go-round” multiple alkylation on aromatic rings via Rh catalysis reported by Oguma *et al.*³⁷

In order to gain further insight into the mechanistic features which underpin these observations, the conversion of **89** into its two structural isomers, **90** and **91**, was modelled by density functional theory (DFT) calculations. The geometries of the complexes were optimised at the bp86/SV(P) level of theory and then single-point energies determined at the pbe0/def2-TZVPP level. The effects of solvation were modelled with COSMO and the resulting energies corrected for the effects of solvation and an empirical dispersion correction applied using Grimme’s D3 method.^{14, 15}

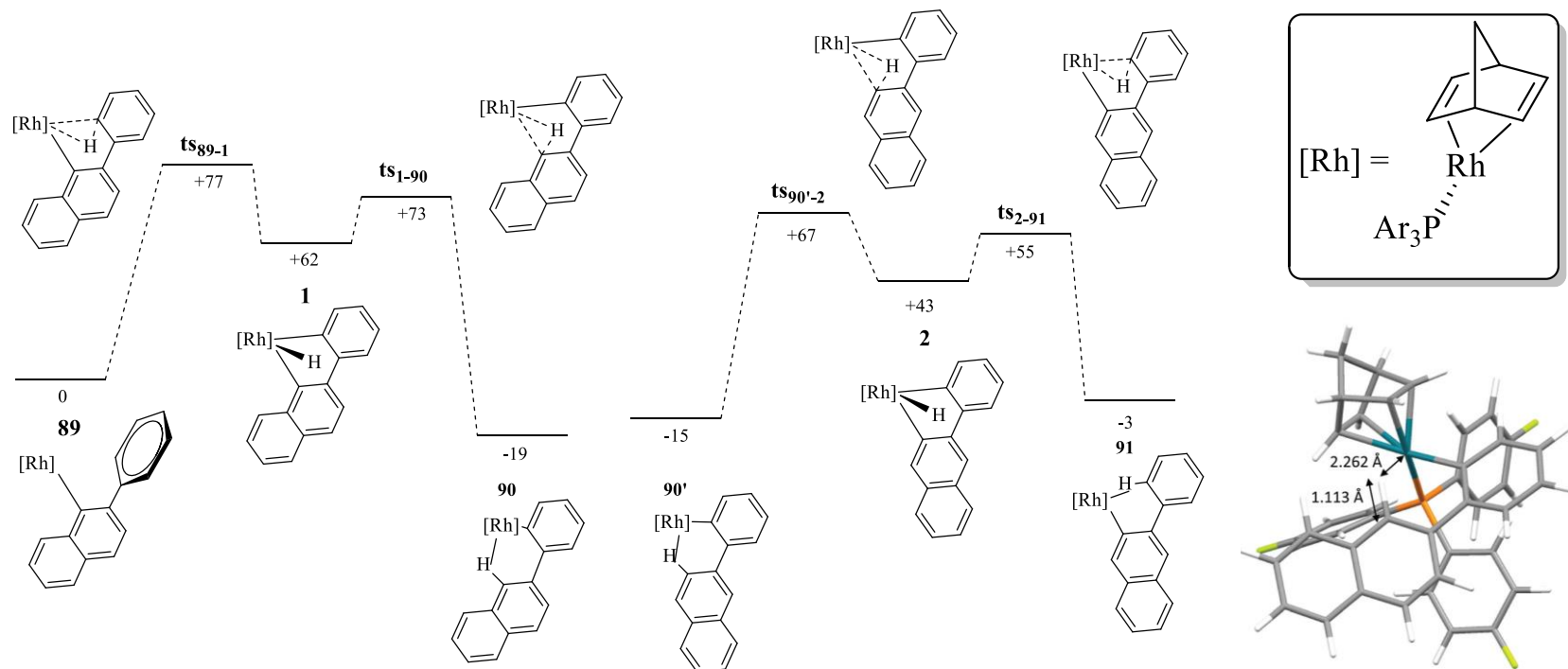


Figure 3-9. DFT-calculated pathway for the conversion of **89** to **90** and **91**. Calculations performed at the D3-pbe0/def2-TZVPP//bp86/SV(P) level with COSMO solvent correction in CH_2Cl_2 . Energies are Gibbs energies at 298 K in units of kJ/mol. $\text{PAr}_3 = \text{P}(\text{4-F-C}_6\text{H}_4)_3$. DFT-predicted structure of **90**, showing the bond metrics of the agostic interaction (carbon grey, hydrogen white, fluorine green, phosphorus orange, rhodium dark green).

As shown in Figure 3-9 the major isomer, complex **90**, has a lower energy (-19 kJ mol⁻¹) than complex **89** (which was taken as the reference state), whereas **91** lies at a relative energy of -3 kJ mol⁻¹. An examination of the DFT-predicted structures of **90**, **90'** and **91** reveals the presence of agostic interactions⁴⁶ between Rh and the 2-naphthylphenyl-1-yl ligand. Using **90** as an example, a Rh-H interaction (2.262 Å) is observed, which is complemented by an elongation of the corresponding C-H bond (1.115 Å), Figure 3-9. No agostic interaction was present in the calculated structure of **89**, with the closest Rh-H distance being 2.970 Å.

The conversion of **89** to **90** proceeds via an intermediate Rh(III)-hydride species, **1**, with an energy of 62 kJ mol⁻¹. Complex **1** lies in a shallow minimum and is connected to **89** and **90** through transition states **ts₈₉₋₁** (+77 kJ mol⁻¹) and **ts₁₋₉₀** (+73 kJ mol⁻¹) respectively. A second, higher energy, pathway was noted involving hydride transfer to the nbd ligand was also observed but was not examined further. The formation of **91** may be rationalised by rotation of the naphthyl group in **90** to give an agostomer⁴⁷ **90'** (-15 kJ mol⁻¹). C-H activation then proceeds through **ts_{90'-2}** (+67 kJ mol⁻¹) to give hydride complex **2**, which only varies from **1** in terms of its connectivity to the naphthyl group. Hydrogen migration through **ts₂₋₉₁** (+55 kJ mol⁻¹) gives **91**. It is also noted that the EXSY peaks observed during NMR characterisation of **90** and **91** are consistent with such a migration/exchange of H atoms between the coloured carbon centres shown in Scheme 3-2 and the predicted structures.

These mechanistic pathways involving a metallocyclic Rh(III)-hydride intermediate are entirely consistent with previous reports concerning such intramolecular migrations involving rhodium.^{37, 40, 48} The calculated energy barriers for the formal 1,4-migration through a hydride intermediate would indicate that the observed distribution of products is entirely under thermodynamic control at 298 K.

The calculations, therefore, support the fact that **90** (possibly in rapid exchange with **90'**) is the major species observed in solution by NMR spectroscopy. Although the calculations broadly reflect the experimental observations, it should be noted that the energy of **91** (-3 kJ mol^{-1}) would imply that its equilibrium concentration with **90** and **90'** would be very low. Moreover, at this level of theory, it is essentially at the same energy as (unobserved and initial target) **89**. However, the differences in energy are, relatively speaking, small and care must be taken when subsequently interpreting data in this fashion due to the non-linear relationship between equilibrium population and Gibbs energy.

3.3.3 Polymerisation Studies

With **90** in-hand we proceeded to determine its efficacy as an initiating species for the polymerisation of phenylacetylene (PA) (accepting that in addition to **90**, the 3-PhNaphth isomer, **91**, and perhaps a third very minor species are also present in solution). To reiterate, while the controlled polymerisation of PA has been reported with a limited number of well-defined, isolated Rh(I)-*vinyl* species, to the best of our knowledge, this is the first example in which an isolated Rh(I)-*aryl* complex has been examined in this specific application. Importantly, any indication of a controlled polymerisation employing **90** has the potential to impact, and significantly enhance, the field of Rh(I) polymerisation catalysis as applied to PA (co)polymerisation. This is due primarily to a large number of commercially available aryl bromides (versus commercially available bromo-triphenylethylenes as employed by Masuda and co-workers) that could be employed in the preparation of new catalytic/initiating species, offering an opportunity for a far more detailed evaluation of structure-activity profiles and access to materials with advanced architectures and topologies.

Table 3-2. Summary of PA polymerisation conditions with **90**, SEC-measured molecular weights and dispersities, initiation efficiencies and NMR measured *cis* contents in the resulting polyphenylacetylene (co)polymers.

Entry	Rh species	[P]/[Rh]	Polym. Temp. (°C)	Polym. solvent	Theoretical MW ^a	M_n (SEC) ^b	M_w (SEC) ^b	Dispersity (\mathcal{D}) ^b	Rh initiation efficiency ^c	<i>cis</i> content (%) ^d
1	90	5	30	Toluene	10,000	15,300	17,800	1.16	0.65	98
2	90	10	30	Toluene	10,000	15,200	17,500	1.15	0.66	98
3	90	20	30	Toluene	15,000	14,100	15,800	1.12	0.67	99
4	90	5	40	Toluene	10,000	15,600	17,100	1.10	0.64	94
5	90	10	40	Toluene	10,000	14,800	16,400	1.11	0.68	95
6	90	20	40	Toluene	20,000	23,560	25,600	1.09	0.85	99
7	90	5	50	Toluene	10,000	15,200	16,900	1.11	0.66	77
8	90	10	50	Toluene	10,000	13,000	15,300	1.18	0.77	76
9	90	20	50	Toluene	20,000	28,100	29,100	1.04	0.71	74
10	90	0	30	Toluene	10,000	nd	nd	nd	nd	nd

a. Calculated as $M_n = \text{mass (g) monomer}/\text{moles of } \mathbf{90}$ and assuming 100% initiation efficiency.

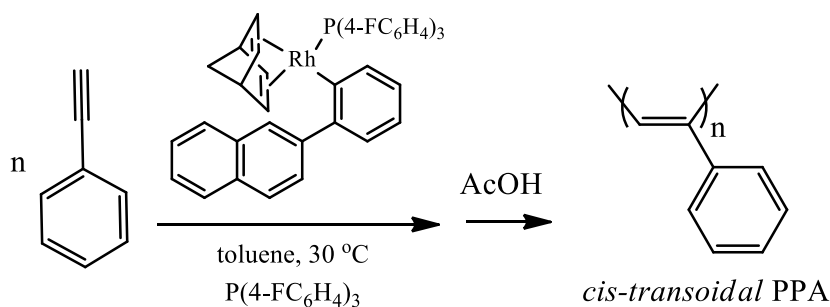
b. As measured by size exclusion chromatography: eluent THF operated at a flow rate of 1.0 mL/min, instrument calibrated with narrow molecular weight distribution polystyrene standards. Dispersity (\mathcal{D}) = M_w/M_n

c. Calculated from the ratio of theoretical to measured (SEC determined) M_n 's.

d. As determined by ¹H NMR spectroscopy according to C. I. Simionescu, V. Percec and S. Dumitrescu, *J. Polym. Sci., Part A: Polym. Chem.*, 1977, **15**, 2497-2509.

e. Not determined

Initially, a control experiment was conducted in which **90** was employed as an initiator for PA homopolymerisation (target molecular weight: 10,000, toluene, 30 °C) in the *absence* of any added free phosphine. Consistent with (co)polymerisations mediated by Rh(I)-vinyl complexes, such as **78b** in the absence of added phosphine,^{24, 49} polymerisation was uncontrolled and yielded a polymer that eluted at the upper limit of the SEC instrument indicating an $M_n > 100,000$ with an unmeasurable dispersity. As such, all further polymerisations were performed in toluene at 30 °C or 40 °C in the presence of added free phosphine as a rate modifier, Scheme 3-4, with polymerisations terminated by the addition of a small volume of acetic acid.



Scheme 3-4. Conditions for the polymerisation of phenylacetylene (PA) with **90**.

Table 3-2 shows a summary of homopolymerisations of PA mediated by **90** performed under experimental conditions such as varying the [P]/[Rh] ratio, and polymerisation temperature (°C), in order to maximise initiation efficiency, IE, as well as control over the molecular weight. It was observed that increasing polymerisation temperature, increases the Rh IE which is expected as increasing temperature increases the rate of initiation which was also observed in the fluorenyl-derivatives reported in Chapter 2. However, a significant decrease in *cis* content (as low as 77 %) was observed as polymerisation temperature increased from 30 °C to 50°C which could be attributed to thermal isomerisation of polyphenylacetylenes (PPAs). This phenomenon is known and has been documented in a study by Percec *et al.*⁵⁰ in which the thermal

isomerisation of PPA at 60 °C was examined under inert conditions (argon and nitrogen-based atmosphere) and air. In that study, it was found that thermal isomerisation occurs overtime even under an inert atmosphere and with degassed solvents, leading to a loss of *cis* content. No significant difference in dispersity, \mathcal{D} , was observed when either parameter changes ([P]/[Rh] ratio or polymerisation temperature). Overall, the highest IE achieved was ca. 0.85 at 40 °C with [P]/[Rh] = 20 in toluene.

In comparison to the Rh(I)-fluorenyl derivatives detailed in Chapter 2, **88b**, **88d**, and **88e** (where **b** = F, **d** = CF₃ or **e** = (CF₃)₂ and refers to the nature of the fluorine species on the phosphine ligand), the IE of **90** ranged from 0.64 to 0.85 and is significantly higher than the highest IE achieved by **88e** which was 0.56. While **90** does not facilitate an examination of the initiating structural feature initially proposed (a freely rotating β -phenyl group), it does appear that when compared to the structurally rigid **88** and its conformationally locked fluorenyl moiety on β -vinyl carbon of the initiating fragment, the analogous β -naphthyl group is structurally beneficial. This demonstrates that the Rh(I)-aryl derivative, **90**, is a good alternative to Rh(I)-vinyl species, **88**, as an initiator for the homopolymerisation of PA. In terms of stereoregularity, PPAs resulting from the polymerisations mediated by **88** and **90** are high in *cis* content (ca. 99 %) with no discernible difference between them.

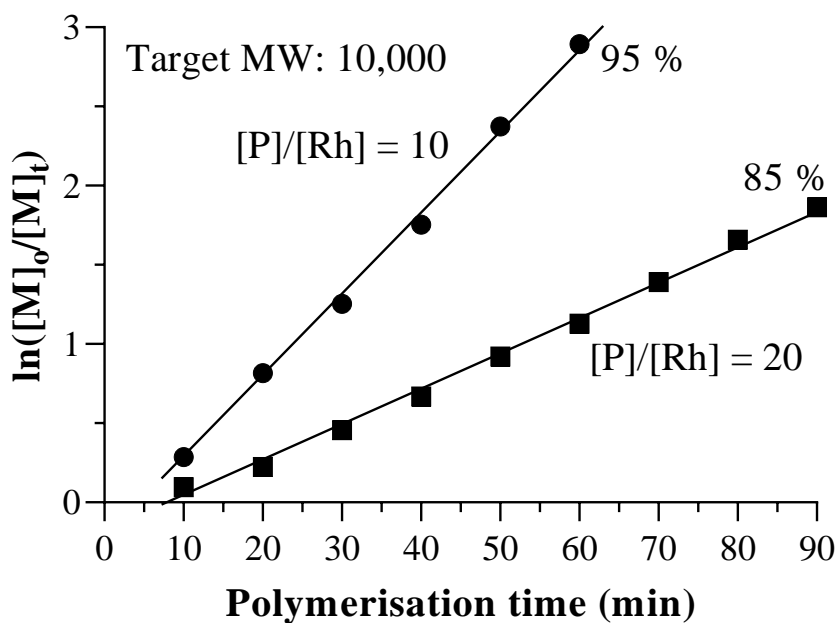
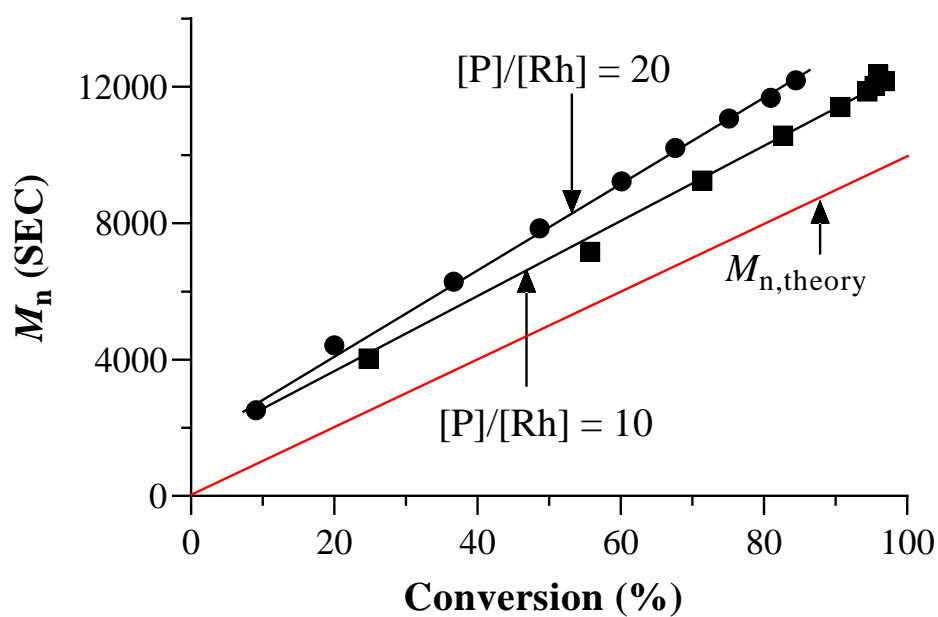
A**B**

Figure 3-10. (A) Pseudo-first-order kinetic plots for the homopolymerisation of PA, with target molecular weight of 10,000 at two different phosphine/Rh ratios; (B) the plots of number average molecular weight (M_n , as measured by SEC and reported as polystyrene equivalents) vs conversion.

Figure 3-10A shows the pseudo-first-order kinetic plots for the homopolymerisation of PA with **90** in toluene at 30 °C in the presence of 10 and 20 equivalents of added free P(4-FC₆H₄)₃ for a target molecular weight of 10,000 at quantitative conversion. Several pertinent features are worth noting. Both plots are linear, even up to near-quantitative conversion, with the homopolymerisation in the presence of 10 equivalents of free phosphine proceeding faster than the polymerisation in the presence of 20 equivalents, as expected. While both plots are linear, confirming a constant number of active propagating species, neither plot passes through the origin, with both exhibiting a short induction period. This is not uncommon and is typically associated with a period of time in which negligible active species are present. The induction period is marginally longer in the case of the polymerisation performed in the presence of 20 equivalents of free phosphine, which is not surprising since the additional free phosphine serves as a monomer-competing binding species. Similar data, and observations, for homopolymerisations with a target molecular weight of 5,000 are given in Figure 3-11

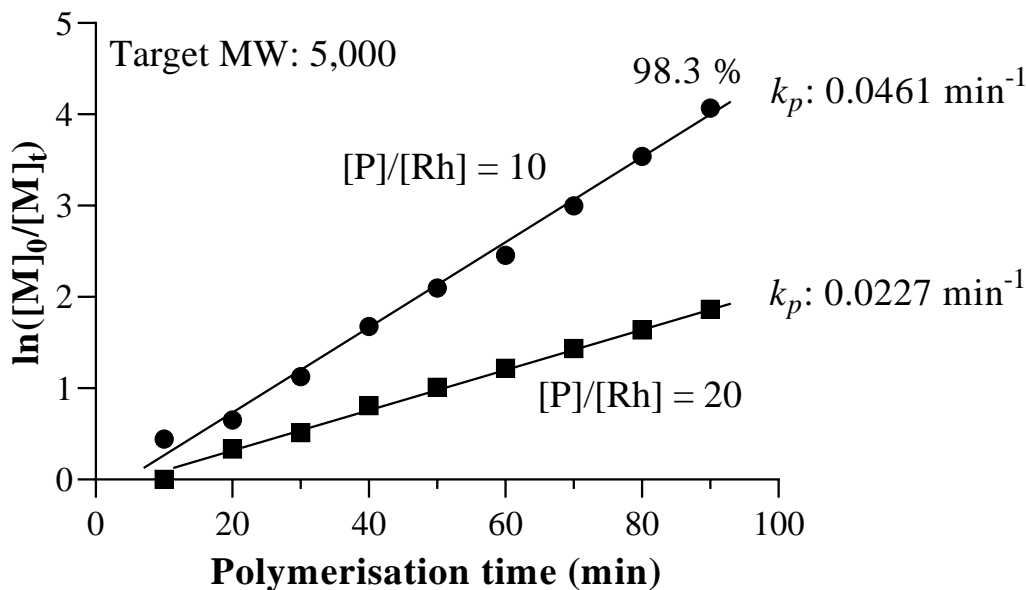


Figure 3-11. Kinetic data for the homopolymerisation of PA with **90** for a target MW of 5,000 at $[P]/[Rh]$ 10 and 20.

The slope of the curve in the pseudo-first order kinetic plots is k_{app} – the apparent propagation rate constant. In the case of the homopolymerisation conducted at a $[P]/[Rh]$ of 10 and target molecular weight of 10,000, the k_{app} is 0.0374 min^{-1} , whereas at $[P]/[Rh]$ of 20, k_{app} is 0.0228 min^{-1} . The k_{app} values for homopolymerisations with a target molecular weight of 5,000 are given in Figure 3-11. In both Figure 3-10A and Figure 3-11, the value k_{app} for $[P]/[Rh]$ of 10 is at least 2 times larger than at $[P]/[Rh]$ of 20, a significant difference but not unexpected.

Figure 3-10B shows the corresponding molecular weight versus conversion plots for the two homopolymerisations with molecular weights reported as the number average (M_n) values as measured by SEC. The theoretical M_n is also shown. In both instances, the evolution of molecular weight is linear, although SEC-measured values are systematically higher than the theoretical molecular weight at all conversions. There are two possible causes for the observed deviation. Firstly, the reported M_n values are polystyrene (PS) equivalents by virtue of the SEC instrument having been

calibrated with a series of narrow molecular weight distribution PS standards and as such may not be accurate hydrodynamic volume equivalents for PPA. However, it has been reported that the dilute solution characteristics of atactic PPA are similar to those of PS of similar tacticity.⁵¹ For example, it has been noted that the molecular weight dependence on the radius of gyration for PS and PPA were very similar with the unperturbed dimensions of the polymers also being almost equal. As such, while the application of PS standards cannot be completely eliminated as the cause for the discrepancy in the theoretical and observed M_n 's it appears PS standards are an extremely good match for PPA regardless of the difference in the chemical nature of the respective polymer backbones. Secondly, the disagreement between the theoretical and measured M_n s could be due to non-quantitative initiation. Assuming the measured M_n values are a genuine reflection of the actual molecular weight of the PPA homopolymers, then the discrepancy suggests an IE for **90** of ca. 0.8. Interestingly, this is exactly the value you would expect assuming that the minor Rh species, 3-PhNaphth, **91**, present in solution is not an active initiator based on the calculated ratio of the two species. If this is the case, the actual IE of **90** is closer to 1.0.

While quantitative initiation is desirable since it facilitates easy tuning of the molecular weight, it is not a formal pre-requisite for a given polymerisation to be accurately described as living (or controlled).⁵² A comparison of the calculated IE with the reported values for complexes **78b**, Figure 3-1, and **88b**, Figure 3-1, indicate that **90** is intermediate of **78b** and **88b** with the former exhibiting essentially quantitative IEs²⁴ while the IE for the latter varies from 0.16-0.56 depending on polymerisation conditions.⁴

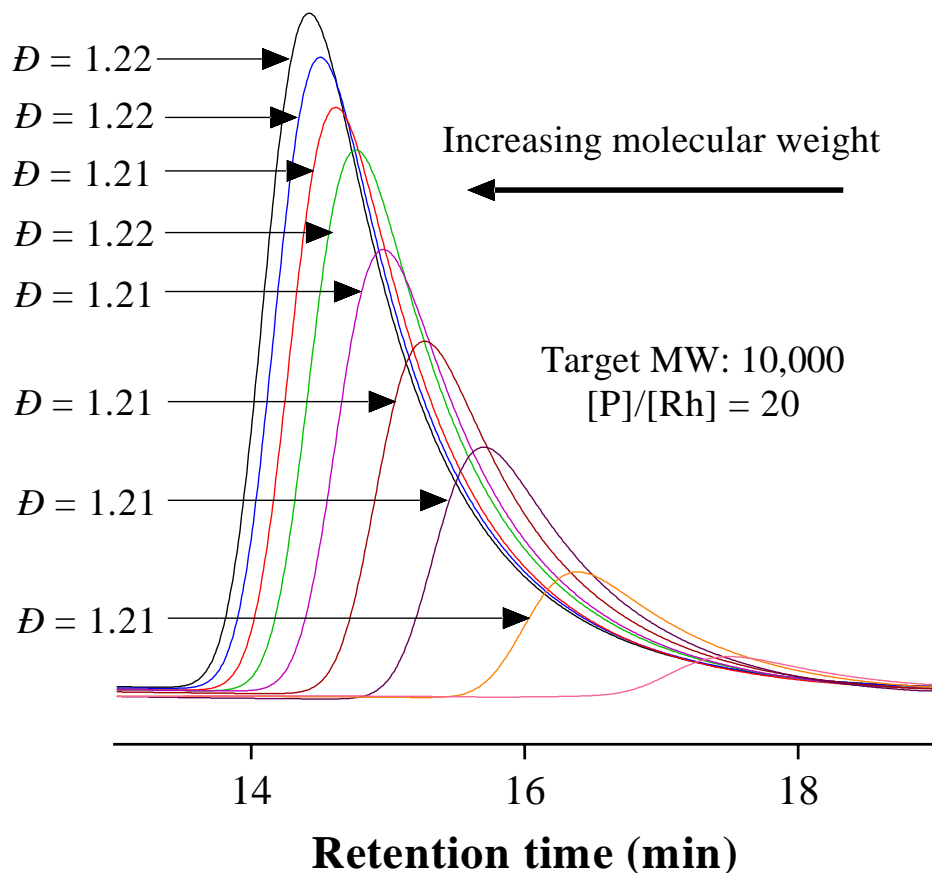


Figure 3-12. A series of SEC traces demonstrating the evolution of the molecular weight distribution with polymerisation time.

In a controlled polymerisation process where $R_i \geq R_p$ (R_i : rate of initiation; R_p : rate of propagation) the resulting (co)polymer will have a narrow molecular weight distribution (assuming there are no side reactions such as termination, chain transfer or branching) in which the dispersity, \bar{D} , decreases as conversion increases.⁵³ Figure 3-12 shows an example of the evolution of the molecular weight distribution in a PA homopolymerisation at $[P]:[Rh]$ of 20 and for a target molecular weight of 10,000. As expected, a systematic shift of the chromatograms to lower retention time (higher molecular weight) was observed with a simultaneous increase in peak intensity with increasing conversion. In this case, the \bar{D} of the distribution remains essentially

constant at ~ 1.21 . While these D values are not as low as some reported in the literature, including by us, for the controlled polymerisation of PA with Rh(I) complexes they are certainly acceptable.

The linearity of the pseudo-first-order kinetic and M_n versus conversion plots, together with the molecular weight distribution chromatograms, when taken together suggest that the polymerisation of PA with the Rh(I)-aryl complex **90** is a controlled process, and validates the further study of new Rh(I)-aryl species in this target application.

There are four possible isomers associated with the geometry and relationship between the backbone C=C and C-C bonds in PPAs. These are referred to as the *cis-cisoidal*, *cis-transoidal*, *trans-transoidal* and *trans-cisoidal* geometric isomers, Figure 3-13.⁵⁴

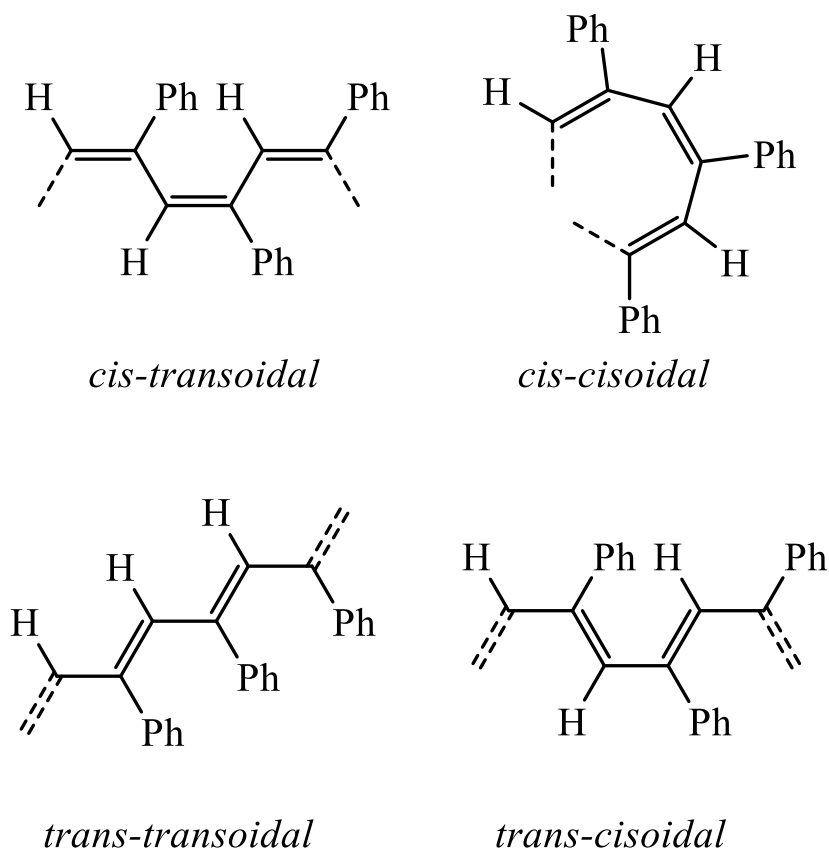


Figure 3-13. The four possible stereoisomers associated with polyphenylacetylenes.

It is known that in polymerisations that proceed via an insertion polymerisation pathway, as with Rh-mediated polymerisations of arylacetylenes, give rise to the *cis-transoidal* form while metathesis-type (co)polymerisation yields the *trans-transoidal/cisoidal* structures.⁵⁴⁻⁵⁶ Figure 3-14 shows the ¹H NMR spectrum, recorded in CDCl₃, of PPA obtained from the homopolymerisation of PA for a target molecular weight of 10,000 and [P]:[Rh] of 20. The key feature in PPAs of high *cis-transoidal* content is the sharp peak at $\delta = 5.83$ ppm that is attributed to the H in the polymer backbone on a *cis* C=C bond, while the remaining peaks are associated with the side chain aromatics and any backbone Hs bonded to a *trans* C=C. This spectrum is entirely consistent with previous reports of PPAs with high *cis-transoidal* stereoregularity, and in this case, the PPA has a calculated⁵⁷ *cis* content of 95 %. In all cases, the *cis* contents of the obtained PPAs were ≥ 95 %.

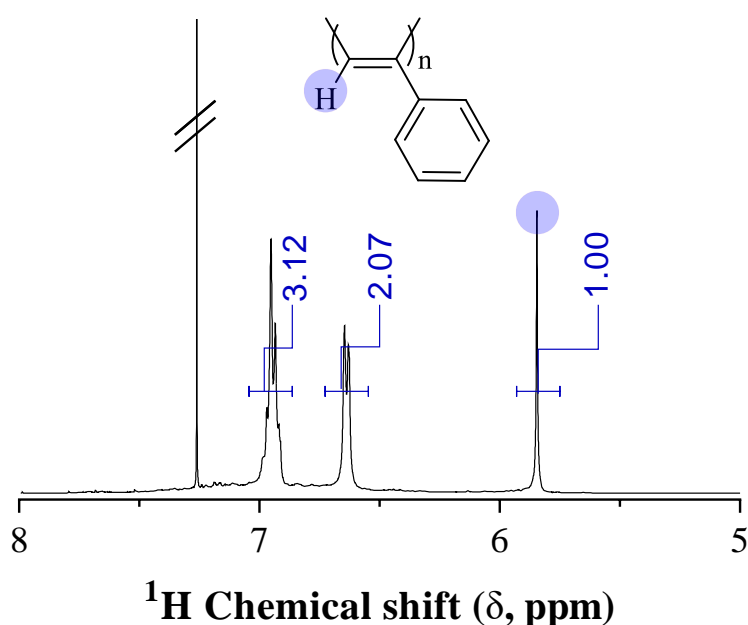


Figure 3-14. ¹H NMR spectrum of polyphenylacetylene, recorded in CDCl₃, prepared with **90** for a target molecular weight of 10,000 and [P]:[Rh] of 20 highlighting the high *cis-transoidal* stereoregularity. Measured integral values given in blue.

3.4 Conclusions

In this chapter we detailed the synthesis of a new Rh(I)-aryl complex and evaluated its use as an initiating species for the controlled, stereospecific polymerisation of phenylacetylene. Interestingly, while targeting a 2-phenylnaphthyl Rh(I) derivative we isolated the isomeric Rh(I)(nbd)(2-naphthylphenyl)(P(4-FC₆H₄)₃) species as determined by X-ray crystal structure analysis. The isolated species was proposed to form from the targeted species via an intramolecular 1,4-Rh atom migration, a supposition that was supported by density functional theory calculations. The isolated complex was characterised in detail by multinuclear NMR spectroscopy which indicated the presence of two principle Rh-P complexes when in solution in an approximate ratio of 4:1 in favour of the 2-naphthylphenyl Rh(I) species. The second, minor, species in solution was identified as a third structural isomer Rh(I)(nbd)(3-phenylnaphthyl)(P(4-FC₆H₄)₃) formed by a proposed second 1,4-Rh atom migration.

The recrystallised species was examined with respect to its ability to initiate the homopolymerisation of phenylacetylene. Pseudo-first-order kinetic plots were linear, albeit with short induction periods, as were the molecular weight vs conversion plots and in all cases the dispersities of the resulting copolymers were ≤ 1.25 suggesting a controlled polymerisation. Initiation efficiencies were not quantitative, but were high (ca. 0.8), with the presence of the second minor Rh species in solution proposed to be the cause. Consistent with Rh-mediated insertion polymerisations, the resulting polyphenylacetylene polymers were highly stereoregular with calculated *cis* contents $\geq 95\%$. This represents, to the best of our knowledge, the first example in which a well-defined isolated Rh(I)-*aryl* complex has been shown to be an effective initiating species for phenylacetylene polymerisation yielding materials with well-defined molecular properties.

3.5 References

1. Misumi, Y.; Kanki, K.; Miyake, M.; Masuda, T., Living polymerization of phenylacetylene by rhodium-based ternary catalysts, (diene)Rh(I) complex/vinyl lithium/phosphorous ligand. effect of catalyst components. *Macromolecular Chemistry and Physics* **2000**, *201* (17), 2239-2244.
2. Yamamoto, M.; Onitsuka, K.; Takahashi, S., Polymerization of aryl isocyanides possessing bulky substituents at an *ortho* position initiated by organorhodium complexes. *Organometallics* **2000**, *19* (23), 4669-4671.
3. Onitsuka, K.; Yamamoto, M.; Mori, T.; Takei, F.; Takahashi, S., Living polymerization of bulky aryl isocyanide with arylrhodium complexes. *Organometallics* **2006**, *25* (5), 1270-1278.
4. Tan, N. S. L.; Simpson, P. V.; Nealon, G. L.; Sobolev, A. N.; Raiteri, P.; Massi, M.; Ogden, M. I.; Lowe, A. B., Rhodium(I)- α -phenylvinylfluorenyl complexes : synthesis, characterization, and evaluation as initiators in the stereospecific polymerization of phenylacetylene. *European Journal of Inorganic Chemistry* **2019**, *2019* (5), 592-601.
5. Császár, P.; Pulay, P., Geometry optimization by direct inversion in the iterative subspace. *Journal of Molecular Structure* **1984**, *114*, 31-34.
6. Ahlrichs, R.; Bär, M.; Häser, M.; Horn, H.; Kölmel, C., Electronic structure calculations on workstation computers: the program system turbomole. *Chemical Physics Letters* **1989**, *162* (3), 165-169.
7. Deglmann, P.; Furche, F.; Ahlrichs, R., An efficient implementation of second analytical derivatives for density functional methods. *Chemical Physics Letters* **2002**, *362* (5-6), 511-518.
8. Deglmann, P.; May, K.; Furche, F.; Ahlrichs, R., Nuclear second analytical derivative calculations using auxiliary basis set expansions. *Chemical Physics Letters* **2004**, *384* (1-3), 103-107.
9. Eichkorn, K.; Treutler, O.; Öhm, H.; Häser, M.; Ahlrichs, R., Auxiliary basis sets to approximate Coulomb potentials. *Chemical Physics Letters* **1995**, *240* (4), 283-290.
10. Eichkorn, K.; Weigend, F.; Treutler, O.; Ahlrichs, R., Auxiliary basis sets for main row atoms and transition metals and their use to approximate Coulomb potentials. *Theoretical Chemistry Accounts* **1997**, *97* (1-4), 119-124.
11. Treutler, O.; Ahlrichs, R., Efficient molecular numerical integration schemes. *The Journal of Chemical Physics* **1995**, *102* (1), 346-354.
12. von Arnim, M.; Ahlrichs, R., Geometry optimization in generalized natural internal coordinates. *The Journal of Chemical Physics* **1999**, *111* (20), 9183-9190.

13. Klamt, A.; Schuurmann, G., COSMO: a new approach to dielectric screening in solvents with explicit expressions for the screening energy and its gradient. *Journal of The Chemical Society, Perkin Transactions 2* **1993**, 2, 799-805.
14. Grimme, S.; Ehrlich, S.; Goerigk, L., Effect of the damping function in dispersion corrected density functional theory. *Journal of Computational Chemistry* **2011**, 32 (7), 1456-1465.
15. Grimme, S.; Antony, J.; Ehrlich, S.; Krieg, H., A consistent and accurate ab initio parametrization of density functional dispersion correction (DFT-D) for the 94 elements H-Pu. *The Journal of Chemical Physics* **2010**, 132 (15), 154104.
16. Harris, R. K.; Becker, E. D.; Cabral de Menezes, S. M.; Granger, P.; Hoffman, R. E.; Zilm, K. W., Further conventions for NMR shielding and chemical shifts (IUPAC recommendations 2008). *Magnetic Resonance in Chemistry* **2008**, 46 (6), 582-598.
17. Carlton, L., Rhodium-103 NMR. In *Annual Reports on NMR Spectroscopy*, Webb, G. A., Ed. Academic Press: Cambridge, US, 2008; Vol. 63, pp 49-178.
18. Sheldrick, G. M., Crystal structure refinement with *SHELXL*. *Acta Crystallographica Section C : Structural Chemistry* **2015**, 71 (1), 3-8.
19. Rietveld, H., A profile refinement method for nuclear and magnetic structures. *Journal of Applied Crystallography* **1969**, 2 (2), 65-71.
20. Loopstra, B. O.; Rietveld, H., The structure of some alkaline-earth metal uranates. *Acta Crystallographica Section B* **1969**, 25 (4), 787-791.
21. Coelho, A. A., TOPAS and TOPAS-Academic: an optimization program integrating computer algebra and crystallographic objects written in C++. *Journal of Applied Crystallography* **2018**, 51 (1), 210-218.
22. Rowles, M. R.; Buckley, C. E., Aberration corrections for non-Bragg-Brentano diffraction geometries. *Journal of Applied Crystallography* **2017**, 50 (1), 240-251.
23. Dollase, W. A., Correction of intensities for preferred orientation in powder diffractometry: application of the March model. *Journal of Applied Crystallography* **1986**, 19 (4), 267-272.
24. Miyake, M.; Misumi, Y.; Masuda, T., Living polymerization of phenylacetylene by isolated rhodium complexes, Rh[C(C₆H₅)=C(C₆H₅)₂](nbd)(4-XC₆H₄)₃P (X = F, Cl). *Macromolecules* **2000**, 33 (18), 6636-6639.
25. Cirera, J.; Ruiz, E.; Alvarez, S., Continuous shape measures as a stereochemical tool in organometallic chemistry. *Organometallics* **2005**, 24 (7), 1556-1562.

26. Drover, M. W.; Schafer, L. L.; Love, J. A., Isocyanate deinsertion from κ 1-O amidates: facile access to perfluoroaryl rhodium(I) complexes. *Dalton Transactions : An International Journal of Inorganic Chemistry* **2015**, 44 (45), 19487-19493.
27. Kumazawa, S.; Rodriguez Castanon, J.; Onishi, N.; Kuwata, K.; Shiotsuki, M.; Sanda, F., Characterization of the polymerization catalyst [(2,5-norbornadiene)Rh{C(Ph)=CPh₂}(PPh₃)] and identification of the end structures of poly(phenylacetylenes) obtained by polymerization using thie catalyst. *Organometallics* **2012**, 31 (19), 6834-6842.
28. Ujwaldev, S. M.; Harry, N. A.; Divakar, M. A.; Anilkumar, G., Cobalt-catalyzed C–H activation: recent progress in heterocyclic chemistry. *Catalysis Science and Technology* **2018**, 8 (23), 5983-6018.
29. Cano, R.; Mackey, K.; McGlacken, G. P., Recent advances in manganese-catalysed C–H activation: scope and mechanism. *Catalysis Science and Technology* **2018**, 8 (5), 1251-1266.
30. Li, H.; Li, B.-J.; Shi, Z.-J., Challenge and progress: palladium-catalyzed sp³ C–H activation. *Catalysis Science and Technology* **2011**, 1 (2), 191-206.
31. Yang, L.; Huang, H., Asymmetric catalytic carbon–carbon coupling reactions via C–H bond activation. *Catalysis Science and Technology* **2012**, 2 (6), 1099-1112.
32. Chen, Z.; Wang, B.; Zhang, J.; Yu, W.; Liu, Z.; Zhang, Y., Transition metal-catalyzed C–H bond functionalizations by the use of diverse directing groups. *Organic Chemistry Frontiers* **2015**, 2 (9), 1107-1295.
33. Gensch, T.; Hopkinson, M. N.; Glorius, F.; Wencel-Delord, J., Mild metal-catalyzed C–H activation: examples and concepts. *Chemical Society Reviews* **2016**, 45 (10), 2900-2936.
34. Zhao, J.; Campo, M.; Larock, R. C., Consecutive vinylic to aryl to allylic palladium migration and multiple C-H activation processes. *Angewandte Chemie International Edition* **2005**, 44 (12), 1873-1875.
35. Ma, S.; Gu, Z., 1,4-migration of rhodium and palladium in catalytic organometallic reactions. *Angewandte Chemie International Edition* **2005**, 44 (46), 7512-7517.
36. Zhang, J.; Liu, J.-F.; Ugrinov, A.; Pillai, A. F. X.; Sun, Z.-M.; Zhao, P., Methoxy-directed aryl-to-aryl 1,3-rhodium migration. *Journal of The American Chemical Society* **2013**, 135 (46), 17270-17273.
37. Oguma, K.; Miura, M.; Satoh, T.; Nomura, M., Merry-go-round multiple alkylation on aromatic rings via rhodium catalysis. *Journal of The American Chemical Society* **2000**, 122 (42), 10464-10465.
38. Hayashi, T.; Inoue, K.; Taniguchi, N.; Ogasawara, M., Rhodium-catalyzed hydroarylation of alkynes with arylboronic acids: 1,4-shift of rhodium from 2-aryl-1-

alkenylrhodium to 2-alkenylarylrhodium intermediate. *Journal of The American Chemical Society* **2001**, *123* (40), 9918-9919.

39. Matsuda, T.; Shigeno, M.; Murakami, M., Asymmetric synthesis of 3,4-dihydrocoumarins by rhodium-catalyzed reaction of 3-(2-hydroxyphenyl)cyclobutanones. *Journal of The American Chemical Society* **2007**, *129* (40), 12086-12087.

40. Matsuda, T.; Suda, Y.; Takahashi, A., Double 1,4-rhodium migration cascade in rhodium-catalysed arylyative ring-opening/spirocyclisation of (3-arylcyclobutylidene)acetates. *Chemical Communications* **2012**, *48* (24), 2988-2990.

41. Sasaki, K.; Hayashi, T., Asymmetric conjugate addition of cis-2-arylethenylboronic acids catalyzed by chiral diene/rhodium complexes: 1,4-rhodium shift from alkenylrhodium to arylrhodium intermediates. *Tetrahedron : Asymmetry* **2012**, *23* (5), 373-380.

42. Seiser, T.; Cramer, N., Rhodium(I)-catalyzed 1,4-silicon shift of unactivated silanes from aryl to alkyl: enantioselective synthesis of indanol derivatives. *Angewandte Chemie International Edition* **2010**, *49*, 10163-10167.

43. Panteleev, J.; Menard, F.; Lautens, M., Ligand control in enantioselective desymmetrization of bicyclic hydrazines: rhodium(I)-catalyzed ring-opening versus hydroarylation. *Advanced Synthesis and Catalysis* **2008**, *350* (18), 2893-2902.

44. Tobisu, M.; Hasegawa, J.; Kita, Y.; Kinuta, H.; Chatani, N., 1,5-migration of rhodium via C–H bond activation in catalytic decyanative silylation of nitriles. *Chemical Communications* **2012**, *48* (93), 11437-11439.

45. Ishida, N.; Shimamoto, Y.; Yano, T.; Murakami, M., 1,5-rhodium shift in rearrangement of N-arenesulfonylazetidins into benzosultams. *Journal of The American Chemical Society* **2013**, *135* (51), 19103-19106.

46. Minkin, V. I., Glossary of terms used in theoretical organic chemistry. *Pure and Applied Chemistry* **1999**, *71* (10), 1919.

47. van der Eide, E. F.; Yang, P.; Bullock, R. M., Isolation of two agostic isomers of an organometallic cation: different structures and colors. *Angewandte Chemie International Edition* **2013**, *52* (39), 10190-10194.

48. Sasaki, K.; Takahiro, N.; Shintani, R.; Kantchev, E. A. B.; Hayashi, T., Rhodium/diene-catalyzed tandem 1,4-shift/1,4-addition of (*E*)-1,2-diphenylethenylboronic acid to enones: density functional theory modeling and asymmetric catalysis. *Chemical Science* **2012**, *3* (4), 1278-1283.

49. Misumi, Y.; Masuda, T., Living polymerization of phenylacetylene by novel rhodium catalysts. quantitative initiation and introduction of functional groups at the initiating chain end. *Macromolecules* **1998**, *31* (21), 7572-7573.

50. Percec, V.; Rudick, J. G.; Nombel, P.; Buchowicz, W., Dramatic decrease of the cis content and molecular weight of cis-transoidal polyphenylacetylene at 23 °C in solutions prepared in air. *Journal of Polymer Science Part A: Polymer Chemistry* **2002**, *40* (19), 3212-3220.
51. Rédrová, D.; Sedláček, J.; Žigon, M.; Vohlídal, J., Unperturbed dimensions of atactic poly(phenylacetylene). *Collection of Czechoslovak Chemical Communications* **2005**, *70* (11), 1787-1798.
52. Jenkins, A. D.; Kratochvíl, P.; Stepto, R. F. T.; Suter, U. W., Glossary of basic terms in polymer science. *Pure and Applied Chemistry* **1996**, *68* (12), 2287-2311.
53. Quirk, R. P.; Lee, B., Experimental criteria for living polymerizations. *Polymer International* **1992**, *27* (4), 359-367.
54. Ke, Z.; Abe, S.; Ueno, T.; Morohuma, K., Rh-catalyzed polymerization of phenylacetylene : theoretical studies of the reaction mechanism, regioselectivity, and stereoregularity. *Journal of The American Chemical Society* **2011**, *133* (20), 7926-7941.
55. Kishimoto, Y.; Eckerle, P.; Miyatake, T.; Kainosho, M.; Ono, A.; Ikariya, T.; Noyori, R., Well-controlled polymerization of phenylacetylenes with organorhodium(I) complexes : mechanism and structure of the polyenes. *Journal of The American Chemical Society* **1999**, *121* (51), 12035-12044.
56. Onishi, N.; Shiotsuki, M.; Masuda, T.; Sano, N.; Sanda, F., Polymerization of phenylacetylenes using rhodium catalysts coordinated by norbornadiene linked to a phosphino or amino group. *Organometallics* **2013**, *32* (3), 846-853.
57. Simionescu, C. I.; Percec, V.; Dumitrescu, S., Polymerization of acetylenic derivatives. XXX. isomers of polyphenylacetylene. *Journal of Polymer Science Part A : Polymer Chemistry* **1977**, *15* (10), 2497-2509.

Every reasonable effort has been made to acknowledge the owners of copyright material. I would be pleased to hear from any copyright owner who has been omitted or incorrectly acknowledged.

Chapter 4

Synthesis, Characterisation, and Application of Rh(I)(2,5-norbornadiene)(biphenyl)(*tris*(4-fluorophenyl)phosphine) as an Initiator in the Stereoregular (Co)Polymerisation of Phenylacetylenes.

The content of this chapter has been published in:

ACS Macro Letters (2020) with the title “Rh(I)(2,5-norbornadiene)(biphenyl)(*tris*(4-fluorophenyl)phosphine): Synthesis, Characterization, and Application as an Initiator in the Stereoregular (Co)Polymerization of Phenylacetylenes” (refer to Appendix C)

4.1 Introduction

In Chapter 2, the synthesis and application of three new Rh(I)- α -phenylvinylfluorenyl complexes bearing fluorine functionalised phosphine ligands, **88** Figure 4-1, was detailed. Although meeting the general structural requirements¹ for highly efficient initiators, these complexes exhibited initiation efficiencies (IEs) (as determined by SEC) in the range 0.13 to 0.56 for PA homopolymerisation. The unexpectedly low IEs were attributed to steric hindrance resulting from the conformationally locked fluorenyl moiety of the initiating fragment, which prevented the facile coordination of monomer. Despite this, the resulting polymers prepared with

88 possessed narrow molecular weight distributions with high *cis-transoidal* stereoregularity (ca. > 90 %).

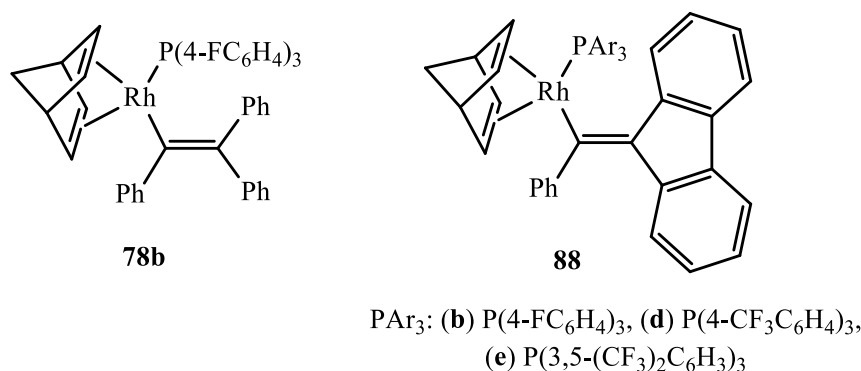


Figure 4-1. Chemical structures of Masuda-type Rh(I)-vinyl complexes, **78b** and **88**, recently reported Rh(I)aryl species **90**, and the structurally related aryl complex **92** (the focus of this chapter).

To address the low IEs observed for **88**, in Chapter 3, we described the attempted synthesis of the Rh(I)-*aryl* species, Rh(I)(2,5-norbornadiene)(2-phenylnaphthyl)(*tris*(4-fluorophenyl)phosphine), as a potential new initiator for the controlled polymerisation of PA. Following recrystallisation, single crystal X-ray diffraction (XRD) revealed that a structural isomer, Rh(nbd)(2-NaphthPh)($P(4-FC_6H_4)_3$), **90**, (2-NaphthPh = 2-naphthylphenyl) was isolated instead.

The proposed mechanism behind its formation was via a 1,4-Rh atom migration from the targeted species, with the concurrent formation of a second

structural isomer, (3-phenylnaphthalen-1-yl)rhodium(I)(2,5-norbornadiene) tris(*para*-fluorophenylphosphine) as evidenced by ^{31}P - $^{103}\text{Rh}\{^1\text{H}, ^{103}\text{Rh}\}$ HMQC NMR spectroscopy. While not the target, the activity of **90** was examined, and it was demonstrated to be an effective initiator for the polymerisation of PA with measured IEs of ca. 0.8 with the resulting polyphenylacetylenes having high *cis-transoidal* stereoregularity (99 %). Pseudo-first order kinetic plots and molecular weight evolution vs time plots were linear, indicative of a controlled polymerisation process.

In this chapter, the synthesis of a new Rh(I) biphenyl derivative, Rh(I)(nbd)(Biphenyl)(P(4-FC₆H₄)₃), is detailed. This species was hypothesised to eliminate the possible formation of multiple ((in)active) Rh complexes via migratory processes in solution. While **92**, Figure 4-1, might still be susceptible to 1,4-Rh atom migrations, the result from this occurrence will be a structurally identical species. Subsequently, the efficacy of the Rh(I)-biphenyl complex as a mediator in the (co)polymerisation of PA was investigated and finally, its ability to form well-defined AB di-block copolymers, in a stereoregular manner, was examined by sequential monomer addition.

4.2 Experimental

4.2.1 Materials

n-Butyllithium (*n*-BuLi, 1.6 M solution in hexane, Sigma-Aldrich), 1-bromobiphenyl (C₁₂H₉Br) (98 % Tokyo Chemical Industry), [Rh(nbd)Cl]₂ (nbd = 2,5-norbornadiene, 98 %, Strem Chemicals), and tris(*para*-fluorophenyl)phosphine (P(4-FC₆H₄)₃, 98 %, Sigma-Aldrich) were used as received. Phenylacetylene (CH≡CPh, 98 %, Sigma-Aldrich) was purified by passage over a column of basic alumina and stored in a fridge until needed. 4-Fluorophenylacetylene (4-FC₆H₄C≡CH), 98%, Sigma-Aldrich) was used as received.

THF, diethyl ether and CH₂Cl₂ were dried using a PureSolv MD5 solvent purification system (Innovative Technology, Inc.), collected, degassed via the freeze-pump-thaw technique and stored under dry nitrogen until needed. Toluene (99.8 %, Sigma-Aldrich) was degassed via the freeze-pump-thaw technique and stored under dry nitrogen until needed. All glassware was pre-dried in an oven at 120 °C and then flamed dried under vacuum before use. All reactions were performed using standard Schlenk line techniques.

4.2.2 Synthesis of Rh(I)(nbd)(Biphenyl)(P(4-FC₆H₄)₃)

Rh(I)(nbd)(Biphenyl)(P(4-FC₆H₄)₃), **92** Figure 4-1, was prepared following the procedure reported for the preparation of the Rh(I)-naphthyl derivatives detailed in Chapter 3.²

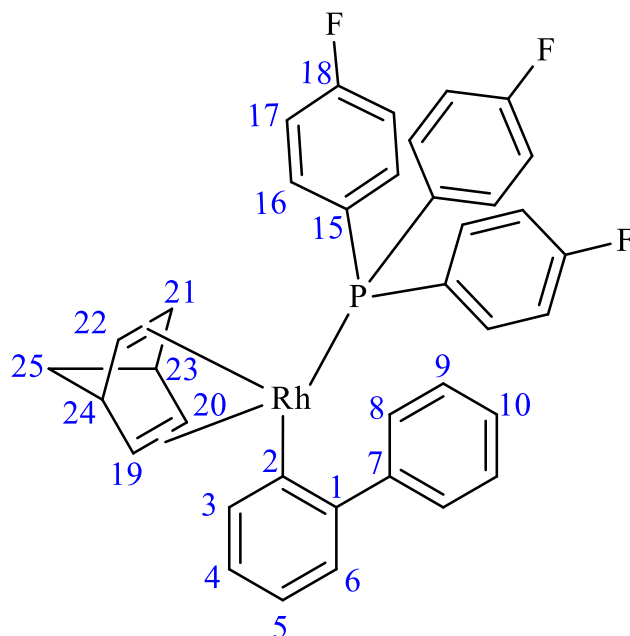
To a round-bottomed flask equipped with a Teflon-coated magnetic stir bar was added 2-bromobiphenyl (233.1 mg, 1.00 mmol) and diethyl ether (20.0 mL) under a dry nitrogen atmosphere. The flask was cooled to 0 °C, and *n*-BuLi (1.6 M solution

in hexane, 0.71 mL, 1.13 mmol) was cannula transferred and the mixture allowed to react for 45 min yielding $C_6H_5(C_6H_4Li)$.

To a separate round-bottomed flask equipped with a magnetic stir-bar containing dry toluene (15.0 mL) was added $[Rh(nbd)Cl]_2$ (115 mg, 0.25 mmol) and $P(4-FC_6H_4)_3$ (316.26 mg, 1.00 mmol). The mixture was stirred vigorously for 15 min at ambient temperature yielding the intermediate Rh species, $Rh(nbd)(P(4-FC_6H_4)_3)Cl$.

The lithiated species, $C_6H_5(C_6H_4Li)$, was added, via cannula, to the solution containing $Rh(nbd)(P(4-FC_6H_4)_3)Cl$ and allowed to stir at ambient temperature for two hours. Subsequently, the reaction solution was cannula transferred and filtered through a short plug of neutral activated alumina 90, under an inert atmosphere, to give a clear orange solution. Solvents were concentrated under high vacuum on a Schlenk line yielding a dark red viscous liquid. To the residue was added CH_2Cl_2 (2.5 mL) and the target compound isolated by recrystallisation from CH_2Cl_2 /methanol via a solvent layering technique. Yield: 161.1 mg, 97 %. CH elemental analysis: %C_{theor}: 66.88, %C_{found}: 66.96; %H_{theor}: 4.40, %H_{found}: 4.16. 1H NMR (600 MHz, CD_2Cl_2), δ (ppm): 7.71-7.66 (m, 2H, H8), 7.35-7.31 (m, 3H, H9,10), 7.11 (d, $J = 7.6$ Hz, 1H, H3), 6.97 (dd, $J = 7.5, 1.5$ Hz, 1H, H6), 6.92-6.87 (m, 6H, H17), 6.87-6.83 (m, 6H, H16), 6.82-6.80 (m, 1H, H5), 6.75 (td, $J = 7.3, 1.5$ Hz, 1H, H4), 4.85 (q, $J = 3.5$ Hz, 1H, H21), 3.85 (t, $J = 3.9$ Hz, 1H, H20), 3.84-3.82 (m, 1H, H22), 3.82-3.80 (m, 1H, H24), 3.80-3.78 (m, 1H, H23), 3.58 (q, $J = 4.6$ Hz, 1H, H19), 1.51 (d, $J = 8.1$ Hz, 1H, H25), 1.31 (d, $J = 8.1$ Hz, 1H, H25'); ^{13}C NMR (151 MHz, CD_2Cl_2), δ (ppm): 171.5 (dd, $J = 33.3, 13.6$ Hz, C2), 163.8 (dd, $J = 249.5, 1.6$ Hz, C-F), 148.1 (C7), 147.2 (C1), 136.2 (C3), 135.8 (dd, $J = 14.1, 8.1$ Hz, C16), 130.4 (dd, $J = 34.5, 2.3$ Hz, C-P), 129.3 (C9), 127.2 (C6), 126.8 (C10), 125.2 (C4), 122.2 (C8), 122.0 (C5), 115.4 (dd, $J = 21.0, 10.2$ Hz, C17), 74.82 (d, $J = 5.6$ Hz, C19), 73.6 (t, $J = 4.2$ Hz, C20), 71.8 (d, $J = 14.2$ Hz, C21),

65.1 (t, $J = 4.6$ Hz, C25), 55.9 (dd, $J = 19.4, 7.1$ Hz, C22), 51.1 (d, $J = 3.3$ Hz, C23), 51.0 (d, $J = 3.7$ Hz, C24); ^{19}F NMR (565 MHz, CD_2Cl_2), δ (ppm): -111.06 (d, $J = 3.3$ Hz); $^{31}\text{P}\{^1\text{H}\}$ NMR (162 MHz, C_6D_6), δ (ppm): 23.91 (dq, $J_{\text{P-Rh}} = 191.5, J_{\text{P-F}} = 3.3$ Hz); ^{103}Rh NMR (19 MHz, d_8 -toluene), δ (ppm): -7699 (536 ppm if referenced to Rh metal).



4.2.3 Polymerisation Studies

All (co)polymerisations were performed under a dry nitrogen atmosphere in glassware pre-dried in an oven set at 120 °C. Below is a typical procedure for the homopolymerisation of phenylacetylene with **92**:

A solution of phenylacetylene (0.184 g, 1.80 mmol) in toluene (2.5 mL) was added to a solution of **92** (0.015 g, 0.02 mmol) and free phosphine ($\text{P}(4\text{-FC}_6\text{H}_4)_3$) (0.031 g, 0.10 mmol) dissolved in toluene (2.5 mL) in a Schlenk flask equipped with a magnetic stir bar. The flask was then immersed in a pre-heated oil bath set at 30 °C and polymerisation allowed to proceed for 90 min. An aliquot (0.1 mL) was withdrawn every 5-10 min and added to a vial of deuterated chloroform (0.5 mL) containing a

small volume of acetic acid (2.0 μL). After 90 min, the polymerisation was terminated by the addition of acetic acid. The final polymer was isolated by precipitation into a large volume of methanol, isolated by gravity filtration and dried to constant weight in a vacuum oven at 40 $^{\circ}\text{C}$ overnight. Monomer conversions were determined by ^1H NMR spectroscopy, and molecular weights and dispersity were determined by size exclusion chromatography.

4.2.4 NMR Measurements

NMR spectra were recorded at 298K on a Bruker Avance IIIHD (600 MHz for ^1H). The data were processed with Bruker's TopSpin 3.5 or MestReNova software packages. ^1H , ^{13}C , ^{19}F , and ^{31}P spectra were collected on a commercial broadband probe, whereas the ^{103}Rh NMR was acquired at 19.1 MHz using a commercial 5 mm triple resonance broadband probe (doubly tuned $^1\text{H}/^{31}\text{P}$ outer coil with inner broadband coil) with 90° pulses of 27.5 μs and 18.4 μs for ^{103}Rh and ^{31}P respectively. ^{103}Rh chemical shifts, δ , are given in ppm relative to $\mathcal{E} = 3.186447^3$ and derived indirectly from the ^{31}P - ^{103}Rh HMQC experiments by four pulse ^{31}P - ^{103}Rh HMQC experiments with ^{103}Rh and ^1H decoupling during acquisition. The transmitter frequency offset and t_1 increments were varied to ensure that no signals were folded. Exponential line broadening of 10 Hz was applied to 1D ^{103}Rh data, with 2D data zero filled, Gaussian broadened by 10 Hz and treated with spine-squared window function during processing. Coupling constants reported herein are given as absolute values but are likely to be negative in sign for $^1J_{\text{Rh-P}}$.⁴

4.2.5 Crystallography

A crystal, $0.36 \times 0.16 \times 0.16 \text{ mm}^3$, was selected and mounted on a suitable support on an Xcalibur, Ruby, Gemini ultra diffractometer. The crystal was kept at a steady $T = 96(1) \text{ K}$ during data collection. Data were measured using ω scans using MoK α radiation. The total number of runs and images was based on the strategy calculation from the program CrysAlisPro (Rigaku, V1.171.40.53, 2019) and the unit cell was refined using CrysAlisPro (Rigaku, V1.171.40.53, 2019) on 77012 reflections, 42 % of the observed reflections. The maximum resolution that was achieved was $\theta = 32.736^\circ$ (0.66 Å). CCDC195957 contains the supplementary crystallographic data for this paper. These data can be obtained free of charge from The Cambridge Crystallographic Data Centre via www.ccdc.cam.ac.uk/structures.

The structure was solved and the space group $P2_1/n$ (# 14) determined by the olex2.solve⁵ structure solution program using Charge Flipping and refined by Least Squares using version 2018/3 of ShelXL.⁶ All non-hydrogen atoms were refined anisotropically. Hydrogen atom positions were calculated geometrically and refined using the riding model.

Crystal data for Rh(I)(nbd)(Biphenyl)(P(4-FC₆H₄)₃): C₃₇H₂₉F₃PRh, $M_r = 664.48$, monoclinic, $P2_1/n$ (No. 14), $a = 13.00900(10) \text{ \AA}$, $b = 16.53910(10) \text{ \AA}$, $c = 13.51040(10) \text{ \AA}$, $\beta = 92.7580(10)^\circ$, $\alpha = \gamma = 90^\circ$, $V = 2903.49(4) \text{ \AA}^3$, $T = 96(1) \text{ K}$, $Z = 4$, $Z' = 1$, $\mu(\text{MoK}\alpha) = 0.689$, 183463 reflections measured, 10430 unique ($R_{int} = 0.0467$) which were used in all calculations. The final wR_2 was 0.0702 (all data) and R_1 was 0.0294 ($I > 2(I)$).

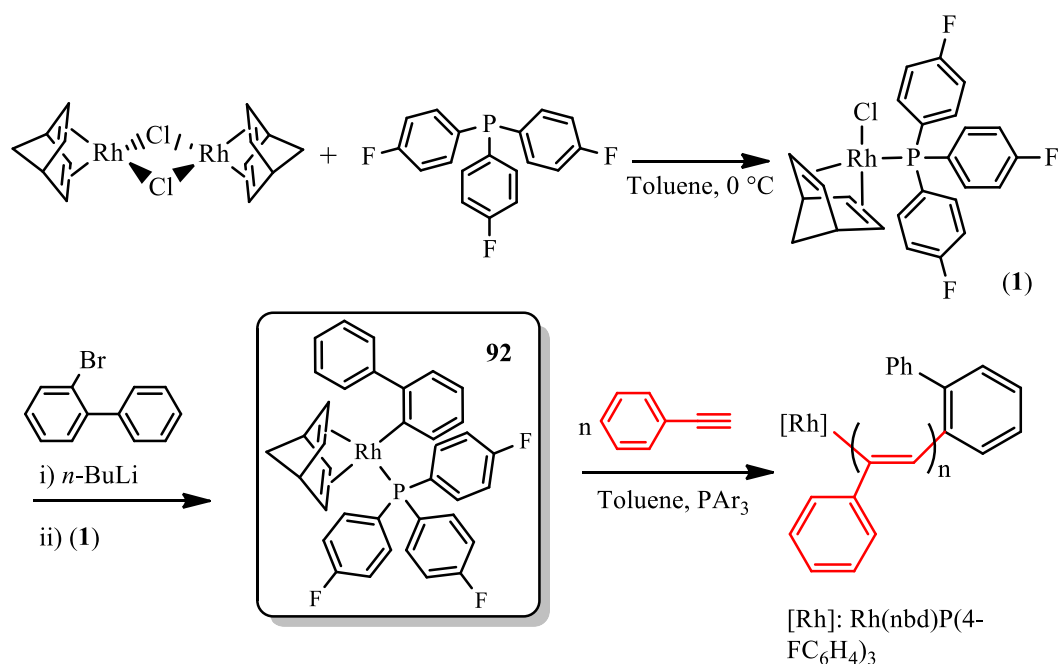
4.2.6 Elemental Analysis

Elemental microanalyses were performed on a Perkin Elmer 2400 Series II CHNS/O Analyser in CHN mode with helium as a carrier gas.

4.2.7 Size Exclusion Chromatography (SEC)

SEC was performed on a Shimadzu modular system consisting of a 4.0 mm × 3.0 mm Phenomenex Security Guard™ Cartridge guard column and two linear phenogel columns (10^3 and 10^4 Å pore size) in tetrahydrofuran (THF) operating at a flow rate of 1.0 mL/min and 40 °C using a RID-20A refractive index detector, a SPD-M20A prominence diode array detector and a miniDAWN TREOS multi-angle static light scattering (MALLS) detector. The system was calibrated with a series of narrow molecular weight distribution polystyrene standards with molecular weights ranging from 0.27 to 66 kg mol⁻¹. Chromatograms were analysed by Lab Solutions SEC software.

4.3 Results and Discussion



Scheme 4-1. Outline for the synthesis of the biphenyl derivative, **92**.

The synthetic route to the target biphenyl functionalised complex and its subsequent use as a polymerisation initiator is shown in Scheme 4-1. Reaction of $[\text{Rh}(\text{nbd})\text{Cl}]_2$ with *tris*(4-fluorophenyl)phosphine gave the intermediate tetracoordinate $\text{Rh}(\text{nbd})(\text{P}(\text{4-FC}_6\text{H}_4)_3)\text{Cl}$ complex, (**1**). Treatment of 2-bromo-1,1'-biphenyl with *n*-BuLi yielded the lithiated biaryl species which when reacted with (**1**) gave the target Rh(I)-aryl complex, $\text{Rh}(\text{nbd})(\text{Biphenyl})\text{P}(\text{4-FC}_6\text{H}_4)_3$, **92** Scheme 4-1. Recrystallisation of **92** from CH_2Cl_2 /methanol yielded X-ray quality crystals enabling the solid-state structure to be determined, Figure 4-2. Consistent with reported Rh(I)(nbd)PAr₃-alkynyl, -vinyl and -aryl complexes detailed previously, **92** adopts a slightly distorted square planar geometry.

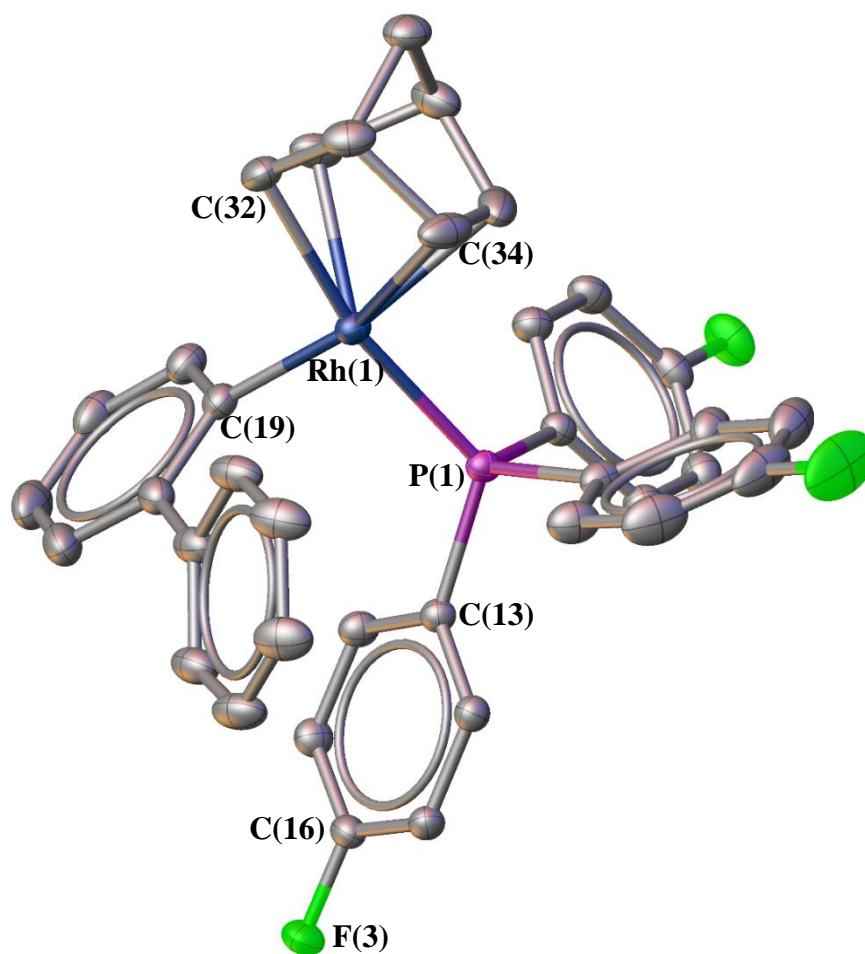


Figure 4-2. OLEX² representation of the X-ray crystal structure of **92** with 50 % probability ellipsoids and H-atoms omitted for clarity. Selected bond lengths (Å): Rh(1)-P(1), 2.297(4); Rh(1)-C(32), 2.177(15); P(1)-C(13), 1.832(14); C(16)-F(3), 1.361(16). Selected bond angles (deg): C(32)-Rh(1)-P(1), 167.84(4); C(34)-Rh(1)-P(1), 104.96(5); C(19)-Rh(1)-P(1), 92.68(4).

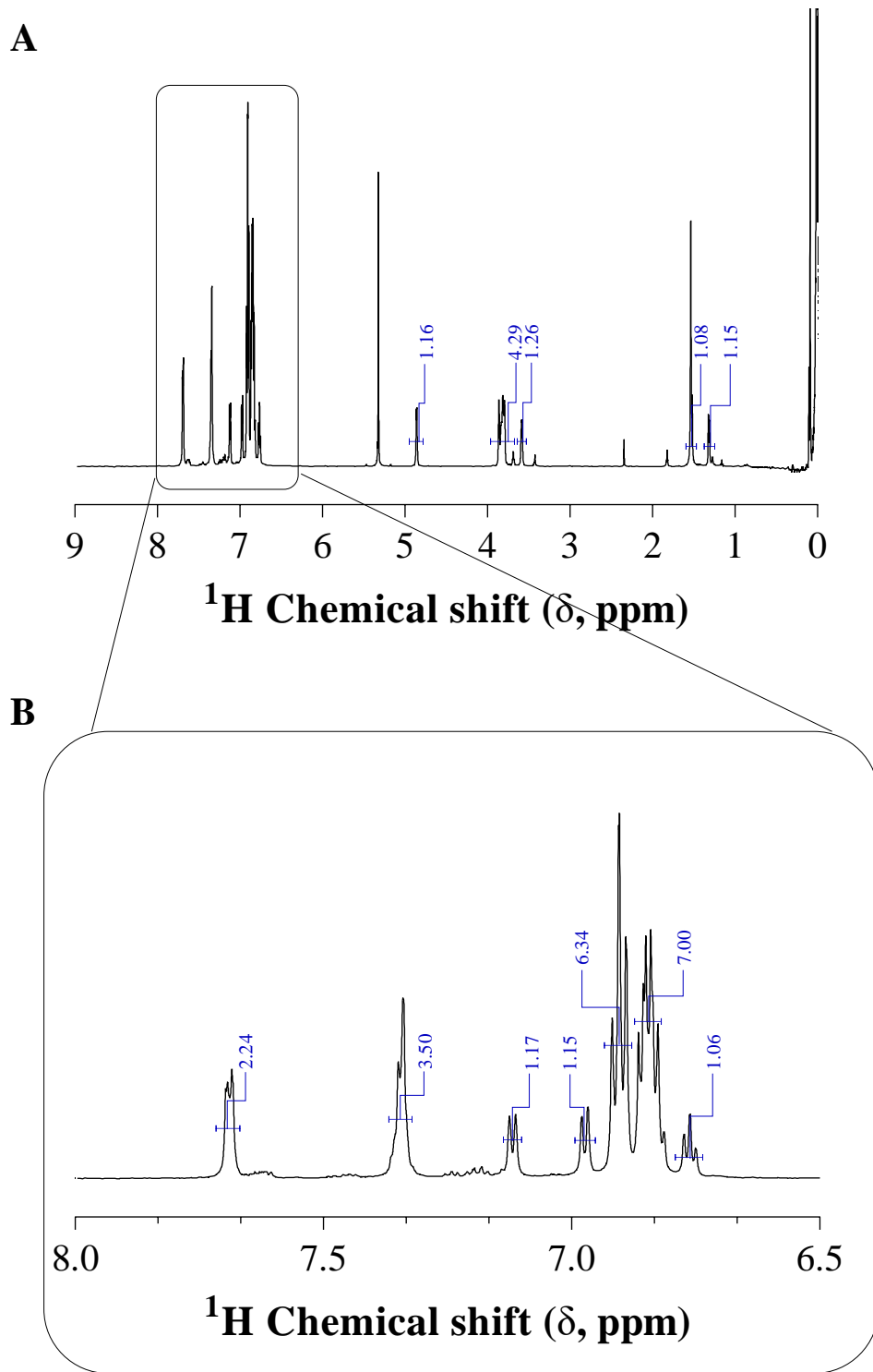


Figure 4-3. (A) ¹H NMR spectrum of Rh(I)(nbd)(Biphenyl)(P(4-FC₆H₄)₃) recorded in CD₂Cl₂. (B) Expanded view of the aromatic region between δ = 8.0 - 6.5 ppm. Measured integral values are annotated in blue.

Multinuclear NMR spectroscopy (^1H , ^{13}C , ^{19}F , ^{31}P , and 2D techniques) was employed to characterise **92**. Figure 4-3 shows the ^1H NMR spectrum of **92** recorded in CD_2Cl_2 ; the full ^1H NMR spectrum is given at the top with an expansion of the aromatic region (plotted between $\delta = 8.0$ to 6.5 ppm) given directly below. Comparatively, the signals within this aromatic region are less complex than the previous Rh(I)-derivatives, **88b** (Chapter 2) and **90** (Chapter 3), and assignment of the peaks was relatively easier to perform. Looking at the expanded view, Figure 4-3B the signals appearing from $\delta = 6.92$ to 6.83 ppm, which appear as two sets of multiplets, integrate to 12 H's and are associated with the phosphine ligand. The remaining signals within this region integrate to 9 H's which belong to the biphenyl moiety; its full assignment is given in the experimental section. All signals integrate to the expected ratio, confirming the structure.

The $^{31}\text{P}\{^1\text{H}\}$ NMR spectrum of **92** is shown in Figure 4-4A. A pair of doublets of quartets is observed at $\delta = 25$ and 23 ppm with a corresponding $^1J_{\text{Rh-P}}$ value of 191.5 Hz. Both the chemical shift and coupling constants of **92** are consistent with previously reported values for the Rh(I)-2-naphthylphenyl derivative, **90** presented in Chapter 3. The ^{19}F NMR spectrum, Figure 4-4B, shows one distinct signal at $\delta = -111.5$ ppm.

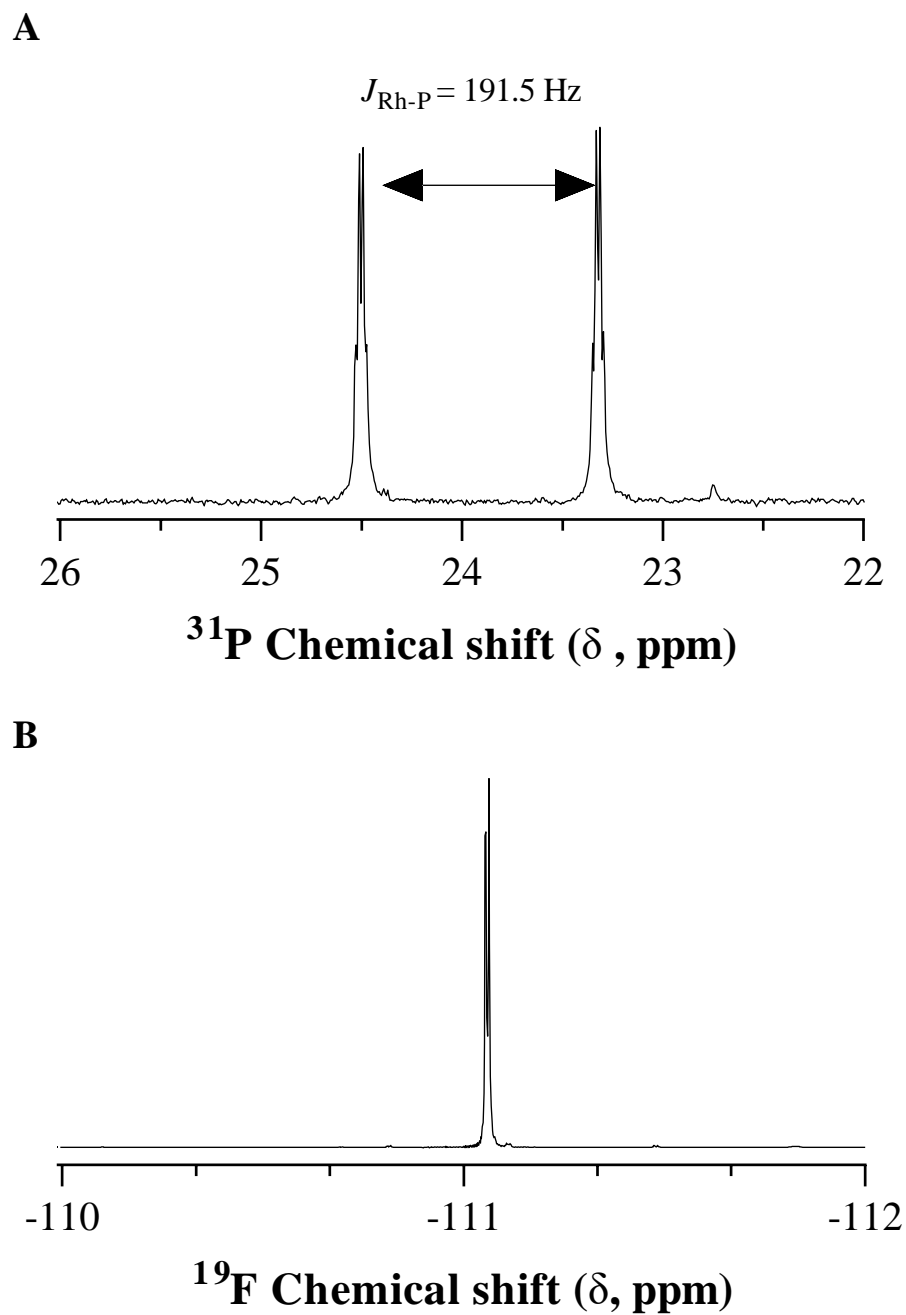


Figure 4-4. (A) ^{31}P NMR spectrum of $\text{Rh(I)(nbd)(Biphenyl)(P(4-FC}_6\text{H}_4)_3)$ recorded in C_6D_6 , showing a doublet of quartets; (B) ^{19}F NMR spectrum of $\text{Rh(I)(nbd)(Biphenyl)(P(4-FC}_6\text{H}_4)_3)$ recorded in C_6D_6 .

While the ^1H , ^{13}C , ^{19}F , ^{31}P NMR spectra and elemental analysis data confirms the structure and purity of **92**, further characterisation by multinuclear NMR spectroscopy was performed such as ^{103}Rh and ^{31}P - $^{103}\text{Rh}\{^1\text{H}\}$ NMR spectroscopy, Figure 4-5. The ^{103}Rh spectrum reveals a doublet due to coupling with ^{31}P , and is centred around $\delta = -7699$ ppm (536 ppm if referenced to Rh metal), Figure 4-5A. This is consistent with the ^{103}Rh chemical shifts we reported for the series of fluorenyl-functionalised Rh(I) complexes, **88**, as well as, the 2-naphthylphenyl Rh(I) derivative, **90**, shown in Figure 4-1, which had measured shifts spanning the range $\delta = -7861$ to -7870 ppm.

To verify this observation and confirm purity, a complementary 2D ^{31}P - $^{103}\text{Rh}\{^1\text{H}\}$ heteronuclear multiple quantum coherence (HMQC) experiment was conducted, Figure 4-5B. The HMQC spectrum clearly shows the presence of single Rh and P species with direct coupling between the two nuclei, confirming the purity and stability of **92** in solution.

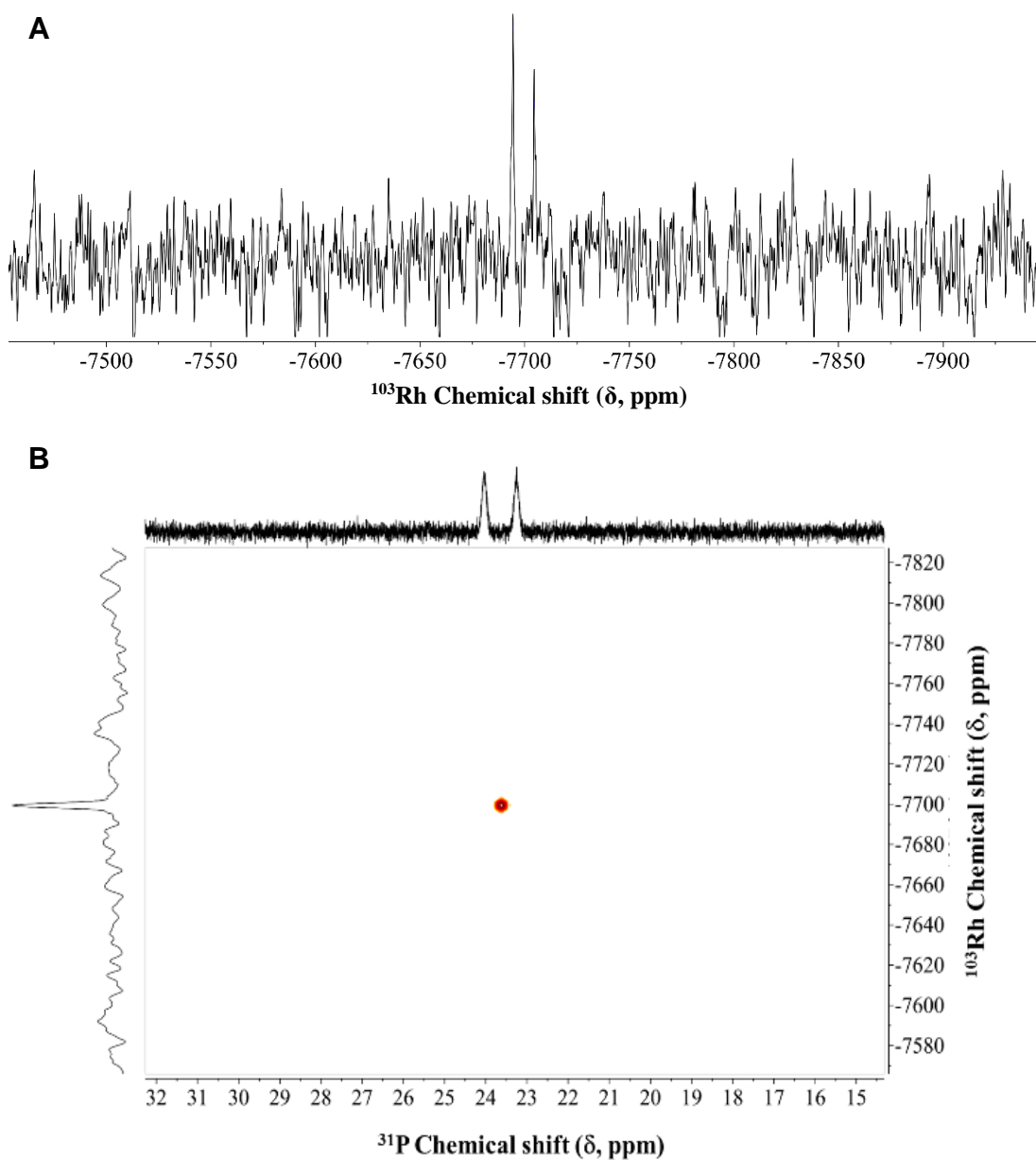


Figure 4-5. (A) ^{103}Rh spectrum (19.1 MHz) recorded in CD_2Cl_2 , and (B) ^{31}P - $^{103}\text{Rh}\{^1\text{H}\}$ HMQC spectrum of complex **92**.

With complex **92** in-hand its efficacy as an initiator for the homopolymerisation of PA was evaluated. It is known that when conducting such 2,1-insertion^{7, 8} (co)polymerisations, it is necessary to add additional free phosphine to serve as a rate modifier if controlled polymerisation is desirable. For example, Miyake, Misumi and Masuda⁹ reported that in polymerisations of PA with **78b**, Figure 4-1, it was necessary to add a minimum of 5 equivalents of free phosphine, relative to Rh, in order to obtain (co)polymers with a low dispersity. Increasing the ratio higher had no discernible effect on the dispersity but impacted the kinetics with polymerisations slowing the higher the free phosphine content.

Similar observations were made in the previous chapters concerning the (co) polymerisation of phenylacetylene with complexes **88b** and **90**, Figure 4-1.^{2, 10} To confirm this general feature a control experiment was initially performed in which PA was homopolymerised for a target M_n of 10,000 in toluene at 30 °C in the absence of added free P(4-FC₆H₄)₃, (Table 4-1, entry 12). Under these conditions polymerisation was rapid reaching ca. 97 % conversion within 30 sec and yielded a PA homopolymer that eluted at the upper column limits of the SEC instrument indicating an M_n in excess of 100,000 and a non-controlled polymerisation process. All further experiments were conducted in the presence of added free phosphine.

Table 4-1. Summary of PA polymerisation conditions with **92**, SEC-measured molecular weights and dispersities, initiation efficiencies and NMR measured *cis* contents in the resulting polyphenylacetylene (co)polymers.

Entry	Rh species	[P]/[Rh]	Polym. Temp. (°C)	Polym. solvent	Theoretical MW ^a	M_n (SEC) ^b	M_w (SEC) ^b	Dispersity (\mathcal{D}) ^b	Rh initiation efficiency ^c	<i>cis</i> content (%) ^d
1	92	5	30	THF	9,090	12,300	13,300	1.08	0.74	94
2	92	20	30	THF	8,830	23,300	26,800	1.15	0.38	98
3	92	5	30	Toluene	9,990	11,600	14,200	1.22	0.86	92
4	92	10	30	Toluene	9,790	11,200	13,100	1.17	0.87	96
5	92	20	30	Toluene	9,990	10,200	11,300	1.11	0.98	99
6	92	5	40	Toluene	9,090	12,800	14,100	1.10	0.71	94
7	92	10	40	Toluene	9,360	12,100	13,500	1.12	0.77	95
8	92	20	40	Toluene	9,360	18,800	19,800	1.05	0.50	96
9	92	5	50	Toluene	9,360	14,400	16,700	1.16	0.65	86
10	92	10	50	Toluene	9,090	17,400	18,700	1.07	0.52	85
11	92	20	50	Toluene	8,930	18,000	19,200	1.07	0.50	79
12	92	0	30	Toluene	9,360	nd ^e	nd ^e	nd ^e	nd ^e	nd ^e

a. Calculated as M_n = mass (g) monomer/moles of **92** and assuming 100 % initiation efficiency.

b. As measured by size exclusion chromatography: eluent THF operated at a flow rate of 1.0 mL/min, instrument calibrated with narrow molecular weight distribution polystyrene standards. Dispersity (\mathcal{D}) = M_w/M_n .

c. Calculated from the ratio of theoretical to measured (SEC determined) M_n 's.

d. As determined by ¹H NMR spectroscopy according to C. I. Simionescu, V. Percec and S. Dumitrescu, *J. Polym. Sci., Part A: Polym. Chem.*, 1977, **15**, 2497-2509.

e. Not determined

The initiating ability of **92** was examined under various experimental conditions, such as [P]/[Rh] ratio, polymerisation temperature and polymerisation solvent, in order to maximise the IE. Interestingly, the polymerisation of PA in toluene resulted in higher IE with values as high as 0.98 but had a negligible impact on the stereoregularity with measured *cis* contents as high as 99 %. These results are consistent with previous Rh(I) complexes (**88b**¹⁰ and **90**², Figure 4-1) detailed in Chapters 2 and 3, in that polymerisation solvent (toluene vs THF) does impact the level of control for PA polymerisations with better control in the less polar solvent.

Next, the effect of [P]/[Rh] ratio and temperature on the homopolymerisation of PA were investigated. At 30 °C, increasing the [P]/[Rh] ratio from 5 to 20 improved the IE from 0.86 to 0.98 (Table 4-1, entries 3-5). At 40 °C (Table 4-1, entry 8) and 50 °C (Table 4-1, entry 11), the IE was significantly reduced when the [P]/[Rh] ratio was increased from 5 to 20 with IE values as low as 0.50 for polymerisations at [P]/[Rh] ratio of 20 at 50 °C. In comparison, the IEs with the Rh(I)- α -phenylvinylfluorenyl,¹⁰ and the Rh(I)-naphthyl² derivatives were shown to increase with increasing [P]/[Rh] ratio. This data suggests that the rate of propagation, R_p , is impacted more than the rate of initiation, R_i , as the temperature increases. It should be noted that the dispersity ($\bar{D} = M_w/M_n$) was observed to decrease at elevated temperatures with values typically around $\bar{D} = 1.07$. In Chapter 2, it was noted that while an increase in IE was observed in the fluorenyl derivatives, **88** Figure 4-1, when polymerisation temperature was increased, it was still not quantitative. While in Chapter 3, increasing polymerisation temperature resulted in a decrease in the IEs overall for **90** with a concomitant detrimental effect on the *cis*-content which was attributed to thermal isomerisation of PPA in solution, a phenomenon studied, and noted by others.¹¹⁻¹⁴

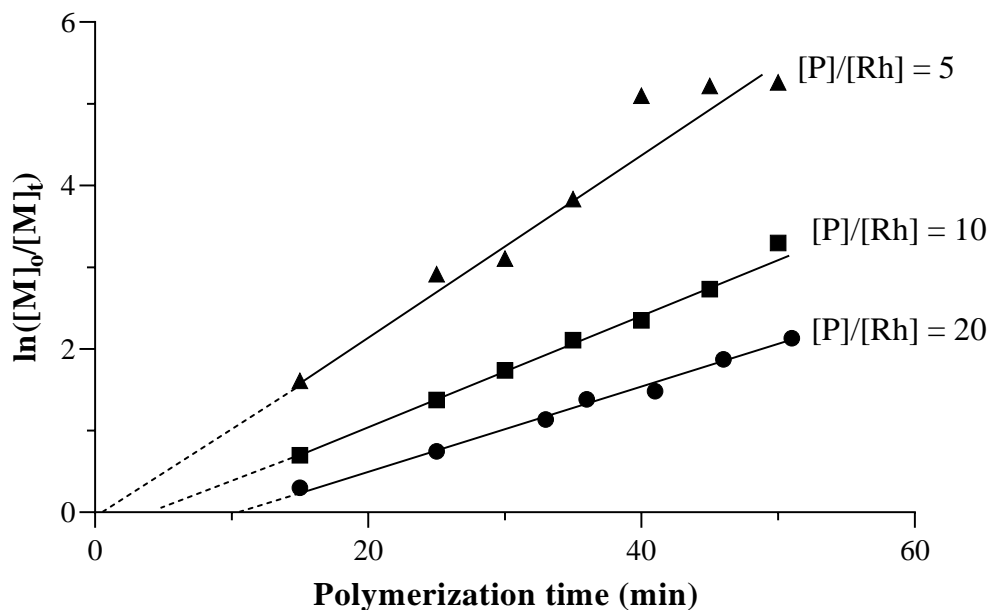
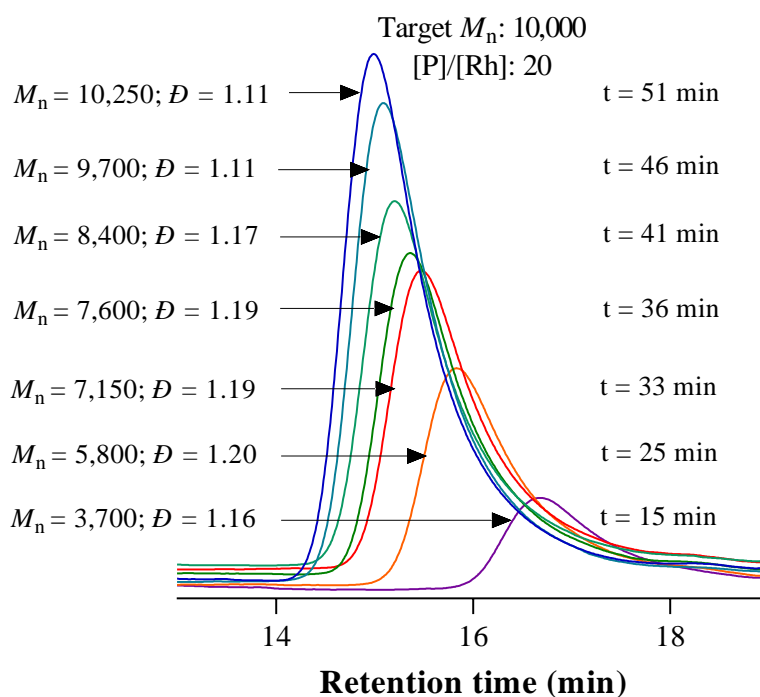
A**B**

Figure 4-6. (A) Pseudo first-order kinetic plots for the homopolymerisation of PA in toluene at 30 °C with [P]/[Rh] = 5, 10 and 20; (B) evolution of the molecular weight distribution in the homopolymerisation of PA for a target molecular weight of 10,000 and [P]/[Rh] = 20. ([P] = [P(4-FC₆H₄)₃])

Figure 4-6A shows the pseudo-first-order kinetic plots associated with the homopolymerisation of PA with **92** in toluene at 30 °C at [P]/[Rh] of 5, 10 and 20. As expected, the homopolymerisation at [P]/[Rh] = 5 was the fastest ($k_{app} = 0.1140 \text{ min}^{-1}$) and reached 98 % conversion after 35 min with the final, isolated material having an SEC measured \bar{D} of 1.25 and M_n of 11,560 which corresponds to an IE of 0.86 (Table 4-1, entry 3). The value of the IE for this Rh(I)-aryl complex is significantly higher than complexes **88b** and **90**, Figure 4-1, and is approaching the benchmark Masuda Rh(I)-vinyl species. In the case of homopolymerisation conducted at [P]/[Rh] = 10, the rate is decreased ($k_{app} = 0.0720 \text{ min}^{-1}$) and a short induction period of ca. 5 min was observed, similar to that observed previously with complex **90**, Figure 4-1. However, polymerisation was still rapid, reaching just over 96 % conversion after 50 min. An improvement in dispersity of 1.18 and a final M_n of 11,250 was observed, which equates to an IE of 0.87 (Table 4-1, entry 6).

A further improvement in the dispersity (and decrease in rate, $k_{app} = 0.0480 \text{ min}^{-1}$, and a slightly increased induction time) was observed at [P]/[Rh] = 20 with the final sample having an SEC-measured \bar{D} of 1.11, and M_n of 10,250. This corresponds to a near-quantitative IE of 0.98 (Table 4-1, entry 9); such efficiencies in this application have only previously been reported for certain Masuda-type Rh(I)-vinyl initiators. The evolution of the molecular weight distribution for this polymerisation is highlighted in Figure 4-6B, the molecular weight distributions are unimodal and a systematic shift to lower retention time (higher molecular weight) is observed, accompanied by increasing height of the chromatograms which is an indication of increasing polymer yields in the aliquots. There was a general decrease in dispersities with increasing conversions. The SEC-measured M_n vs conversion plots for [P]/[Rh] = 5, 10, and 20 homopolymerisations at 30 °C are given in Figure 4-7. The M_n vs

conversion plots shows the molecular weight increasing proportionally to the monomer conversion and are essentially linear, which indicates that neither chain transfer nor chain termination events have occurred.

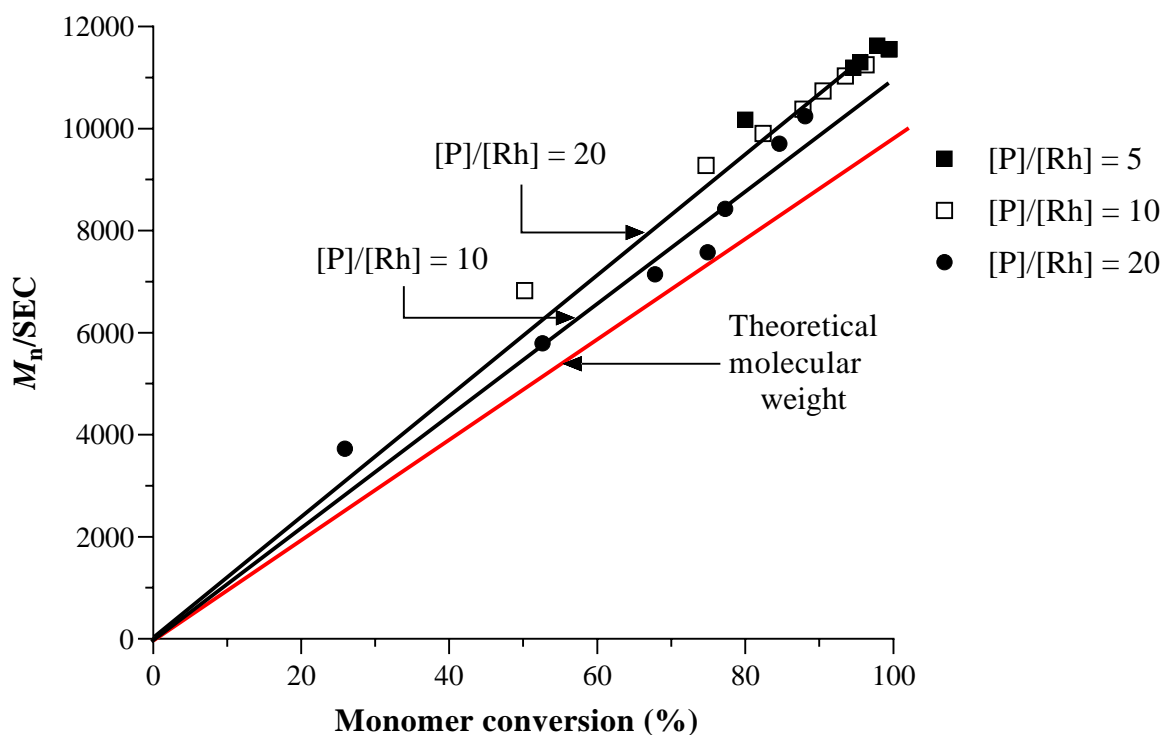


Figure 4-7. M_n vs conversion plot for homopolymerisation of PA at 30 °C in toluene with (A) $[P]/[Rh] = 5$ (■); (B) $[P]/[Rh] = 10$ (□); (C) $[P]/[Rh] = 20$ (●), ($[P] = [P(4-FC_6H_4)_3]$).

Collectively, the kinetic and molecular weight data suggest that the homopolymerisation of PA with **90** in the presence of added free $P(4-FC_6H_4)_3$ proceeds in a controlled fashion with higher ratios of $[P]/[Rh]$ giving better control albeit at the expense of polymerisation rate.

Table 4-2. A comparison between **90** and **92** with their relevant k_{app} values listed. All polymerisations were conducted at 30 °C in toluene.

Rh catalyst	[P]/[Rh]	k_{app} (min ⁻¹)
90	10	0.0360
92	10	0.0720
90	20	0.0228
92	20	0.0480

The measured k_{app} values for **90** (from Chapter 3) and **92** with [P]/[Rh] = 10 and 30 for polymerisations performed in toluene at 30 °C are presented in Table 4-2. The homopolymerisation of PA by **92** is faster than **90** by a factor of 2 at both [P]/[Rh] ratios which suggests that **92** has a much higher activity in the homopolymerisation of PA. In Chapter 3, we described the 1,4-Rh atom migratory processes which **90** underwent in solution, resulting in the formation of multiple ((in)active) species that adversely affected the efficacy of **90** as an initiator for the homopolymerisation of PA. Certainly, **92** might undergo such migratory processes; however, such an event yields a structurally identical species. As a result, a near quantitative IE and doubling in polymerisation rate can be seen while retaining the desirable traits such as low \bar{D} and highly stereoregular *cis-transoidal* polyphenylacetylenes.

A distinguishing feature of phenylacetylene (co)polymers prepared by Rh-mediated insertion polymerisation is the highly stereoregular nature of the final materials with polymers adopting a *cis-transoidal* structure.¹⁵ This key structural feature was observed in the case of the polyphenylacetylene homopolymers prepared herein with calculated *cis* contents of 92 % ([P]/[Rh] = 5), 96 % ([P]/[Rh] = 10) and

99 % ($[P]/[Rh] = 20$) suggesting a correlation between stereoregularity and the polymerisation rate or overall level of control.

To highlight the broader utility of **92** with a functional substrate, 4-fluorophenylacetylene (4-FPA) was homopolymerised for a target M_n of 5,000 and $[P]/[Rh] = 20$, Figure 4-8. Consistent with PA homopolymerisations, polymerisation proceeded rapidly yielding a well-defined homopolymer with a narrow molecular weight distribution ($\mathcal{D} = 1.07$) and high *cis-transoidal* stereoregularity (calculated *cis* content of 96 %).

In a final demonstration of the ability of **92** to mediate the (co) polymerisation of phenylacetylenes in a controlled fashion, an AB diblock copolymer of PA with 4-FPA was prepared via sequential monomer addition to demonstrate retention of chain-end activity, Figure 4-9. PA was first homopolymerised in toluene at 30 °C with $[P]/[Rh] = 20$ and target M_n of 5,000 at quantitative conversion. An aliquot was withdrawn after 60 min and analysed by SEC which indicated a homopolymer with an M_n of 6,200 and \mathcal{D} of 1.10. 4-FPA was subsequently added and block polymerisation allowed to proceed for a further 60 min. The copolymerisation was terminated by the addition of a small volume of acetic acid, and an aliquot removed for SEC analysis.

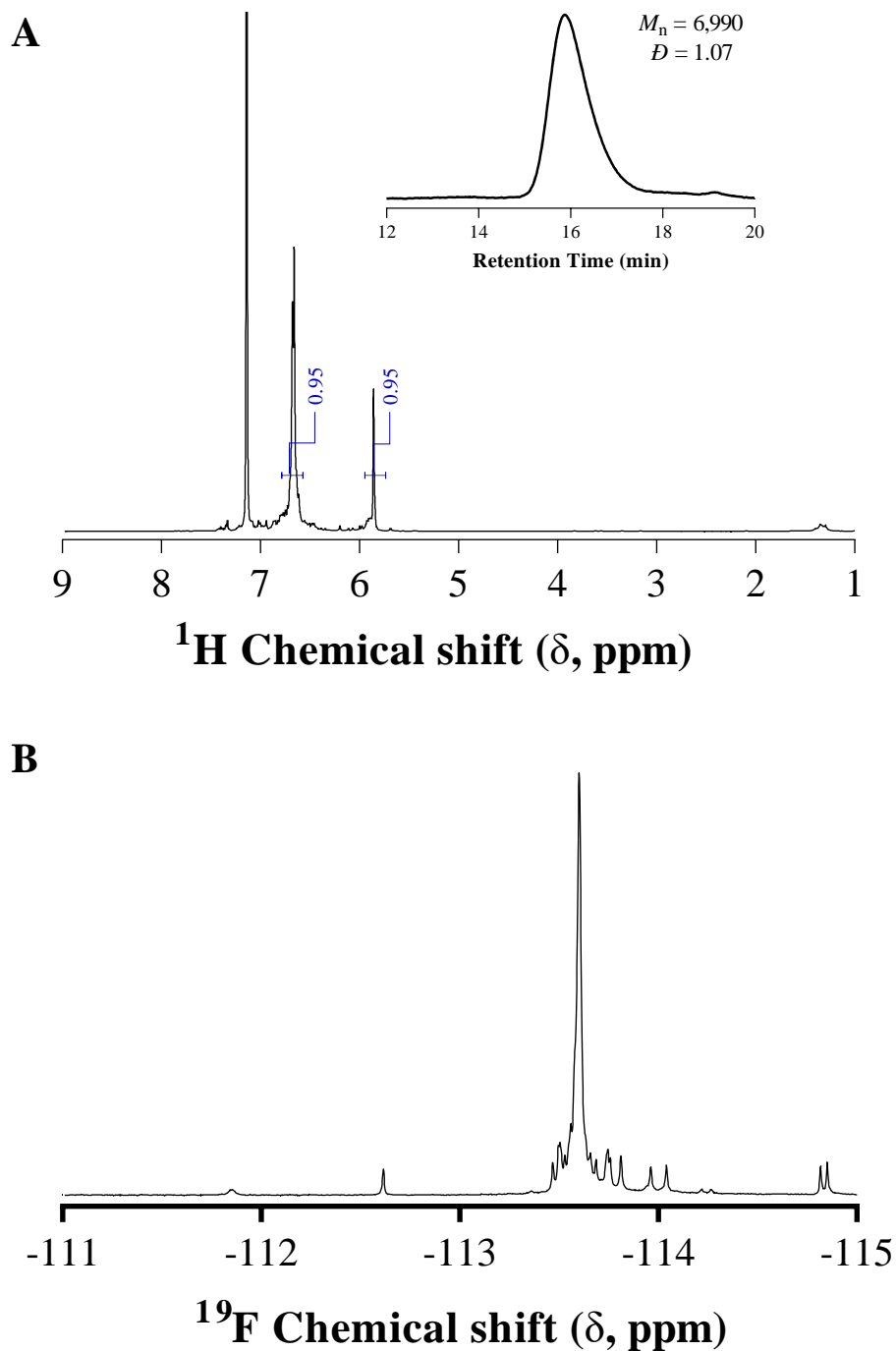


Figure 4-8. (A) ^1H NMR, recorded in C_6D_6 , of poly(4-fluorophenylacetylene) homopolymer, with the SEC trace of the homopolymer shown inset. Calculated *cis* content of 96 %. Measured integral values given in blue. (B) ^{19}F NMR of the poly(4-fluorophenylacetylene) homopolymer.

Block copolymer formation was verified by the systematic shift of the molecular weight distribution, which can be seen in Figure 4-9, to shorter retention time with no evidence of any residual homopolymer ‘impurity’ confirming retention of chain-end activity after PA homopolymerisation and quantitative crossover efficiency. The product AB diblock copolymer had a measured M_n of 15,900 and \mathcal{D} of 1.09.

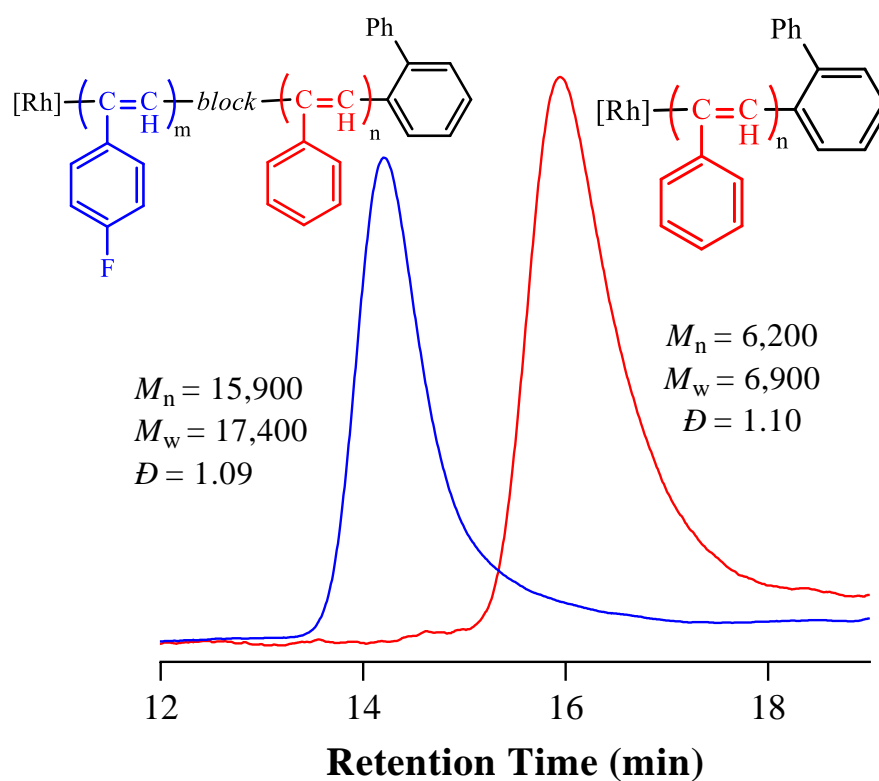


Figure 4-9. SEC traces for a polyphenylacetylene homopolymer (red) and an AB diblock copolymer with 4-fluorophenylacetylene formed by sequential monomer addition (blue).

Figure 4-10 shows the ^1H NMR spectrum, with the ^{19}F spectrum shown inset, recorded in C_6D_6 , of the poly(PA-*block*-4-FPA) copolymer. The stereoregular nature of the copolymer is evidenced by the well-resolved aromatic hydrogens covering the range $\delta = 6.9\text{-}6.2$ ppm, but more importantly, by the two signals at $\delta = 6.0$ and 5.8 ppm. The very sharp, former signal, is associated with backbone hydrogens in the *cis* configuration on the PA block while we assign the latter, broader signal to *cis* hydrogens of the 4-FPA block. The more poorly resolved *cis*-H signal associated with the 4-FPA block is indicative of a less stereoregular microstructure but, nonetheless, is still predominantly *cis*- the overall *cis* content of the copolymer was determined to be 76 %.

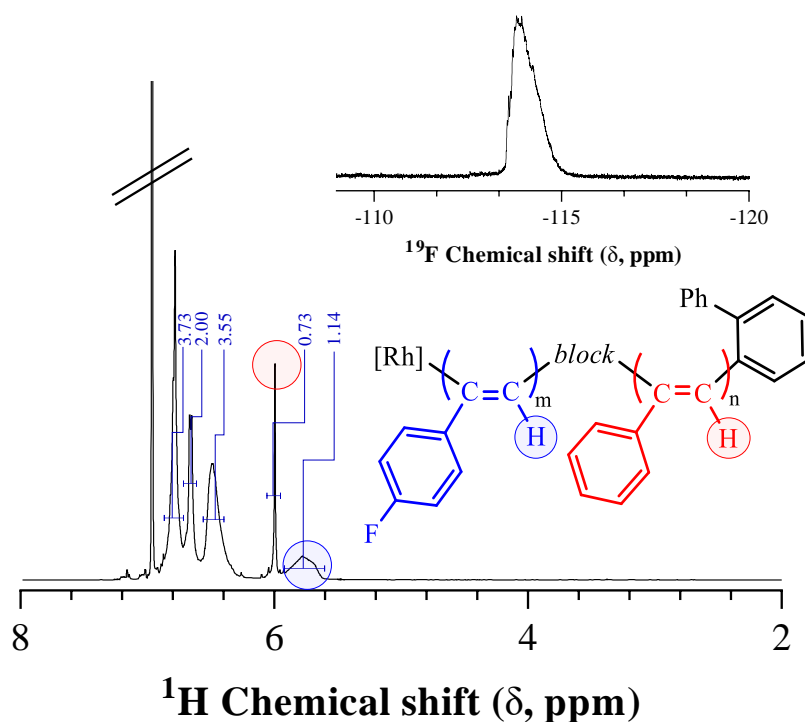


Figure 4-10. ^1H NMR spectrum, recorded in C_6D_6 , of poly(phenylacetylene-*block*-4-fluorophenylacetylene) highlighting the *cis-transoidal* stereoregular nature of the copolymer microstructure with the relevant measured integral values (blue). The ^{19}F NMR spectrum of the block copolymer is shown inset.

4.4 Conclusions

In summary, in this chapter we have reported the synthesis of a new, well-defined, readily isolable, Rh(I)-aryl complex that serves as a highly efficient initiator for the controlled (co)polymerisation of phenylacetylenes. Successful synthesis, isolation and purity of Rh(nbd)(Biphenyl)(P(4-FC₆H₄)₃), **92**, was confirmed by a combination of elemental analysis, X-ray crystal structure analysis, and multinuclear NMR spectroscopy.

The efficacy of **92** was examined under a range of experimental conditions and it was found that the homopolymerisation of phenylacetylene (PA) performed in toluene at 30 °C with [P]/[Rh] = 20 resulted in a system with near-quantitative IE and yielded polymer with a low dispersity ($\mathcal{D} = 1.11$). The calculated *cis* content of the resulting PA homopolymer was calculated to be 99 %. This work detailed herein also reveals that increasing polymerisation temperature had an adverse effect on the initiation efficiencies, which was attributed to a more pronounced impact on the rate of propagation compared to the the rate of initiation at elevated temperature, however, the dispersities were found to decrease at elevated temperatures. It was also noted that the homopolymerisation of PA by **92** was influenced by solvent and experiments conducted in a polar protic solvent like THF, adversely impacted the IEs, which were typically in the range of 0.38 to 0.74. This observation was consistent with **88** in that solvent polarity, or dielectric constant, did impact the level of control attained.

The ability of **92** to mediate the controlled (co)polymerisation of phenylacetylenes was verified from the pseudo-first-order kinetic profiles, the molecular weight vs conversion plots and the ability to prepare an AB diblock copolymer with quantitative reinitiation. The rate of PA polymerisation mediated by **92** was determined to be double the rate observed for the polymerisations initiated by

90, which was evident from the k_{app} values determined from the pseudo first-order kinetic plots. The broader applicability of **92**, was demonstrated by the homopolymerisation of a functional PA derivative, 4-fluorophenylacetylene (4-FPA), mediated by **92**, performed in toluene at 30 °C with $[P]/[Rh] = 20$, yielding poly(4-FPA)s with a \bar{D} of 1.07 and high *cis-transoidal* stereoregularity (*cis* content = 96 %). The stereoregular, *cis-transoidal* structure of the product, poly(phenylacetylene-*block*-4-fluorophenylacetylene), was confirmed by 1H NMR spectroscopy was determined to be 76 % overall.

To conclude, **92** was targeted to circumvent the 1,4-Rh atom migration that afflicted **90** (which was proposed to be responsible for the lower than expected IEs (ca. 0.85) due to the formation of multiple ((in)active) species), and the data presented within this chapter confirms that **92** is indeed a more efficient initiator than **90**. This contribution represents only the second example in which a well-defined Rh(I)-aryl complex has been employed specifically as an initiator for the controlled polymerisation of phenylacetylenes and, at present, exhibits the highest initiation efficiency.

4.5 References

1. Misumi, Y.; Kanki, K.; Miyake, M.; Masuda, T., Living polymerization of phenylacetylene by rhodium-based ternary catalysts, (diene)Rh(I) complex/vinylolithium/phosphorous ligand. effect of catalyst components. *Macromolecular Chemistry and Physics* **2000**, *201* (17), 2239-2244.
2. Tan, N. S. L.; Nealon, G. L.; Lynam, J. M.; Sobolev, A. N.; Rowles, M. R.; Ogden, M. I.; Massi, M.; Lowe, A. B., A (2-(naphthalen-2-yl)phenyl)rhodium(I) complex formed by a proposed intramolecular 1,4-ortho-to-ortho' Rh metal-atom migration and its efficacy as an initiator in the controlled stereospecific polymerisation of phenylacetylene. *Dalton Transactions : An International Journal of Inorganic Chemistry* **2019**, *48* (43), 16437-16447.
3. Harris, R. K.; Becker, E. D.; Cabral de Menezes, S. M.; Granger, P.; Hoffman, R. E.; Zilm, K. W., Further conventions for NMR shielding and chemical shifts (IUPAC recommendations 2008). *Magnetic Resonance in Chemistry* **2008**, *46* (6), 582-598.
4. Carlton, C., *Annual Reports on NMR Spectroscopy*. Elsevier: 2008; Vol. 63.
5. Bourhis, L. J.; Dolomanov, O. V.; Gildea, R. J.; Howard, J. A.; Puschmann, H., The anatomy of a comprehensive constrained, restrained refinement program for the modern computing environment - Olex2 dissected. *Acta Crystallographica Section A: Foundations and Advances* **2015**, *71* (Pt 1), 59-75.
6. Sheldrick, G., Crystal structure refinement with SHELXL. *Acta Crystallographica Section C* **2015**, *71* (1), 3-8.
7. Ke, Z.; Abe, S.; Ueno, T.; Morokuma, K., Rh-catalyzed polymerization of phenylacetylene: theoretical studies of the reaction mechanism, regioselectivity, and stereoregularity. *Journal of the American Chemical Society* **2011**, *133*, 7926-7941.
8. Sanda, F.; Shiotsuki, M.; Masuda, T., Controlled polymerization of phenylacetylenes using well-defined rhodium catalysts. *Macromolecular Symposia* **2015**, *350*, 67-75.
9. Miyake, M.; Misumi, Y.; Masuda, T., Living polymerization of phenylacetylene by isolated rhodium complexes, Rh[C(C₆H₅)=C(C₆H₅)₂](nbd)(4-XC₆H₄)₃P (X = F, Cl). *Macromolecules* **2000**, *33* (18), 6636-6639.
10. Tan, N. S. L.; Simpson, P. V.; Nealon, G. L.; Sobolev, A. N.; Raiteri, P.; Massi, M.; Ogden, M. I.; Lowe, A. B., Rhodium(I)- α -phenylvinylfluorenyl complexes: synthesis, characterization, and evaluation as initiators in the stereospecific polymerization of phenylacetylene. *European Journal of Inorganic Chemistry* **2019**, *2019* (5), 592-601.
11. Simionescu, C. I.; Percec, V., Thermal cis-trans isomerization of cis-transoidal polyphenylacetylene. *Journal of Polymer Science : Polymer Chemistry Edition* **1980**, *18* (1), 147-155.

12. Percec, V.; Rudick, J. G.; Nombel, P.; Buchowicz, W., Dramatic decrease of the cis content and molecular weight of cis-transoidal polyphenylacetylene at 23 °C in solutions prepared in air. *Journal of Polymer Science Part A: Polymer Chemistry* **2002**, *40* (19), 3212-3220.
13. Simionescu, C. I.; Percec, V.; Dumitrescu, S., Polymerization of Acetylenic Derivatives. XXX. Isomers of Polyphenylacetylene. *Journal of Polymer Science Part A: Polymer Chemistry* **1977**, *15*, 2497-2509.
14. Karim, S. M. A.; Nomura, R.; Masuda, T., Degradation behavior of stereoregular cis–transoidal poly(phenylacetylene)s. *Journal of Polymer Science Part A: Polymer Chemistry* **2001**, *39* (18), 3130-3136.
15. Bondarev, D.; Zedník, J.; Plutnarova, I.; Vohlídal, J.; Sedláček, J., Molecular weight and configurational stability of poly[(fluorophenyl)acetylene]s prepared with metathesis and insertion catalysts. *Journal of Polymer Science Part A : Polymer Chemistry* **2010**, *48* (19), 4296-4309.

Every reasonable effort has been made to acknowledge the owners of copyright material. I would be pleased to hear from any copyright owner who has been omitted or incorrectly acknowledged.

Chapter 5

Controlled (Co)Polymerisation of Phenylacetylenes and Other Substituted Arylacetylenes by Rhodium(I)(tetrafluorobenzobarrelene)(biphenyl)(*tris*(4-fluorophenyl)phosphine).

5.1 Introduction

The thesis has, thus far, discussed the synthesis and evaluation of five new Rh(I) derivatives based on the Masuda structural motif, **78**, Figure 5-1, as initiators for the polymerisation of phenylacetylenes (PAs), and in all cases, homopolymers of PA have high *cis-transoidal* stereoregularity, low dispersities ($\mathcal{D} < 1.20$), and the polymerisations mediated by these Rh(I)-vinyl and -aryl derivatives were demonstrated to be controlled, as evidenced by the ability to prepare block copolymers.

In Chapter 1, three new Rh(I)- α -phenylvinylfluorenyl complexes, **88b**, **88d** and **88e**, Figure 5-1, were synthesised, whose initiating fragment fulfils the substitution patterns outlined by Misumi *et al.*¹ for efficient initiators. While they were determined to be active initiators for PA homopolymerisations, they had lower than expected initiation efficiencies (IEs), and spanned the range 0.13 to 0.56. The study demonstrated that the IE is not only governed by substitution patterns but also influenced by geometric or electronic factors.

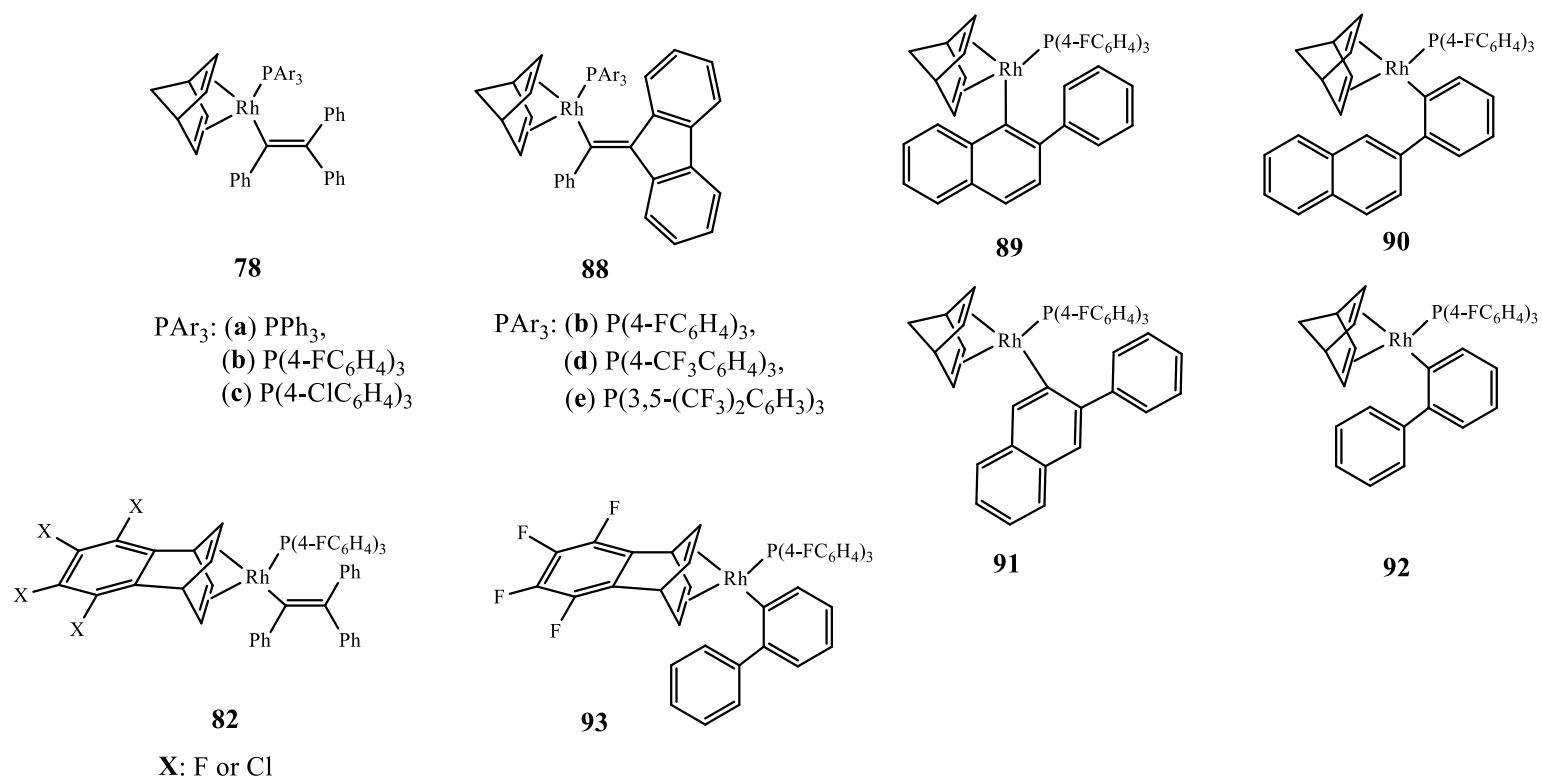


Figure 5-1. Chemical structure of isolable Rh(I)-based complexes described in this thesis with different diene moiety and initiating fragment. Norbornadiene (nbd) variant (top row), Rh(I)-vinyl complexes, **76** and **88**, and recently reported Rh(I)-aryl complexes, **90** and **92**. Tetrafluorobenzobarralene (tfb)/Tetrachlorobenzobarralene (tcb) variant (bottom row), Rh(I)-vinyl complex, **82** reported by Saeed *et al.*² and Rh(I)-aryl complex, **93**, whose synthesis and evaluation as initiator for the homopolymerisation of PA will be discussed in this chapter.

To address the low IEs observed for the Rh(I)- α -phenylvinylfluorenyl complexes, we targeted the synthesis of the Rh(I)-2-phenylnaphthyl derivative, **89**, Figure 5-1, whose initiating fragment has a freely rotating phenyl group on the β -carbon, and was hypothesised to facilitate facile monomer insertion. However, single crystal X-ray diffraction data indicated that we isolated a structural isomer of **89**, namely the Rh(I)-2-naphthylphenyl derivative, **90**, Figure 5-1, and upon further characterisation with 2D NMR spectroscopy (^{31}P - $^{103}\text{Rh}\{^1\text{H}, ^{103}\text{Rh}\}$ HMQC NMR) a second isomeric species, the Rh(I)-2-naphthylphenyl derivative, **91**, Figure 5-1, was identified and a possible 3rd isomeric species observed only in ^{31}P and ^{19}F NMR experiments. The formation of these structural isomers of **89** was attributed to 1,4-Rh atom migrations whose mechanism was discussed in detail in Chapter 3. The evaluation of the new Rh(I)-aryl species, **90**, as an initiator for the homopolymerisation of PA was carried out and the IE was determined to be 0.85. This less than quantitative IE was attributed to the formation of multiple (in)active species such as **91**.

In Chapter 4, to address the Rh-atom migrations, the synthesis of the Rh(I)-biphenyl derivative, **92**, was targeted. Recognising that this Rh(I)-aryl species is susceptible to such migratory processes, the incorporation of a structurally symmetrical initiating fragment, suggested that the IE might be improved. This hypothesis was confirmed when the investigation revealed that **92** exhibited a near-quantitative IE of 0.98, a significant improvement over **90**. We also demonstrated the broader utility with a successful homo- and block (co)polymerisation of a functional PA derivative.

It is evident that these Rh(I) initiators are effective for the polymerisation of PA, however, there is much to be explored in terms of structure-activity studies. The commonality between the Rh(I)-vinyl and -aryl derivatives reported in previous

chapters is their norbornadiene (nbd) ligands which are π -acidic in nature. It is documented that Rh(I)-vinyl species bearing tetrafluorobenzobarralene (tfb) diene ligands, **82**, Figure 5-1, are significantly more active than their nbd diene ligand counterparts due to a higher π -acidity.^{3,4}

Based on the supposition that substituting the nbd ligand with tfb diene ligand will significantly increase the activity of the Rh(I)-biphenyl derivative by virtue of the higher π -acidity of the tfb diene ligand, in this chapter, the synthesis, and characterisation of a new Rh(I)-biphenyl derivative, Rh(I)(tfb)(Biphenyl)(P(4-FC₆H₄)₃), **93**, Figure 5-1, is described. Subsequently, the efficacy of Rh(I)(tfb)-biphenyl species as an initiator for the controlled (co)polymerisation of PA and other substituted aryacetylenes will be investigated, and its ability to mediate block (co)polymerisation will be examined by sequential monomer addition.

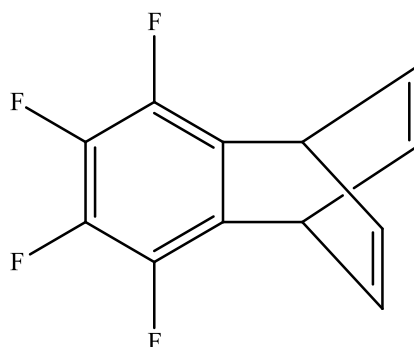
5.2 Experimental

5.2.1 Materials

n-Butyllithium (*n*-BuLi, 1.6 M solution in hexane, Sigma-Aldrich), 2-bromobiphenyl (C₁₂H₉Br) (98 % Tokyo Chemical Industry), and tris(*para*-fluorophenyl)phosphine (P(4-FC₆H₄)₃, 98 %, Sigma-Aldrich) were used as received. Phenylacetylene (CH≡CPh, 98 %, Sigma-Aldrich) was purified by passage over a column of basic alumina and then stored in a fridge until needed.

THF, diethyl ether and CH₂Cl₂ were dried using a PureSolv MD5 solvent purification system (Innovative Technology, Inc.), collected, degassed via the freeze-pump-thaw technique and stored under dry nitrogen until needed. Toluene (99.8 %, Sigma-Aldrich) was degassed via the freeze-pump-thaw method and stored under dry nitrogen until required. All glassware was pre-dried in an oven at 120 °C and then flamed dried under vacuum before use. All reactions were performed using standard Schlenk line techniques

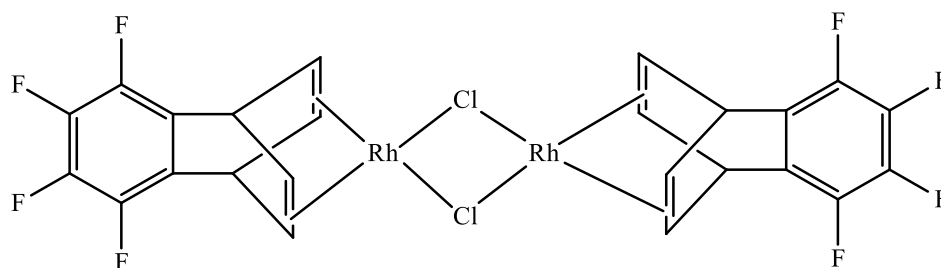
5.2.2 Synthesis of Tetrafluorobenzobarrelene (tfb).



The target compound was prepared via a modification of a previously reported synthesis.^{5,6}

To a round-bottomed flask equipped with a Teflon-coated magnetic stir bar, bromopentafluorobenzene (5 g, 0.02 mol) was added to benzene (63.0 mL, 0.7 mmol) and stirred for 10 minutes under a dry nitrogen atmosphere at 0 °C. To this was added *n*-BuLi (12.5 mL, 0.02 mol) to produce an ethereal light orange solution which was stirred at 0 °C for 2 hours. Subsequently, the solvent was removed via rotary evaporation yielding an orange residue which was extracted with hexane and filtered through a column containing neutral activated alumina 90 (80.0 g, activity I). This process was repeated until white solids remain in the reaction flask, which was discarded, and the yellow coloured fraction was kept. The yellow fraction was reduced via rotary evaporation to afford yellow crystals. It was then sublimed at 60 °C using a cold finger setup and yielded pure white crystals of tetrafluorobenzobarrelene (2.5 g, yield: 55 %). ¹H NMR (400 MHz, CDCl₃) δ (ppm): 6.88 (dd, *J* = 4.3, 3.0 Hz, 4H), 5.29 (ttt, *J* = 4.1, 3.0, 1.0 Hz, 2H); ¹⁹F NMR (376 MHz, CDCl₃) δ (ppm): -149.96 (d, *J* = 7.5 Hz), -150.00 (d, *J* = 7.6 Hz), -162.61 (d, *J* = 7.6 Hz), -162.65 (d, *J* = 7.7 Hz).

5.2.3 Synthesis of $[\text{Rh}(\text{tfb})\text{Cl}]_2$



The target compound was prepared based on a procedure reported by Saeed *et al.*⁴

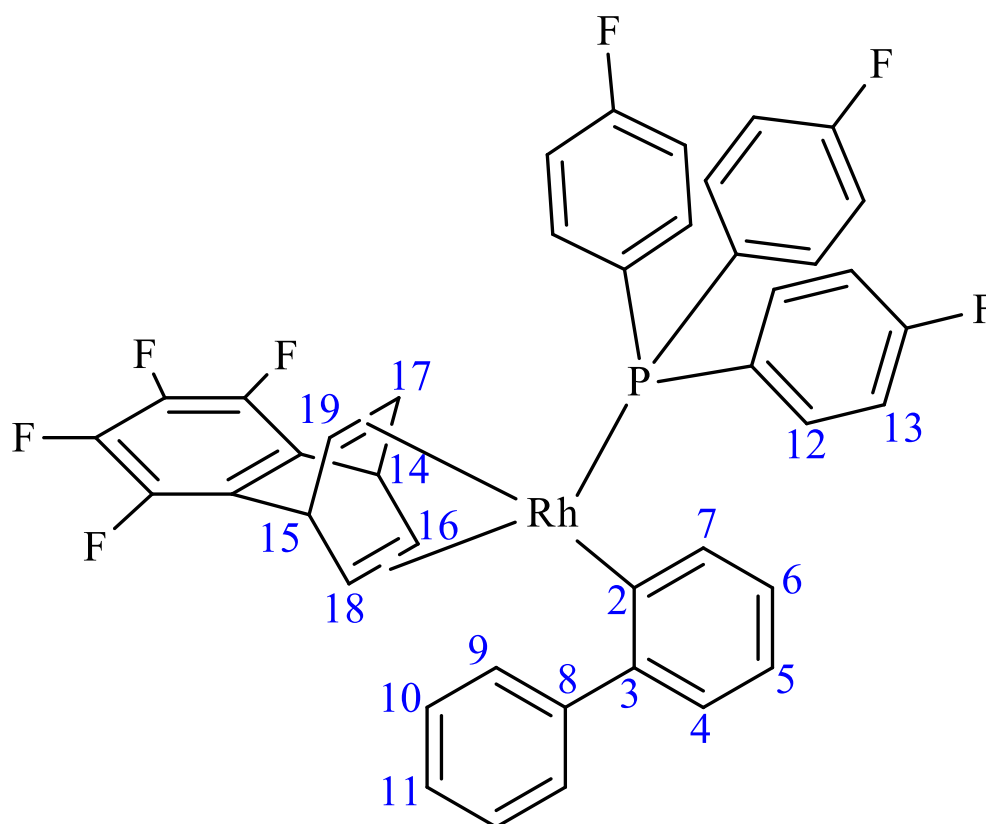
To a round-bottomed flask equipped with a Teflon-coated magnetic stir bar was added $\text{RhCl}_3 \cdot 6\text{H}_2\text{O}$ (679 mg, 2.58 mmol) and tetrafluorobenzobarrelene (1.17 g, 5.16 mmol) in ethanol (15.0 mL) and Milli-Q water (3.0 mL, 18 Ω), forming a purple mixture which was stirred for 30 min at room temperature under a normal air atmosphere. The reaction mixture was then refluxed for 3 h which afforded an orange precipitate. The precipitate was collected via gravity filtration and washed with methanol (30.0 mL) three times. The precipitate was then purified by recrystallisation from CH_2Cl_2 /methanol via a solvent layering technique which afforded the target compound as orange crystals (846 mg, yield: 90 %). ^1H NMR (400 MHz, CDCl_3) δ (ppm): 5.65 (s, 2H), 3.79 (s, 4H); ^{19}F NMR (376 MHz, CDCl_3) δ (ppm): -146.67 (d, J = 7.3 Hz), -146.71 (d, J = 7.2 Hz), -158.69 (d, J = 6.8 Hz), -158.73 (d, J = 7.7 Hz).

5.2.4 Synthesis of Rh(I)(tfb)(Biphenyl)(P(4-FC₆H₄)₃)

The target complex, **93**, was prepared following the procedure described in previous chapters.⁷

To a round-bottomed flask equipped with a Teflon-coated magnetic stir bar was added 2-bromobiphenyl (172.4 μ L, 1.00 mmol) in dry diethyl ether (20.0 mL). The flask was cooled to 0 °C, and *n*-BuLi (1.6 M solution in hexane, 0.71 mL, 1.13 mmol) was cannula transferred and the mixture allowed to react for 45 min yielding an ethereal solution of C₆H₅(C₆H₄Li). To a separate round-bottomed flask equipped with a Teflon-coated magnetic stir bar, a solution of [Rh(tfb)Cl]₂ (182.3 mg, 0.25 mmol) and P(4-FC₆H₄)₃ (316.3 mg, 1.00 mmol) was prepared in dry toluene (15.0 mL). The mixture was then stirred vigorously at 0 °C for 15 min. To this was added the ethereal solution of C₆H₅(C₆H₄Li) via cannula transfer at 0 °C and the mixture was stirred for 4 hours. Subsequently, the reaction solution was quenched with methanol (1.0 mL) and the solution cannula transferred and filtered through a short plug of neutral activated alumina 90 (activity I) under an inert atmosphere, yielding a clear orange solution. Solvents were concentrated under high vacuum on a Schlenk line affording a dark orange viscous liquid. To this residue was added methanol (150 mL) and the mixture stirred vigorously with a magnetic stir bar yielding orange precipitates. The target complex was isolated by recrystallisation from CH₂Cl₂/methanol via a solvent layering technique (0.371 g, yield: 92 %). CH elemental analysis: %C_{theor.}: 63.17, %C_{found.}: 63.21; %H_{theor.}: 3.24, %H_{found.}: 3.34; ¹H NMR (600 MHz, CD₂Cl₂) δ (ppm): 7.73-7.67 (m, 2H, H9), 7.46-7.44 (m, 3H, H10,11), 7.12 (dt, *J* = 7.4, 1.1 Hz, 1H, H7), 7.06 (dd, *J* = 7.5, 1.4 Hz, 1H, H4), 7.01-6.95 (m, 12H, H12,13), 6.86 (t, *J* = 7.3 Hz, 1H, H5), 6.76 (td, *J* = 7.3, 1.4 Hz, 1H, H6), 5.47 (t, 5.6 Hz, 1H, H15), 5.16 (t, *J* = 5.6 Hz, 1H, H14), 4.61 (q, *J* = 4.4 Hz, 1H, H18), 3.65 (t, *J* = 5.4 Hz, 1H, H17),

3.54 (q, $J = 5.5$ Hz, 1H, H16), 3.45 (q, $J = 5.5$ Hz, 1H, H19); $^{13}\text{C}\{^1\text{H}\}$ NMR (151 MHz, CD_2Cl_2) δ (ppm): 169.8 (dd, $J = 32.5, 13.4$ Hz, C2), 164.0 (dd, $J = 250.6, 1.9$ Hz, C-F), 148.2 (C8), 147.0 (t, $J = 1.7$ Hz, C3), 136.9 (dd, $J = 3.5, 1.3$ Hz, C7), 135.8 (dd, $J = 14.1, 8.1$ Hz, C12), 129.9 (dd, $J = 37.2, 3.0$ Hz, C-P), 129.5 (C10), 127.6 (C4), 127.2 (C11), 125.4 (d, $J = 2.0$ Hz, C6), 122.6 (C5), 122.4 (C9), 115.8 (dd, $J = 21.1, 10.4$ Hz, C13), 75.2 (d, $J = 5.7$ Hz, C19), 73.6 (d, $J = 5.4$ Hz, C17), 70.4 (dd, $J = 14.5, 2.7$ Hz, C18), 58.8 (dd, $J = 19.8, 7.2$ Hz, C16), 41.4 (d, $J = 3$ Hz, C15), 40.8 (C14); ^{19}F NMR (376 MHz, C_6D_6) δ (ppm): -110.11 (d, $J = 3.2$ Hz), -147.88 (dd, $J = 22.5, 15.8$ Hz), -148.20 (dd, $J = 22.4, 15.7$ Hz), -160.32 (dd, $J = 22.5, 19.2$ Hz), -160.54 (dd, $J = 22.5, 19.0$ Hz); $^{31}\text{P}\{^1\text{H}\}$ NMR (243 MHz, CD_2Cl_2) δ (ppm): 23.6 (dm, $J_{\text{P-Rh}} = 193.4$ Hz); $^{103}\text{Rh}\{^{31}\text{P}\}$ NMR (19 MHz, CD_2Cl_2) δ (ppm): -7674.



5.2.5 Homopolymerisation of Phenylacetylene

All (co)polymerisations were performed using standard Schlenk line techniques, under a nitrogen atmosphere in glassware pre-dried in an oven set at 120 °C. Below is a typical procedure for the homopolymerisation of phenylacetylene with Rh(tfb)(Biphenyl)(P(4-FC₆H₄)₃), **93**.

A solution of phenylacetylene (0.25 g, 2.45 mmol) in toluene (2.5 mL) was cannula transferred under a nitrogen atmosphere to a solution of Rh(tfb)(Biphenyl)(P(4-FC₆H₄)₃) (0.015 g, 0.02 mmol) and free phosphine, P(4-FC₆H₄)₃, (160 mg, 0.50 mmol) dissolved in toluene (2.5 mL) in a Schlenk flask equipped with a magnetic stir bar. The flask was then immersed in a pre-heated oil bath set at 30 °C and polymerisation allowed to proceed for 90 min. An aliquot (0.1 mL) was withdrawn every 5-10 min and added to a vial of deuterated chloroform (0.5 mL) containing a small volume of acetic acid (2.0 µL). After 90 min, the polymerisation was terminated by the addition of acetic acid. The product polymer was isolated by precipitation into a large volume of methanol, isolated by gravity filtration and dried to a constant weight in a vacuum oven at 40 °C overnight. Monomer conversions were determined by ¹H NMR spectroscopy, and molecular weights and dispersity were measured by size exclusion chromatography.

5.2.6 Self-blocking of Polyphenylacetylene (PPA) with PA

A solution of phenylacetylene (0.25 g, 2.45 mmol) in toluene (2.5 mL) was cannula transferred under a nitrogen atmosphere to a solution of Rh(tfb)(Biphenyl)(P(4-FC₆H₄)₃) (0.015 g, 0.02 mmol) and free phosphine, P(4-FC₆H₄)₃, (160 mg, 0.50 mmol) dissolved in toluene (2.5 mL) in a Schlenk flask equipped with a magnetic stir bar. The flask was then immersed in a pre-heated oil

bath set at 30 °C. After 1 h an aliquot (0.1 mL) was taken and the polymer isolated by precipitation into methanol (20.0 mL) containing a small volume of acetic acid as the terminating agent. Subsequently, a second feed of phenylacetylene (0.25 g, 2.45 mmol) in toluene (2.5 mL) was added to the remaining polymerisation solution and ‘block’ copolymerisation allowed to proceed for 1 hour. The copolymerisation was terminated via the addition of acetic acid, and the copolymer precipitated into a large volume of methanol. The product was isolated by filtration and dried to a constant weight in vacuo.

5.2.7 NMR Measurements

^1H , ^{31}P , and ^{19}F NMR spectra were recorded at 298K on a Bruker Avance 400 spectrometer. The data were processed with Bruker’s TopSpin 3.5 or MestReNova software packages. ^{103}Rh NMR was acquired at 298K on a Bruker Avance IIIHD (600 MHz for ^1H) at 19.1 MHz using a commercial 5 mm triple resonance broadband probe (doubly tuned $^1\text{H}/^{31}\text{P}$ outer coil, with inner broadband coil) with 90° pulses of 27.5 μs and 18.4 μs for ^{103}Rh and ^{31}P respectively. ^{103}Rh chemical shifts, δ , are given in ppm relative to $\mathcal{E} = 3.186447^8$ and derived indirectly from the ^{31}P - ^{103}Rh HMQC experiments by four pulse ^{31}P - ^{103}Rh HMQC experiments with ^{103}Rh and ^1H decoupling during acquisition. The transmitter frequency offset and t_1 increments were varied to ensure that no signals were folded. Exponential line broadening of 10 Hz was applied to 1D ^{103}Rh data, with 2D data zero filled, Gaussian broadened by 10 Hz and treated with spine-squared window function during processing. Coupling constants reported herein are given as absolute values but are likely to be negative in sign for $^1J_{\text{Rh-P}}$.⁹

5.2.8 Crystallography

A suitable crystal, $0.25 \times 0.17 \times 0.10 \text{ mm}^3$, was selected and mounted on a support on an XtaLAB Synergy, Single source at home/near, HyPix diffractometer. The crystal was kept at a steady $T = 120.01(10) \text{ K}$ during data collection. The structure was solved with the ShelXT structure solution program using the Intrinsic Phasing solution method and by using Olex² as the graphical interface. The model was refined with version 2018/3 of ShelXL using Least Squares minimisation.

Crystal data for Rh(I)(tfb)(Biphenyl)(P(4-FC₆H₄)₃): C₄₂H₂₇F₇PRh, $M_r = 798.51$, monoclinic, $C2/c$ (No. 15), $a = 26.3019(3) \text{ \AA}$, $b = 10.31750(10) \text{ \AA}$, $c = 25.1310(4) \text{ \AA}$, $\beta = 94.7320(10)^\circ$, $\alpha = \gamma = 90^\circ$, $V = 6796.55(15) \text{ \AA}^3$, $T = 120.01(10) \text{ K}$, $Z = 8$, $Z' = 1$, $\mu(\text{CuK}\alpha) = 5.115$, 60027 reflections measured, 6909 unique ($R_{int} = 0.0921$) which were used in all calculations. The final wR_2 was 0.1489 (all data) and R_I was 0.0490 ($I > 2(I)$).

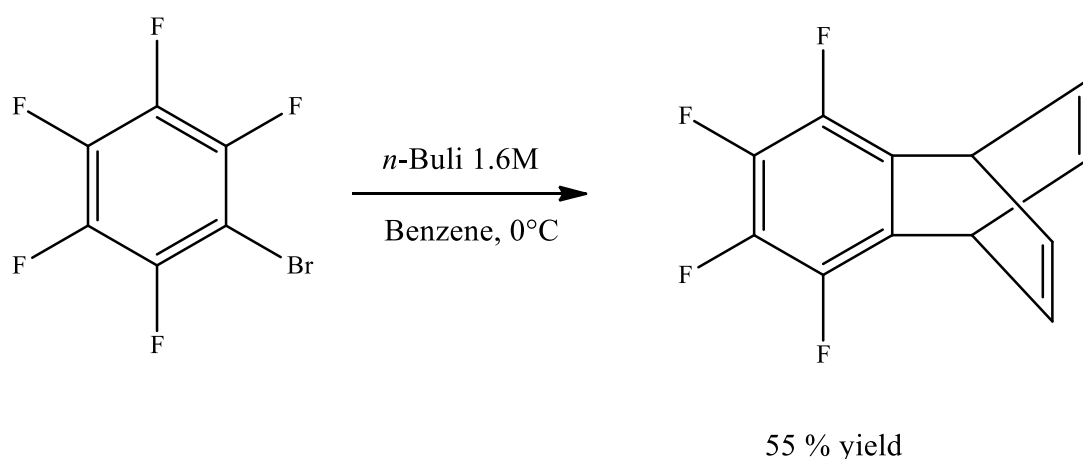
5.2.9 Size Exclusion Chromatography (SEC)

SEC was performed on a Shimadzu modular system consisting of a $4.0 \text{ mm} \times 3.0 \text{ mm}$ Phenomenex Security GuardTM Cartridge guard column and two linear phenogel columns (10^3 and 10^4 \AA pore size) in tetrahydrofuran (THF) operating at a flow rate of 1.0 mL/min and $40 \text{ }^\circ\text{C}$ using a RID-20A refractive index detector, a SPD-M20A prominence diode array detector and a miniDAWN TREOS multi-angle static light scattering (MALLS) detector. The system was calibrated with a series of narrow molecular weight distribution polystyrene standards with molecular weights ranging from 0.27 to 66 kg mol^{-1} . Chromatograms were analysed by Lab Solutions SEC software.

5.3 Results and Discussion

5.3.1 Synthesis of Dimer Complex $[\text{Rh}(\text{tfb})\text{Cl}]_2$

Tetrafluorobenzobarrelene was synthesised following the literature procedure outlined in Scheme 5-1.^{5, 6} The reaction between pentafluorobromobenzene and *n*-butyllithium 1.6 M at 0 °C leads to the formation of pentafluorophenyllithium, a thermally unstable compound,⁵ which then reacts, yielding a highly reactive intermediate, tetrafluorobenzynes through the elimination of lithium fluoride. This intermediate then reacts additively with benzene in a [4+2] cycloaddition yielding tetrafluorobenzobarrelene (tfb).



Scheme 5-1. Reaction of pentafluorobromobenzene with *n*-BuLi 1.6M in benzene to afford tetrafluorobenzobarrelene (tfb).

Regarding the isolation and purification of the target compound, the literature procedure described by Tomlinson *et al.*⁵ requires a significant amount of time to accomplish and resulted in significant yield loss due to the sticky nature of the crude product. On the other hand, the method of Brewers *et al.*⁶ was relatively faster but resulted in lower purity product. A modified approach was developed for the

purification of this volatile compound by a selective combination of Brewers and Tomlinson reported procedures.

In the final stages of purification, the benzene solvent was removed by evaporation *in vacuo*, leaving an orange residue. This was followed by extraction of the residue with hexanes (repeated 5 to 6 times), and filtering through activated neutral alumina (activity I). The solvent from the filtrate was removed via rotary evaporation which afforded faint yellow-tinged crystals. The yellow colouring is associated with reaction side products, which were identified as 2,2',3,3',4,4',5,5'6-nonafluorobiphenyl.^{5, 6} Finally, the separation of the target compound from the impurities was achieved by sublimation using the Tomlinson method, with a cold finger setup. The target compound was isolated when heated *in vacuo* at 60 °C, leaving behind the yellow oily residue. This increases the final yield to 75 % from the reported 50 - 55 % yields and a reduction in synthesis time.

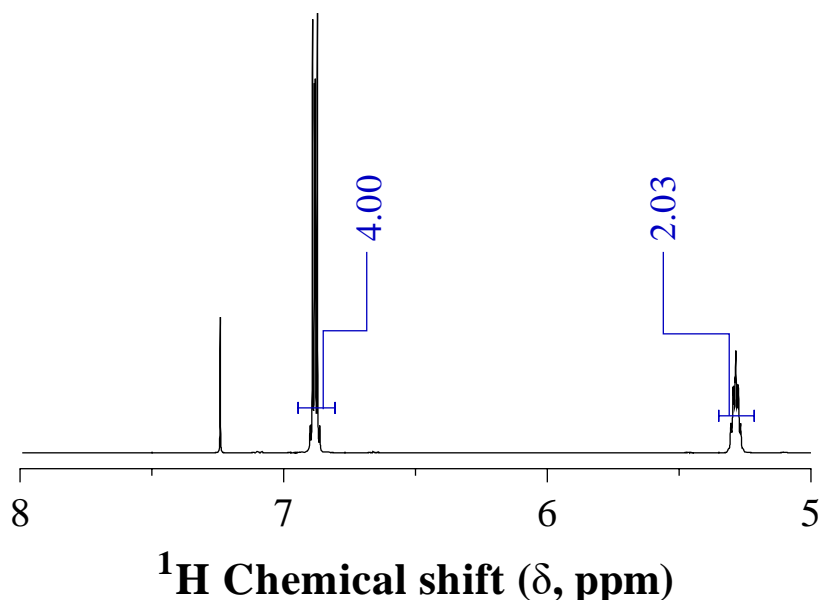


Figure 5-2. ¹H NMR spectrum recorded in CDCl₃ for purified tfb ligand with measured integral values given in blue.

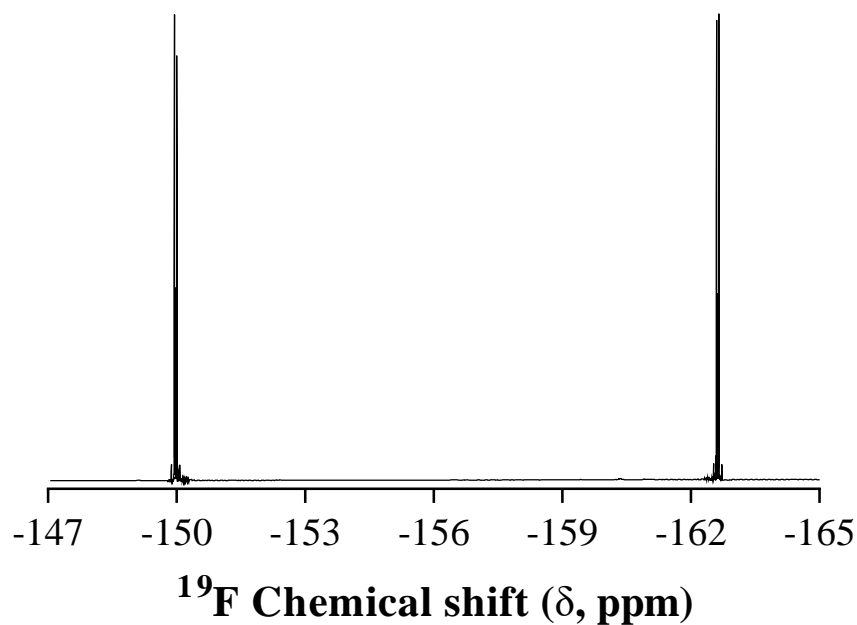


Figure 5-3. ^{19}F NMR spectrum of purified tfb ligand in CDCl_3 .

The ^1H NMR spectra, Figure 5-2, shows two sets of signals, doublets of doublets attributed to the olefinic protons and triplets of triplets of triplets associated with the methine protons, at $\delta = 6.88$ and 5.29 ppm respectively. The ^{19}F NMR spectra, Figure 5-3, shows four pairs of doublets at $\delta = -149.96$, -150.00 , -162.61 and -162.65 ppm. All signals integrate to the expected ratio, confirming the structure.

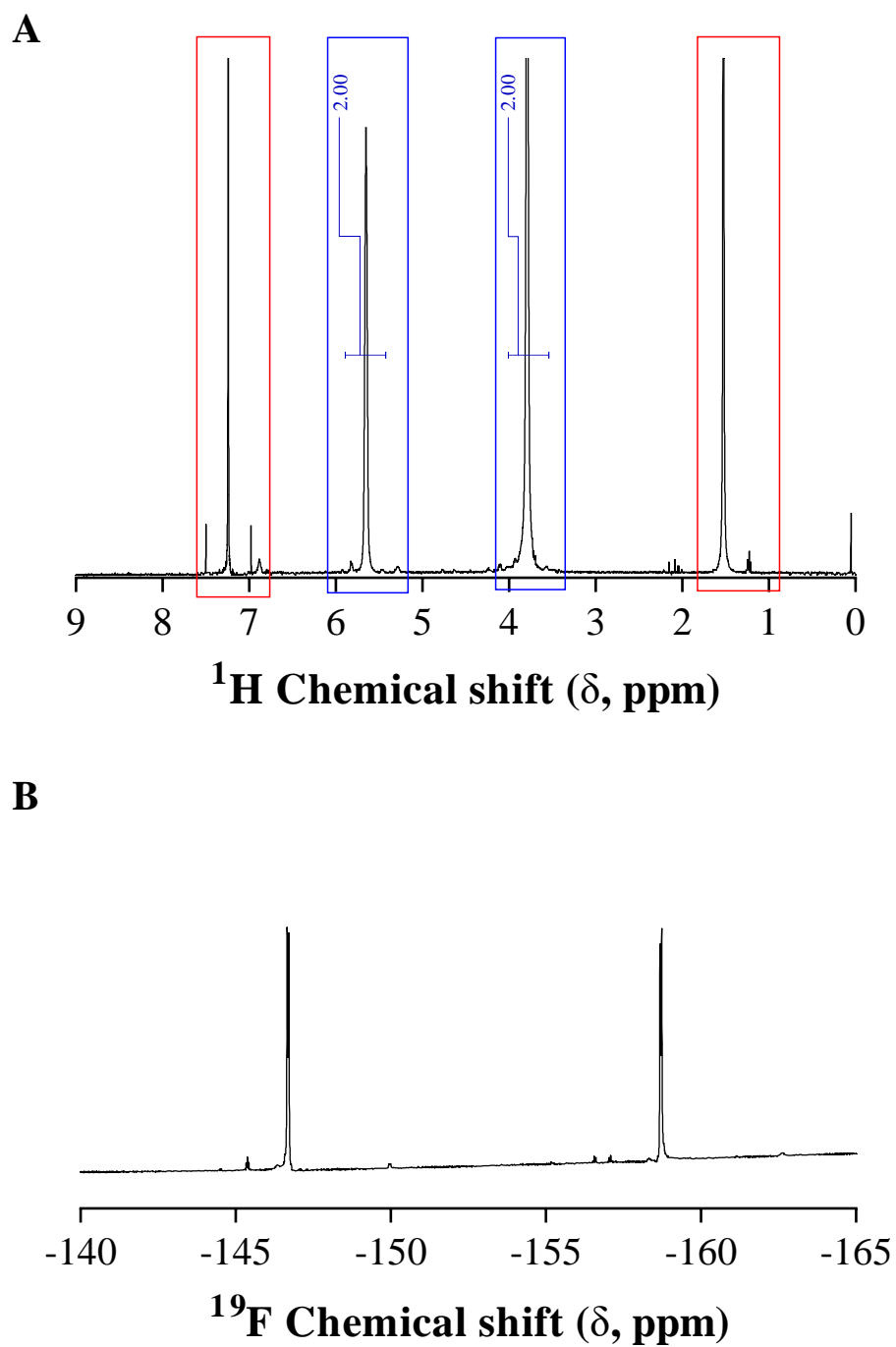
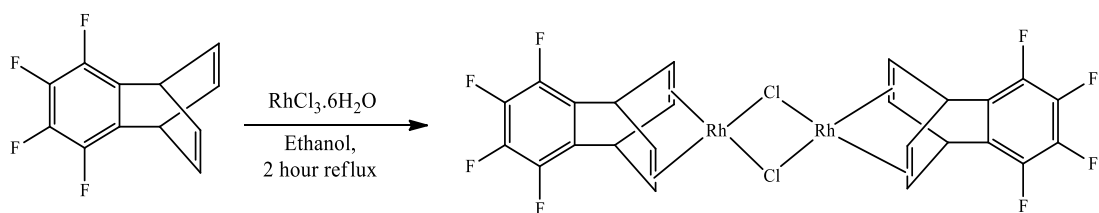


Figure 5-4. (A) ^1H NMR spectrum of $[\text{Rh}(\text{tfb})\text{Cl}]_2$ in CDCl_3 ; (B) ^{19}F NMR spectrum of $[\text{Rh}(\text{tfb})\text{Cl}]_2$ in CDCl_3 . Relevant peaks highlighted in blue boxes with measured integral values. Two intense peaks at $\delta = 7.26$ and 1.56 ppm (indicated with red boxes) are CHCl_3 and HDO respectively.

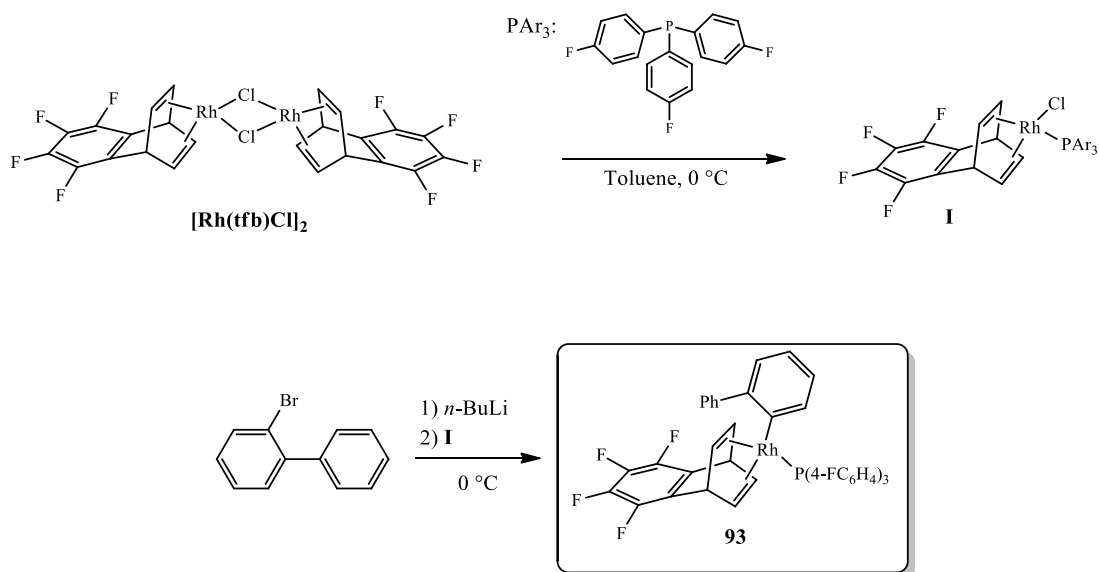


Scheme 5-2. Synthetic pathway employed for the preparation of the Rh dimer $[\text{Rh}(\text{tfb})\text{Cl}]_2$.

With the purified tfb ligand available, the next step in the synthesis was the preparation of the bridged Rh dimer, $[\text{Rh}(\text{tfb})\text{Cl}]_2$. The synthetic pathway adopted, Scheme 5-2, follows a previously reported procedure.⁴ $[\text{Rh}(\text{tfb})\text{Cl}]_2$ was readily prepared by refluxing tfb and $\text{RhCl}_3 \cdot 6\text{H}_2\text{O}$ in ethanol and water for 2 hours, before filtering the yellow precipitate, washing it with methanol and recrystallising it from CH_2Cl_2 and methanol.

Spectroscopic characterisation by ^1H NMR showed two set of singlets, Figure 5-4A, at $\delta = 5.65$ and 3.79 ppm, stemming from the olefinic and methine protons respectively. The ^{19}F NMR spectrum, Figure 5-4B reveals two sets of multiplets at $\delta = -147.18$ and -159.44 ppm. All signals integrated to the expected ratio, and is consistent with previously reported values,⁴ confirming the structure.

5.3.2 Synthesis of Target Complex Rh(I)(tfb)(Biphenyl)(P(4-FC₆H₄)₃)



Scheme 5-3. Overview of the synthetic pathway adopted for the preparation of the target Rh complex $\text{Rh}(\text{I})(\text{tfb})(\text{Biphenyl})(\text{P}(\text{4-FC}_6\text{H}_4)_3)$.

The target complex, $\text{Rh}(\text{I})(\text{tfb})(\text{Biphenyl})(\text{P}(\text{4-FC}_6\text{H}_4)_3)$, was prepared according to Scheme 5-3. The reaction between $[\text{Rh}(\text{tfb})\text{Cl}]_2$ and *tris*(4-fluorophenyl)phosphine gave the intermediate, tetracoordinate, mononuclear species $\text{Rh}(\text{tfb})(\text{P}(\text{4-FC}_6\text{H}_4)_3)\text{Cl}$ (**I** Scheme 5-3). In the final step, *n*-butyllithium-mediated lithiation of 2-bromobiphenyl and subsequent reaction with **I** gave the target complex $\text{Rh}(\text{I})(\text{tfb})(\text{Biphenyl})(\text{P}(\text{4-FC}_6\text{H}_4)_3)$. The complex was isolated/purified via elution through a short plug, packed with neutral alumina as the stationary phase, and recrystallisation from CH_2Cl_2 /methanol using a solvent layering technique.

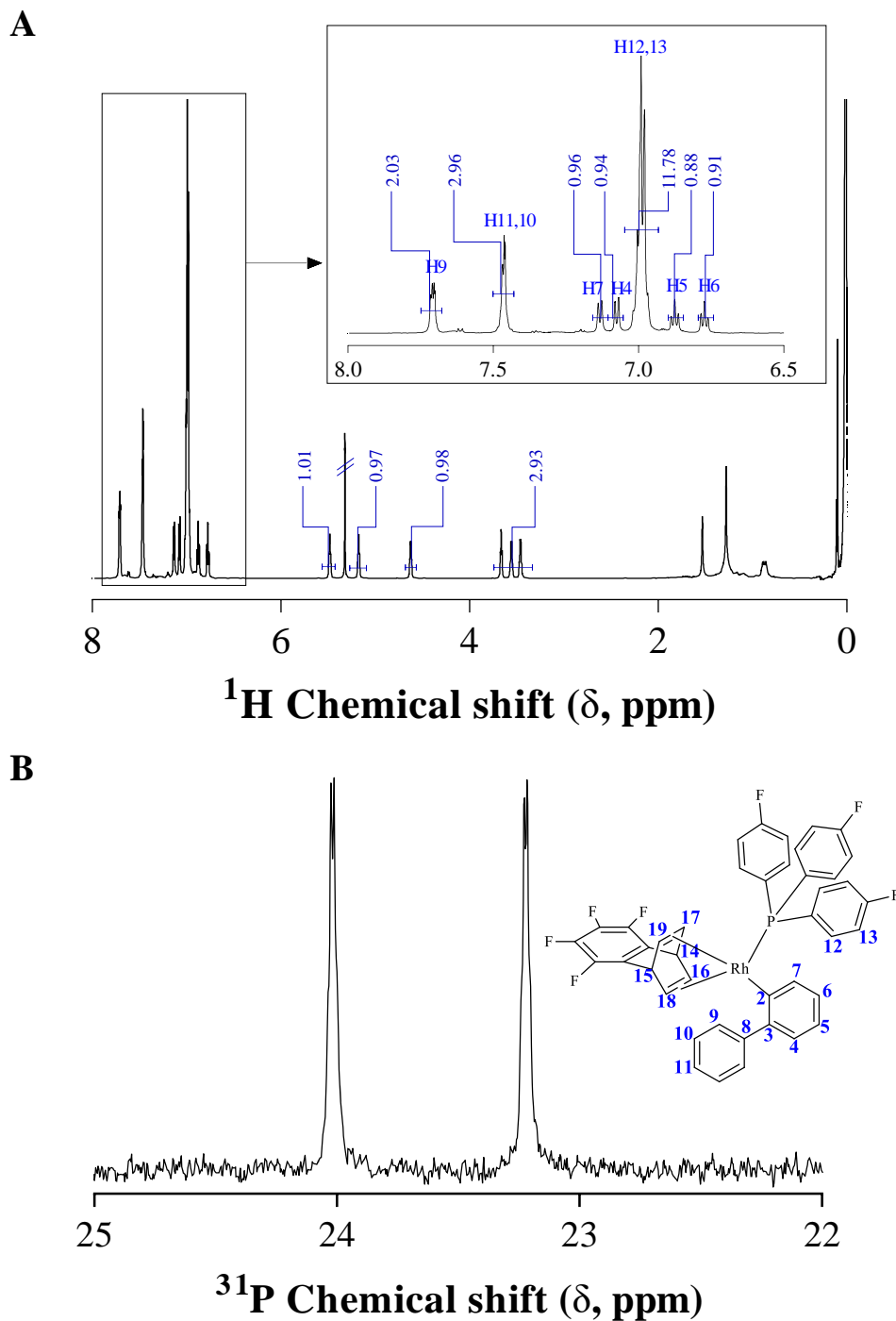


Figure 5-5. (A) ^1H NMR spectrum of $\text{Rh}(\text{I})(\text{tfb})(\text{Biphenyl})(\text{P}(4\text{-FC}_6\text{H}_4)_3)$ with the expanded aromatic region shown inset and measured integral values given in blue; (B) ^{31}P NMR spectrum of $\text{Rh}(\text{I})(\text{tfb})(\text{Biphenyl})(\text{P}(4\text{-FC}_6\text{H}_4)_3)$ showing a doublet of doublets around $\delta = 23.6$ ppm with $J_{\text{P-Rh}} = 193.4$ Hz.

Multinuclear NMR spectroscopy (^1H , ^{13}C , ^{19}F , ^{31}P , and various 2D techniques) were employed to characterise the recrystallised complex, **93**. Figure 5-5A shows the ^1H NMR spectrum of **93** recorded in CD_2Cl_2 ; an expansion of the aromatic region (plotted between $\delta = 6.5$ to 8.0 ppm) is shown inset. The splittings within the aromatic region are similar to **92** reported in Chapter 4; the multiplet around $\delta = 6.9$ to 7.0 ppm integrates to 12H which are associated with the phosphine ligand. The remaining signals within this region are attributed to the biphenyl functional group. The signals between $\delta = 3.0$ to 5.6 ppm are associated with the protons on the tfb ligand. All signals integrated to the expected ratio, confirming the structure.

The $^{31}\text{P}\{^1\text{H}\}$ NMR spectrum of **93** is shown in Figure 5-5B. A pair of doublets of multiplets is observed around $\delta = 23.6$ ppm with a corresponding $^1J_{\text{Rh-P}}$ value of 193.4 Hz. Both chemical shift and coupling constants of **93** are entirely consistent with previously reported values for **90** and **92**.

Figure 5-6 shows the ^{19}F NMR spectrum recorded in CD_2Cl_2 ; The singlet at $\delta = -110.1$ ppm is associated with the fluorine atoms on the phosphine ligand while the four pairs of doublets of doublets shown inset are associated with the fluorine atoms on the tfb ligand. The integrations for these signals are in the expected ratio, further confirming the structure.

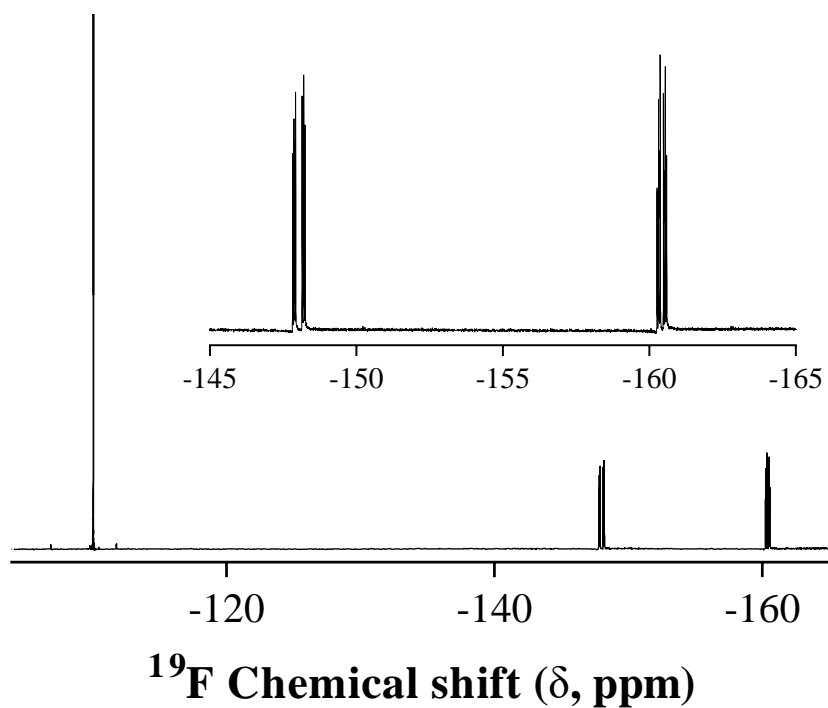


Figure 5-6. ¹⁹F NMR spectrum of Rh(I)(tfb)(Biphenyl)(P(4-FC₆H₄)₃), **93** with an expansion of the region from δ = -145 to -165 ppm shown inset.

The complex was subsequently characterised by a combination of single-crystal X-ray diffraction, ¹⁰³Rh and ³¹P-¹⁰³Rh heteronuclear multiple quantum coherence (HMQC) NMR spectroscopy and elemental analysis. Figure 5-7 shows the experimentally determined X-ray crystal structure of **93**, and its geometry is consistent with previously reported examples of structurally related rhodium(I)-vinyl and -aryl complexes **88b**, **88d**, **88e**, **90**, **91** and **92**.^{7, 10-12}

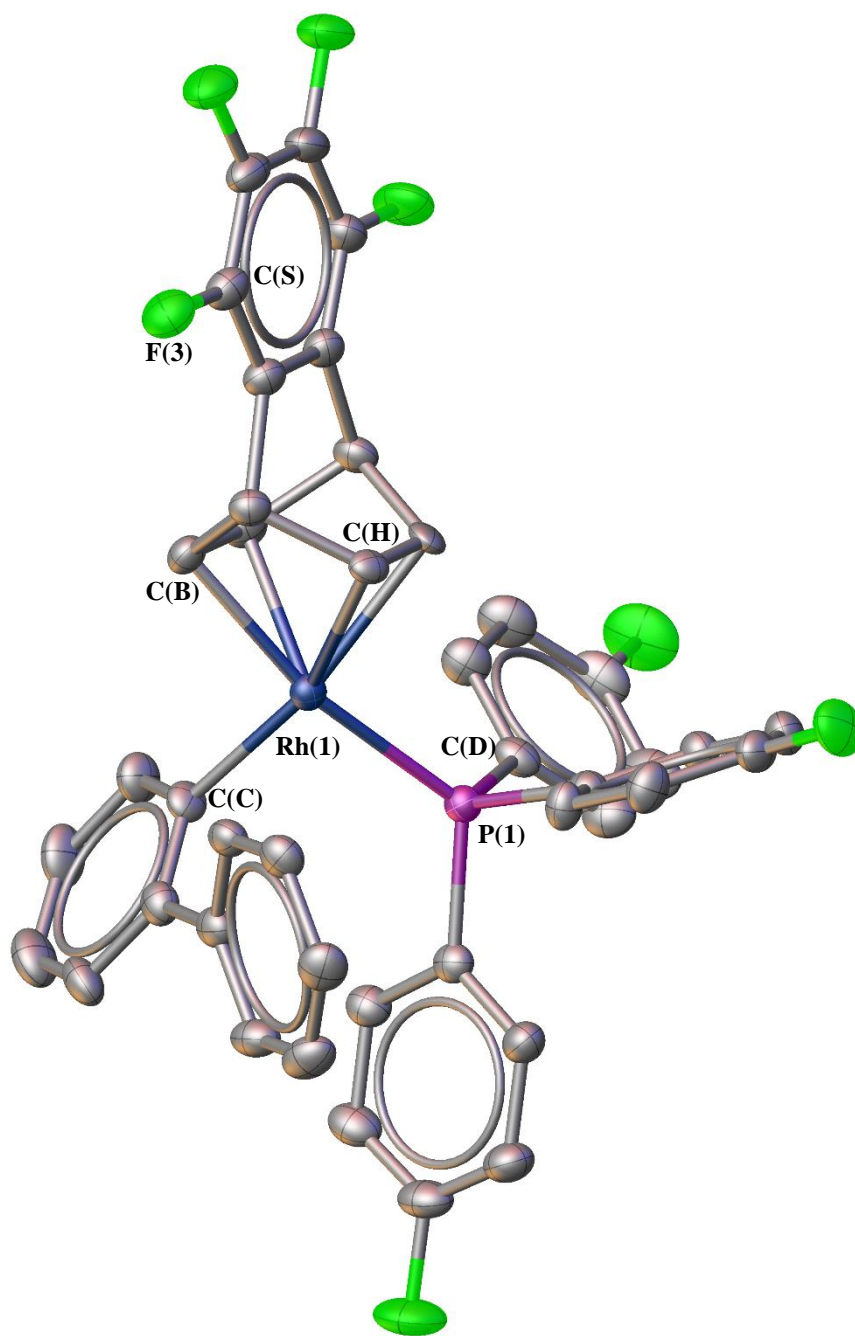


Figure 5-7. OLEX² representation of Rh(I)(tfb)(Biphenyl)(P(4-FC₆H₄)₃), **93**, at 50 % probability ellipsoids and H atoms omitted for clarity. Selected bond lengths (Å): Rh(1)-P(1), 2.323(10); Rh(1)-C(C), 2.093(4); Rh(1)-C(H), 2.236(4); P(1)-C(D), 1.822(5); C(S)-F(3), 1.353(6). Selected bond angles (deg): C(B)-Rh(1)-P(1), 166.19(12); C(H)-Rh(1)-P(1), 111.11(12); C(C)-Rh(1)-P(1), 91.23(13).

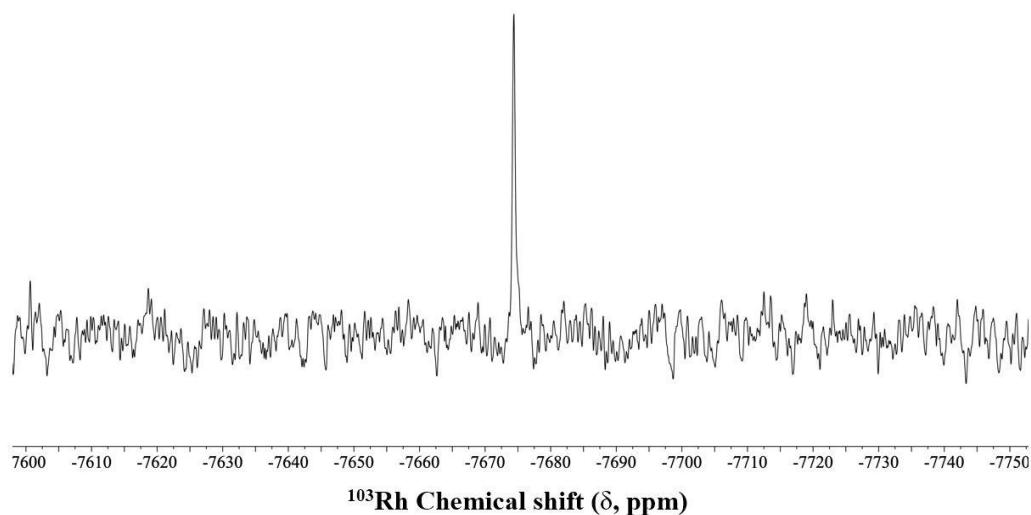


Figure 5-8. $^{103}\text{Rh}\{^1\text{H}\text{-}^{31}\text{P}\}$ NMR spectrum of $\text{Rh}(\text{I})(\text{tfb})(\text{Biphenyl})(\text{P}(4\text{-FC}_6\text{H}_4)_3)$, **93**, recorded in CD_2Cl_2 .

Figure 5-8 shows the $^{103}\text{Rh}\{^1\text{H}\text{-}^{31}\text{P}\}$ NMR spectrum of **93**; a singlet, centred around $\delta = -7674$ ppm (561 ppm if referenced to Rh metal), is observed. This is consistent with previously reported Rh(I) complexes reported in Chapter 2 (**88b**, **88d** and **88e**; $\delta = -7862, -7870, -7861$ ppm respectively; 372, 365 and 373 ppm respectively if reference to Rh metal), Chapter 3 (**90**, $\delta = -7688$ ppm; 547 ppm if reference to Rh metal) and Chapter 4 (**92**, $\delta = -7699$ ppm; 536 ppm if reference to Rh metal).

Figure 5-9 shows the complementary $^{31}\text{P}\text{-}^{103}\text{Rh}$ HMQC NMR spectrum of **93** which clearly indicates the presence of a single Rh and P species with direct coupling between the two nuclei, further confirming the purity and stability of complex **93** in solution.

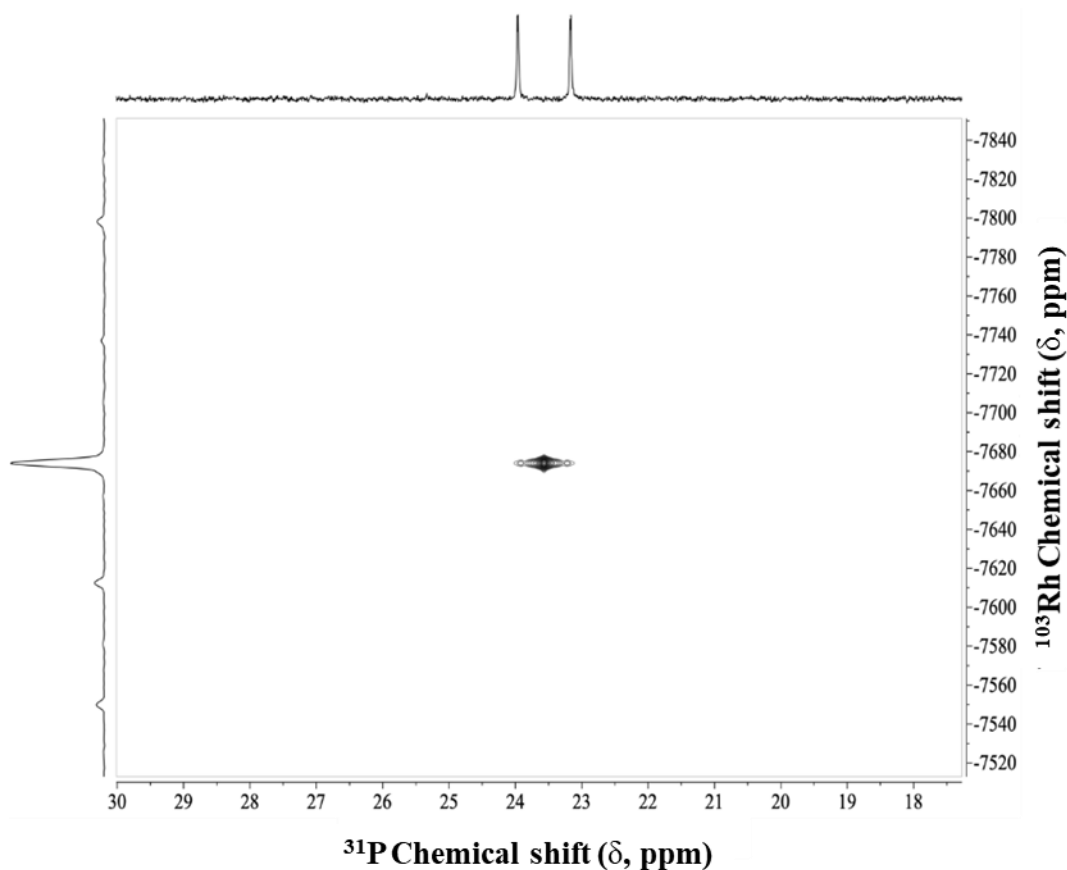


Figure 5-9. ^{31}P - ^{103}Rh HMQC NMR spectrum of $\text{Rh}(\text{I})(\text{tfb})(\text{Biphenyl})(\text{P}(4\text{-FC}_6\text{H}_4)_3)$, recorded in CD_2Cl_2 .

5.3.3 Polymerisation Studies

With **93** in-hand, its efficacy as an initiator in the controlled, stereospecific (co) polymerisation of phenylacetylene(s) was explored. Firstly, a control experiment was conducted in which phenylacetylene (PA) was homopolymerised for a target M_n of 10,000 in toluene at 30 °C in the absence of added free $\text{P}(4\text{-FC}_6\text{H}_4)_3$ (Table 5-1, entry 4). Under these conditions, polymerisation was very rapid reaching ca. 98 % conversion within 30 sec and yielded a homopolymer that eluted at the upper column limits of the SEC instrument, indicating an M_n in excess of 100,000 and a non-controlled polymerisation process. This is consistent with past observations made in

the previous chapters concerning the (co)polymerisation of phenylacetylene with complexes **88b**, **88d**, **88e**, **90**, and **92**, in the absence of free phosphine Figure 5-1.^{7, 10,}

¹² All further experiments were conducted in the presence of added free phosphine.

Table 5-1. Summary of homopolymerisations of PA (**M1**) with **93** conducted at 30 °C, in toluene.

Entry	Rh species	Monomers	[P]/[Rh]	M_n (SEC) ^b	Dispersity (\mathcal{D}) ^b	Rh initiation efficiency ^c	<i>cis</i> content (%) ^d
1	93	M1	5	12,800	1.31	0.78	92
2	93	M1	10	13,100	1.15	0.76	95
3	93	M1	20	10,400	1.15	0.96	99
4	93	M1	0	nd ^e	nd ^f	nd ^f	nd ^f

a. Target M_n is 10,000 which is calculated as $M_n = \text{mass (g) monomer/moles of } \mathbf{93}$ and assuming 100 % initiation efficiency.

b. As measured by size exclusion chromatography: eluent THF operated at a flow rate of 1.0 mL/min, instrument calibrated with narrow molecular weight distribution polystyrene standards. Dispersity (\mathcal{D}) = M_w/M_n .

c. Calculated from the ratio of theoretical to measured (SEC determined) M_n 's.

d. As determined by ¹H NMR spectroscopy according to C. I. Simionescu, V. Percec and S. Dumitrescu, *J. Polym. Sci., Part A: Polym. Chem.*, 1977, **15**, 2497-2509.

Initially, the initiating ability/efficiency of **93** was examined under the same conditions as those employed for the Masuda derivative, **78** (Table 5-1, entry 1).¹¹ The polymerisation proceeded smoothly with a calculated Rh IE of 0.78, yielding a highly stereoregular homopolymer (*cis* content of 92 %) and an SEC-measured M_n of 12,800, but with relatively high dispersity ($\mathcal{D} = 1.31$). At a [P]/[Rh] ratio (where [P] = P(4-FC₆H₄)₃) of 10, no improvement in IE was seen, but we note that the dispersity, \mathcal{D} , decreased from 1.31 to 1.15 (Table 5-1, entry 2). A significant improvement in the IE was observed after increasing the [P]/[Rh] ratio from 5 to 20 (Table 5-1, entry 3), and yielded a PA homopolymer with an SEC-measured M_n of 10,400 which corresponds

to an IE of 0.96. However, no further improvement with \mathcal{D} was observed. Furthermore, the *cis*-content of the resulting polyPA increased from 92 to 99 %. These observations are consistent with the previous Rh(I)-aryl complexes^{7, 12} whereby increasing the [P]/[Rh] ratio improved the polymerisation characteristics overall, leading to better control, albeit at the expense of polymerisation rate.

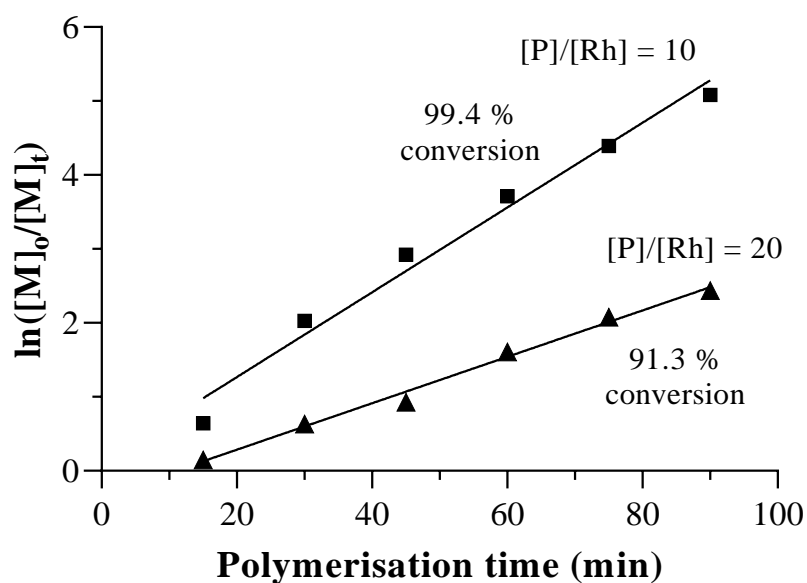


Figure 5-10. Pseudo first-order kinetic plots for the homopolymerisation of PA in toluene at 30 °C with [P]/[Rh] = 10 and 20.

The pseudo-first-order kinetic plots for the homopolymerisation of PA with **93** in toluene at 30 °C at [P]/[Rh] = 10 and 20 are shown in Figure 5-10. As anticipated, the homopolymerisation at [P]/[Rh] = 10 ($k_{app} = 0.600 \text{ min}^{-1}$) proceeded rapidly compared to [P]/[Rh] = 20 ($k_{app} = 0.300 \text{ min}^{-1}$) with a doubling of the polymerisation rate being observed. This is not surprising, as noted in previous chapters, increasing free phosphine concentration results in a decrease in the rate of polymerisation. A short induction period of ca. 10 min for [P]/[Rh] = 20 was observed while for [P]/[Rh] = 10,

there was no observable induction period. Both the kinetic plots are linear, indicating a constant number of active species.

Table 5-2 shows the k_{app} values of the previous Rh(I)-aryl complexes, **90** and **92** bearing an nbd diene ligand and the current Rh(I)-aryl complex, **93**, bearing a tfb diene ligand under otherwise identical conditions for the homopolymerisation of PA. The k_{app} of the polymerisation mediated by **93** was at least ca. 6 times greater than **92** and 16 times higher than **90**, highlighting the increased activity of **93** versus **92** and **90**, Figure 5-1. These results are consistent with reports by Saeed *et al.*³ regarding **82**, Figure 5-1, in which substitution of the nbd diene ligand with the tfb diene ligand to a significantly higher activity than the former, a feature that was attributed to the high π -acidity of the tfb diene ligand.

Table 5-2. The apparent rate constant of propagation, k_{app} and calculated initiation efficiencies, for homopolymerisations of PA mediated by Rh(I)-aryl complexes reported in Chapter 3 and 4 compared to, Rh(I)(tfb)(Biphenyl)(P(4-FC₆H₄)₃), **93**.

Rh species	[P]/[Rh]	k_{app} (min ⁻¹)	Rh initiation efficiency (IE)	Dispersity (\bar{D})
90	10	0.0374	0.82	1.11
92	10	0.0720	0.89	1.18
93	10	0.6000	0.77	1.15
90	20	0.0228	0.85	1.09
92	20	0.0480	0.98	1.11
93	20	0.3000	0.96	1.20

According to the Dewar-Chart-Duncanson model,¹³ the highest occupied molecular orbital (HOMO) of the alkene (diene in the case of tfb), a filled π -orbital,

donates electron density through σ -donation to the metal d-orbital; the metal then donates electron density back from a filled metal d-orbital into the lowest unoccupied molecular orbital (LUMO), a vacant π^* orbital.¹⁴⁻¹⁶ This back-donation results in a decreased electron density around the metal centre, increasing its electrophilic character, and facilitating more facile coordination of the nucleophilic monomer to the rhodium centre.⁴

Further evidence of the strength of the π -acidity of the tfb diene ligand is seen by observing the chemical shift of the olefinic protons of this species. A higher π -acidity ligand results in an upfield chemical shift of the olefinic proton signals. The chemical shift of the olefinic proton of free tfb ligand is $\delta = 6.88$ ppm, Figure 5-2. Upon formation of the target complex, **93**, this signal shifted substantially to $\delta = 3.45$ ppm, Figure 5-5, a difference, $\Delta\delta$, of 3.43 ppm. This is indicative of increased shielding of the olefinic proton as a result of increased backbonding that reduces the π -character of the C=C double bond.¹⁷

A comparison of the calculated IEs and dispersities with the reported values for complexes discussed in Chapter 3, **90**, Figure 5-1, and Chapter 4, **92**, Figure 5-1, are given in Table 5-2. The highest IEs of Rh(I)-aryl complex **93**, Figure 5-1, were typically seen when the $[P]/[Rh] = 20$, however, we note that it is marginally lower than the structurally similar **92**, Figure 5-1, with the latter exhibiting an IE of 0.98. The slightly lower than expected IEs for **93** could be attributed to the significantly higher activity towards PA compared to **92**, resulting in a higher propagation rate in comparison to the initiation rate. We note that quantitative initiation efficiency is not a formal prerequisite for a polymerisation to be accurately term controlled.

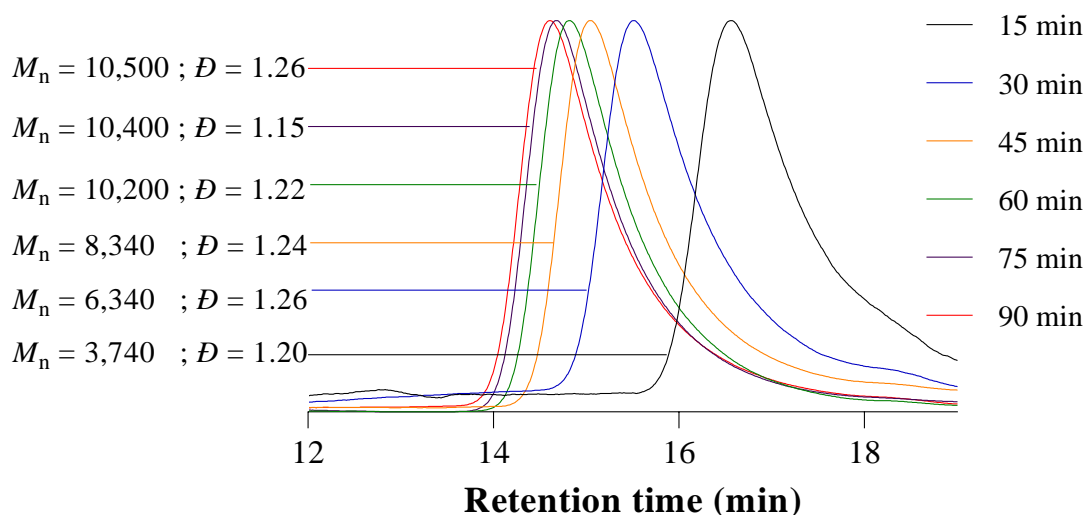


Figure 5-11. Normalised SEC traces showing the evolution of the molecular weight in the homopolymerisation of PA for a target molecular weight of 10,000 and at $[P]/[Rh] = 20$.

Figure 5-11 shows the normalised SEC traces for the aliquots withdrawn from a PA homopolymerisation with **93** with $[P]/[Rh] = 20$ in toluene at 30 °C. All traces are unimodal, with a systematic shift to lower retention time with increasing conversion. No significant change in dispersity, D , was observed, with increasing conversion and D s averaging ca. 1.22. While these D values are not as low as those previously discussed in Chapter 4 for complex **92** ($D = 1.16$), there are certainly acceptable.

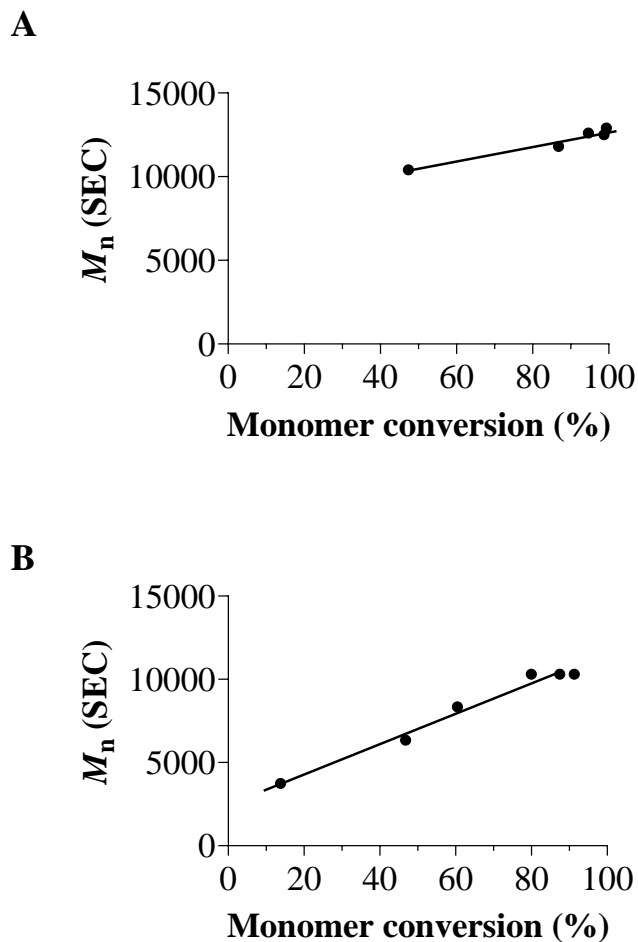


Figure 5-12. M_n vs conversions plots for homopolymerisation of PA at (A) $[P]/[Rh] = 10$; and (B) $[P]/[Rh] = 20$.

Figure 5-12 shows the M_n vs conversion plots for polymerisations of PA conducted with $[P]/[Rh] = 10$ and 20. It can be seen in Figure 5-12A, the plot exhibited non-linearity before 50 % monomer conversions, suggesting non-controlled processes are occurring at lower conversions. When the $[P]/[Rh]$ ratio was increased from 10 to 20, the M_n increased with monomer conversion, exhibiting linearity up to near-quantitative conversion, suggesting increased control over the polymerisation.

A distinguishing feature of controlled polymerisation processes is the ability to prepare block (co)polymers, or more advanced polymer architectures, by sequential

monomer addition. Successful blocking, ideally with quantitative crossover efficiency, confirms retention of active chain ends. Firstly, to demonstrate this ability, a self-blocking experiment was performed in which PA was initially homopolymerised in toluene at 30 °C in the presence of **90** and 20 equivalents of free phosphine, P(4-FC-₆H₄)₃.

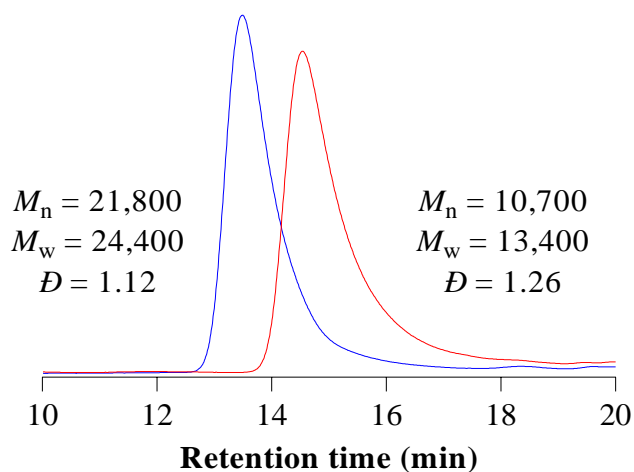


Figure 5-13. SEC-traces for a self-blocking homopolymerisation of PA demonstrating retention of active chain ends.

After 90 minutes, an aliquot was withdrawn and analysed by SEC, Figure 5-13, with the formed PPA having a measured M_n of 10,700 (calculated IE of 0.93) and a corresponding D of 1.26. Then, a second charge of PA was added to the reaction mixture, and the polymerisation was allowed to proceed for another 90 minutes. The polymerisation was quenched with acetic acid and isolated by precipitation in an excess methanol, yielding an orange polymer sample with an SEC-measured M_n of 21,800 and a corresponding D of 1.12. As seen in Figure 5-13, a clear shift in the chromatogram to lower retention time (higher molecular weight) was observed after the addition and polymerisation of the second batch of monomer with little to no

evidence of residual homopolymer ‘impurity’ confirming the retention of chain-end activity after the initial PA homopolymerisation and quantitative crossover efficiency.

Figure 5-14 shows the ^1H NMR spectrum, recorded in CDCl_3 , of the isolated PPA showing a sharp singlet at $\delta = 5.85$ ppm coupled with two sharp resonances at $\delta = 7.0$ to 6.5 ppm indicative of a highly stereoregular structure with, in this instance, a calculated *cis* content of 98 %. This is entirely consistent with previous reports in which the presence of *trans* protons results in a significant broadening in the aromatic region.¹⁸

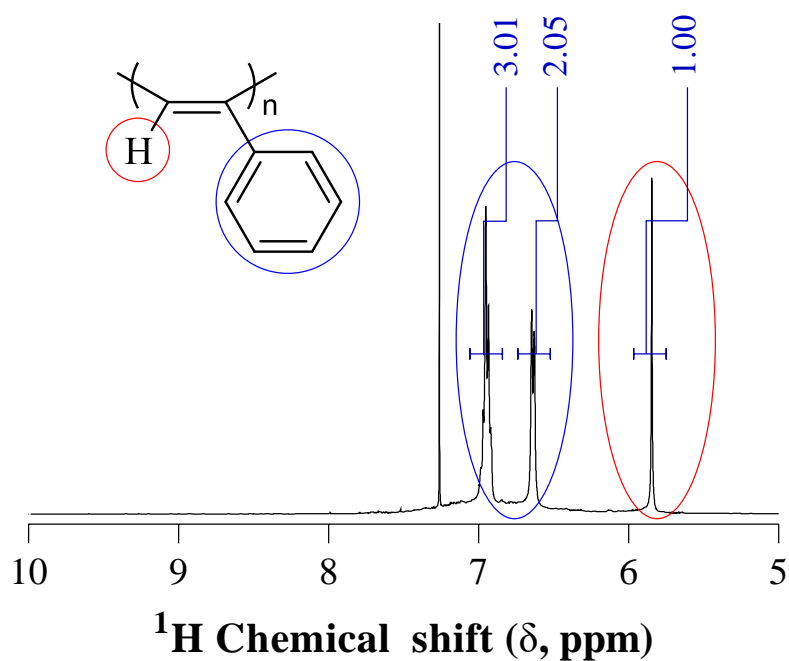


Figure 5-14. ^1H NMR spectrum recorded in CDCl_3 , of a self-block (co)polymer highlighting the *cis-transoidal* stereoregular structure as evidenced by a sharp singlet at $\delta = 6.19$ ppm that is attributed to the proton on the backbone of the polymer in a *cis* conformation. Measured integral values given in blue.

Collectively, the ability to prepare a 'block' copolymer and the kinetic data suggests that **93** mediates the stereospecific controlled polymerisation of PA at $[P]/[Rh] = 20$, in a controlled manner.

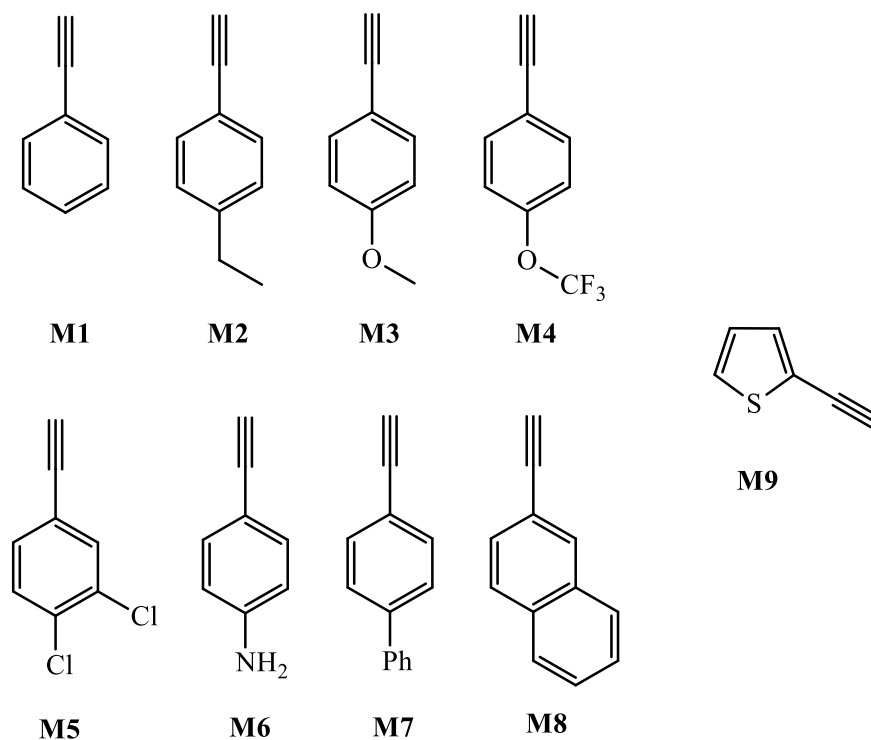


Figure 5-15. Phenylacetylene (**M1**), 1-ethyl-4-ethynylbenzene (**M2**), 4-ethynylanisole (**M3**), 4-(trifluoromethoxy)phenylacetylene (**M4**), 3,4-dichlorophenylacetylene (**M5**), 4-ethynylaniline (**M6**), 4-ethynylbiphenyl (**M7**), 4-ethynyl-naphthalene (**M8**) and 2-ethynylthiophene (**M9**).

The activity of Rh(I)-based complexes bearing a tfb diene ligand remains relatively unexplored even though the activity of such complexes towards PA (co)polymerisation represents amongst the highest recorded in this target application.¹⁹ The activity of **93** in the homopolymerisation of other functional substrates was subsequently investigated, see Table 5-2 with a summary of the polymerisation conditions, k_{app} , M_n , M_w , and \mathcal{D} . The homopolymerisations of functional substrates listed in Figure 5-15 will be detailed herein.

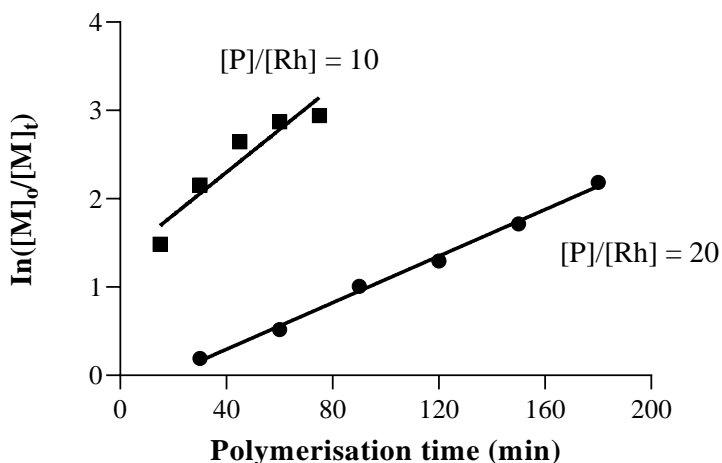


Figure 5-16 Normalised SEC traces of the evolution of molecular weight distribution in the homopolymerisation of **M2** for a target molecular weight of 10,000 with $[P]/[Rh] = 20$.

Figure 5-16A shows the pseudo first-order kinetic plot for the homopolymerisation of 1-ethyl-4-ethynylbenzene, **M2**, in toluene at 30 °C with $[P]/[Rh] = 20$ and 10. Expectedly, the homopolymerisation at $[P]/[Rh] = 10$ (Table 5-3, entry 3) proceeded faster than $[P]/[Rh] = 20$ (Table 5-3, entry 4) and, in both instances, the calculated IEs were near-quantitative, however, the final products had broad MWD at both ratios ($\mathcal{D} = 1.49$). The measured *cis* content showed an improvement from 85 % ($[P]/[Rh] = 10$) to 89 % ($[P]/[Rh] = 20$).

Of all the functional arylacetylenes, the homopolymerisation of **M3** by **93** was the least controlled, with the resulting polymer having an SEC-measured M_n of 9,710 and a very broad molecular weight distribution ($\mathcal{D} = 1.57$) (Table 5-3, entry 5). The pseudo-first-order kinetic plot for the homopolymerisation of **M3** was shown to be linear up to ca. 80 mins, Figure 5-11, but then drops off at the end. This suggest loss of active species, which might account for large \mathcal{D} s observed for the isolated poly(**M3**).

Table 5-3. Summary of homopolymerisations of mono-substituted acetylenes with **93** conducted at 30 °C

Entry	Rh species	Monomers	[P]/[Rh]	Polym. solvent	Theoretical MW ^a	M_n (SEC) ^b	M_w (SEC) ^b	Dispersity (\mathcal{D}) ^b	k_{app} (min ⁻¹)	<i>cis</i> content (%) ^d
1	93	M1	10	Toluene	10,000	13,100	15,000	1.15	0.6000	95
2	93	M1	20	Toluene	10,000	10,370	12,000	1.15	0.3000	99
3	93	M2	10	Toluene	10,000	9,950	14,800	1.49	0.0240	85
4	93	M2	20	Toluene	10,000	10,500	15,800	1.49	0.0132	89
5	93	M3	10	Toluene	10,000	9,710	15,200	1.57	0.0252	97
6	93	M4	10	Toluene	10,000	10,700	11,700	1.09	0.0180	84
7	93	M4	20	Toluene	10,000	8,500	9,100	1.07	0.0084	88
8	93	M5	10	Toluene	10,000	8,530	9,766	1.14	0.0252	84
9	93	M5	20	Toluene	10,000	8,502	9,105	1.07	0.0096	87
10	93	M6	0	Toluene	10,000	nd ^e	nd ^e	nd ^e	nd ^e	nd ^e
11	93	M7	20	Toluene	10,000	insoluble	insoluble	insoluble	insoluble	insoluble
12	93	M8	20	Toluene	10,000	insoluble	insoluble	insoluble	insoluble	insoluble
13	93	M9	10	Toluene	10,000	nd ^e	nd ^e	nd ^e	nd ^e	nd ^e

a. Target M_n is 10,000 which is calculated as $M_n = \text{mass (g) monomer/moles of } \mathbf{93}$ and assuming 100 % initiation efficiency.

b. As measured by size exclusion chromatography: eluent THF operated at a flow rate of 1.0 mL/min, instrument calibrated with narrow molecular weight distribution polystyrene standards. Dispersity (\mathcal{D}) = M_w/M_n

c. Calculated from the ratio of theoretical to measured (SEC determined) M_n 's.

d. As determined by ¹H NMR spectroscopy using a modified approach based on Simonionescu, Percec and Dumitrescu method.²⁰

e. Not determined.

An examination of the M_n vs monomer conversion plot shows an initial increase in M_n followed by a significant decrease before another increase, indicative of undesirable chain-transfer events. The same trend was observed with the SEC data, which clearly indicates a non-controlled process with the dispersity reaching 1.40 after only 15 min and then increasing to 1.66 before finally reaching a final measured value of 1.57. These observations are in contrast to those of Kishimoto *et al.*²¹ who reported that **M3** could be effectively be homopolymerized with 97 % monomer conversion yielded an isolated homopolymer with $\bar{D} = 1.25$ with $\text{Rh}(\text{C}\equiv\text{CC}_6\text{H}_5)(\text{nb})[\text{P}(\text{C}_6\text{H}_5)_3]_2$ (where nb = 2,5-norbornadiene).

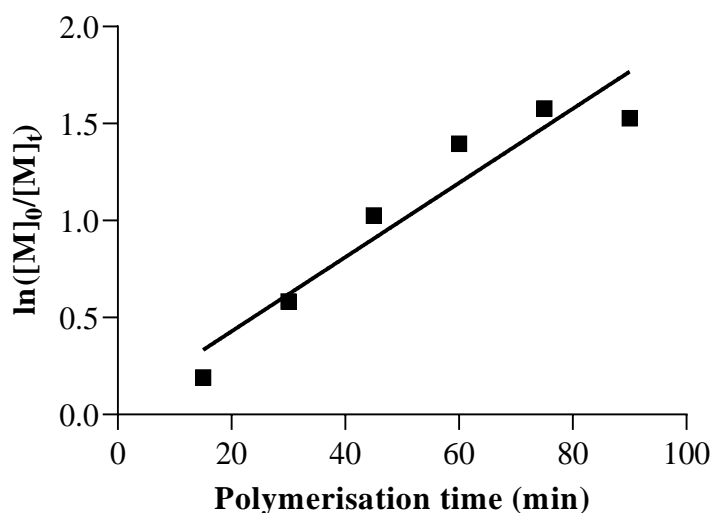


Figure 5-17. Pseudo-first order kinetic plot of homopolymerisation of **M3** in toluene at 30 °C with $[\text{P}]/[\text{Rh}] = 10$.

Surprisingly, the *cis* content was estimated to be 97 % as it can be seen in Figure 5-18A, which shows the ^1H NMR spectrum of the isolated poly(**M3**), recorded in C_6D_6 . The spectrum reveals sharp, distinctive and well-resolved signals, indicative of the stereoregular nature of the poly(**M3**). It was subsequently found that solvent had

a significant effect on the poly(**M3**) stereoisomerism. Poly(**M3**) dissolved in CDCl_3 , Figure 5-18**B**, led to broad signals with a much lower *cis* content.

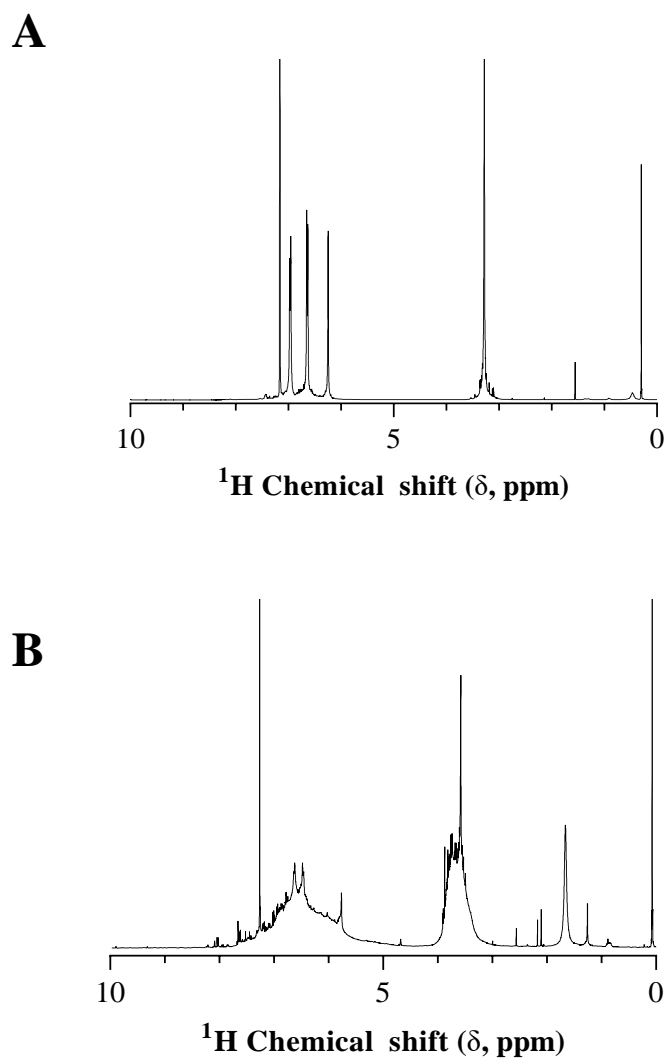


Figure 5-18. ^1H NMR spectrum of poly(4-ethynylansiole), poly(**M3**), (A) recorded in C_6D_6 ; (B) recorded in CDCl_3 .

It should be noted the colour of dissolved poly(**M3**) was dark green in CDCl_3 , whereas in C_6D_6 , the colour was light orange which is consistent with the colour of dissolved PPA and other substituted arylacetylene polymer samples. This observation

suggests that there is solvent-induced change in the backbone geometry of poly(**M3**), and it may have affected data collection, which invariably leads to poor results. Regardless, the current data for the homopolymerisation of **M3**, mediated by **93**, suggest that it is of the uncontrolled nature.

Interestingly, the fluorinated analogue of **M3**, 4-trifluoromethoxyphenylacetylene, **M4**, polymerised with many of the hallmark characteristics of a controlled polymerisation (Table 5-3, entry 6 and 7). For example, Figure 5-19A shows the pseudo-first-order kinetic plots for homopolymerisations in toluene at 30 °C with $[P]/[Rh] = 10$ and 20. The kinetic plots are essentially linear with the polymerisation at $[P]/[Rh] = 10$ proceeding more rapidly. In both cases, a short induction period is observed which is not an uncommon feature of these polymerisations, especially with higher $[P]/[Rh]$ ratios.

A representative series of SEC traces for PA homopolymerisation at $[P]/[Rh] = 10$ with target molecular weight of 10,000 is shown in Figure 5-19B. The SEC traces show a systematic shift to higher molecular weight with decreasing D_s , with the final product having an SEC-measured M_n of 10,700, corresponding IE of 0.93, and D of 1.09. Consistent with the other substituted arylacetylene monomers, **M4** polymerises to give highly stereoregular, *cis* rich poly(**M4**). This is highlighted in the 1H NMR spectrum of poly(**M4**), recorded in $CDCl_3$, Figure 5-20A, which shows a well-defined *cis* proton signal at $\delta = 5.96$ ppm. Similarly, in Figure 5-20B, the ^{19}F NMR spectrum, recorded in $CDCl_3$, displayed a clear distinct signal. While not as stereoregular as PPA homopolymers, the calculated *cis* content for poly(**M4**) was still high at 84 %.

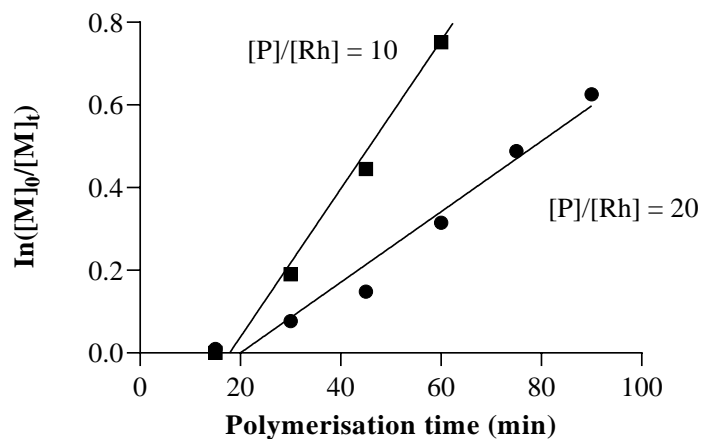
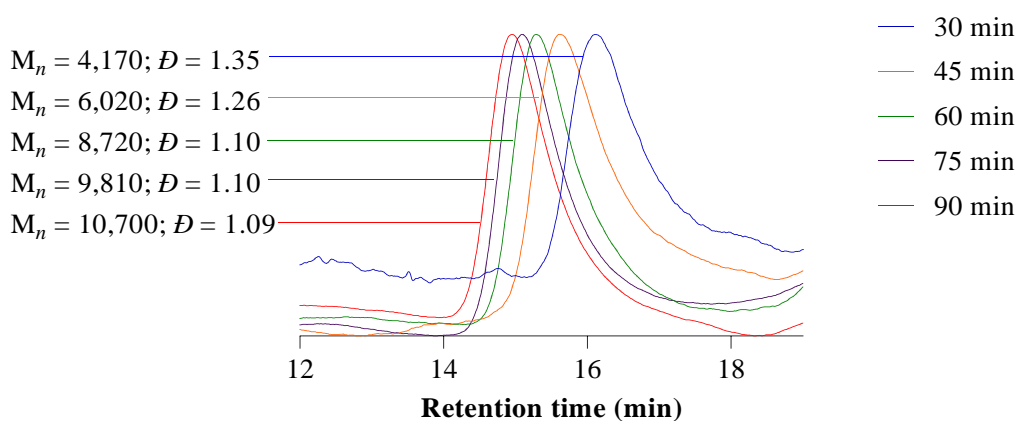
A**B**

Figure 5-19. (A) Pseudo-first order kinetic plots for homopolymerisation of **M4** with $[P]/[Rh] = 10$ and 20; (B) a series of SEC traces for the homopolymerisation of **M4** at $[P]/[Rh] = 10$.

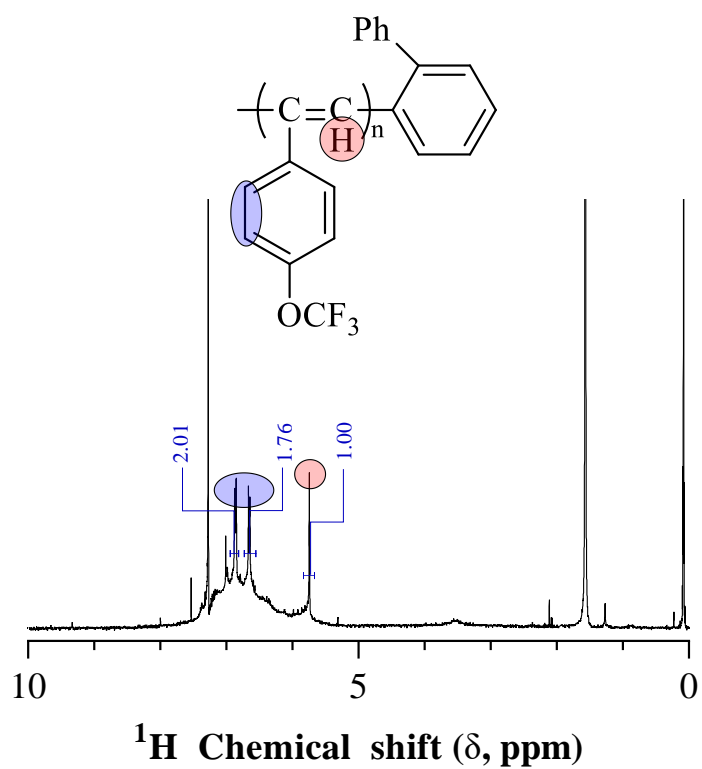
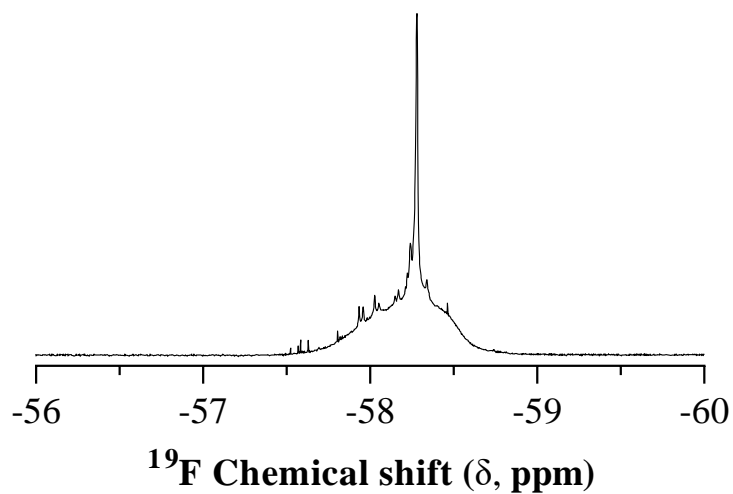
A**B**

Figure 5-20. (A) ^1H NMR spectrum with measured integral values given in blue; (B) ^{19}F NMR spectrum of poly(4-(trifluoromethoxy)phenylacetylene), poly(M4), recorded in CDCl_3 .

3,4-Dichlorophenylacetylene, **M5**, was readily homopolymerised with **93** at [P]/[Rh] = 10 and 20 (Table 5-3, entry 8 and 9). Consistent with the majority of other arylacetylenes examined, the pseudo-first-order kinetic plots are linear with a short induction period observed for [P]/[Rh] = 20. The SEC-measured M_n of aliquots increases systematically in both cases with final samples having an M_n of ca. 8,700. A marginal improvement in dispersity was observed at [P]/[Rh] = 20 with \mathcal{D} of 1.07, compared to 1.14 at [P]/[Rh] = 10. Similarly, the *cis* content for the former is marginally higher at 87 % versus 84 % for the later.

The homopolymerisation of substituted arylacetylenes with a bulky substituent such as 4-ethynylbiphenyl, **M7**, and 4-ethynyl-naphthalene, **M8**, was evaluated next. In this instance, the homopolymerisation of **M7** and **M8** by **93** yielded dark orange, and dark violet coloured polymers respectively after 30 minutes, precipitating during the process and that were insoluble in benzene, THF, dichloromethane and acetone. This prevented the characterisation of the samples, and as such, the results were inconclusive. The insolubility of these polymers had been noted previously.²²⁻²⁵ According to Tabata *et al.*,²³ the solvation of poly(**M8**) (and possibly poly(**M7**)) could be hindered due to the pseudo-hexagonal packed crystal structure and narrow helical pitch width which stems from the *cis-transoidal* nature of the polymer.

The efficacy of **93** as an initiator for the homopolymerisation of 2-ethynylthiophene, **M9**, and 4-ethynylaniline, **M6**, was evaluated next and was found to be inactive toward these monomers with no polymer formation being observed via ¹H NMR or SEC. In regards to the homopolymerisation of **M9**, it has been shown that [Rh(nbd)Cl]/Et₃N, [Rh(cod)Cl]₂/Et₃N and [Rh(acac)Cl]₂ (nbd = norbornadiene; cod = cyclooctadiene; acac = acetylacetonate) were active in the polymerisation of 2-ethynyl- and 3-ethynyl-thiophenes.²⁶⁻²⁹ As for the polymerisation of **M6**, Saeed, Shiotsuki and

Masuda³⁰ performed polymerisation using a variety of synthesised Rh(I)-based catalysts bearing a nbd diene ligand with a heteroatom-containing bidentate ligand based on phenoxy-imine and β -diiminates. The authors reported that the polymerisation of **M6** gave low polymer yields (14-29 %) and noted that the polymer precipitated out of solution during polymerisation.

To demonstrate the ability to prepare functional block copolymers, we prepared two examples with 4-(trifluoromethoxy)phenylacetylene, **M4**, and 3,4-dichlorophenylacetylene, **M5**. In both instances, PA was first homopolymerised in toluene at 30 °C with $[P]/[Rh] = 20$, yielding 'living' PA homopolymers with SEC-measured M_{ns} of 12,200 (poly(**PA1**), Figure 5-21) and 12,100 (poly(**PA2**), Figure 5-22) with a corresponding D s of 1.12 and 1.10.

The addition of **M4** to poly(**PA1**) resulted in a clear, systematic shift of the molecular weight distribution to a lower retention time, Figure 5-21A, with the resulting final copolymer, poly(**PA1**)-*block*-poly(**M4**), having an SEC-measured M_n of 21,200 and D of 1.08. No evidence of residual poly(**PA1**) impurity is observed, indicating retention of chain-end activity after full consumption of PA and a quantitative crossover efficiency to **M4**. The same observations were made for the preparation of poly(**PA2**)-*block*-poly(**M5**) copolymer, Figure 5-22A, which yielded a copolymer (M_n of 20,300 and D of 1.12) with quantitative crossover efficiency. In both examples, the final AB block copolymers had very high *cis-transoidal* stereoregularity as evidenced by the well-defined and sharp signals which are attributed to their respective *cis* protons highlighted in the ¹H NMR spectrums, Figure 5-21B and Figure 5-22B.

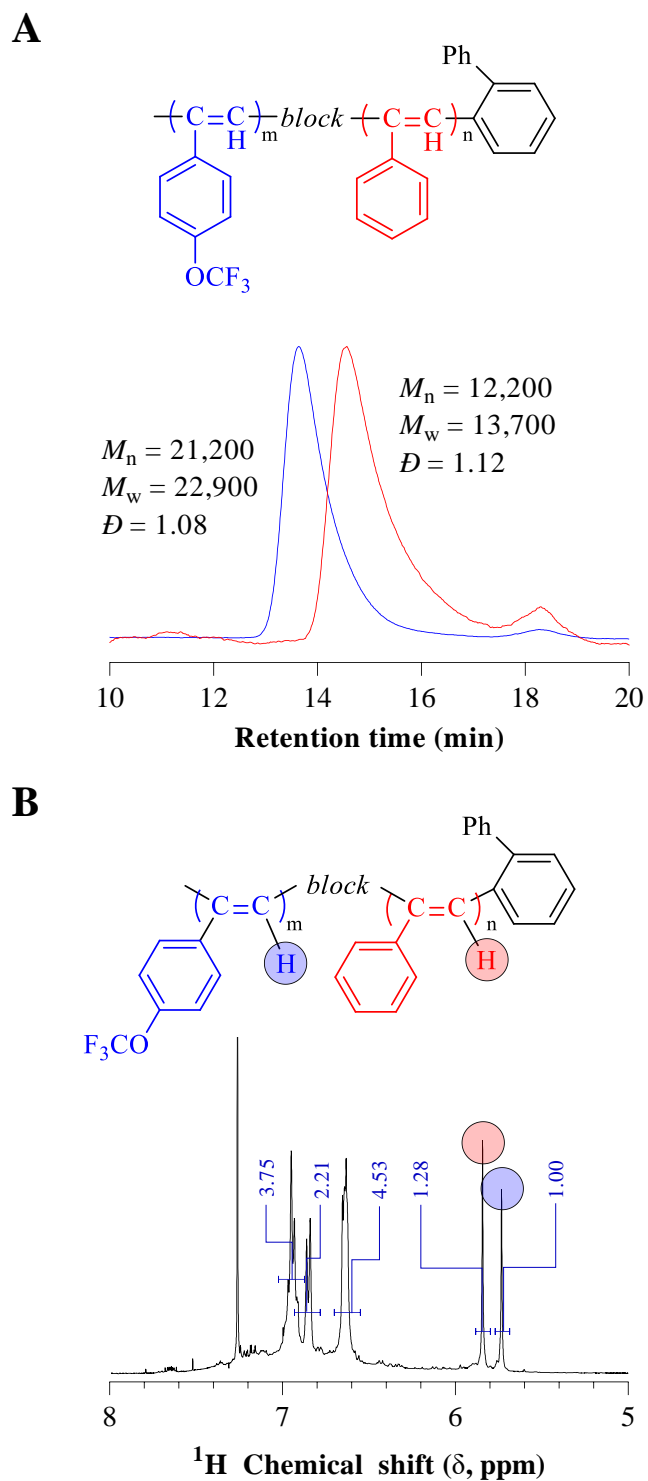


Figure 5-21. (A) SEC traces of a PPA homopolymer, poly(PA1) (red) and a poly(PA1)-*block*-poly(M4) (blue); (B) 1H NMR spectrum, recorded in $CDCl_3$, of poly(PA1)-*block*-poly(M4) with the relevant *cis* protons highlighted.

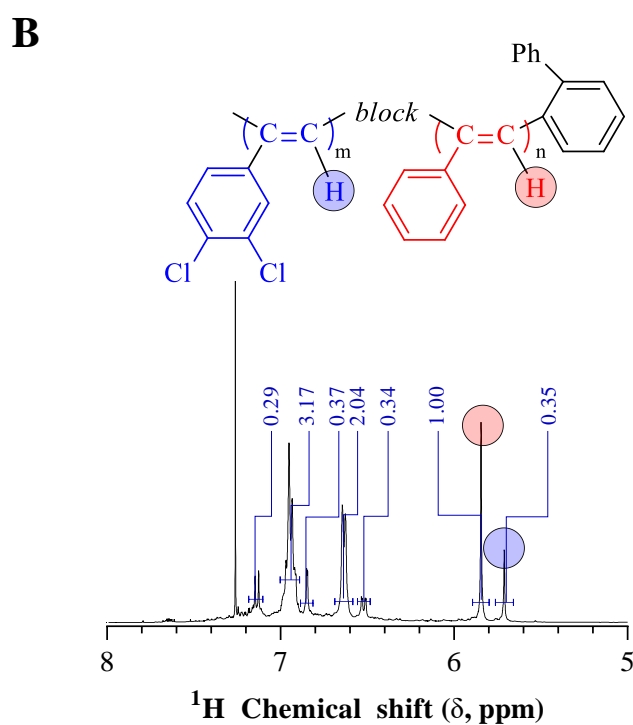
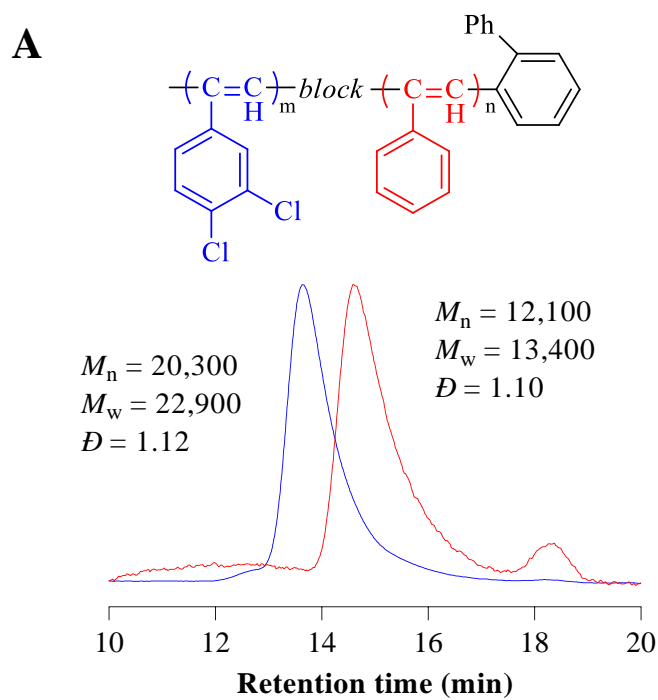


Figure 5-22. (A) SEC traces of a PPA homopolymer, poly(PA2) (red) and a poly(PA2)-block-poly(M5) (blue); (B) ^1H NMR spectrum, recorded in CDCl_3 , of poly(PA2)-block-poly(M5) with the relevant *cis* protons highlighted.

It should be noted that efficient crossover and corresponding block copolymer formation was not achieved with all monomers. For example, the preparation of the block copolymer, poly(**PA3**)-*block*-poly(**M2**) (where **M2** = 1-ethyl-4-ethynylbenzene), was attempted, and while block formation was successful, yielding a final copolymer with an SEC-measured M_n of 26,000 and \mathcal{D} of 1.12, there was evidence of significant PA homopolymer ‘impurities’ present as observed in the SEC trace (blue), Figure 5-23A, which exhibit features of bimodality, indicating possible loss of some chain-end activity and non-quantitative crossover efficiency. Despite this, the resulting final copolymer have high *cis-transoidal* stereoregularity as evidenced by the sharp signals highlighted in the ^1H NMR spectrum, Figure 5-23B.

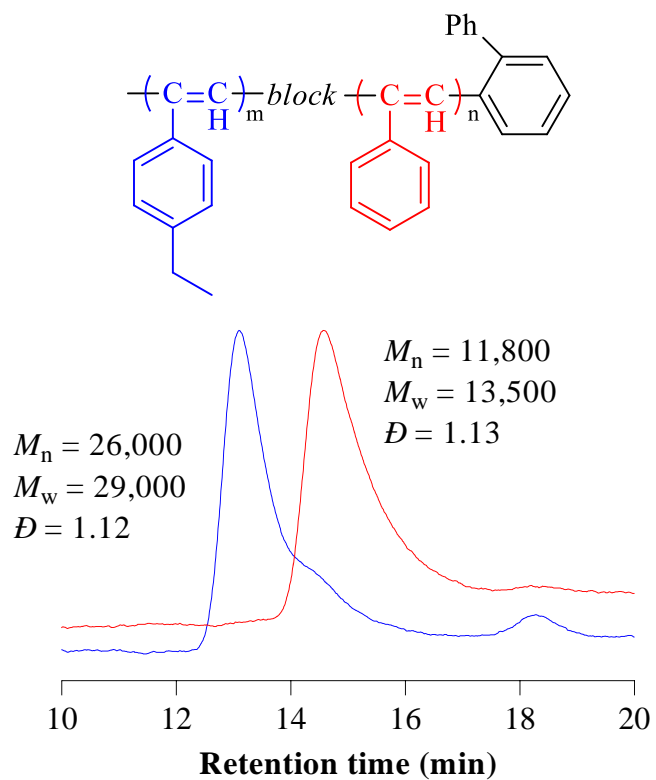
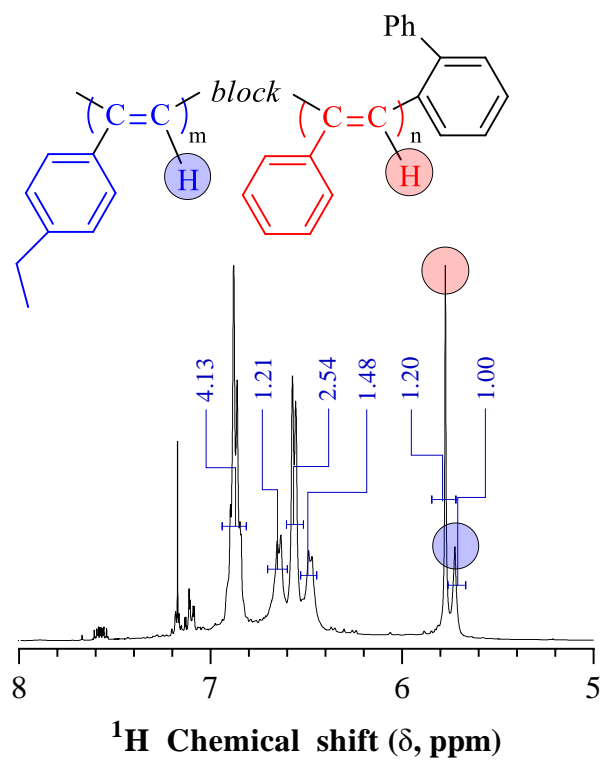
A**B**

Figure 5-23. (A) SEC traces for a PPA homopolymer, poly(**PA3**) (red) and poly(**PA3**)-*block*-poly(**M2**) (blue); (B) ^1H NMR spectrum, recorded in CDCl_3 , of poly(**PA3**)-*block*-poly(**M2**) with the relevant *cis* protons highlighted.

5.4 Conclusions

In summary, the synthesis of a new, well-defined, readily isolable, Rh(I)-aryl complex, $\text{Rh}(\text{tfb})(\text{Biphenyl})(\text{P}(4\text{-FC}_6\text{H}_4)_3)$, was reported, which was characterised in detail via a combination of elemental analysis, X-ray crystal structure analysis, and multinuclear NMR spectroscopy (such as ^1H , ^{19}F , ^{31}P , ^{103}Rh and ^{31}P - ^{103}Rh HMQC NMR spectrum). The ability of **93** to mediate controlled (co)polymerisation of phenylacetylene, specifically at $[\text{P}]/[\text{Rh}] = 20$ (where $[\text{P}] = \text{P}(4\text{-FC}_6\text{H}_4)_3$), was confirmed from the pseudo-first-order kinetic profiles, the molecular weight vs conversion plots, and the ability to form block copolymers through self-blocking demonstrating retention of chain-end activity. In addition, the resulting PA homopolymer was highly stereoregular bearing *cis-transoidal* conformation with a calculated *cis* content of 99 %.

Complex **93** was targeted due to the assumption that substituting the nbd diene ligand with tfb diene ligand in such Rh(I) complexes would increase its activity. This was found to be true with **93** being highly active, as evidenced by the rapid rate of homopolymerisation of PA with calculated k_{appS} (at $[\text{P}]/[\text{Rh}] = 10$) that were at least 8 to 16 times higher than **90** (reported in Chapter 3) and **92** (reported in Chapter 4).

The activity of **93** towards other substituted arylacetylenes was explored and revealed that **93** was active for a range of substituted arylacetylenes including 1-ethyl-4-ethynylbenzene (**M2**), 4-(trifluoromethoxy)phenylacetylene (**M4**), 3,4-dichlorophenylacetylene (**M5**), 4-ethynylbiphenyl (**M7**), and 4-ethynylnaphthalene

(**M8**), however, with varying degrees of control. While the molecular weight distribution for the homopolymer of **M2** was broad ($\mathcal{D} = 1.49$), the homopolymers of **M4** and **M5** had low dispersities ($\mathcal{D} = 1.07$). The homopolymers of **M2**, **M4**, and **M5** all had high stereoregularity with calculated *cis* contents of 89, 88 and 87 % respectively.

Interestingly, the homopolymerisation of 4-ethynylanisole (**M3**) yielded polymer, but the kinetic data displayed inconsistencies, suggesting that the polymerisation was uncontrolled. It was revealed later that the inconsistencies were due to likely polymer degradation in CDCl_3 , resulting in poor data acquisition. However, we noted that the polymerisation of **M3** yielded highly stereoregular *cis-transoidal* polymer with a measured *cis* content of 97 %. The homopolymerisations of 4-ethynyl aniline (**M6**) and 3-ethynylthiophene (**M9**) were attempted but no homopolymer formation was observed in either the SEC analysis, nor via ^1H NMR spectroscopy. The homopolymerisation of 4-ethynylbiphenyl (**M7**) and 4-ethynylnaphthalene (**M8**), in both cases, yielded insoluble polymers, which prevented their characterisation and as such was inconclusive, although the tfb complex clearly initiated polymerisation. The ability to form AB diblock copolymers with other substituted arylacetylenes was demonstrated by the block (co)polymerisation of 'living' PA homopolymer with **M4** and **M5**. Successful block copolymer formation was confirmed by size exclusion chromatography (SEC) with quantitative crossover efficiencies noted and ^1H NMR spectroscopy verifies the high stereoregularity of the final copolymers, which was predominantly *cis* in nature. We noted that in the case of the block copolymerisation of PA with **M2**, SEC data for the resulting block copolymer suggest non-quantitative crossover efficiency, nonetheless, block copolymers formation was successfully achieved.

In summary, the data presented in this chapter confirms that **93** is a highly active initiator for PA homopolymerisation compared to those reported in the previous chapters and under appropriate conditions mediates polymerisation with near-quantitative initiation efficiency.

5.5 References

1. Misumi, Y.; Kanki, K.; Miyake, M.; Masuda, T., Living polymerization of phenylacetylene by rhodium-based ternary catalysts, (diene)Rh(I) complex/vinylolithium/phosphorous ligand. effect of catalyst components. *Macromolecular Chemistry and Physics* **2000**, *201* (17), 2239-2244.
2. Saeed, I.; Shiotsuki, M.; Masuda, T., Remarkable cocatalytic effect of alkali metal amides and alkoxides in the rhodium-catalyzed polymerization of phenylacetylene. *Macromolecules* **2006**, *39* (16), 5347-5351.
3. Saeed, I.; Shiotsuki, M.; Masuda, T., Living polymerization of phenylacetylene with tetrafluorobenzobarrelene ligand-containing rhodium catalyst systems featuring the synthesis of high molecular weight polymer. *Macromolecules* **2006**, *39* (25), 8567-8573.
4. Saeed, I.; Shiotsuki, M.; Masuda, T., Effect of diene ligands in the rhodium-catalyzed polymerization of phenylacetylene. *Macromolecules* **2006**, *39* (26), 8977-8981.
5. Tomlinson, A. J.; Massey, A. G., Perfluorophenyl derivatives of the elements XI. Metal carbonyl derivatives of tetrafluorobenzobicyclo[2.2.2]octatriene. *Journal of Organometallic Chemistry* **1967**, *8* (2), 321-327.
6. Brewer, J. P. N.; Eckhard, I. F.; Heaney, H.; Marples, B. A., Aryne chemistry. part V. some addition reactions of tetrafluorobenzynes. *Journal of The Chemical Society C: Organic* **1968**, 664-676.
7. Tan, N. S. L.; Nealon, G. L.; Lynam, J. M.; Sobolev, A. N.; Rowles, M. R.; Ogden, M. I.; Massi, M.; Lowe, A. B., A (2-(naphthalen-2-yl)phenyl)rhodium(I) complex formed by a proposed intramolecular 1,4-ortho-to-ortho' Rh metal-atom migration and its efficacy as an initiator in the controlled stereospecific polymerisation of phenylacetylene. *Dalton Transactions: An International Journal of Inorganic Chemistry* **2019**, *48* (43), 16437-16447.
8. Harris, R. K.; Becker, E. D.; Cabral de Menezes, S. M.; Granger, P.; Hoffman, R. E.; Zilm, K. W., Further conventions for NMR shielding and chemical shifts (IUPAC recommendations 2008). *Magnetic Resonance in Chemistry* **2008**, *46* (6), 582-598.
9. Carlton, C., *Annual Reports on NMR Spectroscopy*. Elsevier: 2008; Vol. 63.
10. Tan, N. S. L.; Simpson, P. V.; Nealon, G. L.; Sobolev, A. N.; Raiteri, P.; Massi, M.; Ogden, M. I.; Lowe, A. B., Rhodium(I)- α -phenylvinylfluorenyl complexes: synthesis, characterization, and evaluation as initiators in the stereospecific polymerization of phenylacetylene. *European Journal of Inorganic Chemistry* **2019**, *2019* (5), 592-601.

11. Miyake, M.; Misumi, Y.; Masuda, T., Living polymerization of phenylacetylene by isolated rhodium complexes, $\text{Rh}[\text{C}(\text{C}_6\text{H}_5)=\text{C}(\text{C}_6\text{H}_5)_2](\text{nbd})(4\text{-XC}_6\text{H}_4)_3\text{P}$ ($\text{X} = \text{F}, \text{Cl}$). *Macromolecules* **2000**, *33* (18), 6636-6639.
12. Tan, N. S. L.; Nealon, G. L.; Turner, G. F.; Moggach, S. A.; Ogden, M. I.; Massi, M.; Lowe, A. B., $\text{Rh}(\text{I})(2,5\text{-norbornadiene})(\text{biphenyl})(\text{tris}(4\text{-fluorophenyl})\text{phosphine})$: synthesis, characterization, and application as an initiator in the stereoregular (co)polymerization of phenylacetylenes. *American Chemical Society Macro Letters* **2020**, *9* (1), 56-60.
13. Dewar, M. J. S., A review of π complex theory. *Bulletin de la Société Chimique de France* **1951**, *18*, C79.
14. Hartley, F. R., Metal-olefin and -acetylene bonding in complexes. *Angewandte Chemie International Edition* **1972**, *11* (7), 596-606.
15. Stoebenau, E. J.; Jordan, R. F., Nonchelated d^0 zirconium-alkoxide-alkene complexes. *Journal of The American Chemical Society* **2006**, *128* (25), 8162-8175.
16. Chatt, J.; Duncanson, L. A., 586. Olefin co-ordination compounds. Part III. Infra-red spectra and structure: attempted preparation of acetylene complexes. *Journal of The Chemical Society* **1953**, 2622, 2939-2947.
17. Chen, J.; Eldridge, R. B.; Rosen, E. L.; Bielawski, C. W., A study of $\text{Cu}(\text{I})$ -ethylene complexation for olefin-paraffin separation. *AIChE Journal* **2011**, *57* (3), 630-644.
18. Tang, B. Z.; Poon, W. H.; Leung, S. M.; Leung, W. H.; Peng, H., Synthesis of stereoregular poly(phenylacetylene)s by organorhodium complexes in aqueous media. *Macromolecules* **1997**, *30* (7), 2209-2212.
19. Saeed, I.; Shiotsuki, M.; Masuda, T., Living Polymerization of Phenylacetylene with Tetrafluorobenzobarrelene Ligand-Containing Rhodium Catalysts Systems Featuring the Synthesis of High Molecular Weight Polymer. *Macromolecules* **2006**, *39*, 8567-8573.
20. Simionescu, C. I.; Percec, V.; Dumitrescu, S., Polymerization of acetylenic derivatives. XXX. Isomers of polyphenylacetylene. *Journal of Polymer Science: Polymer Chemistry Edition* **1977**, *15* (10), 2497-2509.
21. Kishimoto, Y.; Eckerle, P.; Miyatake, T.; Ikariya, T.; Noyori, R., Living polymerization of phenylacetylenes initiated by $\text{Rh}(\text{C}\equiv\text{CC}_6\text{H}_5)(2,5\text{-norbornadiene})[\text{P}(\text{C}_6\text{H}_5)_3]_2$. *Journal of The American Chemical Society* **1994**, *116* (26), 12131-12132.
22. Karim, S. M. A.; Musikabhumma, K.; Nomura, R.; Masuda, T. In *Synthesis and properties of poly(9-phenanthrylacetylene) and poly(1-pyrenylacetylene)*, Proceedings of the Japan Academy, Series B, Tokyo, JP, The Japan Academy: Tokyo, JP, 1999; pp 97-100.

23. Tabata, M.; Yokota, K.; Namioka, M., An electron spin resonance study of poly(α -ethynynaphthalene) polymerized with [Rh(norbornadiene)Cl]₂ and WCl₆ as catalysts. *Macromolecular Chemistry and Physics* **1995**, *196* (9), 2969-2977.
24. Mawatari, Y.; Motoshige, A.; Yoshida, Y.; Motoshige, R.; Sasaki, T.; Tabata, M., Structural determination of stretched helix and contracted helix having yellow and red colors of poly(2-ethynynaphthalene) prepared with a [Rh(norbornadiene)Cl]₂-triethylamine catalyst. *Polymer* **2014**, *55* (10), 2356-2361.
25. Cataldo, F.; Ursini, O.; Angelini, G., Synthesis and study of the thermal and chiro-optical properties of polyacetylenes with bulky side Groups : poly(1-ethynyl-4-biphenyl), poly(1-ethynyl-4-phenoxybenzene) and poly(1-ethynyl-4-pentylbenzene). *Journal of Macromolecular Science, Part A* **2009**, *46* (9), 860-869.
26. Svoboda, J.; Sedláček, J.; Zedník, J.; Dvořáková, G.; Trhlíková, O.; Rédrová, D.; Balcar, H.; Vohlídal, J., Polymerization of 3-ethynylthiophene with homogeneous and heterogeneous Rh catalysts. *Journal of Polymer Science Part A : Polymer Chemistry* **2008**, *46* (8), 2776-2787.
27. Nakamura, M.; Tabata, M.; Sone, T.; Mawatari, Y.; Miyasaka, A., Photoinduced cis-to-trans isomerization of poly(2-ethynylthiophene) prepared with a [Rh(norbornadiene)Cl]₂ catalyst. ¹H NMR, UV, and ESR studies. *Macromolecules* **2002**, *35* (6), 2000-2004.
28. Imamura, T.; Mawatari, Y.; Fukuda, H.; Tabata, M., Organic thin film transistors with substituted polyacetylenes containing a hetero atom. *E-Journal of Surface Science and Nanotechnology* **2009**, *7*, 767-771.
29. Wang, X.; Yan, Y.; Liu, T.; Su, X.; Qian, L.; Song, Y.; Xu, H., Synthesis and nonlinear optical properties of polyacetylenes containing oxadiazole and thiophene pendant groups with high thermal stability. *Journal of Polymer Science Part A : Polymer Chemistry* **2010**, *48* (23), 5498-5504.
30. Saeed, I.; Shiotsuki, M.; Masuda, T., Nitrogen ligand-containing Rh catalysts for the polymerization of substituted acetylenes. *Journal of Molecular Catalysis A : Chemical* **2006**, *254* (1), 124-130.

Every reasonable effort has been made to acknowledge the owners of copyright material. I would be pleased to hear from any copyright owner who has been omitted or incorrectly acknowledged.

Chapter 6

Conclusions and Future Work

The work presented in this thesis investigated the application of a series of organo-rhodium(I) complexes based on the general Masuda structural motif,¹ **78**, Figure 6-1, in the controlled (co)polymerisations of arylacetylenes. Intrigued by the paucity of reported controlled (co)polymerisations of phenylacetylene (PA) by well-defined isolable rhodium(I) (Rh(I)) complexes, we developed a research program aimed at introducing simple modifications to the initiating fragment of the Masuda catalyst and with systematically increasing complexity, which we then evaluate as initiators for the (controlled) (co)polymerisations of PA and other substituted arylacetylenes.

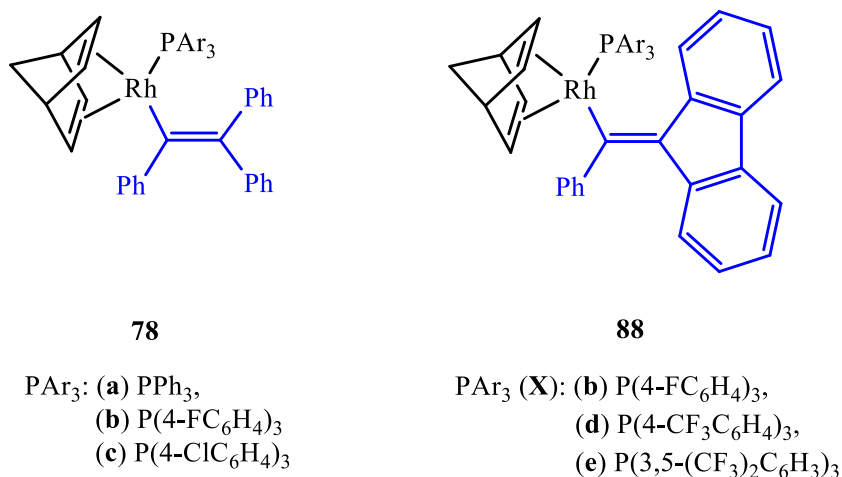


Figure 6-1. The chemical structures of Masuda catalysts¹ (**78**) and three new Rh(I)-fluorenyl complexes bearing a fluorine functionalised phosphine (**88b**, **88d** and **88e** where **b** = P(4-FC₆H₄)₃; **d** = P(4-CF₃C₆H₄)₃; **e** = P(3,5-(CF₃)₂C₆H₃)₃). Initiating fragment highlighted in blue.

In Chapter 2, a series of Rh(I)-fluorenyl complexes, **88b**, **88d** and **88e** (where **b** = P(4-FC₆H₄)₃; **d** = P(4-CF₃C₆H₄)₃; **e** = P(3,5-(CF₃)₂C₆H₃)₃), which contained an α -phenylvinylfluorenyl initiating fragment (highlighted in blue, Figure 6-1) and bears a fluorine-functionalised phosphine ligand. ¹⁰³Rh and ³¹P-¹⁰³Rh 2D NMR spectroscopy was used to characterise **88b**, **88d**, and **88e** along with other complementary characterisation techniques (¹H, ¹⁹F, ³¹P NMR spectroscopy, elemental analysis, x-ray powder diffraction and single-crystal x-ray diffraction). The structural difference of the initiating fragment of **78** and **88** was a bond between the phenyl groups on the β carbon of the vinylic initiating fragment and the initiating ability was examined under a range of experimental conditions. We found that the complexes were active as initiators for the homopolymerisation of PA, but they suffered from low initiation efficiencies (IEs), spanning the range 0.13 to 0.56, but yielding copolymers with dispersities, *D*, as low as 1.03. We proposed that the low IEs were associated with the initial monomer insertion into the Rh-C bond being sterically hindered by the bulky, and conformationally locked fluorenyl moiety. Despite the low IEs, the resulting PA homopolymers have high stereoregularity (*cis* content = 96 %) bearing a *cis-transoidal* configuration. The successful synthesis of AB ‘diblock’ copolymers via a self-blocking experiment demonstrated retention of chain-end activity and quantitative crossover efficiency which is consistent with a controlled polymerisation process. In summary, the series of Rh(I)- α -phenylvinylfluorenyl complexes, **88**, were active initiators for the homopolymerisation of PA. While **88** met the general substitution criteria outlined by Misumi *et al.*² for efficient PA initiators, the results suggest that efficiency is governed not just by substitution patterns (or rather ligand environment) but may also be influenced by other geometric, and perhaps electronic, factors.

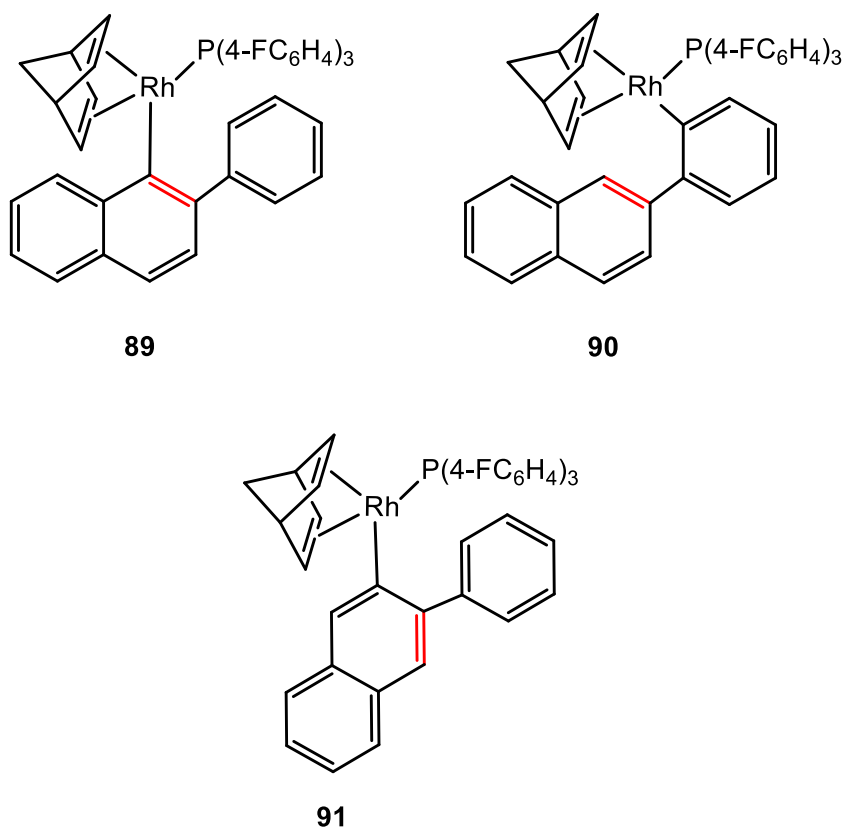


Figure 6-2. Chemical structure of targeted (2-phenylnaphthalene)Rh(I) derivative (**89**), isolated second isomeric form (2-naphthylphenyl)Rh(I) (**90**), and third isomeric form (3-phenylnaphthalene)Rh(I) (**91**) with the ‘vinyl’ moiety highlighted in red.

In Chapter 3, we attempted the synthesis of Rh(I)-2-phenylnaphthyl derivative, **89** Figure 6-2, which was targeted to address the issues of the low IEs of **88** due to the steric hindrance stemming from the bulky, and conformationally locked fluorenyl initiating fragment which prevents facile coordination of PA. Complex **89** is a Rh(I)-aryl complex with an initiating fragment that has a phenyl group on the β -vinyl carbon (recognising that it is part of the aromatic naphthyl group, highlighted in red, that is able to freely rotate. Unexpectedly, we isolated the 2-naphthylphenyl isomer, **90**, after recrystallisation. We proposed that the formation of **90** and **91** proceeded via an intramolecular 1,4-Rh atom migrations or *ortho*-to-*ortho*’ C-H bond activation which

was supported by Density Functional Theory (DFT) calculations. Also, ^1H and ^{31}P - ^{103}Rh NMR spectroscopy indicated that in solution, the 2-naphthylphenyl isomer underwent a second 1,4-Rh atom migration, gaining a third species, the 3-phenylnaphthyl structural isomer, **91**. Accepting the fact that in addition to **90**, a second minor **91** and possibly third species are present in small quantities, we proceeded to examine **90** as an initiator for the homopolymerisation of PA. Consistent with other Rh-mediated insertion polymerisation, the resulting poly(phenylacetylene)s (PPAs) had narrow molecular weight distributions ($\mathcal{D} \leq 1.25$) and possessed high *cis-transoidal* stereoregularity (*cis* content of 99 %) with a corresponding IE of 0.80. The lower than expected IEs were rationalised by the formation of multiple (in)active species via 1,4-Rh atom migratory processes and the calculated ratio of 4:1 in favour of (2-naphthylphenyl)Rh(I) derivative coincides with the overall IE of ca. 0.80. Overall, while not the target species, **90** was an effective initiator for the homopolymerisation of PA, and based on the linearity of pseudo first-order kinetic plots, M_n vs monomer conversion plots, and resulting polymer dispersities ($\mathcal{D} \leq 1.25$) suggests that polymerisations of PA mediated by **90** were controlled and represents a significant improvement over the α -phenylvinylfluorenyl derivative reported in Chapter 2.

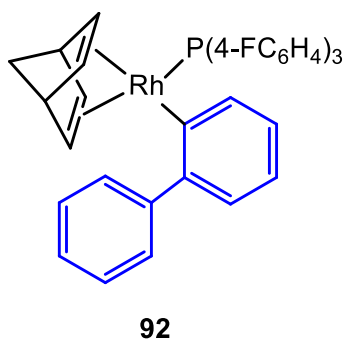


Figure 6-3. Chemical structure of Rh(I)(Biphenyl)(nbd)(P(4-FC₆H₄)₃) (Biphenyl = biphenyl initiating fragment highlighted above in blue).

In an effort to improve the low IEs of **90** associated with formation of additional (in)active species through 1,4-Rh atom migrations, as detailed in Chapter 3, we next targeted **92**, Figure 6-3, with a biphenyl initiating fragment. While still potentially prone to 1,4-migratory processes, the occurrence of such shifts would yield identical species. The target complex, **92**, was successfully synthesised and characterised in detail via methods and techniques highlighted previously. Complex **92** was subsequently evaluated as an initiator for PA (co)polymerisation, and we found that the IEs obtained were near-quantitative (ca. 0.98) with the resulting PA homopolymers also having a low dispersity ($\bar{D} = 1.11$). The pseudo first-order kinetic plots and M_n vs monomer conversion plots for the homopolymerisation of PA were obtained for $[P]/[Rh] = 5, 10$ and 20 and were found to be linear which is consistent with a controlled polymerisation process. To highlight the broader potential use of **92**, we also performed the homopolymerisation of 1-ethynyl-4-fluorobenzene (4-FPA) in toluene at $30\text{ }^\circ\text{C}$ with $[P]/[Rh] = 20$, which was successful in producing poly(4-FPA) with a corresponding IE of 0.71, with polyenes possessing \bar{D} of 1.07 and highly stereoregular structure (*cis-transoidal*, *cis* content = 96 %) that is comparable with PPA. We also demonstrated retention of chain-end activity by successfully performing block (co)polymerisations in the preparation of poly(PA-*block*-4-FPA) which had a predominantly *cis-transoidal* structure with the calculated *cis* content of 76 %. These findings confirm that complex **92** does, successfully, address the issues of 1,4-Rh atom migration noted for complex **90** as detailed in Chapter 3. Further, **92** is the first Rh(I)-aryl complex that exhibits IEs comparable to the Masuda, Rh(I)-triphenylvinyl species.¹

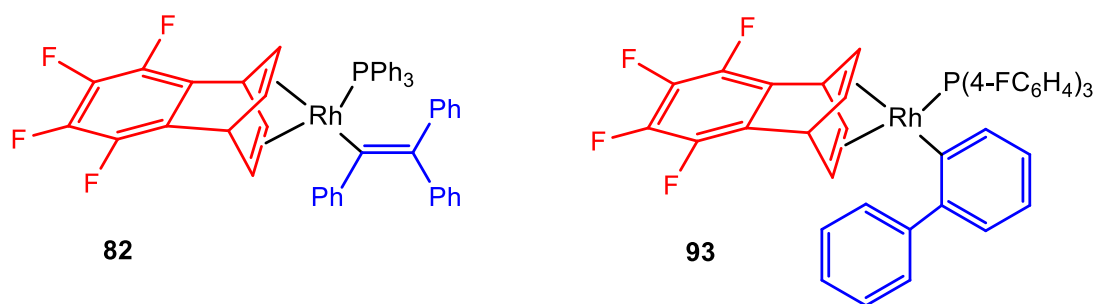


Figure 6-4. Chemical structure of $\text{Rh}(\text{tfb})(\text{PhC}=\text{CPh}_2)(\text{P}(\text{4-FC}_6\text{H}_4)_3)$ (**82**) and $\text{Rh}(\text{tfb})(\text{Biphenyl})(\text{P}(\text{4-FC}_6\text{H}_4)_3)$ (**93**). Tetrafluorobenzobarralene (tfb, highlighted in red) ligand and initiating fragment highlighted in blue, respectively.

In Chapter 5, we built on our recent findings and chose $\text{Rh}(\text{tfb})(\text{BiPh})(\text{P}(\text{4-FC}_6\text{H}_4)_3)$ (where tfb = tetrafluorobenzobarralene), **93**, Figure 6-4, as the final target complex since it was reported by Saeed *et al.*^{3,4} that replacing the norbornadiene (nbd) diene ligand with the tetrafluorobenzobarralene (tfb) ligand significantly improved the activity of the initiator, **82**. The final chapter detailed the synthesis, characterisation and application of **93** as an initiator for the controlled polymerisation of PA. The homopolymerisation of PA mediated by **93** was performed in toluene at 30 °C with $[\text{P}]/[\text{Rh}] = 10$ or 20. It was noted that 20 equivalents of $\text{P}(\text{4-FC}_6\text{H}_4)_3$ was required to achieve near-quantitative IE (0.96), which yielded very high *cis-transoidal* stereoregular PPAs with measured *cis* content of 99 % and low \bar{D} of 1.15. It was also noted that **93** displayed a significantly higher activity towards PA homopolymerisation with k_{app} values generally 8 and 16 times higher than **92** and **90** respectively, in addition, is consistent with the enhanced π -acidity of tfb versus nbd. The pseudo first-order kinetic and M_n vs monomer conversion plots at $[\text{P}]/[\text{Rh}] = 10$ and 20 were linear which meets the criteria for controlled polymerisation as outlined in Chapter 1 of this thesis.

We also utilised **93** to homopolymerise additional arylacetylene monomers, including 1-ethyl-4-ethynylbenzene (**M2**), 4-ethynylanisole (**M3**), 4-(trifluoromethoxy)phenylacetylene (**M4**), 3,4-dichlorophenylacetylene (**M5**), 4-ethynylaniline(**M6**), 4-ethynylbiphenyl (**M7**), 4-ethynylnapthalene (**M8**) and 2-ethynylthiophene (**M9**). The homopolymerisation of **M2**, **M4** and **M5** proceeded smoothly and was found to be consistent with a controlled polymerisation process as confirmed by kinetic studies. Homopolymerisation of **M7** and **M8** yielded insoluble polymers, consistent with previous reports relating to the uncontrolled polymerisation of these monomers.⁵⁻⁸ No evidence of polymerisation for **M6** and **M9** was observed as determined by size exclusion chromatography (SEC). The data for the homopolymerisation of **M3** was inconsistent, and the cause was later determined to be associated with solvent effects which lead to the degradation of the polymers in solution, which prevented the reliable acquisition of data.

Table 6-4. Summary of AB diblock copolymers synthesised by **93** in Chapter 5.

Entry	Polymer	Polymer Yield (%)	M_n	M_w	\bar{D}
1	Poly(PA)- <i>block</i> -poly(M2)	92	26,000	29,100	1.12
2	Poly(PA)- <i>block</i> -poly(M4)	90	21,200	22,900	1.08
3	Poly(PA)- <i>block</i> -poly(M5)	91	20,300	22,700	1.12

As a final demonstration of the controlled nature of the polymerisations mediated by **93**, we successfully performed self-blocking experiments to synthesise AB diblock copolymers via sequential monomer addition (see summary in Table 6-4) with the final copolymers having low dispersities and *cis* contents in the high 90s. This demonstrated the retention of chain-end activity and the broader utility of **93** for the

preparation of new functional materials. Complex **93** represents the most active species among all the Rh(I)-vinyl and -aryl species reported in Chapter 2 (**88**), 3 (**90**) and 4 (**92**).

The data presented in this thesis have demonstrated that the π -acidity of the diene ligand and structural features of the initiating fragment plays a considerable role in regulating the efficiencies of Rh(I)-vinyl and Rh(I)-aryl species as initiators for the polymerisation of arylacetylenes. The facile coordination of the monomer is, in part, greatly affected by the steric hindrance of the initiating fragment, particularly with large bulky aromatic rings which have the potential to limit the synthesis of large aryl end-functionalised homopolymers.

Recently, Taniguchi *et al.*⁹ reported a multi-component catalytic system for living polymerisation of PA is a convenient, highly efficient and versatile method of introducing end-functionalisation to homopolymers of PA and block copolymers which addresses the problem stated above. The method involves a one-pot polymerisation of PA by starting off with reacting $[\text{Rh}(\text{nbd})\text{Cl}]_2$ with a boronic acid of choice and diphenylacetylene in the presence of 50 % (w/v) aqueous solution of KOH and at least 3 equivalents of PPh_3 for 5 minutes at 0 °C before adding PA to start polymerisation process. The diphenylacetylene coordinates to the Rh centre via an insertion process which forms the vinylic portion of the initiating fragment similar to that of the Masuda catalyst, **78**. The formed vinylic portion of the molecule also likely act as a spacer group between the bulky aryl group of the boronic acids and Rh centre. Future research efforts should look at using similar methods described by Taniguchi *et al.*⁹ for previously characterised well-defined isolable Rh(I) initiators that suffer from low IEs such as **88** by investigating if added diphenylacetylenes improve the efficiency of the initiation process.

Finally, it was also demonstrated in Chapter 5 that solvent affects the degradation of poly(**M3**) which should be noted for future work. The thermal isomerisation of PPA in CDCl₃ is well documented by Percec *et al.*¹⁰⁻¹² but there are no specific reports regarding the stability of other functional poly(arylacetylenes). This could present a challenge for future work regarding the acquisition of reproducible data if the groundwork for understanding the stability of substituted poly(arylacetylenes) in a range of solvents are not well understood. This is ever more important since access to substituted poly(arylacetylenes) has been opened with **93** and Taniguchi's multi-component catalytic system.

In summary, this thesis describe the synthesis and detailed characterisation of six new Rh(I)-vinyl and Rh(I)-aryl complexes with a primary emphasis on a systematic evaluation of their ability to mediate the (controlled) (co)polymerisations of PA and other substituted arylacetylene derivatives.

6.1 References

1. Miyake, M.; Misumi, Y.; Masuda, T., Living polymerization of phenylacetylene by isolated rhodium complexes, $\text{Rh}[\text{C}(\text{C}_6\text{H}_5)=\text{C}(\text{C}_6\text{H}_5)_2](\text{nbd})(4\text{-XC}_6\text{H}_4)_3\text{P}$ (X = F, Cl). *Macromolecules* **2000**, *33* (18), 6636-6639.
2. Misumi, Y.; Kanki, K.; Miyake, M.; Masuda, T., Living polymerization of phenylacetylene by rhodium-based ternary catalysts, (diene)Rh(I) complex/vinyl lithium/phosphorous ligand. effect of catalyst components. *Macromolecular Chemistry and Physics* **2000**, *201* (17), 2239-2244.
3. Saeed, I.; Shiotsuki, M.; Masuda, T., Effect of diene ligands in the rhodium-catalyzed polymerization of phenylacetylene. *Macromolecules* **2006**, *39* (26), 8977-8981.
4. Saeed, I.; Shiotsuki, M.; Masuda, T., Living Polymerization of Phenylacetylene with Tetrafluorobenzobarrelene Ligand-Containing Rhodium Catalysts Systems Featuring the Synthesis of High Molecular Weight Polymer. *Macromolecules* **2006**, *39*, 8567-8573.
5. Karim, S. M. A.; Musikabhumma, K.; Nomura, R.; Masuda, T. In *Synthesis and properties of poly(9-phenanthrylacetylene) and poly(1-pyrenylacetylene)*, Proceedings of the Japan Academy, Series B, Tokyo, JP, The Japan Academy: Tokyo, JP, 1999; pp 97-100.
6. Tabata, M.; Yokota, K.; Namioka, M., An electron spin resonance study of poly(α -ethynyl naphthalene) polymerized with $[\text{Rh}(\text{norbornadiene})\text{Cl}]_2$ and WCl_6 as catalysts. *Macromolecular Chemistry and Physics* **1995**, *196* (9), 2969-2977.
7. Mawatari, Y.; Motoshige, A.; Yoshida, Y.; Motoshige, R.; Sasaki, T.; Tabata, M., Structural determination of stretched helix and contracted helix having yellow and red colors of poly(2-ethynyl naphthalene) prepared with a $[\text{Rh}(\text{norbornadiene})\text{Cl}]_2$ -triethylamine catalyst. *Polymer* **2014**, *55* (10), 2356-2361.
8. Cataldo, F.; Ursini, O.; Angelini, G., Synthesis and study of the thermal and chiro-optical properties of polyacetylenes with bulky side Groups : poly(1-ethynyl-4-biphenyl), poly(1-ethynyl-4- phenoxybenzene) and poly(1-ethynyl-4-pentylbenzene). *Journal of Macromolecular Science, Part A* **2009**, *46* (9), 860-869.
9. Taniguchi, T.; Yoshida, T.; Echizen, K.; Takayama, K.; Nishimura, T.; Maeda, K., Facile and versatile synthesis of end-functionalized poly(phenylacetylene)s: a multicomponent catalytic system for well-controlled living polymerization of phenylacetylenes. *Angewandte Chemie International Edition* **2020**, *59* (22), 8670-8680.
10. Simionescu, C. I.; Percec, V., Thermal cis-trans isomerization of cis-transoidal polyphenylacetylene. *Journal of Polymer Science : Polymer Chemistry Edition* **1980**, *18* (1), 147-155.

11. Kunzler, J.; Percec, V., Living polymerization of aryl substituted acetylenes by MoCl₅ and WCl₆ based initiators : The ortho phenyl substituent effect. *Journal of Polymer Science Part A : Polymer Chemistry* **1990**, 28 (5), 1221-1236.
12. Percec, V.; Rudick, J. G.; Nombel, P.; Buchowicz, W., Dramatic decrease of the cis content and molecular weight of cis-transoidal polyphenylacetylene at 23 °C in solutions prepared in air. *Journal of Polymer Science Part A: Polymer Chemistry* **2002**, 40 (19), 3212-3220.

Every reasonable effort has been made to acknowledge the owners of copyright material. I would be pleased to hear from any copyright owner who has been omitted or incorrectly acknowledged.

Appendix A

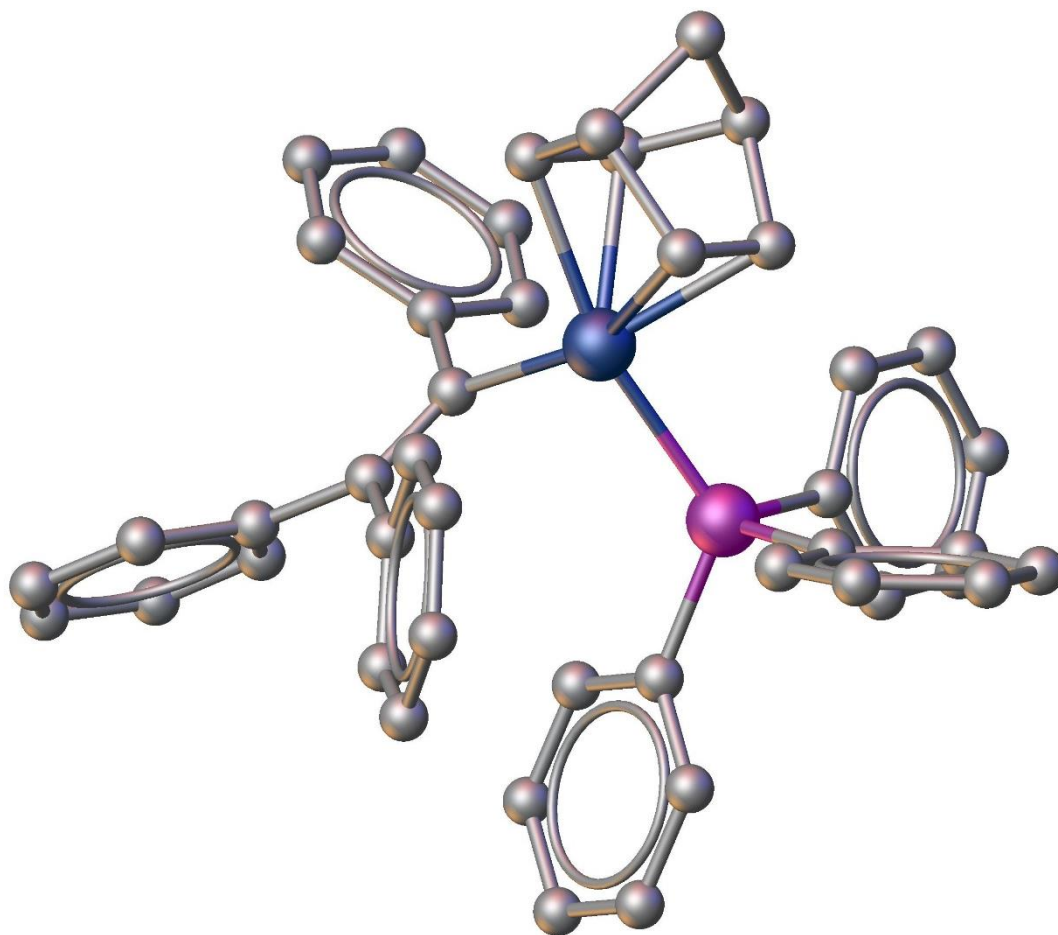


Figure A-1. Reported X-ray crystal structure for the Masuda complex
 $\text{Rh}(\text{nbd})(\text{CPh}=\text{CPh}_2)\text{PPh}_3$, **88a**

See Kumazawa *et al.* *Organometallics* **2012**, *31*, 6834-6842.

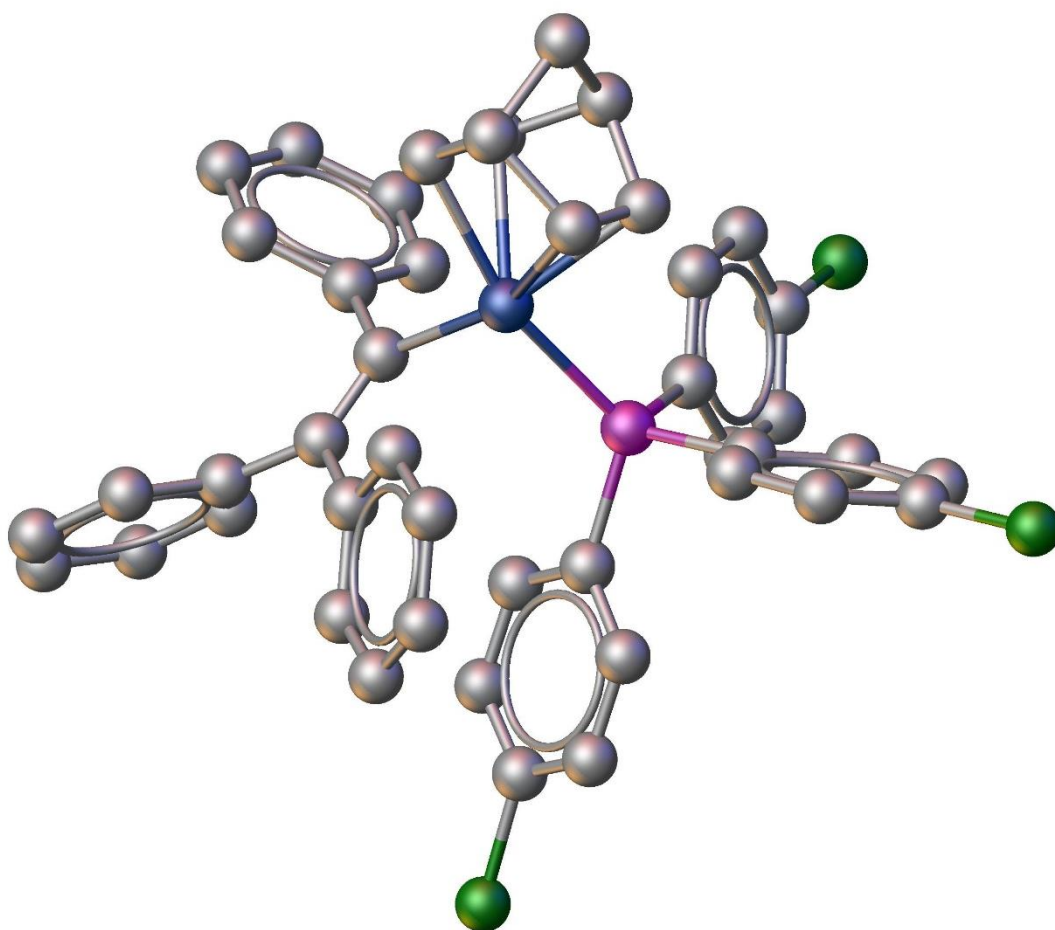


Figure A-2. Reported X-ray crystal structure for the Masuda complex $\text{Rh}(\text{nbd})(\text{CPh}=\text{CPh}_2)\text{P}(4\text{-ClC}_6\text{H}_4)_3$, **88c**.

See Miyake *et al. Macromolecules* **2000**, *33*, 6636-6639.

Appendix B

Chapter 1

Reproduced (adapted) from

Nicholas Sheng Loong Tan, Andrew B. Lowe **‘Polymerizations Mediated by Well-defined Rhodium Complexes’** *Angewandte Chemie, International Edition* **2020**. DOI: 10.1002/anie.201909909.

Nicholas Sheng Loong Tan, Andrew B. Lowe **‘Durch definierte Rhodiumkomplexe vermittelte Polymerisationen’** *Angewandte Chemie*, **2020**. DOI: 10.1002/ange.201909909.

With permission from the *Angewandte Chemie International Edition*. License number: 4901151065618, 3rd September 2020.

With permission from the *Angewandte Chemie*. License number: 4899160217281, 31st August 2020. 4901151158306, 3rd September 2020.

Chapter 2

Reproduced (adapted) from

Nicholas Sheng Loong Tan, Peter V. Simpson, Gareth L. Nealon, Alexandre N. Sobolev, Paolo Raiteri, Massimiliano Massi, Mark I. Ogden, Andrew B. Lowe. **‘Rhodium(I)-a-Phenylvinylfluorenyl Complexes: Synthesis, Characterization, and Evaluation as Initiators in the Stereospecific Polymerization of Phenylacetylene’** *European Journal of Inorganic Chemistry* **2019**, 592-601. DOI: 10.1002/ejic.201801411. Highlighted as a *Very Important Paper*.

With permission from the European Journal of Inorganic Chemistry. License number: 4901150924070, 3rd September 2020.

Chapter 3

Reproduced (adapted) from

Nicholas Sheng Loong Tan, Gareth L. Nealon, Matthew R. Rowles, Alexandre N. Sobolev, Jason M. Lynam, Mark I. Ogden, Massimiliano Massi, Andrew B. Lowe. ‘**A (2-(Naphthalen-2-yl)phenyl)rhodium(I) Complex formed by a Proposed Intramolecular 1,4-Ortho-to-Ortho’ Rh Metal-atom Migration and its Efficacy as an Initiator in the Controlled Stereospecific Polymerization of Phenylacetylene**’ Accepted for publication 18/10/2019. *Dalton Transactions* **2019**, 48, 16437-16447. **DOI:** 10.1039/c9dt02953b.

by permission of The Royal Society of Chemistry.

Chapter 4

Reproduced (adapted) with permission from

Nicholas Sheng Loong Tan, Gareth L. Nealon, Gemma Turner, Stephen Moggach, Mark I. Ogden, Massimiliano Massi, Andrew B. Lowe ‘**Rh(I)(2,5-Norbornadiene)(biphenyl)tris(4-fluorophenyl)phosphine: Synthesis, Characterization and Application as an Initiator in the Stereospecific (Co)Polymerization of Phenylacetylenes**’ *ACS Macro Letters* **2020**, 9, 56-60. **DOI:** 10.1021/acsmacrolett.9b00975.

Copyright (2020) American Chemical Society.

Appendix C



DOI: 10.1002/ejic.201801411



Polymerization Catalysts | Very Important Paper |

Rhodium(I)- α -Phenylvinylfluorenyl Complexes: Synthesis, Characterization, and Evaluation as Initiators in the Stereospecific Polymerization of Phenylacetylene

Nicholas Sheng Loong Tan,^[a,b] Peter V. Simpson,^[a,b] Gareth L. Nealon,^[c] Alexandre N. Sobolev,^[c] Paolo Raiteri,^[b,d,e] Massimiliano Massi,^[a,b] Mark I. Ogden,^[a,b] and Andrew B. Lowe^{*[a,b]}

Abstract: The synthesis, characterization and use, as initiators for phenylacetylene polymerizations, of three new rhodium(I)-vinyl complexes containing fluorenyl functionality with fluorine-functionalized phosphine ligands is described. Rh(nbd)(CPh=CFlu)P(4-FC₆H₄)₃, Rh(nbd)(CPh=CFlu)P(4-CF₃C₆H₄)₃, and Rh(nbd)(CPh=CFlu)P[3,5-(CF₃)₂C₆H₃]₃ (nbd: 2,5-norbornadiene; Flu: fluorenyl) were prepared and isolated as discrete, orange compounds and were readily recrystallized yielding X-ray quality crystals. All complexes were characterized by a combination

of ¹H, ³¹P, ¹⁹F, ¹⁰³Rh NMR spectroscopy and 2D ³¹P-¹⁰³Rh/³¹P-¹⁰³Rh(¹⁰³Rh) heteronuclear multiple-quantum correlation (HMQC) experiments, elemental analysis, and single-crystal X-ray analysis. The complexes were active as initiators in the co-ordination insertion polymerization of phenylacetylene, with initiation efficiencies spanning the range 13–56 %, and yielded polyphenylacetylenes of low dispersity ($\bar{D} = M_w/M_n$) with high *cis-transoidal* stereoregularity.

Introduction

Rhodium catalysts such as [Rh(nbd)Cl]₂ (nbd: 2,5-norbornadiene) in combination with a co-catalyst like triethylamine or 4-(*N,N*-dimethylamino)pyridine (DMAP) are known to serve as initiators for the (co)polymerization of phenylacetylene (PA) and functional derivatives thereof.^[1] Indeed, the literature describing the preparation and properties of poly(phenylacetylene)s (PPAs) is extensive due, in part, to the ease of handling, excellent oxygen tolerance, functional group compatibility and low oxophilicity of the Rh catalysts, coupled with the stability and processability of the resulting PA (co)polymers. While catalysts such as [Rh(nbd)Cl]₂, and derivatives thereof, are versatile such complexes mediate (co)polymerizations in a non-controlled fashion; however, such insertion polymerizations proceed with a high degree of stereoregularity yielding predominantly head-

to-tail *cis-transoidal* materials.^[1d,14] In contrast to the considerable volume of literature detailing non-controlled (co)polymerization of (functional) PAs there is a distinct paucity of reports describing the *controlled* polymerization of this important monomer class.

The first controlled, stereospecific, homopolymerization of PA by a group 9 metal complex was reported by Kishimoto and co-workers employing Rh1, Figure 1.^[2] PPAs were isolated in a near quantitative yield with measured dispersities ($\bar{D} = M_w/M_n$), as determined by size exclusion chromatography (SEC), spanning the range 1.06–1.29; NMR spectroscopy indicated high stereoselectivity with the resulting materials possessing the expected *cis-transoidal* conformation consistent with a 2,1-insertion mechanism. While the dispersity data and the ability to prepare block copolymers via sequential monomer addition (using an isolated PPA homopolymer with an active chain end) demonstrated the controlled nature of the polymerization, the initiation efficiency of Rh1, based on molecular weight data, was estimated to be between 33 and 56 %. The same group subsequently expanded upon this seminal contribution and reported the controlled polymerization of PA with Rh2,^[3] Figure 1. This tetracoordinate complex could not be isolated but was generated in situ in THF at room temperature from the reaction between [Rh(nbd)(OCH₃)₂]₂, PPh₃ and DMAP in the presence of PA. At a Rh/PA feed ratio of 1:50, polymerization proceeded rapidly yielding PPA with an M_n of 6,900, \bar{D} of 1.11 and the expected head-to-tail *cis-transoidal* configuration. While more efficient than Rh1, typical initiator efficiencies for Rh2 were still not quantitative and reported at ca. 72 %. However, the benefit of Rh2 lies in its ease of preparation, i.e. not

[a] Curtin Institute for Functional Molecules and Interfaces (CIFMI), Curtin University, Kent Street, Bentley, Perth, WA 6102, Australia
E-mail: andrew.b.lowe@curtin.edu.au
http://cifmi.curtin.edu.au

[b] School of Molecular and Life Sciences (MLS), Curtin University, Kent Street, Bentley, Perth, WA 6102, Australia

[c] Centre for Microscopy, Characterisation and Analysis (CMCA), M310, University of Western Australia, 35 Stirling Highway, Perth, WA 6009, Australia

[d] Curtin Institute for Computation (CIC), Curtin University, Kent Street, Bentley, Perth, WA 6102, Australia

[e] The Institute for Geoscience Research (TiGeR), Curtin University, Kent Street, Bentley, Perth, WA 6102, Australia

Supporting information and ORCID(s) from the author(s) for this article are available on the WWW under <https://doi.org/10.1002/ejic.201801411>.

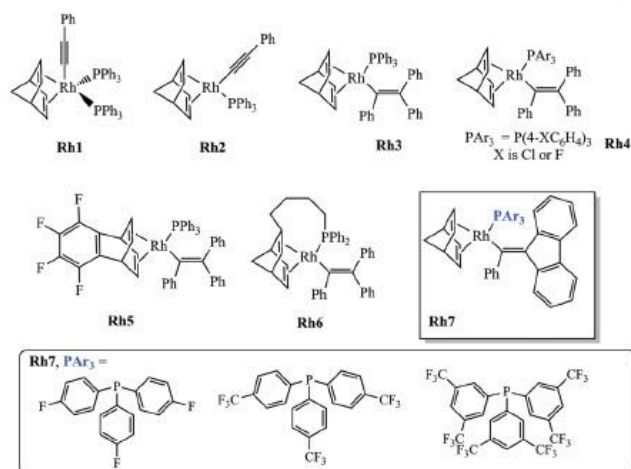


Figure 1. Chemical structures of Noyori's Rh^I-phenylethynyl derivatives (**Rh1** and **Rh2**), Masuda's Rh^I-triphenylvinyl species (**Rh3**–**Rh6**) and new fluororous α -phenylvinylfluorenyl-functional Rh^I complexes (**Rh7**).

requiring the use of a lithiated unsaturated species in its synthesis. A more detailed evaluation of the use of **Rh2** in controlled PA (co)polymerizations and simple *m*- and *p*-substituted PAs was subsequently described by Kishimoto et al.^[4]

Misumi and Masuda reported a novel ternary Rh catalyst system based on $[\text{Rh}(\text{nbd})\text{Cl}]_2$, PPh_3 and $\text{LiCPh}=\text{CPh}_2$ that was able to mediate the stereospecific controlled polymerization of PA with quantitative initiation (as judged by SEC). While the authors did not isolate the active catalytic species they noted that NMR spectroscopic data indicated the active species was **Rh3**, Figure 1.^[5] The authors also demonstrated the ability to introduce functional end-groups by substituting $\text{LiCPh}=\text{CPh}_2$ with $\text{LiCPh}=(4\text{-NMe}_2\text{C}_6\text{H}_4)_2$ in the ternary catalytic mixture. A more detailed examination of the ligand components in this system was subsequently reported by Misumi et al.^[6]

The first reported isolable Rh^I-vinyl complexes from this family of catalysts came from Miyake, Misumi and Masuda.^[7] Complexes **Rh4**, Figure 1, were isolated from mixtures of $[\text{Rh}(\text{nbd})\text{Cl}]_2$, $\text{LiCPh}=\text{CPh}_2$ and $\text{P}(4\text{-XC}_6\text{H}_4)_3$ (X = Cl or F), with the crystal structure of the Cl derivative reported. Both the Cl and F species mediated the polymerization of PA in a controlled fashion with added excess phosphine giving PPA with tunable molecular weights and \mathcal{D} 's as low as 1.05. Homopolymerizations of PA over the temperature range 15–60 °C in a range of solvents all proceeded smoothly.

Subsequently, Masuda and co-workers^[8] reported the controlled polymerization of PA with the tetrafluorobenzobarrelene derivative **Rh5**, Figure 1. **Rh5** could be generated and employed in situ as a ternary system composed of $[\text{Rh}(\text{tbf})\text{Cl}]_2$ (tbf: tetrafluorobenzobarrelene)/ $\text{Ph}_2\text{C}=\text{CPhLi}$ and PPh_3 , or **Rh5** could be isolated and employed as a well-defined catalytic species. In

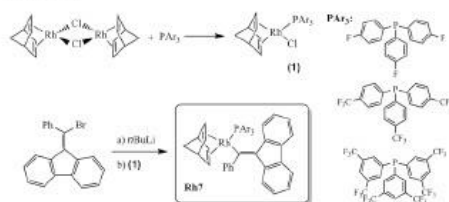
both cases PA polymerizations proceeded with near-quantitative initiation yielding well-defined materials with generally low \mathcal{D} 's. This was the first report of a ternary catalytic system and/or isolated Rh^I vinyl complex containing a diene ligand other than nbd that was effective for the polymerization of PA. A particularly salient feature of **Rh5** was its high activity, even at low concentrations, yielding high molecular weight polymer ($M_n = 401,000$), while still maintaining a low dispersity ($\mathcal{D} = 1.12$).

Rh6, in which the phosphine ligand is tethered to nbd, was reported by Onishi and co-workers.^[9] While active as an initiating species for PA it exhibited significantly reduced activity compared to **Rh3**–**Rh5** and was reported to have less than quantitative initiation efficiencies.

We have a long-standing interest in controlled polymerization processes that yield (co)polymers with low dispersities and interesting properties. Intrigued by the paucity of reported well-defined isolable Rh^I complexes able to mediate the (co)polymerization of PA effectively we recently established a program of research aimed at investigating the synthesis and application of new organo-Rh^I complexes based on the general Masuda structural motif with the aim of investigating the effect of the structure of the vinyl initiating fragment. Herein we detail our results regarding the synthesis of three new Rh^I- α -phenylvinylfluorenyl species bearing fluorine-functionalized phosphine ligands. Interestingly, while meeting the general structural requirements for such Rh^I species able to initiate the polymerization of PA quantitatively these new fluorenyl species exhibited markedly reduced efficiencies suggesting that the structural requirements of the vinyl ligand extend beyond simple substitution patterns^[6] to include geometric considerations.

Results and Discussion

Three new Rh^I- α -phenylvinyl complexes containing fluorenyl functionality on the β -vinyl carbon, in combination with fluorinated triarylphosphine ligands, were synthesized as outlined in Scheme 1.



Scheme 1. Outline for the synthesis of Rh(nbd)(CPh=Flu)P(4-FC₆H₄)₃ (**Rh7-F**), Rh(nbd)(CPh=Flu)P(4-CF₂C₆H₄)₃ (**Rh7-CF₂**) and Rh(nbd)(CPh=Flu)P[3,5-(CF₃)₂C₆H₃]₃ (**Rh7-(CF₃)₂**).

[Rh(nbd)Cl]₂ was first reacted with a fluorine functionalized triphenylphosphine of choice (P(4-FC₆H₄)₃, P(4-CF₂C₆H₄)₃ or P[3,5-(CF₃)₂C₆H₃]₃) to give intermediate tetra-coordinate Rh^I species [Rh(nbd)PAr₃Cl] (**1**). *n*BuLi-mediated lithiation of 9-[bromo(phenyl)methylene]-9H-fluorene followed by reaction with (**1**) gave the target Rh^I- α -phenylvinylfluorenyl-functional complexes [Rh7-X where X = F, CF₂ or (CF₃)₂ and refers to the nature of the fluorine species on the phosphine ligand]. In all instances the Rh^I-vinyl complexes were isolated as orange powders by a washing process with EtOH or in the case of Rh7-(CF₃)₂ by column chromatography, and subsequently recrystallized from CH₂Cl₂/pentane or CH₂Cl₂/methanol solvent mixtures. For all complexes, X-ray quality crystals were obtained facilitating solid-state structure determination, vide infra.

All complexes were characterized via a combination of techniques including multinuclear NMR spectroscopy (¹H, ³¹P, ¹⁹F, ¹⁰³Rh and 2D ³¹P-¹⁰³Rh/³¹P-¹⁰³Rh[¹⁰³Rh] HMQC), elemental analysis and X-ray crystallography. As a representative example, Figure 2 shows the ¹H, ³¹P{¹H}, and ¹⁹F spectra of Rh(nbd)(CPh=CFu)P(4-FC₆H₄)₃ (**Rh7-F**), measured in C₆D₆ with key identifying signals highlighted. Similar data for Rh7-CF₂ and Rh7-(CF₃)₂ verifying their structure, can be found in the Supporting Information. The full ¹H NMR spectrum is given at the top in Figure 2A with an expansion of the aromatic region (plotted between δ = 8.0 and 6.4 ppm) given directly below. In the full spectrum we observe a distinct signal at δ = 9.24 ppm, which appears as a doublet, assigned to a single H labelled A, that is associated with the fluorenyl functional group. The remaining labelled peaks (B, C, D, and E) can be assigned to the norbornadiene ligand, see structure at bottom of Figure 2. All peaks integrate in the expected ratio.

The ¹H NMR spectrum covering the region δ = 8.0–6.4 ppm is complex, Figure 2B. It is within this region that signals associated with the remaining 24 aromatic H's appear, i.e. those present on the phosphine ligand, the α -phenylvinyl group and the remaining fluorenyl H's. However, all signals integrate in the expected ratio, confirming the structure. The ³¹P{¹H} NMR spectrum of Rh7-F is shown in Figure 2C. A set of doublets is

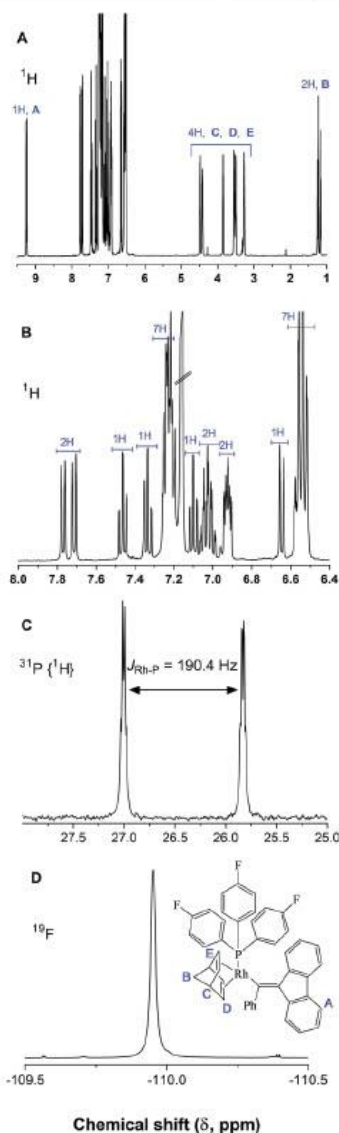


Figure 2. NMR spectra, recorded in C₆D₆, of Rh(nbd)(CPh=CFu)P(4-FC₆H₄)₃ (**Rh7-F**). (A) The full ¹H NMR spectrum with key peaks highlighted and the measured integral values included; (B) the ¹H NMR spectrum covering the aromatic region from δ = 8.0 to 6.4 ppm; (C) the ³¹P{¹H} NMR spectrum with the rhodium-phosphorus coupling constant noted; and (D) the ¹⁹F NMR spectrum with the structure of the complex shown inset.

observed arising from coupling between Rh and P, with signals centered at ≈ 27.0 and 25.8 ppm with a corresponding $^1J_{\text{Rh-P}}$ value of 190.4 Hz. This differs from the Masuda derivative, $\text{Rh}(\text{nbdc})\text{CPh}=\text{CPh}_2(\text{PPh}_3)$, as reported by Kumazawa et al.,^[10] in which the $^{31}\text{P}\{^1\text{H}\}$ NMR spectrum presents as a pair of doublets at 26.9 and 26.3 ppm and ambient temperature (measured in d_6 -toluene) with $^1J_{\text{Rh-P}}$ coupling constants of 183 and 187 Hz; this observation was attributed to the presence of two conformational isomers as determined by variable temperature NMR with the two sets of peaks coalescing at 89 °C. However, both the chemical shifts and coupling constant of **Rh7-F** are consistent with previously reported values for Rh-vinyl complexes with a single phosphine ligand for our target application. The ^{19}F NMR spectrum, Figure 2D, shows a sharp singlet at $\delta = -109.95$ ppm (along with ^{13}C satellites arising from ^{13}C - ^{19}F coupling^[11]). Rhodium has one NMR-active spin $-1/2$ nucleus, ^{103}Rh , which is 100 % abundant. While direct observation of ^{103}Rh is possible, as we demonstrate, it suffers from low sensitivity and a large chemical shift range (of ca. 12,000 ppm). An alternative to direct observation is the application of a 2D polarization transfer technique, such as heteronuclear multiple quantum coherence (HMQC). In such experiments the sensitivity of the ^{103}Rh nuclei can be enhanced considerably if bonded to a nucleus with a high gyromagnetic ratio such as ^{31}P (by a factor of almost 600), ^{19}F or ^1H , facilitating more ready detection of the ^{103}Rh nuclei.^[12] In the case of **Rh7-F** and **Rh7-CF₃** we were able to prepare sufficiently concentrated solutions to directly measure the ^{103}Rh spectra. Figure 3A shows the ^{103}Rh spectrum of **Rh7-F** while 3B shows that of **Rh7-CF₃**. In the case of the former, a doublet is observed centered at $\delta = -7862$ ppm, that arises due to coupling with ^{31}P . The absolute value of the $^1J_{\text{Rh-P}}$ coupling constant was determined to be 190.4 Hz, consistent with the value measured by ^{31}P NMR, vide supra. A similar observation was made for **Rh7-CF₃** with the doublet centered around $\delta = -7870$ ppm with a corresponding $^1J_{\text{Rh-P}}$ coupling constant of 188.8 Hz. We were unable to measure the ^{103}Rh spectrum of **Rh7-(CF₃)₂** in a reasonable timeframe but noted the $^1J_{\text{Rh-P}}$ coupling constant of 198.6 Hz. We were, however, able to readily acquire the ^{31}P - ^{103}Rh HMQC spectrum in CD_2Cl_2 , Figure 3C, giving a ^{103}Rh chemical shift of -7861 ppm and a coupling constant comparable to that determined using ^{31}P NMR spectroscopy. It is known that the ^{103}Rh chemical shift is sensitive to changes in coordination environment, geometry, solvent and temperature.^[12d] The ^{103}Rh chemical shifts for **Rh7-F**, **Rh7-CF₃** and **Rh7-(CF₃)₂** differ by less than 10 ppm, which is consistent with the similarities observed in the metal coordination geometries in the solid state. Furthermore, it appears that the changes in the fluorination pattern of the phosphine ligand do not appreciably alter the electronic environment about the Rh metal center.

While crystal structures of the derivatives $\text{Rh}(\text{nbdc})(\text{CPh}=\text{CPh}_2)\text{PPh}_3$ and $\text{Rh}(\text{nbdc})(\text{CPh}=\text{Ph}_2)\text{P}(4\text{-ClC}_6\text{H}_4)_2$ have been reported,^[7,10] Miyake, Misumi and Masuda noted that they were unable to obtain X-ray quality crystals for the analogous fluorine derivative, $\text{Rh}(\text{nbdc})(\text{CPh}=\text{Ph}_2)\text{P}(4\text{-FC}_6\text{H}_4)_2$.^[7] In contrast, we were able to readily crystallize each of these new fluorine functionalized Rh- α -phenylvinylfluorenyl complexes, enabling the

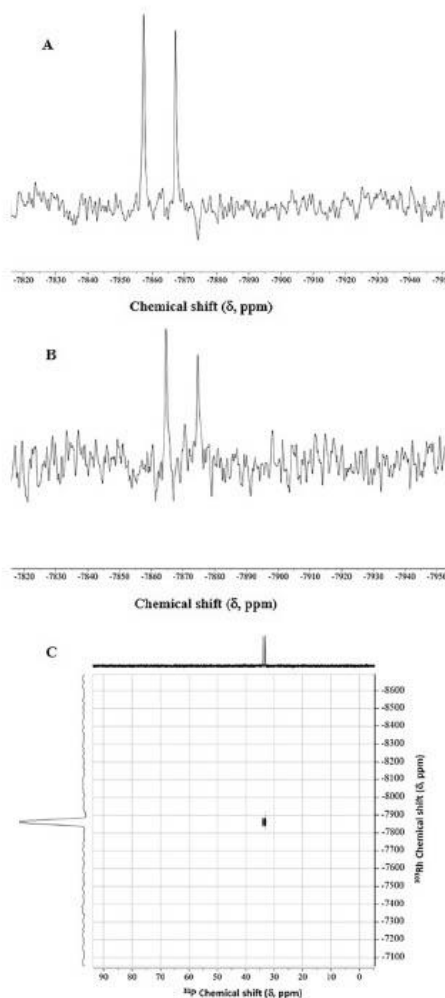


Figure 3. (A) ^{103}Rh NMR spectrum of **Rh7-F**, recorded in C_6D_6 at 298 K; (B) ^{103}Rh NMR spectrum of **Rh7-CF₃**, recorded in CD_2Cl_2 at 298 K; (C) ^{31}P - ^{103}Rh HMQC spectrum of **Rh7-(CF₃)₂** recorded in CD_2Cl_2 at 298 K.

solid-state structures to be determined. Figure 4 shows the X-ray crystal structures obtained for **Rh7-F** and **Rh7-CF₃**; the crystal structure of **Rh7-(CF₃)₂** is given in the Supporting Information. All three complexes have similar solid-state structures adopting a distorted square-planar geometry, consistent with the crystal structures reported for the Masuda derivatives.

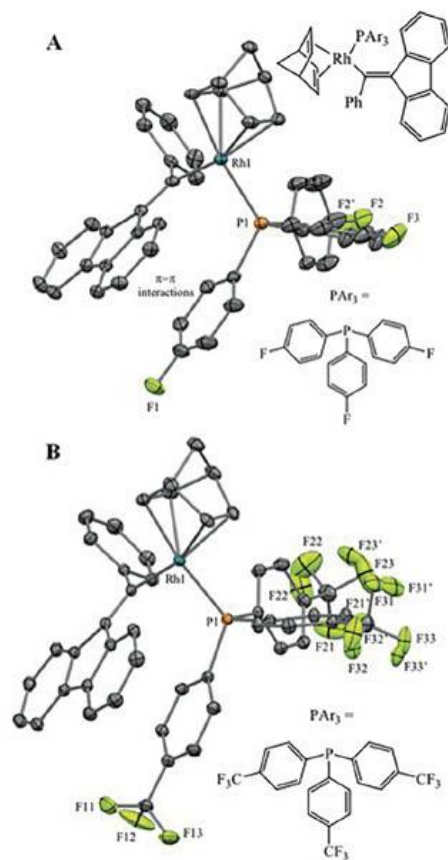


Figure 4. ORTEP representations of the X-ray crystal structures of **Rh7-F** (A) and **Rh7-CF₃** (B) with 50% probability ellipsoids and H atoms omitted for clarity. All bond lengths are given in the Supporting Information.

There are two structural differences between these α -phenylvinylfluorenyl derivatives and the Masuda-type triphenylvinyl analogues. Firstly, the fluorenyl group is conformationally locked and is coplanar with the vinyl bond – such a geometric restriction is not present in the Masuda species with both β -phenyl groups able to freely rotate (the reported crystal structures for **Rh(nbd)(CPh=CPh₂)(PPh₃)** and **Rh(nbd)(CPh=CPh₂)P(4-ClC₆H₄)₃** are shown in the Supporting Information^[7]). Secondly, there is the apparent presence of through-space π - π interactions, at least in the solid state, between the fluorenyl ring and one of the aromatic rings of the phosphine ligand (centroid-centroid distances, interplanar angles: **Rh7-F**, 3.60 Å, 9.65 °; **Rh7-(CF₃)₂**, 3.55 Å, 9.39 °). The presence of these interactions is

supported, at least in part, by gas-phase modeling, vide infra. In all three **Rh7-X** crystal structures we observe positional disorder associated with the fluorine functionality, (F2 and F2') in **Rh7-F** and two of the three CF₃ groups (the F2 and F3 designated species) in **Rh7-CF₃**, Figure 4. Such disorder is not uncommon and can be especially prevalent in species with *tert*-butyl and/or CF₃ functional groups, with the highly symmetrical nature of such functional groups coupled with the relatively low energy barrier for rotation about their threefold symmetry axes the principle cause of the observed disorder.^[13]

The structure and presence of through-space π - π interactions between the fluorenyl functional group and one aromatic group associated with the phosphine ligand was supported by molecular modeling. For example, Figure 5, shows the energy-minimized, gas-phase, modeled geometry of **Rh7-CF₃** and is clearly almost identical to the X-ray crystal structure (phosphine ligand binding energy, ignoring solvent effects was determined to be -31.0 kcal/mol).

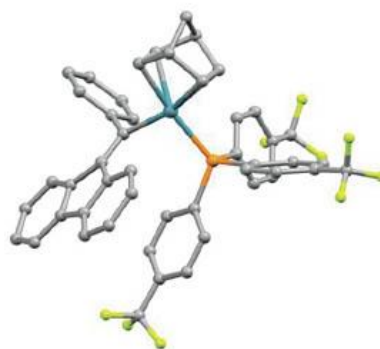
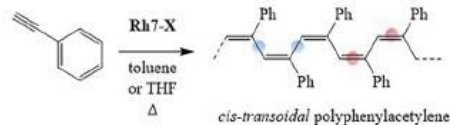


Figure 5. Energy-minimized, gas-phase molecular geometry of **Rh(nbd)(CPh=CFlu)P(4-CF₃C₆H₄)₂** (**Rh7-CF₃**). The corresponding modeled geometry for **Rh7-F** is given in the Supporting Information.

With three new fluorine functional Rh^I- α -phenylvinyl-fluorenyl complexes successfully prepared and characterized we evaluated their efficacy as initiators in the stereospecific (co)-polymerization of phenylacetylene (PA), Scheme 2.



Scheme 2. The homopolymerization of phenylacetylene yielding highly stereoregular polyphenylacetylene with *cis-transoidal* configuration.

Initially we examined the homopolymerization of PA with the Masuda derivative **Rh-4** (X = F) under conditions identical to those reported in the literature (toluene as solvent, $T = 30$ °C, [Rh] = 2.0 mM, [PA] = 0.50 mM, [Rh]/[P] = 1/5, and polymerization time = 60 min.)^[7] to confirm the efficiency and effective-

Table 1. Summary of PA polymerization conditions with **Rh7-F**, **Rh7-CF₃** and **Rh7-(CF₃)₂**, SEC-measured molecular weights and dispersities, initiation efficiencies and NMR measured *cis* contents in the resulting polyphenylacetylene (co)polymers.

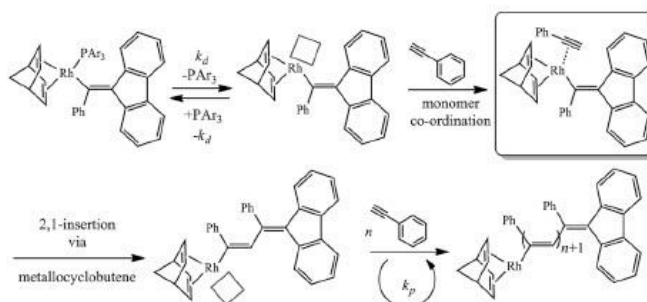
Entry	Rh species	[P]/[Rh]	Polym. Temp. [°C]	Polym. solvent	Theoretical MW ^[a]	M _n [SEC] ^[b]	M _w [SEC] ^[b]	Dispersity [D] ^[b]	Rh initiation efficiency ^[c]	<i>cis</i> content [%] ^[d]
1	Rh4-F	5	30	toluene	25,000	24,500	25,500	1.04	1.00	96
2	Rh4-F	5	30	toluene	9,300	9,100	9,500	1.04	1.00	nd ^[e]
3	Rh7-F	5	30	toluene	10,000	62,800	65,000	1.03	0.16	78
4	Rh7-F	5	40	toluene	9,300	71,000	83,500	1.18	0.13	94
5	Rh7-F	5	50	toluene	9,300	59,500	73,500	1.24	0.16	90
6	Rh7-F	5	60	toluene	9,300	49,000	62,500	1.27	0.19	88
7	Rh7-F	20	60	toluene	9,300	35,900	50,100	1.39	0.26	85
8	Rh7-CF₃	5	30	toluene	9,300	47,900	63,000	1.31	0.19	90
9	Rh7-(CF₃)₂	5	30	THF	9,300	16,500	20,100	1.21	0.56	96
10	Rh7-F	5	30	THF	9,000	19,600	25,500	1.30	0.46	94
11	Rh7-F	5	40	THF	9,000	35,100	43,200	1.23	0.26	92
12	Rh7-F	10	40	THF	9,300	27,300	34,100	1.25	0.34	92
13	Rh7-F	20	40	THF	9,300	18,600	24,100	1.30	0.50	95
14	Rh7-F	10	50	THF	9,300	24,400	41,900	1.22	0.27	92
15	Rh7-F	20	50	THF	9,300	45,800	48,900	1.07	0.20	92

[a] Calculated as M_n = mass (g) monomer/mol of **Rh7-X** and assuming 100% initiation efficiency. [b] As measured by size exclusion chromatography: eluent THF operated at a flow rate of 1.0 mL/min, instrument calibrated with narrow molecular weight distribution polystyrene standards. Dispersity (D) = M_w/M_n. [c] Calculated from the ratio of theoretical to measured (SEC determined) M_n's. [d] As determined by ¹H NMR spectroscopy according to ref^[14] [e] Not determined.

ness of the experimental approach adopted. Under these conditions the resulting PPA has a theoretical M_n of 25,000 at 100% monomer conversion. SEC analysis of the isolated PPA gave an experimentally determined M_n of 24,500, M_w of 25,500 and a corresponding D of 1.04, entry 1 Table 1. ¹H NMR spectroscopic analysis of the obtained PPA indicated that it was highly stereoregular with a calculated^[14] *cis* content of 96%. A second control experiment was conducted targeting a lower PPA MW (M_{n,theor} of 9,300 at quantitative conversion) to confirm the ability to tune MW. This yielded PPA with an SEC-measured M_n of 9,100 and corresponding D of 1.04, Table 1 entry 2.

Subsequently we examined the initiating ability/efficiency of **Rh7-F** under identical conditions to those employed above for **Rh4-F**, Table 1 entry 3. Interestingly, while **Rh7-F** was active it exhibited a low initiation efficiency of ca. 0.16 (based on the molecular weight as determined by SEC) although did yield highly stereoregular PPA with a low dispersity. The low activity is surprising; however, Misumi and co-workers^[9] reported that

changing the substitution pattern on the vinyl group in ternary systems of [Rh(nbd)Cl]₂/vinyl-Li/PPH₃ had a significant effect on the initiation efficiency of the in situ-generated initiating species with values dropping from near quantitative for triphenylvinyl lithium to values more typically in the range 0.2–0.3 even for similar species such as (1,2-diphenylvinyl)lithium, while still maintaining a generally low dispersity. This was proposed to be a direct result of the stability of the vinyl-Li species generated in such ternary systems (with the triphenylvinyl Li species being optimal) and, presumably, the subsequent formation of the actual catalytically active species. However, in these isolated fluorenyl derivatives the low activity cannot be rationalized in terms of the stability of a vinyl-Li species. The low efficiency could, conceivably, be caused by various factors including catalyst decomposition in solution (although this is not consistent with observations regarding **Rh4-X**) but is more likely a result of the energetics associated with the initiation process. The initiation step in such co-ordination polymerization processes is the stage



Scheme 3. The sequence of steps resulting in the formation of polyphenylacetylene from the precursor catalyst/initiator **Rh7-X**.

in which the catalyst (or precatalyst) is converted into the active propagating species. The sequence of processes leading to the formation of PPA is shown in Scheme 3. In solution, Rh7-X becomes "activated" by phosphine ligand dissociation (a reversible process) with an associated rate constant, k_d , resulting in a Rh species with a vacant co-ordination site. In the presence of (excess) PA, the monomer will co-ordinate and undergo a 2,1-insertion into the Rh- α -phenyl carbon bond. The net result of these three processes is chain initiation, and in the presence of excess PA propagation, i.e. chain growth, will ensue.

Since phosphine ligand dissociation and subsequent PA co-ordination is assumed to be rapid, we hypothesize that the low efficiency of the Rh7-X species is associated with the first (perhaps also second) monomer insertion into the Rh-C bond, although such insertions of PA into a Rh-sp² hybridized carbon bond have been reported to be facile.^[15] We propose that the bulky, and conformationally locked, fluorenyl functionality sterically hinders efficient insertion. While 2,1-insertion is the well-established mode of propagation in such polymerizations, theoretical studies suggest that a transition state in which conjugative insertion occurs is energetically favored. This requires the phenyl group of PA to locate on the square planar face of the Rh complex and be coplanar with the PA C=C and the Rh atom.^[15] This may be hindered in these fluorenyl derivatives. However, once PA insertion has occurred subsequent insertions become more energetically favorable as the fluorenyl group moves further away from the active site, the conjugation length increases and, as noted by Onishi et al., the presence of through space electron donation from the phenyl group to the Rh center helps to stabilize the co-ordinatively unsaturated Rh species.^[9] If this proposal is correct then it suggests that a similar level of activity would likely be observed for the Rh7-CF₃ and Rh7-(CF₃)₂. Indeed, for Rh7-CF₃-mediated homopolymerization of PA under the same conditions (Table 1 entry B), the isolated PPA had an SEC-measured M_n of 47,900 (an initiation efficiency of 0.19) with a corresponding \bar{D} of 1.31.

Miyake, Misumi and Masuda^[7] noted that PA homopolymerizations with Rh4-F proceeded smoothly over the temperature range 30–60 °C. In an effort to improve the initiation efficiencies we further examined Rh7-F under conditions noted above except polymerizations were performed at 40, 50 and 60 °C, Table 1 entries 4–6. While an improvement is observed with increasing temperature (initiation efficiency increases from 0.13 at 40 °C to 0.16 at 50 °C and 0.19 at 60 °C) it is still not quantitative and represents only marginal improvements over homopolymerization at 30 °C. There also appears to be an undesirable effect on the dispersity and stereoregularity with increasing polymerization temperature – the former increases from 1.18 to 1.27 and the latter decreases from 94 % to 88 %.

In the same article, the authors reported that the homopolymerization of PA with Rh4 was essentially unaffected by the nature of the polymerization solvent with polymerizations proceeding in a controlled fashion with (near) quantitative initiation efficiencies to give polymers with low dispersities. The only observed effect was related to the kinetics of polymerization with rates falling marginally with increasing dielectric constant of the reaction medium. We subsequently examined PA homo-

polymerizations with Rh7-F in THF, Table 1 entries 10–15. Broadly, the use of THF resulted in higher initiation efficiencies with values spanning the range 0.26–0.50 and increased stereoregularity with *cis* contents as high as 95 %. In the case of polymerizations performed at 40 °C we observed a near doubling of the initiation efficiency when 20 equivalents of free phosphine vs. five were employed albeit at the expense of slightly broader molecular weight distributions. These results suggest that in contrast to the Masuda-type triphenylvinyl derivatives, the polymerization solvent does impact the level of control for PA polymerizations mediated by the fluorenyl derivatives. Next, we conducted a single PA homopolymerization with Rh7-(CF₃)₂ in THF at 30 °C with five equivalents of added free phosphine, Table 1 entry 9. Of all the conditions examined this polymerization proceeded with the highest initiation efficiency (0.56) and yielded the most stereoregular product with a measured *cis* content of 96 %.

While the initiation efficiencies of the Rh7-X complexes were less than quantitative the highly stereoregular nature of the products, their high yields and low dispersities do suggest controlled polymerization. One key feature indicative of a controlled polymerization process is the ability to prepare AB diblock copolymers (or more advanced architectures) by sequen-

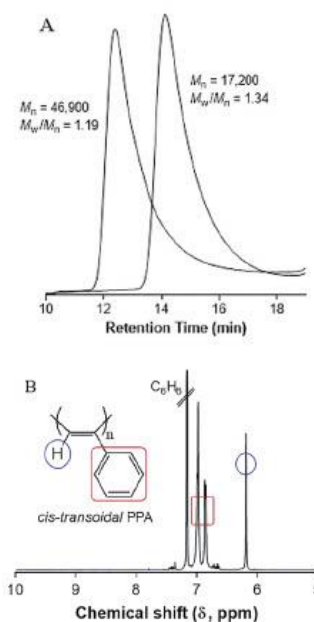


Figure 6. (A) SEC traces (RI signal), measured in THF, of a self-blocked PPA demonstrating retention of active chain ends; (B) ¹H NMR spectrum, recorded in *d*₆-benzene of the final, isolated "block" copolymer highlighting the stereoregular structure as evidenced by the sharp singlet at $\delta = 6.19$ ppm that is attributed to the backbone hydrogen in a *cis* conformation.

tial monomer addition; successful blocking, ideally quantitatively, confirms retention of active chain ends. To examine this feature we performed a self-blocking experiment in which PA was initially homopolymerized in THF at 40 °C in the presence of Rh7-F and 20 equivalents of free phosphine. After 1 h, an aliquot was withdrawn and analyzed by SEC, Figure 6A, with the formed PPA having a measured M_n just over 17,000 and a corresponding \bar{D} of 1.34. Subsequently, a second charge of PA was added to the vessel and the polymerization allowed to proceed for a further 60 min. Termination with acetic acid and isolation by precipitation yielded a final material with an SEC-measured M_n of 46,900 and \bar{D} of 1.19. Importantly, we observe a clear shift in the chromatograms to lower retention time (higher molecular weight) after the addition and polymerization of the second batch of monomer with little, if any, evidence of homopolymer impurity. This confirms retention of active chain ends after the initial homopolymerization of the first batch of PA and also indicates near-quantitative "reinitiation" following the addition of the second charge of monomer; both features are consistent with a controlled polymerization process. Consistent with the prior polymerizations, the isolated material was highly stereoregular with a calculated *cis* content of 96 %. The ^1H NMR spectrum, recorded in C_6D_6 , of the isolated PPA is shown in Figure 6B. The highly regular structure is confirmed by the presence of the sharp singlet at $\delta = 6.19$ ppm coupled with the two sharp resonances at ca. 6.9–7.0 ppm. The former is attributed to the backbone H in a *cis* conformation while the latter are the aromatic hydrogens on the phenyl ring. This is completely consistent with previous reports in which, for example, the presence of any significant *trans* backbone H's results in very significant broadening in the aromatic region.^[14]

Conclusions

Herein we have described the synthesis of three new rhodium(I)- α -phenylvinyl complexes containing various fluorine-functional triarylphosphine ligands. All complexes have been characterized in detail via a combination of NMR spectroscopy (^1H , ^{19}F , ^{31}P , ^{102}Rh , ^{31}P - ^{102}Rh HMQC and ^{31}P - ^{102}Rh HMQC), elemental analysis, and X-ray crystallography. All new species have similar solid-state structures, the general square-planar geometry of which was confirmed by modeling. The complexes were examined as initiators for the stereoregular polymerization of phenylacetylene (PA) with an emphasis on Rh(nbd)(CPh=CFlu)P(4-FC₆H₄)₃ (Rh7-F). All Rh species were active as initiators, yielding polyphenylacetylene with *cis* contents as high as 96 % although initiation efficiencies spanned the range 0.13–0.56 and were dependent on the reaction conditions. The variable activity of these fluorenyl derivatives, as a function of polymerization conditions, was largely unexpected but clearly demonstrates the need to examine new rhodium(I) vinyl species in more detail for this particular target application.

Experimental Section

Materials: *n*-Butyllithium (*n*BuLi, 1.6 M solution in hexane, Sigma-Aldrich), 9-[bromo(phenyl)methylene]-9H-fluorene, (C₁₂H₉)C=CPhBr

(Flu=CPhBr, Matrix Scientific, 95 %), [Rh(nbd)Cl]₂ (nbd = 2,5-norbornadiene, 98 %, Strem Chemicals), tris(*para*-fluorophenyl)phosphine (P(4-FC₆H₄)₃, 98 %, Aldrich), tris(*para*-trifluoromethylphenyl)phosphine (P(4-CF₃C₆H₄)₃, 97 %, Aldrich), and tris[3,5-bis(trifluoromethyl)phenyl]phosphine (P(3,5-(CF₃)₂C₆H₃)₃, 97 %, Strem Chemicals), were used as received. Phenylacetylene (CH=CPh, 98 % Aldrich) was purified by passage over a column of basic alumina and then stored in a fridge until needed. The Masuda complex^[7] Rh(nbd)(CPh=CPh₂)P(4-FC₆H₄)₃ was prepared as detailed below for Rh7-F except triphenylbromoethylene was used in place of Flu=CPhBr.

THF, diethyl ether and CH₂Cl₂ were dried using a PureSolv MD5 solvent purification system (Innovative Technology, Inc.), collected, degassed via the freeze-pump-thaw technique and stored under dry nitrogen until needed. Toluene (99.8 %, Sigma-Aldrich) was degassed via the freeze-pump-thaw technique and stored under dry nitrogen until needed.

All glassware was pre-dried in an oven at 50 °C and flame dried under vacuum prior to use. All reactions were performed using standard Schlenk line techniques.

Rhodium Complexes Rh7

Synthesis of Rh(nbd)(CPh=CFlu)P(4-FC₆H₄)₃: The target complex was prepared according to the method of Miyake et al.^[9] To a round bottomed flask equipped with a Teflon-coated magnetic stir-bar was added Flu=CPhBr (333 mg, 1.0 mmol) and diethyl ether (20.0 mL) under a dry nitrogen atmosphere. The flask was cooled to 0 °C and *n*BuLi (1.6 M solution in hexane, 1.25 mL, 2.0 mmol) was cannula transferred and the mixture allowed to react for 30 min yielding Flu=CPhLi. To a separate round bottomed flask equipped with a magnetic stir-bar containing dry toluene (15.0 mL) was added [Rh(nbd)Cl]₂ (92.2 mg, 0.2 mmol) and P(4-FC₆H₄)₃ (253 mg, 0.8 mmol). The mixture was then stirred vigorously for 15 min at ambient temperature yielding the intermediate Rh species, Rh(nbd)ClP(4-FC₆H₄)₃.

The lithiated species, Flu=CPhLi, was added, via cannula, to the solution containing Rh(nbd)ClP(4-FC₆H₄)₃ and allowed to stir at ambient temperature for 1 h. Subsequently the reaction solution was cannula transferred and filtered through a short plug of neutral activated alumina 90, under an inert atmosphere, to give a clear orange solution. Solvents were removed under high vacuum on a Schlenk line yielding a dark colored viscous liquid. To this crude product was added ethanol (25.0 mL) and the mixture stirred vigorously for 30 min. during which time an orange precipitate formed. The precipitate was collected via a Hirsch funnel and washed with a small amount of additional ethanol. The Rh^I complex Rh(nbd)(CPh=CFlu)P(4-FC₆H₄)₃ (Rh7-F) was isolated by recrystallization from CH₂Cl₂/*n*-pentane employing a solvent layering technique. Yield: 46 %. Anal. Calcd. for C₄₃H₃₃F₃Rh: C, 70.69 %; H, 4.35 %; found C, 70.38 %; H, 4.07 %. ^1H NMR (400.1 MHz, C₆D₆) δ (ppm): 9.24 (dd, $J = 7.4, 1.1$ Hz, 1H), 7.77 (dt, $J = 7.5, 1.0$ Hz, 1H), 7.71 (dt, $J = 7.4, 0.9$ Hz, 1H), 7.46 (td, $J = 7.4, 1.1$ Hz, 1H), 7.33 (td, $J = 7.4, 1.1$ Hz, 1H), 7.26–7.19 (m, 7H), 7.10 (td, $J = 7.4, 1.0$ Hz, 1H), 7.07–6.98 (m, 2H), 6.92 (dddd, $J = 7.3, 4.3, 2.9, 1.2$ Hz, 2H), 6.67–6.63 (m, 1H), 6.60–6.50 (m, 7H), 4.51–4.38 (m, 2H), 3.84 (td, $J = 3.8, 1.9$ Hz, 1H), 3.56–3.48 (m, 2H), 3.30–3.24 (m, 1H), 1.24 (dt, $J = 8.2, 1.6$ Hz, 1H), 1.19–1.14 (m, 1H). ^{31}P NMR (162.0 MHz, C₆D₆) δ (ppm): 25.8 (d, $J = 190.4$ Hz). ^{19}F NMR (376.5 MHz, C₆D₆) δ (ppm): –109.9 (s). ^{102}Rh NMR (19.1 MHz, C₆D₆, 25 °C) δ (ppm): –7862 (d, $J = 190.4$ Hz).

Synthesis of Rh(nbd)(CPh=CFlu)P(4-CF₃C₆H₄)₃: The target complex was prepared as detailed above for Rh7-F except P(4-FC₆H₄)₃ was replaced with P(4-CF₃C₆H₄)₃. The Rh^I complex Rh(nbd)(CPh=C

(CFu)P(4-FC₆H₄)₂ (Rh7-CF₂) was isolated by recrystallization from CH₂Cl₂/n-pentane. Yield 88%. Anal. Calcd for C₄₈H₃₃F₉PRh: C, 63.03%; H, 3.64%; found C, 62.03%; H, 3.57%. ¹H NMR (400.1 MHz, CD₂Cl₂) δ (ppm): 8.76 (dt, *J* = 7.3, 0.8 Hz, 1H), 7.85–7.75 (m, 1H), 7.75–7.68 (m, 1H), 7.56 (dt, *J* = 7.5, 0.9 Hz, 1H), 7.47 (dt, *J* = 7.5, 0.9 Hz, 1H), 7.43–7.37 (m, 6H), 7.37–7.33 (m, 5H), 7.32–7.27 (m, 1H), 7.23 (td, *J* = 7.4, 1.1 Hz, 1H), 7.13 (tt, *J* = 7.4, 1.3 Hz, 1H), 7.02 (qd, *J* = 7.5, 1.3 Hz, 2H), 6.81 (dt, *J* = 7.6, 1.6 Hz, 1H), 6.74 (ddd, *J* = 8.4, 7.2, 1.2 Hz, 1H), 6.33 (dt, *J* = 7.9, 1.5 Hz, 1H), 6.09 (dd, *J* = 7.9, 0.9 Hz, 1H), 4.56 (qd, *J* = 3.7, 1.8 Hz, 1H), 4.43–4.39 (m, 1H), 4.15 (dq, *J* = 3.6, 1.9 Hz, 1H), 3.93 (tq, *J* = 3.3, 1.6 Hz, 1H), 3.78–3.72 (m, 2H), δ 1.56 (dt, *J* = 8.3, 1.5 Hz, 1H), 1.47–1.43 (m, 1H); ³¹P{¹H} NMR (162.0 MHz, C₆D₆, 25 °C) δ (ppm): 29.2 (d, *J* = 188.8 Hz). ¹⁹F NMR (376.5 MHz, C₆D₆, 25 °C) δ (ppm): –62.84 (s). ¹⁰³Rh NMR (19.1 MHz, CD₂Cl₂, 25 °C) δ (ppm): –7870 (d, *J* = 188.8 Hz).

Synthesis of Rh(nbd)(CPh=CFlu)P[3,5-(CF₃)₂C₆H₃]₂: The target complex was prepared as detailed above for Rh7-F except P(4-FC₆H₄)₂ was replaced with P[3,5-(CF₃)₂C₆H₃]₂. The Rh^I complex Rh(nbd)(CPh=CFlu)P[3,5-(CF₃)₂C₆H₃]₂ (Rh7-(CF₃)₂) was purified by recrystallization from CH₂Cl₂/methanol via a solvent layering technique. Yield 25%. Anal. Calcd. for C₅₁H₃₀F₁₈PRh: C, 54.76%; H, 2.70%; found C, 54.12%; H, 2.60%. ¹H NMR (400.1 MHz, C₆D₆) δ (ppm): 8.43 (d, *J* = 7.2 Hz, 1H), 8.11 (dd, *J* = 12.2, 1.6 Hz, 1H), 7.94 (s, 6H), 7.62–7.58 (m, 2H), 7.55 (s, 3H), 7.49 (d, *J* = 7.4 Hz, 1H), 7.45 (dt, *J* = 7.6, 1.0 Hz, 1H), 7.33 (td, *J* = 7.6, 1.2 Hz, 1H), 7.09–7.03 (m, 1H), 6.99 (td, *J* = 7.6, 1.2 Hz, 1H), 6.88 (dt, *J* = 7.7, 1.6 Hz, 1H), 6.82 (td, *J* = 7.7, 1.2 Hz, 1H), 6.57 (d, *J* = 7.9 Hz, 1H), 6.44 (dd, *J* = 7.7, 1.6 Hz, 1H), 4.35 (d, *J* = 4.6 Hz, 1H), 4.32–4.28 (m, 1H), 3.43 (d, *J* = 4.6 Hz, 1H), 3.40 (s, 2H), 3.27 (s, 1H), 1.12 (dt, *J* = 8.5, 1.6 Hz, 1H), 1.05 (dd, *J* = 8.5, 1.7 Hz, 1H). ³¹P{¹H} NMR (162.0 MHz, C₆D₆) δ (ppm): 33.08 (d, *J* = 198.6 Hz). ¹⁹F NMR (376.5 MHz, C₆D₆) δ (ppm): –62.92 (s). ¹⁰³Rh NMR (19.1 MHz, CD₂Cl₂, 25 °C) δ (ppm): –7861 (determined indirectly by HMQC).

Modeling: The geometry of the complexes obtained by single-crystal X-ray crystallography were relaxed in vacuo using the 6-311G** basis set of the light atoms while Rh was treated with the Stuttgart-Dresden effective core potential.^[16] The vibrational frequencies have been calculated to ensure that the final configuration was a stable minimum. The final relaxed geometries were then employed to calculate the bonding energies using the triple-zeta Dunning's correlation consistent basis sets (cc-pVTZ),^[17] the counterpoise correction was also included.^[18]

Polymerizations: All (co)polymerizations were carried out under a dry nitrogen atmosphere in a pre-dried Schlenk flask.

Homopolymerization of Phenylacetylene: Below is given a typical procedure for the homopolymerization of phenylacetylene with a Rh^I-vinyl catalyst.

A solution of phenylacetylene (0.184 g, 1.80 mmol) in THF or toluene (2.5 mL) was added to a solution of Rh catalyst (0.015 g, 0.02 mmol) and free additional phosphine – P(4-FC₆H₄)₂ in the case of Rh(nbd)(CPh=CFlu)P(4-FC₆H₄)₂ for example (0.031 g, 0.10 mmol) dissolved in THF or toluene (2.5 mL) in a Schlenk flask equipped with a magnetic stir bar. The flask was immersed in a pre-heated oil bath set at 30 °C and allowed to react for 1 hour after which the polymerization was stopped via the addition of a small volume of acetic acid. The polymer was isolated by precipitation into a large volume of methanol, filtered by gravity filtration and dried to constant weight in a vacuum oven at 40 °C overnight.

Multistage Self-blocking of Polyphenylacetylene with Phenylacetylene: A solution of phenylacetylene (0.184 g, 1.80 mmol) in

THF (2.5 mL) was added to a solution of Rh catalyst (0.015 g, 0.02 mmol) and free additional phosphine – P(4-FC₆H₄)₂ in the case of Rh(nbd)(CPh=CFlu)P(4-FC₆H₄)₂ for example (124 mg, 0.39 mmol) in THF (2.5 mL) in a Schlenk flask immersed in a pre-heated oil-bath set at 40 °C. After 1 hour an aliquot was withdrawn (1.0 mL) and the polymer isolated by precipitation into methanol (20 mL) containing a small amount of acetic acid. Then, a second feed of phenylacetylene (0.184 g, 1.80 mmol) in THF (2.5 mL) was added to the remaining polymerization solution and “block” copolymerization allowed to proceed for 1 hour. Subsequently the polymerization was quenched with acetic acid and the “copolymer” precipitated into a large volume of methanol. The copolymer was isolated by filtration and dried to a constant weight in vacuo.

NMR Spectroscopic Measurements: ¹H, ³¹P, and ¹⁹F NMR spectra were recorded at 298 K on a Bruker Avance 400 spectrometer. The data were processed with Bruker's TopSpin 3.1 software. ¹⁰³Rh NMR was acquired at 298 K on a Bruker Avance IIIHD (600 MHz for ¹H) at 19.1 MHz using a commercial 5 mm triple resonance broadband probe (doubly tuned ¹H/³¹P outer coil, with inner broadband coil) with 90° pulses of 27.5 μs and 18.4 μs for ¹⁰³Rh and ³¹P respectively. ¹⁰³Rh chemical shifts, δ, are given in ppm relative to Ξ = 3.186447^[19] (as an aide to the reader, the chemical shifts for the commonly used reference Ξ = 3.160000 (Rh metal) are also given in the Supplementary Information) and were determined, where possible, by direct detection (using an anti-ringing experiment, Bruker pulse sequence *aring*) or by four pulse ³¹P-¹⁰³Rh HMQC experiments with and without ¹⁰³Rh decoupling during acquisition. The transmitter frequency offset and t1 increments were varied to ensure that no signals were folded. All ¹⁰³Rh data were processed using Bruker's Topspin 3.5 or MestReNova software packages. Exponential line broadening of 10 Hz was applied to 1D ¹⁰³Rh data, with 2D data zero filled, Gaussian broadened by 10 Hz and treated with sine-squared window function during processing. Coupling constants reported herein are given as absolute values but are likely to be negative in sign for ¹J_{Rh-P}.^[12c]

Crystallography: Crystallographic data for the structures were collected at 100(2) K on an Oxford Diffraction Gemini or Xcalibur diffractometer using Mo-Kα radiation, λ = 0.71073 Å, *Lp*, and absorption corrections applied. Following absorption corrections and solution by direct methods, the structures were refined against *F*² with full-matrix least-squares procedures using the program SHELX-2014.^[20] Unless stated below, anisotropic displacement parameters were employed for the non-hydrogen atoms. All hydrogen atoms were added at calculated positions and refined by use of a riding model with isotropic displacement parameters based on those of the parent atom.

CCDC 1865950 [for Rh7-(CF₃)₂], 1865951 (for Rh7-F), 1865952 (for Rh7-CF₂) contain the supplementary crystallographic data for this paper. These data can be obtained free of charge from The Cambridge Crystallographic Data Centre.

Crystal data for Rh7-F: C₄₈H₃₃F₉PRh, *M* = 764.59, 0.218 × 0.200 × 0.134 mm³, triclinic, space group *P*1̄ (No. 2), *a* = 10.3698(2), *b* = 10.8798(3), *c* = 17.8743(4) Å, α = 76.930(2), β = 77.883(2), γ = 83.054(2)°, *V* = 1914.88(8) Å³, *Z* = 2, *D*_c = 1.326 g cm⁻³, μ = 0.532 mm⁻¹, *F*₀₀₀ = 780, 2θ_{max} = 65.3°, 39697 reflections collected, 12915 unique (*R*_{int} = 0.0456). Final *GooF* = 1.000, *R*₁ = 0.0404, *wR*₂ = 0.0874, *R* indices based on 10608 reflections with *I* > 2σ(*I*) (refinement on *F*²), |Δρ|_{max} = 1.1(1) e Å⁻³, 455 parameters, 1 restraint. CCDC number 1865951.

Crystal Data for Rh7-CF₃: C₄₈H₃₃F₉PRh, *M* = 914.62, orange prism, 0.386 × 0.215 × 0.152 mm³, monoclinic, space group *P*2₁/*c* (No. 14), *a* = 19.6621(3), *b* = 16.2263(2), *c* = 12.5354(2) Å, β = 104.996(2)°, *V* = 3863.13(10) Å³, *Z* = 4, *D*_c = 1.573 g cm⁻³, μ = 0.563 mm⁻¹, *F*₀₀₀ = 1848, 2θ_{max} = 65.4°, 85622 reflections collected, 13411 unique (*R*_{int} = 0.0380). Final *Goof* = 1.002, *R*1 = 0.0337, *wR*2 = 0.0861, *R* indices based on 11430 reflections with *I* > 2σ(*I*) (refinement on *F*²), |Δρ|_{max} = 0.98(8) e Å⁻³, 586 parameters, 132 restraints. CCDC number 1865952.

Crystal Data for Rh7-(CF₃)₂: C₅₁H₃₀F₁₈PRh, *M* = 1118.63, orange prism, 0.281 × 0.252 × 0.167 mm³, triclinic, space group *P*1 (No. 2), *a* = 12.5332(4), *b* = 13.0550(4), *c* = 16.0370(5) Å α = 79.006(3), β = 69.692(3), γ = 64.893(3)°, *V* = 2225.45(14) Å³, *Z* = 2, *D*_c = 1.669 g cm⁻³, μ = 0.533 mm⁻¹, *F*₀₀₀ = 1116, 2θ_{max} = 64.6°, 41817 reflections collected, 14683 unique (*R*_{int} = 0.0376). Final *Goof* = 1.001, *R*1 = 0.0507, *wR*2 = 0.1157, *R* indices based on 12467 reflections with *I* > 2σ(*I*) (refinement on *F*²), |Δρ|_{max} = 1.6(1) e Å⁻³, 658 parameters, 324 restraints. CCDC number 1865950.

Elemental Analysis: Elemental microanalyses were performed on a Perkin Elmer 2400 Series II CHNS/O Analyzer in CHN mode with helium as a carrier gas.

Chromatography: Size exclusion chromatography (SEC) was performed on a Shimadzu modular system consisting of a 4.0 mm × 3.0 mm Phenomenex Security Guard™ Cartridge guard column and two linear phenogel columns (103 and 104 Å pore size) in tetrahydrofuran (THF) operating at a flow rate of 1.0 mL/min and 40 °C using a RID-20A refractive index detector, a SPD-M20A prominence diode array detector and a miniDAWN TREOS multi-angle static light scattering (MALLS) detector. The system was calibrated with a series of narrow molecular weight distribution polystyrene standards with molecular weights ranging from 0.27 to 66 kg mol⁻¹. Chromatograms were analyzed by Lab Solutions SEC software.

Acknowledgments

A. B. L. kindly thanks the Research Office, Curtin (ROC) for a PhD scholarship for N. S. L. T. Mr. Robert Herman is thanked for conducting the elemental analysis experiments. P. R. thanks the Australian National Computational Infrastructure (NCI) for the provision of computing resources through NCMAS. The authors acknowledge the facilities, and the scientific and technical assistance of Microscopy Australia at the Centre for Microscopy, Characterisation and Analysis, The University of Western Australia, a facility funded by the University, State and Commonwealth Governments.

Keywords: Rhodium · Phenylacetylene · Stereospecific polymerization

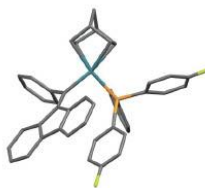
- [1] a) A. Nakazato, I. Saeed, T. Katsumata, M. Shiotsuki, T. Masuda, J. Zednik, J. Vohlidal, *J. Polym. Sci., Part A: Polym. Chem.* **2005**, *43*, 4520–4536; b) J. Liu, J. W. Lam, B. Z. Tang, *Chem. Rev.* **2009**, *109*, 5799–5867; c) M. Shiotsuki, F. Sanda, T. Masuda, *Polym. Chem.* **2011**, *2*, 1044–1058; d) S. Li, K. Liu, G. Kuang, T. Masuda, A. Zhang, *Macromolecules* **2014**, *47*, 3288–3296; e) X. A. Zhang, M. R. Chen, H. G. Zhao, Yuan, Q. Wei, S. Zhang, A. Qin, J. Z. Sun, B. Z. Tang, *Macromolecules* **2011**, *44*, 6724–6737; f) M. N. Bhebbhe, E. A. De Eluate, Y. Pei, D. W. Arrigan, P. J. Roth, A. B. Lowe, *Macromol. Rapid Commun.* **2017**, *38*, 1600450; g) L. Liu, G. Zhang, T. Aoki, Y. Wang, T. Kaneko, m. Teraguchi, C. Zhang, H. Dong, *ACS Macro Lett.* **2016**, *5*, 1281–1285; h) B. Z. Tang, W. H. Poon, S. M. Leung, W. H. Leung, H. Peng, *Macromolecules* **1997**, *30*, 2209–2212; i) S. Abe, K. Hirata, T. Ueno, K. Morino, N. Shimizu, M. Yamamoto, M. Takata, E. Yashima, Y. Watanabe, *J. Am. Chem. Soc.* **2009**, *131*, 6958–6960.
- [2] Y. Kishimoto, P. Eckerle, T. Miyatake, T. Ikariya, R. Noyori, *J. Am. Chem. Soc.* **1994**, *116*, 12121–12132.
- [3] Y. Kishimoto, T. Miyatake, T. Ikariya, R. Noyori, *Macromolecules* **1996**, *29*, 5054–5055.
- [4] Y. Kishimoto, P. Eckerle, T. Miyatake, M. Kainosho, A. Ono, T. Ikariya, R. Noyori, *J. Am. Chem. Soc.* **1999**, *121*, 12035–12044.
- [5] Y. Misumi, T. Masuda, *Macromolecules* **1998**, *31*, 7572–7573.
- [6] Y. Misumi, K. Kanki, M. Miyake, T. Masuda, *Macromol. Chem. Phys.* **2000**, *201*, 2239–2244.
- [7] M. Miyake, Y. Misumi, T. Masuda, *Macromolecules* **2000**, *33*, 6636–6629.
- [8] I. Saeed, M. Shiotsuki, T. Masuda, *Macromolecules* **2006**, *39*, 8567–8573.
- [9] N. Onishi, M. Shiotsuki, T. Masuda, N. Sano, F. Sanda, *Organometallics* **2013**, *32*, 846–853.
- [10] S. Kumazawa, J. R. Castanon, N. Onishi, K. Kuwata, M. Shiotsuki, F. Sanda, *Organometallics* **2012**, *31*, 6824–6842.
- [11] R. K. Harris, *J. Mol. Spectrosc.* **1963**, *10*, 309–319.
- [12] a) J. M. Ernsting, S. Gaemers, C. J. Elsevier, *Magn. Reson. Chem.* **2004**, *42*, 721–736; b) W. v. Philipsborn, *Pure Appl. Chem.* **1986**, *58*, 513–528; c) L. Carlton, in *Annual Reports on NMR Spectroscopy*, Vol. 63, Elsevier Ltd, **2008**, pp. 46–178.
- [13] a) A. Corona-Armenta, M. Ordoñez, J. A. López, J. Cervantes, Q. Serrano, *Helv. Chim. Acta* **2015**, *98*, 359–367; b) R. Eujen, B. Hoge, D. J. Brauer, *Inorg. Chem.* **1997**, *36*, 1464–1475; c) X. Wang, F. B. Mallory, C. W. Mallory, P. A. Beckmann, A. L. Rheingold, M. M. Frand, *J. Phys. Chem. A* **2006**, *110*, 3954–3960; d) E. B. Brouwer, G. D. Enright, C. I. Ratcliffe, J. A. Ripmeester, *Supramol. Chem.* **1996**, *7*, 79–83.
- [14] C. I. Simionescu, V. Percec, S. Dumitrescu, *J. Polym. Sci., Part A: Polym. Chem.* **1977**, *15*, 2497–2509.
- [15] Z. Ke, S. Abe, T. Ueno, K. Morokuma, *J. Am. Chem. Soc.* **2011**, *133*, 7926–7941.
- [16] D. Andrae, U. Haeusslerman, M. Dolg, H. Stoll, H. Preuss, *Theor. Chim. Acta* **1990**, *77*, 123–141.
- [17] T. H. Dunning Jr., *J. Chem. Phys.* **1989**, *90*, 1007–1023.
- [18] S. F. Boys, F. Bernardi, *Mol. Phys.* **1970**, *19*, 553–566.
- [19] R. K. Harris, E. D. Becker, S. M. Cabral de Menezes, P. Granger, R. E. Hoffman, K. W. Zilm, *Pure Appl. Chem.* **2008**, *80*, 59–84.
- [20] G. M. Sheldrick, *Acta Crystallogr., Sect. C-Struct. Chem.* **2015**, *71*, 3–8.

Received: November 19, 2018

Polymerization Catalysts

N. S. L. Tan, P. V. Simpson,
G. L. Nealon, A. N. Sobolev,
P. Raiteri, M. Massi, M. I. Ogden,
A. B. Lowe* 1–11

 **Rhodium(I)- α -Phenylvinylfluorenyl
Complexes: Synthesis, Characteriza-
tion, and Evaluation as Initiators in
the Stereospecific Polymerization of
Phenylacetylene**



Three new well-defined, isolated rhodium(I) vinyl complexes containing fluorenyl functionality in combination with fluorine functionalized phosphine ligands are presented. All complexes are shown to be active as initiators for phenylacetylene yielding highly stereoregular polymers with a *cis-transoidal* structure.

DOI: 10.1002/ejic.201801411

Reproduced from

Nicholas Sheng Loong Tan, Peter V. Simpson, Gareth L. Nealon, Alexandre N. Sobolev, Paolo Raiteri, Massimiliano Massi, Mark I. Ogden, Andrew B. Lowe. ‘**Rhodium(I)- α -Phenylvinylfluorenyl Complexes: Synthesis, Characterization, and Evaluation as Initiators in the Stereospecific Polymerization of Phenylacetylene**’ *European Journal of Inorganic Chemistry* **2019**, 592–601. DOI: 10.1002/ejic.201801411. Highlighted as a *Very Important Paper*.

With permission from the European Journal of Inorganic Chemistry. License number 4987441251105, 14th January 2021.

Cite this: *Dalton Trans.*, 2019, 48,
16437

A (2-(naphthalen-2-yl)phenyl)rhodium(i) complex formed by a proposed intramolecular 1,4-*ortho*-to-*ortho'* Rh metal-atom migration and its efficacy as an initiator in the controlled stereospecific polymerisation of phenylacetylene†

Nicholas Sheng Loong Tan,^a Gareth L. Nealon,^{a,b} Jason M. Lynam,^{a,c}
Alexandre N. Sobolev,^d Matthew R. Rowles,^d Mark I. Ogden,^a
Massimiliano Massi^a and Andrew B. Lowe^{a*}

The synthesis of a novel Rh(i)-aryl complex is detailed and its ability to serve as an initiator in the stereospecific polymerisation of phenylacetylene evaluated. Targeting the Rh(i) species, (2-phenylnaphthalen-1-yl)rhodium(i) (2,5-norborradiene)tris(*para*-fluorophenylphosphine), Rh(nbd)(P(4-FC₆H₄)₃)(2-PhNaph), following recrystallization we obtained the isomeric (2-(naphthalen-2-yl)phenyl)rhodium(i) complex, Rh(nbd)(P(4-FC₆H₄)₃)(2-NaphPh), as determined by X-ray single-crystal structure analysis, and confirmed by X-ray powder diffraction. The isolation of the latter species was proposed to occur from the target (2-PhNaph) derivative via an intramolecular 1,4-Rh atom migration. This supposition was supported by density functional theory (DFT) calculations that indicated the isolated (2-NaphPh) derivative has lower energy (−19 kJ mol^{−1}) than the targeted complex. The structure of the isolated (2-NaphPh) species was confirmed by multinuclear NMR spectroscopy including 2D ³¹P–¹⁰³Rh{¹H, ¹⁰³Rh}, heteronuclear multiple-quantum correlation (HMQC) experiments; however, NMR analysis indicated the presence of a second, minor species in solution in an approximate 1:4 ratio with the 2-NaphPh complex. The minor species was identified as a second structural isomer, the 3-phenylnaphthyl derivative, proposed to be formed under a dynamic equilibrium with the 2-NaphPh derivative via a second 1,4-Rh atom migration. DFT calculations indicate that this 1,4-migration proceeds through a low-energy pathway involved in the oxidative addition of a C–H bond to Rh followed by a reductive elimination with the distribution of the products being thermodynamically controlled. The recrystallized Rh(nbd)(P(4-FC₆H₄)₃)(2-NaphPh) complex was subsequently evaluated as an initiator in the polymerisation of phenylacetylene (PA); gratifyingly, the Rh(i) species was an active initiating species with the pseudo-first-order kinetic and molecular weight evolution vs time plots both linear implying a controlled polymerisation while yielding (co)polymers with low dispersities ($D = M_w/M_n$, typically <1.25) and high *cis-transoidal* stereoregularity (>95%). Typical initiation efficiencies, while not quantitative (as judged by size exclusion chromatography), were nonetheless high at ca. 0.8. The presence of the minor 3-phenylnaphthyl species when in solution is proposed to be the cause of the observed non-quantitative initiation.

Received 18th July 2019.
Accepted 17th October 2019
DOI: 10.1039/c9dt02953b
rsc.li/dalton

Introduction

Poly(phenylacetylene)s (PPAs) are an important subset of conjugated materials with application in areas as diverse as anti-static coatings, corrosion protection, gas sensing, electrochromic displays, electrocatalysis and as artificial muscles.¹ PPAs have long attracted attention in the academic community due to their impressive oxidative stability, solubility in common organic solvents and ease of processing.

There is a significant volume of literature detailing the (co)polymerisation of phenylacetylene (PA), and a wide array of functional derivatives thereof, most commonly via the application of Rh complexes in conjunction with an appropriate co-

^aCurtin Institute for Functional Molecules and Interfaces (CIFMI) and School of Molecular and Life Sciences (MLS), Curtin University, Bentley, Perth, WA, 6102, Australia. E-mail: andrew.b.lowe@curtin.edu.au

^bCentre for Microscopy, Characterisation and Analysis (CMCA), M310, University of Western Australia, 35 Stirling Highway, Perth, WA 6009, Australia. E-mail: gareth.nealon@uwa.edu.au

^cDepartment of Chemistry, University of York, Heslington, York, YO10 5DD, UK. E-mail: jason.lynam@york.ac.uk

^dJohn de Laeter Centre, Curtin University, Bentley, Perth, WA, 6102, Australia

† Electronic supplementary information (ESI) available: Full computational data; ¹H, ¹³C, ¹⁹F, COSY, H2BC, HMBC, HSQC, NOESY NMR spectra; full crystallographic data; shape analysis; powder XRD pattern; kinetic data and rate constants for polymers with targeted M_n of 5k. CCDC 1902529. For ESI and crystallographic data in CIF or other electronic format see DOI: 10.1039/c9dt02953b

catalyst.^{2–6} Rh species are particularly attractive in this application given their general low oxophilicity, high functional group tolerance and high activity at ambient temperatures thus facilitating ready access to a large number of interesting materials under facile conditions. However, while readily executed, (co)polymerisations initiated with catalysts such as $[\text{Rh}(\text{nbd})\text{Cl}]_2$ (nbd: 2,5-norbornadiene), typically in combination with an amine co-catalyst, proceed in a non-controlled fashion, with low initiation efficiencies, yielding (co)polymers with broad molecular weight distributions, limited topology and of basic architecture.

In contrast to the extensive literature describing the non-controlled (co)polymerisation of PAs there is a paucity of reports describing the controlled (co)polymerisation of this monomer class,⁷ and especially with readily isolable, distinct initiating complexes. At present, the best developed, or examined, Rh(i) species that serve as initiators in this target application are those reported by Masuda and co-workers, Fig. 1 I for example.^{7–10} The common structural feature in these complexes is the presence of a $-\text{CPh}=\text{CPh}_2$ ligand that serves as the initiating fragment (more specifically, such complexes are examples of Rh(i)-vinyl species with additional triarylphosphine and diene ligands with the latter most commonly, but not exclusively, being nbd). Under suitable conditions, Masuda-type species initiate the polymerisation of PA essentially quantitatively (as determined by size exclusion chromatography, SEC), with (co)polymerisation proceeding by a head-to-tail 2,1-insertion pathway yielding highly stereoregular *cis-transoidal* polymers with low dispersities ($D = M_w/M_n$).^{11–13} For example, Miyake, Misumi and Masuda⁸ described the synthesis and activity of two isolated Rh(i)-vinyl complexes, namely $[\text{Rh}(\text{CPh}=\text{CPh}_2)(\text{nbd})(\text{P}(4\text{-XC}_6\text{H}_4)_3)]$ ($X = \text{F}$ or Cl). Both species mediated the (co)polymerisation of PA, under a range of experimental conditions, in a controlled manner with essentially quantitative initiation yielding polymers with reported D s as low as 1.05. The only additional requirement for effective control was the addition of at least five equivalents of free phosphine, $\text{P}(4\text{-FC}_6\text{H}_4)_3$ in the case of $[\text{Rh}(\text{CPh}=\text{CPh}_2)(\text{nbd})(\text{P}(4\text{-FC}_6\text{H}_4)_3)]$ for example, as a rate modifier. In the absence of added free phosphine, polymerisation yielded a polymer with a broad molecular weight distribution, *i.e.* $D = ca. 1.50$.

Intrigued by the limited number of isolated Rh(i) complexes detailed to mediate the controlled polymerisation of PA, and simple substituted derivatives, we recently initiated a program

of research focussing on the synthesis and evaluation, as polymerisation initiators, of new Rh(i) complexes. In our first disclosure, we reported the preparation of three new Rh(i)- α -phenylvinylfluorenyl complexes based on the Masuda structural motif, see Fig. 1 II for a representative example.¹⁴ Interestingly, while structurally similar and meeting the general substitution criteria on the vinyl ligand reported for effective initiating species¹⁵ these complexes exhibited low initiation efficiencies (IEs) (as judged by SEC) spanning the range 0.16 to 0.56 depending on polymerisation conditions. These preliminary results suggested that a detailed understanding of the ligand environment, particularly of the initiating fragment, in the mediation of PA polymerisation remains elusive. However, while initiation was non-quantitative, (co)polymerisation with the fluorenyl-functionalized catalysts did yield highly stereoregular *cis-transoidal* PPAs with SEC measured D s as low as 1.03. The observed difference in activity, or IE, between I and II was hypothesized to be due to the conformationally locked nature of the fluorenyl group on the β -vinyl carbon. Specifically, we proposed that the fluorenyl group inhibited the effective co-ordination of incoming monomer. To test this proposition we targeted complex III, Fig. 1, a 2-phenylnaphthyl Rh(i) derivative in which the phenyl group on the β -vinyl carbon (recognizing that the vinyl bond is part of the aromatic naphthyl group, and this is technically a Rh(i)-aryl complex) is able to freely rotate and thus part of the initiating fragment is similar to I.

Herein we detail our results regarding the attempted synthesis of III, a mechanistic rationale for the isolation, *via* recrystallization of (2), *vide infra*, an isomeric 2-naphthylphenylrhodium(i)-aryl derivative and the presence of a third structural isomer, a 3-phenylnaphthyl derivative formed in solution from (2) *via* a second Rh atom migration. Finally, we detail the efficacy of (2) as an initiating species in the controlled, stereospecific polymerisation of PA. This represents, to the best of our knowledge, the first example in which a Rh(i)-aryl complex of this type has been evaluated as a polymerisation initiator for PA although similar Rh(i)-aryl species are known to mediate the polymerisation of bulky aryl isocyanides.^{16,17}

Experimental

Materials

n-Butyllithium (*n*-BuLi, 1.6 M solution in hexane, Sigma-Aldrich), 1-bromo-2-phenylnaphthalene ($\text{C}_{16}\text{H}_{13}\text{Br}$) (98% Tokyo Chemical Industry), $[\text{Rh}(\text{nbd})\text{Cl}]_2$ (nbd = 2,5-norbornadiene, 98%, Strem Chemicals), and tris(*para*-fluorophenyl) phosphine ($\text{P}(4\text{-FC}_6\text{H}_4)_3$, 98%, Sigma-Aldrich) were used as received. Phenylacetylene ($\text{CH}\equiv\text{CPh}$, 98%, Sigma-Aldrich) was purified by passage over a column of basic alumina and then stored in a fridge until needed.

THF, diethyl ether and CH_2Cl_2 were dried using a PureSolv MD5 solvent purification system (Innovative Technology, Inc.), collected, degassed *via* the freeze-pump-thaw technique and

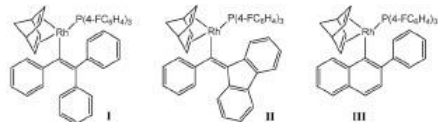


Fig. 1 Examples of a Masuda triphenylvinyl Rh(i) derivative (I), a tan α -phenylvinylfluorenyl Rh(i) derivative (II) and a targeted 2-phenylnaphthyl Rh(i) species (III).

stored under dry nitrogen until needed. Toluene (99.8%, Sigma-Aldrich) was degassed *via* the freeze-pump-thaw technique and stored under dry nitrogen until needed. All glassware was pre-dried in an oven at 120 °C and then flame dried under vacuum before use. All reactions were performed using standard Schlenk line techniques.

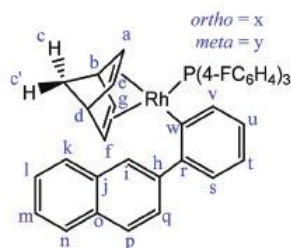
Synthesis of Rh(nbd)(P(4-FC₆H₄)₃)(2-NaphPh) (2)

Rh(nbd)(P(4-FC₆H₄)₃)(2-NaphPh) (2), was prepared following the procedure we recently reported for the preparation of Rh(i)- α -phenylvinylfluorenyl derivatives.¹⁴

To a round-bottomed flask equipped with a Teflon-coated magnetic stir bar was added 1-bromo-2-phenylnaphthalene (293 mg, 1.03 mmol) and diethyl ether (20.0 mL) under a dry nitrogen atmosphere. The flask was cooled to 0 °C, and *n*-BuLi (1.6 M solution in hexane, 1.25 mL, 2.0 mmol) was cannula transferred and the mixture allowed to react for 30 min yielding C₆H₅(C₁₀H₇Li).

To a separate round-bottomed flask equipped with a magnetic stir-bar containing dry toluene (15.0 mL) was added [Rh(nbd)Cl]₂ (210 mg, 0.45 mmol) and P(4-FC₆H₄)₃ (411 mg, 1.30 mmol). The mixture was then stirred vigorously for 15 min at ambient temperature yielding the intermediate Rh species, Rh(nbd)(P(4-FC₆H₄)₃)Cl.

The lithiated species, C₆H₅(C₁₀H₇Li), was added, *via* cannula, to the solution containing Rh(nbd)(P(4-FC₆H₄)₃)Cl and allowed to stir at ambient temperature overnight. Subsequently, the reaction solution was cannula transferred and filtered through a short plug of neutral activated alumina 90, under an inert atmosphere, to give a clear orange solution. Solvents were concentrated under high vacuum on a Schlenk line yielding a dark viscous liquid. To the residue was added CH₂Cl₂ (2.5 mL) and the Rh(i) complex, (2), the 2-naphthyl-phenyl structural isomer was isolated by recrystallisation from CH₂Cl₂/methanol *via* a solvent layering technique. Yield: 64%. CH elemental analysis: %C_{theor}: 68.92, %C_{found}: 68.20; %H_{theor}: 4.37, %H_{found}: 4.33.



¹H NMR (600 MHz, CD₂Cl₂), δ (ppm): 9.14 (s, 1H, H_i), 8.06 (d, *J* = 8.2 Hz, 1H, H_k), 7.89 (d, *J* = 8.1 Hz, 1H, H_n), 7.60 (d, *J* = 8.3 Hz, 1H, H_p), 7.59 (m, 1H, H_l), 7.54 (ddd, *J* = 8.1, 6.8 m 1.3 Hz, 1H, H_m), 7.25 (dt, *J* = 7.2, 1.6 Hz, 1H, H_e), 7.06 (dd, *J* = 7.4, 1.4 Hz, 1H, H_d), 6.99 (dd, *J* = 8.3, 1.8 Hz, 1H, H_q), 6.88

(m, 1H, H_e), 6.84 (td, *J* = 7.2, 1.4 Hz, 1H, H_a), 6.74 (m, 6H, H_j), 4.97–4.94 (m, 1H, H_g), 6.60 (m, 6H, H_x), 4.13 (dt, *J* = 7.5, 3.8 Hz, 1H, H_f), 4.04 (s, 1H, H_d), 3.83 (s, 1H, H_b), 3.55 (m, 1H, H_a), 3.54 (m, 1H, H_e), 1.60 (dt, *J* = 8.1, 1.7 Hz, 1H, H_c), 1.35–1.32 (m, 1H, H_c); ¹³C NMR (151 MHz, CD₂Cl₂), δ (ppm): 172.3 (dd, *J* = 33.5, 13.2 Hz, C_w), 163.4 (dd, *J* = 249.5, 1.9 Hz, C-F), 147.2 (dd, *J* = 3.0, 1.9 Hz, C_e), 145.9 (d, *J* = 2.2 Hz, C_h), 136.2 (dd, *J* = 2.4, 1.8 Hz, C_e), 135.8 (dd, *J* = 14.2, 8.1 Hz, C_e), 135.0 (C_j), 133.2 (C_e), 130.1 (dd, *J* = 35.3, 3.2 Hz, C-P), 128.6 (C_k), 128.1 (C_n), 127.9 (C_p), 127.6 (C_a), 126.4 (C_i), 125.7 (C_m), 125.2 (d, *J* = 1.7 Hz, C_u), 124.7 (C_q), 122.2 (C_i), 116.2 (d, *J* = 1.4 Hz, C_i), 115.2 (dd, *J* = 20.9, 10.2 Hz, C_y), 75.4 (dd, *J* = 5.3, 3.2 Hz, C_a), 75.0 (dd, *J* = 5.7, 1.4 Hz, C_a), 72.4 (dd, *J* = 15.1, 1.4 Hz, C_g), 64.9 (t, *J* = 4.7 Hz, C_z), 55.5 (dd, *J* = 19.1, 6.9 Hz, C_z), 51.5 (d, *J* = 3.3 Hz, C_h), 51.1 (d, *J* = 3.9 Hz, C_d); ¹⁹F NMR (565 MHz, CD₂Cl₂), δ (ppm): -112.4 (m); ³¹P{¹H} NMR (243 MHz, CD₂Cl₂), δ (ppm): 24.4 (dq, *J*_{P-Rh} = 189.9, *J*_{P-F} = 3.3 Hz); ¹⁰³Rh NMR (19.1 MHz, *d*₈-toluene), δ (ppm): -7688 (547 ppm if referenced to Rh metal).

Computational chemistry

All calculations were performed using the TURBOMOLE V6.4 package using the resolution of identity (RI) approximation.^{18–25}

Initial optimizations were performed at the (RI)-BP86/SV(P) level, followed by frequency calculations at the same level. Transition states were located by initially performing a constrained minimization (by freezing internal coordinates that change most during the reaction) of a structure close to the anticipated transition state. This was followed by a frequency calculation to identify the transition vector to follow during a subsequent transition state optimization. A final frequency calculation was then performed on the optimized transition-state structure. All minima were confirmed as such by the absence of imaginary frequencies, and all transition states were identified by the presence of only one imaginary frequency. Dynamic Reaction Coordinate analysis confirmed that transition states were connected to the appropriate minima. Single-point calculations on the (RI)-BP86/SV(P) optimized geometries were performed using the hybrid PBE0 functional and the flexible def2-TZVPP basis set. The (RI)-PBE0/def2-TZVPP SCF energies were corrected for their zero-point energies, thermal energies and entropies (obtained from the (RI)-BP86/SV(P)-level frequency calculations). A 28 electron quasi-relativistic ECP replaced the core electrons of Rh. No symmetry constraints were applied during optimizations. Solvent corrections were applied with the COSMO dielectric continuum model²⁶ and dispersion effects modelled with Grimme's D3 method.^{27,28}

Polymerisation kinetics

All (co)polymerisations were carried out under a dry nitrogen atmosphere in glassware pre-dried in an oven set at 120 °C. Below is given a typical procedure for the homopolymerisation of phenylacetylene with (2):

A solution of phenylacetylene (0.184 g, 1.80 mmol) in toluene (2.5 mL) was added to a solution of (2) (0.015 g, 0.02 mmol) and free phosphine (P(4-FC₆H₄)₃) (0.031 g,

0.10 mmol) dissolved in toluene (2.5 mL) in a Schlenk flask equipped with a magnetic stir bar. The flask was then immersed in a pre-heated oil bath set at 30 °C and polymerisation allowed to proceed for 90 min. An aliquot (0.1 mL) was withdrawn every 5–10 min and was added to a vial of deuterated chloroform (0.5 mL) containing a small volume of acetic acid (2.0 µL). After 90 min the polymerisation was terminated by the addition of acetic acid. The final polymer was isolated by precipitation into a large volume of methanol, isolated by gravity filtration and dried to constant weight in a vacuum oven at 40 °C overnight. Monomer conversions were determined by ¹H NMR spectroscopy, and molecular weights and dispersity were determined by size exclusion chromatography.

NMR measurements

NMR spectra were recorded at 298 K on a Bruker Avance IIIHD (600 MHz for ¹H). The data were processed with Bruker's TopSpin 3.5 or MestReNova software packages. ¹H, ¹³C, ¹⁹F, and ³¹P spectra were collected on a commercial broadband probe, whereas the ¹⁰³Rh NMR was acquired at 19.1 MHz using a commercial 5 mm triple resonance broadband probe (doubly tuned ¹H/³¹P outer coil with inner broadband coil) with 90° pulses of 27.5 µs and 18.4 µs for ¹⁰³Rh and ³¹P respectively. ¹⁰³Rh chemical shifts, δ, are given in ppm relative to ε = 3.186447²⁹ and derived indirectly from the ³¹P-¹⁰³Rh HMQC experiments (as an aide to the reader, the chemical shift for the commonly used reference ε = 3.160000 (Rh metal) is also given) by four pulse ³¹P-¹⁰³Rh HMQC experiments with ¹⁰³Rh and ¹H decoupling during acquisition. The transmitter frequency offset and *t*₁ increments were varied to ensure that no signals were folded. Exponential line broadening of 10 Hz was applied to 1D ¹⁰³Rh data, with 2D data zero filled, Gaussian broadened by 10 Hz and treated with spine-squared window function during processing. Coupling constants reported herein are given as absolute values but are likely to be negative in sign for ¹J_{Rh-P}.³⁰

Crystallography

The crystalline sample of (2) was measured at 100(2) K on an Oxford Diffraction Xcalibur diffractometer using Mo-Kα radiation, λ = 0.71073 Å, *l*_p and absorption corrections applied. The structure was solved and refined against *F*² with full-matrix least-squares using the program suite SHELX-2014.³¹ Anisotropic thermal displacement parameters were employed for the non-hydrogen atoms. All hydrogen atoms were added at calculated positions and refined by the use of a riding model with isotropic displacement parameters based on those of the parent atom. CCDC 1902529† deposit contains supplementary crystallographic data.

Crystal data for Rh(nbd)(P(4-FC₆H₄)₃)(2-NaphPh) (C₄₁H₃₁F₃PRh, CH₂Cl₂). C₄₂H₃₂Cl₂F₃PRh, *M* = 799.46, yellow needle, 0.210 × 0.115 × 0.099 mm³, monoclinic, space group *P*2₁/*n* (No. 14), *a* = 11.7509(1), *b* = 21.0929(2), *c* = 13.9381(1) Å, β = 96.153(1)°, *V* = 3434.80(5) Å³, *Z* = 4, *D*_c = 1.546 g cm⁻³, μ = 0.747 mm⁻¹, *F*₀₀₀ = 1624, *T* = 100(2) K, 2θ_{max} = 64.7°, 71 355 reflections collected, 11 686 unique (*R*_{int} = 0.0492). Final

GoF = 1.000, *R*₁ = 0.0397, *wR*₂ = 0.0916, *R* indices based on 9483 reflections with *I* > 2σ(*I*) (refinement on *F*²), |Δρ|_{max} = 1.1(1) e Å⁻³, 442 parameters, 0 restraints.

Size exclusion chromatography (SEC)

SEC was performed on a Shimadzu modular system consisting of a 4.0 mm × 3.0 mm Phenomenex Security Guard™ Cartridge guard column and two linear phenogel columns (103 and 104 Å pore size) in tetrahydrofuran (THF) operating at a flow rate of 1.0 mL min⁻¹ and 40 °C using a RID-20A refractive index detector, a SPD-M20A prominence diode array detector and a miniDAWN TREOS multi-angle static light scattering (MALLS) detector. The system was calibrated with a series of narrow molecular weight distribution polystyrene standards with molecular weights ranging from 0.27 to 66 kg mol⁻¹. Chromatograms were analyzed by Lab Solutions SEC software.

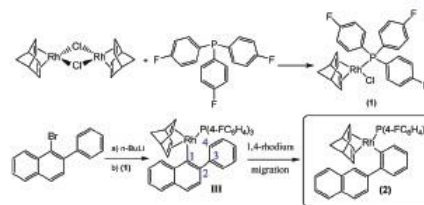
Results and discussion

Catalyst synthesis and characterisation

The synthetic route employed for the preparation of the target Rh(η⁵-aryl) complex III is shown in Scheme 1.

The reaction of commercially available [Rh(nbd)Cl]₂ with the fluorine functionalized phosphine P(4-FC₆H₄)₃ yielded the intermediate tetra-coordinate Rh(η⁵) species Rh(nbd)(P(4-FC₆H₄)₃)Cl (1). Reaction of 1-bromo-2-phenylnaphthalene with *n*-BuLi gave the corresponding lithiated 2-phenylnaphthalene derivative that when reacted with (1) was anticipated to yield the target complex III. Interestingly, after isolation and recrystallization, X-ray single-crystal structure analysis, Fig. 2, indicated the presence of (2), a structural isomer of the target III.

While (2) was not the target species, we did proceed to characterize the complex. We see from the single-crystal structure in Fig. 2 that the recrystallized species has a slightly distorted square planar geometry consistent with previous reports of similar Rh(η⁵) species.^{8,14} X-ray powder diffraction characterization of a bulk sample of (2) was consistent with the single-crystal structure (see ESI, Fig. S1†) with remaining intensity mismatches likely due to large crystallites in the powder or



Scheme 1 Outline for the synthesis of the target 2-phenylnaphthyl derivative, III, and chemical structure of the isolated, isomeric, 2-naphthylphenyl species (2).

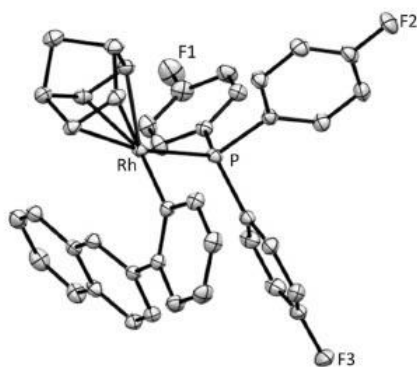


Fig. 2 ORTEP representation of the X-ray crystal structure of (2) with 50% probability ellipsoids and H-atoms omitted for clarity.

slight changes in crystal structure due to the temperature difference between powder and single-crystal data collection. A tetrahedral-square planar continuous shape measure analysis³² was performed comparing (2) to complexes similar to I and II (Fig. 1), as well as the three other structurally characterised Rh(nbd)PR₃(Ar) complexes: Rh(nbd)(PPh₃) (2-Me-1-Naphth),¹⁷ Rh(nbd)(PPh₃)(*m*-xylene)³³ and Rh(nbd)(PCy₃)(C₆H₅)³⁴ (Cy = cyclohexyl). While all are appropriately described as having distorted square planar geometries, complexes with triphenylvinyl ligands, I, are the most significantly distorted towards tetrahedral geometry and those with an aromatic ring directly coordinated the least distorted. Of the latter class, it is notable that (2) is the most distorted of these, presumably because of the bulky naphthyl substituent, placing it amongst the α -phenylvinylfluorenyl derivatives, II (see ESI†).

Multinuclear NMR spectroscopy (¹H, ¹³C, ¹⁹F, ³¹P, and various 2D techniques) was employed to characterize (2). Fig. 3 shows the ¹H NMR spectrum of (2) recorded in CD₂Cl₂;

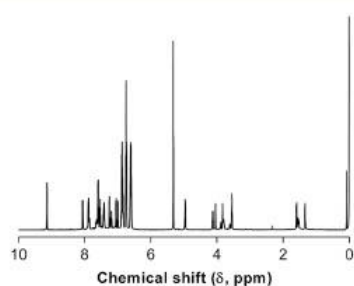


Fig. 3 ¹H NMR, recorded in CD₂Cl₂, of complex (2). Full peak assignments are given in the Experimental section.

full peak assignments are given in the Experimental section along with the ¹³C, ¹⁹F, ³¹P and ¹⁰³Rh chemical shifts of (2) (additional 2D NMR data can be found in the ESI†).

Interestingly, the ¹H, ¹³C, ³¹P{¹H} and ³¹P-¹⁰³Rh{¹H, ¹⁰³Rh} spectra, indicated the presence of more than one species in solution even though samples were prepared with recrystallized complex. Rhodium has one NMR-active spin- $\frac{1}{2}$ nucleus, ¹⁰³Rh, which is 100% abundant. While direct observation of ¹⁰³Rh is possible,¹⁴ it suffers from low sensitivity and a large chemical shift range (of ca. 12 000 ppm). In cases where Rh is bonded to a nucleus with a high gyromagnetic ratio, such as ³¹P, the sensitivity of the Rh nucleus can be enhanced significantly – by a factor of almost 600 in the case of ³¹P. In such instances, it is straightforward to employ a 2D polarization transfer technique, such as heteronuclear multiple quantum coherence (HMQC), to observe the ¹⁰³Rh nuclei. Fig. 4 shows the measured HMQC spectrum of (2). There are clearly two main phosphorus species present, in a ratio of 4 : 1, and both are coupled to Rh (the presence of a third species (ca. 5%) was also detected in the ³¹P{¹H} spectrum of (2), Fig. S8† but was not observable in the HMQC experiment, Fig. S9†). Initially we considered the possibility that the two major species observed in Fig. 4 were rotamers – this has previously been observed by Kumazawa *et al.* in their detailed structural characterization of Rh(nbd)(CPh=CPh₂)(PPh₃).¹¹ However, variable temperature (VT) ³¹P{¹H}, ¹H and ³¹P-¹⁰³Rh HMQC NMR experiments proved inconclusive as compound decomposition took place during heating to 90 °C in *d*₆-toluene. Based, therefore, on the ¹H, ¹³C and 2D techniques employed to characterize (2), we conclude that the major species present in solution is complex (2a) (ca. 75%), while the minor species is a second structural isomer of III, (3-phenylnaphthalen-1-yl)rhodium(i) (2,5-norbornadiene) tris(*para*-fluorophenylphosphine), (2b) (3-PhNaph) (ca. 19%). Finally, we note the presence of a smaller phosphorus peak centred around 25.4 ppm that is not coupled to Rh and is attributed to the presence of phosphine oxide (this is more clearly observed in the full ³¹P{¹H} of the complex and ³¹P{¹H} of the phosphine ligand in the ESI, Fig. S2 and S8†).

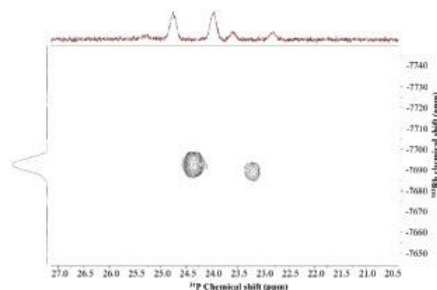


Fig. 4 ³¹P-¹⁰³Rh{¹H, ¹⁰³Rh} HMQC NMR spectrum of (2) recorded in *d*₆-toluene.



Scheme 2 Proposed formation of (2-naphthylphenyl-1-yl)rhodium(I) (2,5-norbornadiene)(tris-*para*-fluorophenylphosphine), (2-NaphPh) and (3-phenylnaphthalen-1-yl)rhodium(I)(2,5-norbornadiene)(tris-*para*-fluorophenyl phosphine), (3-PhNaph) via sequential 1,4-Rh atom migrations. $\text{PAR}_3 = \text{P}(4\text{-FC}_6\text{H}_4)_3$.

The formation of the minor species in solution is proposed to occur *via* sequential 1,4-Rh migrations as outlined in Scheme 2.

While unanticipated, we propose that (2a) and (2b) are formed from III *via* intramolecular 1,4-Rh metal-atom migrations or *ortho-to-ortho'* C-H bond activations. This is an important feature of this synthesis since transition metal-mediated C-H bond activations^{35–40} play an increasingly important role in modern chemical syntheses and, mechanistically, reaction pathways involving metal (catalyst) atom migrations have been proposed to rationalize product formation with pertinent examples including reactions mediated by Pd⁴¹ or Rh catalysts.⁴² In the case of Rh-catalyzed reactions, examples of 1,3-,⁴³ 1,4-,^{44–50} and 1,5-^{51,52} migrations have been reported. For example, Oguma *et al.*⁴⁴ reported that alkylation of phenylboronic acid, with norbornene, catalyzed by [Rh(cod)Cl]₂/dppp (cod: cyclooctadiene; dppp: bis(diphenylphosphino)propane) yielded predominantly, under appropriate conditions, the 1,2,3,4-tetraalkylated product. The formation of the polyalkylated species was rationalized in terms of inser-

tion of the ene into the $\text{sp}^2\text{C-Rh}$ bond (as expected) followed by a 1,4-Rh atom migration to the next adjacent phenyl ring C followed by further norbornene insertion *etc.* Alkylation stopped after four insertion/migration steps due to steric hindrance.

In order to gain further insight into the mechanistic features which underpin these observations, the conversion of III into its two structural isomers, (2a) and (2b), was modelled by density functional theory (DFT) calculations. The geometries of the complexes were optimised at the bp86/SV(P) level of theory and then single-point energies determined at the pbe0/def2-TZVPP level. The effects of solvation were modelled with COSMO and the resulting energies corrected for the effects of solvation and an empirical dispersion correction applied using Grimme's D3 method. As shown in Fig. 5 the major isomer, complex (2a), has a lower energy (-19 kJ mol^{-1}) than complex III (which was taken as the reference state), whereas 2b lies at a relative energy of -3 kJ mol^{-1} . An examination of the DFT-predicted structures of 2a, 2a' (q.v.) and 2b reveals the presence of agostic interactions between Rh and the 2-naphthylphenyl-1-yl ligand. Using 2a as an example, a Rh-H interaction (2.262 Å) is observed, which is complemented by an elongation of the corresponding C-H bond (1.115 Å), Fig. 5. No agostic interaction was present in the calculated structure of III, with the closest Rh-H distance being 2.970 Å.

The conversion of III to (2a) proceeds *via* an intermediate Rh(m)-hydride species, 4, with an energy of 62 kJ mol^{-1} . Complex 4 lies in a shallow minimum and is connected to III and 2a through transition states $\text{ts}_{\text{III-4}}$ ($+77 \text{ kJ mol}^{-1}$) and ts_{4-2a} ($+73 \text{ kJ mol}^{-1}$) respectively. We also note that a second, higher energy, pathway involving hydride transfer to the nbd ligand was observed. See ESI† for details. The formation of (2b) may be rationalised by rotation of the naphthyl group in

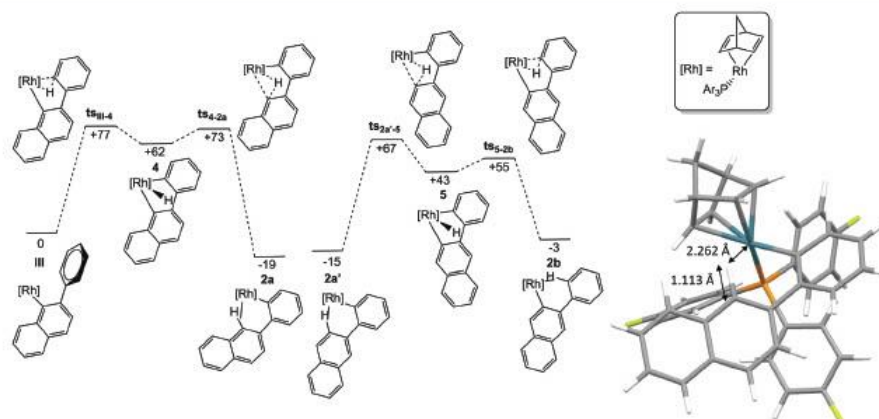


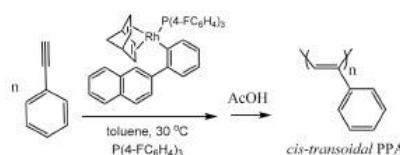
Fig. 5 DFT-calculated pathway for the conversion of III to 2a and 2b. Calculations performed at the D3-pbe0/def2-TZVPP/bp86/SV(P) level with COSMO solvent correction in CH_2Cl_2 . Energies are Gibbs energies at 298 K in units of kJ mol^{-1} . $\text{PAR}_3 = \text{P}(4\text{-F-C}_6\text{H}_4)_3$. DFT-predicted structure of 2a, showing the bond metrics of the agostic interaction (carbon grey, hydrogen white, fluorine green, phosphorus orange, rhodium dark green).

(2a) to give an agostomer⁵³ (2a') (-15 kJ mol^{-1}). C–H activation then proceeds through $\text{ts}_{2a',5}$ ($+67 \text{ kJ mol}^{-1}$) to give hydride complex 5, which only varies from 4 in terms of its connectivity to the naphthyl group. Hydrogen migration through $\text{ts}_{5,2b}$ ($+55 \text{ kJ mol}^{-1}$) gives (2b). We also note that the EXSY peaks observed during NMR characterization of (2a) and (2b) are consistent with such a migration/exchange of H atoms between the coloured carbon centres shown in Scheme 2 and the predicted structures.

These mechanistic pathways involving a metallocyclic Rh(m)-hydride intermediate are entirely consistent with previous reports concerning such intramolecular migrations involving rhodium.^{44,47,54} The calculated energy barriers for the formal 1,4-migration through a hydride intermediate would indicate that the observed distribution of products is entirely under thermodynamic control at 298 K. The calculations, therefore support the fact that 2a (possibly in rapid exchange with 2a') is the major species observed in solution by NMR spectroscopy. Although the calculations broadly reflect the experimental observations, it should be noted that the energy of 2b (-3 kJ mol^{-1}) would imply that its equilibrium concentration with 2a and 2a' would be very low. Moreover, at this level of theory it is essentially at the same energy as (unobserved) III. However, the relative differences in energy are, relatively speaking, small and care must be taken when subsequently interpreting data in this fashion due to the non-linear relationship between equilibrium population and Gibbs energy.

Polymerisation studies

With (2a) in-hand we proceeded to determine its efficacy as an initiating species for the polymerisation of PA (accepting that in addition to (2a), 3-PhNaph, 2b, and perhaps a third very minor species are also present in solution). To reiterate, while the controlled polymerisation of PA has been reported with a limited number of well-defined, isolated Rh(i)-vinyl species, to the best of our knowledge this is the first example in which an isolated Rh(i)-aryl complex has been examined in this specific application. Importantly, any indication of a controlled polymerisation employing (2) has the potential to impact, and significantly enhance, the field of Rh(i) polymerisation catalysis as applied to PA (co)polymerisation. This is due primarily to the large number of commercially available aryl bromides (*versus* commercially available bromo-triphenylethylenes as employed by Masuda and co-workers) that could be employed in the preparation of new catalytic/initiating species, offering an opportunity for a far more detailed evaluation of structure-activity profiles and access to materials with advanced architectures and topologies. Initially we conducted a control experiment in which (2) was employed as an initiator for PA homopolymerisation (target molecular weight: 10 000, toluene, 30 °C) in the absence of any added free phosphine. Consistent with (co)polymerisations mediated by Rh(i)-vinyl complexes, such as I in the absence of added phosphine,^{8,55} polymerisation was uncontrolled and yielded a polymer that eluted at the upper limit of the SEC instrument indicating an $M_n > 100\,000$ with an unmeasurable dispersity. As such, all further



Scheme 3 Conditions for the polymerisation of phenylacetylene with (2a).

polymerisations were performed in toluene at 30 °C in the presence of added free phosphine as a rate modifier, Scheme 3, with polymerisations terminated by the addition of a small volume of acetic acid.

In determining the ability of a species to mediate a polymerisation in a controlled fashion there are specific features that need to be elucidated which, when taken collectively, indicate a living or controlled process: the (pseudo) first-order kinetic plot should be linear with respect to monomer concentration over the full conversion range (this indicates a constant number of active species); the evolution of polymer molecular weight with monomer conversion should be linear; it is often desirable that the product (co)polymer has a narrow molecular weight distribution, *i.e.* $D \leq 1.30$ (although this is not a formal requirement for a controlled polymerisation); and materials with advanced architectures such as AB diblock copolymers should be accessible *via* sequential monomer addition.

Fig. 6(A) shows the pseudo-first-order kinetic plots for the homopolymerisation of PA with (2a) in toluene at 30 °C in the presence of 10 and 20 equivalents of added free $\text{P}(4\text{-FC}_6\text{H}_4)_3$ for a target molecular weight of 10 000 at quantitative conversion. Several pertinent features are worth noting. Both plots are linear, even up to near-quantitative conversion, with the homopolymerisation in the presence of 10 equivalents of free phosphine proceeding faster than the polymerisation in the presence of 20 equivalents, as expected. While both plots are linear, confirming a constant number of active propagating species, neither plot passes through the origin, with both exhibiting a short inhibition period. This is not uncommon and is typically associated with a period of time in which negligible active species are present. The inhibition period is marginally longer in the case of the polymerisation performed in the presence of 20 equivalents of free phosphine, which is not surprising since the additional free phosphine serves as a monomer-competing binding species. Similar data, and observations, for homopolymerisations with a target molecular weight of 5000 are given in the ESI.†

The slope of the curve in the pseudo-first order kinetic plots is k_{app} – the apparent propagation rate constant. In the case of the homopolymerisation conducted at a $[\text{P}]/[\text{Rh}]$ of 10 and target molecular weight of 10 000, the k_{app} is 0.0374 min^{-1} , whereas at $[\text{P}]/[\text{Rh}]$ of 20, k_{app} is 0.0228 min^{-1} . The k_{app} values for homopolymerisations with a target molecular weight of 5000 are given in the ESI, Fig. S20.†

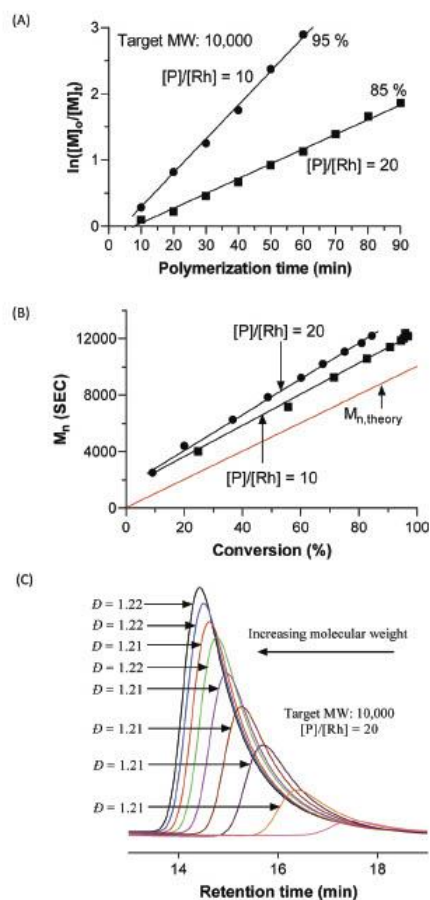


Fig. 6 (A) Pseudo-first-order kinetic plots for the homopolymerisation of PA, with target molecular weight of 10 000 at two different phosphine/Rh ratios; (B) the plots of number average molecular weight (M_n), as measured by SEC and reported as polystyrene equivalents) vs. conversion, and (C) a series of SEC traces demonstrating the evolution of the molecular weight distribution with polymerisation time.

Fig. 6(B) shows the corresponding molecular weight versus conversion plots for the two homopolymerisations with molecular weights reported as the number average (M_n) values as measured by SEC. The theoretical M_n is also shown. In both instances the evolution of molecular weight is linear although SEC-measured values are systematically higher than the theoretical molecular weight at all conversions. There are two possible causes for the observed deviation. Firstly, we note that

the reported M_n values are polystyrene (PS) equivalents by virtue of the SEC instrument having been calibrated with a series of narrow molecular weight distribution PS standards and as such may not be accurate hydrodynamic volume equivalents for PPA. However, it has been reported that the dilute solution characteristics of atactic PPA are similar to those of PS of similar tacticity.⁵⁶ For example, it has been noted that the molecular weight dependence on the radius of gyration for PS and PPA were very similar with the unperturbed dimensions of the polymers also being almost equal. As such, while the application of PS standards cannot be completely eliminated as the cause for the discrepancy in the theoretical and observed M_n 's it appears PS standards are an extremely good match for PPA regardless of the difference in the chemical nature of the respective polymer backbones. Secondly, the disagreement between the theoretical and measured M_n 's could be due to non-quantitative initiation. Assuming the measured M_n values are a genuine reflection of the actual molecular weight of the PPA homopolymers, then the discrepancy suggests an initiation efficiency (IE) for (2) of ca. 0.8. Interestingly, this is exactly the value you would expect assuming that the minor Rh species, 3-PhNaph (2b), present in solution is not an active initiator based on the calculated ratio of the two species. If this is the case, the actual IE of (2a) is 1.0. We note, however, that while quantitative initiation is desirable, it is not a formal pre-requisite for a given polymerisation to be accurately described as living (or controlled).⁵⁷ A comparison of the calculated IE with the reported values for complexes I and II, Fig. 1, indicate that (2) is intermediate of I and II with the former exhibiting essentially quantitative IEs⁹ while the IEs for the latter vary from 0.13–0.56 depending on polymerisation conditions.¹⁴

In a truly living polymerisation processes where $R_i \geq R_p$ (R_i : rate of initiation; R_p : rate of propagation) the resulting (co) polymer will have a narrow molecular weight distribution (assuming there are no side reactions such as termination, chain transfer or branching) in which the dispersity, D , decreases as conversion increases.⁵⁸ Fig. 6(C) shows an example of the evolution of the molecular weight distribution in a PA homopolymerisation at $[P]:[Rh]$ of 20 and for a target molecular weight of 10 000. As expected we observe a systematic shift of the chromatograms to lower retention time (higher molecular weight) with a simultaneous increase in peak intensity with increasing conversion.

In this case, the D of the distribution remains essentially constant at ~ 1.21 . While these D values are not as low as some reported in the literature, including by us, for the controlled polymerisation of PA with Rh(i) complexes they are certainly acceptable.

Collectively, the linearity of the pseudo-first-order kinetic and M_n versus conversion plots, together with the molecular weight distribution chromatograms, when taken together suggest that the polymerisation of PA with the Rh(i)-aryl complex (2) is a controlled process.

There are four possible isomers associated with the geometry and relationship between the backbone C=C and C-C bonds in PPAs. These are referred to as the *cis-cisoidal*,

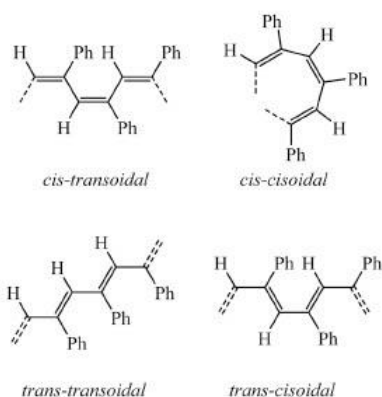


Fig. 7 The four possible stereoisomers associated with polyphenylacetylene.

cis-transoidal, *trans-transoidal* and *trans-cisoidal* geometric isomers, Fig. 7.⁵⁹

It is known that polymerisations that proceed via an insertion pathway, as with Rh-mediated polymerisations of aryl acetylenes, give rise to the *cis-transoidal* form while metathesis-type (co)polymerisation yields the *trans-transoidal/cisoidal* structures.^{10,59,60} Fig. 8 shows the ¹H NMR spectrum, recorded in CDCl₃, of PPA obtained from the homopolymerisation of PA for a target molecular weight of 10 K and [P] : [Rh] of 20. The key feature in PPAs of high *cis-transoidal* content is the sharp peak at $\delta = 5.83$ ppm that is attributed to the H in the polymer backbone on a *cis* C=C bond, while the remaining peaks are associated with the side chain aromatics and any backbone Hs bonded to a *trans* C=C. This spectrum is entirely consistent with previous reports of PPAs with high *cis-transoidal* stereoregularity and in this case the PPA has a calculated⁶¹ *cis* content of 95%. In all cases, the *cis* contents of the obtained PPAs were $\geq 95\%$.

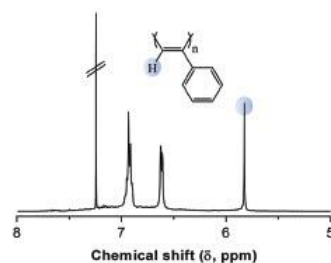


Fig. 8 ¹H NMR spectrum of polyphenylacetylene, recorded in CDCl₃, prepared with (2) for a target molecular weight of 10 K and [P] : [Rh] of 20 highlighting the high *cis-transoidal* stereoregularity.

Conclusions

Herein we have detailed the synthesis of a new Rh(I)-aryl complex and evaluated its use as an initiating species for the controlled, stereospecific polymerisation of phenylacetylene. Interestingly, while targeting a 2-phenylphenyl Rh(I) derivative we isolated the isomeric (2-naphthylphenyl)Rh(I)(nbd) (P(4-FC₆H₄)₃) species as determined by X-ray single-crystal structure analysis. The isolated species was proposed to form from the targeted species via an intramolecular 1,4-Rh atom migration, a supposition that was supported by density functional theory calculations. The isolated complex was characterized in detail by multinuclear NMR spectroscopy which indicated the presence of two principle Rh-P complexes when in solution in an approximate ratio of 4 : 1 in favour of the 2-naphthylphenyl Rh(I) species. The second, minor, species in solution was identified as a third structural isomer (3-phenylphenyl)Rh(I)(nbd)(P(4-FC₆H₄)₃) formed by a proposed second 1,4-Rh atom migration. The recrystallized species was examined with respect to its ability to initiate the homopolymerisation of phenylacetylene. Pseudo-first-order kinetic plots were linear, albeit with short induction periods, as were the molecular weight vs. conversion plots and in all cases the dispersities were ≤ 1.25 suggesting a controlled polymerisation. Initiation efficiencies were not quantitative, but were high (*ca.* 0.8), with the presence of the second minor Rh species in solution proposed to be the cause. Consistent with Rh-mediated insertion polymerisations, the resulting polyphenylacetylene polymers were highly stereoregular with calculated *cis* contents $\geq 95\%$. This report represents, to the best of our knowledge, the first example in which a Rh(I)-aryl complex has been shown to be an effective initiating species for phenylacetylene polymerisation yielding materials with well-defined molecular properties. We are continuing to examine new Rh(I)-aryl species in this specific application.

Conflicts of interest

There are no conflicts to declare.

Acknowledgements

ABL would like to thank the Research Office at Curtin (ROC) for the stipend for NSLT. The authors acknowledge the facilities and the scientific and technical assistance of Microscopy Australia at the Centre for Microscopy, Characterisation and Analysis (CMCA), The University of Western Australia, a facility funded by the University, State and Commonwealth Governments. Dr G. A. Facey of the University of Ottawa is acknowledged for his help with the HMQC experiments. Part of this research was undertaken using the XRD instrumentation (ARC LE0775551) at the John de Laeter Centre, Curtin University. We are grateful to the EPSRC for funding the computational equipment used in this study, grants EP/H011455/1 and EP/K031589/1.

Notes and references

- 1 G. Inzelt, *Conducting Polymers: A New Era in Electrochemistry*, Springer, Berlin, 2nd edn, 2012.
- 2 T. Masuda, *Polym. Rev.*, 2017, 57, 1–14.
- 3 M. Shiotsuki, F. Sanda and T. Masuda, *Polym. Chem.*, 2011, 2, 1044–1058.
- 4 A. Xu, T. Masuda and A. Zhang, *Polym. Rev.*, 2017, 57, 139–159.
- 5 J. Sedláček and H. Balcar, *Polym. Rev.*, 2017, 57, 31–51.
- 6 M. N. Bhebbhe, E. A. De Eulate, Y. Pei, D. W. M. Arrigan, P. J. Roth and A. B. Lowe, *Macromol. Rapid Commun.*, 2017, 38, 1600450.
- 7 F. Sanda, M. Shiotsuki and T. Masuda, *Macromol. Symp.*, 2015, 350, 67–75.
- 8 M. Miyake, Y. Misumi and T. Masuda, *Macromolecules*, 2000, 33, 6636–6639.
- 9 I. Saeed, M. Shiotsuki and T. Masuda, *Macromolecules*, 2006, 39, 8567–8573.
- 10 N. Onishi, M. Shiotsuki, T. Masuda, N. Sano and F. Sanda, *Organometallics*, 2013, 32, 846–853.
- 11 S. Kumazawa, J. R. Castanon, N. Onishi, K. Kuwata, M. Shiotsuki and F. Sanda, *Organometallics*, 2012, 31, 6834–6842.
- 12 S. Kumazawa, J. R. Castanon, M. Shiotsuki, T. Sato and F. Sanda, *Polym. Chem.*, 2015, 6, 5931–5939.
- 13 L. Liu, G. Zhang, T. Aoki, Y. Wang, T. Kaneko, M. Teraguchi, C. Zhang and H. Dong, *ACS Macro Lett.*, 2016, 5, 1381–1385.
- 14 N. S. L. Tan, P. V. Simpson, G. L. Nealon, A. N. Sobolev, P. Raiteri, M. Massi, M. I. Ogden and A. B. Lowe, *Eur. J. Inorg. Chem.*, 2019, 592–601.
- 15 Y. Misumi, K. Kanki, M. Miyake and T. Masuda, *Macromol. Chem. Phys.*, 2000, 201, 2239–2244.
- 16 K. Onitsuka, T. Mori, M. Yamamoto, F. Takei and S. Takahashi, *Macromolecules*, 2006, 39, 7224–7231.
- 17 K. Onitsuka, M. Yamamoto, T. Mori, F. Takei and S. Takahashi, *Organometallics*, 2006, 25, 1270–1278.
- 18 P. Császár and P. Pulay, *J. Mol. Struct.*, 1984, 114, 31–34.
- 19 R. Ahlrichs, M. Bär, M. Häser, H. Horn and C. Kölmel, *Chem. Phys. Lett.*, 1989, 162, 165–169.
- 20 P. Deglmann, F. Furche and R. Ahlrichs, *Chem. Phys. Lett.*, 2002, 362, 511–518.
- 21 P. Deglmann, K. May, F. Furche and R. Ahlrichs, *Chem. Phys. Lett.*, 2004, 384, 103–107.
- 22 K. Eichkorn, O. Treutler, H. Öhm, M. Häser and R. Ahlrichs, *Chem. Phys. Lett.*, 1995, 240, 283–290.
- 23 K. Eichkorn, F. Weigend, O. Treutler and R. Ahlrichs, *Theor. Chem. Acc.*, 1997, 97, 119–124.
- 24 O. Treutler and R. Ahlrichs, *J. Chem. Phys.*, 1995, 102, 346–354.
- 25 M. von Arnim and R. Ahlrichs, *J. Chem. Phys.*, 1999, 111, 9183–9190.
- 26 A. Klamt and G. Schuurmann, *J. Chem. Soc., Perkin Trans.* 2, 1993, 799–805.
- 27 S. Grimme, J. Antony, S. Ehrlich and H. A. Krieg, *J. Chem. Phys.*, 2010, 132, 154104.
- 28 S. Grimme, S. Ehrlich and L. Goerigk, *J. Comput. Chem.*, 2011, 32, 1456–1465.
- 29 R. K. Harris, E. D. Becker, S. M. Cabral de Menezes, P. Granger, R. E. Hoffman and K. W. Zilm, *Pure Appl. Chem.*, 2008, 80, 59–84.
- 30 C. Carlton, *Annual Reports on NMR Spectroscopy*, Elsevier, 2008.
- 31 G. M. Sheldrick, *Acta Crystallogr., Sect. C: Struct. Chem.*, 2015, 71, 3–8.
- 32 J. Cirera, E. Ruiz and S. Alvarez, *Organometallics*, 2005, 24, 1556–1562.
- 33 M. Yamamoto, K. Onitsuka and S. Takahashi, *Organometallics*, 2000, 19, 4669–4671.
- 34 M. W. Drover, L. L. Schafer and J. A. Love, *Dalton Trans.*, 2015, 44, 19487–19493.
- 35 S. M. Ujwaldev, N. A. Harry, M. A. Divakar and G. Anilkumar, *Catal. Sci. Technol.*, 2018, 8, 5983–6018.
- 36 R. Cano, K. Mackey and G. P. McGlacken, *Catal. Sci. Technol.*, 2018, 8, 1251–1266.
- 37 H. Li, B.-J. Li and Z.-J. Shi, *Catal. Sci. Technol.*, 2011, 1, 191–206.
- 38 L. Yang and H. Huang, *Catal. Sci. Technol.*, 2012, 2, 1099–1112.
- 39 Z. Chen, B. Wang, J. Zhang, W. Yu, Z. Liu and Y. Zhang, *Org. Chem. Front.*, 2015, 2, 1107–1295.
- 40 T. Gensch, M. N. Hopkinson, F. Glorius and J. Wencel-Delord, *Chem. Soc. Rev.*, 2016, 45, 2900–2936.
- 41 J. Zhao, M. Campo and R. C. Larock, *Angew. Chem.*, 2005, 117, 1907–1909.
- 42 S. Ma and Z. Gu, *Angew. Chem., Int. Ed.*, 2005, 44, 7512–7517.
- 43 J. Zhang, J.-F. Liu, A. Ugrinov, A. F. X. Pillai, Z.-M. Sun and P. Zhao, *J. Am. Chem. Soc.*, 2013, 135, 17270–17273.
- 44 K. Oguma, M. Miura, T. Satoh and M. Nomura, *J. Am. Chem. Soc.*, 2000, 122, 10464–10465.
- 45 T. Hayashi, K. Inoue, N. Taniguchi and M. Ogasawara, *J. Am. Chem. Soc.*, 2001, 123, 9918–9919.
- 46 T. Matsuda, M. Shigeno and M. Murakami, *J. Am. Chem. Soc.*, 2007, 129, 12086–12087.
- 47 T. Matsuda, Y. Suda and A. Takahashi, *Chem. Commun.*, 2012, 48, 2988–2990.
- 48 K. Sasaki and T. Hayashi, *Tetrahedron: Asymmetry*, 2012, 23, 373–380.
- 49 T. Seiser and N. Cramer, *Angew. Chem., Int. Ed.*, 2010, 49, 10163–10167.
- 50 J. Pantelev, F. Menard and M. Lautens, *Adv. Synth. Catal.*, 2008, 350, 2893–2902.
- 51 M. Tobisu, J. Hasegawa, Y. Kita, H. Kinuta and N. Chatani, *Chem. Commun.*, 2012, 48, 11437–11439.
- 52 N. Ishida, Y. Shimamoto, T. Yano and M. Murakami, *J. Am. Chem. Soc.*, 2013, 135, 19103–19106.
- 53 E. F. van der Eide, P. Yang and R. M. Bullock, *Angew. Chem., Int. Ed.*, 2013, 52, 10190–10194.

- 54 K. Sasaki, T. Nishimura, R. Shintani, E. A. B. Kantchev and T. Hayashi, *Chem. Sci.*, 2012, 3, 1278–1283.
- 55 Y. Misumi and T. Masuda, *Macromolecules*, 1998, 31, 7572–7573.
- 56 D. Ředrová, J. Sedláček, M. Žigon and J. Vohlřídál, *Collect. Czech. Chem. Commun.*, 2005, 70, 1787–1798.
- 57 A. D. Jenkins, P. Kratochvíl, R. F. T. Stepto and U. W. Suter, *Pure Appl. Chem.*, 1996, 68, 2287–2311.
- 58 R. P. Quirk and B. Lee, *Polym. Int.*, 1992, 27, 359–367.
- 59 Z. Ke, S. Abe, T. Ueno and K. Morokuma, *J. Am. Chem. Soc.*, 2011, 133, 7926–7941.
- 60 Y. Kishimoto, P. Eckerle, T. Miyatake, M. Kainosho, A. Ono, T. Ikariya and R. Noyori, *J. Am. Chem. Soc.*, 1999, 121, 12035–12044.
- 61 C. I. Simionescu, V. Percec and S. Dumitrescu, *J. Polym. Sci., Part A: Polym. Chem.*, 1977, 15, 2497–2509.

Reproduced from

Nicholas Sheng Loong Tan, Gareth L. Nealon, Matthew R. Rowles, Alexandre N. Sobolev, Jason M. Lynam, Mark I. Ogden, Massimiliano Massi, Andrew B. Lowe. ‘A (2-(Naphthalen-2-yl)phenyl)rhodium(I) Complex formed by a Proposed Intramolecular 1,4-Ortho-to-Ortho’ Rh Metal-atom Migration and its Efficacy as an Initiator in the Controlled Stereospecific Polymerization of Phenylacetylene’ Accepted for publication 18/10/2019. *Dalton Transactions* 2019, 48, 16437-16447. DOI: 10.1039/c9dt02953b.

by permission of The Royal Society of Chemistry.

Rh(I)(2,5-norbornadiene)(biphenyl)(tris(4-fluorophenyl)phosphine): Synthesis, Characterization, and Application as an Initiator in the Stereoregular (Co)Polymerization of Phenylacetylenes

Nicholas Sheng Loong Tan,[†] Gareth L. Nealon,[‡] Gemma F. Turner,[‡] Stephen A. Moggach,[‡] Mark I. Ogden,[†] Massimiliano Massi,[†] and Andrew B. Lowe*^{†,‡}

[†]Curtin Institute for Functional Molecules and Interfaces (CIFMI) and School of Molecular and Life Sciences (MLS), Curtin University, Kent Street, Bentley, Perth, Western Australia 6102, Australia

[‡]Centre for Microscopy, Characterisation, and Analysis (CMCA) and School of Molecular Sciences, M310, University of Western Australia, 35 Stirling Highway, Perth, Western Australia 6009, Australia

Supporting Information

ABSTRACT: The synthesis of the Rh(I)-aryl complex, Rh(I)(nbd)(Biph)(P(4-FC₆H₄)₃) is reported and its efficacy as an initiator for the (co)polymerization of phenylacetylenes established. The X-ray crystal structure indicates that the complex adopts a slightly distorted square planar geometry whose purity and structure was also confirmed by elemental analysis and ¹H, ¹³C, ³¹P, ¹⁹F, ¹⁰³Rh, and ³¹P-¹⁰³Rh{¹H} HMQC NMR spectroscopy. We demonstrate that Rh(I)(nbd)(Biph)(P(4-FC₆H₄)₃) mediates the (co)polymerization of phenylacetylenes in a controlled fashion with initiation efficiencies as high as 0.98, as evidenced by the pseudo-first-order kinetic and number-average molecular weight versus conversion profiles. The ability to form well-defined AB diblock copolymers, in a stereoregular manner, by sequential monomer addition is verified in the block copolymerization of phenylacetylene with 4-fluorophenylacetylene with quantitative crossover efficiency, as determined by size exclusion chromatography.



Certain Rh complexes are well-known as versatile and efficient catalysts for the (co)polymerization of alkyne functional monomers, including phenylacetylenes, propargyl esters and amides, and phenyl isocyanides.¹ Their common use as initiators for these monomer families is due to their low oxophilicity, impressive functional group tolerance, ease of handling, and generally high activity. While the uncontrolled (co)polymerization of arylacetylenes employing catalytic bridged dimers such as [Rh(nbd)Cl]₂ (nbd: 2,5-norbornadiene) or [Rh(cod)Cl]₂ (cod: 1,5-cyclooctadiene), as well as other Rh derivatives,^{2,3} typically with an amine cocatalyst, is well documented,^{4–8} there are comparatively few reports detailing the use of well-defined Rh(I) catalysts for controlled (co)polymerization of this important monomer class.^{9–18}

The first report detailing the controlled polymerization of phenylacetylene (PA) was from Kishimoto et al.⁹ and employed the pentacoordinate Rh(I)-alkynyl complex, Rh(C≡CPh)(nbd)(PPh₃)₂. While mediating polymerization in a controlled manner, the reported initiation efficiencies (IEs) for this species were nonquantitative and spanned 0.33–0.56. Subsequently, the same group reported that the in situ generated tetracoordinate Rh(I) species, Rh(C≡CPh)(nbd)(PPh₃) likewise effected the controlled polymerization of PA, with IEs as high as 0.72.¹⁹ Following these seminal reports, and based on the assumption that the active propagating center in PA (co)polymerization is a vinylrhodium species, Masuda and co-workers reported the synthesis and application of a series of Rh(I)-vinyl complexes,

most commonly with a triphenylvinyl initiating fragment, see Figure 1, compound A for examples.^{10,12,20,21} Such complexes

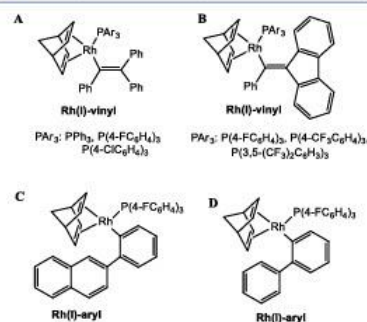


Figure 1. Chemical structures of Masuda-type Rh(I)-vinyl complexes A and B, our recently reported Rh(I)aryl species C, and the structurally related aryl complex D, which is the focus of this report.

Received: December 10, 2019

Accepted: December 16, 2019

are typically readily isolated, exhibit essentially quantitative IEs for the (co) polymerization of PA, and yield highly stereoregular (>95%) *cis-transoidal* polyphenylacetylene (co)polymers.

Inspired by the work of Masuda and co-workers and the dearth of examples of well-defined Rh(I) species as initiators for PA (co) polymerization, we recently reported the synthesis and application of three new Masuda-type Rh(I)- α -phenylvinyl-fluorenyl complexes containing fluorine-functionalized phosphine ligands, Figure 1, compound B.²² Surprisingly, while meeting the general structural requirements for highly efficient initiators,¹¹ these complexes exhibited IEs (as determined by SEC), for PA homopolymerization, in the range 0.13 to 0.56, although the product polymers possessed narrow molecular weight distributions and the expected high *cis-transoidal* stereoregularity. To more clearly understand the difference in IEs for complexes A and B, we subsequently targeted a new complex, Rh(I)(2,5-norbornadiene)(2-phenylnaphthyl)tris(4-fluorophenyl) phosphine, a Rh(I)-*aryl* species. Rh(I)-*aryl* complexes are particularly attractive alternatives in this target application given the large number of commercially available aryl bromides available for the synthesis of new complexes, and have been previously demonstrated to be effective initiators for the polymerization of isocyanides bearing bulky *ortho*-substituents.^{23,24} Interestingly, after recrystallization, X-ray analysis indicated isolation of the structural isomer (C), the Rh(I)-2-naphthylphenyl derivative formed by a 1,4-Rh atom migration from the target complex. Compound C was, however, an active initiator for PA with measured IEs, as determined by SEC, as high as 0.8 and represented the first demonstration of the effectiveness of a well-defined, isolated Rh(I)-*aryl* complex in this specific application.²⁵ Unexpectedly, however, when in solution, compound C underwent a second *ortho-to-ortho* migration to give a third isomer, the 3-phenyl-2-naphthyl derivative. While such Rh-atom migrations are of fundamental mechanistic interest, to eliminate the possible formation of multiple ((in)active) Rh complexes via such migratory processes in solution, herein we report the synthesis and application of a new Rh(I) biphenyl derivative.

The synthetic route to the target biphenyl functionalized complex, and its subsequent use as a polymerization initiator is shown in Scheme 1. Reaction of [Rh(nbd)Cl]₂ with tris(4-fluorophenyl)phosphine gave the intermediate tetracoordinate Rh(nbd)(P(4-FC₆H₄)₃)Cl complex, (I). Treatment of 2-bromo-1,1'-biphenyl with *n*-BuLi yielded the lithiated biaryl species which when reacted with (I) gave the target Rh(I)-*aryl*

Scheme 1. Outline for the Synthesis of Rh(I)(nbd)(BiPh)P(4-FC₆H₄)₃, D, and Its Application as an Initiator for the Homopolymerization of Phenylacetylene



complex, Rh(nbd)(BiPh)(P(4-FC₆H₄)₃), Figure 1, compound D. Recrystallization of D from CH₂Cl₂/methanol yielded X-ray quality crystals, enabling the solid-state structure to be determined, Figure 2. Consistent with previously reported Rh(I)(nbd)PAr₃-alkynyl, -vinyl, and -aryl complexes noted above, D adopts a slightly distorted square planar geometry.

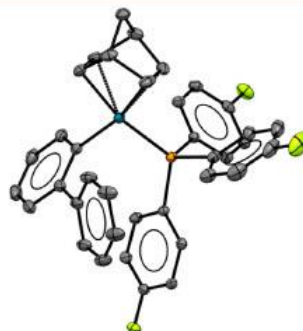


Figure 2. ORTEP representation, with 50% probability ellipsoids, of complex D (CCDC195957). H atoms are omitted for clarity.

Complex D was further characterized by multinuclear NMR spectroscopy. The ¹H, ¹³C, ¹⁹F, and ³¹P data/spectra, and the corresponding assignments are given in the Supporting Information (Figures S1–S4) and confirm the structure and purity of D, while the ¹⁰³Rh and ³¹P-¹⁰³Rh{¹H} spectra are shown in Figure 3. The NMR-active spin -1/2 nucleus ¹⁰³Rh is

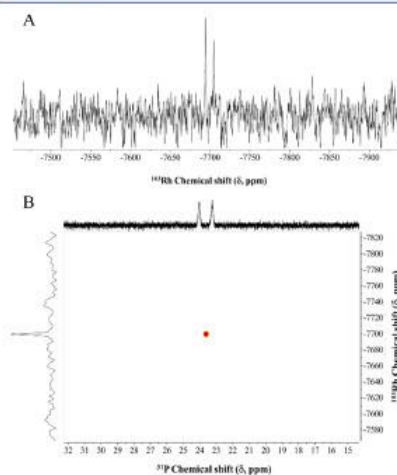


Figure 3. ¹⁰³Rh spectrum (19.1 MHz) recorded in CD₂Cl₂ (A) and ³¹P-¹⁰³Rh{¹H} HMQC spectrum (B) of complex D.

100% abundant, but suffers from extremely low sensitivity and large chemical shift range. However, in this instance, we were able to directly observe the ^{103}Rh signal which appears as a doublet, due to coupling with ^{31}P , centered around $\delta = -7699$ ppm (536 ppm if referenced to Rh metal), Figure 3A. This is consistent with the ^{103}Rh chemical shifts we reported for the series of fluorenyl-functionalized Rh(I) complexes shown in Figure 1, compound B, which had measured shifts spanning the range $\delta = -7861$ to -7870 ppm.²² To verify this observation and confirm purity we conducted a complementary 2D ^{31}P , ^{103}Rh - $\{^1\text{H}\}$ heteronuclear multiple quantum coherence (HMQC) experiment, Figure 3B. In such experiments, the sensitivity of the Rh nucleus is enhanced by a factor of ~ 600 by virtue of being bonded to P with its associated high gyromagnetic ratio. The HMQC spectrum clearly shows the presence of single Rh and P species with direct coupling between the two nuclei, confirming the purity and stability of complex D in solution.

With complex D in-hand we evaluated its efficacy as an initiator for the homopolymerization of PA. It is known that when conducting such 2,1-insertion^{26,27} (co)polymerizations it is necessary to add additional free phosphine to serve as a rate modifier if controlled polymerization is desirable. For example, Miyake, Misumi, and Masuda¹² reported that in polymerizations of PA with A ($\text{PA}_{\text{r}_3} = \text{P}(4\text{-FC}_6\text{H}_4)_3$), Figure 1, it was necessary to add a minimum of 5 equiv of free phosphine, relative to Rh, in order to obtain material with a low dispersity. Increasing the ratio higher had no discernible effect on the dispersity, but impacted the kinetics with polymerizations slowing the higher the free phosphine content. We have made similar observations in our previous reports concerning the (co)polymerization of phenylacetylene with complexes B and C, Figure 1.^{22,25} To confirm this general feature, we performed a control experiment in which PA was homopolymerized for a target M_n of 10000 in toluene at 30 °C in the absence of added free $\text{P}(4\text{-FC}_6\text{H}_4)_3$. Under these conditions, polymerization was rapid, reaching about 97% conversion within 30 s and yielded a homopolymer that eluted at the upper column limits of our SEC indicating an M_n in excess of 100000 and a noncontrolled polymerization process. All further experiments were conducted in the presence of additional free phosphine.

Figure 4A shows the pseudo-first-order kinetic plots associated with the homopolymerization of PA with D in toluene at 30 °C at $[\text{P}]/[\text{Rh}]$ of 5, 10, and 20. As expected, the homopolymerization at $[\text{P}]/[\text{Rh}] = 5$ was the fastest ($k_{\text{app}} = 0.0019 \text{ s}^{-1}$) and reached 98% conversion after 35 min with the final, isolated material having an SEC measured dispersity ($D = M_w/M_n$) of 1.25 and M_n of 11,560 which corresponds to an IE of 0.86. The value of the IE for this Rh(I)-aryl complex is significantly higher than complexes B and C, Figure 1, and is approaching the benchmark Masuda Rh(I)-vinyl species. In the case of homopolymerization conducted at $[\text{P}]/[\text{Rh}] = 10$, the rate is decreased ($k_{\text{app}} = 0.0012 \text{ s}^{-1}$), and we observe a short induction period of about 5 min, similar to that observed previously with complex C, Figure 1. However, polymerization is still rapid, reaching just over 96% conversion after 50 min. We observed an improved dispersity of 1.18 and a final M_n of 11250, which equates to an IE of 0.87. A further improvement in the dispersity (and decrease in rate, $k_{\text{app}} = 0.0008 \text{ s}^{-1}$, and slightly increased induction time) is observed at $[\text{P}]/[\text{Rh}] = 20$ with the final sample having an SEC-measured D of 1.11 and M_n of 10250. This corresponds to a near-quantitative IE of 0.98; such efficiencies have only previously been reported for certain Masuda-type Rh(I)-vinyl initiators. The evolution of the

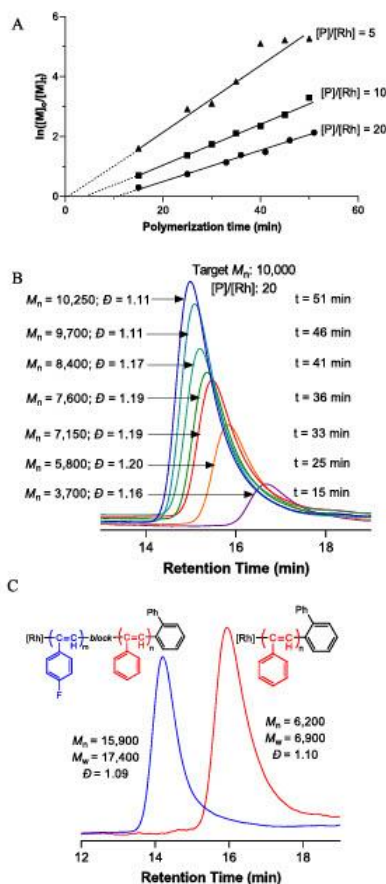


Figure 4. (A) Pseudo-first-order kinetic plots for the homopolymerization of PA in toluene at 30 °C with $[\text{P}]/[\text{Rh}] = 5, 10$ and 20; (B) evolution of the molecular weight distribution in the homopolymerization of PA for a target molecular weight of 10000 and $[\text{P}]/[\text{Rh}] = 20$; (C) SEC traces for a poly(phenylacetylene) homopolymer (red) and an AB diblock copolymer with 4-fluorophenylacetylene formed by sequential monomer addition (blue). $[\text{P}] = [\text{P}(4\text{-FC}_6\text{H}_4)_3]$.

molecular weight distribution for this polymerization is highlighted in Figure 4B, while the SEC-measured M_n versus conversion plots for the three homopolymerizations are given in the Supporting Information (Figures S5–S7). The M_n versus conversion plots are essentially linear for all three homopolymerizations. Collectively, the kinetic and molecular weight data suggest that the homopolymerization of PA with D in the presence of added free $\text{P}(4\text{-FC}_6\text{H}_4)_3$ proceeds in a controlled

fashion with higher ratios of $[P]/[Rh]$, giving better control albeit at the expense of polymerization rate.

A distinguishing feature of phenylacetylene (co)polymers prepared by Rh-mediated insertion polymerization is the highly stereoregular nature of the final materials with polymers adopting a *cis-transoidal* structure.²⁸ This key structural feature was observed in the case of the polyphenylacetylene homopolymers prepared herein with calculated *cis* contents of 92 ($[P]/[Rh] = 5$), 96 ($[P]/[Rh] = 10$), and 99% ($[P]/[Rh]$), suggesting a correlation between stereoregularity and the polymerization rate or overall level of control.

To highlight the broader utility of D with a functional substrate, we subsequently homopolymerized 4-fluorophenylacetylene (4-FPA) for a target M_n of 5000 and $[P]/[Rh] = 20$. Consistent with PA homopolymerizations, polymerization proceeded rapidly yielding a well-defined product with a narrow molecular distribution ($D = 1.07$) and high *cis-transoidal* stereoregularity (calculated *cis* content of 96%), Figures S8–S10.

In a final demonstration of the ability of D to mediate the (co)polymerization of phenylacetylenes in a controlled fashion an AB diblock copolymer of PA with 4-FPA was prepared via sequential monomer addition to demonstrate retention of chain-end activity, Figure 4C. PA was first homopolymerized in toluene at 30 °C with $[P]/[Rh] = 20$ and target M_n of 5000 at quantitative conversion. An aliquot was withdrawn after 60 min and analyzed by SEC, which indicated a homopolymer with an M_n of 6200 and D of 1.10. 4-FPA was subsequently added and block polymerization allowed to proceed for a further 60 min. The copolymerization was terminated by the addition of a small volume of acetic acid, and an aliquot removed for SEC analysis. Block copolymer formation was verified by the systematic shift of the molecular weight distribution to shorter retention time with no evidence of any residual homopolymer “impurity” confirming retention of chain-end activity after PA homopolymerization and quantitative crossover efficiency. The product AB diblock copolymer had a measured M_n of 15900 and D of 1.09.

Figure 5 shows the 1H NMR spectrum, with the ^{19}F spectrum shown inset, recorded in C_6D_6 of the poly(PA-*block*-4-FPA) copolymer. The stereoregular nature of the copolymer is evidenced by the well-resolved aromatic hydrogens covering the range $\delta = 6.9$ –6.2 ppm, but more importantly, by the two signals at $\delta = 6.0$ and 5.8 ppm. The very sharp, former signal, is associated with backbone hydrogens in the *cis* configuration on the PA block while we assign the latter, broader signal to *cis* hydrogens of the 4-FPA block. The more poorly resolved *cis*-H signal associated with the 4-FPA block is indicative of a less stereoregular microstructure but, nonetheless, is still predominantly *cis*; the overall *cis* content of the copolymer was determined to be 76%. Such observations have been made previously for poly(fluorophenylacetylene)s prepared via insertion and metathesis catalysts.²⁸

In summary, we have reported the synthesis of a new, well-defined, readily isolable, Rh(I)-aryl complex that serves as a highly efficient initiator for the controlled (co)polymerization of phenylacetylenes. Successful synthesis, isolation, and purity of Rh(nbd)(BiPh)(P(4-FC₆H₄))₃, D, was confirmed by a combination of elemental analysis, X-ray crystal structure analysis, and multinuclear NMR spectroscopy. The ability of D to mediate the controlled (co)polymerization of phenylacetylenes was verified from the pseudo-first-order kinetic profiles, the molecular weight vs conversion plots and the ability

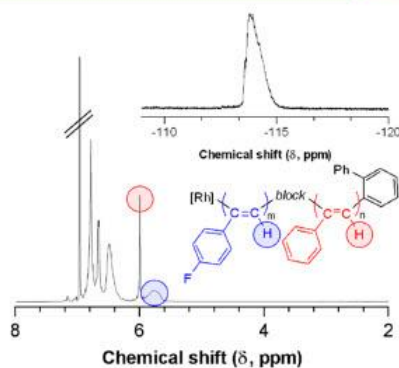


Figure 5. 1H NMR spectrum, recorded in C_6D_6 of poly(phenylacetylene-*block*-4-fluorophenylacetylene), highlighting the *cis-transoidal* stereoregular nature of the copolymer microstructure. The ^{19}F NMR spectrum of the block copolymer is shown in the inset.

to prepare an AB diblock copolymer with quantitative reinitiation. The stereoregular, *cis-transoidal* structure of the product (co)polymers was confirmed by 1H NMR spectroscopy. This contribution represents only the second example in which a well-defined Rh(I)-aryl complex has been employed specifically as an initiator for the controlled polymerization of phenylacetylenes and, at present, exhibits the highest initiation efficiency. We continue to examine new, novel Rh(I)-aryl complexes in this specific target application.

■ ASSOCIATED CONTENT

Supporting Information

The Supporting Information is available free of charge at <https://pubs.acs.org/doi/10.1021/acsmacrolett.9b00975>.

Experimental details, instrument (SEC/NMR) information, select NMR spectra, and full crystallographic details (PDF)

■ AUTHOR INFORMATION

Corresponding Author

*E-mail: andrew.b.lowe@curtin.edu.au

ORCID

Mark I. Ogden: 0000-0001-5317-1637

Massimiliano Massi: 0000-0001-6949-4019

Andrew B. Lowe: 0000-0002-7874-2050

Notes

The authors declare no competing financial interest.

■ ACKNOWLEDGMENTS

A.B.L. kindly thanks the Research Office, Curtin for a stipend for NSLT. The authors acknowledge the facilities and the scientific and technical assistance of Microscopy Australia at the Centre for Microscopy, Characterisation and Analysis (CMCA), the University of Western Australia, a facility funded by the University, State and Commonwealth Governments.

REFERENCES

- (1) Tan, N. S. L.; Lowe, A. B. Polymerizations Mediated by Well-defined Rhodium Complexes. *Angew. Chem., Int. Ed.*, DOI: 10.1002/anie.201909909 and DOI: 10.1002/ange.201909909.
- (2) Tang, B. Z.; Poon, W. H.; Leung, S. M.; Leung, W. H.; Peng, H. Synthesis of Stereoregular Poly(phenylacetylene)s by Organorhodium Complexes in Aqueous Media. *Macromolecules* 1997, 30, 2209–2212.
- (3) Wu, X.; Zhang, P.; Yang, Z.; Zhang, S.; Liu, H.; Chi, W.; Li, X.; Dong, Y.; Qiu, N.; Yan, L. Polymerization of phenylacetylenes by binuclear rhodium catalysts with different *para*-binucleating phenoximinato linkages. *Polym. Chem.* 2019, 10, 4163–4172.
- (4) Bhebbé, M. N.; De Eulate, E. A.; Pei, Y.; Arrigan, D. W. M.; Roth, P. J.; Lowe, A. B. Reactive Conjugated Polymers: Synthesis, Modification, and Electrochemical Properties of Poly(pentadienylphenylacetylene) (Co)Polymers. *Macromol. Rapid Commun.* 2017, 38, 1600–1650.
- (5) Masuda, T. Substituted Polyacetylenes: Synthesis, Properties, and Functions. *Polym. Rev.* 2017, 57, 1–14.
- (6) Freire, F.; Quaiñó, E.; Rigueira, R. Supramolecular Assemblies from Poly(phenylacetylene)s. *Chem. Rev.* 2016, 116, 1242–1271.
- (7) Liu, L.; Zang, Y.; Jia, H.; Aoki, T.; Kaneko, T.; Hadano, S.; Teraguchi, M.; Miyata, M.; Zhang, G.; Namikoshi, T. Helix-Sense-Selective Polymerization of Axial Phenylacetylenes and Unique Properties of the Resulting Cis-Isoidal Polymers. *Polym. Rev.* 2017, 57, 89–118.
- (8) Masuda, T. Substituted Polyacetylenes. *J. Polym. Sci., Part A: Polym. Chem.* 2007, 45, 165–180.
- (9) Kishimoto, Y.; Eckerle, P.; Miyatake, T.; Ikariya, T.; Noyori, R. Living Polymerization of Phenylacetylenes Initiated by Rh-(C≡C₂H₅)(2,5-norbornadiene)[P(C₆H₅)₃]₂. *J. Am. Chem. Soc.* 1994, 116, 12131–12132.
- (10) Misumi, Y.; Masuda, T. Living Polymerization of Phenylacetylene by Novel Rhodium Catalysts Quantitative Initiation and Introduction of Functional Groups at the Initiating Chain End. *Macromolecules* 1998, 31, 7572–7573.
- (11) Misumi, Y.; Kanki, K.; Miyake, M.; Masuda, T. Living Polymerization of Phenylacetylene by Rhodium-Based Ternary Catalysts, (Diene)Rh(I) Complex/Vinylithium/Phosphorous Ligand. Effect of Catalyst Components. *Macromol. Chem. Phys.* 2000, 201, 2239–2244.
- (12) Miyake, M.; Misumi, Y.; Masuda, T. Living Polymerization of Phenylacetylene by Isolated Rhodium Complexes, Rh[(C₆H₅)₃]=C(C₆H₅)₂(nb)(4-XC₆H₄)₂P (X = F, Cl). *Macromolecules* 2000, 33, 6636–6639.
- (13) Saeed, I.; Shiotsuki, M.; Masuda, T. Living Polymerization of Phenylacetylene with Tetrafluorobenzoborelene Ligand-Containing Rhodium Catalysts Systems Featuring the Synthesis of High Molecular Weight Polymer. *Macromolecules* 2006, 39, 8567–8573.
- (14) Onishi, N.; Shiotsuki, M.; Masuda, T.; Sano, N.; Sanda, F. Polymerization of Phenylacetylenes Using Rhodium Catalysts Coordinated by Norbornadiene Linked to a Phosphino or Amino Group. *Organometallics* 2013, 32, 846–853.
- (15) Kumazawa, S.; Castanon, J. R.; Onishi, N.; Kuwata, K.; Shiotsuki, M.; Sanda, F. Characterization of the Polymerization Catalysts [(2,5-norbornadiene)Rh(C(Ph)=CPh₂)(PPh₃)₂] and Identification of the End Structures of Poly(phenylacetylene)s Obtained by Polymerization Using this Catalyst. *Organometallics* 2012, 31, 6834–6842.
- (16) Krebs, F. C.; Jørgensen, M. Conducting Block Copolymers. Towards a Polymer *pn*-Junction. *Polym. Bull.* 2003, 50, 359–366.
- (17) Shiotsuki, M.; Onishi, N.; Sanda, F.; Masuda, T. Living Polymerization of Phenylacetylenes Catalyzed by Cationic Rhodium Complexes Bearing Tetrafluorobenzoborelene. *Polym. J.* 2011, 43, 51–57.
- (18) Jiménez, M. V.; Pérez-Torrente, J. J.; Bartolomé, M. L.; Viñe, E.; Lahoz, F. J.; Oro, L. A. Cationic Rhodium Complexes with Hemilabile Phosphine Ligands as Polymerization Catalyst for High Molecular Weight Stereoregular Poly(phenylacetylene). *Macromolecules* 2009, 42, 8146–8156.
- (19) Kishimoto, Y.; Miyatake, T.; Ikariya, T.; Noyori, R. An Efficient Rh(I) Initiator for Stereospecific Living Polymerization of Phenylacetylenes. *Macromolecules* 1996, 29, 5054–5055.
- (20) Kanki, K.; Masuda, T. Synthesis of Conjugated Star Polymer and Star Block Copolymers Based on the Living Polymerization of Phenylacetylenes with a Rh Catalyst. *Macromolecules* 2003, 36, 1500–1504.
- (21) Saeed, I.; Shiotsuki, M.; Masuda, T. Living Polymerization of Phenylacetylene with Tetrafluorobenzoborelene Ligand-Containing Rhodium Catalyst Systems Featuring the Synthesis of High Molecular Weight Polymer. *Macromolecules* 2006, 39, 8567–8573.
- (22) Tan, N. S. L.; Simpson, P. V.; Nealon, G. L.; Sobolev, A. N.; Raiteri, P.; Massi, M.; Ogden, M. I.; Lowe, A. B. Rhodium(I)- α -Phenylvinylfluorenyl Complexes: Synthesis, Characterization, and Evaluation as Initiators in the Stereospecific Polymerization of Phenylacetylene. *Eur. J. Inorg. Chem.* 2019, 592–601.
- (23) Yamamoto, M.; Onitsuka, K.; Takahashi, S. Polymerization of Aryl Isocyanides Possessing Bulky Substituents at an *ortho* Position Initiated by Organorhodium Complexes. *Organometallics* 2000, 19, 4669–4671.
- (24) Onitsuka, K.; Yamamoto, M.; Mori, T.; Takei, F.; Takahashi, S. Living Polymerization of Bulky Aryl Isocyanide with Arylrhodium Complexes. *Organometallics* 2006, 25, 1270–1278.
- (25) Tan, N. S. L.; Nealon, G. L.; Lyman, J. M.; Sobolev, A. N.; Rowles, M. R.; Ogden, M. I.; Massi, M.; Lowe, A. B. A (2-(Naphthalen-2-yl)phenyl)rhodium(I) Complex formed by a Proposed Intramolecular 1,4-Ortho-to-Ortho' Rh Metal-atom Migration and its Efficacy as an Initiator in the Controlled Stereospecific Polymerization of Phenylacetylene. *Dalton Trans* 2019, 48, 16437–16447.
- (26) Ke, Z.; Abe, S.; Ueno, T.; Morokuma, K. Rh-Catalyzed Polymerization of Phenylacetylene: Theoretical Studies of the Reaction Mechanism, Regioselectivity, and Stereoregularity. *J. Am. Chem. Soc.* 2011, 133, 7926–7941.
- (27) Sanda, F.; Shiotsuki, M.; Masuda, T. Controlled Polymerization of Phenylacetylenes Using Well-Defined Rhodium Catalysts. *Macromol. Symp.* 2015, 350, 67–75.
- (28) Bondarev, D.; Zedník, J.; Plutnarova, I.; Vohlidal, J.; Sellič, J. Molecular Weight and Configurational Stability of Poly-[(fluorophenyl)acetylene]s Prepared with Metathesis and Insertion Catalysts. *J. Polym. Sci., Part A: Polym. Chem.* 2010, 48, 4296–4309.

Reprinted (adapted) with permission from

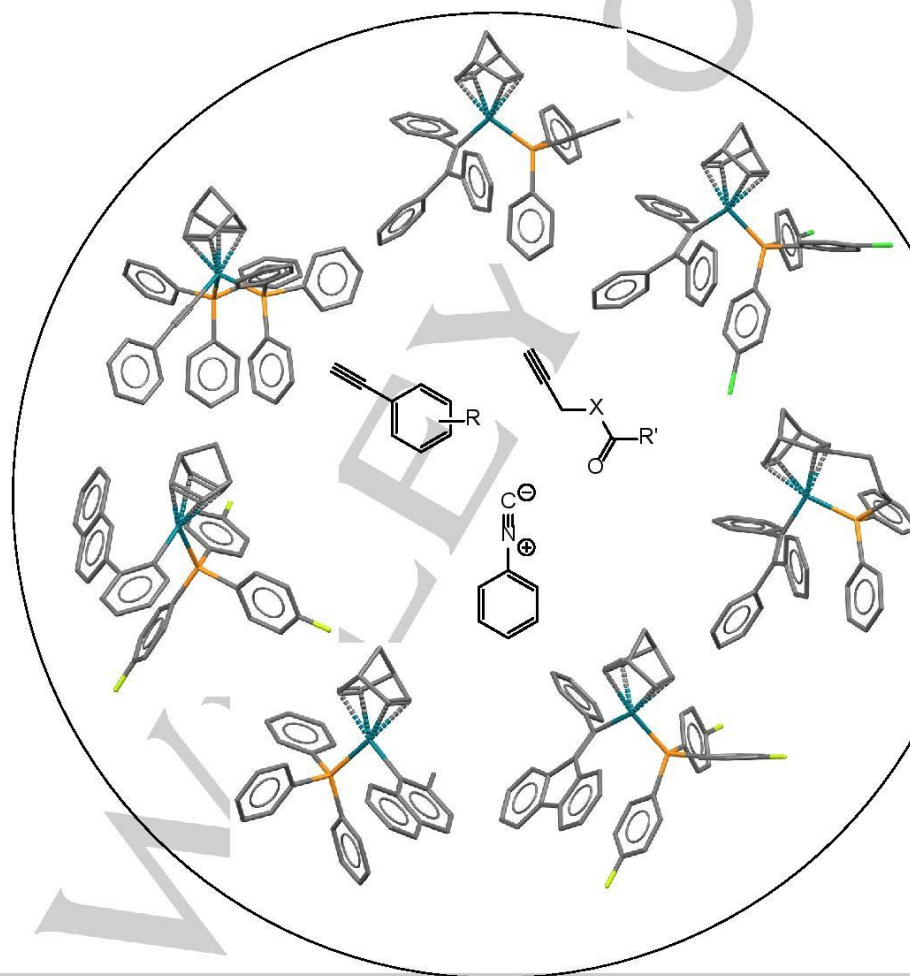
Nicholas Sheng Loong Tan, Gareth L. Nealon, Gemma Turner, Stephen Moggach, Mark I. Ogden, Massimiliano Massi, Andrew B. Lowe ‘**Rh(I)(2,5-Norbornadiene)(biphenyl)tris(4-fluorophenyl)phosphine: Synthesis, Characterization and Application as an Initiator in the Stereospecific (Co)Polymerization of Phenylacetylenes**’ *ACS Macro Letters* 2020, 9, 56-60.

DOI: 10.1021/acsmacrolett.9b00975.

Copyright (2020) American Chemical Society.

Polymerisationen vermittelt durch wohl-definierte Rhodium Komplexe

Nicholas Sheng Loong Tan^[a] and
Andrew B. Lowe^{*[a]}



Accepted Manuscript

Abstract: Dieser Minireview detailliert den aktuellen Stand von (Co)polymerisationen vermittelt durch wohl-definierte Rh(I) ethynyl-, vinyl-, und aryl Komplexe. Insbesondere fokussieren wir auf Rh(I) Verbindungen, die sich für die (Co)polymerisation von Phenylazetylenen, Arylisocyaniden und Propargylestern und Amidien eignen.

1. Einleitung

Die Möglichkeit, neue (Co)polymere in einer kontrollierten (oder lebenden) Art darzustellen, d.h. mit fortschrittlichen Architekturen, Topologien, vorbestimmten molekularen Eigenschaften und mit ortsspezifischen funktionellen Gruppen, oft für gezielte Anwendungen, ist ein zentrales Thema in der modernen synthetischen Polymerwissenschaft geworden. Das grundlegende Prinzip einer kontrollierten Polymerisation ist nicht neu; Ziegler hat 1936 vorgeschlagen, dass die anionische Polymerisation initiiert mit einem Lithiumalkyl in der Abwesenheit von Transfer und Terminierungen ablaufen sollte;^[1] diese zwei Eigenschaften formen die Basis der aktuellen IUPAC Definition einer lebenden Kettenwachstumspolymerisation.^[2]

Nicholas S. L. Tan hat einen BSc (Hons) Abschluss in Chemie von Curtin University. Er ist aktuell Doktorand im dritten Jahr und arbeitet unter der Aufsicht von Prof. Andrew Lowe in der School of Molecular and Life Sciences, wo er Mitglied des Curtin Institute for Functional Molecules and Interfaces ist. Seine Forschung basiert auf der Synthese von neuen Rh(I) Komplexen für die kontrollierte Polymerisation von Phenylazetylenen.



Andrew B. Lowe hat BSc (Hons), DPhil und DSc Abschlüsse von der University of Sussex Sussex, UK. Er hatte akademische Positionen an der University of Southern Mississippi und der University of New South Wales, Sydney, inne. Aktuell ist er Direktor und Professor am Curtin University Institute for Functional Molecules and Interfaces.



[a] Mr. N. S. L. Tan and Prof. A. B. Lowe*
Curtin Institute for Functional Molecules and Interfaces (CIFMI)
& School of Molecular and Life Sciences (MLS)
Curtin University
Bentley, Perth, WA 6102, Australia.
E-mail: andrew.b.lowe@curtin.edu.au

Es war allerdings nicht bis zu den Pionierarbeiten von Swarc und Mitarbeiter*innen, dass solche lebenden anionischen Polymerisationen experimentell bestätigt wurden.^[3] Seit diesen einschneidenden Beiträgen sind viele Vorgehensweisen entwickelt worden, die (Co)polymerisation der meisten (üblichen) Monomertypen in einer kontrollierten Weise ermöglichen (siehe SI für die Kriterien einer kontrollierten Polymerisation).

Polymerisationstechniken wie zum Beispiel pseudo-lebende kationische,^[4] Gruppentransfer,^[5] „unsterbliche“,^[6] *N*-carboxyanhydrid ring-öffnende,^[7] lebende ring-öffnende Metathese,^[8] lebende Koordination,^[9] und die reversiblen Deaktivierung radikalischen Prozesse (stabile radikalische Polymerisation (SRP),^[10] ATRP,^[11] RAFT,^[12] und TERP/SBRP^[13]) sind heute wohl-etabliert und ermöglichen gemeinsam die kontrollierte (Co)polymerisation der meisten üblichen Monomerklassen. (Co)polymere mit vollständig konjugierten Rückgraten stellen eine wichtige Materialfamilie dar. Solche Materialien (üblicherweise verschiedenartig bezeichnet als leitfähige Polymere, halb-leitende Polymere, oder selbstleitende Polymere) haben einzigartige und einstellbare Eigenschaften und von daher weite Anwendungsmöglichkeiten.^[14] Eine wichtige Untereinheit dieser Materialfamilie sind solche, die auf dem strukturellen Phenylazetylenmotiv basieren. Diese Substratfamilie hat signifikante Aufmerksamkeit auf sich gezogen wegen ihrer beeindruckenden Löslichkeitseigenschaften, einfachen Verarbeitbarkeit und Oxidationsstabilität. Phenylazetylen ist für eine Reihe an Polymerisationen geeignet, einschließlich radikalischer,^[15] Metathese^[16] und Einschub^[17] Prozesse, wobei die letzteren als Übergangsmetall-vermittelte Pfade bevorzugt sind. Von diesen Vorgehensweisen wird Einschubpolymerisation, typischerweise vermittelt von Rh-Verbindungen, am häufigsten verwendet. In der Tat macht deren hohe Toleranz für funktionelle Gruppen, einfache Handhabbarkeit, hohe Aktivität, und niedrige Oxophilie Rh-Verbindungen ideale Katalysatoren/Initiatoren für gezielte Anwendungen.

Die nicht-kontrollierte Einschubpolymerisation von Phenylazetylenen und deren funktionellen Derivaten ist gut dokumentiert.^[18] Eine Reihe von kommerziell erhältlichen Rh-Komplexen ist angewendet worden, typischerweise in Verbindung mit einer Base mit zum Beispiel Triethylamin (NEt₃) oder *N,N*-4-Dimethylaminopyridin (DMAP). Abbildung 1 zeigt die chemischen Strukturen der zwei am häufigsten für die Synthese von Phenylazetylen-basierten (Co)polymeren verwendeten Rh-Spezies, (1)^[19] und (2),^[19c, 19d, 19h, 19k, 20] die auch als Vorstufen für andere Rh-Komplexe dienen.^[21] Sowohl (1) als auch (2) sind Beispiele von Halogen-überbrückten binuklearen Rh-Komplexen mit stabilisierenden Dien Liganden—bicyclisches 2,5-Norbornadien (nbd) in (1) und 1,5-Cyclooctadien (cod) im Fall von (2).

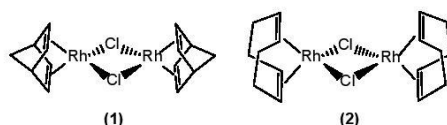


Abbildung 1. Chemische Strukturen vom 2,5-Norbornadienrhodium(I) chlorid dimer, $[\text{Rh}(\text{nbd})\text{Cl}]_2$ (1), und 1,5-cyclooctadienrhodium(I) chlorid dimer, $[\text{Rh}(\text{cod})\text{Cl}]_2$ (2).

Als Folge der verschiedenen möglichen Übergangsmetal-vermittelten Reaktionspfaden, nämlich Einschub und Metathese, gibt es vier mögliche verschiedene stereoreguläre Strukturen der resultierenden Poly(phenylazetylene)—zwei als Resultat des Einschubprozesses und zwei produziert durch Metathese (Co)polymerisation, deren Strukturen sich unterscheiden in der Natur der Verbindungen zwischen den Wiederholungseinheiten siehe Abbildung 2.

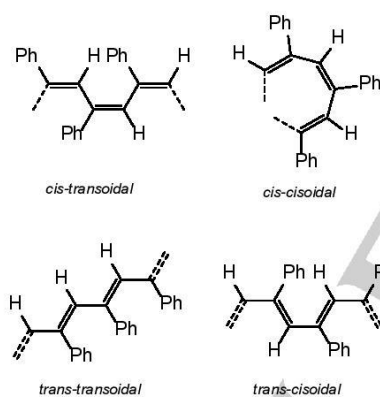


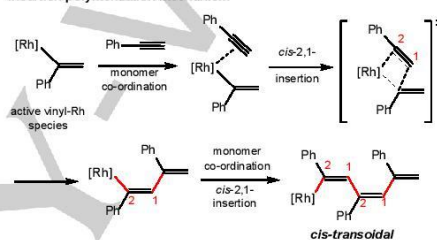
Abbildung 2. Vier mögliche stereoisomere von Polyphenylazetylen.

Die *cis-transoidal* und *cis-cisoidal* Spezies sind mit dem Einschubprozess verbunden wobei die Wiederholungseinheiten durch die Bildung von neuen C–C Bindungen verbunden werden, während die *trans-transoidal* und *trans-cisoidal* Strukturen von der Metathesepolymerisation herrühren, bei der die Wiederholungseinheiten durch die Bildung von neuen C=C Bindungen verbunden werden.^[22] Die generell akzeptierten 2,1-Einschub- und Metathesemechanismen sind in Schema 1 gezeigt wobei die jeweils neuen C–C und C=C Bindungen in rot hervorgehoben sind.

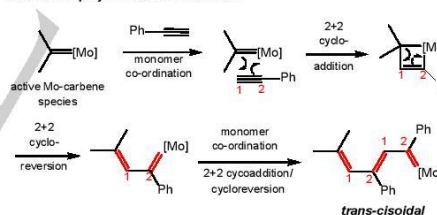
Isozyanide, R–NC, die auch als Isonitrile bekannt sind, haben seit langem die Aufmerksamkeit von Polymerwissenschaft und organischer Chemie auf sich gezogen.

Von diesen Monomeren abgeleitete Polymere formen helikale Strukturen,^[23] während die Monomere auch Schlüsselreagenzien in Ugi und Passerini Multikomponentenreaktionen und Varianten dieser Reaktionen wie zum Beispiel die Ugi-Smiles, Ugi-Joullié und Ugi-Heck Prozesse sind.^[24] Von einer Materialperspektive sind eine weite Reihe an Übergangsmetallspezies effektive Initiatoren für die Polymerisation dieser Substratfamilie, einschließlich Ni Komplexe,^[25] heteronukleare Pt/Pd^[26] Spezies und gewisse Rh Initiatoren.^[23b] Das Produkt einer Isozyanidpolymerisation ist eigenartig für ein ungesättigtes Substrat, da jedes Kohlstoffatom im Polymerrückgrat einen Substituenten trägt, Schema 2, wobei die Polymerisationstriebe die Umsetzung eines formal bivalenten Kohlenstoffs im Monomeren zu einem tetravalenten Kohlenstoff im Polymeren ist.

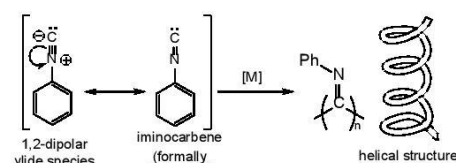
Insertion polymerization mechanism



Metathesis polymerization mechanism



Schema 1. Die Mechanismen der Rh-vermittelten Einschubpolymerisation von Phenylazetylen (oben) und der Mo-vermittelten Metathesepolymerisation von Phenylazetylen (unten).



Schema 2. Die zwitterionischen und Iminocarbon kanonischen Formen von Phenylisocyaniden und Struktur des resultierenden Homopolymers, das die Substituierung jedes Kohlenstoffatoms im Rückgrat hervorhebt. [M] = Metallkatalysator.

Eine dritte Klasse von alky-funktionellen Monomeren, die für (Co)polymerisation mit Rh spezies geeignet ist, sind gewisse propargyl-Derivate,^[27] siehe Abbildung 3.



Abbildung 3. Generische Strukturen von Propargylester- (links) und Propargylamidmonomeren (rechts).

Zum Beispiel, Monomere wie Prop-2-yn-1-ylazetat, Prop-2-yn-1-ylbenzoat, Prop-2-yn-1-ylheptanoat und *N*-(Prop-2-yn-1-yl)hexanamid sind in unkontrollierter Weise mit (1), dem phenoxy-überbrückten Rh Derivat (3) und dem zwitterionischen Komplex (4) polymerisiert worden, siehe Abbildung 4.^[21a, 28] Ähnlich zu Phenylazetylenen verläuft die Rh-vermittelte Polymerisation von Propargylestern und -amiden meist in hochstereoselektiver Weise und liefert Materialien mit hohem *cis* Anteil, wobei jedoch the Endanteil an Stereoregularität vom eingesetzten Katalysator und Lösungsmittel abhängt.

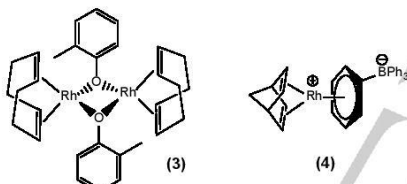


Abbildung 4. Chemische Strukturen vom 1,5-Cyclooctadienrhodium(I) 2-methylphenoxy Dimer (3) und von 2,5-Norbornadienrhodium(I) tetraphenylborat (4).

2. Rhodium(I)-Alkynyl Komplexe

2.1. Phenylazetylene

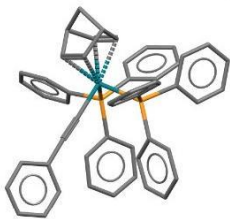
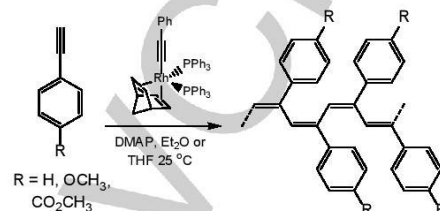


Abbildung 5. Röntgenkristallstruktur von Rh(C≡CPh)(nbd)(PPh₃)₂.

Das erste Literaturbeispiel einer kontrollierten stereospezifischen Phenylazetylenpolymerisation mit einer Rh Spezies war von Kishimoto et al.^[29] Rh(C≡CPh)(nbd)(PPh₃)₂ wurde in 77%-iger Ausbeute durch Reaktion von [Rh(nbd)Cl]₂, PPh₃ und LiC≡CPh in Diethylether dargestellt. Im Festzustand nimmt der Komplex eine leicht verzerrte trigonale bipyramidale Geometrie an mit dem Phenylethynyl Liganden und einer C=C Bindung von nbd in die axialen Positionen, siehe Abbildung 5.



Schema 3. Die Polymerisation von Phenylazetylenen mit (C≡CPh)(nbd)(PPh₃)₂ in der Gegenwart von DMAP ergibt stereoreguläre Polymere.

Die Homopolymerisation von Phenylazetylen und einigen *para*-substituierten Derivaten mit Rh(C≡CPh)(nbd)(PPh₃)₂ in der Gegenwart von DMAP wurde beschrieben wobei Polymerisationen bei Raumtemperatur in Diethylether schnell abließen und Homopolymere in quantitativer Ausbeute und mit SEC-gemessenen *M_n* von 14.900 und *D* = *M_w*/*M_n* von 1,15 ergaben. Ähnliche Ergebnisse wurden vermerkt für Polymerisationen in THF und mit alternativen Phenylazetylen substraten. Während die Polymerisationen allgemein Eigenschaften typisch für kontrollierte Polymerisationen hatten, vermerkten die Autor*innen, dass die Initiatoreffizienzen (IE) nicht quantitativ und im Bereich von 33–56% waren (wobei wir jedoch anmerken dass quantitative Initiierung *keine* formale Bedingung ist um eine Polymerisation zutrefflich als kontrolliert zu bezeichnen).

Nachdem sie bemerkten, dass die aktive Initiatorspezies nicht der fünffach-koodinierte Komplex in Abbildung 5, sondern die vierfach-koodinierte Spezies gebildet durch die rasche, reversible Dissoziation eines PPh₃ Liganden war, Abbildung 6, haben Kishimoto und Koautor*innen ein ternäres Katalysatorsystem beschrieben, in dem die aktive Spezies *in situ* generiert wurde.^[30]

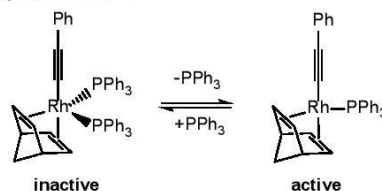


Abbildung 6. Die reversible Dissoziation von PPh₃ vom inaktiven Rh(C≡CPh)(nbd)(PPh₃)₂ zum aktiven Rh(C≡CPh)(nbd)(PPh₃).

Die Homopolymerisation von Phenylazetylen verlief rasch bei Raumtemperatur in THF mit $[\text{Rh}(\text{nbd})(\text{OCH}_3)_2]$, PPh_3 und DMAP in einem Verhältnis von 1:1:10 und ergab Kopf-Schwanz verbundenes, *cis-transoidal* stereoreguläres Polymer mit gemessenem M_n von 6.900 und \bar{D} von 1,11. Basierend auf den SEC-Ergebnissen wurde die IE für dieses ternäre System auf ~0,72 geschätzt, fast doppelt so hoch wie der Wert für $\text{Rh}(\text{C}\equiv\text{CPh})(\text{nbd})(\text{PPh}_3)_2$. Während die Autor*innen die Bildung der aktiven vierfach-kordinierten Spezies klar demonstrierten, konnte sie wegen Instabilität nicht isoliert werden. Jedoch wurde eine oligomere Verbindung mit einer vierfach-kordinierten Rh-Endgruppe isoliert, die bestätigte, dass die Initiierungs- und Fortpflanzungsreaktionen für dieses ternäre System identisch waren mit denen für $\text{Rh}(\text{C}\equiv\text{CPh})(\text{nbd})(\text{PPh}_3)_2$.

Nach diesen anfänglichen Veröffentlichungen hat dieselbe Gruppe eine detaillierte Studie zum Mechanismus und der Struktur der resultierenden Polyenen der durch die obigen Organorhodium(I)-Komplexe vermittelten Polymerisationen berichtet.^[31] Durch stöchiometrische Studien wurde gezeigt, dass DMAP in der Rolle als Cocatalysator kritisch für das Erreichen einer kontrollierten Polymerisation mit niedrigen \bar{D} Werten ist. Obgleich der fünf-fach-kordinierte Komplex $\text{Rh}(\text{C}\equiv\text{CPh})(\text{nbd})(\text{PPh}_3)_2$ in der Abwesenheit von DMAP moderat aktiv für die Polymerisation von Phenylazetylen ist, resultierte die Abwesenheit des Cocatalysators in einer Fraktion an hochmolekulargewichtigem Polymer mit gemessenem M_n von 175.000 und \bar{D} von 2,45. Die geringe Kontrolle in der Abwesenheit von DMAP wurde auf die Bildung eines bimolekularen Rhodacyclopentadien-Komplexes, der nicht als Initiator aktiv war, zurückgeführt.

3. Rhodium(I)-vinyl Komplexe

3.1. Phenylazetylene

Die Initiatorsysteme von Kishimoto et al, obgleich einschneidende Arbeiten, sind bestreitbar limitiert in Bezug auf deren IEs und hinsichtlich der Darstellbarkeit von end-funktionalisierten (Co)polymeren. Letzteres ist bedingt durch die Tatsache, dass, obwohl eine Untersuchung des aktiven vierfach-kordinierten Komplexes den Anschein erweckt, dass die Polymerisation über Monomereinschub in die Rh-Phenylethynyl Bindung verläuft (d.h. die Phenylethynylgruppe kann als Initiatorfragment angesehen werden und deshalb sollten end-funktionalisierte Polymere zugänglich sein durch Einsatz von funktionellen Phenylethynyliganden), die resultierenden Polymere Hydride am initiiertem Ende tragen, welche einen mehrstufigen Initiierungsprozess implizieren, der schließlich nicht in dem Einbau der Phenylethynylgruppe resultiert.

Auf der Annahme basierend, dass die aktive Stelle in der Rh-vermittelten Polymerisation von Phenylazetylen eine Vinylrhodiumverbindung ist, haben Misumi und Masuda^[32] ein ternäres Katalysatorsystem dargestellt aus $[\text{Rh}(\text{nbd})\text{Cl}]_2$, PPh_3 und $\text{LiCPh}=\text{CPh}_2$ in Benzol oder Toluol berichtet, das Homo- und Copolymerisationen von Phenylazetylen in kontrollierter

Weise vermittelte und Polymere mit niedrigen \bar{D} Werten und mit quantitativer Initiierung ergab. Während die Kristallstruktur in dieser ersten Veröffentlichung nicht berichtet wurde, wurde vermerkt, dass eine Rhodiumverbindung aus dem ternären Gemisch isoliert wurde und deren Struktur basierend auf NMR spektroskopischer Analyse als $\text{Rh}(\text{nbd})(\text{CPh}=\text{CPh}_2)\text{PPh}_3$ bestätigt wurde. Die Kristallstruktur von diesem Komplex, Abbildung 7, wurde einige Zeit später von Kumazawa et al.^[33] beschrieben, der*die auch eine detaillierte Untersuchung zur Endgruppenstruktur von Polyphenylazetylenen dargestellt mit wohl-definierten isolierten Katalysatoren führte.

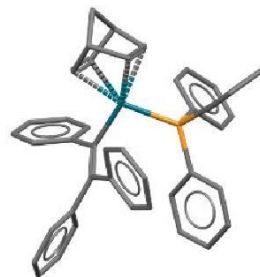


Abbildung 7. Kristallstruktur von $\text{Rh}(\text{nbd})(\text{CPh}=\text{CPh}_2)\text{PPh}_3$

Zusätzlich zur Demonstration einer quantitativen Initiierung, hoben Misumi und Masuda auch die Möglichkeit, end-funktionelle Polyphenylazetylene darzustellen, hervor. Dies wurde erreicht durch Ersetzen von $\text{LiCPh}=\text{CPh}_2$ durch das amino-funktionelle Vinylolithium $\text{LiCPh}=\text{C}(4\text{-NMe}_2\text{-C}_6\text{H}_4)_2$ im ternären katalytischen Gemisch (siehe **Schema S1**). Indem sie auf ein Produkt mit niedrigem Molekulargewicht abzielten, haben die Autor*innen klar den effizienten (quantitativen) Einbau dieser funktionellen Gruppe durch ^1H NMR Spektroskopie demonstriert. Obgleich dies ein effizienter Zugang zu end-funktionalen Polyphenylazetylenen ist, ist ein großes Hindernis dieser synthetischen Route der Mangel an kommerziell erhältlichen funktionellen Triarylvinylobromiden, die als Vorstufe für die Vinylolithiumverbindungen dienen, und dass diese dargestellt werden müssen. Im Falle des obigen Beispiels wurde die $\text{BrCPh}=\text{C}(4\text{-NMe}_2\text{-C}_6\text{H}_4)_2$ Vorstufe in einer mehrstufigen Prozedur mit einer Ausbeute von 10.5% dargestellt. Die Synthese von Polyphenylazetylen-*block*-poly(β -propiolacton) Copolymeren wurde von Kanki, Misumi und Masuda^[34] berichtet, die das ternäre katalytische System $[\text{Rh}(\text{nbd})\text{Cl}]_2/p\text{-tert-BuMe}_2\text{SiOC}_6\text{H}_4(\text{Ph})\text{C}=\text{CPhLi}/\text{PPh}_3$ benutzten. Die Anwendung dieser silyloxy-funktionellen Verbindung ergab wohl-definierte Polyphenylazetylene, die die siloxy-funktionelle Gruppe am initiiertem Ende trugen; deren Einbau wurde durch ^1H NMR Analyse als praktisch quantitativ ermittelt. Entfernung der Silyloxy-Schutzgruppe ergab das korrespondierende Phenol-endfunktionelle Material das, nach Behandlung mit NaH um das

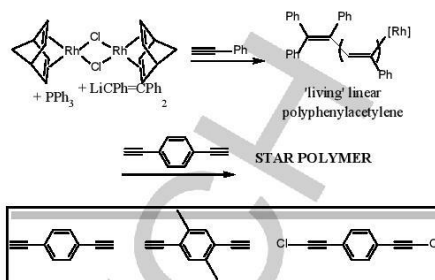
korrespondierende Phenolat zu erhalten, als Makroinitiator für eine anschließende Ring-öffnende Polymerisation von β -propiolacton eingesetzt wurde. Blockcopolymerisation wurde bestätigt durch eine Kombination von NMR und FTIR spektroskopischer Analyse. Leider wurden keine Übergangseffizienzen oder D Werte für das endgültige Blockcopolymer berichtet.

Nach diesem ersten Bericht,^[32] publizierten Misumi und Mitarbeiter*innen^[35] eine detaillierte Studie zu den Auswirkungen von jeder Komponente in solchen ternären katalytischen Systemen. Im Fall der En/Dien Komponente in Rh(diene/ene)/LiPh=CPh₂/PPh₃, wurde beschrieben, dass ein Austausch von Norbornadien mit 1,5-Cyclooctadiene ein aktives katalytisches System ergab, das in 100% Umsatz von Phenylazetylen in das korrespondierende Polymer resultierte, allerdings zu Kosten eines Kontrollverlusts über die Molekulargewichtsverteilung, wobei das Produkt eine gemessene D von 2,45 hatte, während ein Austausch von Norbornadien mit zwei Cyclooctenliganden eine inaktive Spezies ergab.

Die Auswirkungen von Substituenten in den α und β Positionen von Vinylolithiumverbindungen wurde ebenfalls untersucht. Es wurden gefunden, dass sterisch anspruchsvolle Substituenten in der α Position (vorzugsweise eine Ph Gruppe) zusammen mit mindestens einem Substituenten in der β Position nötig waren, um eine gut-kontrollierte Polymerisation von Phenylazetylen zu erreichen. Allerdings ergaben nur Triphenylvinylverbindungen, d.h. das originale [Rh(nbd)Cl]₂/LiPh=CPh₂/PPh₃ ternäre Gemisch, Systeme, die quantitative Initiierung zeigten, wobei die verbleibenden ternären Gemische aktive Spezies mit IEs im Bereich von 0,072–0,30 ergaben.

Die Auswirkung der Strukturen der Phosphinliganden auf die Kontrolle in solch ternären katalytischen Systemen ist weniger stark ausgeprägt, zumindest für PPh₃ und simple tris *para*-substituierte Derivate. Zum Beispiel ergab der Einsatz von PPh₃, P(4-ClC₆H₄)₃, P(4-FC₆H₄)₃, P(4-CH₃C₆H₄)₃, und P(4-MeOC₆H₄)₃ in ternären Gemischen in allen Fällen aktive Spezies und vollständigen Umsatz von Phenylazetylen mit 100% IE und praktisch identischen D Werten von 1,16. Es gab allerdings einen beobachteten, aber nicht unerwarteten, kinetischen Einfluss im Zusammenhang mit einer Veränderung der Phosphinligandenstruktur. Mit abnehmender Basizität der Phosphinliganden stieg die Polymerisationsrate, eine Besonderheit verbunden mit der Tatsache, dass der Phosphinligand mit der Bindung zum Monomer konkurriert—je niedriger die Basizität des Phosphins, desto niedriger die Bindungstendenz und desto höher die Polymerisationsrate. Für die beschriebenen Liganden, unter identischen Bedingungen, nahm die Polymerisationsrate in der Reihenfolge P(4-FC₆H₄)₃ > PPh₃ > P(4-ClC₆H₄)₃ > P(4-CH₃C₆H₄)₃ > P(4-MeOC₆H₄)₃ zu.

Die breitere Nützlichkeit des [Rh(nbd)Cl]₂/LiPh=CPh₂/PPh₃ katalytischen Systems für die Darstellung von Polymeren mit fortschrittlichen Architekturen und speziell für sternförmige Homo- und Copolymere wurde von Kanki und Masuda beschrieben, Schema 4.^[36]



Schema 4. Die Synthese von sternförmigen Polymeren durch Homopolymerisation von Phenylazetylen gefolgt von Vernetzen mit einem bifunktionellen Arylalkin.

Polymerisation von Phenylazetylen mit einem angestrebten M_n von 5.100 ($[M]_0/[Rh] = 50$) gab „lebendes“ Polyphenylazetylen mit einem SEC-gemessenem M_n von 5.350 und D von 1,13. Anschließend Zugabe von fünf Äquivalenten 1,4-Diethynylbenzol (DEB) (basierend auf [Rh]) resultierte in Vernetzen und Aufarbeiten eines neuen Materials mit einem M_n von 37.500 und D von 1,2 (diese Spezies beinhaltete <3% lineare Polyphenylazetylenketten). Der Austausch von DEB mit 1,4-Diethynyl-2,5-dimethylbenzol ergab auch sternförmige Produkte, allerdings mit bis zu 25% linearen Ketten. Dies wurde auf die im Vergleich zu Phenylazetylen reduzierte Reaktivität von 2-Methylphenylazetylen gegenüber Rh-Katalysatoren zurückgeführt. Bildung von sternförmigen Polymeren wurde nicht beobachtet wenn 1,4-Bis(chloerthynyl)benzol als Vernetzer zugegeben wurde.

Folgend auf den Bericht über den Einfluss der individuellen Komponenten in ternären katalytischen Gemischen des Typs Rh-Komplex/Phosphin/Vinylolithium haben Miyake, Misumi und Masuda^[37] Katalysatoren mit halogen-funktionellen Phosphinliganden nachgeprüft. Ins Besondere haben sich die Autor*innen auf die Synthese, Aufarbeitung, und Anwendung von Rh(nbd)(CPh=CPh₂)P(4-XC₆H₄)₃ konzentriert, wobei X = F oder Cl darstellt. Beide Rh(I) vinyl-Katalysatoren wurden aus den korrespondierenden ternären Gemischen isoliert und, im Fall des Chlor-Derivats, wurde eine Kristallstruktur berichtet, Abbildung 8, wobei der Komplex eine verzerrte quadratisch-planare Geometrie annahm konsistent mit der übergeordneten Rh(nbd)(CPh=CPh₂)PPh₃ Verbindung. Es wurde anschließend gezeigt, dass die Cl und F Derivate die kontrollierte Polymerisation von Phenylazetylen mit praktisch quantitativer Initiierung effektiv vermittelten und hoch-stereoreguläre (*cis-transoidale*) Polymere mit einstellbaren Molekulargewichten und niedrigen D ergaben. Interessanterweise wurde berichtet, dass die wohl-definierten, isolierten Rh(I)-Verbindungen noch effektiver waren als die korrespondierenden ternären Gemische, welche insbesondere deutlich niedrigere IEs hatten.

Es sollte vermerkt werden, dass Polymerisationen mit den isolierten Rh Komplexen typischerweise in der Gegenwart von einem Überschuss an Phosphin ausgeführt werden, der als kontrollierendes Agens und Geschwindigkeitsmodifizierer dient. Zum Beispiel wurde berichtet, dass ein Verhältnis $[P(4\text{-XC}_6\text{H}_4)_3]/[\text{Rh}]$ von mindestens 5 nötig war um eine lebende Polymerisation von Phenylazetylen und niedrigen \bar{D} zu erreichen. Polymerisationen, die mit höheren Verhältnissen von freiem Phosphin durchgeführt wurden, verliefen auch in einer kontrollierten Weise aber mit einer reduzierten Geschwindigkeit, da der Einfluss des kompetitiven Bindens des Phosphins dominanter wird.

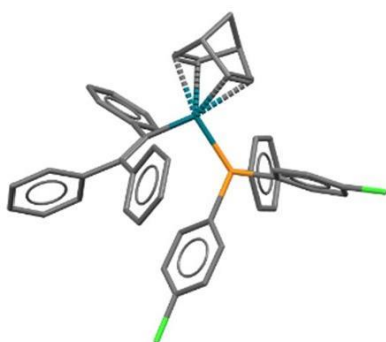
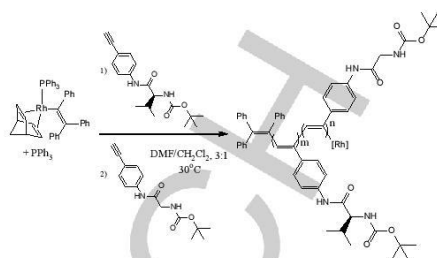


Abbildung 8. Kristallstruktur des Masuda Komplexes $\text{Rh}(\text{nb}d)(\text{CPh}=\text{CPh}_2)\text{P}(4\text{-ClC}_6\text{H}_4)_3$

Während Phenylazetylen, und in manchen Fällen simple substituierte Derivate, die Monomere der Wahl sind, um die Effektivität von neuen Rh(I)-Komplexen als Initiatoren zu demonstrieren, haben diese Substrate jedoch auch eine breitere Anwendbarkeit, bleiben allerdings auch noch weitgehend unterbenutzt. Zum Beispiel haben Kumazawa und Mitarbeiter*innen^[38] die Anwendung von $\text{Rh}(\text{nb}d)(\text{CPh}=\text{CPh}_2)\text{PPh}_3/\text{PPh}_3$ als initiiierende Spezies in der Blockcopolymerisation des chiralen Monomers *N*-tert-Butoxycarbonyl-L-valin 4-ethynylanilid mit dem achiralen Comonomer *N*-tert-Butoxycarbonylglycin 4-ethynylanilid detailliert. Eine Serie von Homo- und Copolymeren, Abbildung 5, mit einstellbaren Zusammensetzungen und Molekulargewichten wurde dargestellt und in den meisten Fällen hatten die Endprodukte niedrige Molekulargewichtverteilungen mit $\bar{D} \leq 1,25$. Interessanterweise zeigten die Autor*innen Chiralitätsverstärkung in den Blockcopolymeren wobei Chiralitätstransfer vom chiralen Block zum achiralen Block klar offensichtlich war. Der Chiralitätstransfer wurde rationalisiert durch die Energiedifferenz zwischen Konformeren mit und ohne Helixwindung, wie durch DFT Berechnung gezeigt wurde.



Schema 5. Blockcopolymerisation eines chiralen Arylazetylderivats mit einem achiralen Comonomer durch sequenzielle Monomergabe mit $\text{Rh}(\text{nb}d)(\text{CPh}=\text{CPh}_2)\text{PPh}_3/\text{PPh}_3$ als Initiatorsystem.

In einer ähnlichen Studie berichteten Liu et al.^[39] die Verwendung von $\text{Rh}(\text{nb}d)(\text{CPh}=\text{CPh}_2)\text{P}(4\text{-FC}_6\text{H}_4)_3$ als initiiierende Spezies in der Darstellung von AB Diblock Copolymeren, in denen der A-Block eine chirale Verbindung basierend auf (((1*S*,5*S*)-6,6-Dimethylbicyclo[3.1.1]heptan-2-yl)methyl)(4-ethynylphenyl)-dimethylsilan ((a) **Abbildung S1**) war und der B-Block auf dem achiralen (2-(Dodecyloxy)-5-ethynyl-1,3-phenylen)dimethanol ((b) **Abbildung S1**) basierte. Wohl-definierte AB Diblock Copolymeren mit einstellbaren Zusammensetzungen und mit gemessenen \bar{D} im Bereich $1,29 \leq \bar{D} \leq 1,73$ wurden dargestellt. Ähnlich zu der Arbeit von Kumazawa und Mitarbeiter*innen^[38] induzierte die Verwendung des von (a) abgeleiteten chiralen Blocks A Chiralität im B-Block, der aus Monomer (b) bestand. Allerdings, im Unterschied zur ersten Publikation, hatte das poly((a)-*b*(b)) Copolymer eine *cis-transoidal*((a) Block)/*cis-cisoidal*((b) Block) stereoreguläre Struktur—das erste Beispiel dieser Art dargestellt durch Helixrichtung-selektive Polymerisation.

Die bis hierher vorgestellten Rh(I) vinyl-Komplexe vom Masuda-Typ geben optimale Kontrolle in Bezug auf ein einstellbares Molekulargewicht, hohen IEs und niedrige Molekulargewichtverteilungen der resultierenden Copolymeren wenn sie in Verbindung mit mindestens fünf Äquivalenten (in Bezug auf [Rh]) an zusätzlichem freien Phosphin verwendet werden. Wir haben angemerkt, dass das zusätzliche Phosphin als Geschwindigkeitsmodifizierer funktioniert, indem es kompetitiv an Monomere bindet—im Wesentlichen kontrolliert es die effektiven Initiierungs- und Fortpflanzungsraten und ermöglicht kontrollierte Polymerisation.

Onishi und Mitarbeiter*innen^[40] berichteten über eine Serie von neuen Rh(I)-Katalysatoren, die eine Butylenbrücke zwischen dem nbd Liganden und einem koordinierendem Phosphin oder einer Aminogruppe enthalten, mit der allgemeinen Formel $[(\text{nbd}-(\text{CH}_2)_4-\text{X})\text{RhR}]$ wobei (5): X = PPh₂, R = Cl; (6): X = NPh₂, R = Cl; (7): X = PPh₂, R = Triphenylvinyl, Abbildung 9, mit den berichteten Röntgenkristallstrukturen der Triphenylvinyl-derivate (7) in Abbildung 10 gezeigt.

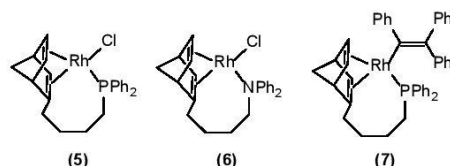


Abbildung 9. Chemische Strukturen von Rh(I)-Komplexen mit Butylenbrücken zwischen dem nbd Liganden und einem koordinierenden Phosphin oder einer Aminogruppe

Im Gegensatz dazu polymerisierte das Stickstoffanalogon, $\text{Rh}(\text{nbd}-(\text{CH}_2)_4-\text{NPh}_2)\text{Cl}$, (6) Abbildung 9, Phenylazetylen quantitativ mit einer Ausbeute von 83%, \bar{D} von 1,7 und einer Initiator-effizienz von 0,21. Das Rh(I) vinyl Derivat, $\text{Rh}(\text{CPh}=\text{CPh}_2)(\text{nbd}-(\text{CH}_2)_4-\text{PPh}_2)$, (7) Abbildung 9, ergab Polymerausbeuten von 94% mit quantitativem Monomerumsatz und einer relativen niedrigen \bar{D} von 1,3. Die IE jedoch, obwohl höher als für (6), war nicht quantitativ mit 0,6. Laut der Autor*innen war die niedrige beobachtete IE für den $\text{Rh}(\text{nbd}-(\text{CH}_2)_4-\text{NPh}_2)\text{Cl}$ Komplex bedingt durch einen geringen Bestand am aktiven 14e mononuklearen Komplex, der durch Koordination der Aminogruppe zum Rh-Zentrum generiert wurde, ähnlich zu NEt_3 im $[\text{Rh}(\text{nbd})\text{Cl}]_2/\text{NEt}_3$ katalytischen System. Im Fall von (5), $\text{Rh}(\text{nbd}-(\text{CH}_2)_4-\text{PPh}_2)\text{Cl}$, wurde die geringe Aktivität einer langsamen Bildung der Rh-C≡CPh Spezies zugeschrieben, die als initierende Spezies in der Polymerisation von Phenylazetylen dient. Im Gegensatz dazu und konsistent mit vorherigen Beispielen von Rh(I) vinyl-Komplexen (Masuda Typ), ermöglicht die $\text{Rh}(\text{CPh}=\text{CPh}_2)(\text{nbd}-(\text{CH}_2)_4-\text{PPh}_2)$ Spezies mit einer einer strukturellen Ähnlichkeit zum aktiven fortpflanzenden Kettenende einen glatten Einschub von Phenylazetylen in die Rh-C Bindung des Metallzentrums und der Triphenylvinylgruppe. Initiator (7) ist das erste Beispiel eines wohl-definierten Rh-Komplexes mit einem dreizähligen Liganden für diese spezielle Anwendung und ist auch das einzige aktuelle Beispiel eines Rh(I) Triphenylvinyl-Komplexes geeignet um eine kontrollierte Polymerisation von Phenylazetylen ohne Zugabe von freiem Phosphin zu vermitteln.

Abbildung 10. Kristallstruktur von $\text{Rh}(\text{CPh}=\text{CPh}_2)(\text{nbd}-(\text{CH}_2)_4-\text{PPh}_2)$

Alle drei dieser Verbindungen wurden als Initiatoren in der (Co)polymerisation von Phenylazetylen untersucht. Der $\text{Rh}(\text{nbd}-(\text{CH}_2)_4-\text{PPh}_2)\text{Cl}$ Komplex, (5), Abbildung 9, in der Abwesenheit von Zusatzstoffen, zeigte eine niedrige katalytische Aktivität mit einem gemessenen Monomerumsatz von <1% nach 24 h in THF bei 30 °C.

Abbildung 11. Kristallstruktur von $\text{Rh}(\text{nbd})(\text{CPh}=\text{CFlu})\text{P}(4-\text{FC}_6\text{H}_4)_3$

Fasziniert von der geringen Anzahl an beschriebenen wohl-definierten Rh(I) vinyl-Komplexen, die als Initiator für die kontrollierte Polymerisation von PA dienen, haben wir kürzlich drei neue Rh(I)- α -Phenylvinylfluorenylverbindungen basierend auf Masudas strukturellem Motif, nämlich Rh(nbd)(CPh=CFlu)P(X-C₆H₄)₃, (wobei X = 4-F, 4-CF₃, 3,5-(CF₃)₂) beschrieben.^[41] Abbildung 11 zeigt die Röntgenkristallstruktur des Rh(nbd)(CPh=CFlu)P(4-FC₆H₄)₃ Komplexes. Der Komplex nimmt im Festzustand eine verzerrte quadratisch-planare Geometrie an, wobei die unbewegliche Fluorenylgruppe am β -vinyl-Kohlenstoff komplanar mit der Vinylbindung ist. Zusätzlich gibt es π - π Wechselwirkungen durch den Raum zwischen der Fluorenylgruppe und einem Arylring des Phosphinliganden. Diese zwei Eigenschaften grenzen die Fluorenylivate von Komplexen vom Masuda-Typ, welche einen Triphenylvinyligenen mit frei-rotierenden β -Phenylgruppen tragen, ab.

Die Homopolymerisation von Phenylazetylen mit den drei Fluorenylderivaten wurde untersucht unter Bedingungen identisch zu denen von Matsuda und Mitarbeiter*innen.^[37] Interessanterweise und trotz Erfüllens der generellen strukturellen Bedingungen der hocheffizienten Masuda-Komplexe, waren die IEs dieser Komplexe im Bereich 0,16–0,56. Allerdings hatten die produzierten Polymere eine sehr hohe *cis-transoidale* Stereoregularität und niedrige \bar{D} Werte. Wir führten die niedrigen IE zurück auf die Energetik des Initiationsprozesses, in dem die konformativ gesperrte Fluorenylgruppe einen effizienten Einschub von Phenylazetylen behindert, was der etablierte Fortpflanzungsweg für diese Polymerisationen ist, Schema 1. Neueste molekulare Berechnungen zu diesen Polymerisationen regen an, dass der Übergangszustand, in dem der konjugative Einschub stattfindet, energisch bevorzugt ist und voraussetzt, dass das hinzukommende Phenylazetylenmonomer komplanar mit C \equiv C und dem Rh-Atom ist.^[17] In den Fluorenylderivaten könnte dies signifikant gehemmt sein durch die konformative Sperrung der Fluorenylgruppe aber es wird energisch bevorzugt sobald Einschub- und Fortpflanzungsschritte ablaufen, bei denen sich die Fluorenylgruppe vom Rh-Zentrum fortbewegt. Obwohl diese IEs suboptimal sind, suggeriert dieser Bericht, dass die strukturellen Bedingungen für effiziente Initiierung durch den Rh(I)-vinyl Typ komplexer sind als ursprünglich von Misumi et al. dargestellt^[35] und geometrische Faktoren einschließen, die ursprünglich nicht berücksichtigt wurden. Zusätzlich zur Phenylazetylenhomopolymerisation wurde die kontrollierte Natur der Polymerisationsprozesse durch selbst-Block Experimente begründet, in denen Phenylazetylen in THF bei 40 °C mit einem [Phosphin]/[Rh] Verhältnis von 5 homopolymerisiert wurde und ein Polyphenylazetylen mit einem M_n von 17.000 und \bar{D} von 1,34 ergab; anschließend wurde eine weitere Charge Phenylazetylen hinzugefügt und die Polymerisation begann wieder und formte ein selbst-geblocktes Polyphenylazetylen mit einem SEC-gemessenen M_n von 46.900 und \bar{D} von 1,19.

Alle bisher vorgestellten Beispiele in diesem Minireview waren Rh-basierte Komplexe, die nbd oder cod als Dien-Liganden enthalten. Wir vermerken, dass, obwohl nbd-

Katalysatoren die Polymerisation von Phenylazetylen (und Derivaten) in einer kontrollierten Art vermitteln, bewirken cod-basierte Katalysatoren nur unkontrollierte (Co)polymerisationen—es gibt keine bekannten Beispiele von wohl-definierten cod-Analoga der in Abbildungen 5, 7, 8, 10 und 11 gezeigten Komplexe, die fähig sind, eine kontrollierte Polymerisation von Arylazetylenen zu vermitteln. Der Einfluss der Dien-Liganden in Komplexen des Typs [Rh(diene)Cl]₂ auf die Polymerisation von Phenylazetylen wurde mit der Reihe der in Abbildung 12 gezeigten Diene von Saeed, Shiotsuki und Masuda^[42] berichtet, mit dem grundlegenden Ziel, neue katalytische Systeme zu entwickeln.

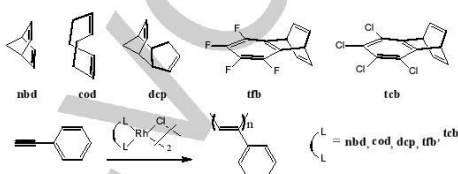


Abbildung 12. Chemische Strukturen von Dien-Liganden: 2,5-Norbornadien (nbd); 1,5-Cyclooctadien (cod); endo-Dicyclopentadien (dcp); Tetrafluorobenzobarrelen (tfb) und Tetrachlorobenzobarrelen (tcb), und die Homopolymerisation von Phenylazetylen mit überbrückten Rh-Komplexen [Rh(diene)Cl]₂.

Es wurde gezeigt, dass die tfb- und tcb-Derivate [Rh(tfb)Cl]₂ und [Rh(tcb)Cl]₂ deutlich mehr aktiv waren als die konventionellen [Rh(nbd)Cl]₂ und [Rh(cod)Cl]₂ Spezies. Zum Beispiel ergaben Polymerisationen, die in Toluol bei 30 °C für eine Minute in der Gegenwart von einem Äquivalent NEt₃ unter sonst identischen Bedingungen durchgeführt wurden, Polyphenylazetylen mit den nbd Katalysator in 69% Ausbeute (SEC-gemessenes M_n von 118.000, \bar{D} von 1,85), während der cod Katalysator Polyphenylazetylen in 5% Ausbeute ergab (M_n von 22.000, \bar{D} von 2,16); der dcp Komplex ergab nur eine Spur Polymer, während die tfb und tcb Derivate beide quantitative Umsätze ergaben, wobei der erstere ein Homopolymer mit M_n von 281.000 und \bar{D} von 1,70 und der tcb Komplex eines mit M_n von 227.000 and korrespondierendem \bar{D} von 1,79 ergaben (Bemerkung: Alle Polymere hatten einen erwarteten hohen Anteil an *cis-transoidaler* Stereoregularität). Dies war die erste Beschreibung eines katalytischen Systems, das höhere Aktivität zeigte als der wohl-etablierte [Rh(nbd)Cl]₂ Komplex. Die Autor*innen untersuchten ebenfalls den Einfluss von Lösungsmittel und Cokatalysator, wobei Aktivitätsprofile in allen Fällen demselben Trend folgten mit zunehmender Katalysatoraktivität in der Reihenfolge tfb = tcb > nbd > cod > dcp. Basierend auf diesen Beobachtungen schlugen die Autor*innen vor, dass die unterschiedlichen Katalysatoraktivitäten zwischen den Komplexen zurückzuführen waren auf die unterschiedliche π Azidität dieser Dien-Liganden. Das Bindungsmodell für solche Metall-Alkenkomplexe ist in Abbildung 13 gezeigt.

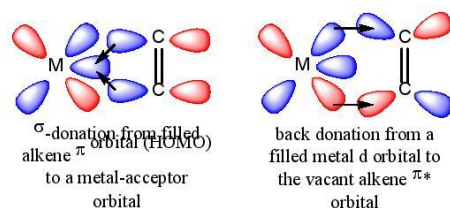


Abbildung 13. Das Dewar-Chatt-Duncanson Bindungsmodell zwischen einem Metallzentrum und einem Alken.

Das Nettoergebnis der Rückbindung from Metall zum Alken führt zu einer Reduktion der Elektronendichte am Metallzentrum d.h. eine Zunahme an Elektrophilität. Das Ausmaß an Rückbindung wird bestimmt, zumindest zum Teil, durch die π -Azidität des Alkens, d.h. die Fähigkeit des Liganden, Elektronen in das π^* (LUMO) Orbital anzunehmen ($d-\pi^*$ Überlappen).

Von daher kann die π -Azidität abgeschätzt werden durch die Energie des LUMOs. In dieser Veröffentlichung berichteten die Autor*innen die LUMO Energiewerte (in eV) (in aufsteigender Reihenfolge) 0,21 (tfb) < 0,48 (tcb) < 0,79 (nbd) < 0,90 (cod) < 1,09 (dcp), vollkommen übereinstimmend mit der obigen Reihenfolge von beobachteten Polymerisationsaktivitäten, was hervorhob, dass von den fünf Liganden tfb erwartbar die höchste π -Azidität hatte.

Als eine natürliche Erweiterung der obigen Studie detaillierten dieselben Autor*innen die Synthese eines wohl-definierten tfb-basierten Rh katalytischen Systems.^[43] Saeed, Shiotsuki und Masuda berichteten ein ternäres katalytisches System abgeleitet von $[\text{Rh}(\text{tfb})\text{Cl}]_2$, PPh_3 und $\text{LiCPh}=\text{CPh}_2$ zusammen mit dem wohl-definierten Rh(I) vinyl-Katalysator $\text{Rh}(\text{tfb})\text{CPh}=\text{CPh}_2(\text{PPh}_3)$, der aus dem ternären Gemisch isoliert wurde. Obgleich die Kristallstruktur von $\text{Rh}(\text{tfb})\text{CPh}=\text{CPh}_2(\text{PPh}_3)$ nicht berichtet wurde, wurde eine quadratisch planare Geometrie angenommen, in Einklang mit den oben behandelten Rh(I) vinyl-Spezies.

Eine Auswertung der katalytischen Aktivität der ternären Mischung in der Homopolymerisation von Phenylazetylen enthüllte, dass unter diesen Bedingungen dargestellte Polyphenylazetylene mit praktisch quantitativer Initiierung entstanden (geschätzte IEs von 0,96), d.h. mit kontrollierbaren Molekulargewichten und \bar{D} so niedrig wie 1,03 und mit *cis-transoidalem* Gehalt $\geq 99\%$. Für das ternäre katalytische System und auch den isolierten Komplex wurden mehrstufige Polymerisationsexperimente von Phenylazetylen durchgeführt, die die lebende Natur der Polymerisationen bestätigten, genau so wie pseudo-erster Ordnung kinetische Auftragungen und die Entwicklung der \bar{D} als Funktion des Umsatzes. Eine besonders vorstehende und etwas außergewöhnliche Eigenschaft der mit $\text{Rh}(\text{tfb})\text{CPh}=\text{CPh}_2(\text{PPh}_3)$

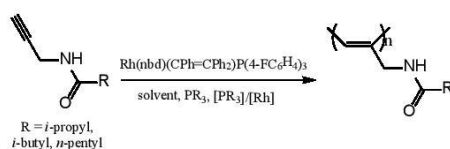
PPh_3 durchgeführten Polymerisationen war die beobachtete hohe Aktivität und hohe IE selbst bei niedrigen Konzentrationen. Zum Beispiel gab Homopolymerisation von Phenylazetylen mit $[\text{M}_0]/[\text{Rh}]$ von 4.000 (theoretisches M_n von 408.560) ein Homopolymer mit einem SEC-gemessenem M_n von 401.000 (berechnete IE von 0,98) und \bar{D} von 1,12.

Während andere Berichte existieren, die die Benutzung von tfb-funktionellen Rh Katalysatoren für die Darstellung von Polyphenylazetylenen beschreiben^[26b, 44] (typischerweise in unkontrollierter Weise), bleibt der oben beschriebene Bericht nach bestem Wissen das einzige Beispiel in dem ein wohl-definierter isolierbarer Rh(I) vinyl-Komplex, oder ein ternäres Gemisch in dem die aktive tfb-Rh(I) Spezies *in situ* gebildet wird, beschrieben wurde und effektive Kontrolle in der Polymerisation von Phenylazetylen demonstriert wurde mit Darstellung von Materialien mit fast-vollständiger *cis-transoidaler* Stereoregularität. Dies suggeriert signifikanten Spielraum und Gelenheiten für eine weitere Entwicklung und Bewertung von neuen tfb, tcb-basierenden katalytischen Systemen für gezielte Anwendungen.

3.2. Propargyl-basierte Monomere

Während gewisse Rh-Katalysatoren deutlich effektive Spezies für die (un)kontrollierte (Co)polymerisation von Arylazetylen substraten sind, reicht deren Anwendbarkeit nicht über diese wichtige Monomerfamilie hinaus. Zusätzlich zu Arylazetylenen wurden auch Propargylester und -amide als geeignete Substrate beschrieben, obwohl sie typischerweise in einer unkontrollierten Weise polymerisieren und Polymere mit reduzierter Stereoregularität (verglichen mit Phenylazetylenen) ergeben. Zum Beispiel wurde eine Serie von Poly(propargylestern) dargestellt mit dem nbd-Tetraphenylborat Rh-Katalysator (4) (Abbildung 4) von Zhang et al. beschrieben.^[26] Zum Beispiel ergab eine Homopolymerisation von Propargylhexanoat mit (4) in THF unter einer Reihe von Bedingungen Poly(propargylhexanoat) with Ausbeuten von 42–77%, SEC-gemessenen M_n von 4.900–28.000, \bar{D} im Bereich von 1,83 bis 4,70 und *cis* Anteil von 48–88% mit wenig, wenn überhaupt, klarem Zusammenhang zwischen diesen Merkmalen. Arbeiten von Masuda und Mitarbeiter*innen,^[45] die denselben Katalysator für Propargylester und -amide benutzten, haben sich eher auf Aminosäure-abgeleitete Monomer konzentriert und die Struktur und Eigenschaften der Endprodukte hervorgehoben, als auf fundamentale Eigenschaften der Polymerisation einzugehen. Dennoch vermerken wir, dass in diesen Arbeiten Beispiele gegeben sind, in denen Polymere mit 100% Ausbeute isoliert wurden und mit beobachteten $\bar{D} < 1,20$, was suggeriert, dass unter bestimmten Bedingungen Polymerisationen dieser Monomerfamilie in kontrollierter (oder pseudo-kontrollierter) Weise ablaufen.

Nakazato und Mitarbeiter*innen^[46] berichteten über die Anwendung des wohl-definierten Masuda Komplexes $\text{Rh}(\text{nbd})(\text{CPh}=\text{CPh}_2)\text{P}(\text{4-FC}_6\text{H}_4)_3$, das Fluor-Analogon der in Abbildung 8 gezeigten Katalysatoren, für die Polymerisation von drei simplen Alkylpropargylamid Monomeren. Schema 6.



Schema 6. Die Polymerisation von Propargylamid-Monomeren mit dem wohl-definierten Masuda Rh(I) vinyl-Komplex $\text{Rh}(\text{nbd})(\text{CPh}=\text{CPh}_2)\text{P}(4\text{-FC}_6\text{H}_4)_3$.

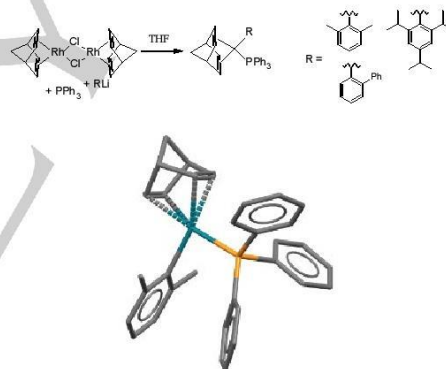
Als repräsentatives Beispiel ergab die Polymerisation des Isobutylderivats in CHCl_3 bei $30\text{ }^\circ\text{C}$ mit fünf Äquivalenten zugegebenem PPh_3 als Geschwindigkeitsmodifizierer Polymerprodukt in 100% Ausbeute mit einem M_n von 17.300 (IE von 0,8, wobei wir vermerken dass Molekulargewichte per SEC gemessen wurden und als Polystyroläquivalente berichtet wurden) und \mathcal{D} von 1,36. Die fundamentalen Eigenheiten dieser Polymerisation wurden unter identischen Bedingungen untersucht, mit der Ausnahme, dass Polymerisationen bei $0\text{ }^\circ\text{C}$ durchgeführt wurden. Unter diesen Bedingungen war die Polymerisation des Isobutylmonomers nach 60 min vollständig und zeigte eine lineare pseudo-erster Ordnung Kinetik (obwohl der Graph nicht durch den Ursprung verlief, was nicht-ideale Polymerisation suggeriert), \mathcal{D} nahm mit zunehmendem Umsatz ab (obwohl Werte konsistent höher als erwartet waren), und die Polymerisation fuhr fort nachdem eine zweite Charge Monomer zugegeben wurde, die ebenfalls vollständig polymerisierte. Während die Autor*innen den Verlauf von Molekulargewicht mit Umsatz als linearen Graph präsentierten, sollte er wohl besser als zwei-stufiger Graph gesehen werden mit einem anfänglichen steilen Zuwachs des gemessenen Molekulargewichts. Dies ist wahrscheinlich auch konsistenter mit dem nicht-idealen kinetischen Verlauf und suggeriert, dass unkontrollierte Polymerisation in den ersten Momenten des Polymerisationsprozesses stattfindet. Jedoch ist es klar, dass die Polymerisationen mit vielen der wesentlichen Eigenschaften von kontrollierten Polymerisationen vorzugehen scheinen und wir wiederholen, dass weder quantitative Initiierung noch niedrige Dispersität Vorbedingungen einer Polymerisation sind, um „kontrolliert“ genannt zu werden. Die Autor*innen schlugen vor, dass die sub-idealen Dispersitäten wahrscheinlich auf ein höheres k_p/k_t Verhältnis als normalerweise mit anderen kontrollierten Polymerisationen verbunden ist, zurückzuführen waren.

4. Rhodium(I) Aryl-Komplexe

4.1. Arylisozyanide

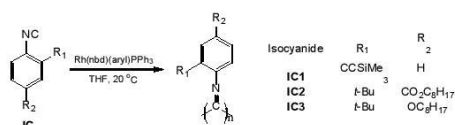
Arylisozyanide haben seit langem Aufmerksamkeit in den Polymergemeinschaft auf sich gezogen, weil Materialien aus diesen Monomeren leicht helikale Strukturen bilden.^[23a, 47] Die

Übergangsmetall-vermittelte kontrollierte (Co)polymerisation von Isozyaniden ist gut dokumentiert,^[23b] wobei Komplexe basierend auf $\text{Ni}(\text{II})$,^[48] $\text{Pt}(\text{II})$,^[49] und gewissen binuklearen $\text{Pt}(\text{II})$ - $\text{Pd}(\text{II})$ Spezies^[50] besonders nützlich sind. Im Kontext dieses Minireviews fokussieren wir auf Beispiele von Rh(I) Aryl-Komplexen, die effektiv in der (Co)polymerisation von sterisch anspruchsvollen Arylisozyaniden sind.^[51] Yamamoto, Onitsuka und Takahashi^[51c] berichteten über die Synthese von drei Rh(I) Aryl-Komplexen und deren Anwendung als Initiatoren für die Polymerisation von drei unterschiedlich substituierten Arylisozyanidmonomeren. Schema 4 zeigt die synthetische Route für die Darstellung der Rh-Komplexe zusammen mit der berichteten Röntgenkristallstruktur des $\text{Rh}(\text{nbd})(2,6\text{-Me}_2\text{C}_6\text{H}_3)\text{PPh}_3$ Derivats. Solche Rh(I) Aryl-Komplexe werden in derselben generellen Weise dargestellt wie die oben beschriebenen wohl-definierten Rh(I) vinyl-Komplexe, nämlich durch Reaktion von $[\text{Rh}(\text{nbd})\text{Cl}]_2$ mit einem Triarylphosphin (PPh_3) und einer Aryllithiumverbindung (im Gegensatz zu Vinylolithium das für Rh(I) vinyl-Komplexe benutzt wird), wobei der oben genannte $\text{Rh}(\text{nbd})(2,6\text{-Me}_2\text{C}_6\text{H}_3)\text{PPh}_3$ Komplex in 96% Ausbeute isoliert wurde. Die berichtete Kristallstruktur dieses Rh(I) aryl-Komplexes zeigt, dass der Komplex eine quadratisch-planare Geometrie hat, die vollständig mit der von Rh(I) vinyl-Komplexen konsistent ist.



Schema 7. Die generelle synthetische Route für die Darstellung von Rh(I) aryl-Komplexen des Typs $\text{Rh}(\text{nbd})(\text{aryl})\text{PPh}_3$ und die berichtete Festkörperstruktur des $\text{Rh}(\text{nbd})(2,6\text{-Me}_2\text{C}_6\text{H}_3)\text{PPh}_3$ Derivats.

Alle drei Rh(I) aryl-Komplexe wurden anschließend als Initiatoren für die Polymerisation von drei unterschiedlichen Arylisozyaniden untersucht, siehe Schema 8.



Schema 8. Die Polymerisation von 2,4-substituierten Arylisocyanidmonomeren mit Rh(nbd)(aryl)PPh₃ Komplexen.

Die Polymerisation von IC1 ((Trimethylsilyl)ethynyl)phenylisocyanid) mit Rh(nbd)(2,6-Me₂C₆H₃)PPh₃ verlief grundsätzlich glatt, vorausgesetzt, dass sie mit 10 Äquivalenten freiem PPh₃ durchgeführt wurde. Zum Beispiel resultierte eine Polymerisation mit einem IC1/Rh Verhältnis von 25 und PPh₃/Rh von 10 unter den in Schema 8 gegebenen Bedingungen in 100% Monomerumsatz und einem Polymerprodukt mit einem SEC-gemessenen M_n von 4.700 und \bar{D} von 1,12. Obwohl diese Werte als Polystyroläquivalente berichtet wurden, bemerken wir, dass die Autor*innen eine Endgruppenanalyse durchführen konnten und eine praktisch quantitative IE für Rh(nbd)(aryl)PPh₃/PPh₃ begründeten. In der Abwesenheit von zugegebenem PPh₃ war der Umsatz geringer und zusätzlich zu Polymeren wurde eine signifikante Menge an Oligomeren geformt, was zeigt, dass zugegebenes Phosphin nötig ist, um eine glatte Polymerisation zu gewährleisten. Eine Erhöhung des IC1/Rh Verhältnisses zu 50, 75, und schließlich 100 resultierte in einem systematischen Anstieg des endgültigen Polymerelementarwichts, wurde allerdings von einem bemerkbaren Anstieg von \bar{D} von 1,19 zu 1,26 zu 1,47 bei IC1/Rh = 100 begleitet. Ähnliche Polymerisationsergebnisse wurden für Homopolymerisationen der Monomere IC2 und IC3 gefunden. Versuche, Blockcopolymere darzustellen, um zumindest zum Teil deren kontrollierte Natur nachzuweisen, schlugen fehl, was suggerierte, dass Polymerisationen nicht kontrolliert waren und dass es während der Polymerisation wahrscheinlich zu Endgruppenzersetzung kam. Leider wurden keine kinetischen Daten berichtet, die diese Annahme hätten unterstützen oder belegen können.

In einer folgenden Publikation berichteten Onitsuka et al. eine Studie, in der sie die Anzahl an Katalysatoren und Arylisocyaniden ausweiteten. Abbildung 14 zeigt die Strukturen der sechs untersuchten Rh-Komplexe und beinhaltet die drei in Abbildungen 7 gezeigten Spezies, zwei neue Derivate Rh(nbd)(2-MeNaphthyl)PPh₃ und Rh(nbd)(9-Anthra)PPh₃ und den ursprünglichen wohl-definierten Masuda Komplex Rh(nbd)(CPh=CPh₂)PPh₃. Abbildung 15 zeigt die berichtete Röntgenkristallstruktur des Rh(nbd)(2-MeNaphthyl)PPh₃ Komplexes.

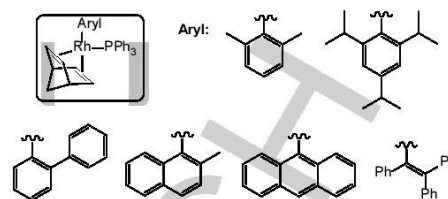


Abbildung 14. Generelle Struktur des von Onitsuka und Mitarbeiter*innen berichteten Rh(nbd)(PPh₃(aryl) Komplexes.

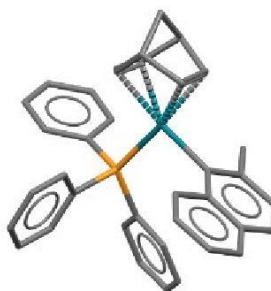


Abbildung 15. Röntgenkristallstruktur des Rh(2-MeNaphthyl)(nbd)(PPh₃) Komplexes.

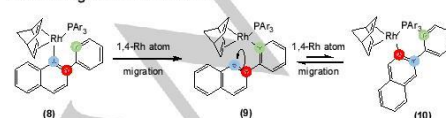
Als generelle Beobachtung wurde gefunden, dass alle dieser Komplexe (inklusive des Masuda Vinylderivats) die Polymerisation von Arylisocyaniden effektiv vermittelten, vorausgesetzt, dass das Isocyanidmonomer einen sterisch anspruchsvollen Substituenten in einer seiner *ortho*-Positionen hatte. Versuchte Polymerisationen von 2,6-Dimethylphenylisocyanid mit Rh(nbd)(2,6-Me₂C₆H₃)PPh₃, zum Beispiel, hatten keinen beobachtbaren Umsatz. In Fällen von erfolgreichen Polymerisationen hatten die resultierenden Polymere einstellbare Molekulargewichte und \bar{D} Werte im Bereich von 1,16–1,53. In keinem Fall der obigen Komplexe wurden oligomere Nebenprodukte beobachtet. Die kontrollierte Natur der Polymerisationen wurde klar demonstriert durch den linearen Verlauf von M_n mit dem Umsatz wobei für alle Umsätze die gemessenen Werte fast perfekt mit den theoretischen übereinstimmten. Im Einklang mit dem einleitenden Bericht schlugen anfängliche Versuche, Blockcopolymere durch sequenzielle Monomerzugabe zu bewirken, fehl, was zusätzlich bestätigte, dass sich das aktive Zentrum langsam zersetzte und bei hohen Umsätzen besonders problematisch wurde. Dennoch demonstrierten die Autor*innen, dass das aktive Kettenende durch Zugabe eines großen Überschusses an PPh₃ effizient stabilisiert werden konnte, was die Darstellung von

Blockcopolymeren ermöglichte. Zum Beispiel berichteten die Autor*innen, dass drei schrittweise sequenzielle Zugaben von 50 Äquivalenten an IC2 zu $\text{Rh}(\text{nbd})(2,4,6\text{-}i\text{-Pr}_3\text{C}_6\text{H}_2)\text{PPh}_3$ in der Gegenwart von 400 Äquivalenten PPh_3 in einer schrittweisen Bildung von Polymeren mit Molekulargewichten von 21.300, 38.000 und 50.900 und korrespondierenden \bar{D} Werten von 1,19, 1,20 und 1,29 resultierte. Zusätzlich wurde ein AB Diblockcopolymer aus IC2 (A Block) mit 2-*tert*-Butyl-4-(cyclohexyloxy-carbonyl)phenylisozyanid (B Block) erfolgreich und quantitativ unter ähnlichen Bedingungen ($\text{Rh}(\text{nbd})(2,4,6\text{-}i\text{-Pr}_3\text{C}_6\text{H}_2)\text{PPh}_3$ als Initiator, 400 Äquivalenten an PPh_3 , THF, 20 °C) dargestellt.

Das tri-*iso*-propyl Rh-Derivat $\text{Rh}(\text{nbd})(2,4,6\text{-}i\text{-Pr}_3\text{C}_6\text{H}_2)\text{PPh}_3$ ist auch als Initiator in der Helixrichtung-selektiven (Co)polymerisation von sterisch anspruchsvollen Arylisozyanidmonomeren mit chiralen Ester- oder Amidgruppen eingesetzt worden, was Materialien mit variablen Molekulargewichten und niedrig bis mittleren Dispersitäten ergab.^[51b] Zum Beispiel resultierte die Polymerisation von (*S*)-Octan-2-yl 3-(*tert*-butyl)-4-isozyanobenzoat (100 Äquivalente) mit $\text{Rh}(\text{nbd})(2,4,6\text{-}i\text{-Pr}_3\text{C}_6\text{H}_2)\text{PPh}_3$ mit 40 Äquivalenten PPh_3 basierend auf $[\text{Rh}]$ in THF bei 20 °C in quantitativem Monomerumsatz, wobei das Homopolymer ein M_n von 43.600 und \bar{D} von 1,40 hatte. Der spezifische Drehwert $[\alpha]_D$ des chiralen Monomers wurde als +32 ermittelt, während $[\alpha]_D$ für das korrespondierende Homopolymer als -178 gemessen wurden, was anzeigte, dass die Polymerisation in der Bildung von Chiralität zusätzlich zu der der Esterseitengruppen resultierte. Das CD (*circular dichromism*) Spektrum des Homopolymers zeigte einen starken Cottoneneffekt im Bereich 250–400 nm, wohingegen für das Monomer nichts in diesem Bereich beobachtet wurde. Die Autor*innen vermerkten dass der Cottoneneffekt im Bereich um 350 nm mit einem $n\text{-}\pi^*$ Übergang von Iminogruppen typisch für helikale Polyarylisozyanide zusammenhängt. Die Autor*innen demonstrierten auch, dass die Struktur der chiralen Estergruppen und besonders die Monomerreinheit, genaue Lage des chiralen Zentrums und Länge der Alkylketten einen direkten Einfluss auf die Helixrichtung-Selektivität hatten.

4.2. Phenylazetylene

Im Bestreben, die oben beschriebene geringere IE in der $\text{Rh}(\text{I})$ - α -Phenylvinylfluorenylkomplex-vermittelten Polymerisation von Phenylazetylen (siehe Abbildung 12) besser zu verstehen, haben wir kürzlich einen neuen $\text{Rh}(\text{I})$ Komplex untersucht, Schema 9, mit dem Ziel, den geometrischen Einfluss um das Initiatorfragment zu beurteilen.^[52]



Schema 9. Chemische Struktur des 2-Phenyl-naphthyl $\text{Rh}(\text{I})$ -Derivats (8), und Strukturen der isomeren 2-Naphthylphenyl (9) und 3-Phenyl-2-naphthyl (10),

Komplexe, die durch vorgeschlagene 1,4-Wanderungen des Rh-Atoms geformt werden.

Der Komplex (8), Schema 9, wurde 'dargestellt' in derselben generellen synthetischen Route wie für all die anderen oben-berichteten $\text{Rh}(\text{I})$ vinyl- und $\text{Rh}(\text{I})$ aryl-Komplexe, nämlich durch Lithierung des korrespondierenden Vinyl-/Arylbromids (1-Bromo-2-phenyl-naphthalen in diesem Fall), gefolgt von der Reaktion mit der vierfach-koordinierten Spezies gebildet aus der Reaktion von $[\text{Rh}(\text{nbd})\text{Cl}]_2/\text{P}(\text{4-FC}_6\text{H}_4)_3$. Interessanterweise zeigte Röntgenstrukturaufklärung, dass nach Umkristallisieren nicht der beabsichtigte Komplex isoliert wurde, sondern der isomere 2-Naphthylphenyl-Komplex (9), Schema 9. Die Röntgenkristallstruktur des isolierten $\text{Rh}(\text{I})$ aryl-Komplexes ist in Abbildung 16 gezeigt.

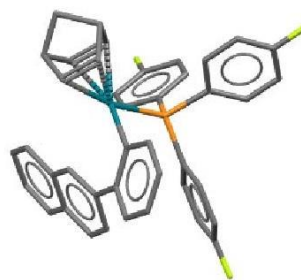
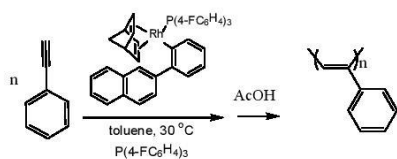


Abbildung 16. Die Röntgenkristallstruktur von $\text{Rh}(\text{nbd})(2\text{-NaphthPh})\text{P}(\text{4-FC}_6\text{H}_4)_3$

Wie schlugen vor, dass der isolierte Komplex durch *ortho*-zu-*ortho*' (oder 1,4-) Rh-Atomwanderung gebildet wurde; ein Annahme, die durch durch DFT Berechnungen unterstützt wurde, welche zeigten dass der isolierte Komplex eine niedrigere Energie (-19 kJmol^{-1}) als der ursprünglich anvisierte Komplex hatte. Obwohl es nicht die beabsichtigte Verbindung war, untersuchten wir diese neue Spezies detailliert. Interessanterweise identifizierten wir durch NMR -Untersuchung in Lösung ein drittes Isomer, nämlich das 3-Phenyl-2-naphthyl Derivat (10), Schema 9, das vermutlich durch eine zweite 1,4-Rh-Atomwanderung aus Komplex (9) gebildet wurde.

Während Komplex (9) es uns nicht erlaubte, wie zuerst beabsichtigt den besonderen geometrischen Einfluss der Struktur des Initiatorfragments zu untersuchen, konnten wir dennoch die Fähigkeit von (9), Polymerisationen von Phenylazetylen zu initiieren, untersuchen (wobei bemerkt werden muss dass auch (10) wahrscheinlich in Lösung vorlag), Schema 10.



Schema 10. Homopolymerisation von Phenylazetylen mit $\text{Rh}(\text{nbd})(2\text{-NaphthPh})\text{P}(4\text{-FC}_6\text{H}_4)_2\text{P}(4\text{-FC}_6\text{H}_4)_3$

Der $\text{Rh}(\text{I})$ aryl-Komplex (**9**) erwies sich als ein effektiver Initiator in der Polymerisation von Phenylazetylen. Die pseudo-erste Ordnung Kinetik und Molekulargewicht-gegen-Umsatz Graphen waren linear, was einen kontrollierten Polymerisationsprozess zeigte. Die gemessenen \bar{D} Werte der resultierenden Polyphenylazetylene waren niedrig und generell $\leq 1,25$, während eine hoch-stereospezifische Struktur durch ^1H NMR Spektroskopie nachgewiesen wurde, wobei Produkte eine $>95\%$ *cis-transoidale* Struktur hatten. Berechnete IEs, obwohl nicht quantitativ, waren hoch mit etwa 0,8. Dieser Report stellt die erste detaillierte Untersuchung eines $\text{Rh}(\text{I})$ aryl-Komplexes spezifisch für die kontrollierte Polymerisation von Phenylazetylen dar und suggeriert dass diese generelle Komplexfamilie eine breitere Anwendbarkeit als bislang wahrgenommen hat

5. Zusammenfassung und Ausblick

Hierin haben wir einen Überblick über den aktuellen Stand der (kontrollierten) Polymerisationsprozesse mit wohl-definierten $\text{Rh}(\text{I})$ vinyl- und aryl-Komplexen gegeben. Die $\text{Rh}(\text{I})$ triarylvinyl-Derivate, die allgemein als Masuda-Typ bezeichnet werden, sind hoch-effizient darin, kontrollierte Polymerisationen von Phenylazetylen und (funktionellen) Derivaten zu vermitteln. Obwohl die unterschiedlichen Ligandenkomponenten solcher Verbindungen variiert wurden und deren Effektivitäten untersucht wurden, verbleibt noch immer ein großer Spielraum für eine weitere Entwicklung von neuen Komplexen und offensichtlich gibt es ein Gelehenheiten in der Darstellung von neuen Endgruppen-funktionellen Materialien, als auch von neuen Polymeren mit Architekturen über Arylazetylen-basierte Homopolymere, statistische Copolymere und simple AB Diblockcopolymere hinaus. Basierend auf der berichteten Wirksamkeit des Masuda Derivats $\text{Rh}(\text{nbd})(\text{CPh}=\text{CPh}_2)\text{P}(4\text{-FC}_6\text{H}_4)_3$, kontrollierte Polymerisationen von gewissen Propargylamiden zu vermitteln, scheint es ähnliche Gelegenheiten für diese generelle Monomerfamilie zu geben. Neuen Initiatoren können und sollten dargestellt und untersucht werden und synthetische Routen für die Darstellung von Materialien mit fortschrittlichen Architekturen entwickelt werden. Die Verbindung der innewohnenden helikalen Struktur mit neuen Topologien und Architekturen bietet Gelegenheiten für die

Darstellung von komplexeren und möglicherweise interessanten (Ko)polymeren.

Ähnlich zur kontrollierten Rh -vermittelten Polymerisation von Arylazetylen und Propargylamiden und -estern, gibt es relativ wenige Berichte, die eine kontrollierte Polymerisation von Arylisozyaniden mit wohl-definierten $\text{Rh}(\text{I})$ aryl-Komplexen beschreiben und nach bestem Wissen nur einen Bericht, der den Einsatz einer $\text{Rh}(\text{I})$ Verbindung dieser Art in einer kontrollierten Polymerisation von Phenylazetylen beschreibt.

Basierend auf der großen Anzahl kommerziell erhältlicher Arylbromide, gibt es Gelegenheiten für zusätzliche Beiträge in (mechanistischer) organometallischer Synthese, die ein rationales Design und Anwendung als Polymerisationsinitiatoren beinhalten, sowie die Synthese von neuen funktionellen (Co)polymeren mit bislang unbekanntem Architekturen und, als Folge davon, die Entwicklung von neuen Materialien mit potentiell neuen oder neuartigen Eigenschaften. Seit der einschneidenden Arbeit von Kishimoto und Mitarbeiter*innen in 1994 und der folgenden Pionierarbeit von Masuda et al. hat es deutliche und signifikante Fortschritte im Bereich der $\text{Rh}(\text{I})$ Komplexkatalyse gegeben und speziell darin, solche wohl-definierten $\text{Rh}(\text{I})$ vinyl- und aryl-Komplexe als Katalysatoren/Initiatoren für die kontrollierte Polymerisation von Alkin-funktionellen Monomeren zu benutzen. Während es effektive Katalysatoren, die die Polymerisation der drei hierin aufgeführten Monomertypen vermitteln, gibt, gibt es neue zusätzliche Komplexe, die dargestellt und untersucht werden könnten; es scheint unwahrscheinlich, dass der effizienteste, aktivste, und meist-einsetzbare Rh Komplex für diese Anwendungen schon gefunden worden ist, basierend auf der relativ kleinen Anzahl an bereits berichteten Beispielen.

Acknowledgements

ABL bedankt sich beim Research Office at Curtin (ROC) für ein Promotionsstipendium für NSLT.

Keywords: Polyphenylacetylene • Rh complex • Controlled polymerization • Stereoregularity • Arylisozyanide

- [1] K. Ziegler, *Angew. Chem.* **1936**, *49*, 499-502.
- [2] A. D. Jenkins, P. Kratochvíl, R. F. T. Stepto, U. W. Suter, *Pure & Appl. Chem.* **1996**, *68*, 2287-2311.
- [3] a) M. Szwarc, M. Lecy, R. Milkovich, *J. Am. Chem. Soc.* **1956**, *78*, 2656-2657; b) M. Szwarc, *Nature* **1956**, *178*, 1168-1169.
- [4] S. Aoshima, S. Kanaoka, *Chem. Rev.* **2009**, *109*, 5245-5287.
- [5] a) O. W. Webster, W. R. Hertler, D. Y. Sogah, W. B. Farnham, T. V. RajanBabi, *J. Am. Chem. Soc.* **1983**, *105*, 5706-5708; b) O. W. Webster, *J. Polym. Sci., Part A: Polym. Chem.* **2000**, *38*, 2855-2860.
- [6] S. Inoue, *J. Polym. Sci., Part A: Polym. Chem.* **2000**, *38*, 2861-2871.
- [7] T. J. Deming, *J. Polym. Sci., Part A: Polym. Chem.* **2000**, *38*, 3011-3018.
- [8] C. W. Bielawski, R. H. Grubbs, *Prog. Polym. Sci.* **2007**, *32*, 1-29.
- [9] G. J. Domski, J. M. Rose, G. W. Coates, A. D. Bolig, M. Brookhart, *Prog. Polym. Sci.* **2007**, *32*, 30-92.

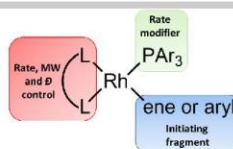
- [10] J. Nicolas, Y. Guillauneuf, C. Lefay, D. Bertin, D. Gimes, B. Charleux, *Prog. Polym. Sci.* **2013**, *38*, 63-235.
- [11] K. Matyjaszewski, *Adv. Mater.* **2018**, *30*, 1706441.
- [12] a) G. Moad, E. Rizzardo, S. H. Thang, *Aust. J. Chem.* **2012**, *65*, 985-1076; b) J. Chiefari, Y. K. Chong, F. Ercole, J. Krstina, J. Jeffery, T. P. T. Le, R. T. A. Mayadunee, G. F. Meijs, C. L. Moad, G. Moad, E. Rizzardo, S. H. Thang, *Macromolecules* **1998**, *31*, 5559-5562.
- [13] S. Yamago, *J. Polym. Sci., Part A: Polym. Chem.* **2006**, *44*, 1-12.
- [14] G. Inzelt, *Conducting Polymers, Monographs in Electrochemistry*, Springer, Verlag Berlin Heidelberg, **2012**.
- [15] S. Amdur, A. T. Y. Cheng, C. J. Wong, P. Ehrlich, *J. Polym. Sci., Polym. Chem. Ed.* **1978**, *16*, 407-414.
- [16] T. Masuda, A. Zhang, in *Handbook of Metathesis, Vol. 3: Polymer Synthesis*, 2 ed. (Eds.: R. H. Grubbs, E. Khosravi), Wiley-VCH, **2015**, pp. 375-390.
- [17] Z. Ke, S. Abe, T. Ueno, K. Morohuma, *J. Am. Chem. Soc.* **2011**, *133*, 7926-7941.
- [18] a) T. Masuda, *Polym. Rev.* **2017**, *57*, 1-14; b) F. Freire, E. Quiñoá, R. Riguera, *Chem. Rev.* **2016**, *116*, 1242-1271; c) L. Liu, Y. Zang, H. Jia, T. Aoki, T. Kaneko, S. Hadano, M. Teraguchi, M. Miyata, G. Zhang, T. Namikoshi, *Polym. Rev.* **2017**, *57*, 89-118; d) T. Masuda, *J. Polym. Sci., Part A: Polym. Chem.* **2007**, *45*, 165-180.
- [19] a) S. Li, K. Liu, G. Kuang, T. Masuda, A. Zhang, *Macromolecules* **2014**, *47*, 3288-3296; b) Y. Zang, T. Aoki, M. Teraguchi, T. Kaneko, L. Ma, H. Jia, *Polymer* **2015**, *56*, 199-206; c) T. Sone, R. D'Amato, Y. Mawatari, M. Tabata, A. Furlani, M. V. Russo, *J. Polym. Sci., Part A: Polym. Chem.* **2004**, *42*, 2365-2376; d) X. A. -Zhang, H. Zhao, Y. Gao, J. Tong, L. Shan, Y. Chen, S. Zhang, A. Qin, J. Z. Sun, B. Z. Tang, *Polymer* **2011**, *52*, 5290-5301; e) J. Chen, K. K.-L. Cheuk, B. Z. Tang, *J. Polym. Sci., Part A: Polym. Chem.* **2006**, *44*, 1153-1167; f) H. Jia, J. Li, Y. Zang, T. Aoki, M. Teraguchi, T. Kaneko, *J. Polym. Sci., Part A: Polym. Chem.* **2012**, *50*, 5134-5143; g) Y. Qu, J. Hua, Y. Jiang, H. Tian, *J. Polym. Sci., Part A: Polym. Chem.* **2009**, *47*, 1544-1552; h) X. A. Zhang, M. R. Chen, H. Zhao, Y. Gao, Q. Wei, S. Zhang, A. Qin, J. Z. Sun, B. Z. Tang, *Macromolecules* **2011**, *44*, 6724-6737; i) A. C. Pauly, P. Theato, *Polym. Chem.* **2012**, *3*, 1769-1782; j) M. Bhebe, E. A. De Eulate, Y. Pei, D. W. M. Amigan, P. J. Roth, A. B. Lowe, *Macromol. Rapid Commun.* **2017**, *38*, 1600528; k) M. Tabata, T. Sone, Y. Sadahiro, *Macromol. Chem. Phys.* **1999**, *200*, 265-282; l) I. Saeed, M. Shiotsuki, T. Masuda, *Macromolecules* **2006**, *39*, 5347-5351.
- [20] J. G. Rodríguez, A. Lafuente, J. Arranz, *J. Polym. Sci., Part A: Polym. Chem.* **2005**, *43*, 6438-6444.
- [21] a) A. Nakazato, I. Saeed, T. Katsumata, M. Shiotsuki, T. Masuda, J. Zednik, J. Vohlidal, *J. Polym. Sci., Part A: Polym. Chem.* **2005**, *43*, 4530-4536; b) H. Gulyás, A. C. Bényei, J. Bakos, *Inorg. Chim. Acta* **2004**, *357*, 3094-3098; c) G. Zamora, J. Pons, J. Ros, *Inorg. Chim. Acta* **2004**, *357*, 2899-2904; d) N. I. Nikishin, J. Huskens, W. Verboom, *Polymer* **2013**, *54*, 3175-3181.
- [22] D. Bondarev, J. Zednik, I. Plutnarova, J. Vohlidal, J. Sedláček, *J. Polym. Sci., Part A: Polym. Chem.* **2010**, *48*, 4296-4309.
- [23] a) E. Schwartz, M. Koepf, H. J. Kito, R. J. M. Nolte, A. E. Rowan, *Polym. Chem.* **2011**, *2*, 33-47; b) M. Suginome, Y. Ito, *Adv. Polym. Sci.* **2004**, *171*, 77-136.
- [24] J. Zhu, Q. Wang, M.-X. Wang, Wiley-VCH, Weinheim, Germany, **2015**.
- [25] a) P. C. J. Kamer, R. J. M. Nolte, W. Drenth, *J. Am. Chem. Soc.* **1988**, *110*, 6818-6825; b) T. J. Deming, B. M. Novak, *J. Am. Chem. Soc.* **1993**, *115*, 9101-9111; c) S. Asaoka, A. Joza, S. Mnagawa, L. Song, Y. Suzuki, T. Iyoda, *ACS Macro Lett.* **2013**, *2*, 906-911.
- [26] a) K. Onitsuka, K.-i. Yabe, N. Ohshiro, A. Shimizu, R. Okumura, F. Takei, S. Takahashi, *Macromolecules* **2004**, *37*, 8204-8211; b) N. Onishi, M. Shiotsuki, F. Sanda, T. Masuda, *Macromolecules* **2009**, *42*, 4071-4076; c) O. Nobuaki, S. Atsushi, O. Reiko, T. Fumie, K. Onitsuka, T. Shigetoshi, *Chem. Lett.* **2000**, *29*, 786-787.
- [27] Y. Yoshida, Y. Mawatari, M. Tabata, *Polymers* **2019**, *11*, 93-103.
- [28] W. Zhang, J. Tabel, M. Shiotsuki, T. Masuda, *Polym. Bull.* **2006**, *57*, 463-472.
- [29] Y. Kishimoto, P. Eckerle, T. Miyatake, T. Ikariya, R. Noyori, *J. Am. Chem. Soc.* **1994**, *116*, 12131-12132.
- [30] Y. Kishimoto, T. Miyatake, T. Ikariya, R. Noyori, *Macromolecules* **1996**, *29*, 5054-5055.
- [31] Y. Kishimoto, P. Eckerle, T. Miyatake, M. Kainosho, A. Ono, T. Ikariya, R. Noyori, *J. Am. Chem. Soc.* **1999**, *121*, 12035-12044.
- [32] Y. Misumi, T. Masuda, *Macromolecules* **1998**, *31*, 7572-7573.
- [33] S. Kumazawa, J. R. Castanon, N. Onishi, K. Kuwata, M. Shiotsuki, F. Sanda, *Organometallics* **2012**, *31*, 6834-6842.
- [34] K. Kanki, Y. Misumi, T. Masuda, *Inorg. Chim. Acta* **2002**, *336*, 101-104.
- [35] Y. Misumi, K. Kanki, M. Miyake, T. Masuda, *Macromol. Chem. Phys.* **2000**, *201*, 2239-2244.
- [36] K. Kanki, T. Masuda, *Macromolecules* **2003**, *36*, 1500-1504.
- [37] M. Miyake, Y. Misumi, T. Masuda, *Macromolecules* **2000**, *33*, 6636-6639.
- [38] S. Kumazawa, J. R. Castanon, M. Shiotsuki, T. Sato, F. Sanda, *Polym. Chem.* **2015**, *6*, 5931-5939.
- [39] L. Liu, G. Zhang, T. Aoki, Y. Wang, T. Kaneko, M. Teraguchi, C. Zhang, H. Dong, *ACS Macro Letts.* **2016**, *5*, 1381-1385.
- [40] N. Onishi, M. Shiotsuki, T. Masuda, N. Sano, F. Sanda, *Organometallics* **2013**, *32*, 846-853.
- [41] N. S. L. Tan, P. V. Simpson, G. L. Nealon, A. N. Sobolev, P. Raiteri, M. Massi, M. I. Ogden, A. B. Lowe, *Eur. J. Inorg. Chem.* **2019**, 592-601.
- [42] I. Saeed, M. Shiotsuki, T. Masuda, *Macromolecules* **2006**, *39*, 8977-8981.
- [43] I. Saeed, M. Shiotsuki, T. Masuda, *Macromolecules* **2006**, *39*, 8567-8573.
- [44] a) M. V. Jiménez, J. J. Pérez-Torrente, M. I. Bartolomé, E. Vispe, F. J. Lahoz, L. A. Oro, *Macromolecules* **2009**, *42*, 8146-8156; b) M. Shiotsuki, N. Onishi, F. Sanda, T. Masuda, *Polym. J.* **2011**, *43*, 51-57.
- [45] a) F. Sanda, K. Terada, T. Masuda, *Macromolecules* **2005**, *38*, 8149-8154; b) F. Sanda, H. Araki, T. Masuda, *Macromolecules* **2005**, *38*, 10605-10608; c) F. Sanda, H. Araki, T. Masuda, *Macromolecules* **2004**, *37*, 8510-8516; d) G. Gao, F. Sanda, T. Masuda, *Macromolecules* **2003**, *36*, 3932-3937.
- [46] A. Nakazato, I. Saeed, M. Shiotsuki, F. Sanda, T. Masuda, *Macromolecules* **2004**, *37*, 4044-4047.
- [47] E. Yashima, K. Maeda, H. Iida, Y. Furusho, K. Nagai, *Chem. Rev.* **2009**, *109*, 6102-6211.
- [48] a) A. Sadayuki, J. Ayako, M. Sakiko, S. Lijun, S. Yukimitsu, I. Tomokazu, *ACS Macro Letts.* **2013**, *2*, 906-911; b) J. Lee, S. Shin, T.-L. Choi, *Macromolecules* **2018**, *51*, 7800-7806.
- [49] Y.-X. Xue, J.-L. Chen, Z.-Q. Jiang, Z. Yu, N. Liu, J. Yin, Y.-Y. Zhu, Z.-Q. Wu, *Polym. Chem.* **2014**, *5*, 6435-6438.
- [50] a) T. Fumie, Y. Koichi, O. Kiyotaka, T. Shigetoshi, *Chem. Eur. J.* **2000**, *6*, 983-993; b) O. Nobuaki, S. Atsushi, O. Reiko, T. Fumie, O. Kiyotaka, T. Shigetoshi, *Chem. Lett.* **2000**, *29*, 786-787; c) K. Onitsuka, A. Shimizu, F. Takei, S. Takahashi, *J. Inorg. Organomet. Polym.* **2009**, *19*, 98-103.
- [51] a) K. Onitsuka, M. Yamamoto, T. Mori, F. Takei, S. Takahashi, *Organometallics* **2006**, *25*, 1270-1278; b) K. Onitsuka, T. Mori, M. Yamamoto, F. Takei, S. Takahashi, *Macromolecules* **2006**, *39*, 7224-7231; c) M. Yamamoto, K. Onitsuka, S. Takahashi, *Organometallics* **2000**, *19*, 4669-4671.
- [52] N. S. L. Tan, G. L. Nealon, J. M. Lynam, A. N. Sobolev, M. I. Ogden, M. Massi, A. B. Lowe, **2019**, Submitted.

Entry for the Table of Contents

Layout 1:

REVIEW

Dieser Minireview bietet eine Zusammenfassung des aktuellen Stands in (kontrollierter) Polymerisation von Alkin-basierten Monomeren durch wohl-definierte Rh Komplexe.



Nicholas Sheng Loong Tan, Andrew B. Lowe*

Page No. – Page No.

Polymerisationen vermittelt durch wohl-definierte Rhodium Komplexe

Accepted Manuscript

This article is protected by copyright. All rights reserved.

Reproduced (adapted) from

Nicholas Sheng Loong Tan, Andrew B. Lowe **‘Durch definierte Rhodiumkomplexe vermittelte Polymerisationen’** *Angewandte Chemie*, **2020**. DOI: 10.1002/ange.201909909.

With permission from the Angewandte Chemie. License number: 4987450508587, 31st August 2020. 4901151158306, 14th January 2021.



A Journal of the Gesellschaft Deutscher Chemiker

Angewandte Chemie

GDCh

International Edition

www.angewandte.org

Accepted Article

Title: Polymerizations Mediated by Well-defined Rhodium Complexes

Authors: Nicholas Sheng Loong Tan and Andrew B. Lowe

This manuscript has been accepted after peer review and appears as an Accepted Article online prior to editing, proofing, and formal publication of the final Version of Record (VoR). This work is currently citable by using the Digital Object Identifier (DOI) given below. The VoR will be published online in Early View as soon as possible and may be different to this Accepted Article as a result of editing. Readers should obtain the VoR from the journal website shown below when it is published to ensure accuracy of information. The authors are responsible for the content of this Accepted Article.

To be cited as: *Angew. Chem. Int. Ed.* 10.1002/anie.201909909
Angew. Chem. 10.1002/ange.201909909

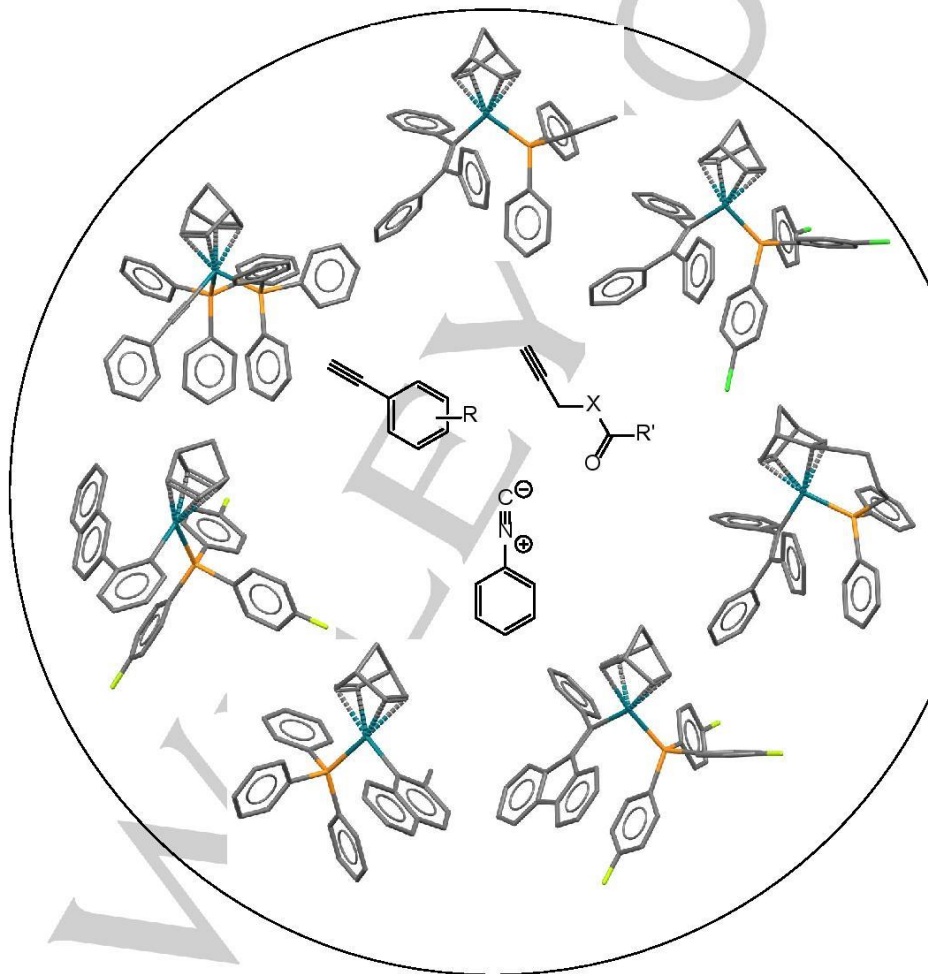
Link to VoR: <http://dx.doi.org/10.1002/anie.201909909>
<http://dx.doi.org/10.1002/ange.201909909>

WILEY-VCH

MINIREVIEW

Polymerizations Mediated by Well-defined Rhodium Complexes

Nicholas Sheng Loong Tan^[a] and Andrew B. Lowe^{*[a]}



Accepted Manuscript

MINIREVIEW

Abstract: This minireview details the current state-of-the-art relating to (co)polymerizations mediated by well-defined Rh(I)-ethynyl, vinyl and aryl complexes. In particular we focus on Rh(I) species suitable for the (co)polymerization of phenylacetylenes, arylisocyanides and propargyl esters and amides.

1. Introduction

The ability to prepare new (co)polymers in a controlled (or living) fashion, i.e. with advanced architectures, topologies, predetermined molecular characteristics and with site-specific functionality, often for targeted applications has become a central theme in modern synthetic polymer science. The basic concept of a controlled polymerization is not new; Ziegler proposed in 1936 that the anionic polymerization of styrene initiated with an alkyl lithium should proceed in the absence of transfer and termination events;^[1] these two features form the basis of the current IUPAC definition of a living chain growth polymerization process.^[2]

However, it was not until the pioneering work of Szwarc, and co-workers, that such living anionic polymerization was demonstrated experimentally.^[3] Since these seminal contributions numerous approaches have been developed that enable the (co)polymerization of most (common) monomer types in a controlled manner (see SI for criteria regarding a controlled polymerization). Polymerization techniques such as pseudo-living cationic,^[4] group transfer,^[5] immortal,^[6] *N*-carboxyanhydride ring-opening,^[7] living ring-opening metathesis,^[8] living coordination,^[9] and the suite of reversible deactivation radical polymerization processes (stable radical polymerization (SRP),^[10] ATRP,^[11] RAFT,^[12] and TERP/SBRP^[13]) are today well established, and collectively facilitate the controlled (co)polymerization of most common monomer classes.

(Co)Polymers with fully conjugated backbones represent an important family of materials. Such materials (commonly referred to variously as conducting polymers, semi-conducting polymers, or intrinsically conducting polymers) possess unique and tuneable properties, and as a result have a broad application base.^[14] An important sub-set of this family of materials are those based on the phenylacetylene structural motif. This family of substrates has attracted significant attention due to their impressive solubility characteristics, ease of processing and oxidative stability. Phenylacetylene is susceptible to polymerization by a number of routes including radical,^[15] metathesis^[16] and insertion^[17] processes with the latter, transition metal-mediated pathways being favoured. Of these two approaches, insertion polymerization, typically mediated by Rh species, is most commonly adopted. Indeed, the high functional group tolerance, ease of handling, high activity, and low oxophilicity of Rh species renders them ideal catalysts/initiators in this target application.

The *non-controlled*, insertion, (co)polymerization of phenylacetylene, and functional derivatives thereof, is well documented.^[18] A variety of commercially available Rh complexes have been employed, typically in partnership with a base such as triethylamine (NEt₃) or *N,N*-4-dimethylaminopyridine (DMAP). Figure 1 shows the chemical structures of two of the most commonly employed Rh species, **(1)**^[19] and **(2)**,^[19c, 19d, 19h, 19k, 20] for synthesizing phenylacetylene-based (co)polymers and that likewise serve as precursors to alternative Rh complexes.^[21] Both **(1)** and **(2)** are examples of halogen-bridged dinuclear Rh complexes with stabilizing diene ligands – bicyclic 2,5-norbornadiene (nbd) for **(1)** and 1,5-cyclooctadiene (cod) in the case of **(2)**.

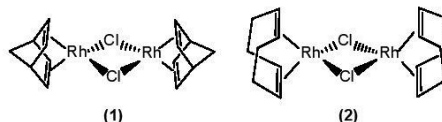


Figure 1. Chemical structures of 2,5-norbornadienerhodium(I) chloride dimer, [Rh(nbd)Cl]₂ (**1**), and 1,5-cyclooctadienerhodium(I) chloride dimer, [Rh(cod)Cl]₂ (**2**).

Nicholas S. L. Tan holds a BSc (Hons) degree in Chemistry from Curtin University. He is currently a third year PhD student working under the supervision of Prof.

Andrew Lowe in the School of Molecular and Life Sciences where he is affiliated with the Curtin Institute for Functional Molecules and Interfaces. His research is based on the synthesis of new Rh(I) complexes for the controlled polymerization of phenylacetylenes



Andrew B. Lowe holds BSc (Hons), DPhil and DSc degrees from the University of Sussex, UK. He has held academic appointments at the University of Southern Mississippi and the University of New South Wales, Sydney. Currently he serves as Director and Professor of the Curtin University Institute for Functional Molecules and Interfaces.



[a] Mr. N. S. L. Tan and Prof. A. B. Lowe*
Curtin Institute for Functional Molecules and Interfaces (CIFMI)
& School of Molecular and Life Sciences (MLS)
Curtin University
Bentley, Perth, WA 6102, Australia.
E-mail: andrew.b.lowe@curtin.edu.au

MINIREVIEW

As a result of the different transition metal-mediated polymerization pathways available, i.e. insertion versus metathesis, there exists four possible stereoregular structures for resulting poly(phenylacetylene)s – two as a result of the insertion process and two produced via metathesis (co)polymerization, Figure 2, whose structures differ in the nature of the bonds connecting the repeat units.

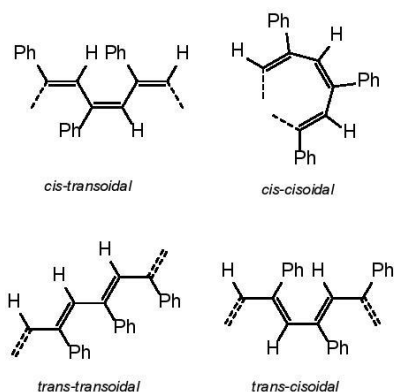
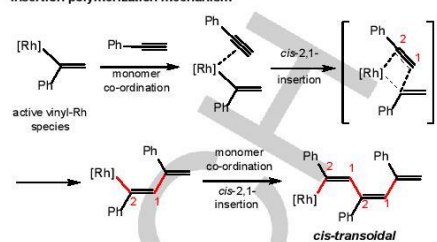


Figure 2. The four possible stereoisomers of polyphenylacetylene.

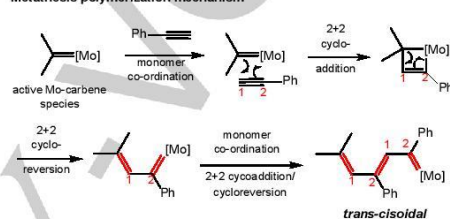
The *cis-transoidal* and *cis-cisoidal* species are associated with the insertion process with repeat units linked by the formation of a new C-C bond, while the *trans-transoidal* and *trans-cisoidal* structures result from metathesis polymerization with repeat units linked by the generation of new C=C bonds.^[22] The generally accepted 2,1-insertion and metathesis polymerization mechanisms are shown in Scheme 1 with the new C-C and C=C bonds highlighted in red.

Isocyanides, R-NC, also known as isonitriles, have long attracted attention in the polymer science and organic chemistry communities; polymers derived from these monomers form helical structures,^[23] while they are also key reagents in the Ugi and Passerini multicomponent reactions as well as variants of these reactions such as the Ugi-Smiles, Ugi-Joullié and Ugi-Heck processes.^[24] From a materials perspective, a wide range of transition metal species are effective initiators for the polymerization of this family of substrates including Ni complexes,^[25] heteronuclear Pt/Pd^[26] species and certain Rh initiators.^[29b] The product from the polymerization of isocyanides is somewhat unique for an unsaturated substrate, with every carbon atom in the polymer backbone bearing a substituent, Scheme 2, with the driving force for polymerization being the conversion of the formally divalent carbon in the monomer to tetravalent carbon in the polymer.

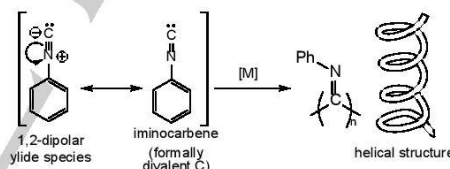
Insertion polymerization mechanism



Metathesis polymerization mechanism



Scheme 1. The mechanisms for the Rh-mediated insertion polymerization of phenylacetylene (TOP) and the Mo-mediated metathesis polymerization of phenylacetylene (BOTTOM).



Scheme 2. The zwitterionic and iminocarbene canonical forms of phenylisocyanide and structure of the resulting homopolymer highlighting the substituted nature of every C atom in the backbone structure. [M] = metal catalyst.

A third family of alkyne-functional monomers that are susceptible to (co)polymerization with Rh species are certain propargyl derivatives,^[27] Figure 3.



Figure 3. Generic structure of propargyl ester (left) and propargyl amide (right) monomers.

MINIREVIEW

For example, monomers such as prop-2-yn-1-yl acetate, prop-2-yn-1-yl benzoate, prop-2-yn-1-yl heptanoate and *N*-(prop-2-yn-1-yl)hexanamide have been polymerized in a non-controlled fashion with (1), the phenoxy bridged Rh derivative (3) and the zwitterionic complex (4), Figure 4.^[21a, 28] Similar to phenylacetylenes, the Rh-mediated (co)polymerization of propargyl esters/amides often proceeds in a highly stereoselective manner yielding materials with high *cis* contents although the final degree of stereoregularity is dependent on the catalyst and solvent employed.

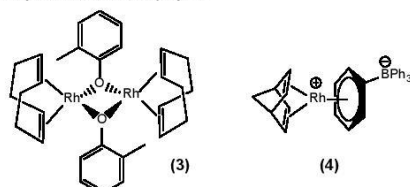


Figure 4. Chemical structures of 1,5-cyclooctadienerhodium(I) 2-methylphenoxy dimer (3) and of 2,5-norbornadienerhodium(I) tetraphenylborate (4).

2. Rhodium(I)-Alkynyl Complexes

2.1. Phenylacetylenes

The first literature example concerning the controlled, stereospecific polymerization of phenylacetylene by a rhodium species was from Kishimoto et al.^[29] $\text{Rh}(\text{C}\equiv\text{CPh})(\text{nbnd})(\text{PPh}_3)_2$ was prepared from the reaction of $[\text{Rh}(\text{nbnd})\text{Cl}]_2$, PPh_3 and $\text{LiC}\equiv\text{CPh}$ in diethyl ether and isolated in a 77% yield. The complex adopts a slightly distorted trigonal bipyramidal geometry in the solid state with the phenylethynyl ligand and one C=C associated with nbnd occupying the axial positions, Figure 5.

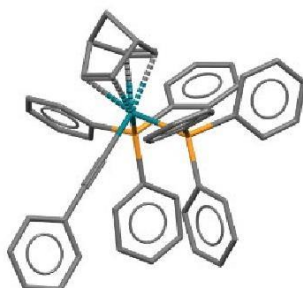
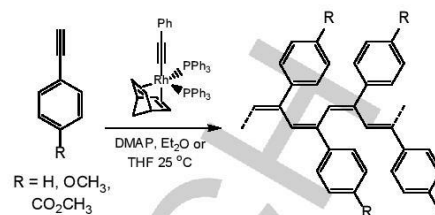


Figure 5. X-ray crystal structure of $\text{Rh}(\text{C}\equiv\text{CPh})(\text{nbnd})(\text{PPh}_3)_2$.



Scheme 3. The polymerization of phenylacetylenes with $\text{Rh}(\text{C}\equiv\text{CPh})(\text{nbnd})(\text{PPh}_3)_2$ in the presence of DMAP yielding stereoregular polymer.

The homopolymerization of phenylacetylene, and several *para*-substituted derivatives, with $\text{Rh}(\text{C}\equiv\text{CPh})(\text{nbnd})(\text{PPh}_3)_2$ in the presence of DMAP was reported with polymerizations proceeding rapidly at ambient temperatures, in diethyl ether, yielding homopolymer essentially quantitatively with an SEC-measured M_n of 14,900 and $\bar{D} = M_w/M_n$ of 1.15. Similar results were noted for polymerizations in THF and with alternative phenylacetylene substrates. While broadly exhibiting features associated with a controlled polymerization, the authors noted that initiation efficiencies (IE) were non-quantitative and reported to be in the range 33–56% (although we note that quantitative initiation is *not* a formal requirement for a polymerization to be accurately termed controlled).

Recognizing that the active initiating species is not the pentacoordinate complex in Figure 5 but the tetracoordinate species formed by the rapid, reversible dissociation of one of the PPh_3 ligands, Figure 6, Kishimoto and co-workers subsequently reported a ternary catalytic system in which the active species was generated *in situ*.^[30]

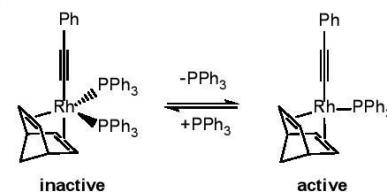


Figure 6. The reversible dissociation of PPh_3 from inactive $\text{Rh}(\text{C}\equiv\text{CPh})(\text{nbnd})(\text{PPh}_3)_2$ to active $\text{Rh}(\text{C}\equiv\text{CPh})(\text{nbnd})(\text{PPh}_3)$.

Homopolymerization of phenylacetylene proceeded rapidly at RT in THF with $[\text{Rh}(\text{nbnd})(\text{OCH}_3)_2]$, PPh_3 and DMAP in a ratio of 1:1:10 yielding a head-to-tail, *cis-transoidal* stereoregular polymer with a measured M_n of 6,900 and \bar{D} of 1.11. Based on the SEC results, the IE of this ternary system was estimated to be ~0.72, almost double that observed for $\text{Rh}(\text{C}\equiv\text{CPh})(\text{nbnd})(\text{PPh}_3)_2$. While the authors clearly demonstrated the formation of the active tetracoordinate species in solution it could not be isolated due to

MINIREVIEW

its instability. However, an oligomeric species bearing a tetracoordinate Rh end-group was isolated and confirmed that the initiation and propagation steps for this ternary system was identical to those for $\text{Rh}(\text{C}\equiv\text{CPh})(\text{nbd})(\text{PPh}_3)_2$.

Following these initial disclosures, the same group reported a detailed study on the mechanism and structure of the resulting polyenes in polymerizations mediated by the above organorhodium(I) complexes.^[31] Through stoichiometric studies, the role of DMAP as a cocatalyst was shown to be critical in achieving a controlled polymerization yielding materials with low \bar{D} s. Although the pentacoordinate complex $\text{Rh}(\text{C}\equiv\text{CPh})(\text{nbd})(\text{PPh}_3)_2$, in the absence of DMAP, was moderately active for the polymerization of phenylacetylenes, the absence of the cocatalyst yielded a high molecular weight polymer fraction with a measured M_n of 175,000 and \bar{D} of 2.45. The reduced level of control in the absence of DMAP was attributed to the formation of a binuclear rhodacyclopentadiene complex which was not an active initiator.

3. Rhodium(I)-vinyl Complexes

3.1. Phenylacetylenes

The initiating systems described by Kishimoto et al., while clearly seminal contributions, are arguably limited in terms of the reported IEs and with respect to accessible end-functional (co)polymers. The latter is due to the fact that while inspection of the active tetracoordinate complex might suggest that polymerization proceeds via monomer insertion into the Rh-phenylethynyl bond (i.e. the phenylethynyl group can be viewed as the initiating fragment and thus end-functional polymers should be accessible by using a functional phenylethynyl ligand), the resulting polymers bear hydride at the initiating terminus implying a multistep initiation process that ultimately does not result in incorporation of the phenylethynyl group.

Based on the assumption that the active site in the Rh-mediated polymerization of phenylacetylene is a vinylrhodium species, Misumi and Masuda^[32] reported a ternary catalytic system prepared from $[\text{Rh}(\text{nbd})\text{Cl}]_2$, PPh_3 and $\text{LiCPh}=\text{CPh}_2$ in benzene or toluene that was shown to mediate the homo- and copolymerization of phenylacetylene in a controlled fashion yielding polymers with low \bar{D} s and with quantitative initiation. While the crystal structure was not reported in this initial disclosure, it was noted that a Rh species was isolated from the ternary mixture and its structure confirmed to be $\text{Rh}(\text{nbd})(\text{CPh}=\text{CPh}_2)\text{PPh}_3$ based on NMR spectroscopic analysis. The crystal structure of this complex, Figure 7, was reported sometime later by Kumazawa et al.^[33] who also conducted a detailed examination of the end-group structure in polyphenylacetylenes prepared with the well-defined isolated catalyst.

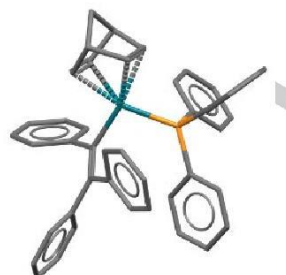


Figure 7. Crystal structure of $\text{Rh}(\text{nbd})(\text{CPh}=\text{CPh}_2)\text{PPh}_3$

In addition to demonstrating quantitative initiation, Misumi and Masuda highlighted the ability to prepare end-functional polyphenylacetylene. This was accomplished by replacing $\text{LiCPh}=\text{CPh}_2$ with the amino-functional vinylolithium $\text{LiCPh}=\text{C}(4\text{-NMe}_2\text{-C}_6\text{H}_4)_2$ in the ternary catalytic mixture (see Scheme S1). Targeting a low molecular weight product the authors clearly demonstrated the efficient (quantitative) incorporation of this functional group via ^1H NMR spectroscopy. While an effective approach for the preparation of end-functional polyphenylacetylenes, the major drawback of this synthetic route is the lack of commercially available functional triarylvinyllithiums that serve as the precursors to the vinylolithium species, and as such need to be synthesized. In the case of the above example, the target $\text{BrCPh}=\text{C}(4\text{-NMe}_2\text{-C}_6\text{H}_4)_2$ precursor was prepared via a multistep procedure and isolated in a 10.5% yield. The synthesis of polyphenylacetylene-*block*-poly(β -propiolactone) copolymers was reported by Kanki, Misumi and Masuda^[34] employing the $[\text{Rh}(\text{nbd})\text{Cl}]_2/p\text{-tert-BuMe}_2\text{SiOC}_2\text{H}_4(\text{Ph})\text{C}=\text{CPhLi}/\text{PPh}_3$ ternary catalytic system. The use of this siloxy-functional triarylvinyllithium species yielded well-defined polyphenylacetylene bearing the siloxy functional group at the initiating chain end; its incorporation, as determined by ^1H NMR analysis, was determined to be essentially quantitative. Removal of the protecting siloxy group yielded the corresponding phenol-end-functional material which, after treatment with NaH to yield the corresponding phenolate, was employed as a macroinitiator for the subsequent ring-opening polymerization of β -propiolactone. Block copolymerization was verified by a combination of NMR and FTIR spectroscopic analysis. Unfortunately, no cross-over efficiencies were reported nor any \bar{D} data provided for the final block copolymers.

Following the initial report,^[32] Misumi and co-workers^[35] reported a detailed study of the effects of each component in such ternary catalytic systems. In the case of the ene/diene ligand component in $\text{Rh}(\text{diene/ene})/\text{LiPh}=\text{CPh}_2/\text{PPh}_3$, it was reported that substituting norbornadiene for 1,5-cyclooctadiene gave an active catalytic system resulting in 100% conversion of phenylacetylene to the corresponding polymer but at the expense of losing control associated with the molecular weight distribution with the product having a measured \bar{D} of 2.45, while replacing

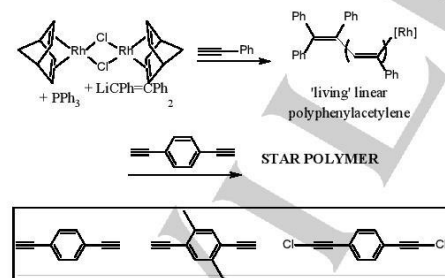
MINIREVIEW

norbornadiene with two cyclooctene ligands yielded an inactive species.

The effect of substituents at the α and β positions on the vinyl lithium species was likewise investigated. It was found that bulky substituents at the α position (preferably a Ph group) with at least one substituent on the β position were necessary to achieve a well-controlled polymerization of phenylacetylene. However, only the triphenylvinyl species, i.e. the original $[\text{Rh}(\text{nbd})\text{Cl}]_2/\text{LiPh}=\text{CPh}_2/\text{PPh}_3$ ternary mixture, gave a system that exhibited quantitative initiation with the remaining ternary mixtures yielding active species with IEs covering the range 0.072–0.30.

The effect of the structure of the phosphine ligand has a less pronounced effect on the level of control in such ternary catalytic systems at least for PPh_3 and simple *para*-substituted derivatives. For example, the use of PPh_3 , $\text{P}(4\text{-ClC}_6\text{H}_4)_3$, $\text{P}(4\text{-FC}_6\text{H}_4)_3$, $\text{P}(4\text{-CH}_3\text{C}_6\text{H}_4)_3$, and $\text{P}(4\text{-MeOC}_6\text{H}_4)_3$ in ternary mixtures yielded, in all instances, active species giving quantitative conversion of phenylacetylene with 100% IE and essentially identical \mathcal{D} s of 1.16. There was, however, an observed, but not unexpected, kinetic impact associated with changing the phosphine ligand structure. As the basicity of the phosphine ligand decreases the rate of polymerization increases, a feature associated with the fact that the phosphine ligand serves as a competitive binding species with monomer—the lower the basicity of the phosphine the lower the effective competitive binding and thus increase in rate of polymerization. For the ligands noted, and under identical polymerization conditions, the rate of polymerization increased in the order: $\text{P}(4\text{-FC}_6\text{H}_4)_3 > \text{PPh}_3 > \text{P}(4\text{-ClC}_6\text{H}_4)_3 > \text{P}(4\text{-CH}_3\text{C}_6\text{H}_4)_3 > \text{P}(4\text{-MeOC}_6\text{H}_4)_3$.

The broader utility of the $[\text{Rh}(\text{nbd})\text{Cl}]_2/\text{LiPh}=\text{CPh}_2/\text{PPh}_3$ ternary catalytic system for the preparation of polymers with advanced architectures, and specifically star and star-block copolymers, was reported by Kanki and Masuda, Scheme 4.^[96]



Scheme 4. The synthesis of star polymers via the homopolymerization of phenylacetylene followed by crosslinking with a difunctional arylalkyne.

Polymerization of phenylacetylene for a target M_n of 5,100 ($[\text{M}]_0/[\text{Rh}] = 50$) yielded "living" polyphenylacetylene with an SEC-measured M_n of 5,350 and \mathcal{D} of 1.13. Subsequent addition of five equivalents 1,4-diethynylbenzene (DEB) (based on Rh) resulted

in crosslinking and isolation of a new material with an M_n of 37,500 and \mathcal{D} of 1.2 (this species contained <3% of linear polyphenylacetylene chains). Substituting DEB with 1,4-diethynyl-2,5-dimethylbenzene also yielded star products although with up to 25% linear chains. This was attributed to the reduced reactivity of 2-methylphenylacetylene towards Rh catalysts compared to phenylacetylene. No star formation was observed when 1,4-bis(chloroethynyl)benzene was employed as the linking agent.

Following the report regarding the effect of the individual components in ternary catalytic mixtures of the general type Rh complex/phosphine/vinyl lithium, Miyake, Misumi and Masuda^[97] reexamined catalysts bearing halogen functionalized phosphine ligands. In particular the authors focused on the synthesis, isolation and application of $\text{Rh}(\text{nbd})(\text{CPh}=\text{CPh}_2)\text{P}(4\text{-XC}_6\text{H}_4)_3$, where X = F or Cl. Both Rh(I)-vinyl catalysts were isolated from the corresponding ternary mixtures, and in the case of the chloro derivative a crystal structure was reported, Figure 8, with the complex adopting a distorted square planar geometry consistent with the "parent" $\text{Rh}(\text{nbd})(\text{CPh}=\text{CPh}_2)\text{PPh}_3$ species. The Cl and F derivatives were subsequently shown to effectively mediate the controlled polymerization of phenylacetylene with essentially quantitative initiation yielding highly stereoregular (*cis-transoidal*) polymers with tunable molecular weights and low \mathcal{D} s. Interestingly, the well-defined, isolated Rh(I) species were reported to be more effective than the corresponding ternary mixtures which, most notably, exhibited markedly lower IEs.

It should be noted that polymerizations performed with the isolated Rh complexes are typically conducted in the presence of added excess phosphine that serves as a co-controlling agent and rate modifier. For example, it was reported that a ratio of $[\text{P}(4\text{-XC}_6\text{H}_4)_3]/[\text{Rh}]$ of at least 5 was essential in achieving the living polymerization of phenylacetylene as well as low \mathcal{D} s. Polymerizations conducted with higher ratios of free phosphine also proceeded in a controlled manner but at a reduced rate as the effect of competitive phosphine binding becomes more dominant.

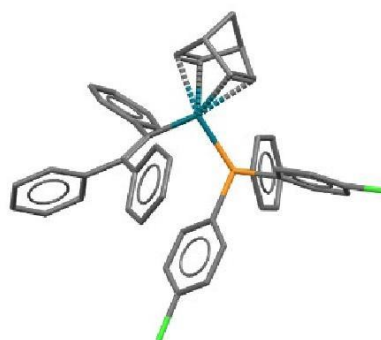
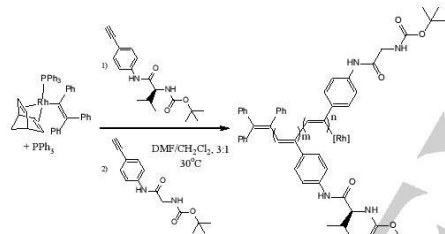


Figure 8. Crystal structure of the Masuda complex $\text{Rh}(\text{nbd})(\text{CPh}=\text{CPh}_2)\text{P}(4\text{-ClC}_6\text{H}_4)_3$

MINIREVIEW

While phenylacetylene, and in some instances simple substituted derivatives, are the monomer substrates of choice when demonstrating the effectiveness of new Rh(I) complexes as initiators such species do exhibit a broader applicability although still remain largely under-utilized. For example, Kumazawa and co-workers^[38] detailed the application of Rh(nbd)(CPh=CPh₂)PPh₂/PPh₃ as the initiating species in the block copolymerization of the chiral monomer *N*-tert-butoxycarbonyl-L-valine 4-ethynylanilide with the achiral comonomer *N*-tert-butoxycarbonylglycine 4-ethynylanilide. A series of homo- and block copolymers, Scheme 5, were prepared of tunable composition and molecular weight and, in most instances, the final materials possessed narrow molecular weight distributions with $\bar{D} \leq 1.25$. Interestingly, the authors demonstrated chirality amplification in the block copolymers with chirality transfer from the chiral block to the achiral block clearly evident. The chirality transfer was rationalized in terms of the energy difference between conformers with and without a helix turn as determined by DFT calculations.



Scheme 5. Block copolymerization of a chiral arylacetylene derivative with an achiral comonomer via sequential monomer addition with Rh(nbd)(CPh=CPh₂)PPh₂/PPh₃ as the initiating system.

In related work Liu et al.^[39] reported the use of Rh(nbd)(CPh=CPh₂)P(4-FC₆H₄)₃ as an initiating species in the preparation of AB diblock copolymers in which the A block was a chiral species based on (((1*S*,5*S*)-6,6-dimethylbicyclo[3.1.1]heptan-2-yl)methyl)(4-ethynylphenyl)-dimethylsilane (**(a)** Figure S1) and the B block on achiral 2-(dodecyloxy)-5-ethynyl-1,3-phenylene)dimethanol (**(b)**, Figure S1). Well defined AB diblock copolymers of tunable composition were prepared with measured \bar{D} s in the range $1.29 \leq \bar{D} \leq 1.73$. Similar to the work of Kumazawa and co-workers,^[38] the use of a chiral A block derived from (**a**) induced chirality in the B block of monomer (**b**). However, distinct from the previous report, the poly(**(a)**-**(b)**) copolymers possessed a *cis-transoidal*(**(a)** block)/*cis-cisoidal*(**(b)** block) stereoregular structure – the first example of its kind prepared by helix-sense selective polymerization.

The Masuda-type Rh(I)-vinyl complexes highlighted thus far give optimal control, in terms of tunable molecular weight, high IE and low dispersity of resulting copolymers, when used in conjunction with at least five equivalents of added free phosphine (based on [Rh]). We have noted that the added phosphine serves as a rate modifier by acting as a monomer-competing binding species – in essence it controls the effective rates of initiation and propagation facilitating controlled polymerization.

Onishi and co-workers^[40] reported a series of novel Rh(I) catalysts containing a butylene bridge between the nbd ligand and a co-ordinating phosphine or amino functional group, of general formula [(nbd-(CH₂)₄-X)RhR] where (**5**): X = PPh₂, R = Cl; (**6**): X = NPh₂, R = Cl; (**7**): X = PPh₂, R = triphenylvinyl, Figure 9, with the reported X-ray crystal structure of the triphenylvinyl derivative, (**7**), is shown in Figure 10.

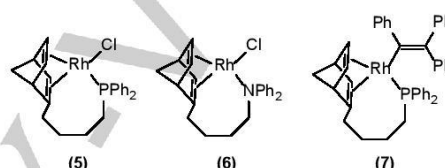


Figure 9. Chemical structures of Rh(I) complexes with butylene bridges between the nbd ligand and coordinating phosphine or amino groups

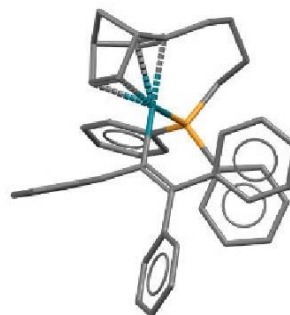


Figure 10. Crystal structure of Rh(CPh=CPh₂)(nbd-(CH₂)₄-PPh₂)

All three of these species were evaluated as initiators in the (co)polymerization of phenylacetylene. The Rh(nbd-(CH₂)₄-PPh₂)Cl complex, (**5**) Figure 9, in the absence of any additive, displayed low catalytic activity with a measured monomer conversion of <1% after 24 h in THF at 30 °C.

MINIREVIEW

In contrast, the nitrogen analogue, $\text{Rh}(\text{nbdc}(\text{CH}_2)_4\text{-NPh}_2)\text{Cl}$, (**6**) Figure 9, polymerized phenylacetylene quantitatively with an isolated yield of 83%, D of 1.7 and initiation efficiency of 0.21. The $\text{Rh}(\text{I})$ -vinyl derivative, $\text{Rh}(\text{CPh}=\text{CPh}_2)(\text{nbdc}(\text{CH}_2)_4\text{-PPh}_2)$, (**7**) Figure 9, gave polymer yields of 94% with quantitative conversion of monomers and a relatively low D of 1.3.; however, the IE, while higher than (**6**), was non-quantitative at 0.6. According to the authors, the low IE observed for the $\text{Rh}(\text{nbdc}(\text{CH}_2)_4\text{-NPh}_2)\text{Cl}$ complex was due to a low population of the active 14e mononuclear complex generated via coordination of the amino group to the Rh centre akin to NEt_3 in the $[\text{Rh}(\text{nbdc})\text{Cl}]_2/\text{NEt}_3$ catalyst system. In the case of (**5**), $\text{Rh}(\text{nbdc}(\text{CH}_2)_4\text{-PPh}_2)\text{Cl}$, the low activity was attributed to the slow formation of the $\text{Rh}-\text{C}\equiv\text{CPh}$ species which serves as the initiating species in the polymerization of phenylacetylene. In contrast, and consistent with previous examples of $\text{Rh}(\text{I})$ -vinyl, Masuda-type, complexes, the $\text{Rh}(\text{CPh}=\text{CPh}_2)(\text{nbdc}(\text{CH}_2)_4\text{-PPh}_2)$ species with a structural resemblance to the active propagating chain end facilitates the smooth insertion of phenylacetylene monomer into the $\text{Rh}-\text{C}$ bond of the metal centre and triphenylvinyl group. Initiator (**7**) is the first example of a well-defined Rh complex with a tridentate ligand for this specific application and also represents the only current example of a $\text{Rh}(\text{I})$ -triphenylvinyl complex able to mediate the controlled polymerization of phenylacetylene without the addition of extra free phosphine.

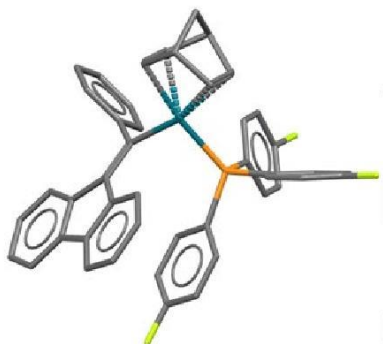


Figure 11. Crystal structure $\text{Rh}(\text{nbd})(\text{CPh}=\text{CFu})\text{P}(4\text{-FC}_6\text{H}_4)_3$

Intrigued by the limited number of reported well-defined $\text{Rh}(\text{I})$ -vinyl complexes that serve as initiators for the controlled polymerization of PA, we recently reported three new $\text{Rh}(\text{I})$ - α -phenylvinylfluorenyl species based on the Masuda structural motif, i.e. $\text{Rh}(\text{nbd})(\text{CPh}=\text{CFu})\text{P}(\text{X}-\text{C}_6\text{H}_4)_3$, (where $\text{X} = 4\text{-F}$, 4-CF_3 , $3,5\text{-}(\text{CF}_3)_2$).^[41] Figure 11 shows the X-ray crystal structure for the $\text{Rh}(\text{nbd})(\text{CPh}=\text{CFu})\text{P}(4\text{-FC}_6\text{H}_4)_3$ complex. The complex adopts a distorted square planar geometry in the solid state with the conformationally locked fluorenyl group on the β -vinyl carbon being coplanar with the vinyl bond. Additionally, there is the presence of through-space π - π interactions between the fluorenyl group and one aryl ring of the phosphine ligand. These two features distinguish the fluorenyl derivatives from the Masuda-

type complexes bearing a triphenylvinyl ligand with freely rotating β -phenyl groups.

The homopolymerization of phenylacetylene with the three fluorenyl derivatives was examined under identical conditions to those reported by Masuda and co-workers.^[37] Interestingly, while meeting the general structural requirements for highly efficient Masuda-type complexes^[35] the IEs reported for the three complexes covered the range 0.16-0.56; however, the polymers produced had very high *cis-transoidal* stereoregularity and low D s. We attributed the low IE to the energetics of the initiation process, whereby the conformationally locked fluorenyl group hinders the efficient 2,1-insertion of phenylacetylene, the established mode of propagation for these polymerizations, Scheme 1. Recent molecular modelling studies of these polymerizations suggest that a transition state whereby conjugative insertion occurs is energetically favourable and requires the incoming phenylacetylene monomer to be coplanar with the $\text{C}\equiv\text{C}$ and Rh-atom.^[17] In these fluorenyl derivatives, this might be hindered to a significant extent due to the conformationally locked nature of the fluorenyl functional group but becomes more energetically favourable once insertion and initial propagation steps take place with the fluorenyl moiety moving away from the Rh centre. While these IEs are less than ideal, this report does suggest that the structural requirements for efficient initiating complexes of the $\text{Rh}(\text{I})$ -vinyl type is more complex than those originally outlined by Misumi et al.^[36] and include geometric factors not originally considered. In addition to phenylacetylene homopolymerization, the controlled nature of the polymerization process was established through self-blocking experiments in which phenylacetylene was homopolymerized in THF at 40°C with a [phosphine]/[Rh] ratio of 5 being employed yielding a polyphenylacetylene with an M_n of 17,000 and D of 1.34; subsequently a second charge of phenylacetylene was added and polymerization recommenced forming a self-blocked polyphenylacetylene with a final SEC-measured M_n of 46,900 and D of 1.19.

All examples highlighted thus far in this mini-review have been Rh-based catalysts containing nbd or cod as the diene ligand. We note that while nbd catalysts are able to mediate the polymerization of phenylacetylene (and derivatives) in a controlled or non-controlled fashion, cod-based catalysts only effect non-controlled (co)polymerization – there are no known examples of well-defined cod-analogues of the complexes shown in Figure 5, 7, 8, 10 or 11 capable of mediating the controlled polymerization of arylacetylenes. The effect of diene ligands in complexes of the type $[\text{Rh}(\text{diene})\text{Cl}]_2$ for the polymerization of phenylacetylene employing the series of dienes shown in Figure 12 was reported by Saeed, Shiotsuki and Masuda,^[42] with the principle aim of developing novel catalytic systems.

MINIREVIEW

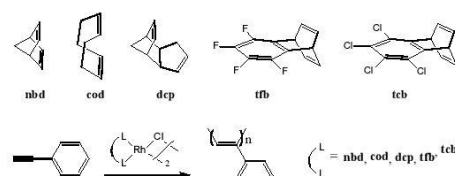


Figure 12. Chemical structures of diene ligands: 2,5-norbornadiene (nbd); 1,5-cyclooctadiene (cod); endo-dicyclopentadiene (dcp); tetrafluorobenzobarrelene (tfb) and tetrachlorobenzobarrelene (tcb), and the homopolymerization of phenylacetylene with bridged Rh complexes [Rh(diene)Cl]₂.

The **tfb** and **tcb** derivatives, [Rh(**tfb**)Cl]₂ and [Rh(**tcb**)Cl]₂, were found to be significantly more active than the conventional [Rh(**nbd**)Cl]₂ and [Rh(**cod**)Cl]₂ species. For example, in polymerizations conducted in toluene at 30 °C for one minute in the presence of one equivalent of NEt₃ under otherwise identical conditions yielded for the **nbd** catalyst, polyphenylacetylene in a yield of 69 % (SEC-measured *M_n* of 118,000, *D* of 1.85); while the **cod** catalyst yielded polyphenylacetylene in a 5 % yield (*M_n* of 22,000, *D* of 2.16), the **dcp** complex only gave a trace of polymer while the **tfb** and **tcb** derivatives both effected quantitative conversion with the former yielding a homopolymer with an *M_n* of 281,000 and *D* of 1.70, while the **tcb** complex yielded a homopolymer with an *M_n* of 227,000 and corresponding *D* of 1.79 (note: all polymers have the expected high degree of *cis-transoidal* stereoregularity). This was the first demonstration of catalytic systems exhibiting a superior activity over the well-established [Rh(**nbd**)Cl]₂ complex. The authors also examined the effect of solvent and co-catalyst additive with, in all cases the activity profiles following the same trend with catalyst activity increasing in the order **tfb** ≈ **tcb** > **nbd** > **cod** > **dcp**. Based on this observation, the authors proposed that the difference in catalytic activity between the different complexes was due to the difference in π-acidity of the diene ligands. The bonding model in such metal-alkene complexes is shown in Figure 13.

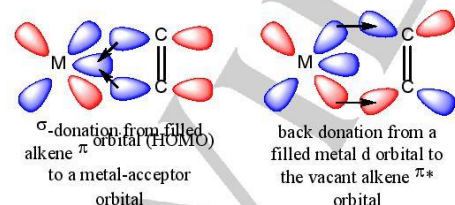


Figure 13. The Dewar-Chat-Duncanson model of bonding between a metal centre and an alkene.

The net result of the back-donation from the metal to the alkene is a reduction in the electron density at the metal centre, i.e. an increase in electrophilic character. The degree of back-

donation is determined, at least in part, by the π-acidity of the alkene, i.e. the ability of the ligand to accept electrons into the π* (LUMO) orbital (d-π* overlap). As such, the π-acidity can be estimated from the energy of the LUMO. In this contribution the authors reported the LUMO energies (in eV) to be (in order from lowest to highest): 0.21 (**tfb**) < 0.48 (**tcb**) < 0.79 (**nbd**) < 0.90 (**cod**) < 1.09 (**dcp**), entirely consistent with the above order of observed polymerization activity and highlights that of the five ligands **tfb** is expected to be the most π-acidic.

As a natural extension of the above study, the same authors detailed the synthesis of a well-defined **tfb**-based Rh catalytic system.^[43] Saeed, Shiotsuki and Masuda reported a ternary catalyst system derived from [Rh(**tfb**)Cl]₂, PPh₃ and LiCPh=CPh₂ along with the well-defined Rh(I)-vinyl catalyst, Rh(**tfb**)CPh=CPh₂(PPh₃), isolated from the ternary mixture. Although the crystal structure of Rh(**tfb**)CPh=CPh₂(PPh₃) was not reported it was presumed to have a square planar geometry in line with the above highlighted Rh(I)-vinyl species.

An evaluation of the activity of the ternary catalytic mixture in the homopolymerization of phenylacetylene revealed that polyphenylacetylenes prepared under such conditions yielded product with essentially quantitative initiation (estimated IE of 0.96), i.e. controllable molecular weights, *D*s as low as 1.03, and *cis-transoidal* contents ≥ 99%. For both the ternary catalyst system and the isolated complex, multistage polymerization of phenylacetylene experiments were conducted and confirmed the living nature of the polymerizations as did the pseudo-first order kinetic plots and evolution of *D* as a function of conversion. A particularly salient, and somewhat unique, feature of polymerizations conducted with the Rh(**tfb**)CPh=CPh₂(PPh₃)/PPh₃ initiating system was the observed high activity, and IE, even at low concentration. For example, homopolymerization of phenylacetylene at [M₀]/[Rh] of 4,000 (theoretical *M_n* of 408,560) yielded a polymer with an SEC-measured *M_n* of 401,000 (calculated IE of 0.98) and *D* of 1.12.

While other reports exist detailing the use of **tfb**-functional Rh catalysts for the preparation of polyphenylacetylenes^[26b, 44] (typically in a non-controlled fashion), the above highlighted report remains, to the best of our knowledge, the only example in which a well-defined isolable Rh(I)-vinyl complex, or ternary mixture with the *in situ* generation of the active **tfb**-Rh(I)-vinyl species, has been noted and that has been demonstrated to be effective in the controlled polymerization of phenylacetylene yielding materials with near-quantitative *cis-transoidal* stereoregularity. This suggests that there is significant scope and opportunity for the further development and evaluation of new **tfb**, **tcb**-based catalytic systems for this target application.

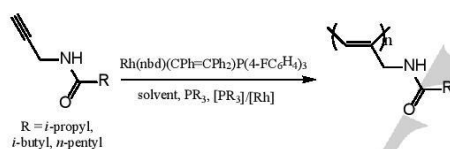
3.2. Propargyl-based monomers

While certain Rh catalysts are clearly highly effective species for the (non)controlled (co)polymerization of arylacetylene substrates their applicability does extend beyond this important family of monomers. In addition to arylacetylenes, propargyl esters and amides have been reported to be suitable substrates although typically polymerize in a non-controlled fashion yielding polymers

MINIREVIEW

with reduced stereoregularity (compared to phenylacetylenes). For example, a series of poly(propargyl ester)s were reported by Zhang et al.^[28] obtained using the nbd-tetraphenylborate Rh catalyst, (4) Figure 4. For example, homopolymerization of propargyl hexanoate with (4) in THF under a range of conditions yielded poly(propargyl hexanoate) with yields of 42-77%, SEC-measured M_n s of 4,900-28,000, D s spanning the range 1.83 to 4.70 and *cis* contents of 48-88% with little, if any, clear direct correlation between any of these features. Reports employing the same catalyst for both propargyl esters and amides, from Masuda and co-workers,^[45] have focused on amino-acid derived monomers and emphasized the structure and properties of the final materials rather than the fundamental features of polymerization. However, we note that within this body of work examples are given in which polymers are isolated with 100% monomer conversion and reported D s < 1.20 which suggests that under certain conditions polymerization of this monomer family proceeds in a controlled (or pseudo-controlled) manner.

Nakazato et al.^[46] reported the application of the well-defined Masuda complex $Rh(nbd)(CPh=CPh_2)P(4-FC_6H_4)_3$, the fluorine analogue of the catalysts shown in Figure 8, for the polymerization of three simply alkyl propargyl amide monomers, Scheme 6.



Scheme 6. The polymerization of propargyl amide monomers with the well-defined Masuda Rh(I)-vinyl complex, $Rh(nbd)(CPh=CPh_2)P(4-FC_6H_4)_3$.

As a representative example, the polymerization of the *i*-butyl derivative, in $CHCl_3$ at 30 °C with five equivalents of added PPh_3 as a rate modifier gave a 100% yield of polymer product with an M_n of 17,300 (IE of 0.8, although we note that molecular weights were measured by SEC and reported as polystyrene equivalents) and D of 1.36. The fundamental features of this polymerization were examined under identical conditions except polymerization was conducted at 0 °C. Under such conditions, the polymerization of the *i*-butyl monomer was complete after 60 min, exhibited linear pseudo-first order kinetics (although the plot did not pass through the origin suggesting non-ideal polymerization), D decreased with conversion (although are consistently higher than might be expected), and polymerization resumed upon the second charge of monomer which also polymerized to completion. While the authors presented the molecular weight vs. conversion plot as a linear plot it is, arguably, better represented as a two-stage plot with an initial steep increase in the measure molecular weight. This is perhaps also more consistent with the non-ideal kinetic plot and suggests that there may be some non-controlled polymerization occurring in the early stages of the polymerization process. However, it is clear that the polymerizations do appear to proceed with many of the key hallmark features associated with

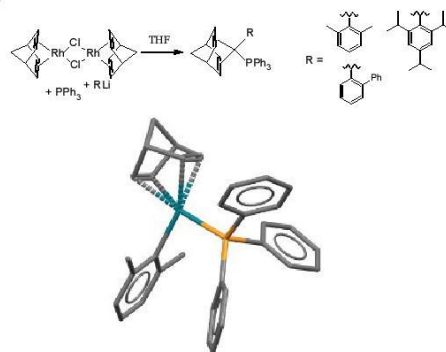
a controlled polymerization and we reiterate that quantitative initiation nor low dispersity are formally prerequisites for a polymerization to be termed 'controlled'. The authors proposed that the less-than ideal dispersities were likely due to a larger k_p/k_t ratio than might be commonly associated with alternative controlled polymerizations.

4. Rhodium(I)-Aryl Complexes

4.1. Arylisocyanides

Arylisocyanides have long attracted attention in the polymer community due to the propensity of materials formed from such monomers to form helical structures.^[23a, 47] The transition metal-mediated controlled (co)polymerization of arylisocyanides is well-documented,^[23b] with complexes based on Ni(II),^[48] Pt(II),^[49] and certain dinuclear Pt(II)-Pd(II) species^[50] being particularly useful. In the context of this mini-review, we will highlight examples of Rh(I)-aryl complexes that have been shown to be effective in promoting the (co)polymerization of bulky arylisocyanides.^[51]

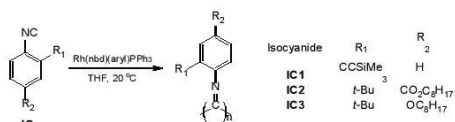
Yamamoto, Onitsuka and Takahashi^[51c] reported the synthesis of three Rh(I)-aryl complexes and their application as initiators for the polymerization of three different, substituted arylisocyanides monomers. Scheme 7 shows the synthetic outline for the preparation of the Rh complexes along with the reported X-ray crystal structure of the $Rh(nbd)(2,6-Me_2C_6H_3)PPh_3$ derivative. Such Rh(I)-aryl species are prepared via the same general route as the well-defined Rh(I)-vinyl complexes described earlier, namely, reaction between $[Rh(nbd)Cl]_2$, a triarylphosphine (PPh_3) and an aryllithium (versus a vinylolithium in the case of the Rh(I)-vinyl complexes), with the noted $Rh(nbd)(2,6-Me_2C_6H_3)PPh_3$ complex isolated in a 96% yield. The reported crystal structure of this Rh(I)-aryl species shows that the complex adopts a square planar geometry that is entirely consistent with the Rh(I)-vinyl complexes.



Scheme 7. The general synthetic route for the preparation of Rh(I)aryl complexes of the type $Rh(nbd)(aryl)PPh_3$ and the reported solid state structure for the $Rh(nbd)(2,6-Me_2C_6H_3)PPh_3$ derivative.

MINIREVIEW

All three Rh(I)-aryl complexes were subsequently evaluated as initiating species in the polymerization of three different arylisocyanides, Scheme 8.



Scheme 8. The polymerization of 2,4-disubstituted arylisocyanides monomers with Rh(nbd)(aryl)PPh₃ complexes.

The polymerization of **IC1** (2-((trimethylsilyl)ethynyl)phenyl isocyanide) with Rh(nbd)(2,6-Me₂C₆H₃)PPh₃ generally proceeded smoothly provided the polymerization was performed with 10 equivalents of added free PPh₃. For example, for a **IC1**/Rh of 25 and PPh₃/Rh of 10, under the conditions noted in Scheme 8, resulted in 100% conversion of monomer to polymer with the product having an SEC measured *M_n* of 4,700 and *D* of 1.12. While this is reported as a polystyrene-equivalent molecular weight we note that the authors were able to perform end-group analysis and established that the IE for Rh(nbd)(aryl)PPh₃/PPh₃ was essentially quantitative. In the absence of added PPh₃, the yield dropped and in addition to polymer a significant amount of oligomers were formed highlighting the need for added phosphine in order to ensure smooth polymerization. Increasing the **IC1**/Rh ratio to 50, 75 and finally 100 resulted in a systematic increase in the final *M_n* of the polymer although was accompanied by a noticeable increase in the *D* from 1.19 to 1.26 to 1.47 at **IC1**/Rh = 100. Similar polymerization results were obtained for the homopolymerizations of monomers **IC2** and **IC3**. Attempts to prepare block copolymers, verifying at least in part, the controlled nature of the polymerizations, failed suggesting that polymerization was not controlled and that chain end decomposition was likely occurring during polymerization. Unfortunately, no kinetic data was reported that would have supported, or verified, this supposition.

In a follow-up paper Onitsuka et al.^[519] detailed a study in which they expanded both the catalyst pool and the number of arylisocyanides. Figure 14 shows the structures of the six Rh complexes examined and includes the three species shown in Scheme 7, two new derivatives Rh(nbd)(2-MeNaphthyl)PPh₃ and Rh(nbd)(9-Anthra)PPh₃ and the original well-defined Rh(I)-vinyl Masuda complex, Rh(nbd)(CPh=CPh₂)PPh₃. Figure 15 shows the reported X-ray crystal structure for the Rh(nbd)(2-MeNaphthyl)PPh₃ complex.

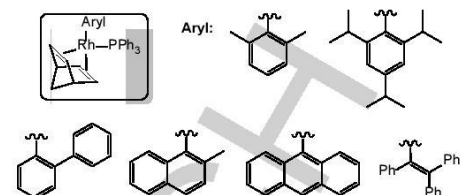


Figure 14. General structure of Rh(nbd)(PPh₃)(aryl) complexes reported by Onitsuka and co-workers.

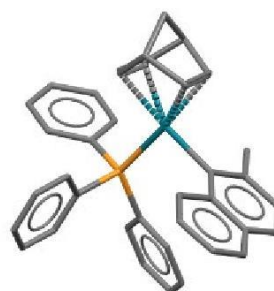


Figure 15. The X-ray crystal structure of the Rh(2-MeNaphthyl)(nbd)(PPh₃) complex.

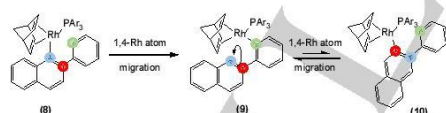
As a general observation, all the noted complexes (including the Masuda-vinyl derivative) effectively mediated the polymerization of arylisocyanides provided there was a bulky substituent in one of the *ortho* positions in the isocyanide monomer. Attempted polymerization of 2,6-dimethylphenylisocyanide with Rh(nbd)(2,6-Me₂C₆H₃)PPh₃, for example, resulted in no observed conversion. In cases where polymerization was effective, the resulting polymers had tunable molecular weights and *D*s spanned the range 1.16-1.53. In no instance was any oligomeric by-product observed for the above complexes. The controlled nature of the polymerizations was clearly demonstrated with the *M_n* vs conversion plots being linear and measured values agreeing almost perfectly with the theoretical values at all conversions. Consistent with the preliminary report, initial attempts to effect block copolymer formation by sequential monomer addition failed, further confirming that the active site slowly decomposed, and became particularly problematic at high conversion. However, the authors demonstrated that the active chain end could be efficiently stabilized in the presence of a large excess of added PPh₃ allowing block copolymer formation. For example, the authors reported that the three-step sequential addition of 50 equivalents of **IC2** to Rh(nbd)(2,4,6-*i*-Pr₃C₆H₂)PPh₃ in the presence of 400 equivalents of PPh₃ resulted in the step-wise formation of polymer with *M_n*s of 21,300, 38,000 and 50,900 with corresponding *D*s of 1.19, 1.20 and 1.29. Further, an AB diblock copolymer of **IC2** (A

MINIREVIEW

block) with 2-*tert*-butyl-4-(cyclohexyloxycarbonyl)phenyl isocyanide (B block) was successfully prepared, quantitatively, under similar conditions with $(\text{Rh}(\text{nbd})(2,4,6\text{-}i\text{-Pr}_3\text{C}_6\text{H}_2)\text{PPh}_3)$ as initiator, 400 equivalents of PPh_3 , THF, 20 °C). The tri-*iso*-propyl Rh derivative, $(\text{Rh}(\text{nbd})(2,4,6\text{-}i\text{-Pr}_3\text{C}_6\text{H}_2)\text{PPh}_3)$, has also been employed as the initiating species in the helix sense selective (co)polymerization of bulky aryl isocyanide monomers with chiral ester or amide groups, yielding materials of variable molecular weight and low-to-medium dispersities.^[5,16] For example, polymerization of (*S*)-octan-2-yl 3-(*tert*-butyl)-4-isocyanobenzoate (100 equivalents) with $(\text{Rh}(\text{nbd})(2,4,6\text{-}i\text{-Pr}_3\text{C}_6\text{H}_2)\text{PPh}_3)$ with 40 equivalents of PPh_3 based on $[\text{Rh}]$ in THF at 20 °C resulted in quantitative conversion of monomer to polymer with the homopolymer having an M_n of 43,600 and \mathcal{D} of 1.40. The specific rotation, $[\alpha]_D$, of the chiral monomer was determined to be +32 while $[\alpha]_D$ for the corresponding homopolymer was measured at -178 indicating that the polymerization resulted in the generation of chirality other than that associated with the pendent ester groups. The CD (circular dichroism) spectrum of the homopolymer exhibited a strong Cotton effect in the 250-400 nm region while nothing was observed for the monomer in this region. The authors noted that the Cotton effect around 350 nm is associated with the $n\text{-}\pi^*$ transition of imino groups characteristic of helical poly(aryl isocyanide)s. The authors also demonstrated that the structure of the chiral ester groups, and specifically the monomer purity, precise location of the chiral centre and the length of the alkyl chain, had a direct impact on the helical sense selectivity.

4.2. Phenylacetylenes

In an effort to further understand the reduced IE observed in the $\text{Rh}(\text{I})\text{-}\alpha\text{-phenylvinylfluorenyl}$ complex-mediated polymerization of phenylacetylene highlighted above (see Figure 12) we recently targeted a new $\text{Rh}(\text{I})$ complex, Scheme 9, with the aim of evaluating the geometric effect around the initiating fragment.^[52]



Scheme 9. Chemical structure of the target 2-phenyl-2-naphthyl $\text{Rh}(\text{I})$ derivative, (8), and structures of the isomeric 2-naphthylphenyl, (9), and 3-phenyl-2-naphthyl, (10), complexes formed by proposed 1,4-Rh atom migrations.

The target complex, (8) Scheme 9, was 'prepared' following the general synthetic route employed for all the above reported $\text{Rh}(\text{I})\text{-vinyl}$ and $\text{Rh}(\text{I})\text{-aryl}$ complexes namely lithiation of the corresponding vinyl/aryl bromide (1-bromo-2-phenyl-2-naphthalene in this instance) followed by reaction with the tetracoordinate species formed the reaction of $[\text{Rh}(\text{nbd})\text{Cl}]_2/\text{P}(4\text{-FC}_6\text{H}_4)_3$. Interestingly, after recrystallization, X-ray structural characterization revealed isolation not of the target complex but

the isomeric 2-naphthylphenyl complex, (9) Scheme 9. The X-ray crystal structure of the isolated $\text{Rh}(\text{I})\text{-aryl}$ complex is given in Figure 16.

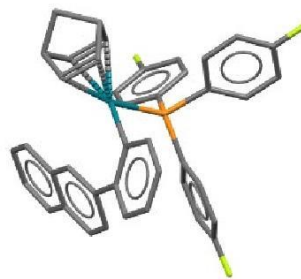
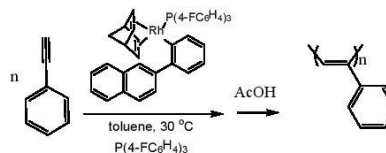


Figure 16. The X-ray crystal structure of $\text{Rh}(\text{nbd})(2\text{-NaphthPh})\text{P}(4\text{-FC}_6\text{H}_4)_3$.

We proposed that the isolated complex was formed by a *ortho-to-ortho* (or 1,4-) Rh atom migration, a supposition that was supported by DFT calculations that indicated the isolated complex had a lower energy (-19 kJmol^{-1}) compared to the target species. While not the target complex we did characterize this new species in detail. Interestingly, during NMR solution characterization we identified a third structural isomer, the 3-phenyl-2-naphthyl derivative, (10) Scheme 9, formed, presumably, via a second 1,4-Rh atom migration from complex (9).

While complex (9) did not allow for us to evaluate the specific geometric effect relating to the structure of the initiating fragment as initially intended we did proceed to examine the ability of (9) to initiate the polymerization of phenylacetylene (recognizing that (10) was also likely present when in solution), Scheme 10.



Scheme 10. Homopolymerization of phenylacetylene with $\text{Rh}(\text{nbd})(2\text{-NaphthPh})\text{P}(4\text{-FC}_6\text{H}_4)_3/\text{P}(4\text{-FC}_6\text{H}_4)_3$.

The $\text{Rh}(\text{I})\text{-aryl}$ complex (9) proved to be an effective initiator for the polymerization of phenylacetylene. The pseudo first order kinetic and molecular weights vs conversion plots were linear indicating a controlled polymerization process. The measured \mathcal{D} s of the resulting polyphenylacetylenes were low and typically ≤ 1.25 while the highly stereoregular structure was confirmed by ¹H NMR spectroscopy with products having >95% *cis-transoidal*

MINIREVIEW

structure. Calculated IEs, while not quantitative, were high at ca. 0.8. This report represents the first detailed evaluation of a Rh(I)-aryl complex specifically for the controlled polymerization of phenylacetylene and suggests that this general family of complexes may have a broader utility than currently appreciated.

5. Summary and Outlook

Herein we have provided an overview of the current state-of-the-art relating to (controlled) polymerization processes with well-defined Rh(I)-vinyl and Rh(I)-aryl complexes. The Rh(I)-triarylvinyl derivatives, broadly referred to as Masuda-type complexes, are highly effective at mediating the controlled polymerization phenylacetylene and (functional) derivatives thereof. While the various ligand components in such species have been varied and their efficacy evaluated, there still remains significant scope for the further development of new complexes and clearly opportunities are present in the preparation of novel end-group functional materials as well as new polymers with architectures beyond arylacetylene-based homopolymers, statistical copolymers or simple AB diblock copolymers.

Given the reported efficacy of the Masuda Rh(nbd)(CPh=CPh₂)P(4-FC₆H₄)₃ derivative in mediating the controlled polymerization of certain propargyl amides it seems that similar opportunities exist for this general family of monomers. New initiators can, and should, be prepared and evaluated as well as the development of synthetic approaches for the preparation of materials with advanced architectures. The combination of inherent helical structure with new topologies and architectures presents opportunities for the preparation of more complex and potentially interesting (co)polymers.

As with the controlled, Rh-mediated polymerization of arylacetylenes and propargyl amides and esters, there are relatively few reports detailing the controlled polymerization of arylisocyanides with well-defined Rh(I)-aryl complexes and, to the best of our knowledge, only one report describing the use of a member of this family of Rh(I) species in the controlled polymerization of phenylacetylene. Given the large, and varied, number of commercially available arylbromides there exists opportunities for additional contributions in (mechanistic) organometallic synthesis, involving rationale design and application as polymerization initiators, the synthesis of new, functional (co)polymers with currently unknown architectures and, as a consequence, the generation of new materials with potentially new or novel properties.

Since the seminal contribution from Kishimoto and co-workers in 1994 and the subsequent pioneering work from Masuda et al. there have clearly been significant advances in the field of Rh(I)-complex catalysis and specifically regarding the use of such well-defined Rh(I)-vinyl and Rh(I)-aryl complexes as catalysts/initiators for the controlled polymerization of alkyne-based monomers. While effective catalysts are available for effecting the controlled polymerization of the three monomer families described herein, there are new, additional, complexes that could be prepared and examined; it seems unlikely that the most efficient, active, and broadly applicable Rh complexes for

these target applications would have been discovered based on the comparatively limited number of examples reported thus far.

Acknowledgements

ABL thanks the Research Office at Curtin (ROC) for a PhD stipend for NSLT.

Keywords: Polyphenylacetylene • Rh complex • Controlled polymerization • Stereoregularity • Arylisocyanide

- [1] K. Ziegler, *Angew. Chem.* **1936**, *49*, 499-502.
- [2] A. D. Jenkins, P. Kratochvíl, R. F. T. Stepto, U. W. Suter, *Pure & Appl. Chem.* **1996**, *68*, 2287-2311.
- [3] a) M. Szwarc, M. Lécy, R. Milkovich, *J. Am. Chem. Soc.* **1956**, *78*, 2656-2657; b) M. Szwarc, *Nature* **1956**, *178*, 1168-1169.
- [4] S. Aoshima, S. Kanaoka, *Chem. Rev.* **2009**, *109*, 5245-5287.
- [5] a) O. W. Webster, W. R. Hettler, D. Y. Sogah, W. B. Farnham, T. V. RajanBabu, *J. Am. Chem. Soc.* **1983**, *105*, 5706-5708; b) O. W. Webster, *J. Polym. Sci., Part A: Polym. Chem.* **2000**, *38*, 2855-2860.
- [6] S. Inoue, *J. Polym. Sci., Part A: Polym. Chem.* **2000**, *38*, 2861-2871.
- [7] T. J. Deming, *J. Polym. Sci., Part A: Polym. Chem.* **2000**, *38*, 3011-3018.
- [8] C. W. Bielawski, R. H. Grubbs, *Prog. Polym. Sci.* **2007**, *32*, 1-29.
- [9] G. J. Domski, J. M. Rose, G. W. Coates, A. D. Bolig, M. Brookhart, *Prog. Polym. Sci.* **2007**, *32*, 30-92.
- [10] J. Nicolas, Y. Guillauneuf, C. Lefay, D. Bertin, D. Gimes, B. Charleux, *Prog. Polym. Sci.* **2013**, *38*, 63-235.
- [11] K. Matyjaszewski, *Adv. Mater.* **2018**, *30*, 1706441.
- [12] a) G. Moad, E. Rizzardo, S. H. Thang, *Aust. J. Chem.* **2012**, *65*, 985-1076; b) J. Chiefari, Y. K. Chong, F. Ercole, J. Kristina, J. Jeffery, T. P. T. Le, R. T. A. Mayadunee, G. F. Mejs, C. L. Moad, G. Moad, E. Rizzardo, S. H. Thang, *Macromolecules* **1998**, *31*, 5559-5562.
- [13] S. Yamago, *J. Polym. Sci., Part A: Polym. Chem.* **2006**, *44*, 1-12.
- [14] G. Inzelt, *Conducting Polymers, Monographs in Electrochemistry*, Springer, Verlag Berlin Heidelberg, **2012**.
- [15] S. Amdur, A. T. Y. Cheng, C. J. Wong, P. Ehrlich, *J. Polym. Sci., Polym. Chem. Ed.* **1978**, *16*, 407-414.
- [16] T. Masuda, A. Zhang, in *Handbook of Metathesis, Vol. 3: Polymer Synthesis*, 2 ed. (Eds.: R. H. Grubbs, E. Khosravi), Wiley-VCH, **2015**, pp. 375-390.
- [17] Z. Ke, S. Abe, T. Ueno, K. Morohuma, *J. Am. Chem. Soc.* **2011**, *133*, 7926-7941.
- [18] a) T. Masuda, *Polym. Rev.* **2017**, *57*, 1-14; b) F. Freire, E. Quiñoa, R. Riguera, *Chem. Rev.* **2016**, *116*, 1242-1271; c) L. Liu, Y. Zang, H. Jia, T. Aoki, T. Kaneko, S. Hadano, M. Teraguchi, M. Miyata, G. Zhang, T. Namikoshi, *Polym. Rev.* **2017**, *57*, 89-118; d) T. Masuda, *J. Polym. Sci., Part A: Polym. Chem.* **2007**, *45*, 165-180.
- [19] a) S. Li, K. Liu, G. Kuang, T. Masuda, A. Zhang, *Macromolecules* **2014**, *47*, 3288-3296; b) Y. Zang, T. Aoki, M. Teraguchi, T. Kaneko, L. Ma, H. Jia, *Polymer* **2015**, *56*, 199-206; c) T. Sone, R. D'Amato, Y. Mawatari, M. Tabata, A. Furlani, M. V. Russo, *J. Polym. Sci., Part A: Polym. Chem.* **2004**, *42*, 2365-2376; d) X. A. -Zhang, H. Zhao, Y. Gao, J. Tong, L. Shan, Y. Chen, S. Zhang, A. Qin, J. Z. Sun, B. Z. Tang, *Polymer* **2011**, *52*, 5290-5301; e) J. Chen, K. K.-L. Cheuk, B. Z. Tang, *J. Polym. Sci., Part A: Polym. Chem.* **2006**, *44*, 1153-1167; f) H. Jia, J. Li, Y. Zang, T. Aoki, M. Teraguchi, T. Kaneko, *J. Polym. Sci., Part A: Polym. Chem.* **2012**, *50*, 5134-5143; g) Y. Qu, J. Hua, Y. Jiang, H. Tian, *J. Polym. Sci., Part A: Polym. Chem.* **2009**, *47*, 1544-1552; h) X. A. Zhang, M. R. Chen, H. Zhao, Y. Gao, Q. Wei, S. Zhang, A. Qin, J. Z. Sun, B. Z. Tang, *Macromolecules* **2011**, *44*, 6724-6737; i) A. C. Pauly, P. Theato, *Polym. Chem.* **2012**, *3*, 1769-1782; j) M. Bhebe, E. A. De Eulate, Y. Pei, D. W. M. Arrigan, P. J.

MINIREVIEW

- Roth, A. B. Lowe, *Macromol. Rapid Commun.* **2017**, *38*, 1600528; k) M. Tabata, T. Sone, Y. Sadahiro, *Macromol. Chem. Phys.* **1999**, *200*, 265-282; l) I. Saeed, M. Shiotsuki, T. Masuda, *Macromolecules* **2006**, *39*, 5347-5351.
- [20] J. G. Rodríguez, A. Lafuente, J. Arranz, *J. Polym. Sci., Part A: Polym. Chem.* **2005**, *43*, 6438-6444.
- [21] a) A. Nakazato, I. Saeed, T. Katsumata, M. Shiotsuki, T. Masuda, J. Zednik, J. Vohlidal, *J. Polym. Sci., Part A: Polym. Chem.* **2005**, *43*, 4530-4536; b) H. Gulyás, A. C. Bényei, J. Bakos, *Inorg. Chim. Acta* **2004**, *357*, 3094-3098; c) G. Zamora, J. Pons, J. Ros, *Inorg. Chim. Acta* **2004**, *357*, 2899-2904; d) N. I. Nikishin, J. Huskens, W. Verboom, *Polymer* **2013**, *54*, 3175-3181.
- [22] D. Bondarev, J. Zednik, I. Plutnarova, J. Vohlidal, J. Sedláček, *J. Polym. Sci., Part A: Polym. Chem.* **2010**, *48*, 4296-4309.
- [23] a) E. Schwartz, M. Koepf, H. J. Kitto, R. J. M. Nolte, A. E. Rowan, *Polym. Chem.* **2011**, *2*, 33-47; b) M. Sugimoto, Y. Ito, *Adv. Polym. Sci.* **2004**, *171*, 77-136.
- [24] J. Zhu, Q. Wang, M.-X. Wang, Wiley-VCH, Weinheim, Germany, **2015**.
- [25] a) P. C. J. Kamer, R. J. M. Nolte, W. Drenth, *J. Am. Chem. Soc.* **1988**, *110*, 6818-6825; b) T. J. Deming, B. M. Novak, *J. Am. Chem. Soc.* **1993**, *115*, 9101-9111; c) S. Asacka, A. Joza, S. Minagawa, L. Song, Y. Suzuki, T. Iyoda, *ACS Macro Lett.* **2013**, *2*, 906-911.
- [26] a) K. Onitsuka, K.-I. Yabe, N. Ohshiro, A. Shimizu, R. Okumura, F. Takei, S. Takahashi, *Macromolecules* **2004**, *37*, 8204-8211; b) N. Onishi, M. Shiotsuki, F. Sanda, T. Masuda, *Macromolecules* **2009**, *42*, 4071-4076; c) O. Nobuaki, S. Atsushi, O. Reiko, T. Fumie, K. Onitsuka, T. Shigetoshi, *Chem. Lett.* **2000**, *29*, 786-787.
- [27] Y. Yoshida, Y. Mawatari, M. Tabata, *Polymers* **2019**, *11*, 93-103.
- [28] W. Zhang, J. Tabei, M. Shiotsuki, T. Masuda, *Polym. Bull.* **2006**, *57*, 463-472.
- [29] Y. Kishimoto, P. Eckerle, T. Miyatake, T. Ikariya, R. Noyori, *J. Am. Chem. Soc.* **1994**, *116*, 12131-12132.
- [30] Y. Kishimoto, T. Miyatake, T. Ikariya, R. Noyori, *Macromolecules* **1996**, *29*, 5054-5055.
- [31] Y. Kishimoto, P. Eckerle, T. Miyatake, M. Kainosho, A. Ono, T. Ikariya, R. Noyori, *J. Am. Chem. Soc.* **1999**, *121*, 12035-12044.
- [32] Y. Misumi, T. Masuda, *Macromolecules* **1998**, *31*, 7572-7573.
- [33] S. Kumazawa, J. R. Castanon, N. Onishi, K. Kuwata, M. Shiotsuki, F. Sanda, *Organometallics* **2012**, *31*, 6834-6842.
- [34] K. Kanki, Y. Misumi, T. Masuda, *Inorg. Chim. Acta* **2002**, *336*, 101-104.
- [35] Y. Misumi, K. Kanki, M. Miyake, T. Masuda, *Macromol. Chem. Phys.* **2000**, *201*, 2239-2244.
- [36] K. Kanki, T. Masuda, *Macromolecules* **2003**, *36*, 1500-1504.
- [37] M. Miyake, Y. Misumi, T. Masuda, *Macromolecules* **2000**, *33*, 6636-6639.
- [38] S. Kumazawa, J. R. Castanon, M. Shiotsuki, T. Sato, F. Sanda, *Polym. Chem.* **2015**, *6*, 5931-5939.
- [39] L. Liu, G. Zhang, T. Aoki, Y. Wang, T. Kaneko, M. Teraguchi, C. Zhang, H. Dong, *ACS Macro Lett.* **2016**, *5*, 1381-1385.
- [40] N. Onishi, M. Shiotsuki, T. Masuda, N. Sano, F. Sanda, *Organometallics* **2013**, *32*, 846-853.
- [41] N. S. L. Tan, P. V. Simpson, G. L. Nealon, A. N. Sobolev, P. Raiteri, M. Massi, M. I. Ogden, A. B. Lowe, *Eur. J. Inorg. Chem.* **2019**, 592-601.
- [42] I. Saeed, M. Shiotsuki, T. Masuda, *Macromolecules* **2006**, *39*, 8977-8981.
- [43] I. Saeed, M. Shiotsuki, T. Masuda, *Macromolecules* **2006**, *39*, 8567-8573.
- [44] a) M. V. Jiménez, J. J. Pérez-Torrente, M. I. Bartolomé, E. Vispe, F. J. Lahoz, L. A. Oro, *Macromolecules* **2009**, *42*, 8146-8156; b) M. Shiotsuki, N. Onishi, F. Sanda, T. Masuda, *Polym. J.* **2011**, *43*, 51-57.
- [45] a) F. Sanda, K. Terada, T. Masuda, *Macromolecules* **2005**, *38*, 8149-8154; b) F. Sanda, H. Araki, T. Masuda, *Macromolecules* **2005**, *38*, 10605-10608; c) F. Sanda, H. Araki, T. Masuda, *Macromolecules* **2004**, *37*, 8510-8516; d) G. Gao, F. Sanda, T. Masuda, *Macromolecules* **2003**, *36*, 3932-3937.
- [46] A. Nakazato, I. Saeed, M. Shiotsuki, F. Sanda, T. Masuda, *Macromolecules* **2004**, *37*, 4044-4047.
- [47] E. Yashima, K. Maeda, H. Iida, Y. Furusho, K. Nagai, *Chem. Rev.* **2009**, *109*, 6102-6211.
- [48] a) A. Sadaoyuki, J. Ayako, M. Sakiko, S. Lijun, S. Yukimitsu, I. Tomokazu, *ACS Macro Lett.* **2013**, *2*, 906-911; b) J. Lee, S. Shin, T.-L. Choi, *Macromolecules* **2018**, *51*, 7800-7806.
- [49] Y.-X. Xue, J.-L. Chen, Z.-Q. Jiang, Z. Yu, N. Liu, J. Yin, Y.-Y. Zhu, Z.-Q. Wu, *Polym. Chem.* **2014**, *5*, 6435-6438.
- [50] a) T. Fumie, Y. Koichi, O. Kiyotaka, T. Shigetoshi, *Chem. Eur. J.* **2000**, *6*, 983-993; b) O. Nobuaki, S. Atsushi, O. Reiko, T. Fumie, O. Kiyotaka, T. Shigetoshi, *Chem. Lett.* **2000**, *29*, 786-787; c) K. Onitsuka, A. Shimizu, F. Takei, S. Takahashi, *J. Inorg. Organomet. Polym.* **2009**, *19*, 98-103.
- [51] a) K. Onitsuka, M. Yamamoto, T. Mori, F. Takei, S. Takahashi, *Organometallics* **2006**, *25*, 1270-1278; b) K. Onitsuka, T. Mori, M. Yamamoto, F. Takei, S. Takahashi, *Macromolecules* **2006**, *39*, 7224-7231; c) M. Yamamoto, K. Onitsuka, S. Takahashi, *Organometallics* **2000**, *19*, 4669-4671.
- [52] N. S. L. Tan, G. L. Nealon, J. M. Lynam, A. N. Sobolev, M. I. Ogden, M. Massi, A. B. Lowe, **2019**, Submitted.

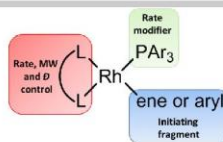
MINIREVIEW

Entry for the Table of Contents

Layout 1:

REVIEW

This mini-review provides a summary of the current state-of-the-art relating to the (controlled) polymerization of alkyne-based monomers by well-defined Rh complexes.



Nicholas Sheng Loong Tan, Andrew B. Lowe*

Page No. – Page No.

Polymerizations Mediated by Well-defined Rh Complexes

Accepted Manuscript

This article is protected by copyright. All rights reserved.

Reproduced (adapted) from

Nicholas Sheng Loong Tan, Andrew B. Lowe **‘Polymerizations Mediated by Well-defined Rhodium Complexes’** *Angewandte Chemie, International Edition* **2020**. DOI: 10.1002/anie.201909909.

With permission from the Angewandte Chemie International Edition.

License number: 498740331324, 14th January 2021.